NTNU – Trondheim
Norwegian University of
Science and Technology

Investigations into 3-*O*-protected monosaccharides

Marcus de Bourg

June 2019

Department of Chemistry
Norwegian University of Science and Technology

Supervisor: Nebojša Simić

Co-Supervisor: Sondre Nervik

Preface

The work herein has been conducted independently and in accordance with the exam regulations of the Norwegian University of Science and Technology. The work was performed during the spring of 2019 at the Department of Chemistry at NTNU under the supervision of Nebojša Simić, and co-supervised by Sondre Nervik.

It has been a pleasure working in such a great(ly toxic) working environment, compounded by my two colleagues Sondre Nervik and Edvard Stenset. I would like to thank Roger Aarvik for supplying equipment and good moods, Susana Villa Gonzales for running MS samples and Rudolf Schmid for lending equipment. Last but not least, it is thanks to the support and guidance of my parents, God and Country that I am here today.

Abstract

The work presented herein aims to facilitate the total synthesis towards 1-*O*-(3-*O*-linolenoyl-6-deoxy-6-sulfo-α-D-glucopyranosyl)-glycerol (**CDA**), a potent anti-inflammatory drug. Focusing on the initial stages of the total synthesis, the work addresses anomeric separation, mechanistic aspects of a key rearrangement-glycosylation reaction and the effect of 3-*O*-protecting groups on yields and anomeric ratios. Due to scant literature, an exploratory look into procedures for synthesis of furanosides is also presented. Additionally, methods for insertion of chirally pure glycerol acetonides in the anomeric position were investigated.

Anomeric resolution by chromatography was achieved by two derivatisation strategies. Global acetylation allowed for anomeric separation in high yields, but was constrained to medium scales (< 5 g). This featured is magnified by 4,6-*O*-acetals, allowing for larger scales (5-20 g). Insight into the rearrangement-glycosylation reaction progression was achieved by studying a wide range of 3-*O*-protected substrates. Although the exact mechanistics were found highly dependent on conditions, furanosides were generally kinetically favoured. Allyl 3-*O*-benzyl glucofuranoside was found to exhibit unusual properties in terms of selectivity and chromatographic behaviour. Viable alternatives to 3-*O*-benzyl protection were found, adding versatility to the total synthesis. None of the alternatives facilitated direct anomeric separation, although some aided work-up by imparting crystallinity. In scoping reaction conditions for furanoside synthesis, promising starting points for further optimisation were found. Lastly, Schmidt glycosylation was shown to be a viable strategy for stereochemical control of the glycerol moiety.

During the work, 44 compounds were synthesised, of which 19 are novel. In addition, 13 more intermediates and/or by-products were isolated and identified, of which 11 are novel. In total, a large amount of knowledge about glycosylation reactions have been provided, as well as insight into more exotic protecting groups with desirable properties.

Følgende arbeid har som målsetting å tilrettelegge for totalsyntesen av 1-*O*-(3-*O*-linolenoyl-6-deoksy-6-sulfo-α-D-glukopyranosyl)-glyserol (**CDA**), legemiddel med potent betennelsesdempende effekt. Med fokus på de tidligere stadiene av totalsyntesen, adresserer arbeidet anomerseparasjon, mekanistiske aspekter av en viktig glykosylering-omleiringsreaksjon, og virkningen av 3-*O*-beskyttelsesgrupper på utbytte og anomerforhold. Grunnet manglende publisert litteratur angående syntese av glukofuranosider, presenteres en utforskende studie av furanosidsyntese. Attpåtil ble metoder for å sette inn et kiralt ren glyserolacetonid i anomerisk posisjon undersøkt.

To derivatiseringsstrategier førte til anomerseparasjon ved hjelp av kromatografi. Fullstendig acetylering gjorde anomerseparasjon i høyt utbytte mulig, men strategien var begrenset til eksperimenter i mellomskala (< 5 g). Denne egenskapen er foredlet av 4,6-*O*-acetaler, som tillater oppskalering til 5-20 g. Forståelse for reaksjonsframgangen i glykosylering-omleiringsreaksjonen ble tilvirket ved å studere en rekke 3-*O*-beskyttede substrater. Selv om de eksakte mekanistiske forholdene er sterkt avhengige av reaksjonsbetingelser, eksisterer generelt en kinetisk preferanse for furanosider. Uvanlige egenskaper med tanke på selektivitet og kromatografisk natur ble funnet for allyl 3-*O*-benzyl glukofuranosid. Gode alternativer til 3-*O*-benzylbeskyttelse ble funnet, noe som gir allsidighet til syntesen. Ingen alternativer tillot direkte anomerseparasjon, men enkelte assisterte opparbeidelse ved å tilføre krystallinitet. Lovende utgangspunkt for videre optimalisering ble funnet under utforsking av reaksjonsbetingelser. Til sist ble det vist at Schmidtglykosylering er en levedyktig strategi for stereokjemisk kontroll over glyserolgruppa.

I løpet av arbeidet ble 44 stoffer syntetisert, hvorav 19 er nye. I tillegg ble 13 intermediater eller biprodukter isolert og identifisert, hvorav 11 er nye. Til samme ble en stor mengde kunnskap rundt glykosyleringsreaksjoner tilført prosjektet, i tillegg til nye forståelse for mer eksotiske beskyttelsesgrupper med ønskede egenskaper.

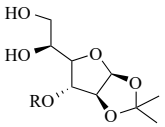

MC-1: R = Bn
MC-2: R = *p*-Ph-benzyl

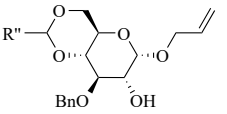

9i: R" = *p*-NO_2-Ph
9j: R" = antracene

Acid

TsOH
R"$CH(OMe)_2$

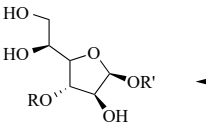

R'-OH
Promotor

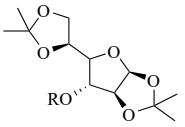

All-OH
HCl

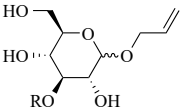

3a: R = Bn, R' = All
3c: R = *p*-Ph-benzyl, R' = All
3f: R = *t*-Bu-diphenylsilyl, R' = All
3μ: R = Bn, R' = Me

2a: R = Bn
2b: R = 2-naphthyl
2c: R = *p*-Ph-benzyl
2d: R = (3,5-di-*t*-Bu)benzyl
2e: R = *t*-Bu-dimethylsilyl
2f: R = *t*-Bu-diphenylsilyl
2g: R = triisopropylsilyl
2i: R = *p*-nitrobenzyl
2j: R = (9'-anthracenyl)methylene

4a: R = Bn
4b: R = 2-naphthyl
4c: R = *p*-Ph-benzyl
4d: R = (3,5-di-*t*-Bu)benzyl
4f: R = *t*-Bu-diphenylsilyl
4i: R = *p*-nitrobenzyl

Pyridine
Ac_2O

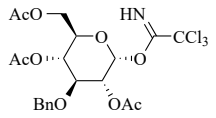

IC-5

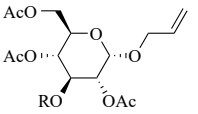

8a: R = Bn
8b: R = 2-naphthyl

Contents

Symbols and abbreviations 1

Synthesised and isolated compounds 3

1 Introduction 7
- 1.1 General description and nomenclature for carbohydrates . . . 9
- 1.2 Reactivity at the anomeric centre . . . 12
- 1.3 Glycosylation reactions . . . 15
  - 1.3.1 Fischer . . . 15
  - 1.3.2 Koenigs-Knorr . . . 16
  - 1.3.3 Thioglycoside . . . 16
  - 1.3.4 Schmidt . . . 17
- 1.4 Mechanism of glycosylation . . . 21
- 1.5 Protecting groups . . . 24
  - 1.5.1 Ethers . . . 24
  - 1.5.2 Acetals . . . 32
  - 1.5.3 Esters . . . 34
- 1.6 Status quo . . . 35

2 Results and discussion 37
- 2.1 Anomeric separation of allyl 3-*O*-benzyl-D-glucopyranoside (**4a**) . . . 37
  - 2.1.1 Global acylation . . . 38
  - 2.1.2 4,6-*O*-acetals . . . 40
- 2.2 The 3-*O*-protecting group . . . 44
  - 2.2.1 Protection of 3-OH . . . 48
  - 2.2.2 Rearrangement and glycosylation of 3-*O*-protected monosaccharides . . . 55
  - 2.2.3 3-*O*-protected furanosides . . . 63
  - 2.2.4 Furanoside syntheses . . . 72
- 2.3 Schmidt glycosylation . . . 78
  - 2.3.1 Preparation for glycosylation . . . 81
  - 2.3.2 Schmidt glycosylation . . . 83
- 2.4 Discussions on spectroscopic data . . . 87
  - 2.4.1 Optical rotation . . . 88
  - 2.4.2 NMR of furanose diacetonides . . . 91
  - 2.4.3 NMR of furanosides . . . 92

2.4.4 NMR of pyranosides 98
2.4.5 NMR of miscellaneous pyranoids 102
2.4.6 4,6-*O*-acetals 109
2.4.7 Infrared spectroscopy 117
2.4.8 Mass spectroscopy 117

3 Conclusion and further work 118

4 Experimental 120
4.1 General materials and methods 120
4.1.1 Thin-layer chromatography (TLC) 120
4.1.2 High-performance liquid chromatography (HPLC) 120
4.1.3 Flash chromatography 121
4.1.4 IR spectroscopy 121
4.1.5 Melting point analysis 121
4.1.6 MS spectroscopy 121
4.1.7 NMR spectroscopy 122
4.1.8 Optical rotation 122
4.2 Preparation of protecting groups 123
4.2.1 9-(Chloromethyl)anthracene (**RC-1**) . . . 123
4.2.2 *p*-Nitrobenzaldehyde dimethyl acetal (**RC-2**) 124
4.2.3 9-Anthraldehyde dimethyl acetal (**RC-3**) 124
4.3 Synthesis of 3-*O*-protected monosaccharides . . 125
4.3.1 General procedure for introducing benzyl-like ethers 125
4.3.2 3-*O*-Benzyl-1,2;5,6-di-*O*-isopropylidene-α-D-glucofuranose (**2a**) 126
4.3.3 3-*O*-(2-Naphthyl)methyl-1,2;5,6-di-*O*-isopropylidene-α-D-glucofuranose (**2b**) . . . 127
4.3.4 3-*O*-(*p*-Phenyl)benzyl-1,2;5,6-di-*O*-isopropylidene-α-D-glucofuranose (**2c**) 128
4.3.5 3-*O*-(3,5-Di-*tert*-butyl)benzyl-1,2;5,6-di-*O*-isopropylidene-α-D-glucofuranose (**2d**) . 129
4.3.6 3-*O*-*p*-Nitrobenzyl-1,2;5,6-di-*O*-isopropylidene-α-D-glucofuranose (**2i**) 130
4.3.7 3-*O*-(9'-Anthracenyl)methyl-1,2;5,6-di-*O*-isopropylidene-α-D-glucofuranose (**2j**) . . 131

4.3.8 3-*O*-(*t*-Butyl-dimethylsilyl)-1,2;5,6-di-*O*-isopropylidene-α-D-glucofuranose (**2e**) . . . 132
4.3.9 1,2-*O*-Isopropylidene-5-*O*-triisopropylsilyl-α-D-xylofuranose (**IC-1**) 133
4.3.10 1,2-*O*-Isopropylidene-3-*O*-benzyl-5-*O*-tri-iso-propylsilyl-α-D-xylofuranose (**IC-2**) . 134
4.3.11 1,2-*O*-Isopropylidene-3-*O*-benzyl-α-D-xylofuranose (**2ø**) 134
4.3.12 3-*O*-Benzyl-1,2;5,6-di-*O*-isopropylidene-α-D-allofuranose (**2ð**) 135
4.3.13 1,2-*O*-Isopropylidene-3-*O*-benzyl-α-D-glucofuranose (**MC-1**) 136
4.3.14 1,2-*O*-Isopropylidene-3-*O*-(*p*-phenyl)benzyl-α-D-glucofuranose (**MC-2**) 137
4.3.15 General procedure for introducing silyl ethers 138
4.3.16 3-*O*-(*t*-Butyl-diphenylsilyl)-1,2;5,6-di-*O*-isopropylidene-α-D-glucofuranose (**2f**) . . . 138
4.3.17 3-*O*-(Triisopropylsilyl)-1,2;5,6-di-*O*-isopropylidene-α-D-glucofuranose (**2g**) 139
4.4 Glycosylation of 3-*O*-protected monosaccharides 140
4.4.1 General procedure for Fischer glycosylation 140
4.4.2 General procedure for deacetylation . . . 140
4.4.3 Allyl 3-*O*-benzyl-2,4,6-tri-*O*-acetyl-α,β-D-glucopyranoside (**8a**) 140
4.4.4 Allyl 3-*O*-benzyl-α,β-D-glucopyranoside (**4a**) 142
4.4.5 Allyl 3-*O*-(2-naphthyl)methyl-2,4,6-tri-*O*-acetyl-α,β-D-glucopyranoside (**8b**) 143
4.4.6 Allyl 3-*O*-(2-naphthyl)methyl-α,β-D-glucopyranoside (**4b**) 145
4.4.7 Allyl 3-*O*-(*p*-phenyl)benzyl-D-glucopyranoside (**4c**) 146
4.4.8 Allyl 3-*O*-(3,5-di-*tert*-butyl)benzyl-D-glucopyranoside (**4d**) 147
4.4.9 Allyl 3-*O*-*p*-nitrobenzyl-D-glucopyranoside (**4i**) 148

4.4.10 Methyl 3-*O*-benzyl-2,4,6-tri-*O*-acetyl-α,β-D-glucopyranoside (**8μ**) 150
4.4.11 Methyl 3-*O*-benzyl-α,β-D-glucopyranoside (**4μ**) 151
4.4.12 Allyl 3-*O*-benzyl-α-D-xylopyranoside (**4ø**) 152
4.4.13 Allyl 3-*O*-benzyl-β-D-allopyranoside (**4ð**) and allyl 3-*O*-benzyl-β-D-allofuranoside (**3ð**) 153
4.4.14 Allyl 3-*O*-benzyl-β-D-glucofuranoside (**3a-β**) 154
4.4.15 1,2,4,6-Tetra-*O*-acetyl-3-*O*-benzyl-D-glucopyranose (**IC-3**) 155
4.4.16 3-*O*-Benzyl-2,4,6-tri-*O*-acetyl-D-glucopyranose (**IC-4**) 157
4.4.17 *O*-(3-*O*-Benzyl-2,4,6-tri-*O*-acetyl-α-D-glucopyranosyl)trichloroacetimidate (**IC-5**) . 158
4.5 Acetal protection of 1,3-diols 159
4.5.1 Allyl 3-*O*-benzyl-4,6-*O*-(*p*-nitrobenzylidene)-α,β-D-glucopyranoside (**9i**) 159
4.5.2 Allyl 3-*O*-benzyl-4,6-*O*-(9'-anthracenyl)methylene-α,β-D-glucopyranoside (**9j**) 160

Appendices i

Appendix A Experimental data i
A.1 Intermediates and byproducts isolated from the glycosylation reactions i
A.1.1 General procedure for isolating glycosylation intermediates i
A.1.2 Allyl 3-*O*-benzyl-α-D-glucofuranoside (**3a-α**) i
A.1.3 Allyl 3-*O*-(*p*-phenyl)benzyl-α,β-D-glucofuranoside (**3c**) ii
A.1.4 Methyl 3-*O*-benzyl-α,β-D-glucofuranoside (**3μ**) iii
A.1.5 Allyl 3-*O*-(*t*-butyl-diphenylsilyl)-α,β-D-glucofuranoside (**3f**) iv
A.1.6 Allyl 3-*O*-(*t*-butyl-diphenylsilyl)-α,β-D-glucopyranoside (**4f**) vi

A.1.7 Allyl 3-*O*-benzyl-5,6-*O*-isopropylidene-β-D-glucofuranoside (**MC-3**) vii
A.1.8 Allyl 3-*O*-benzyl-5,6-*O*-isopropylidene-β-D-glucofuranoside (**MC-3**) viii
A.2 Other byproducts viii
A.2.1 *N*-Benzyl-3-*O*-benzyl-4,6-di-*O*-acetyl-β-D-glucopyranosylamine viii
A.2.2 3-*O*-Benzyl-4-*O*-trichloroacetimidate-1,2,6-tri-*O*-acetyl-α, β-D-glucopyranose ix

Appendix B Spectroscopic data **xi**
B.1 Spectroscopic data for compound **2a** xi
B.2 Spectroscopic data for compound **2b** xix
B.3 Spectroscopic data for compound **2c** xxvi
B.4 Spectroscopic data for compound **2d** xxxiii
B.5 Spectroscopic data for compound **2e** xl
B.6 Spectroscopic data for compound **2f** xlvii
B.7 Spectroscopic data for compound **2g** liv
B.8 Spectroscopic data for compound **2i** lxi
B.9 Spectroscopic data for compound **2j** lxviii
B.10 Spectroscopic data for compound **2ð** lxxv
B.11 Spectroscopic data for compound **2ø** lxxxii
B.12 Spectroscopic data for compound **3a-α** lxxxix
B.13 Spectroscopic data for compound **3a-β** xcvi
B.14 Spectroscopic data for compound **3c-α** ciii
B.15 Spectroscopic data for compound **3c-β** cxi
B.16 Spectroscopic data for compound **3f-α** cxix
B.17 Spectroscopic data for compound **3f-β** cxxv
B.18 Spectroscopic data for compound **3µ-α** cxxxii
B.19 Spectroscopic data for compound **3µ-β** cxl
B.20 Spectroscopic data for compound **3ð** cxlviii
B.21 Spectroscopic data for compound **IC-1** clv
B.22 Spectroscopic data for compound **IC-2** clxii
B.23 Spectroscopic data for compound **MC-1** clxix
B.24 Spectroscopic data for compound **MC-2** clxxvi
B.25 Spectroscopic data for compound **MC-3** clxxxiii
B.26 Spectroscopic data for compound **MC-4** clxxxix
B.27 Spectroscopic data for compound **4a-α** cxcvi
B.28 Spectroscopic data for compound **4a-β** cciii

B.29 Spectroscopic data for compound **4b-α** ccx
B.30 Spectroscopic data for compound **4b-β** ccxvii
B.31 Spectroscopic data for compound **4c** ccxxiv
B.32 Spectroscopic data for compound **4d** ccxxxi
B.33 Spectroscopic data for compound **4f-α** ccxxxviii
B.34 Spectroscopic data for compound **4f-β** ccxliv
B.35 Spectroscopic data for compound **4i** ccli
B.36 Spectroscopic data for compound **4μ-α** cclviii
B.37 Spectroscopic data for compound **4μ-β** cclxv
B.38 Spectroscopic data for compound **4ø** cclxxii
B.39 Spectroscopic data for compound **4ð** cclxxix
B.40 Spectroscopic data for compound **8a-α** cclxxxvi
B.41 Spectroscopic data for compound **8a-β** ccxciii
B.42 Spectroscopic data for compound **8μ-α** ccc
B.43 Spectroscopic data for compound **8μ-β** cccvii
B.44 Spectroscopic data for compound **8b-α** cccxiv
B.45 Spectroscopic data for compound **8b-β** cccxxi
B.46 Spectroscopic data for compound **IC-3** cccxxviii
B.47 Spectroscopic data for compound **IC-4** cccxxxv
B.48 Spectroscopic data for compound **IC-5** cccxlii
B.49 Spectroscopic data for compound **9j** cccxlix
B.50 Spectroscopic data for compound **9j-α** ccccl
B.51 Spectroscopic data for compound **9j-β** ccclx
B.52 Spectroscopic data for compound **9i-α** ccclxvii
B.53 Spectroscopic data for compound **9i-β** ccclxxiv
B.54 Spectroscopic data for glucopyranosylamine . . . ccclxxxi
B.55 Spectroscopic data for compound **RC-3** ccclxxxix
B.56 Spectroscopic data for compound **RC-2** cccxcvi
B.57 Spectroscopic data for compound **RC-1** . . . . . cdiii
B.58 Spectroscopic data for 4-*O*-TCAI . . . . . cdvii

Symbols and abbreviations

Table 1: Symbols and abbreviations.

Abbreviation	Explanation
ANT	9-(methyl)anthracene
CAN	cerium ammonium nitrate
CSA	camphosulfonic acid
DBU	1,8-diazabicyclo[5.4.0]undec-7-ene
DCA	dichloroacetic acid
DCM	dichloromethane
DMF	*N*,*N*-dimethylformamide
DMSO	dimethylsulfoxide
DTB	(3,5-di-*t*-butyl)benzyl
DDQ	2,3-dichloro-5,6-dicyano-1,4-benzoquinone
DMAP	4-dimethyl aminopyridine
DMSO	dimethyl sulfoxide
DTB	3,5-di-*tert*-butylbenzyl
FMOC	fluorenylmethyloxycarbonyl
GLF	glucofuranoside
HPLC	high-performance liquid chromatography
LdB-AvE	Lobry de Bruyn–Alberda–van Ekenstein
LC	liquid chromatography
NAP	2-naphthyl
NBS	*N*-bromosuccinimide
NIS	*N*-iodosuccinimide
OTf	trifluoromethanesulfonyl
OTs	toluenesulfonyl
PG	protecting group
PMB	*p*-methoxybenzyl
PNB	*p*-nitrobenzyl
PPB	*p*-phenylbenzyl
rt	room temperature
SQAG	sulfoquinovosyl acylglycerol
SQDG	sulfoquinovosyl diacylglycerol

Table 2: Symbols and abbreviations (continued).

Abbreviation	Explanation
TBAF	tetra-*n*-butylammonium fluoride
TBDMS	*tert*-butyldimethylsilyl
TBDPS	*tert*-butyldiphenylsilyl
TCA	trichloroacetic acid
TCAI	trichloroacetimidate
TCAN	trichloroacetonitrile
TCT	2,4,6-trichloro-1,3,5-triazine
TEA	triethylamine
TEABr	tetraethylammonium bromide
TFA	trifluoroacetic acid
THF	tetrhydrofuran
TIPS	triisopropylsilyl
TLC	thin-layer chromatography
TMS	trimethylsilyl
TMSCl	trimethylsilyl chloride
Troc	2,2,2-trichloroethoxycarbonyl
TMS	trimethylsilyl

Synthesised and isolated compounds

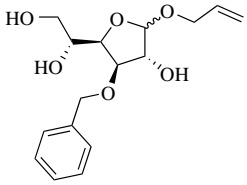

3a

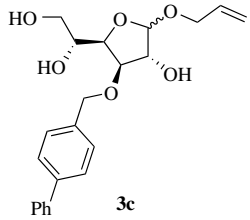

3c

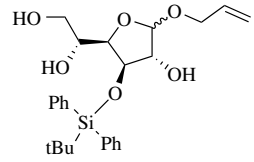

3f

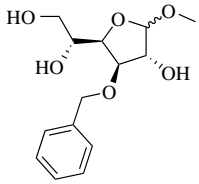

3µ

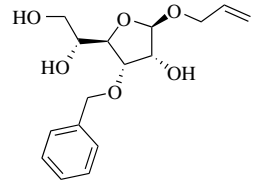

3ð

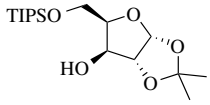

IC-1

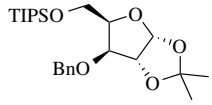

IC-2

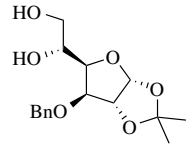

MC-1

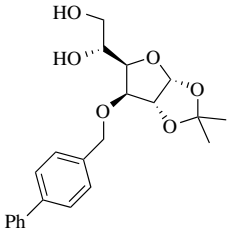

MC-2

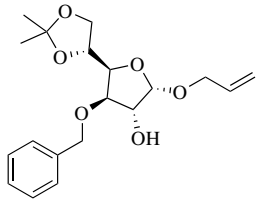

MC-3

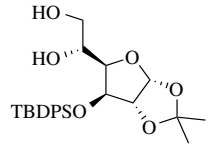

MC-4

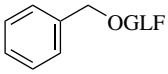

2a

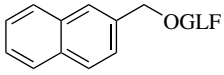

2b

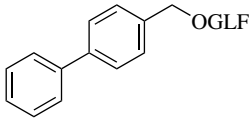

2c

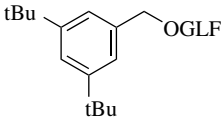

2d

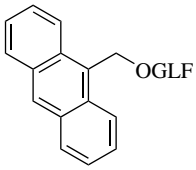

2j

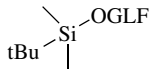

2e

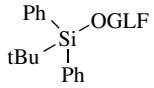

2f

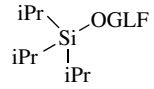

2g

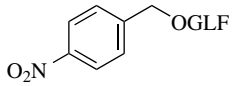

2i

GLF =

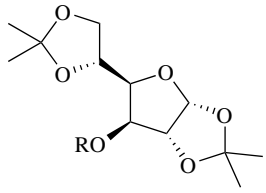

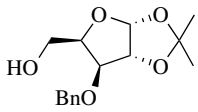

2ø

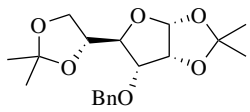

2ð

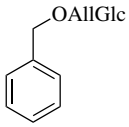

4a

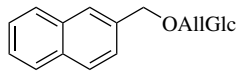

4b

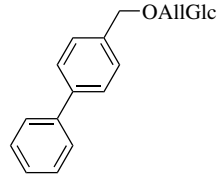

4c

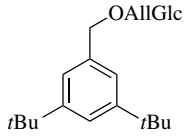

4d

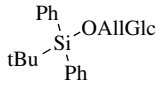

4f

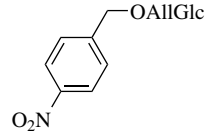

4i

AllGlc =

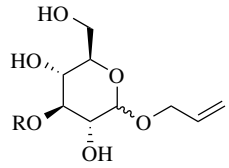

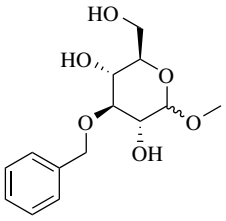

4µ

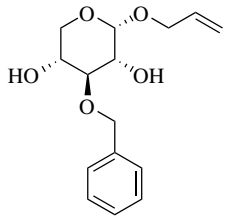

4ø

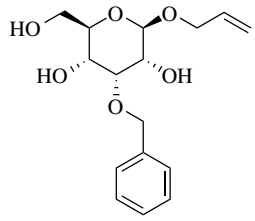

4ð

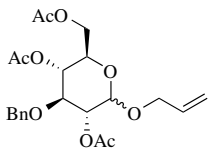

8a

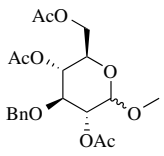

8μ

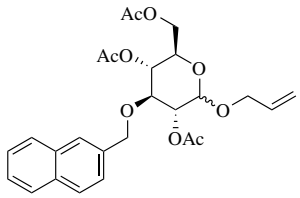

8b

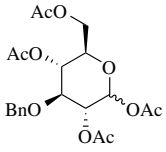

IC-3

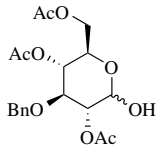

IC-4

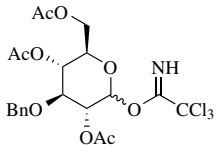

IC-5

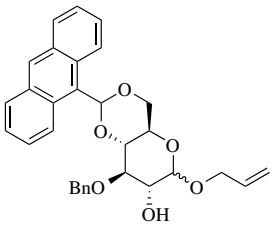

9j

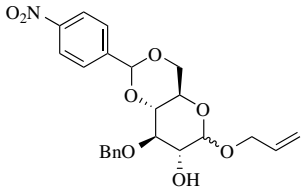

9i

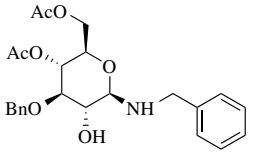

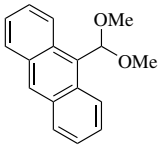

RC-3

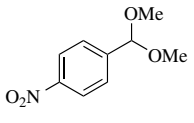

RC-2

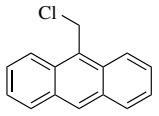

RC-1

1 Introduction

Carbohydrates compounds have seen a long history of medical use. Clinical use of carbohydrate based drugs dates back to the 17th century, at least, when extracts from foxglove, *Digitalis purpurea*, were deemed medicinally relevant. It was not until 1926 that the active component, digitoxin (**10w**, Figure 1), was identified.[1] Digitoxin has a saponin-like structure, consisting of a trisaccharide (blue) coupled to a steroid moitey (red), and has been used as a cardiac drug.[2] More recent carbohydrate drugs include the antithrombotic drug idraparinux (**10x**). The drug consists of a pentasaccharide backbone derivatised with sulfonyl esters and methyl ethers, as well as carboxylic acid groups.[3] Modifications to the carbohydrate backbone, can make more drug-like carbohydrate analogs, such as oseltamivir (Figure 2, **10y**). Perhaps better known by its brand name, Tamiflu, oseltamivir inhibits influenza neuraminidases. Here, the carbohydrate backbone is modified, such that the molecule becomes more hydrophobic, while retaining its biological activity.[4]

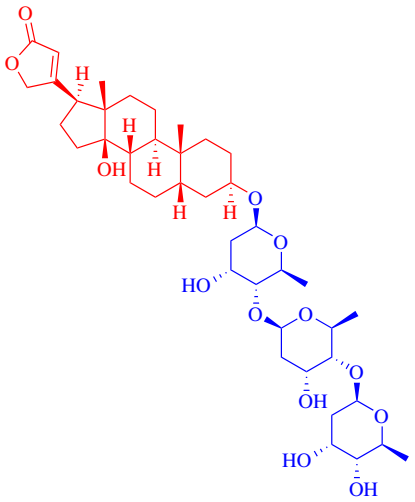

10w

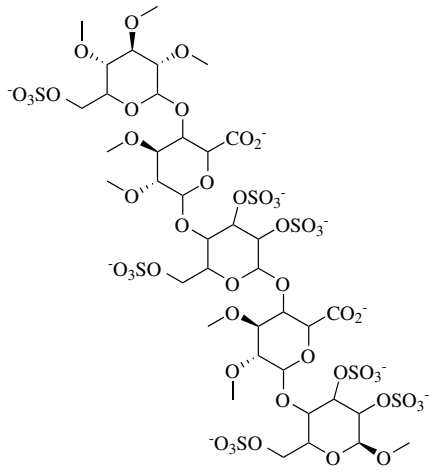

10x

Figure 1: Carbohydrate drugs dixitoxin (**10w**) and idraparinux (**10x**).

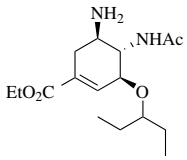

10y

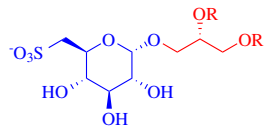

10z: R = oleyl

Figure 2: Carbohydrate and carbohydrate-based drugs oseltamivir (**10y**) and a sulfoquinovosyl diacyl glycerol (**10z**).

Another class of drugs based on carbohydrates, are the glycoglycerolipids, which are prevalent in plant-like species. These are carbohydrates with a glycerol moiety bearing fatty acid esters. Glycoglycerolipids have been shown to have a wide range of bioactivities, such as anti-tumor and anti-viral activity.[5] A prominent subgroup of glycoglycerolipids, is sulfoquinovosyl acyl glycerols (SQAG), which includes sulfoquinovosyl diacyl glycerols (SQDG).[5] An example of an SQAG is **10z**, which has anti-HIV activity.[6] SQAGs consist of sulfoquinovose (**10z**, in blue), with a diacylglycerol moiety (in red). The acyl groups can be both saturated and unsaturated fatty acids.[5]

In 2015, a novel compound, **CDA** (Figure 3), sharing many properties with SQAGs, was isolated from the common hardgrass *S. dura*. It was determined that **CDA** exhibits anti-inflammatory properties. The mechanism of said effect was not known, but it was found that *CDA* reduces activity of PLA2 enzymes, which are normally involved in early stage of inflammation.

The mechanism of said effect is undetermined, however, inhibition of arachidonic acid release was found to be involved.[7] The structural likeness with SQDGs, differing in the placement of the acyl group, along with the wide range of bioactivities of SQDGs, makes **CDA** and other sulfoquinovosylglycerols with fatty acids attached to the sugar backbone, very interesting as potential drugs.

In order to explore the structure-activity relationship of **CDA**-like compounds, a total synthesis strategy has to be devised. This would facilitate the synthesis of a range of

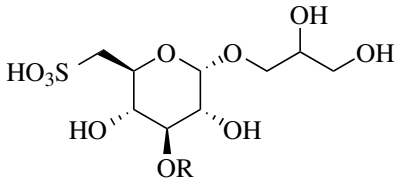

CDA: R = linolenate

Figure 3: Potential SQDG-like drug exhibiting anti-inflammatory properties.[7]

CDA-analogs. Although total syntheses of various SQDGs are found[5], placing the acyl group on the sugar introduces additional difficulties in terms of selectivity and compatibility. To give an understanding of the processes required in the syntheses of carbohydrate derivatives, a brief description of carbohydrate properties, their reactions and common protecting group manipulations used to achieve selectivity in carbohydrate chemistry will be presented.

1.1 General description and nomenclature for carbohydrates

Carbohydrates, as their name suggests, can be described by the formula $(CH_2O)_n$. In their simplest form, carbohydrates are carbon chains with multiple hydroxyl groups (Figure 4), bearing an aldehyde (*aldose*, left) or keto (*ketose*, right) group. The length of the carbon chain is typically, but not limited to, five or six carbon atoms. Numbering starts at the end closest to the carbonyl group. A carbohydrate having a substituent on C-*n*, would be *n-C*-substituted, for example, where C-*n* is carbon number *n*. More commonly, the substituents are on the hydroxyl oxygens. When the substituent is on the hydroxyl group on C-*m*, the carbohydrate is considered *m-O*-substituted (exemplified in Figure 4). Differing stereochemistry at the hydroxyl-bearing carbons gives rise to the different carbohydrate configurations.[8] The gluco-configuration (left in Figure 4) is the most relevant to the work presented herein.

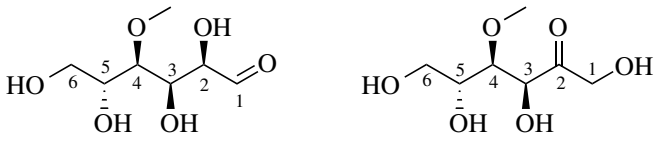

Figure 4: D-Glucose (left) and D-fructose (right), bearing 4-*O*-methyl groups.

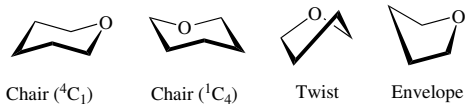

Figure 5: Chair conformations of pyranose rings (left and middle left) and conformations of furanose rings (middle right and right).[11]

Not long after the discovery of the previously described carbohydrate structure, it was noted that the carbonyl group would react very sluggishly, having a reactivity far lower than expected.[9] This phenomena was attributed to ring closing, via the formation of an intramolecular hemicacetal. It was found that the open-chain form is almost negligible, while the furanose and pyranose forms are dominant.[10] Due to their stability, five-membered (*furanose*) and six-membered (*pyranose*) rings are favoured under most circumstances (Figure 1). Upon ring closing, a new chiral centre is formed at C-1 (the *anomeric centre*), resulting in two epimers, the α- and β-*anomers*. Under certain conditions, interconversion between all forms (open-chain form and both anomers of furanose and pyranose) occurs.[8]

Upon ring closure, the resulting pyranose ring can theoretically take on 26 different conformations: two chair, six boat, six skew and 12 half-chair. Only the chair conformations will be discussed here, as only the chair conformations are relevant for the vast majority of pyranose sugars. Of the two chair conformations, the $^4C_1$ (Figure 5) is dominant for most D-pyranoses (the D-enantiomers being prevalent for carbohydrates in nature, as opposed to the L-enantiomers).[11] Due to the lower barrier to conformational change in fu-

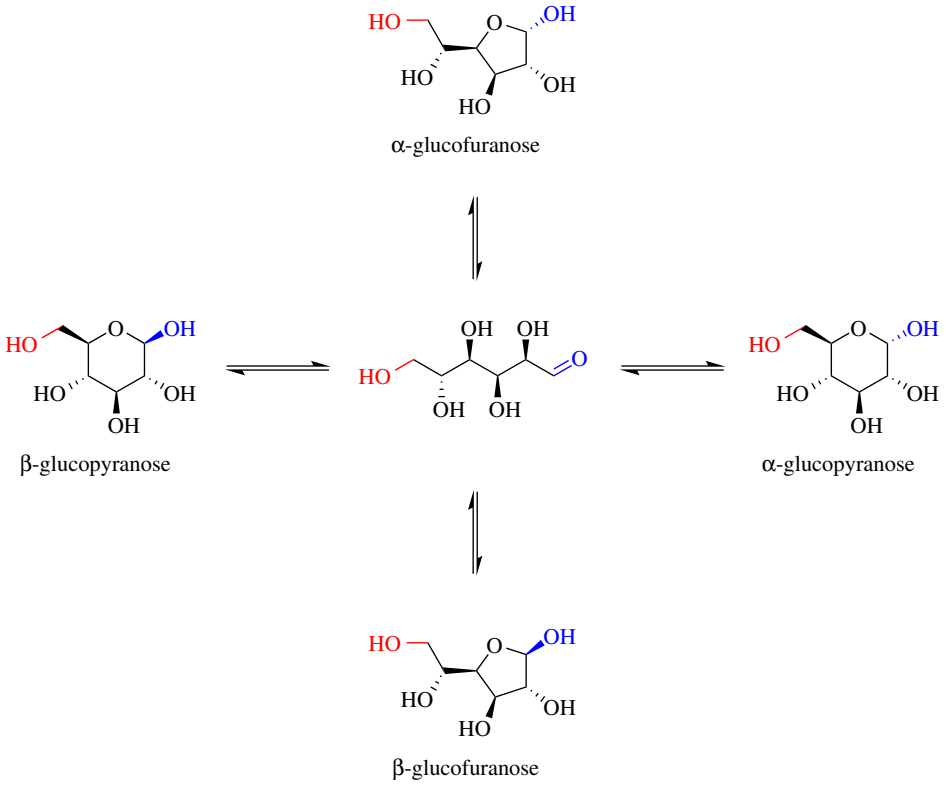

Scheme 1: Equilibrium between open-chain, and anomers of the furanose and pyranose forms of D-glucose. Positions one and six are highlighted in blue and red, respectively.

ranose rings, conformations are more dynamic. Multiple twist and envelope conformations (Figure 5) are possible. Conformations are highly dependent on the sugar configuration and substitution pattern.[12] Due to the compounds studied most extensively in this work being of the same gluco-configuration and having similar substitution patterns, carbohydrate conformations will not be extensively covered here.

1.2 Reactivity at the anomeric centre

In the middle of the 19th century, it was discovered that for a solution of pure α-D-glucose, the optical rotation would decline over time,[13] a phenomenon later dubbed *mutarotation* by T. M. Lowry.[14] The explanation was later found to be a reversible interconversion between the α- and β-anomers.[15]

After equilibrium between the anomers has been established, the ratio of anomers (RA) is dependent on the relative stabilities of the anomers.[11] Sterically demanding substituents give rise to a preference for equatorial positions (i.e. the β-anomer for the anomeric substituent) due to steric factors. Nevertheless, a disproportionate preference for the α-anomer was observed.[16] The preference for the α-anomer was dubbed the *anomeric effect* by N. J. Chu,[17] who studied it extensively. The mechanism behind the anomeric effect has been the subject of lengthy debate. Two models compete: orbital interactions with endocyclic oxygen lone pairs, and minimisation of dipole moment. In the orbital interaction model, favourable orbital interactions takes place between the endocyclic oxygen lone pairs and the orbitals of the bond between C-1 and 1-OH in the α-anomer (Scheme 2). The dipole minimisation model explains the preference for the α-anomer by its lower dipole moment, relative to the β-anomer (Scheme 3). The models are not necessarily mutually exclusive; both could be operative at the same time.[18]

Regardless of mechanism, some aspects of the anomeric effect are undisputed. Increased electron withdrawing properties of the anomeric substituent, results in bias for the α-anomer.[19] The C-2 substituent also influences the anomeric

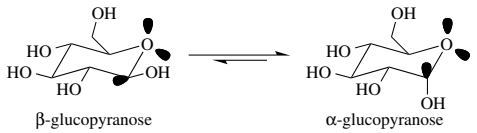

Scheme 2: Orbital interaction model in equilibrium between α- and β-gluopyranose.

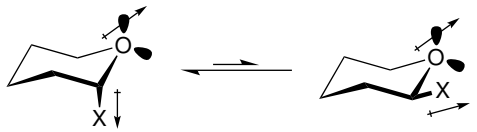

Scheme 3: Dipole minimisation model in equilibrium between generalised α- and β-gluopyranose.

affect, where an axial group on C-2 imparts the anomeric effect.[20] A small effect is observed for the C-5 subtituent.[12] Other substituents have not been observed to play an important role.[21] Solvent polarity and temperature are significant influencers, with increased temperature and reduced solvent polarity amplifying the anomeric effect.[18]

In order for interconversion between the anomers to even occur, it was found by T. M. Lowry[22] that both an acid and a base catalyst is required. Multiple mechanisms for the action of the acid and base have been proposed to account for kinetic isotope effect findings, ranging from concerted acid-base action, to general acid-catalysis.[23] An interesting side-story is the bifunctional catalyst, 2-pyridinol, which is capable of acting as both an acid and a base in a concerted manner (Scheme 4). Due to its bifunctional nature, 2-pyridinol is a much better mutarotation catalyst than acids and bases of approximately equal strength.[24]

Exchange of O-1 with solvent oxygen occurs, albeit at a lower rate than than mutarotation itself. This was theorised to be the result of relatively slow solvation of the open-chain form, compared to ring-closing.[25] Although the open-chain aldehyde form has been considered an important intermediate for years, observations of said form have been elusive.[23] In a series of experiments, Los et al.[26] determined that

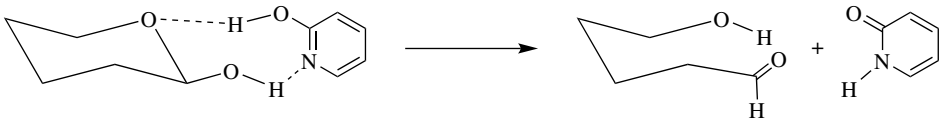

Scheme 4: 2-Pyridinol as bifunctional catalyst for mutarotation.[24]

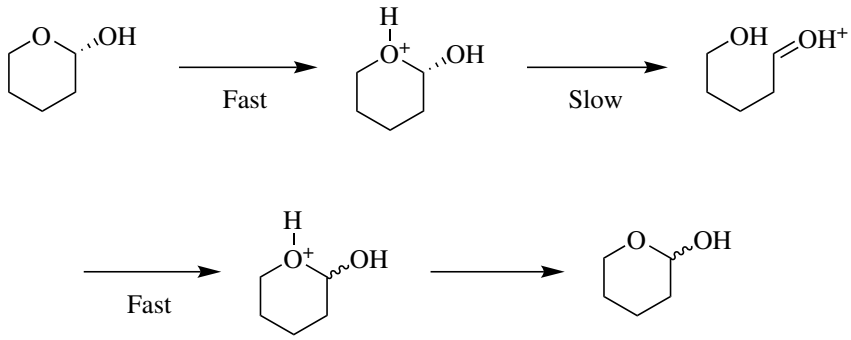

Scheme 5: Suggested mechanism for mutarotation in sugars. The exact order of protonation-deprotonation is undetermined, and an arbitrary choice was made here.[23]

for glucose, the open-chain form represented approximately 0.0026%. Ring closing was observed to be significantly faster than ring-opening.

In a review by Isbell and Pigman, using data collected from multiple sources, a mechanism for mutarotation is proposed (Figure 5) accounting for the previously mentioned observations. The first step involves protonation or deprotonation of the sugar, and then slow cleavage of the bond between C-1 and the ring oxygen. Upon cleavage of the ring-oxygen bond, an intermediate with a conformation close to the starting compound (similar to an early transition state), is formed. For the intermediate, dubbed *pseudo-acyclic*, ring-closing is significantly faster than ring-opening. The open-chain form is thought to have an almost transition-state like nature.[23]

Substituting the hydroxyl group at C-1 for a better leaving group, leaves C-1 more susceptible to intermolecular nucleophilic attack. This is what occurs in the *glycosylation* reaction, a key reaction in carbohydrate chemistry. The nu-

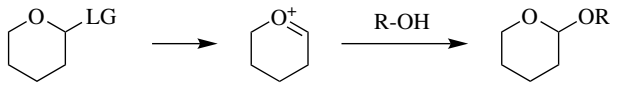

Scheme 6: Commonly used, simplified glycosylation mechanism.

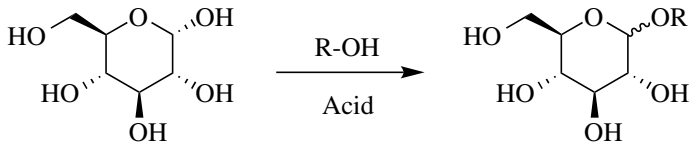

Scheme 7: Fischer glycosylation of α-D-glucose.

cleophile is the *glycosyl donor*, the carbohydrate is the *glycosyl acceptor* and the final product is the *glycoside* (not to be confused with *glucoside*, which is the glycoside of glucose). The substituent in anomeric position is often referred to as the *aglycone*.[8] Commonly, the glycosylation reaction is described to proceed via the following mechanism (Scheme 6): leaving group in anomeric position exit to form an oxocarbenium ion. Nucleophilic attack on the oxocarbenium ion yields the glycoside.[27]

1.3 Glycosylation reactions

In practice, glycosylation reactions are among the most commonly used reactions in carbohydrate chemistry.[8] Practical aspects of some common types of glycosylation reactions will be presented here.

1.3.1 Fischer

Fischer glycosylation represents glycosylation in its simplest form (Scheme 7), where the glycoside donor is the solvent. The acid acts as a promotor, turning the anomeric hydroxyl group into a good leaving group, followed by displacement by the solvent alcohol. Advantages of the Fischer glycosylation include selectivity for anomeric position and inexpensive reagents. Only simple alcohols can be used as glycosyl

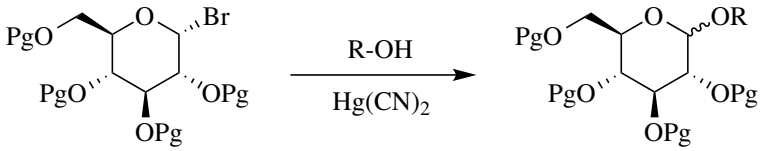

Scheme 8: Koenigs-Knorr glycosylation. Pg = protecting group.

donors, however. The usability of the reactions is also limited by the harsh conditions required (i.e. strong acid and high temperature). Stereoselectivity in Fischer glycosylations are dictated by the anomeric effect, thereby offering little in terms of tuning capabilities.[28]

1.3.2 Koenigs-Knorr

Due to these shortcomings, alternatives to Fischer glycosylation have been developed. An early glycosylation method that still sees wide use to this day, is the Koening-Knorr method (Scheme 8). It involves activation of the glycosyl acceptor by forming a glycosyl halide (either bromide or chloride). Heavy metal salts, most commonly silver and mercury salts, are used as promotors, alongside with an acid-scavenger and drying agent. Some tuning in terms of anomeric selectivity is possible, for example via neighbouring group participation. Conversion to glycosyl halides is possible. Drawbacks of the Koenigs-Knorr method primarily involve the use of toxic and expensive heavy metal salts. It does not offer great opportunities in terms of anomeric selectivity, however.[29] The method has been expanded to use Lewis acids and phase transfer catalysts as promotors as well.[30]

1.3.3 Thioglycoside

The relatively high stability of the thioglycoside and the mild conditions used in the glycosylation reaction has resulted in widespread use of the thioglycoside method (Scheme 10). A wide array of alkyl and aryl thioglycosides, with corresponding thiophilic promotors can be used.[30] Thioglycosides have the ability to be used in sequential glycosylation reactions

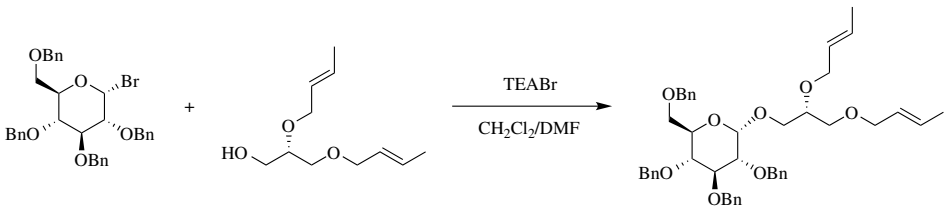

Scheme 9: Koenigs-Knorr glycosylation with labile glycosyl donor and phase transfer catalyst in Mannock's monoglycosyldiacylglycerol synthesis.[5] TEABr = tetraethylammonium bromide.

(Figure 11).[31] Good anomeric selectivity can be achieved by modifying reaction conditions and additives.[32]

1.3.4 Schmidt

Discovered in the 1980s, the trichloroacetimidate (or Schmidt) method, has quickly become a popular glycosylation method. It is initiated by activation of the glycosyl acceptor with trichloroacetonitrile (Scheme 12) and a base. Glycosylation occurs under mild Lewis acid promotion.[30]

Excellent anomeric control for the glycosyl trichloroacetimidate (TCAI) can be achieved. The β-anomer is favoured under kinetic conditions, while the α-anomer under thermodynamic conditions. Formation of the β-glycosyl TCAI is thought to be reversible, allowing the β-anomer to act as an intermediate in the formation of the thermodynamic α-anomer (Scheme 13). Varying the base also impacts the glycosyl TCAI ratio of anomers, where for example K_2CO_3 and DBU can help facilitate selectivity for the β-anomer, while NaH often favours the α-anomer.[33]

Glycosylation occurs by addition to the glucosyl TCAI, usually in the presence of an acid catalyst. Only a mild Lewis acid catalyst is required, however, such as $BF_3 \cdot OEt_2$ at low concentrations (Scheme 14 illustrates glycoslation in the presence of labile triethylsilyl ethers). At lower temperatures, glycosylation protomoted by $BF_3 \cdot Et_2O$ primarily gives inversion at the anomeric centre. The stronger acid TMS-OTf, on the other hand results in the preference for

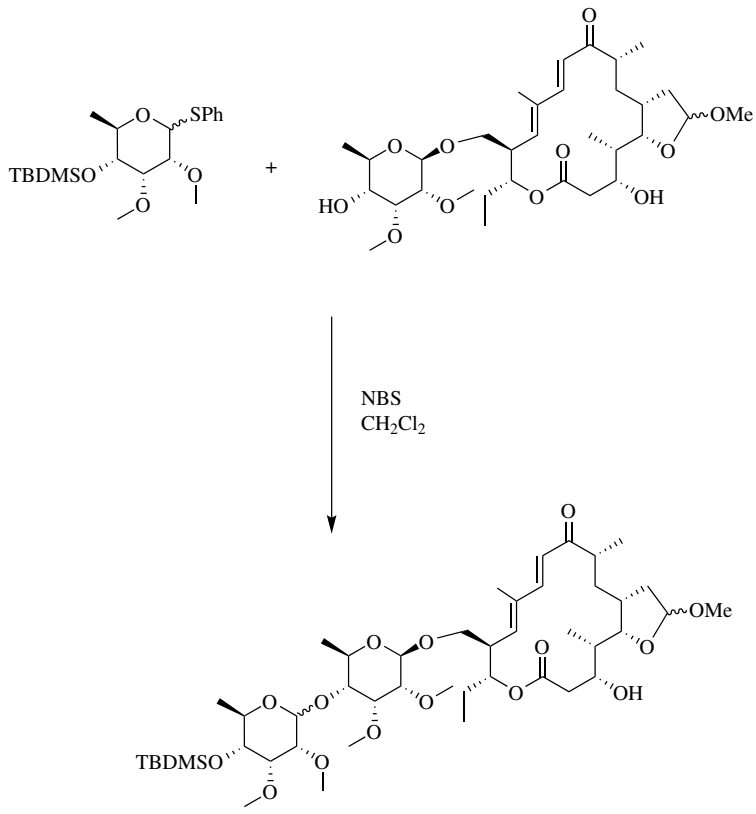

Scheme 10: Thioglycoside method in Toshima's synthesis of a tylosin derivative.[30] NBS = *N*-bromosuccinimide.

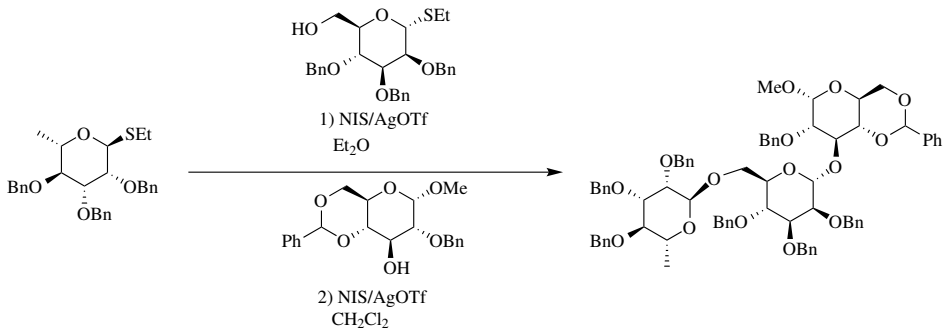

Scheme 11: Thioglycosides in sequential trisaccharide synthesis.[32] NIS = *N*-iodosuccinimide.

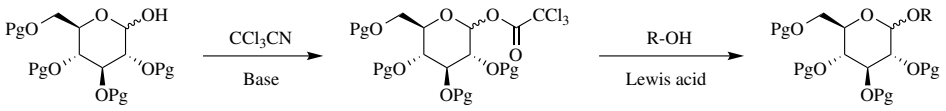

Scheme 12: Schmidt glycosylation. Pg = protecting group.

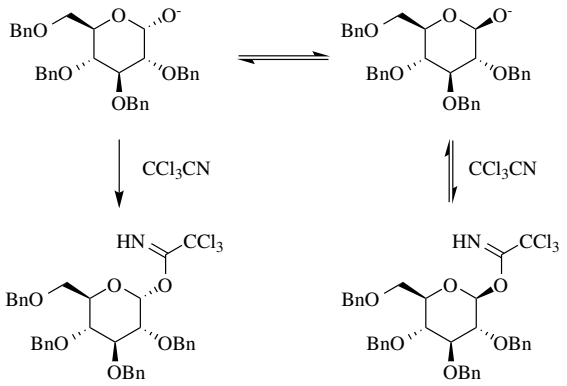

Scheme 13: Dynamics of glycosyl trichloroacetimidate formation, according to Schmidt.[33]

the thermodynamic product (usually α-glucosides for gluco-configurations). In the presence of acetyl or other participating neighbouring groups, selectivity is to a large extent determined by neighbouring group participation. For example high α-selectivity is achieved for mannosides.[33] Other activators, such as pyridinium *p*-toluenesulfonate (PPTS) have also been developed.[30] The glucosyl TCAIs are often sufficiently labile to allow glycosylation with carboxylic acids as nucleophiles as well.[33]

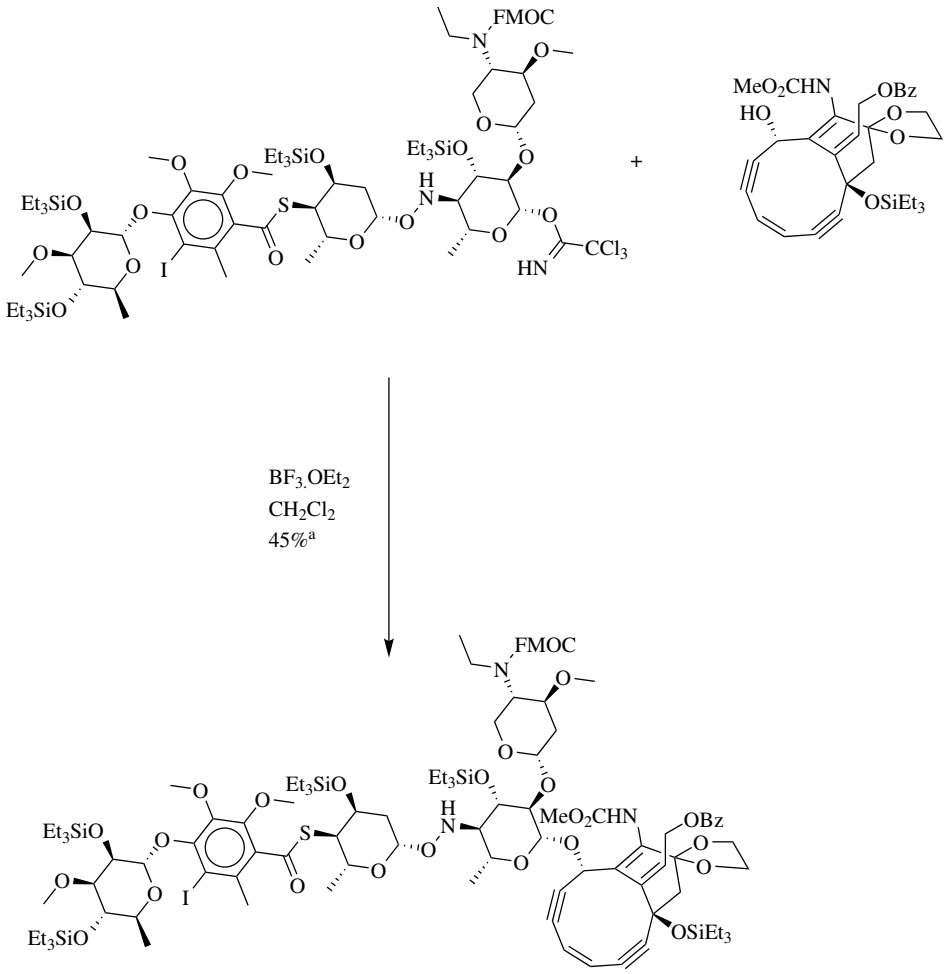

Scheme 14: Schmidt glycosylation in one of the last steps of Nicolaou's Calicheamicin γ^1 synthesis.[34] FMOC = fluorenylmethyloxycarbonyl. [a] 45% yield plus 31% monodesilylated product.

Figure 6: Methoxymethyl cation.

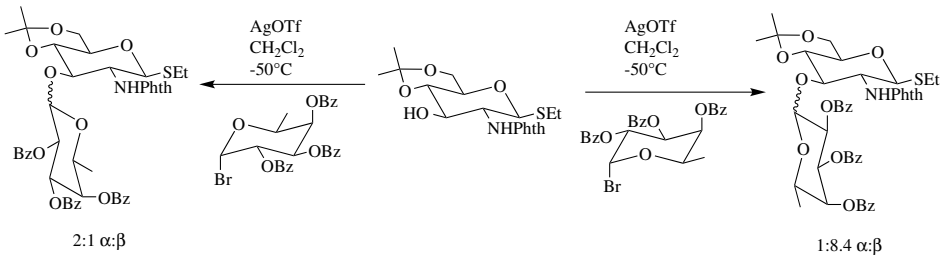

Scheme 15: Large difference in selectivity from enantiomer pair of glycosyl acceptors.[27] NPhth = phthalimide.

1.4 Mechanism of glycosylation

The existence of the previously discussed oxocarbenium ions (Section 1.2) has been a highly debated topic for a long time. Despite the research into the topic, glycosyl oxocarbenium ions have not been observed in organic solvents. Thought to be approximately as stable as glycosyl oxocarbenium ions, the methoxymethyl cation, on the other hand, has been observed by NMR.[27]

Results from some types of glycosylation gives credence to an S_N1-type mechanism. Fischer glycosylations (discussed in Section 1.3.1) proceed with racemisation at the anomeric centre. Resulting ratio of anomers are only decided by the relative stabilities of the anomers.[8] It is usually difficult to achieve selectivity for Koenigs-Knorr glycosylations (discussed in Section 1.3.2).[30] Unexpected selectivites are sometimes observed in Koenings-Knorr reactions. For example in a disaccharide synthesis, the two enantiomers of the glycosyl acceptors gave widely different selectivity (Scheme 15).[27]

Schmidt glycosylations (discussed in Section 1.3.4), on the other hand, proceeds primarily with retention at the anomeric centre, at least under kinetic control.[33] The observed retention is often attributed to an "exploded" transition state (Figure 7).[27]

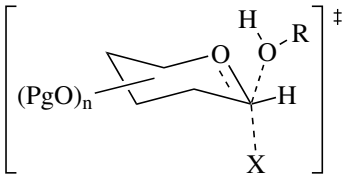

Figure 7: Exploded transition state during glycosylation.[27]

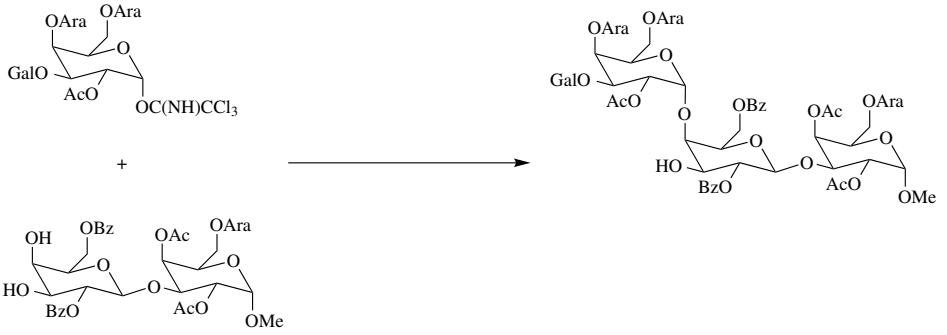

Scheme 16: Pure α-product in spite of 2-*O*-acetyl group.[35] Gal = perbenzoyl-galactosyl. Ara = perbenzoyl-arabinosyl.

The previously mentioned selectivity is not universal. When a neighbouring group capable of anchimeric assistance is present, the 1,2-*trans* product is formed almost exclusively.[33] In an oligosaccharide synthesis by Yang et al., however, instead of the expected 1,2-*trans* product (β-anomer), only the α anomer is seen (Scheme 16).[35]

The glycosyl donor also plays a large part in determining stereoselectivity. A series of experiments with donors of decreasing nucleophilicity, from ethanol to trifluoroethanol were conducted.[36] The effect of the donor nucleophilicty is highly dependent on the nature of the acceptor, though. For the 4,6-*O*-benzylidene protected thioglycoside, a sharp increase in α-selectivity is seen with decreasing donor nucleophilicity. With the same protecting group pattern on a thiglycoside acceptor with the *manno* configuration, no influence of donor nucleophile strength was observed. Substituting the acceptor for a mannonic acid ester or the donor for allyl-TMS also have dramatic impacts on selectivity.[36]

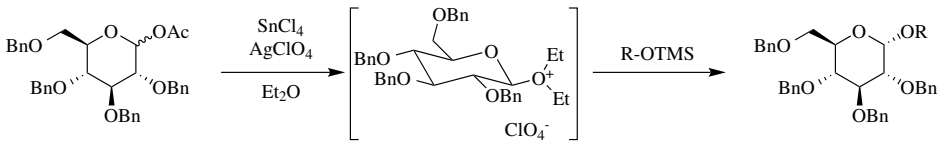

Scheme 17: Solvent participation and ion pair used to explain stereochemical outcome of reaction.[38] R = cholestanyl.

In addition to neighbouring groups, solvent and additives can also take part in glycosylation reactions.[11] Acetonitrile[27] and DMF[37] modify the selectivity of glycosylation reactions by direct participation. Solvent and additives could also interact with the reaction at the same time. The α-selectivity achieved in glycosylations with a Lewis acid and $AgClO_4$ was explained by participation of the solvent (diethyl ether) combined with the perchlorate ion blocking the path leading to the other stereochemical outcome (Scheme 17).[38]

A mounting body of evidence shows that the oxocarbenium mechanism is a gross simplification. Glycosylation reactions spans the entire continuum between S_N1 and S_N2 and contact ion pair mechanisms span the gap between the two extremes. Many of the mechanistic aspects of glycosylation reaction are covered in-depth in a recent, comprehensive review by Adero et al.[36] Although it is possible to determine the mechanistic aspects of a specific reaction with fairly high certainty, it can be difficult to make good predictions about the outcome of a reaction. A large number of factors impact the outcome; glycosyl donor nucleophilicity and stereoelectronic effects, acceptor conformation and neighbouring groups, temperature and a wide range of solvent effects, among others.[36]

Some examples of the large effects that small changes in conditions can incur on the outcome, have been presented in this section. A parallel can be drawn between the selectivity in glycosylation reactions and the field of *chaos theory* in mathematics dealing with *chaotic systems*. Although deterministic, chaotic systems exhibit a dramatic effect of initial variables on the final outcome. Changes in initial conditions smaller than the rounding error in numerical computations,

have large effects on the outcome. As a result, predictions about the outcome are difficult, if not impossible, to make.[39]

Although glycosylation reactions arguably resemble chaotic systems, recent advances in technology have allowed for greater degrees of automation in studies of glycosylation reactions. Automation permits the construction of empirical models covering a wider range of conditions. In an excellent study by Chatterjee et al.[40], a microreactor setup with automated HPLC analysis was employed. As a result, a large group of substrates and conditions could be surveyed with less effort. The study provides an empirical understanding of glycosylation with glycosyl trichloroacetimidates.[40] Applying the same methodology to a wider range of substrates could allow for making empirical interpolations, resulting in better predictions of outcome for glycosylation reactions.

1.5 Protecting groups

The primary challenge in carbohydrate synthesis lies in achieving selectivity for the desired hydroxyl group. Only the primary hydroxymethyl (e.g. 6-OH in glucose-derivatives) can be manipulated in a selective manner, due to steric accessibility factors. Some selectivity can be achieved for the anomeric position as well through certain glycosylation reactions. In order to accomplish selectivity for most positions on the carbohydrate backbone, a series of protecting group manipulations is required. Non-participating protecting groups have to be compatible with subsequent operations. Despite not participating in the reaction, protecting groups can affect other manipulations through anchimeric assistance and stereoelectronic effects. Bridging groups can affect conformation and structure of the carbohydrate.[28] Some useful protecting groups will be presented in the following sections.

1.5.1 Ethers

1.5.1.1 Benzyl ethers are among the most commonly used protecting groups in carbohydrate chemistry. This is due to their excellent stability to a wide range of conditions, and

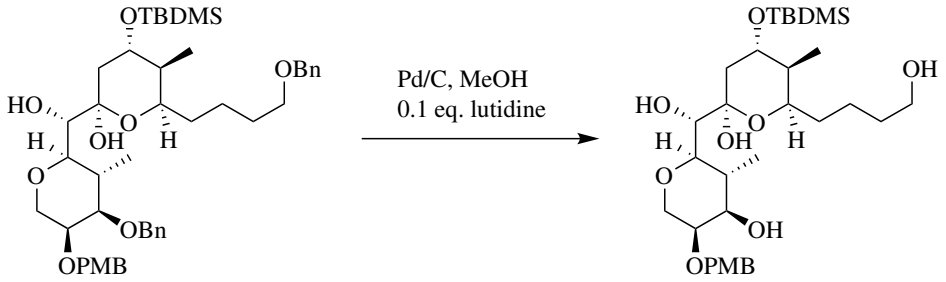

Scheme 18: Selective catalytic hydrogenation of benzyl ethers in the presence of *p*-methoxybenzyl (PMB) ethers in the total synthesis of (+)-Spongistatin 1. Lutidine serves to partially poison the catalyst.[42]

the possibility for selective removal in the presence of many other functionalities. Introduction is usually carried out with benzyl bromide with NaH in DMF. Other polar aprotic solvents and bases are possible. Should the substrate be base-sensitive, Ag_2O can serve as the base, or introduction can go via benzyl trichloroacetimidate, as in Schmidt glycosylation. Regioselectivity can be achieved by forming a benzylidene acetal, followed by regioselective reductive cleavage (Figure 27 in Section 1.5.2). Catalytic hydrogenation on a heterogeneous palladium catalyst allows for cleavage in the presence of many other functionalities. While catalytic hydrogenation is very mild, some functionalities, like nitro groups and aromatic halides, can be affected. Selectivity in the presence of more electron-rich benzyl groups, such as *p*-OMe-benzyl, is possible with some tuning (Scheme 18). Birch-like reductions, Raney nickel, oxidative conditions and Lewis acids are also capable of removing benzyl ethers (Scheme 18).[41]

1.5.1.2 2-Naphthyl (NAP) and *p*-phenylbenzyl (PPB)

ethers share many qualities with benzyl ethers. These protecting groups, with more electron-rich aromatic systems than benzyl groups, have proven to be useful protecting groups. Both benzyl-like ethers share some of the benzyl ether's resistance to cleavage under acidic conditions. These two protecting groups have the advantage of allowing for removal

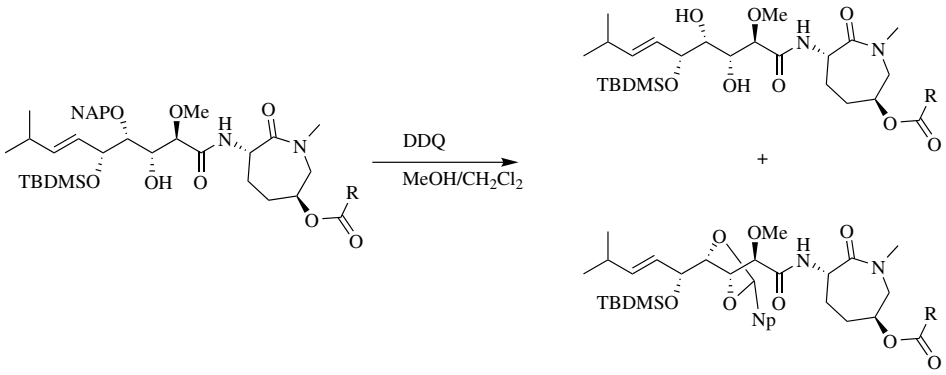

Scheme 19: Use of 2-naphthyl (NAP) ether in Bengamide B synthesis. Acetal side product is also formed.[43] DDQ = 2,3-dichloro-5,6-dicyano-1,4-benzoquinone. Np = 2-naphthalene. R = tridecyl.

under oxidative conditions, in addition to the methods used to cleave benzyl ethers. Introduction is carried out via regular Williamson ether synthesis from the corresponding bromide or chloride, or by Fischer glycosylation. Cleavage occurs under similar conditions to benzl ethers, e.g. catalytic hydrogenation, Birch reduction etc. In addition, NAP and PPB ethers can be removed in the presence of benzyl ethers. Oxidative cleavage occurs with 2,3-dichloro-5,6-dicyano-1,4-benzoquinone (DDQ), typically in DCM-methanol. Allylic alcohols may be oxidised with DDQ, but this can often be avoided, such as in Scheme 19.[41]

1.5.1.3 *p*-Methoxybenzyl (PMB) ethers are more ephemeral alternatives to the benzyl ether. PMB ethers exhibit significantly higher acid-lability than benzyl ethers. Introduction via Williamson ether synthesis from PMB-Cl or PMB-Br is preferred. An advantage of PMB ethers is the possibility of facile cleavage under oxidative conditions with DDQ or cerium ammonium nitrate (CAN). PMB ethers can be cleaved selectively in the presence of both NAP and benzyl ethers (Scheme 20). Benzyl ethers are regularly not removed with DDQ. Silyl ethers are also spared.[41] Although PMB ethers

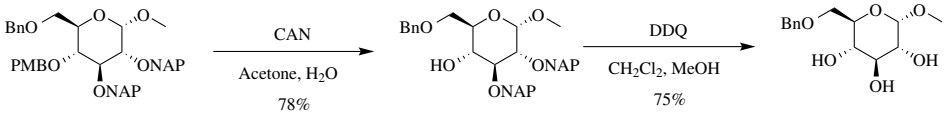

Scheme 20: Selective oxidative cleavage of *p*-OMe-benzyl with cerium ammonium nitrate (CAN) and 2,3-dichloro-5,6-dicyano-1,4-benzoquinone (DDQ).[45]

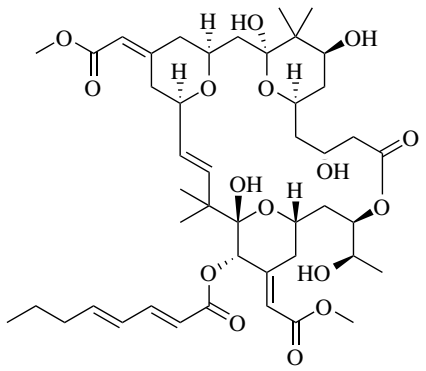

Figure 8: Bryostatin 2.[44]

are acid-labile, some acid-catalysed reactions are possible to carry out with PMB ethers present. In Evans'[44] Bryostatin 2 (Figure 8) synthesis, a PMB ether is present though over ten reaction steps, of which some are acid-catalysed.

1.5.1.4 *p*-Nitrobenzyl (PNB) and *p*-halobenzyl ethers are modified versions of the benzyl ether, with electron withdrawing substituents, augmenting their acid-stability. In addition, increased acid-resitance is observed for such ethers. *p*-Nitrobenzyl (PNB) and *p*-halobenzyl ethers have the ability to be cleaved under relatively mild conditions (Scheme 21), and in the case of PNB ethers, in the presence of benzyl ethers. The ethers also have a propensity to impart crystallinity, aiding product purification.[41, 45] The PNB ether can be cleaved orthogonally to benzyl ethers by first reducing the nitro group to get an amine. As the PNB ether is more labile to catalytic hydrogenation than the benzyl ether, it is

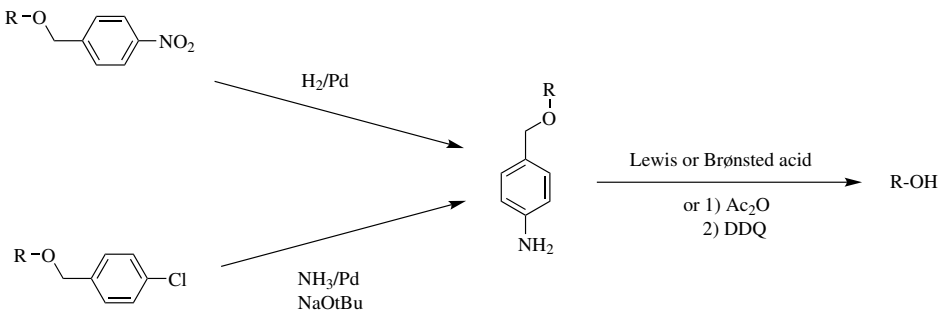

Scheme 21: Cleavage of *p*-nitrobenzyl and *p*-halobenzyl ethers.[45, 46]

possible to achieve selectivity this way. Zn-Cu can also be used to reduce the PNB ether selectively. Removal of the *p*-aminobenzyl is facilitated by acetic anhydride, giving an amide, which is cleaved with DDQ.[46] Kakitsubata's dermatan sulfate trisaccharide synthesis is an example of the usefulness PNB ethers, where it is removed in the presence of benzyl ethers, a trichloroethoxycarbonyl (Troc) group, a benzoyl ester and a TBDMS ether (Scheme 22).[47]

The base sensitivity of PNB ethers makes regular Williamson ether synthesis conditions inviable. Formation of PNB ethers usually takes place from PNB-Br and Ag_2O in an apolar solvent. Substituting silver oxide for silver triflate, or using PNB trichloroacetimidate are also possibilities. Reductive cleavage of *p*-nitrobenzylidene acetals can give selective formation of PNB ethers.[46]

p-Halobenzyl ethers (Cl, Br), on the other hand, can be introduced under regular, basic Willamson ether synthesis conditions. Cleavage of *p*-halobenzyl ether can be achieved by palladium-catalysed amination, followed by acid hydrolysis or acetic anhydride and DDQ.[45] A major benefit of *p*-halobenzyl ethers, is the possibility of introducing other functionalities through cross-coupling reactions. Using Suzuki coupling, *p*-halobenzyl ethers can be transoformed into biphenyl groups, which allow for facile cleavage (Scheme 23).[48]

1.5.1.5 Allyl ethers see wide use in carbohydrate chemistry. They are stable under a wide range of conditions,

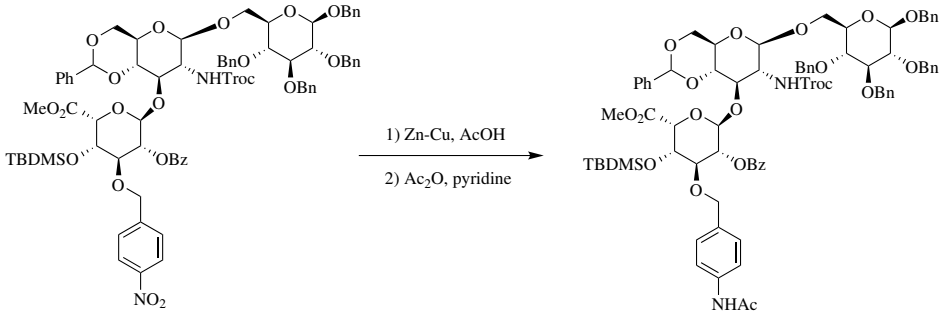

Scheme 22: Selective transformation of *p*-nitrobenzyl (PNB) ether, in the presence of benzyl and Troc groups, to the more labile acetylaniline group, which can be removed with 2,3-dichloro-5,6-dicyano-1,4-benzoquinone (DDQ).[47] Troc = 2,2,2-trichloroethoxycarbonyl.

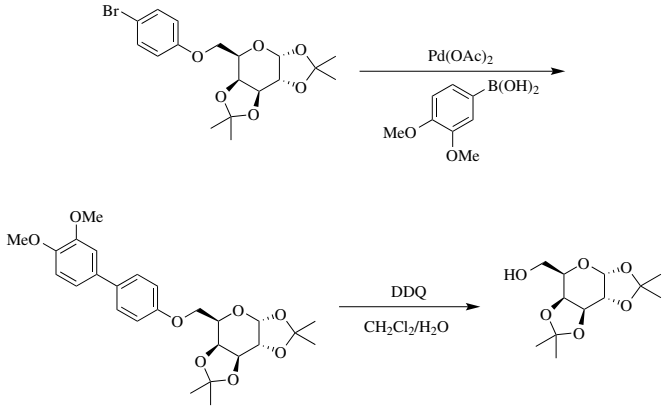

Scheme 23: Transforming *p*-bromobenzyl ether into biphenyl ether, followed by oxidative cleavage.[48] DDQ = 2,3-dichloro-5,6-dicyano-1,4-benzoquinone

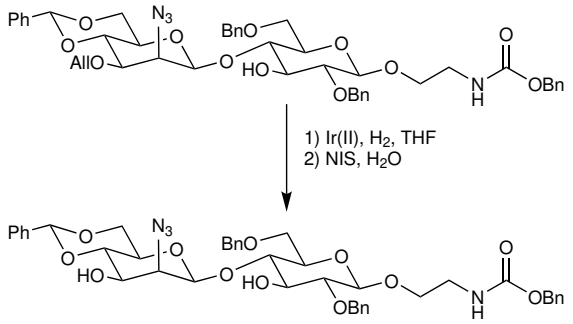

Scheme 24: Deallylation in the presence of other important protecting groups.[45]

including moderately basic and acidic conditions. Unwanted interactions may occur under reductive and oxidative conditions, such as catalytic hydrogenation or elemental bromine. Formation of allyl ethers is usually carried out with allyl bromide in a Williamson ether synthesis manner. Fischer glycosylation in allyl alcohol is also possible, in order to selectively induce the allyl group in anomeric position. Orthogonal removal is possible with a wide range of other protecting groups, such as benzyl ethers (Scheme 24). Cleavage often occurs in a two-step process, involving isomerisation to an enol ether, followed by solvolysis. Isomerisation is carried out with either metal catalysts, such as Ir(II), Wilkinson's catalyst or heterogeneous palladium, or a hindered base, such as *t*-BuOK. The enol ether can be cleaved under mildly acidic conditions, such as NIS in water or methanol. If acidic conditions are undesirable, mercury salts can be used.[45]

1.5.1.6 Other ether protecting groups that see use in carbohydrate chemistry include trityl, methoxymethyl (MOM), tetrahydropyran (THP) and methyl ethers. The trityl (triphenylmethyl) ether primarily serves as a selective protecting group for primary hydroxyls. Good selectivity for primary positions can be achieved with trityl chloride in pyridine. Due to the extreme acid-lability of the trityl group, however, its usage is limited to acting as a temporary protecting group. Cleavage is usually carried out with weak Brøndsted

or Lewis acids.[28] Trityl ethers are labile even to the point of being cleaved on silica gel, which can both be problematic or employed as a method of deprotection.[49] Methoxymethyl (MOM) and tetrahydropyran (THP) ethers serve as commonly used protecting groups in general organic synthesis, but see less usage as carbohydrate protecting groups. These are resistant to a wide range of conditions, and allow for cleavage by Brønsted acids. Introduction usually happens with methoxymethyl chloride (MOM-Cl) and 3,4-dihydropyran for MOM and THP ether, respectively. It should be noted that THP ether introduces a new chiral centre in the molecule.[41] Methyl ethers see some use in carbohydrate chemistry. Their use is limited by lack of selective cleavage methods. Most use cases involve permanently capping hydroxyl groups. Methyl ethers are most commonly formed with iodomethane or dimethyl sulfate with NaH in THF.[41]

1.5.1.7 Silyl ethers see widespread use in carbohydrate chemistry, due to the mild conditions used to both introduce and remove them. Preparation is usually carried out with the silyl chloride, promoted by dimethylaminopyridine (DMAP) or imidazole. Should the hydroxyl be sterically hindered, particularly with a bulky silyl group, use of silyl triflates with 2,6-lutidine may be required. Cleavage is accomplished by fluoride donors, such as ammonium fluoride, or the stronger tetrabutylammonium fluoride (TBAF). This method is very mild, but acyl groups may be affected, either via deacylation or acyl migration.[45] Aqueous acids[41] or Lewis acids[50] may be employed for cleavage as well. Silyl ethers are, depending on the substituents on the silicon, anywhere from very to moderately acid and base labile. Triethylsilyl ethers does not see widespread use in carbohydrate chemistry due to their lability, only as temporary protecting groups in some situations (e.g. Scheme 14). *tert*-butyldimethylsilyl (TBDMS) ethers are most commonly used, due to their moderate stability. *tert*-butyldiphenylsilyl (TBDPS) and triisopropylsilyl (TIPS) are more hardy, where TBDPS ethers are the most acid-stable and TIPS the most base stable.[41] Using the bulky TIPS and TBDPS ethers, it is possible to selectively manip-

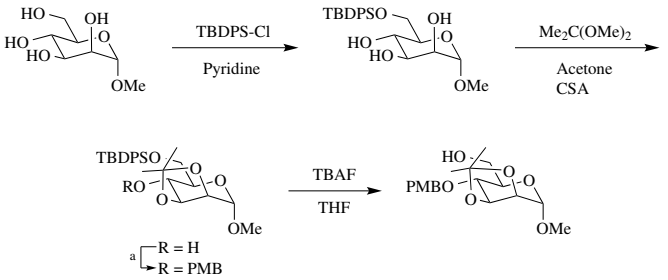

Scheme 25: Orthogonal protection strategy exploiting the selectivity of the bulky TBDPS ether for primary positions. a) *p*-methoxybenzyl (PMB) bromide, NaH.[28] TBAF = tetrabutylammonium fluoride.

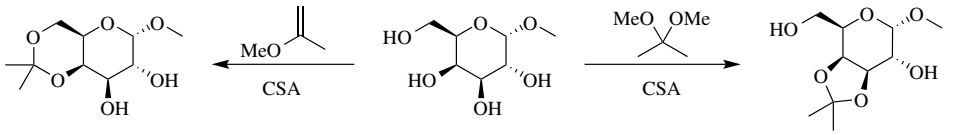

Scheme 26: Selectivity can be optimised for either 1,2- or 1,3-diols.[45]

ulate the primary position (Scheme 25).[28] Silyl ethers, but to a lower extent TBDPS and TIPS, have been observed to migrate under basic protic, but also acidic conditions.

1.5.2 Acetals

Acetal protecting groups are primarily used for protecting 1,2- or 1,3-diols. Isopropylidene acetals are some of the most commonly used acetal protecting groups. Formation is usually carried out with acetone dimethyl acetal, in the presence of an acid catalyst. It is possible to modify selectivity by changing the reagent (Scheme 26). Using methoxypropene favours the kinetic 1,3-acetal (left), while acetone dimethyl acetal favours the 1,2-acetal (right). Cleavage usually happens by acid hydrolysis, but other methods, such as oxidation with DDQ are also possible.

Benzylidene acetals share some properties with isopropylidene acetals, but benzylidene acetals have two additional benefits. As opposed to isopropylidene acetals, benzylidene

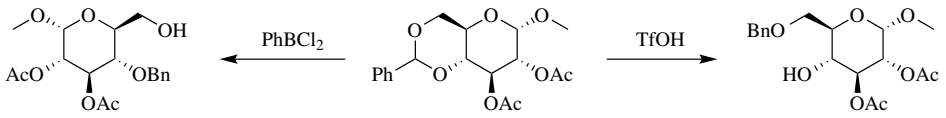

Scheme 27: Regioselective reductive benzylidene cleavage. Triethylsilane as a reducing agent and CH_2Cl_2 as solvent were used in both cases.[51] CSA = camphosulfonic acid.

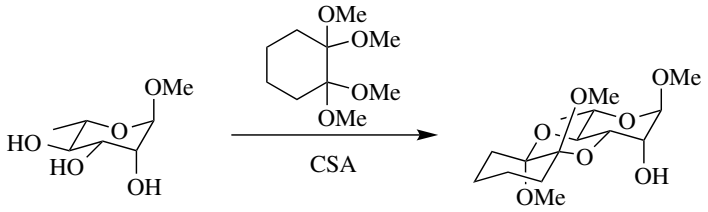

Scheme 28: Selective protection of *trans*-1,2-diols with cyclohexane-1,2-diacetal.[52]

acetals favour 1,3-diols rather than 1,2-diols. Benzylidene acetals are usually introduced from benzylidene dimethyl acetal under acid-catalysis. Cleavage can occur by catalytic hydrogenation, without the need for acids. Benzylidene acetals can also be regioselectively opened under reductive conditions (Scheme 27). Selectivity for selective opening can be tuned by modifying reducing agent, type of acid, acid strength and solvent.[41]

Selective protection of *trans*-1,2-diols is possible with dispiroketals[41] and cyclohexane-1,2-diacetals[52] (Scheme 28). The two protecting groups share many properties with the isopropylidene acetals, but differ mostly in selectivity. In the case of cyclohexane-1,2-diacetals, introduction is facilitated by 1,2-cyclohexanedione dimethyl acetal. Dispiroketals are formed from bisdihydropyran. Introduction of both groups is facilitated by a Brøndsted acid, such as CSA. Cleavage is generally carried out with acids as well, for example TFA.

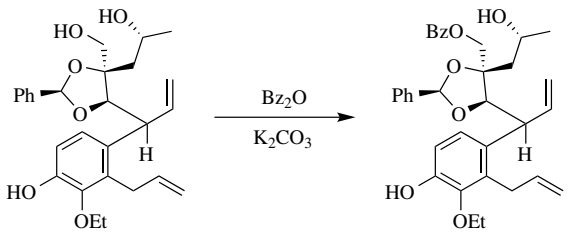

Scheme 29: Selective benzoylation of primary hydroxyl in synthesis towards Resiniferatoxin.[53]

1.5.3 Esters

Due to their ability to be introduced under mild conditions, with little prior purification, ester groups are frequently used in carbohydrate chemistry. Benzoyl and acetyl groups are the most common ester protecting groups. In addition to acting as protecting groups, acetyl and benzoyl groups are sometimes used to aid purification and structure elucidation by masking hydroxyl groups and thereby reducing polarity. Drawbacks to acyl groups, is their propensity to migrate under acidic and basic conditions. Acetyl groups are usually prepared with acetic anhydride and pyridine. DMAP can be used to catalyse sluggish reactions.[28]

Benzoyl groups are introduced with benzoyl chloride or benzoyl anhydride. Compared to acetyl, benzoyl esters are significantly less prone to migration. As opposed to acetylation, benzoylation can also be performed with some selectivity (Scheme 29). As well as selectivity for primary positions, axial vs. equatorial selectivty is also possible.[41] Another advantage of acyl groups, is the possibility of selectively accessing the anomeric position by 1-*O*-deacylation (Scheme 30).[47] Deacylation is carried out with a strong nucleophile. Sodium methoxide in methanol is the most commonly used method.[28] Benzoyl groups can also facilitate anomeric resolution, where enzymatic deacylation occurs at one of the anomers, followed by isolation of the deprotected anomer.[54]

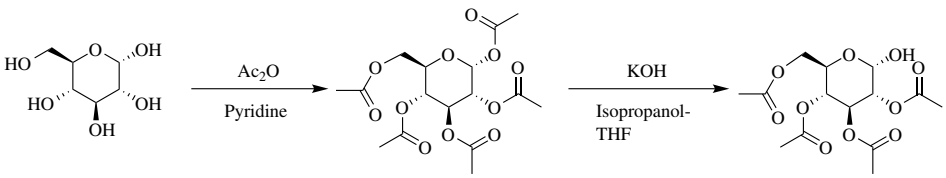

Scheme 30: Global acetylation, followed by selective 1-*O*-deacetylation in order to get a free anomeric hydroxyl.[47]

1.6 Status quo

A synopsis of the planned synthesis towards **CDA** is as follows (Scheme 31). The benzyl group was chosen as a 3-*O*-protecting group due to its acid resistance and ability for selective cleavage by catalytic hydrogenation. In order to attain selectivity for 3-OH, the isopropylidene protected glucofuranose (**1**) was benzylated (Scheme 32) in excellent yields ($> 95\%$). Collumn chromatography was not needed to purify **2a**. The isopropylidene groups of **2a** were hydrolysed and the sugar glycosylated to get **4a** in good yields (74%). Anomeric resolution is desirable to achieve as early as possible in the synthesis. Anomeric separation of **4a** by chromatography and crystallisation have been attempted without success. Derivatisation of **4a** to facilitate anomeric resolution is subject for further investigation.

Further, introduction of the thioacetate group in 6-position should take place, followed by oxidation of the allyl group (Scheme 31, steps c). Deprotection of the benzyl group, esterification of 3-*O*-position and oxidation of the thioacetate group should be performed next (steps d). Some of the previously described steps could be problematic. First of all, resolution of the diastereomers at the glycerol C-2 has proven problematic.[55, 56] An alternative to dihydroxylation of the allyl group (steps c) would be to introduce an enantiomerically pure glycerol group through glycosylation. Catalytic hydrogenation for cleavage of the benzyl group (steps d) could result in side-reactions on both the silyl and the thioacetyl groups. Accordingly, it may be necessary to substitute the benzyl group for an alternative protecting group. Lastly,

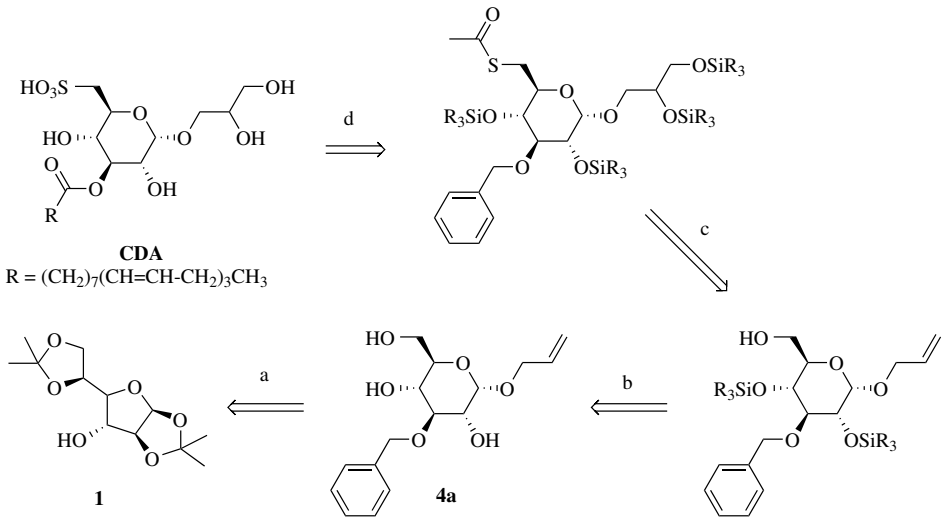

Scheme 31: Current retrosynthetic plan for synthesising **CDA**.

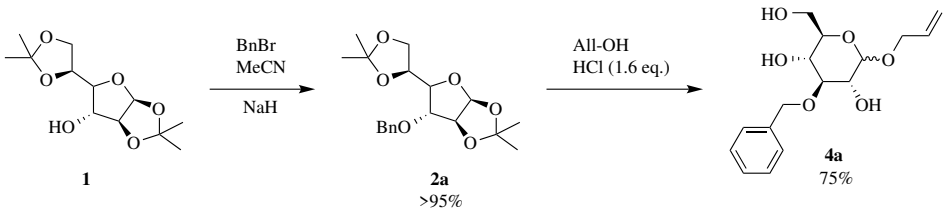

Scheme 32: Initial work on the total synthesis towards **CDA**.

upon desilylation with a fluoride source, in the final step (steps d), migration of the fatty acid could occur. An alternative protecting group that does not induce acyl migration on deprotection would be desirable.

Some investigation and optimisation effort has previously been carried out on the rearrangement-glycosylation reaction on the 3-*O*-benzyl protected compound (**2a** to **4a**). The focus has been on optimising catalyst and reaction conditions, in order to maximise yield of the α-anomer. Alternatives to the 3-*O*-benzyl group have not been explored.

2 Results and discussion

This work was focused on the initial parts of the total synthesis towards **CDA** (step a, Scheme 31). The work can be divided into four parts: anomeric resolution of allyl 3-*O*-protected glucopyranoside, development of alternative 3-*O*-protecting groups, exploring alternative carbohydrate backbones for a future structure-activity relationship study, and introduction of enantiomerically pure glycerol moitey in anomeric position.

Primary focus was put on anomeric resolution, as this is essential to the synthesis of **CDA** (Section 2.1). After adequate procedures for anomeric resolution had been found, alternative 3-*O*-protecting groups were thoroughly investigated (Section 2.2). An exploratory look into alternative carbohydrate backbones was performed, scoping out potential alternatives to glucopyranosides (Section 2.2.4, minor discussion in Section 2.2.2). Some additional work on finding a tentative glycosylation procedure for inserting an enantiomerically pure glycerol moiety was also performed (Section 2.3).

Compounds in the main series were numbered in a consecutive manner. The alphabetical suffix signifies the protecting group pattern. For example, in **4b**, **4** represents an allyl 3-*O*-protected glucopyranoside, and **b** represents the 2-naphthyl group in 3-*O*-position. In the case where the protection group pattern differs significantly or the sugar is of a different configuration from those suffixed **a**-**j**, a letter from a non-latin alphabet was chosen, in a similar fashion to how spin systems are descibed (AB, AX, etc.). Due to the branched nature of the synthesis work, not all compounds were named in accordance with this system.

2.1 Anomeric separation of allyl 3-*O*-benzyl-D-glucopyranoside (4a)

Anomeric separation is an essential part of the total synthesis that remains unresolved. Separation by chromatography has been extensively investigated by the research group. Silica gel chromatography, as well as other normal phase sys-

tems, such as silica or alumina, have been attempted with a wide range of mobile phases to no avail. Reverse phase chromatography (C18-SiO_2) has proven capable of anomeric separation on HPLC. Scaling to low-pressure VersaFlash cartridges failed, so C18-silica was disregarded on that basis. The lack of anomeric separation using normal phase chromatography, was hypothesised to be the result of the comparatively high retention from the primary 6-OH group, relative to the area near the anomeric centre. Consequently, the following derivatisations were proposed: global acylation and insertion of 4,6-*O*-acetals.

2.1.1 Global acylation

Due to the lack of work-up required for acetylation, this was the derivatisation procedure attempted first (Scheme 33). Acetylation of the crude rearrangement-glycosylation product (**4a**) in acetic anhydride-pyridine resulted in the fully acetylated product (**8a**). For this derivative, baseline separation was achieved using column chromatography (SiO_2). The yield for the acetylation procedure were slightly higher than for the underivatised compound (79% vs. 74%). The increased yield was hypothesised to be from a reduction in loss from irreversible adsorption on the silica gel. Due to the similar retention of the anomers, large quantities of silica gel was required (50:1 to 100:1, silica to loaded compound, by mass) to achieve good anomeric separation. As a result, scaling above 3-6 g compound, was problematic for this method.

Global deacetylation, was a mostly effortless procedure. The acetylated compound was added to NaOMe (0.2 M) in MeOH, and stirred at room temperature until completion, monitored by TLC (Table 3), followed by quenching with an acidic ion exchange resin. Reaction times of 30 to 90 min were common. By-products from the deacetylation reaction were volatile and easily removed under reduced pressure. Despite the benzyl ether being touted as base and nucleophile resistant[41], some cleavage of the benzyl group was observed (multiple entries). Debenzylation was possible to minimise by shortening reactions times (entry 7), however. Alternatively,

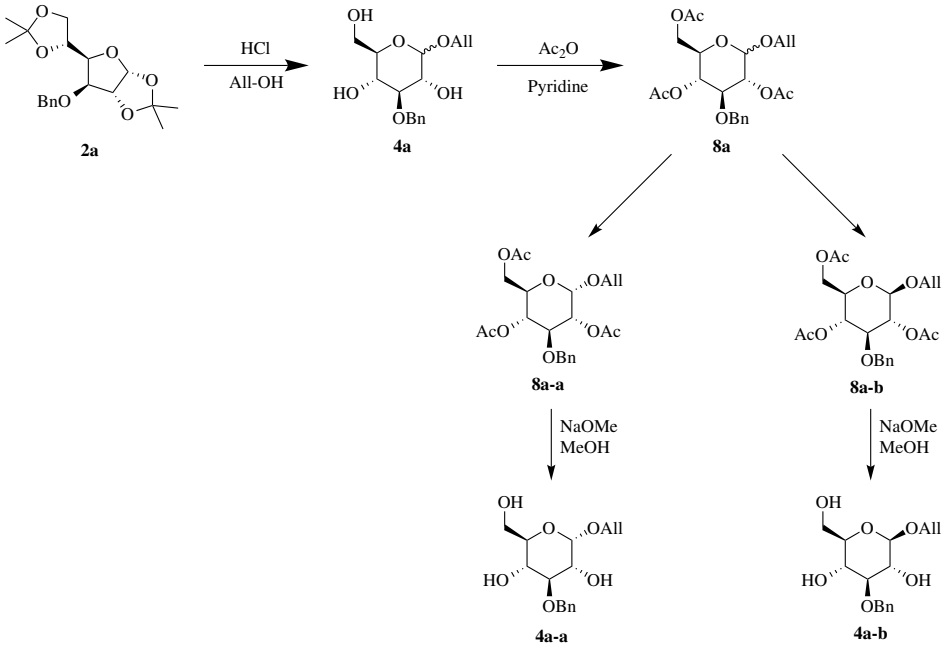

Scheme 33: Anomeric separation of **4a**, starting from **2a**, facilitated by global acetylation.

Table 3: Deacetylation of allyl 3-*O*-benzyl-D-glucopyranoside (**4b**). Detection by NMR. Trace = $< 5\%$. Significant = 5% to 10%.

Entry	Anomer	c NaOMe [M]	Time	Completion	Debenzylation
0	$\alpha + \beta$	0.01	16 h	No	Not detected
1	$\alpha + \beta$	0.02	16 h	Yes	Trace
2	$\alpha + \beta$	0.10	5 h	Yes	Significant
3	$\alpha + \beta$	0.20	2 h	Yes	Significant
4	α	0.10	4 h	Yes	Significant
5	β	0.10	4 h	No	Trace
6	α	0.20	2 h	Yes	Significant
7	α	0.20	1.5 h	Yes	Trace
8	β	0.20	2 h	Yes	Significant

a reduced sodium methoxide concentration facilitated more control over reaction progression, at the cost of prolonged reaction times (entry 1 or 4).

2.1.2 4,6-*O*-acetals

Due to the preference of benzylidene acetals for 1,3-diols,[41] benzylidene-like acetals (Figure 9) were chosen. Prior research by the group has discovered that the 4,6-*O*-benzylidene group imparted crystallinity for allyl glucopyranoside. Consequently, benzylidene (**9a**), *p*-nitrobenzylidene (**9i**) and (9'-anthracenyl)methylene (**9j**) acetals were investigated, of which, the work on the benzylidene acetal was performed simultaneously by another member of the group. The anthracene group, in addition to claims about its crystallinity, exhibits fluorescence, greatly simplifying detection for chromatography.[57]

While benzaldehyde dimehtyl acetal was commercially available, *p*-nitrobenzaldehyde (**RC-2**) and 9-anthraldehyde (**RC-3**) dimethyl acetals were synthesised from commercially available aryl aldehydes with trimethyl orthoformate, in methanol (Scheme 34, Table 4). A procedure, based on one by Ito et al., using TsOH as the acid catalyst was attempted.[58]

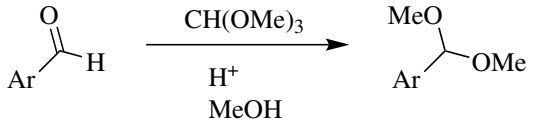

Scheme 34: Acid-catalysed acetal formation of aromatic aldehydes, with trimethyl orthoformate.

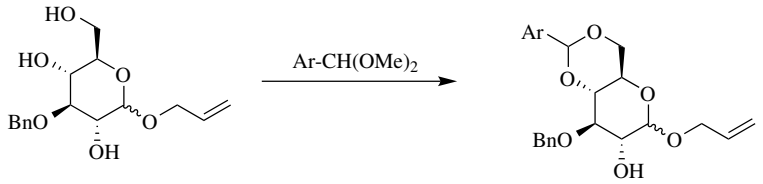

Scheme 35: Introduction of 4,6-*O*-acetals to allyl 3-*O*-benzyl-D-glucopyranoside (**2a**).

For **RC-2**, this procedure was successful, resulting in a good yield (82%, entry 1). Starting from 9-anthraldehyde, however, the former procedure did not result in any reaction whatsoever (entry 2). The same procedure was attempted, with more acid and higher temperature (entries 3, 4), but it did not result in any reaction either. A procedure based on findings by U. Ellervik[59], which used an acidic ion exchange resin, in catalytic quantities, caused the reaction to proceeded smoothly (entry 6). A mechanistic explanation for the preference for heterogeneous acid catalysis was not immediately obvious and was considered out of scope for this work.

Trans-acetalisation in MeCN with TsOH (Scheme 35) was successful for introducing benzylidene and *p*-nitrobenzylidene in 4,6-*O*-position (Table 5). Nevertheless, with anthracene as the aryl group, low yields (34%) were achieved. A similar procedure was used by Jakab et al.[57], using camphorsulfonic acid (CSA) in lieu of TsOH, furnished 4,6-*O*-acetals in 79% yield. Different substituents are used by Jakab et al. and it was possible that such high yields are viable following some optimisation.

All 4,6-*O*-acetals improved chromatographic separation of

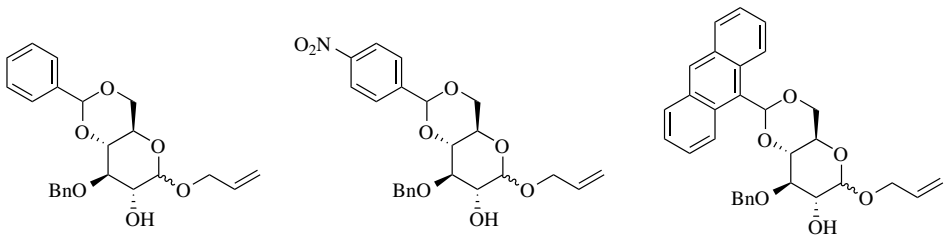

Figure 9: 4,6-*O*-Acetal protected allyl 3-*O*-benzyl-D-glucopyranosides.

Table 4: Transacetalisation reaction (Scheme 34) between aryl aldehyde and trimethyl orthoformate (2 equiv) in MeOH (0.75 M). Reaction time: 2-4 h. NR: no reaction.

Entry	Aryl group	Catalyst	Temp.	Yield
0	*p*-Nitrophenyl (**RC-2**)	TsOH (0.03 equiv)	rt	82%
1	Anthracene (**RC-3**)	TsOH (0.03 equiv)	rt	NR
2	Anthracene (**RC-3**)	TsOH (0.2 equiv)	reflux	NR
3	Anthracene (**RC-3**)	HCl (3 equiv)	reflux	NR
4	Anthracene (**RC-3**)	Amberlyst-15 (0.1 equiv)	rt	low
5	Anthracene (**RC-3**)	Amberlyst-15 (0.2 equiv)	reflux	87%

Table 5: Introduction of 4,6-*O* aryl acetals to **2a** (Scheme 35).

Aryl group	Yield	Anomer sep. by chrom.	ΔR_F [d]	Anomer sep. by cryst.
Ph (**9a**)	62%[a,c]	Yes	0.151	Yes
p-NO_2-Ph (**9i**)	63%[b,c], 72%[a]	Yes	0.148	No
Anthracene (**9j**)	34%[b]	Yes	0.151	No

[a] Purification by crystallisation. [b] Purification by chromatography. [c] Only α-anomer. [d] ΔR_F of anomers with 2:1 *n*-pentane:EtOAc.

the anomers by a large margin (Table 5), and baseline separation proceeded effortlessly for either acetal protected glucoside. Accordingly, slightly larger quantities of **9a**, **9i** and **9j** could be separated using column chromatography.

The disadvantage of using acetal protecting groups to aid chromatography, was that the introduction reactions of acetals entailed more prior purification work, relative to acetylation. In terms of crystallinity, all acetals gave a significant improvement. The *p*-nitrophenyl group (**9i**) was the most crystalline, with a yield of 72% achieved, starting from **4a**. That said, both anomers precipitated readily, and made isolation of the α-anomer impossible. For the benzylidene protected derivative (**9a**), the α-anomer precipitated over the course of the reaction, and yielded anomerically pure **4a** in 62% yield by simple filtration. Lastly, for anthracene derivative **9j**, chromatographic separation of anomers was as facile as for the two other 4,6-*O*-acetal derivatives, though crystallisation yields were lower. The lack of anomeric separation by crystallisation, mediocre yield and necessity for preliminary reagent synthesis portrayed the anthracene acetal as an inferior derivatisation strategy for the total synthesis. It was subsequently discovered that benzylidene (**9a**) and *p*-nitrobenzylidene (**9i**) acetals could be inserted to crude **4a**, greatly simplifying the procedure, without proving detrimental to the yield.

Removal of the 4,6-*O*-acetals was achieved in 80% AcOH

in water overnight in yields of 60-85%. Passing the product through a short column or a pad of silica was necessary for the final purification step. As a result, the 4,6-*O*-acetal strategy could be used as a low-effort procedure for making anomerically pure **4a**.

In conclusion, the acetylation procedure was a viable method for achieving anomeric separation. It had the added benefit of also isolating the β-anomer, but had limitied potential for scaling, due to the challenging chromatographic separation required. In order to scale the reaction somewhat further, chromatographic anomeric separation could be performed on either of the 4,6-*O*-acetals. Further scaling was possible by precipitating the benzylidene-protected sugar (**9a-α**). This procedure had the added benefit of not requiring tedious column chromatography, and has enabled syntheses of **4a-α** in 20 g batches.

2.2 The 3-*O*-protecting group

While the rearrangement-glycosylation reaction, in the initial parts of the total synthesis towards **CDA** (Scheme 36), had been heavily scrutinised by the research group, this work had been focused on optimisation of the main synthesis pathway (Scheme 46 in Section 1.6). This involved benzylation of the 3-*O*-position, followed by later removal with catalytic hydrogenation for esterification (left path, Scheme 37). Little focus had been put on investigations into alternative strategies, however.

Following the main strategy, a maximal ratio of anomers (RA) of 75:25 (α : β), had been achieved. Varying the 3-*O*-group could influence the RA, potentially increasing the fraction of the desired α-anomer, or even eliminating the β-anomer completely, which would greatly simplify the total synthesis. Little information about the influence of the 3-*O*-substituent on the RA was available,[21] thus, a study on the effect of the 3-*O*-substituent, would be of great interest from a chemical point of view.

Achieving anomeric separation was, as discussed in Section 2.1, challening for **4a**, without resorting to derivatisa-

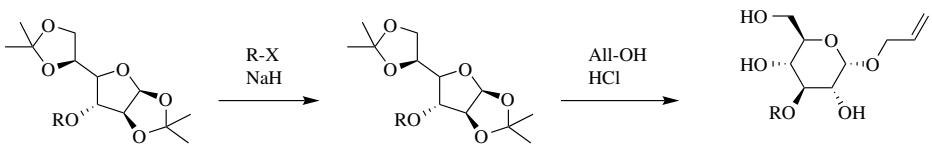

1

2a: R = Bn
2b: R = (2-naphthyl)methyl
2c: R = *p*-Ph-benzyl
2d: R = (3,5-di-*t*-Bu)benzyl
2e: R = *t*-Bu-dimethylsilyl
2f: R = *t*-Bu-diphenylsilyl
2g: R = triisopropylsilyl
2i: R = *p*-nitrobenzyl
2j: R = (9'-anthracenyl)methylene

4a: R = Bn
4b: R = (2-naphthyl)methyl
4c: R = *p*-Ph-benzyl
4d: R = (3,5-di-*t*-Bu)benzyl
4f: R = *t*-Bu-diphenylsilyl
4i: R = *p*-nitrobenzyl

Scheme 36: Initial parts of the synthesis towards **CDA**.

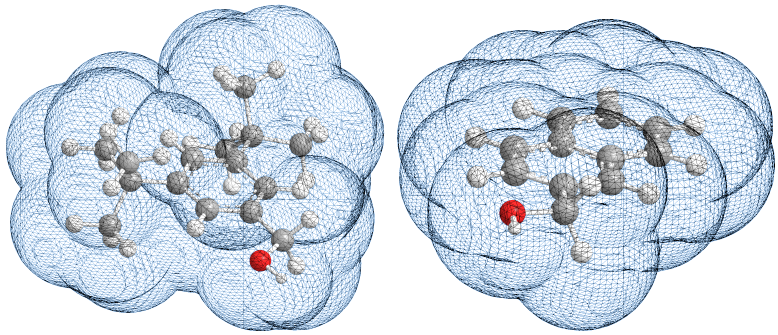

Figure 10: Solvent-accessible surface map from Chem3D of (3,5-di-*t*-Bu)benzyl (left) and 2-naphthyl (right) alcohols.

tions. It was hypothesised that other 3-*O*-protecting groups could facilitate anomeric separation, either by means of chromatography or crystallisation.

A third reason to develop alternatives to the benzyl group in 3-*O*-position, was the potential complications that could arise from selective deprotection of the benzyl group (left path, Scheme 37). Although the conditions for removal of the benzyl group is a well established method, which is supposed to be compatible with a wide range of protecting groups[41], is has not yet been definitively established that benzyl ether cleavage by catalytic hydrogenation will be compatible with the overall protection strategy.

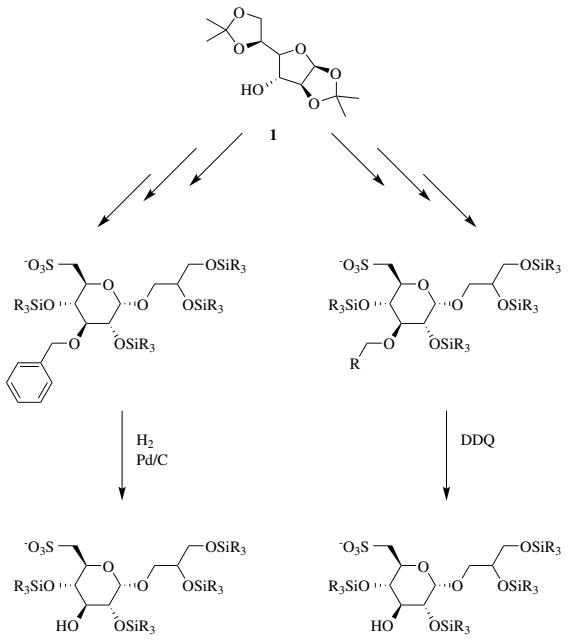

Scheme 37: Alternative synthesis towards sulfoquinovosyl glycerols. R = 2-naphthalene (NAP) or *p*-biphenyl (PPB).

Table 6: Available literature properties of 3-*O*-protecting groups (Figure 11).[41, 46, 60, 61] Cat. H_2 is catalytic hydrogenation. UK = Unknown.

Entry	Group	Acid-stability	Cleavage options
0	Bn	High	Cat. H_2
1	NAP	High	Cat. H_2, DDQ
2	PPB	High	Cat. H_2, DDQ
3	DTB	UK	UK
4	TBDMS	Low	Fluoride, acid
5	TBDPS	Moderate	Fluoride
6	TIPS	Moderate	Fluoride
7	PNB	Very high	Cat. H_2
8	ANT	UK	UK

In case deprotection of the benzyl group should prove problematic, other protecting groups, which could be removed under different conditions, would be investigated. A list of potential alternatives to the benzyl group was formulated (Figure 11). Requirements were mainly focused on acid-stability and orthogonal deprotection. Five benzyl-like ethers were chosen: 2-naphthyl (NAP), (*p*-Ph)benzyl (PPB), (3,5-di-*t*-Bu)benzyl (DTB), *p*-nitrobenzyl (PNB) and (9'-anthracenyl)methylene (ANT). Cleavage of NAP, PPB and PNB ethers by catalytic hydrogenation is documented in literature (entries 0-2 and 7, Table 6),[41] however, due to their similarity it was reasonable to expect the cleavage of the remaining aforementioned groups under the same conditions. The *tert*-butyl groups might block access for the catalyst to the π-system in DTB ethers, though.

In terms of acid-stability, PNB ethers were more durable than benzyl ethers (entry 7),[46] while NAP and PPB ethers were similar to benzyl ethers (entries 1,2). DTB ethers (entry 3) were close to benzyl, NAP and PPB in terms of electronic properties, and was expected to behave in a similar fashion. The DTB group was included primarily to gauge the effect of

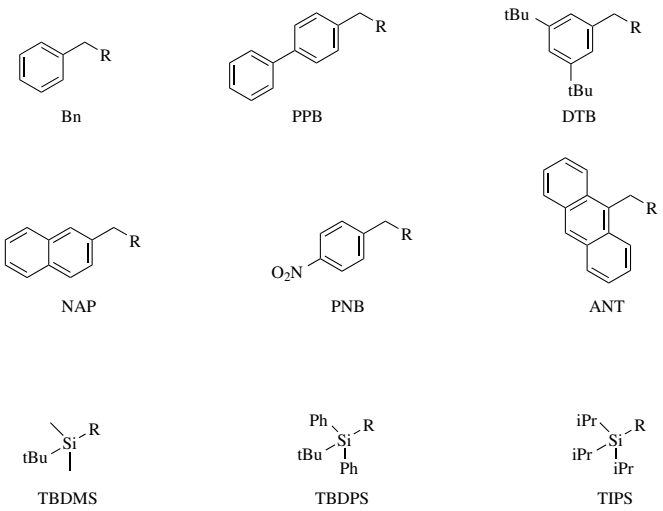

Figure 11: 3-*O*-protecting protecting groups employed.

a non-planar bulk (Figure 10) on the 3-*O*-protecting group, rather than being theorised to have any particular benefits. As a consequence of its electron-rich aromatic group, ANT ethers could be less hardy than desired, and no data on the acid-stability of ANT ethers was found in literature (entry 8). Three silyl ethers were also investigated: *tert*-butyldimethyl, *tert*-butyldiphenyl and triisopropyl silyl ethers (entries 4-6). The silyl ethers were all capable of being introduced and removed orthogonally, and were chosen on the basis of covering a range of acid-stabilities, with TBDPS being the most resilient, and TBDMS the least.[41]

2.2.1 Protection of 3-OH

In order to get 3-OH selectively protected, a 3-*O*-protecting group was applied to D-glucose diacetonide (**1**), which can be further rearranged into glucopyranosides. All benzyl-like ethers except *p*-nitrobenzyl, were introduced through regular Williamson ether synthesis (Scheme 36) from the alkyl halide (R = Cl, Br in Scheme 36). The benzyl, PPB, DTB and NAP halides were commercially available, but 9-(chloromethyl)anthracene (**RC-1**) was not. Producing **RC-1** from commercially

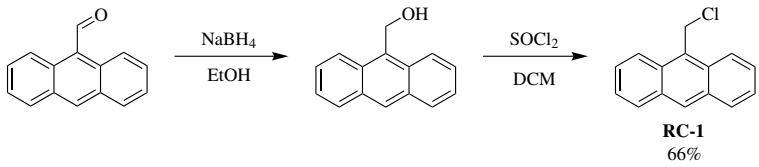

Scheme 38: Reduction, followed by hydroxyl substitution of 9-anthraldehyde.

available 9-anthraldehyde (Scheme 38) was straightforward, however.

Reduction of the aldehyde group to a primary alcohol was quick and facile, and no work-up beyond extraction was needed before proceeding to the next step. During column chromatography (19:1 *n*-pentane:EtOAc), **RC-1** partially co-eluted with an aromatic byproduct, such that the overall yield was somewhat lowered (66%). A weaker eluent should be used in subsequent syntheses of **RC-1**.

As shown in Table 7, all syntheses of benzyl-like ethers proceeded as expected with good to excellent yields. Tetrabutylammonium iodide (TBAI) was added when synthesising the PPB ether, which used the alkyl chloride as starting material. TBAI catalysis resulted in increased reaction rate (time reduced from overnight to 3 h), but was also associated with formation of impurities (Figure 12), complicating chromatographic purification to an undesired degree.

As opposed to the simple ether synthesis of previous benzyl-like ethers, PNB ethers required special procedures. The low tolerance towards basic conditions for *p*-nitrobenzyl bromide and corresponding PNB ethers, presented compatibility issues with the sodium hydride catalysed reactions hitherto described (Scheme 36). Rather than a strong base in polar media, heavy metal reagents are used in a nonpolar solvent, such as DCM or toluene.[46] Employing Ag_2O in excess at reflux resulted in high conversions, making the experimental procedure itself straightforward. Silver(I) oxide, however, was required in large quantities, making the procedure significantly more costly than regular ether synthesis procedures.

The introduction of silyl groups on 3-OH was equally

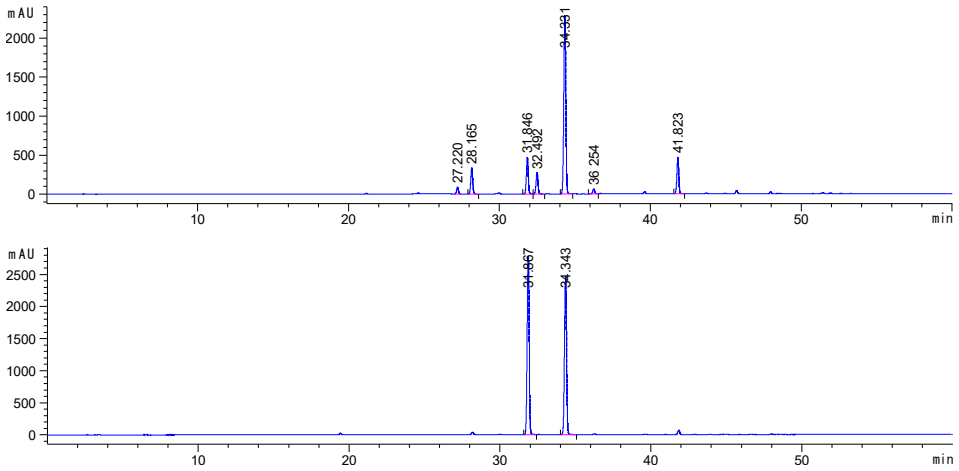

Figure 12: HPLC (Method *X*, 210 nm) chromatogram of crude product from ether synthesis of 1,2;5,6-di-*O*-isopropylidene-α-D-glucofuranose (**1**) and *p*-phenylbenzyl chloride (Scheme 36). Top: with tetrabutylammonium iodide (TBAI) added. Bottom: without TBAI. The product is at 34.3 min and reactant at 31.9 min.

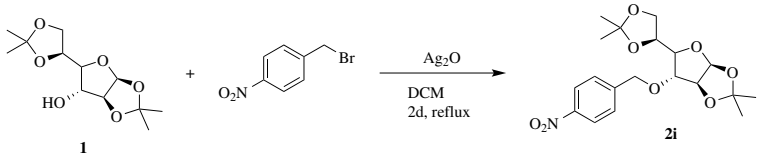

1 **2i**

Scheme 39: Protecting 1,2;5,6-di-*O*-isopropylidene-α-D-glucofuranose (**1**) with a *p*-nitrobenzyl ether.

Table 7: Comparison of protecting groups for 3-OH of 1,2;5,6-di-*O*-isopropylidene-α-D-glucofuranose (**1**).

Entry	3-*O*-R	Yield [%]	Notes
0	Benzyl	95	
1	2-Naphthyl	91	
2	*p*-Phenylbenzyl	88	
3	(3,5-Di-*tert*-butyl)benzyl	80	Expensive reactant
4	*t*-Butyldimetyhsilyl	74	
5	*t*-Butyldiphenylsilyl	88	
6	Triisopropylsilyl	54	Difficult sepration
7	*p*-Nitrobenzyl	71	Expensive reagent
8	(9'-Anthracenyl)methyl	86	

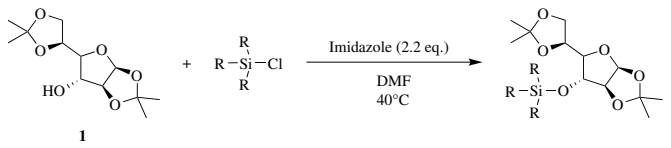

1

Scheme 40: Protecting 1,2;5,6-di-*O*-isopropylidene-α-D-glucofuranose (**1**) with silyl ethers.

facile. Introduction of TBDPS (**2f**) and TIPS (**2g**) was carried out with silyl chlorides in DMF at 40°C, catalysed by imidazole (Scheme 40). The TBDMS derivative (**2e**) was procured by the use of TBDMS triflate in DCM at 0°C with 2,6-lutidine as base. Yields for silylation of **1** were generally high (Table 7), with the exception of the TIPS group, where overlap with residual silylating agent during column chromatography proved somewhat detrimental to the yield.

Alternative carbohydrate backbones for **CDA** have been considered for futher structure-activity studies. Two alternatives to the *gluco* configuration were chosen on the basis of allowing for facile selective protection of 3-OH: allose and xylose. Allose is the C-3 epimer of glucose, and xylose has the *gluco* configuration, but with one less carbon atom on the backbone. D-Allose diacetonide and 1,2-*O*-isopropylidene-α-D-xylofuranose were commercially available. Benzy-

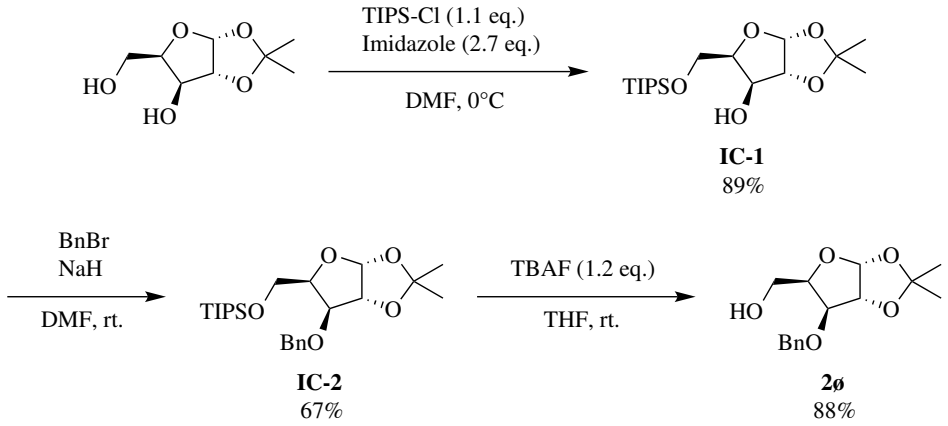

Scheme 41: Selectively protecting 3-OH of xylose. Performing the reaction in a one-pot manner, gives a yield of 69% over all three steps.

lation of D-allose diacetonide in 3-*O*-position was achieved in exactly the same manner as when benzylating **1** (Scheme 36). Attaining selective 3-*O*-benzylation of xylose required some protecting group manipulation (Scheme 41).

The preference of triisopropylsilyl (TIPS) ethers for primary alcohols (Section 1.5.1) was exploited in order to attain selectivity for 5-OH. Excellent selectivity was observed on NMR for this reaction and separation from excess silylating agent and imidazole was achieved with a short pad of silica gel (89% yield). Subsequent benzylation of 3-*O*-positions was carried out using the standard method, and **IC-2** was easily isolated by column chromatography. An unexpectedly low yield (67%) was noted for this reaction. It was hypothesised that this could be due to cleavage of the TIPS group, followed by benzylation of 5-OH. While TIPS ethers are subject to some base sensitivity, it only pertains to aqueous solutions.[41] Lastly, the TIPS group was removed using tetrabutylammonium fluoride (TBAF) in THF, resulting in a good yield (88%).

Chromatographic purification of intermediates **IC-1** and **IC-2** proved unnecessary, as the reaction yielded more 3-*O*-benzyl xylose (**2ø**) when performed without chromatographic

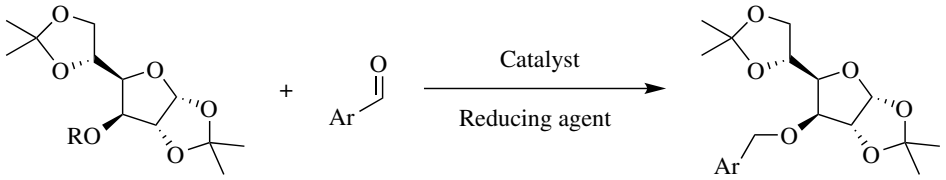

R = H, TBDMS

Scheme 42: Protection of 3-OH by reductive etherification.

Table 8: Attempts at protecting 3-OH in 1,2;5,6-di-*O*-isopropylidene-α-D-glucofuranose (**1**) by reductive etherification (Scheme 42). The TBDMS-protected, rather than the TMS-protected alcohol were used for the Savela procedure[62]. NR = No reaction.

Entry	Ar	Procedure	Red. agent	Outcome
0	Anthracene	Savela[62]	Et_3SiH	NR
1	Anthracene	Zhao[63]	Et_3SiH	Non-ether coupling
2	*p-nitrobenzyl*	Zhao[63]	Et_3SiH	Non-ether coupling
3	Anthracene	Zhao[63]	$BH_3{-}NH_3$	Reduction of C=O

separation until the final step (69% over three steps). In an attempt to minimise cleavage of the TIPS group, reaction progression was monitored more closely, and greater care was taken to avoid moisture. Employing this procedure presented no observable decrease in purity, so the method was considered superior by all measures.

Due to the relative difficulty and/or expense of forming ANT and PNB ethers using previously described methods, the possibility of coupling aryl aldehydes to sugars via reductive etherification (Scheme 42, Table 8) emerged as desirable. A procedure by Savela and Leino[62] couples TMS ethers to aldehydes with a $FeCl_3$-TMS-Cl catalyst system and Et_3SiH. Their substrate scope includes a reaction between TMS-menthol and *p*-Ph-benzaldehyde, which while not a carbohydrate, is a comparable system as a secondary, somewhat hindered alcohol and a large aryl aldehyde are involved.

Attempting this procedure, the TBDMS-GLF (**2e**) was used

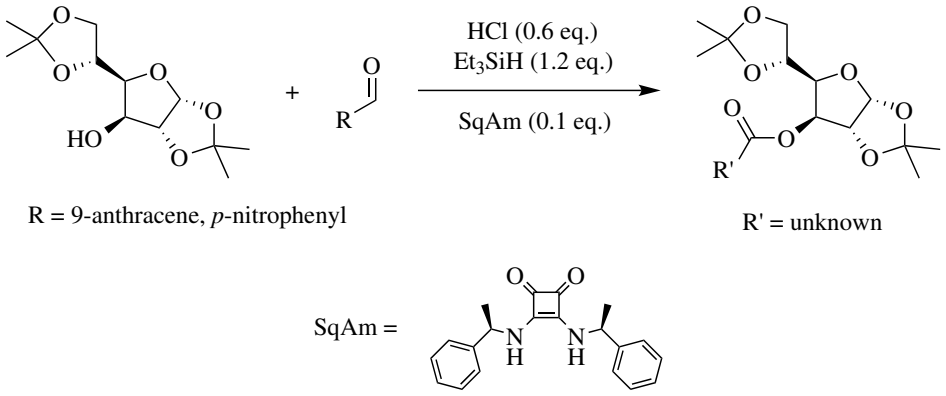

Scheme 43: Attempted reductive etherification, using the Zhao procedure.[63]

rather than TMS, due to it having been synthesised previously. Little information on nucleophile strengths of TBDMS relative to TMS was found. Some instances of procedures where TMS and TBDMS ethers are interchangeable were found.[64–66] TMS ethers were most frequently employed, however.[62, 67–70] Applying the Savela conditions on **2e** and 9-anthraldehyde, no desired reaction was observed (entry 0). NMR showed some homocoupling of the aldehyde and cleavage of the isopropylidenes. The lack of reaction, coupled with the prevalence of undesired side-reactions resulted in abandonment of the Savela method for reductive etherifaction.

Another method by Zhao et al. uses a catalyst system consisting of HCl and a thiourea organocatalyst (Scheme 43). The thiourea catalyst was substituted for a squaramide catalyst (structure shown in Schem 43) with similar properties.[71] Using both 9-antraldehyde and *p*-nitrobenzaldehyde, coupling between the anthracene moiety and sugar did occur (entry 1 and 2). Coupling to both 3-OH and 6-OH (resulting from cleavage of the 5,6-*O*-isopropylidene) was observed. Although the exact structure of the products was not determined, it was for certain that the reaction did not proceed as desired. No diastereotopic benzylic protons were observed, proving that no ether linkage was formed. Strong indications

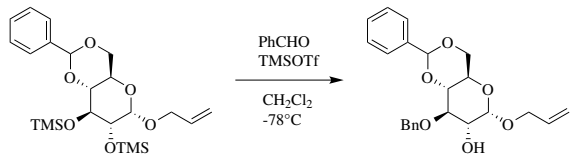

Scheme 44: Benzylation of 3-*O*-position by reductive etherification.[73]

of an ester or conjugated carbonyl was present in the form of a strong carbonyl peak on IR (1730 cm^{-1}), and a carbon peak at 160 ppm, which coupled to the sugar H-6. MS did not fit with any expected product, however, and the proton shifts of the aromatic protons were changed. Is was apparent that a more complex reaction governed by an unknown mechaism had occured. Similar results were produced when using *p*-nitrobenzaldehyde (entry 2). It is theoretically possible to produce esters from an aldehyde and an alcohol, but oxidative conditions are required for such a reaction.[72] While these results were chemically interesting, the desired ether coupling was not produced, and identifying products and elucidating mechanisms for such reactions was far out of scope for this work. In a final, unsuccessful attempt, triethylsilane was substituted for the slightly stronger reducing agent ammonia borane. Reduction of the aldehyde group to an alcohol followed (entry 3).

A promising procedure for reductive etherification in 3-*O*-position of carbohydrates by Wang et al (Scheme 44), was later discovered, but at this point it was too late to carry out any further experiments on the subject.[73]

2.2.2 Rearrangement and glycosylation of 3-*O*-protected monosaccharides

In order to synthesise allyl 3-*O*-protected glucopyranosides (**4a-i**), 3-*O*-protected glucose diacetonides (**2a-j**) were refluxed in allyl alcohol in the presence aqueous HCl (Scheme 36). During this process, the acetals are hydrolysed, the carbohydrate backbone is rearranged into the more thermodynamically stable pyranose form and glycosylation occurs, though not necessarily in that order. All 3-*O*-protected GLFs

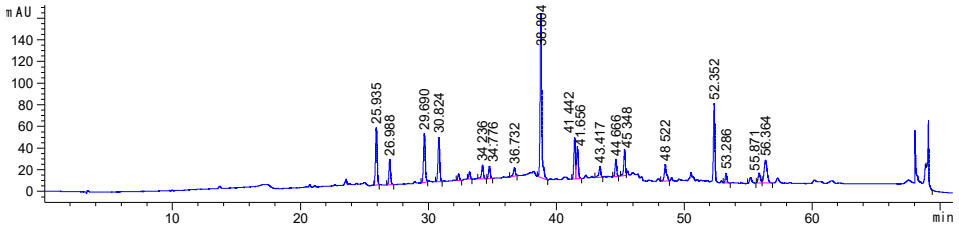

Figure 13: HPLC (Method *X*, 254 nm) chromatogram after rearrangement and glycosylation of **2j** with allyl alcohol (Scheme 36).

(**2a-j**) were subjected to reflux in allyl alcohol with 1.6 equiv aqueous HCl. Protecting groups that exhibited little cleavage were **4a-d** and **4i** (Table 9). The benzyl-like ethers proved vastly more tolerant towards the acidic conditions than the silyl ethers, which was expected (see Introduction Section 1.5.1). The benzyl, NAP and PNB ethers were the most resistant (entries 0, 1, 7), exhibiting no detectable cleavage. Survival in the case of the PPB and DTB ethers was moderately good (entries 2,3). None of the silyl ethers were compatible with these conditions, however, the TBDPS derivative (**4f**) did exhibit some survival (entry 5). The TBDMS (**4e**) and TIPS (**4g**) ethers (entries 4, 6) were completely hydrolysed.

Subjecting the ANT group to the glycosylation reaction (Scheme 36), produced a myriad of side-reactions (Figure 13). Although the products from the reaction were not isolated and characterised, the multitude of aromatic compounds detected at 254 nm showed that the extent at which side reactions occurred must be very high, as the only significant UV active (254 nm) component present before the reaction, was **2j**. Recrystallisation in EtOAc was attempted, but no carbohydrate compounds, only various aromatics, precipitated. TLC also showed a large number of species with little potential for isolationo of pure compounds. As a result, isolation of products from the reaction was considered to be ineffective use of time. There is some evidence of ANT protecting groups taking part during glycosylation, however. Kulkarni et al.[74] found that glycosylation with a 2-*O*-ANT group present, yielded a conjugated addition on the central anthracene ring, resulting in a high yield and high stereoselec-

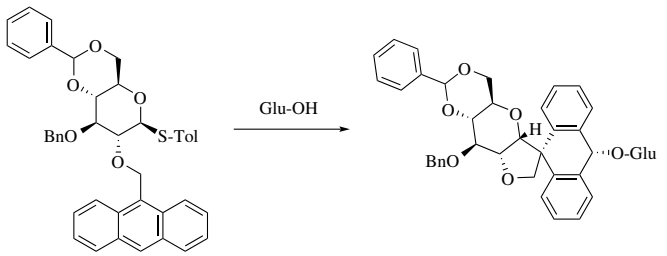

Scheme 45: Neighbouring group participation, where conjugated addition to the anthracene group occurs.[74]

tivity of a C-glycoside (Scheme 45).

Literature on acid-stability of the protecting groups considers benzyl and NAP[41] ethers to be of high stability. PNB ethers are very acid-stable.[46] PPB is of quite high acid stability.[41] No information was available about the DTB group, but with two weakly electron-donating substituents, it was expected to be somewhat less acid-stable than benzyl. As for the silyl groups, TBDMS ethers are of low acid-stability. TIPS and TBDPS ethers are approximately 35 and 250 times as acid-stable as TBDMS, exhibiting moderate acid-stability. Silyl ethers are more susceptible to acid-catalysed deprotection in aqueous media[11] The results from rearranging and glycosylating all 3-*O*-protected GLFs in allyl alcohol did conform with available information about the acid-stability of those protecting groups. While the lack of compatibility for TBDMS and TIPS ethers was somewhat disappointing, NAP and PPB ethers, which can be deprotected oxidatively in the presence of many other protecting groups, were discovered to be compatible. The DTB group could be possible to cleave oxidatively, but no investigation into deprotection was carried out.

The following 3-*O*-protecting groups were determined to be compatible with Fischer glycosylation: benzyl, NAP, PPB, DTB and PNB. All other protecting groups proved too labile. A number of properties were evaluated for the aforementioned protecting groups: yield, ratio of anomers, isolation by crystallisation, and anomeric separation by chromatography and crystallisation (Table 11).

Table 9: Protecting group survival, estimated from crude NMR analyses, in allyl alcohol at reflux with 0.42 M aqueous HCl for 30 min. Minimal = No cleavage detected by NMR. Low = < 10% cleavage. High = 40-80% cleavage.

Entry	Group	Cleavage
0	Bn	Minimal
1	NAP	Minimal
2	PPB	Low
3	DTB	Low
4	TBDMS	Complete
5	TBDPS	High
6	TIPS	Complete
7	PNB	Minimal
8	ANT	High

When separating the products as anomeric mixtures by column chromatography, good yields were achieved for benzyl and NAP (entries 0, 1). DTB and PPB exhibited slightly lower yields (entries 3, 2), presumably owing to more rapid cleavage of the 3-*O*-protecting group. Good yields were obtained for the PNB group from recrystallisation. Global acetylation of the crude before chromatography resulted gave slightly higher yields (entry 0, 1).

The effect of the 3-*O*-protecting group on the ratio of anomers resulting from the glycosylation-rearrangement reaction, was also investigated. A ratio of anomers of 73:27 (α : β) was seen for most protecting groups. The PNB ether displayed a slightly increased fraction of α-anomer, but this could be the result of more α-anomer being crystallised, rather than any actual difference in ratio of anomers. For the DTB group, on the other hand, a significant increase in ratio of anomers was observed (entry 3).

In terms of anomeric separation by chromatography, no alternative protecting group resulted in any improvement over benzyl ether. Using silica gel as the stationary phase, anomeric

Table 10: Some crystallisation attempts of allyl 3-*O*-protected glucopyranosides **4c** (PPB) and **4i** (PNB).

Entry	Compound	Yield [%]	$\alpha : \beta$	Solvent
0	PPB	20	83:17	EtOH-H_2O
1	PPB	14	86:14	Acetone-H_2O
2	PNB	69	76:27	EtOAc
3	PNB	30	80:20	Acetone

separation was approximately the same as for the benzyl ether (i.e. more or less none). On HPLC, the benzyl ether did best, with baseline separation of the anomers possible. The TBDMS-protected furanosides (**4f**) were separated on HPLC, but the α-furanoside (**3f-α**) and α-pyranoside (**4f-α**) overlapped partially. No separation whatsoever was observed on C18-silica for all other protecting groups.

Crystallisation proved tough for the benzyl, NAP and DTB-protected sugars (entries 0, 1, 3). In their neat forms, the α-anomer of the benzyl and NAP ethers would eventually precipitate, but no significant quantities could be precipitated from solution. All efforts to obtain a crystalline form of the DTB ether were unfruitful. The PPB ether could be crystallised as an anomeric mixture in quite low yields (20%, in ethanol-water), but all attempts at precipitating only the α-anomer failed (entries 0-1, Table 10). The PNB group imparted very high crystallinity. Precipitation of an anomeric mixture was possible in very good yields in relation to yields from chromatograpy (entry 2). Due to the highly crystalline nature of both anomers, however, anomeric separation by precipitation was not achieved.

In order to determine the usefulness of the 3-*O*-protecting groups under investigation to the total synthesis of **CDA** (Scheme 46), a number of factors had to be taken into consideration. Figure 14 attempts to summarise the properties of some of the most promising 3-*O*-protecting group. Most importantly, they had to be compatible with subsequent reaction conditions used in the total synthesis. The most demanding steps in the synthesis (Scheme 46) were the glycosylation-

Table 11: *Ac yield* is yield achieved when fully acetylating before chromatography.

Entry		$\alpha : \beta$	Yield [%]	Ac yield [%]	Crystallinity	Anomer sep. by chrom.	Anomer sep. by cryst.
0	**4a**	73:27	74	79	Low	Low	Difficult
1	**4b**	73:27	73	78	Low	Low	Difficult
2	**4c**	73:27	54	-	Medium	Low	Difficult
3	**4d**	81:19	49	-	Oil	Low	No
4	**4i**	76:27*	69	-	Very high	Low	No

* Purified by crystallisation.

rearrangement in HCl at reflux in allyl alcohol (step a) and oxidation of the thioacetyl group with Oxone (step d).

The ANT group and silyl groups were determined to be incompatible with highly acidic conditions, and thus disregarded. Benzyl, NAP, PPB, DTB and PNB ethers demonstrated acceptable acid-resistance. Cleavage of benzyl, NAP, PPB and PNB is possible using hydrogenation on palladium.[41] It was theorised that DTB ethers could be removed in the same manner, due to the similarity with the previously mentioned benzyl-like ethers, but testing was not carried out. Regardless, the DTB ether was included primarily as an exercise to study the effect of a bulky 3-*O*-protecting group on the rearrangement reaction, rather than looking particularly promising for the total synthesis project. NAP, PPB[41] and PNB[46] carried the added advantage of being orthogonally cleavable in the presence of benzyl ethers, making them candidates for use orthogonally to the 3-*O*-benzyl group in the synthesis. NAP[60] and PPB[61] can, in addition to with catalytic hydrogenation, be deprotected oxidatively, using DDQ. A stochiometric oxidant, such as $Mn(OAc)_3$ can also be used along with DDQ, making the procedure more cost-efficient.[61] For the synthesis towards **CDA**, should catalytic hydrogenation, to remove the benzyl ether, prove incompatible with, e.g., the thioacetyl group, the benzyl group

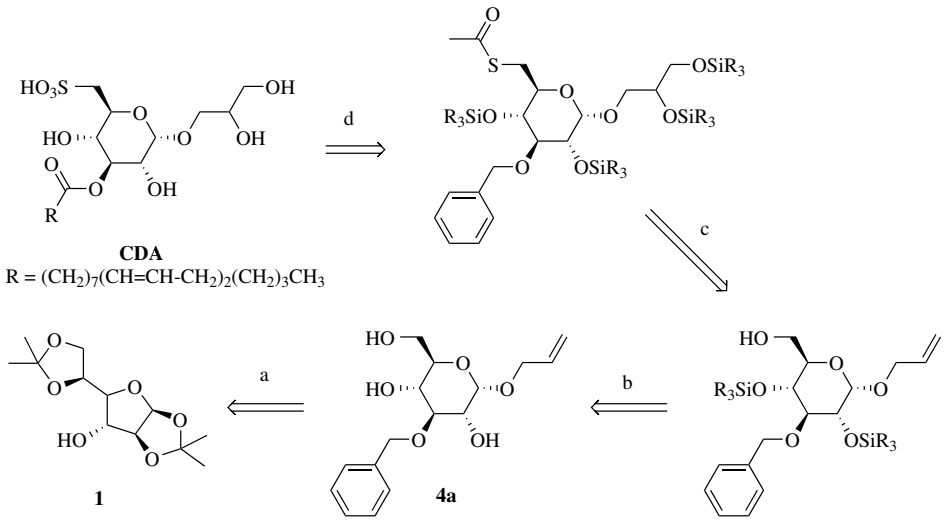

Scheme 46: Tentative total synthesis strategy towards **CDA**. Conditions a-d represent multiple steps.

can be substituted for a DDQ-cleavable protecting group, such as NAP and PPB. Selective cleavage of PNB ethers, in the presence of benzyl ethers, is also possible, in a two-step process, by exploiting the lability of PNB ethers for catalytic hydrogenation. [46]

In terms of ratio of anomers, no notably large increase was seen for either 3-*O*-protecting group. While the DTB ether resulted in slightly more α-anomer, the increase was not large enough to warrant substituting the benzyl ether for the more expensive, untested DTB ether. The practical usefulness of the crystallinity seen for the PPB and PNB compounds, appeared somewhat limited. Substituting the 3-*O*-benzyl group for PNB would be beneficial in terms of product purification, but it would likely block any attempts at selective crystallisation of the α-anomer, by imparting great crystallinity to both anomers. The PPB group appeared to increase the crystallinity, relative to benzyl ethers, but due to low crystallisation yields and co-precipitation of both anomers, no practical use of crystallisation has yet been established for the purposes of the toatl synthesis.

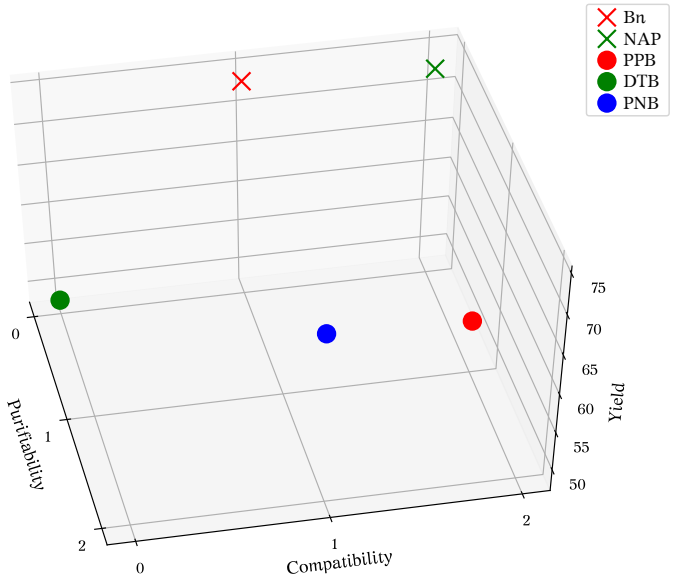

Figure 14: 3-*O*-Protecting group suitability chart. Compatibility (with the total synthesis) is relative to the benzyl group, where 1 is equal to benzyl, 0 is less and 2 is more compatible. *Purifiability*: 2 means anomeric separation is possible by crystallisation, 1 means an anomeric mixture can be purified by crystallisation, 0 means neither is possible. Yield in percent.

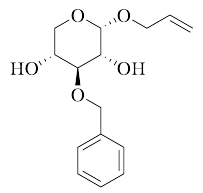

4ø

Figure 15: Allyl 3-*O*-benzyl-α-D-xylopyranoside (**4ø**).

The allo (**2ð**) and xylo (**2ø**) furanoses were also subjected to the rearrangement-glycosylation reaction, in order to scope their viability as alternative carbohydrate backbones for **CDA**. Refluxing the xylofuranose (**2ø**) in allyl alcohol with HCl afforded the pyranosides, with no appreciable furanoside forms. The α-anomer of the pyranoside (**4ø-α**) was precipitated in acceptable yields (31%), allowing for facile work-up. Since the primary hydroxyl of the pyranoside of the xylo configuration was unavailable for subsequent derivatisation (Figure 15), an alternative procedure for glycosylation had to be devised in order to proceed with the synthesis towards **CDA**. The product distribution from the rearrangement-glycosylation of the allofuranose (**2ð**) was markedly different from the glucofuranosides. Both the α-anomer of the pyranoside and the furanoside were not separable by chromatography due to overlap and low prevalence. The β-anomers of the furanoside (**3ð**) and pyranoside (**4ð**) were isolated in modest yields (19% and 23%, respectably). In subsequent structure-activity relationship studies, the two allosides could prove useful. A major advantage of the aforementioned syntheses, is the possibility of isolating anomerically pure allyl 3-*O*-benzyl compounds without the need for further derivatisation procedures.

In conclusion, perhaps the most promising alternative to benzyl ethers, were the NAP and PPB ethers. Other protecting groups were not all that practically viable. Investigations have revealed that NAP ethers behaved almost identically to benzyl ethers in the conditions tested, while having more deprotection options. This likeness to the benzyl group means that the two groups likely can be interchanged without modifying any procedures. The same is mostly true for the PPB group, which could also help facilitate crystallisation.

2.2.3 3-*O*-protected furanosides

In an effort for better understanding of the reaction progress and kinetics, the rearrangement-glycosylation reaction (Scheme 36) of 3-*O*-benzyl-protected glucofuranose (**2a**) in allyl alcohol was slowed down by decreasing the temperature to

rt. When running the reaction at reflux in allyl alcohol, only minuscule quantities of any carbohydrate intermediates and/or by-products were present along with the glucopyranoside (**4a**). At room temperature, however, the picture became dramatically more complicated, with eight different intermediates or by-products identified, in addition to the starting material present. Isolation was achieved by stopping the reaction at various points in the reaction pathway.

After 70 min, **MC-1** represented almost the entirety of the reaction carbohydrate composition. Purification of **MC-1** was facile, and could be achieved by a short silica gel column. Being an expected intermediate, structure elucidation of **MC-1** was unproblematic.

After 5-12 h, the β-anomer of the glycosylated furanoside (**3a-β**) was quite prevalent. During column chromatography the compounds co-eluted with **4a** in several fractions, however, a lesser amount of pure **3a-β** was isolated (14%). Although low, the yield was comparable to common literature yields of glucofuranoses and glucofuranosides (20-35%).[75, 76] Structure elucidation of said compounds was complicated by confusing NMR-data regarding the configuration at C-1. Furthermore, due to their reported instability, it was not entirely expected to find molecules in the furanoside form.

Since there were few procedures on producing glucofuranosides available, the notion of producing **3a-β** in at least moderate yields was interesting. Isolating the compound, however, proved to be difficult. After approximately 12 h, **3a-β** was near its maximum, but at that point **4a** was present in significant quantities. Due to overlap, separation of the two on silica gel was impractical in scales beyond approximately 100 mg.

Multiple normal phase eluent systems were attempted, but with little success. Derivatisation through acetylation resulted in diminished separation potential. Although the difference in retention time on analytical HPLC was moderately high (approx. 2 min difference on Bonus-RP column, and less on the XDB, using Method *X* for both columns) of **MC-1**, **3a-β**, and **4a**, applying C18-silica column chromatography in 1 g scale resulted in significant overlap due to line

broadening. The only reliable way of isolating **3a-β**, was by preparative HPLC, which is not viable for scales larger than approx. 100 mg. In addition to the monosaccharides described previously, unglucosylated glucopyranose (**UG-P**) was also observed. Derivatisation through acetylation was used to facilitate isolation of the glucopyranose, due to its high polarity.

Despite being a simple reaction on the face of it, the rearrangement-glycosylation reaction presented a complex set of equilibria, consisting of many species, most of which were anomeric mixtures. The possible reaction pathways are illustrated in Scheme 47.

In general terms, the 5,6-*O*-isopropylidene was opened first (step a). Hydrolysis of the 1,2-*O*-isopropylidene follows, but it was not clear to what extent the reaction proceeded through the following: simple isopropylidene cleavage to give the glucose (step b), concerted isopropylidene cleavage-glycosylation to give furanoside (step c_1) or pyranoside (step c_2). The glucose form (**UG-P**) was only observed in pyranose form, but it may theoretically exist on furanose form as well. Fischer glycosylation of the glucose, to give the furanoside (step d_1) or pyranoside (step d_2), can then occur. In addition, isomerisation between the furanoside and pyranoside forms (step e) was apparent.

Cleavage of the 1,2-*O*-isopropylidene first (step f) did also occur, followed by hydrolysis of the 5,6-*O*-acetal (step g). Only very small quantities of the 1,2-*O*-cleaved compounds (**MC-3**) were observed for the HCl-catalysed reaction. Using $FeCl_3$ (Section 2.2.4) as the catalyst, however, yielded more **MC-3** early in the reaction pathway. None of the unglycosylated form was observed, only the furanoside (**MC-3**), so either isopropylidene cleavage and glycosylation occurred in a concerted fashion, or the glycosylation of the furanose was much more rapid than isopropylidene hydrolysis. Although only the α-anomer of **3a** was observed at room temperature; minor amounts of **3a** with a RA of 1:1 (α : β) was observed when the reaction was run at reflux.

The reaction was most extensively studied in allyl alcohol with aqueous HCl as the catalyst at room temperature

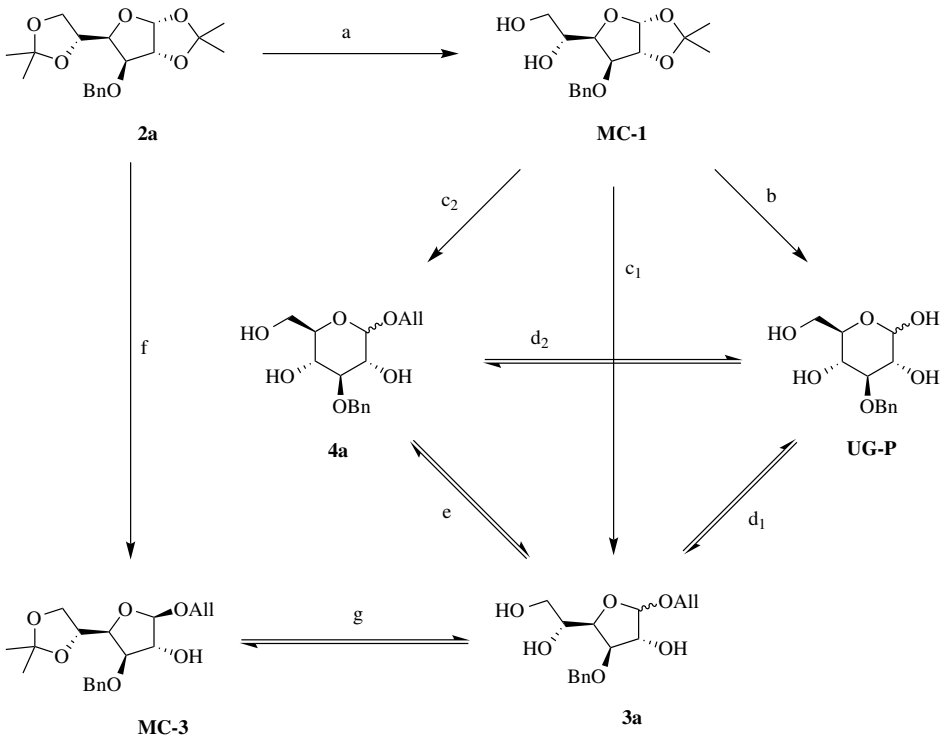

Scheme 47: Possible reaction paths for glycosylation-rearrangement reaction of **2a** in allyl alcohol. **UG-P** was observed in its acetylated form (**IC-3**). Some reactions are illustrated as irreversible due to the equilibrium appearing to be heavily shifted towards the product.

(Figure 16). Under these conditions, the 5,6-*O*-acetal was rapidly cleaved, and most starting material (**2a**) disappeared rather quickly. The glucofuranosides (**3a** and **MC-3**) were formed quickly at first, but seemed to approach equilibrium after about 24 h. Net increase of **4a** happened, slowly, in a linear fashion, appearing to follow zero-order kinetics. As for the unglycosylated pyranose (**UG-P**), the data showed a high degree of uncertainty. A clear increase was seen from $t = 0$ to after 24 h, but it was not clear whether an equilibrium would reached after some time, or if it followed an inverse U-curve.

Similar observations were made when carrying out the same reaction in methanol (Figure 17). The furanoside forms appeared to be somewhat more favoured in methanol, with **3**μ peaking at just over 50%, compared to 40% for **3a**. Formation of the pyranoside, although occurring linearly, just as in allyl alcohol, was significantly slower in methanol.

A comparison of the two glycosyl donors could be made by studying the reaction kinetics. Presumably, due to the multitude of equilibria present, most compounds could not be described by simple kinetic equations. Consumption of **MC-1** was approximated well by first-order kinetics, assuming that the reaction is irreversible:

$$\frac{dC}{dt} = kC$$

Where C is concentration, t is time and k is the rate constant. After integration, the rate equations becomes:

$$\log C = kt$$

Plotting log C against t gave $k_A = -0.058$ in allyl alcohol and $k_M = -0.063$ in methanol, with a good fit. An increase was observed when going from allyl alcohol to methanol, but the difference between the two values was arguably smaller than the uncertainty in the data. Increased reaction rate would be expected for the more polar solvent, however. As the pyranosides (**4a** and **4μ**) both increased linearly, a comparison can be drawn between the two as well. The slopes of the mole fraction of **4a** and **4μ** were $k'_A = 0.0031$ and

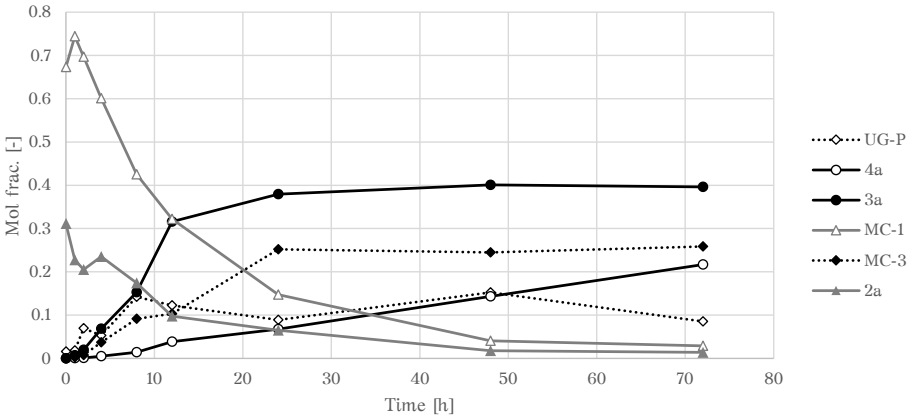

Figure 16: Mole fractions of products and intermediates, starting from **2a** in allyl alcohol with 1.6 equiv HCl (37%) at room temperature.

$k'_M = 0.0006$, respectively. Now, the rates of pyranoside formation can be compared quantitatively. The pyranoside was formed about 5 times as fast in allyl alcohol as in methanol. It appeared the furanosides were favoured as kinetic products to a greater extent in methanol. Some support for this claim can be found in the literature, as most methods claiming furanoside selectivity, use methanol as glycosyl donor.[77, 78]

Following the ratio of anomers over time on HPLC, can also give some insight into the reaction. In allyl alcohol (Figure 18), the ratio of anomers of both furanosides (**3a** and **MC-3**) remaied unchanged. A small increase was seen at 2-5 h for **MC-3**, but it was not significant. The ratio of anomers of **3a** was not plotted in Figure 18, as only the α-anomer was present at all times. Both pyranoids (**4a** and **UG-P**) followed the same pattern, where the α-anomer was favoured early in the reaction progress, but reached an equilibrium after some time. In methanol, however, an almost opposite pattern emerged. The pyranoside (**4μ**) had a constant ratio of anomers (RA), while the furanosides (**3μ**) and **X-1**) appeared to be slightly higher and lower, respectively, at first, before flatlining. Although the error margin in the data for **UG-**

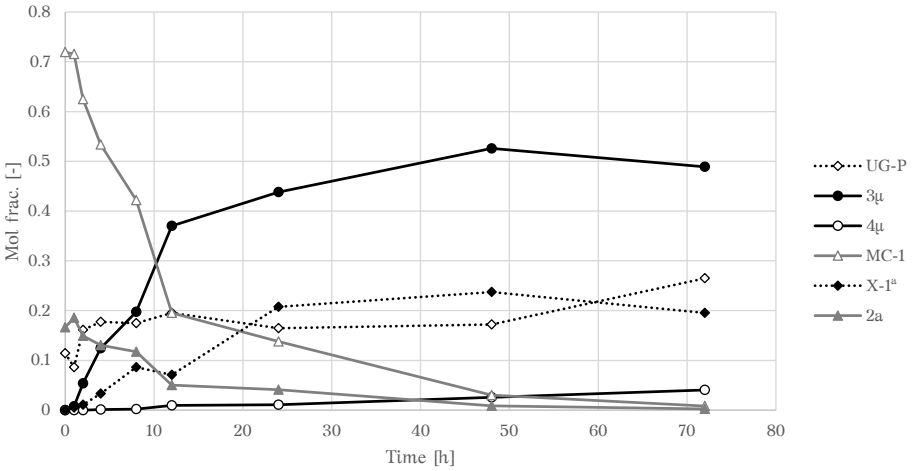

Figure 17: Mole fractions of products and intermediates, starting from **2a** in methanol with 1.6 equiv HCl (37%) at room temperature. [a] Methyl 3-*O*-benzyl-5,6-*O*-isopropylidene-D-glucofuranoside.

P was quite high, a trend of declining ratio of anomers was evident, as was the case in allyl alcohol as well. Very similar patterns were seen by Bishop et al. for methyl xylosides.[79]

Some interesting observations were made by following the reactions on HPLC, but it was difficult to draw any conclusions from the data. The observation of the furanosides being favoured relatively early in the reaction path can be explained. Furanosides are often kinetic products in glycosylation reactions. [79–81] This appeared to be the case here as well. Some support for this statement was found in the data gathered. The ratio of anomers was observed to be fairly uniform for furanoid species, except **3a**, where a small change was seen over the first 12 h. Allyl 3-*O*-benzyl-β-D-glucofuranoside (**3a**) appeared to be a special case, however, as only the α-anomer was observed at room temperature. An extreme deviation in retention time between the anomers of **3a** (less than a minute is common) was also observed. There could be some conformational differences between **3a** and the other furanoids, which will be discussed further in Sec-

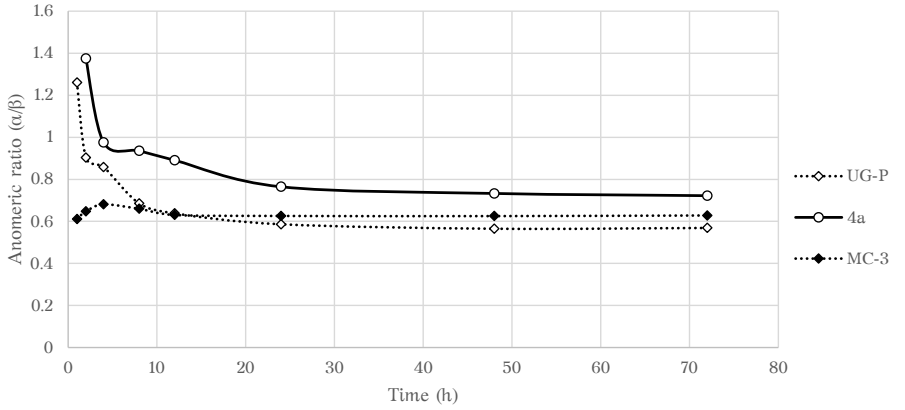

Figure 18: Ratios of anomer of products and intermediates, starting from **2a** in allyl alcohol with 1.6 equiv HCl (37%) at room temperature.

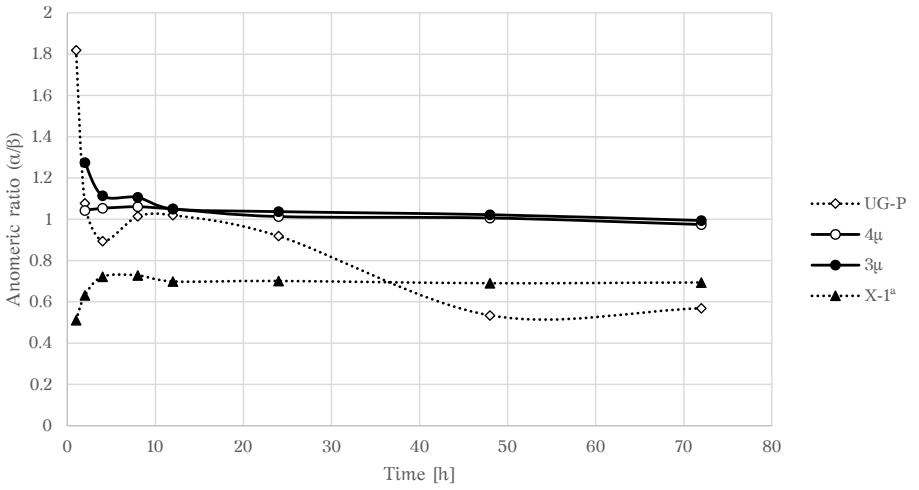

Figure 19: Ratios of anomer of products and intermediates, starting from **2a** in methanol with 1.6 equiv HCl (37%) at room temperature. [a] Methyl 3-*O*-benzyl-5,6-*O*-isopropylidene-D-glucofuranoside.

Table 12: Ratios of anomers of glucofuranosides after 16 h of glycosylation in allyl alcohol at room temperature. R_1 = Anomeric group. R_3 = 3-*O*-group.

Entry	R_1	R_3	$\alpha : \beta$
0	Bn	All	β
1	Bn	Me	57:43
2	(*p*-Ph)Bn	All	52:48
3	TBDPS	All	53:47

tion 2.4. The question remains whether allyl 3-*O*-benzyl is a special case, in terms of possibility for producing furanosides at more kinetic conditions.

A short series of 3-*O*-protected glucofuranosides were prepared: benzyl (**2a**), PPB (**2c**) and TBDPS (**2f**). These would be subjected to the same conditions that produce **3a**-β with some selecitivty, that is in allyl alcohol with 1.6 equiv of HCl (Table 12). It was observed earlier that when glycosylating under the previously mentioned conditions, only the β-anomer of **3a** was present. This observation led to the question of whether the high β-selectivity is present for other protecting group combinations.

Interestingly, all other combinations of 3-OH and anomeric protecting groups resulted in furanoside anomeric mixtures (entries 1-3). Furanosides with other protecting group patterns were also isolated to study the anomeric ratio (Table 12). An approximately 1:1 ratio of anomers was observed for the other furanosides than **3a**, with only a small excess of the α-anomer. By substituting the benzyl group in **3a** for the similar PPB group, a dramatic change in anomeric composition was seen. Differences between the furanosides will be discussed further in Section 2.4.3.

Even though separation of mixtures consisting of both anomers of both the furanoside and pyranoside forms is extremely difficult, a method for producing the furanoside form selectively would greatly simplify the separation effort. Further investigations into selectively making furanosides were considered, as there are few procedures for producing them.

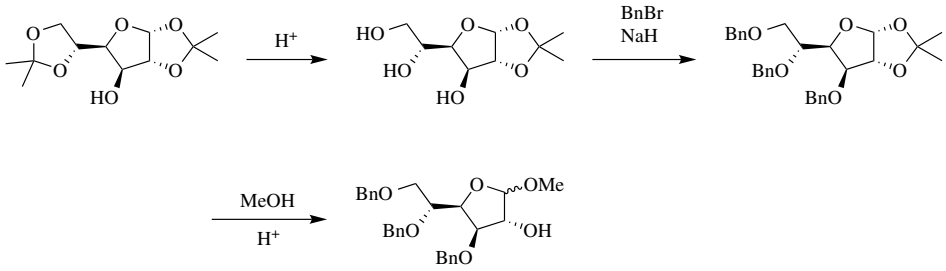

Scheme 48: Multi-step procedure for producing furanosides by Lee et al.[82]

Furanosides could also be considered for replacing the pyranoside backbone in **CDA**.

2.2.4 Furanoside syntheses

As previously discussed, it is possible to produce glucofuranosides by exploiting the fact that they are kinetic products in many cases, although high selectivity is required for isolation of the desired product to be viable. Few literature procedures for producing furanosides with high selectivity currently exists. The majority of the attempted furanoside syntheses were performed on the model substrate **2a**, additional substrates were prepared to scope general applicability. Unless otherwise stated, **2a** was the starting material, and allyl alcohol was employed as the glucosyl donor (Scheme 49).

The most obvious method for retaining the furanose configuration involves protecting the 5-hydroxyl functionality, thereby blocking ring closure towards the pyranoside. A method by Lee et al.[82] illustrates the procedure (Scheme 48). Starting with a glucose diacetonide, 5-OH is protected by an acid-resistant protecting group, such that glycosylation can take place without rearrangement to the pyranoid form. While straightforward, this method has the disadvantage of introducing additional steps. This procedure was disregarded, as it would confer compatibility issues with the total synthesis.

Multiple promotor and solvent combinations along with subsequent product distributions of calculated HPLC yields,

are shown in Table 13. Two data points (16 and 36 h) from the reaction of **2a** in allyl alcohol with HCl were included for comparison purposes (entry 0 and 1).

A widely-cited methodology for preparing glucofuranosides involves the use of trivalent iron as a promotor. By varying the solvent, selectivity can be tuned for furanoside and pyranoside, and their ratio of anomers, all in high yields. Using octyl alcohol as the glycosyl donor, pure α-glucofuranoside can supposedly be achieved using DCM as the solvent, albeit in a low yield. By changing to *p*-dioxane, an anomeric mixture (approx. 1:1 (α : β)) of furanosides was achieved.[80] The glycosylation of **2a** with allyl alcohol by this procedure gave results in accordance with the claims of the authors (entries 2,3). Dioxane gave good selectivity for the furanoside forms, with an approximately 1:1 ratio of anomers (entry 2). After multiple days of reaction time, however, the reaction struggled to proceed beyond opening the 5,6-*O*-acetal. Using DCM, good selectivity for the β-glucofuranoside was achieved (entry 3). The unglycosylated form was favoured, though, and some α-furanoside and pyranoside were present. Better conversions could possibly be attained by starting from 3-*O*-benzyl-glucose, without the isopropylidene groups.

A complicating factor was encountered in the scarce information regarding work-up in the literature. An example of this is the work of Ferrières et al.[80], which describes no work-up procedure at all. A work-up procedure was devised, involving multiple washes with saturated bicarbonate solution during extraction, for adequate neutralisation of all iron species. The heavy extraction procedure on relatively polar sugars, led to significant product loss. To adress the loss of yield associated with extraction, acetylation of the crude product was attempted in pyridine-Ac_2O. Acetylation proved unsuccesful, presumably due to interference from iron species present, and a plethora of byproducts were obtained alongside **3a** from column chromatography.

Compared to the previously described Fischer glycosylation (entry 0, 1), the method of Ferrières et al. presented no significant improvement in terms of isolated furanoside yields. By tuning the solvent, both anomers of **3a** could be

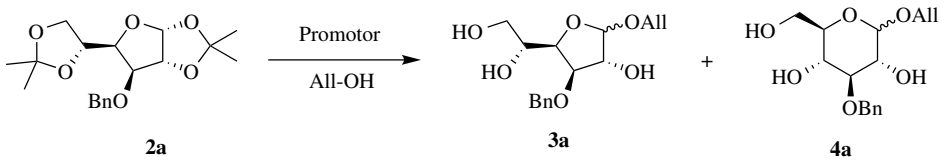

Scheme 49: Glycosylation of **2a** with allyl alcohol.

produced, however, making it one of the few methods for producing **3a-α** in non-marginal yields. In conclusion, the method using $FeCl_3$ looks good on paper, but presented major drawbacks in terms of practically isolating the products in good yields.

Using a DMSO and cyanuric chloride (TCT) catalyst system, Shi et al.[77] was able to tune reactivity to either glucofuranoside or glucopyranoside by varying the DMSO concentration. In methanol, the reactivity could be tuned to both furanoid and pyranoid forms, while the use of longer alkyl chains (ethanol, etc.), was associated with loss of selectivity. Allyl alcohol, however, was not included in the study. Since the DMSO-cyanuric chloride catalyst system is presumably not capable of hydrolysing acetals, **2a** could not be applied as the starting material in this case. Starting from an anomeric mixture (73:27 α : β) of **4a**, the procedure favouring the furanoside was used, in order to investigate whether any isomerisation to the furanoside form (**3a**) occurred (entry 4). Furanoside production was marginal, but present, giving some credence to the method. 3-*O*-Benzyl-glucopyranose was prepared by deacetylating 3-*O*-benzyl-1,2,4,6-tetra-*O*-acetyl-glucopyranose (**IC-3**), followed by quenching and filtering. Without further purification, Shi's procedure was carried out on the product (entry 5). A furanoside-pyranoside ratio of about 1:4 was achieved. Although better than the 1:9 achieved by Shi et al. using *n*-propanol, it is not selective enough to allow for facile separation. Despite low yields and insufficient selectivity, the results indicated that this procedure could be optimised somewhat in future studies.

A final, prominent, method for selectively producing glucofuranosides, utilises molecular iodine in methanol. Acting

as a soft acid, the iodine cleaves acetals, and at higher temperatures catalyse glycosylation reactions. By refluxing **1** in methanol, moderately good selectivity for the glucofuranoside can be attained.[78] Since molecular iodine is incompatible with the allyl group under most circumstances, little chance of modifying the procedure for allyl alcohol was expected. Regardless, the procedure was attempted on **2a** in allyl alcohol (entry 6). Only minuscule amounts of glycosylated compounds were observed. Plentiful side reactions were observed, and, accordingly, the procedure was disregarded.

With the exception of the method employing iron(III) chloride, the other two methods involve methanol as the glycosyl donor. Whereas good reactivity and selectivity are seen for methanol, substituting with allyl alcohol, or any other aliphatic alcohol, appears to have a detrimental effect on selectivity. The difference in nucleophilicity between the methanol, ethanol and allyl alcohol is not great[83], so the difference in nucleophile strength was not thought to be determining. Solvent polarity, on the other hand, has been shown to have a large effect on furanoside vs. pyranoside selectivity.[77] The present data were insufficient to draw any conclusion in regards to the effect of the glycosyl acceptors properties on the furanoside-pyranoside equilibrium. Due to the limited number of glycosyl donors of interest for the total synthesis, a wider scope of donors will not be screened.

The iron(III) chloride promoted method produced moderate yields and good selectivity. In order to make the method desirable, however, optimisation and better procedures are required.

Other promotors and conditions were also explored in terms of selectivity (Table 13), based on previous observations[84] that at reflux, different Brønsted acid catalysts could result in different product compositions. The rationale for this was not clear and may be attributed to a number of factors, such as acid strength, water content, nature of the counterion, etc. Lewis acids, such as $SnCl_2$ and $ZnCl_2$, had also been employed previously in an attempt to optimise the anomeric ratio of pyranose products.

At reflux temperatures, the TsOH promoted reaction re-

Table 13: Effect of promotor and solvent on product distribution, starting from **2a** at room temperature, unless stated otherwise. TFA = trifluoroacetic acid, DCA = dichloroacetic acid, TCT = 2,4,6-trichloro-1,3,5-triazine, TsO = *p*-toluenesulfonyl, DMSO = dimethylsulfoxide.

Entry	Promotor	Loading	Solvent	Time [h]	**2a**[a]	**MC-1**[a]	**3a-β**[a]	**3a-α**[a]	**4a**[a]	**UG-P**[a]
0	HCl	1.6 equiv	All-OH	36	0	6	56	0	23	11
1	HCl	1.6 equiv	All-OH	16	19	48	17	0	2	13
2	$FeCl_3$	3 equiv	*p*-Dioxane	96	0	62	12	15	0	3
3	$FeCl_3$	3 equiv	CH_2Cl_2	96	0	23	34	4	5	24
4[c]	TCT/DMSO	2.0/1.5 equiv	All-OH	4	0	0	1.5	1.5	96	0
5[d]	TCT/DMSO	2.0/1.5 equiv	All-OH	4	0	0	4	4	23	69
6	I_2*	1%[e]	All-OH	12	9	20	2	1	2	16
7	TsOH*	1.6 equiv	All-OH	16	0	40	5	0	0	23
8	TFA	50%[b]	All-OH	168	0	4	12	0	0	76
9	DCA	50%[b]	All-OH	168	0	20	19	1	16	38
10	$SnCl_4$	1 equiv	Et_2O	168	32	34	11	4	2	13
11	$Bi(NO_3)_3$*	0.25 equiv	CH_2Cl_2	168	0	17	0	0	0	32

[a] Calculated yield. [b] Volume percent. [c] Starting from allyl 3-*O*-benzyl-D-glucopyranoside. [d] Starting from 3-*O*-benzyl-D-glucopyranose. [e] Weight over volume percent. * Unidentified side-products.

sulted in a myriad of byproducts (entry 7). It was hypothesised that the rather low water content of TsOH, in its monohydrate form, could by some mechanism make a difference to the product distribution. Using TsOH at 1.6 eq surprisingly little glycosylation was seen (entry 7). The unglycosylated form (**UG-P**) and the partially cleaved isopropylidene furanose (**MC-1**) represented most of product distribution. Comparing this result to when using HCl (entry 1), little glycosides are observed.

Two weaker acids were considered: trifluoroacetic (TFA) and dichloroacetic (DCA) acid. In terms of solvent properties, both acids are similar, mostly differing in acid strength. In spite of their similarity, the two acids gave dramatically different results. In TFA, the unglycosylated sugar (**UG-P**) was produced with high selectivity (entry 8), whereas the other species represented a small portion of the product distribution. In DCA, however, a distribution fairly even among all products was noted (entry 9). The prevalence of the unglycosylated form (**UG-P**), which requires two equivalents of water, posed questions about the role of water in the rearrangement-glycosylation reaction. In lieu of further speculation on the topic of the role of water, a proper study, using known quantities of water, should be carried out. Regardless, results from both TFA and DCA were unsatisfactory.

The viability of Lewis acids as acetal hydrolysis and glycosylation catalysts was also considered. Bismuth(III) nitrate, a mild Lewis acid catalyst, has been successfully applied as a glycosylation catalyst, but not in the tandem acetal cleavage-glycosylation reaction in question. [85] The same applies to the stronger $SnCl_4$.[38] $SnCl_4$ (entry 10) and $Bi(NO_3)_3 \cdot 5\,H_2O$ (entry 11) were applied as promotors in Et_2O and DCM, respectively, using stochiometric amounts of allyl alcohol. With $Bi(NO_3)_3 \cdot 5\,H_2O$, the 5,6-*O*-isopropylidene acetal was hydrolysed to some extent, but most compounds produced were unidentified. No glucosides were detected, and $Bi(NO_3)_3 \cdot 5\,H_2O$ was deemed an unsuitable promotor for the reaction. Due to the difference in solvent, the selectivites were not directly comparable to the standard reaction in allyl alcohol and the long reaction times required presented a

slight inconvenience. Moderately good selectivity for furanosides was attained using $SnCl_4$ (entry 10). The ability of the tin catalyst to effectively catalyse the reaction with only stochiometric quantities of glycoside donor, does allow for more free tuning of solvent polarity, relative to traditional Fischer glycosylation. Should further optimisation into the reaction be performed, $SnCl_4$ is a promising candidate.

Although none of the screened methods produced the desired results, two did show some potential. Both Lewis acids $FeCl_3$ and $SnCl_4$ exhibited acceptable selectivity for furanosides. In order to produce good yields, reaction conditions will need to be tuned to produce furanosides with high selectivity. This is necessary, since separation of anomeric mixtures of both furanosides and pyranosides is highly problematic. As selectivity appears to be highly dependent on reaction conditions, procedures are not necessarily generally applicable, as seen when trying to modify literature procedures to those relevant for the total synthesis towards **CDA**. The research conducted here highlights the need for optimisation, but shows that a targeted effort towards producing the desired furanosides may very well result in respectable yields.

2.3 Schmidt glycosylation

In addition to the investigations into glycosylation-rearrangement of the 3-*O*-protected compounds, an additional study in relation to the total synthesis project was conducted. Although the following work is not reflected in the title of the thesis, it carries high importance for the total synthesis project. In order to get a glycerol moiety as the aglycone of **CDA**, the current strategy is to glycosylate with allyl alcohol, followed by dihydroxylation of the double bond at an appropriate point in the total synthesis (left path, Scheme 50). This approach is not entirely unproblematic, as dihydroxylation generally produces two diastereomers, owning to the chiral centre at the glycerol secondary carbon atom.[86] At this point, Sharpless asymmetric dihydroxylation (AD) has been attempted on the allyl group by the research group. Although

successful, the procedure does confer problems related to the stereochemistry at the glycerol moiety. Sharpless AD produced hardly any diastereomeric excess, and the subsequent separation of those diastereomers was proven to be problematic.[84] Optimisation of AD is unlikely to result in an acceptable diastereomeric excess (de) on the glycerol moiety, since a) the method often produces mediocre stereoselctivity for terminal alkenes,[87–91] b) existing chiral centres in substrates can be detrimental to selectivity,[88, 92] and c) AD has been attempted on similar substrates without acceptable results.[56, 93] Alternative ligands are available, but desired stereoselectivity (> 95% de) is rarely achieved for terminal alkenes and compounds with existing chiral centres.[56, 89–91]

An alternative to glucosylation with allyl alcohol and oxidation of the double bond, is introducing the glycerol acetonide moiety via a mild glycosylation procedure (right path, Scheme 50). By incorporating glucosylation with glycerol acetonide, complete control over the stereochemistry at the glycerol aglycon can be achieved, since both enantiomers of the glycerol acetonide are commercially available. A number of SQDG syntheses incorporate procedures that involve glycosylation with glycerol acetonide.[93–96] The Schmidt glycosylation procedure was chosen due to the mild reaction conditions and lack of expensive and hazardous heavy metal salts needed[33] in the Koenigs-Knorr glycosylation procedure. The use of Schmidt glycosylation for insertion of the glycerol moiety is well established in the literature, and applied to SQDG syntheses in multiple instances.[93–95] Although similar, all literature procedures differ substantially in carbohydrate configuration, protection group pattern, desired stereochemistry, etc. As a result, optimal reaction conditions for the glycosylation of the 3-*O*-protected compounds in question were not immediately obvious. Thus, reaction conditions were chosen somewhat arbitrarily. Only an exploratory look into the glucosylation with glycerol acetonide would be permitted within the allotted timeframe, and would only be considered complementary to the work carried out.

In order to introduce a glycerol moiety to a 3-*O*-protected

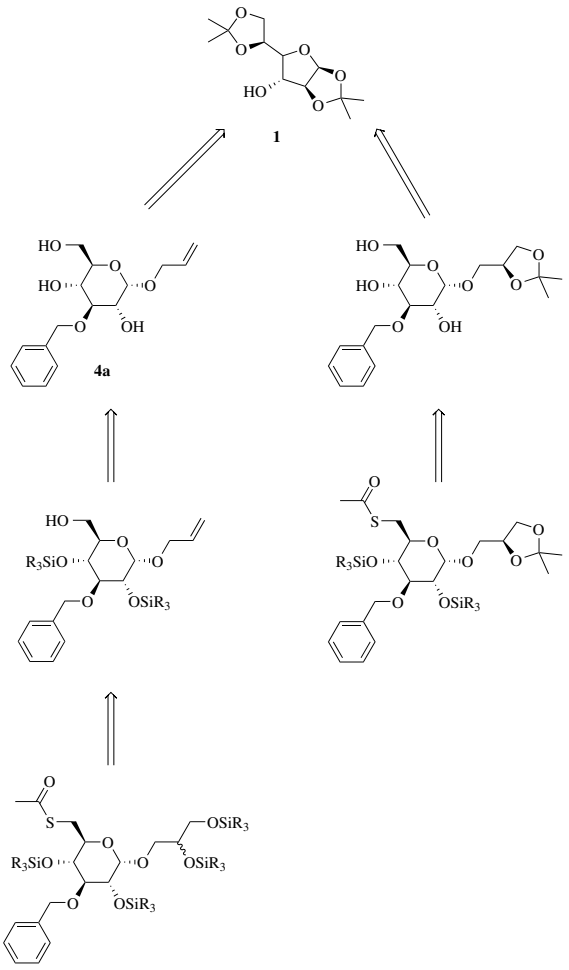

Scheme 50: Alternative syntheses towards **CDA**. In the route on the left, an anomeric allyl group is introduced, then oxidised to afford a glycerol group, whereas in the right route, an isopropylidene-protected glycerol group is introduced directly.

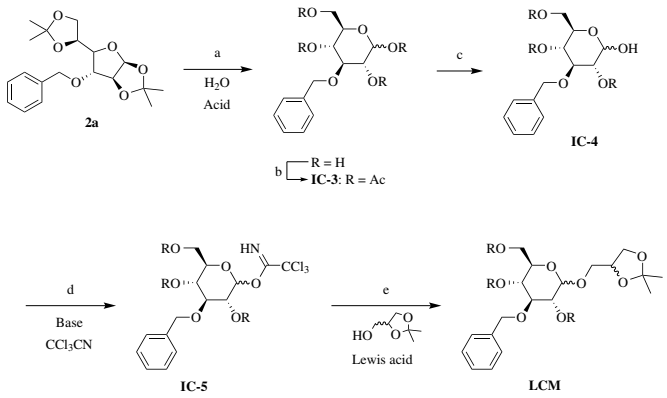

Scheme 51: General strategy for introducing an isopropylidene-protected glycerol group to a 3-*O*-benzyl-glucopyranoside.

glucose, a suitable protection strategy is required. A general procedure is shown in Scheme 51. After rearranging **2a** (step a), temporary protection groups, orthogonal to the existing benzyl group, are required on all other positions (step b). Then, the anomeric protection group is to be removed (step c), followed by activation with trichloroacetonitrile (step d), and glycosylation (step e).

2.3.1 Preparation for glycosylation

A tentative approach, involving acetyl groups, was devised (Scheme 51) on the basis of its simplicity and their known compatibility with the procedure.[95] In addition to facile introduction and removal, the anomeric acetyl group can be removed selectively, taking away the need for multiple protection groups. Alternatively, a different temporary protecting group, such as PMB ethers, could be employed, but this would require additional steps in order to get the anomeric position unprotected.

Refluxing **2a** in water with HCl afforded 3-*O*-benzyl-D-glucose, which was subsequently acetylated. Purifcation by chromatography gave **IC-3** in a good yield (80%). Anomeric separation on silica gel was poor, compared to the acetylated allyl and methyl pyranosides (**8a**, **8b** and **8μ**), where baseline

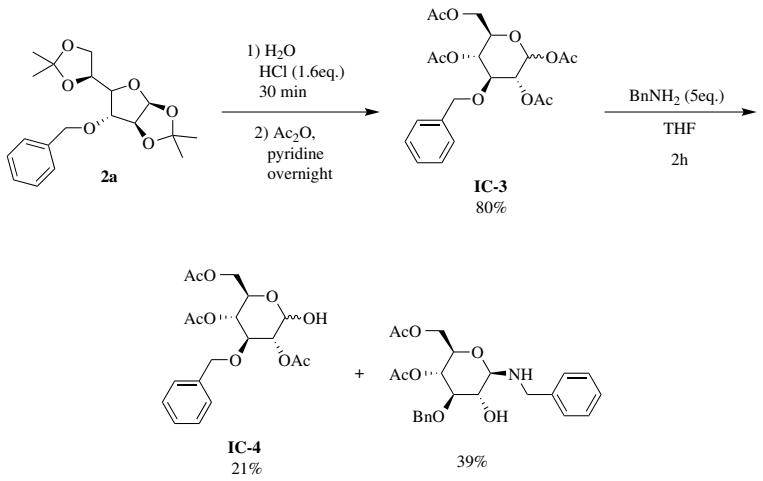

Scheme 52: Experimental procedure for producing a protected glucose, for use in Schmidt glycosylation.

or partial anomeric separation was possible. The β-anomer was favoured under these conditions (30:70 (α : β)), an observation that could be explained by the anomeric effect, owing to the polarity of the solvent.

A number of procedures were available for removing the anomeric acetyl group selectively. All involve a moderately good nucleophile. Benzylamine was ultimately chosen, in a decision based purely on availability of the reagent. That said, the most common reagents (e.g. $BnNH_2$, NH_3 and hydrazinium monoacetate) appear to fare similarly in terms of yield (70-90%). Ammonia and hydrazinium monoacetate have the advantage of being more easily removed during work-up, though.[97–99]

Using 5 equiv benzylamine in THF at room temperature for 2 h (Scheme 52), resulted in the reaction proceeding too far. The major product was a *N*-benzyl glucopyranoside, and the desired product (**IC-4**) was only isolated in a low yield. Only the β-anomer of the *N*-benzyl byproduct was observed, which coupled with the fact that the 2-*O*-acetyl group was removed, could indicate some involvement of the 2-*O*-acetyl group in the reaction. That being said, further experiments are necessary to determine the role of the 2-*O*-acetyl group,

if any.

Optimisation of the removal of the anomeric acetyl group could be carried out by simply closely monitoring the reaction by TLC, and stopping at an appropriate time. Five equivalents of benzylamine was presumably excessive as well. It is reasonable to expect an increase in yield from these optimisation measures, as Cai et al. obtained 92% yield for a similar reaction, using benzylamine (1.1 equiv).[97] Substituting benzylamine for a base that is more easily removed during work-up, such as ammonia[98], hydrazinium monoacetate[99] or 3-(dimethylamino)-1-propylamin[100], could also be desirable. Upon removing the anomeric acetyl group, the ratio of anomers was changed from 30:70 to about 75:25 (α : β). This change could possibly be attributed to the anomeric effect as well, following the decrease in solvent polarity when switching from water to THF.

2.3.2 Schmidt glycosylation

Once the anomeric position is unprotected, the Schmidt glycosylation can commence. A trial procedure was established, loosely based on Lafont[95] and Hanashima's[93] SQDG syntheses. The first step of the Schmidt glycosylation proceudre, involves forming the trichloroacetimidate (TCAI), a better leaving group, from trichloroacetonitrile and a base (Scheme 53). DBU was chosen as the base, due to successful applications in multiple SQDG syntheses. DBU is of suitably low nucleophilicity[101] and has seen effective use in other syntheses that involve acetyl groups[95].

Carrying out the trichloroacetonitrile (TCAN) activation of **IC-4** with 0.46 equiv DBU in DCM at 0°C (entry 1, Table 14), was successful. The NMR spectrum of crude **IC-5** showed that full conversion had been attained (entry 1, Table 14). Isolated yield, however, was only 42%, indicating that there was significant product loss during work-up, i.e. on column. It was hypothesised that slightly acidic silica gel would activate **IC-5** for nucleophilic attack, causing loss on column. It might be desirable to purify TCAIs by passing it through only a pad, or a very short column of silica, in order

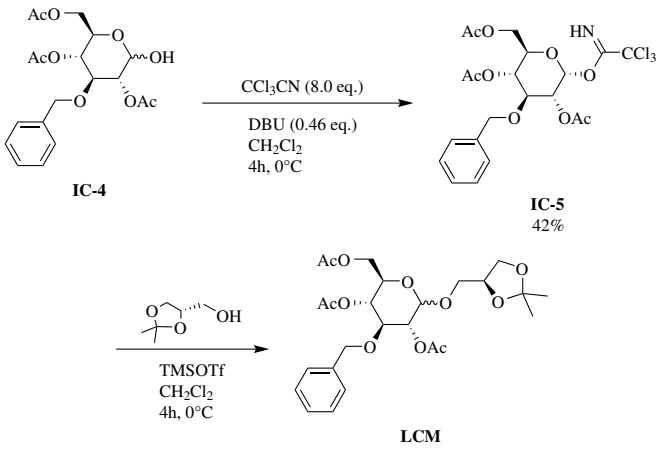

Scheme 53: Experimental procedure for Schmidt glycosylation with isopropylidene-*sn*-glycerol.

to minimise contact time, and thus avoid product loss. Purification by reverse-phase chromatography faces comparable problems, with TCAIs being reactive towards water as well.

Preparation of **IC-5** was also attempted directly from **IC-3**, by in-situ deacetylation, followed by reaction with CCl_3CN (Scheme 54, Table 14). A first attempt, using the same conditions as when starting with **IC-4** (entry 1), was made (entry 2). The attempt was unfruitful, affording only a byproduct with TCAI in 4-*O*-position rather than anomeric (Scheme 54). Increasing the DBU concentration to 0.80 equiv (entry 3), however, resulted in moderate crude yields of **IC-5**, and similar byproduct formation to the the previous experiment (entry 2). Isolated yield, on the other hand, likewise to other TCAI experiments, was significantly lower than the calculated yield. The continued product loss during work-up emphasised the need to improve the work-up procedure for TCAI sugars. Product isolation was particularly difficult when directly reacting TCAN with **IC-3**, since **IC-3** and **IC-5** eluted quite closely. The mechanistic aspects of in-situ deacetylation, followed by activation with TCAN, were not known, yet some hypotheses were be made based on prior knowledge. While acetyl groups are susceptible to removal

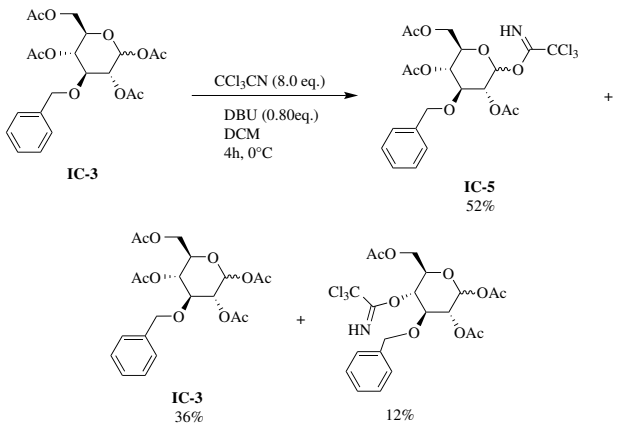

Scheme 54: TCAI formation from fully acetylated glucose. All yields are NMR yield.

by nucleophilic bases, DBU is widely regarded as a non-nucleophilic base, so effective deacetylation by direct reaction with DBU is unlikely. However, nucleophilic behaviour from DBU has been observed previously, and can not be completely ruled out.[101] Regardless, fact that conversion was significantly augmented by increasing the DBU concentration, showed that DBU somehow had some involvement in the process.

A by-product with the TCAI in 4-*O*-position was also formed in minor quantities. Interestingly, the acetyl group in 4-*O*-position, which is the least sterically accessible, was converted into TCAI, rather than the more readily accessible primary hydroxyl. This observation may be attributed to acetyl migration, where the primary acetyl is cleaved, followed by acetyl migration from 4-*O*-position, which is known to occur.[45] The phenomena is not unknown, minor deacetylation in 4-*O*-position is known to occur in the presence of a base.[102]

Finally, the glycosylation of **IC-5** was carried out with isopropylidene-*sn*-glycerol (Scheme 53). Reaction conditions previously used for introducing isopropylidene-glycerol varies by a large margin, from 0.6 equiv TMS-OTf at room temperature for 72 h[94] where the α-anomer is desired, to 2.5 mol%

Table 14: Reaction with trichloroacetonitrile of **IC-4** (Scheme 53), and the fully acetylated **IC-3** (Scheme 54). *Product* is the glycosyl acceptor with trichloroacetimidate in anomeric position (**IC-5**), *Biproduct* is the glucoside acceptor with trichloroacetimidate in 4-*O*-position (biproduct in Scheme 54). DBU: 1,8-diazabicyclo[5.4.0]undec-7-ene. ND: none detected.

	equiv DBU	Product[a]	Biproduct[a]	Yield product[b]
IC-4	0.47	Quantitative	ND	42%
IC-3	0.47	ND	14%	0%
IC-3	0.80	52%	12%	24%

[a] NMR yield. [b] Isolated yield.

at -20°C for 4 h[95] where the β-anomer is desired. In order to produce both anomers, a middle ground of 0.2 equiv of TMS-OTf at 0°C to room temperature, and a reaction time of 4 h were ultimately chosen. Unfortunately, separation of the product (**LCM**) was complicated by overlap with a significant impurity. Complete isolation was not carried out due to time constraints. Some information could be gleaned from the impure NMR spectrum, however, which will be discussed further in Section 2.4. Under these conditions selectivity for the β-anomer was observed, however the ratio of anomers could potentially by optimised for the α-anomer. As previously mentioned, the ratio of anomers (RA) in the starting TCAI can have an impact on the final RA, i.e. there is some kind of inversion of stereochemistry. This inversion is more prevalent under kinetic conditions[103], a possible explanation for the observed β-selectivity. In addition to the usual factors imparted by the anomeric effect, modifying the RA, both the type of Lewis acid promotor and concentration can affect the RA of the product glycoside.[33] The 2-*O*-acetyl group could potentially complicate the picture even further. Acetyl groups have been shown to interact with the glycosylation reaction by anchimeric assistance, which could possibly be the case here.[33]

Further optimisation on the glycosylation procedures with

glycerol acetonide should address the anomeric effect on the final glycoside (**LCM**). Firstly, a procedure for producing both anomers of the glucosyl TCAI (**IC-5**) should be devised. The base, temperature and solvent should be varied in order to produce both anomers of **IC-5**. Subsequently, the effect of the TCAI **(IC-5)**, on the RA on the product glycoside (**LCM**), should be investigated. Finally, conditions favouring the α-anomer during glycosylation should be looked into. Alternative promotors, in addition to TMS-OTf, such as TBDMS-OTf and $BF_3 \cdot Et_2O$ should be tested. Ideally, a procedure for producing pure **LCM-α** should be devised, negating the need for a method of achieving anomeric separation. It might be necessary to substitute the acetyl group with more inert, temporary protecting groups, such as PMB. Although the α-anomer is the main focus of the total synthesis, the β-anomer is also desired for potential structure-activity relationship studies of **CDA**.

2.4 Discussions on spectroscopic data

Due to the amount of data generated, most spectroscopic data will only be discussed in general terms, with comparisons being drawn between analogous compounds. The non-carbohydrate reagents (**RC-1**, **RC-2**, **RC-3**) will not be discussed beyond MS, as these matched reference data and are of little interest. The sugars with configuration differing from the *gluco*-configuration (xylo, allo), are, when available, included in the tables to give an indication of the variance *between* different carbohydrate configurations, relative to the variance within different protecting group patterns for the glucosides and glucoses.

Of the 3-*O*-protected diacetone glucoses, only the DTB (**2d**) and ANT (**2j**) ethers were novel, so little time will be spent on justifying the structure of said group of compounds. Most 3-*O*-protected glycopyranosides were novel compounds, with the exception of allyl (**4a**) and methyl (**4μ**) 3-*O*-benzylpyranosides, for which limited NMR data were found in the literature. All sugars with xylo and allo configurations had previously been described in the literature. Reference data for

the series of furanosides were lacking. Only data for methyl 3-*O*-benzyl glucofuranoside (**3μ**) was found. More data were available for the series of acetylated compounds, with only allyl 3-*O*-NAP (**8b**) being novel. The two compounds used for the Schmidt glycosylation (**IC-4** and **IC-3**), and the 4,6-*O*-acetal protected furanosides (**8i** and **8j**) were novel as well.

Spectroscopic data were incomplete for a handful of compounds. IR spectra and optical rotation were missing for **MC-3**, **3f-α** and **4f-α** due to being isolated in insufficient quantities to perform all the desired analyses. Due to lack of instrument availability, **MC-3**, and both anomers of **3f** and **4f** were characterised using a 400 MHz instrument for NMR. NMR data for **3f-α** did not allow for an assertive structure determination, as **3f-α** was isolated in insufficient amounts to produce good quality ^{13}C and HMBC spectra. A tentative structure determination of allyl 3-*O*-TBDPS-α-D-glucofuranoside was used. MS was not run of **IC-5**, as it is unsuitable due to its unstability. The HMBC spectrum of **3a-α** was inadequate, but a structure determination could still be made with the available information. MS was performed on an anomeric mixture of **9j**, and this was considered sufficient, since the spectrum showed only constituents with equal mass.

2.4.1 Optical rotation

Comparing the specific rotation of the furanosides, a general trend emerged (Table 15). The α-anomer had a positive values, meanwhile the β-anomers typically had a negative, slightly larger specific rotation. The opposite sign of the α and β-anomers were presumably coincidental, as they are not enantiomers. Inverting the configuration at C-3 of **3a**, to give **3ð** did not appear to have a large impact on the optical rotation. Due to the lack of literature data for the synthesised compounds, methyl 3,5,6-tri-*O*-benzyl-D-glucofuranoside was included as a reference.

A larger dataset was available for the pyranosides (Table 16), as more were isolated as pure anomers. The α-anomers had moderate to large positive values (+30 to +80°), while

Table 15: Optical rotation of furanosides. Concentration range 0.5 or 1.0 g/100 mL in CH_2Cl_2.

α	Compound	β
+68°	**3a**	-71°
+80°	**3c**	-104°
+76°	**3μ**	-112°
+29°	Ref.[a]	-55°
	3f	-112°
	3ð	-36°

[a] Reference value for methyl 3,5,6-tri-*O*-benzyl-D-glucofuranoside.[104]

the β-anomers had low negative values. Most compounds fell within a fairly narrow range of values ±25°. Data for **9a** was included as a reference for the 4,6-*O*-acetal protected pyranosides. Literature data for both anomers of **4μ** were available: -25°(β-anomer)[105] and +58° (α-anomer),[106] both in chloroform. Recorded data were consistent with the literature when allowing for some variation from difference in solvent and concentration.

Optical rotation of isopropylidene protected furanoses are presented in Table 17. All compounds here are α-anomers. Most compounds fell within a very small range of about 20-35°. Not unexpectedly, the other sugar configurations (**2ø** and **2ð**) differed significantly. The TBDPS-protected furanoside (**2f**) differed by a large margin, as could be said of the ANT-protected furanoside (**2j**) as well. These are relatively sterically demanding groups, so some difference in conformation could be expected.

It was noted that the diacetonide α-furanoses (**2a-j**) are closer in optical rotation to the β-furanosides (**3a-f**)). Optical rotation is a function of conformation of molecule[108] and the isopropylidene acetals modify the conformation, such that the acetal protected furanoses (**2a-j**) will not necessarily share optical rotation power with the α-furanosides (**3a-f**).

Table 16: Optical rotation of pyranosides. Concentration 0.5 or 1.0 g/100 mL in CH_2Cl_2.

α	Compound	β
+98°	**4a**	-28°
+85°	**4b**	-26°
	4f	-52°
+96°	**4µ**	-2°
	4ð	-8°
+55°	**9i**	-28°
+88°	**9j**	-24°
+78°	**9a**[a]	-37°
+76°	**8a**	-20°
+58°	**8b**	+10°
+52°	**8µ**	-8°
+72°	**4ø**	

[a] Reference value from Peer et al.[107]

Table 17: Optical rotation of isopropylidene protected furanoses. Concentration 1.0 g/100 mL in CH_2Cl_2.

Compound	Optical rotation
2a	-26°
2b	-24°
2c	-32°
2d	-24°
2e	-16°
2f	32°
2g	-20°
2i	-34°
2j	-9°
2ø	-64°
2ð	98°

Table 18: Sugar ring proton shifts in $CDCl_3$ for isopropylidene protected furanosides, relative to TMS. *Bn-b* and *Bn-a* are benzylic protons.

	H-1	H-2	H-3	H-4	H-5	H-6b	H-6a	Bn-b	Bn-a
2a	5.90	4.58	4.02	4.15	4.37	4.00	4.11	4.64	4.68
2b	5.93	4.63	4.08	4.16	4.42	4.03	4.14	4.79	4.85
2c	5.91	4.61	4.06	4.16	4.39	4.02	4.13	4.68	4.73
2d	5.89	4.60	4.04	4.18	4.41	4.05	4.12	4.63	4.66
2e	5.87	4.35	4.24	4.03	4.23	3.95	4.11	-	-
2f	5.80	4.06	4.43	4.03	4.46	4.00	4.17	-	-
2g	5.87	4.42	4.41	4.03	4.32	3.96	4.11	-	-
2i	5.92	4.62	4.04	4.12	4.36	4.02	4.14	4.76	4.81
2j	5.85	4.63	4.24	4.14	4.38	4.00	4.07	5.59	5.68
2ø	6.00	4.65	4.02	4.28	-	3.86[a]	3.95[b]	4.50	4.72
2ð	5.75	4.58	3.89	4.14	4.37	3.97	4.01	4.59	4.78

[a] H-5b. [b] H-5a.

2.4.2 NMR of furanose diacetonides

NMR data for the isopropylidene-protected furanoses are presented in Table 18 (proton shifts), Table 19 (vicinal coupling constants) and Table 20 (^{13}C shifts). For most of the isopropylidene-protected furanoses, such as the benzyl-protected (**2b**) and PNB-protected (**2i**), reference data were available. Sources can be found in the Experimental section. No significant deviations from literature data were found for either of the compounds. Having made a sizeable series of 3-*O*-protected furanoses, some patterns started to emerge. All compounds with benzyl-like ethers had almost the same proton and ^{13}C shifts, as well as coupling constants. Only the benzylic shifts changed significantly between the analogues, which seemed plausible due to the different electronic properties of the aromatic systems.

Substituting one of the benzyl-like ethers with a silyl ether, on the other hand, has a pronounced effect on the sugar ring signals, especially around C-3. The result was

Table 19: Sugar ring proton coupling constants in Hz, in $CDCl_3$, for isopropylidene protected furanosides. UR: unresolved.

	$J_{1,2}$	$J_{2,3}$	$J_{3,4}$	$J_{4,5}$	$J_{5,6b}$	$J_{5,6a}$
2a	3.7	0.0	3.1	7.8	5.8	6.1
2b	3.7	0.0	3.1	7.8	5.7	6.2
2c	3.7	0.0	3.1	7.8	5.8	6.2
2d	3.7	0.0	3.1	7.4	5.4	6.3
2e	3.5	0.0	2.7	8.2	6.0	6.1
2f	3.5	0.0	2.5	8.4	6.0	6.3
2g	3.5	0.0	2.7	8.1	6.2	6.3
2i	3.7	0.0	3.0	8.6	5.5	6.2
2j	3.7	0.0	3.0	8.4	5.3	6.3
2ø	3.8	0.0	3.6	UR	3.8	4.7
2ð	3.9	0.0	8.6	3.2	7.1	8.2

a reduction in chemical shift of H-2, increase in H-3, and reduction in H-4. TBDMS (**2e**) and TIPS (**2g**) deviated somewhat from the TBDPS (**2f**) GLF, which could have been due to electronic or steric effects of the phenyl groups. The opposite pattern was seen for the ^{13}C shifts, with increase at C-2, decrease at C-3 and increase at C-4. Differences in the coupling constants around C-3 were also observed from the silyl ethers relative to the benzyl-like ethers. As coupling constants depend on both conformational factors, as well stereo-electronic factors[109], the difference in coupling constants between benzyl-like ethers and silyl ethers could possibly be attributed to both.

2.4.3 NMR of furanosides

A small array of furanosides was also prepared, and the NMR data are presented in Table 21 (proton shifts), Table 22 (vicinal coupling constants) and Table 23 (^{13}C shifts).

Proton shifts were rather similar for all investigated substitution patterns. The same effects as with other sugars were seen from methyl, allyl, silyl ethers, etc. For the H-1 signals,

Table 20: Sugar ring carbon shifts in $CDCl_3$ for isopropylidene protected furanosides, relative to TMS.

	C-1	C-2	C-3	C-4	C-5	C-6	Benzylic
2a	105.3	82.7	81.7	81.4	72.5	67.4	72.4
2b	105.3	82.8	81.6	81.4	72.5	67.5	72.5
2c	105.3	82.7	81.7	81.4	72.5	67.5	72.1
2d	105.3	82.6	81.9	81.4	72.7	67.2	73.2
2e	105.3	85.6	75.5	82.3	72.2	67.8	-
2f	105.0	84.5	76.5	82.6	72.2	67.9	-
2g	105.1	85.6	76.1	82.5	72.0	67.8	-
2i	105.3	82.6	82.4	81.3	72.3	67.7	71.1
2j	105.4	83.6	81.6	81.7	72.4	67.6	65.1
2ø	105.1	82.5	82.8	80.0	61.0	-	71.9
2ð	103.9	77.8	77.5	78.0	74.8	65.0	72.2

variation within the anomers was large in comparison to the variation between the anomers, making H-1 proton shifts unreliable for anomer determination.

NOESY spectra were employed in an attempt to determine the configuration at C-1 for the furanosides. The spectra provided a somewhat ambiguous answer. Applying the methyl furanoside (**3μ**) as an example, correlation between H-1 and H-2 was observed for both the α-anomer (Figure 20) and the β-anomers (Figure 20). Correlation between H-1 and H-3 was present for one of the anomers, and was not observed for the other, although overlap made an unequivocal determination difficult to make. The correlation between H-1 and H-3 gave a good indication that this was the β-anomer. As an additional example, take the allyl 3-*O*-PPB furanosides (**3c**). Correlation from H-1 to H-2 was observed for both anomers, on the other hand no correlation to H-3 was present. A conclusive determination could not be made due to overlap with the allylic signals, however. The sum of the evidence gathered from the NOESY spectra did give an indication that the anomers with the higher $J_{1,2}$ and lower carbon shift at C-1 were the α-anomer. Meanwhile, the β-anomers were theo-

Table 21: Sugar ring proton shifts in $CDCl_3$ for furanosides, relative to TMS.

	H-1	H-2	H-3	H-4	H-5	H-6b	H-6a
			α-anomers				
3a	5.11	4.29	4.19	4.17	3.93	3.66	3.79
3c	5.12	4.32	4.23	4.19	3.96	3.68	3.81
3μ	4.95	4.28	4.17	4.14	3.94	3.67	3.79
Ref.[a]	5.02						
3f	5.16	4.06	4.48	4.07	3.99	3.72	3.84
			β-anomers				
3a	4.92	4.35	4.17	4.25	4.03	3.70	3.82
3c	4.94	4.40	4.22	4.28	4.07	3.72	3.84
3-μ	4.79	4.31	4.17	4.24	4.02	3.71	3.84
Ref.[a]	4.79						
MC-3	4.95	4.27	3.95	4.38	4.41	4.04	4.07
3f	4.74	4.08	4.43	4.20	4.21	3.79	3.87
3ð	5.01	4.08	4.38	4.11	3.87	3.67	3.71

[a] Reference: methyl 3,5,6-tri-*O*-benzyl-D-glucofuranoside.[104]

Table 22: Sugar ring proton coupling constants in Hz, in $CDCl_3$, for furanosides. UR: unresolved.

	$J_{1,2}$	$J_{2,3}$	$J_{3,4}$	$J_{4,5}$	$J_{5,6b}$	$J_{5,6a}$
			α-anomers			
3a	4.6	UR	6.5	UR	5.8	3.5
3c	4.6	4.1	6.5	7.9	5.6	3.6
3-μ	4.7	4.2	6.5	7.7	5.1	3.5
Ref.[a]	4.5					
3f	4.2	3.9	UR	UR	5.7	UR
			β-anomers			
3a	1.8	2.9	6.6	8.9	5.5	3.3
3c	1.8	3.2	6.6	8.8	5.6	3.2
3μ	<2	2.9	6.6	8.9	5.4	3.4
Ref.[a]	s					
MC-3	1.3	2.1	5.1	5.5	6.2	6.2
3f	2.0	3.8	5.6	8.9	5.6	3.0
3ð	<2	UR	UR	UR	UR	UR

[a] Methyl 3,5,6-tri-*O*-benzyl-D-glucofuranoside.[104]

rised to be the compounds with $J_{1,2} < 2$ Hz and the higher carbon shift at C-1.

Comparing the hypothetical anomeric determination made previously with available reference data, confirmed this hypothesis. Spectroscopic data from Arevalo et al.[110] for the methyl furanosides (**3μ**) confirmed the determination made here. Although literature information on glucofuranosides was scarce, an additional reference compound was included in order to solidify the conclusion made. Reference data for methyl 3,5,6-tri-*O*-benzyl-D-glucofuranoside from Ghorai et al.[104] also confirmed the judgements made previously.

For the coupling constant $J_{1,2}$, as opposed to the proton shift of H-1, determination of anomer appeared to be possible, judging from the gathered data. The α-anomers had $J_{1,2}$

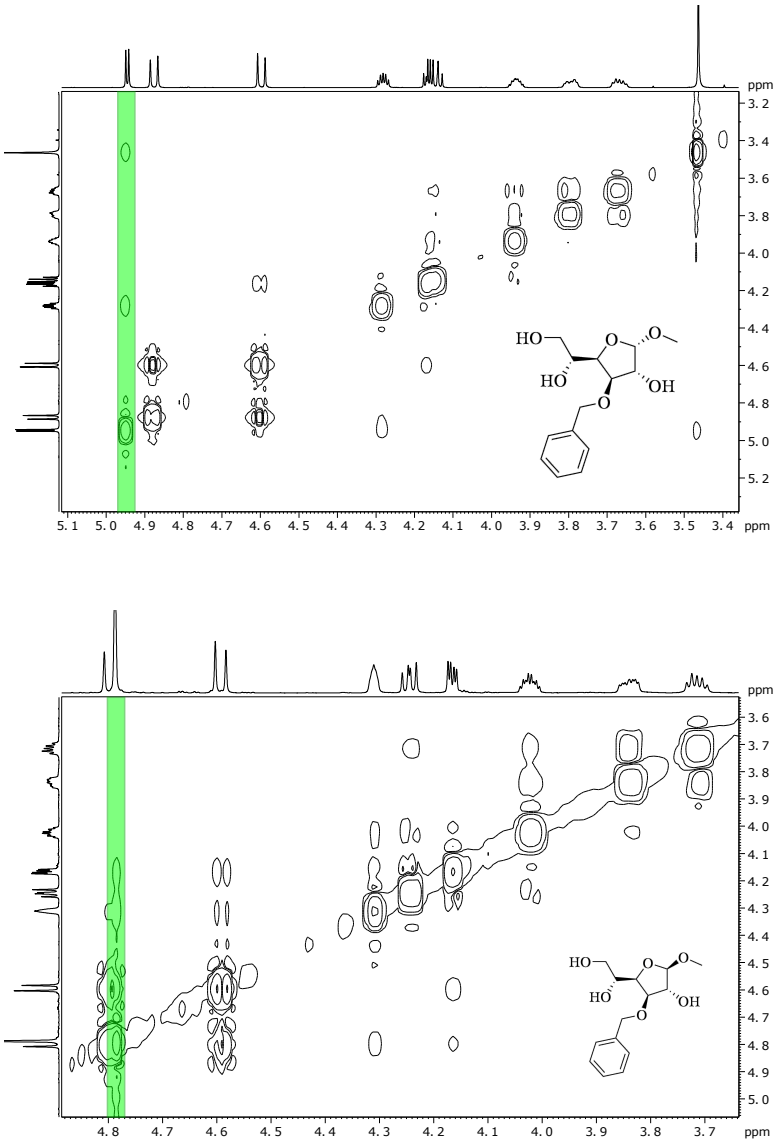

Figure 20: NOESY spectra of the α-anomer (left) and β-anomer (right) of the methyl glucofuranoside (**3μ**).

Table 23: Sugar ring carbon shifts in $CDCl_3$ for furanosides, relative to TMS.

	C-1	C-2	C-3	C-4	C-5	C-6
			α-anomers			
3a	99.9	77.6	84.3	76.9	70.8	64.1
3c	99.9	77.6	84.4	76.9	70.8	64.1
3μ	101.7	77.5	84.3	76.8	70.8	64.1
3f	100.5	79.6	79.0	77.4	69.6	64.5
			β-anomers			
3a	107.5	79.2	84.5	79.3	71.1	64.1
3c	107.4	79.5	84.6	79.3	71.1	64.2
3μ	109.6	79.4	84.4	79.3	71.0	64.2
MC-3	107.6	79.3	83.1	81.9	74.1	66.9
3f	107.3	81.9	80.4	80.3	70.9	64.3
3ð	107.1	73.5	78.2	82.7	72.2	63.3

near 4.6 Hz, while the β-anomers had a very small coupling constant (< 2 Hz). Carbon shifts at C-1 shared the same property, with the α-anomers having a shift near 100 ppm, and the β-anomers just under 110 ppm.

In combination with reference data and NOESY spectra, $J_{1,2}$ and the carbon shift of C-1 were used to identify the configuration at C-1. The compound for which reference data are available (**3μ**)[110] and the reference (Methyl 3,5,6-tri-*O*-benzyl-D-glucofuranoside)[104] were both consistent with each other, as well as the determination made using NOESY.

The available NMR spectra for what was presumed to be **3f-α** was of poor quality. Sample quantities were insufficient for proper ^{13}C and HMBC spectra. Using information already present from the series of furanosides synthesised, the carbon shifts could be hesitantly assigned, and a tentative opinion about its structure was made. Further spectroscopic data are required to make a confident conclusion, however.

2.4.4 NMR of pyranosides

NMR data for various acetylated pyranosides and pyranoses are presented in Table 24 (proton shifts), Table 25 (vicinal coupling constants) and Table 29 (^{13} shifts).

While NMR data for all pyranosides substituted with benzyl-like ethers conformed to a tight standard, the differing electronic properties of the silyl group resulted in significant deviations for all shifts. The silyl-protected pyranosides (**3f**) particularly deviated around C-3, as expected, due to the change in substituent being on C-3.

All NMR data for the pyranosides conformed to expectations, with the exception of $J_{5,6}$ for the TBDPS (**4f**) and PNB (**4i**) pyranosides. An unusually small $J_{5,6b}$ (3.9 Hz) was observed for (**4f-α**) and abnormally large $J_{5,6a}$ (8.8 Hz) for (**4i-α**). The deviations could have been brought forth by conformational changes or stereoelectronic effects, resulting from the 3-*O*-protecting group.

In order to facilitate structure elucidation and assignment of anomeric mixtures, two primary techniques were employed: selective TOCSY (total correlation spectroscopy) and difference spectra. For challenging anomeric separations, sufficient anomeric separation to isolate pure anomers can be impossible to attain. Even if no anomerically pure fraction could be obtained, the first and last fractions were often enriched in one of the anomers. This feature was exploited in order to produce difference spectra, where one anomer was subtracted from the spectrum, affording a spectrum of a pure anomer. Applying said procedure to an anomeric mixture of peracetyl 3-*O*-benzyl glucopyranose (**IC-3**) acquired spectra showed the isolated resonances of both anomers (Figure 21). This process yielded high-resolution spectra showing only the α-anomer (middle, blue) and β-anomer (top, red). Although some noise was present, the resonances of interest were of significantly higher intensity, and all desired information could be extracted. When the circumstances allowed for their production, difference spectra were more desirable than selective TOCSY experiments, due to the higher resolution of the former. The circumstances which allow for producing difference spectra were limited to compounds which

Table 24: Pyranoside proton shifts in ppm, in $CDCl_3$, relative to TMS.

	H-1	H-2	H-3	H-4	H-5	H-6	Benzylic
				α-anomers			
4a	4.92	3.68	3.61	3.56	3.70	3.78, 3.84	4.73, 5.05
4b	4.93	3.73	3.67	3.61	3.70	3.78, 3.84	4.90, 5.21
4c	4.93	3.70	3.65	3.59	3.71	3.80, 3.85	4.78, 5.09
4d	4.93	3.70	3.63	3.56	3.70	3.78, 3.84	4.70, 5.03
4f	4.83	3.58	3.77	3.65	3.50	3.73, 3.75	-
4ı	4.93	3.70	3.63	3.67	3.71	3.80, 3.89	4.90, 5.16
4μ	4.76	3.68	3.59	3.55	3.64	3.79, 3.90	4.73, 5.03
				β-anomers			
4a	4.36	3.54	3.42	3.59	3.35	3.77, 3.87	4.76, 5.00
4b	4.37	3.58	3.48	3.63	3.63	3.78, 3.88	4.93, 5.17
4c	4.39	3.57	3.46	3.64	3.39	3.82, 3.91	4.80, 5.07
4d	4.38	3.58	3.43	3.58	3.38	3.78, 3.90	4.71, 5.01
4f	4.22	3.50	3.59	3.65	3.20	3.73, 3.83	-
4ı	4.38	3.56	3.47	3.68	3.40	3.74, 3.92	4.90, 5.14
4μ	4.24	3.50	3.42	3.60	3.38	3.79, 3.91	3.76, 5.01
4ð	4.76	3.56	4.12	3.62	3.67	3.75, 3.87	4.69, 5.07

Table 25: Pyranoside coupling constants in Hz, in $CDCl_3$, relative to TMS.

	$J_{1,2}$	$J_{2,3}$	$J_{3,4}$	$J_{4,5}$	$J_{5,6b}$	$J_{5,6a}$
			α-anomers			
4a	3.9	9.3	8.9	9.2	4.7	3.7
4b	3.8	9.3	9.0	9.2	4.7	3.9
4c	3.9	9.3	9.1	9.4	4.6	3.6
4d	3.8	9.4	9.1	9.2	4.7	3.9
4f	3.9	9.5	9.2	9.4	3.9	3.9
4ι	3.8	9.5	8.8	8.9	4.2	8.8
4μ	3.9	9.0	8.9	9.2	4.7	3.7
			β-anomers			
4a	7.8	9.1	9.2	9.4	4.9	3.6
4b	7.7	9.1	9.1	9.4	5.0	3.6
4c	7.7	8.9	9.1	9.3	5.4	3.8
4d	7.8	8.7	8.9	9.2	4.9	3.7
4f	7.7	8.3	8.5	8.9	4.8	3.5
4ι	7.9	9.1	9.3	9.6	4.7	3.8
4μ	7.7	9.1	9.1	9.4	5.0	3.9
4ð	7.8	3.0	3.1	9.6	5.0	3.3

Table 26: Pyranoside carbon shifts in ppm, in $CDCl_3$, relative to TMS.

	C-1	C-2	C-3	C-4	C-5	C-6
			α-anomers			
4a	97.7	72.9	82.9	70.3	71.1	62.5
4b	97.7	73.0	82.9	70.3	71.1	62.6
4c	97.7	73.0	83.0	70.3	71.2	62.6
4d	97.8	72.9	82.9	70.3	71.2	62.6
4f	97.7	72.6	77.2	71.6	71.0	62.4
4ι	97.6	72.9	83.5	70.3	71.0	62.4
4μ	99.6	73.0	82.8	70.3	70.9	62.6
			β-anomers			
4a	102.0	74.5	83.7	70.1	75.2	62.5
4b	102.0	74.6	83.5	70.3	75.2	62.6
4c	102.0	74.6	83.7	70.3	75.2	62.7
4d	102.0	74.5	84.0	70.3	75.3	62.8
4f	101.8	74.3	79.1	71.6	74.7	62.5
4ι	101.9	74.6	84.0	70.4	75.1	62.6
4μ	104.0	74.6	83.6	70.3	75.2	62.7
4ð	100.0	72.7	78.2	68.0	74.9	62.9

were partially separated, however. In addition, it can be challenging to record multiple spectra such that resonances exhibit exactly the same chemical shift and shape, as that would require identical experimental conditions for each run.

In cases where no fractions with significantly differing anomer compositions could be obtained, such as when the products were precipitated, selective TOCSY was employed. Selective TOCSY is an NMR experiment when one or more resonances are irradiated. This produces a spectrum with only resonances from the same spin system as the irradiated resonance(s). By employing selective TOCSY to an anomeric mixture, the carbohydrate backbone of either anomer can be irradiated, resulting in a spectrum of a pure anomer. Two selective TOCSY spectra, along with a standard proton spectrum is shown in Figure 22. Irradiating the hydroxyl in 2-position (2.19 ppm) produced the best result for the α-anomer (red, on top). All carbohydrate backbone resonances except for H-6 of the α-anomer were induced. In order to highlight the β-anomer, H-5 of the β-anomer (3.39 ppm) was irradiated (blue, in middle). Accordingly, all carbohydrate backbone resonances from the β-anomer are induced. As a result, resonances from both anomers could be identified, despite overlap between the anomers.

In practice, however, less than ideal spectra were produced, with artefacts prevalent and spectra of low resolution. All resonances in a spin system were not necessarily induced in the selective TOCSY spectrum.

2.4.5 NMR of miscellaneous pyranoids

In addition to acting as a protecting strategy, acetylation conferred a number of advantages to the work-up and analytic effort (see Section 1.5.3), such as modifying the chemical shifts of the sugar ring protons. The change in chemical shift could be observed for **4a-β** (Figure 23). The shifts of the sugar ring protons for the acetylated groups were shifted upfield, relative to when underivatised, which was apparent for H-2 and H-4, changing from approximately 3.6 ppm, up to near 5.1 ppm. Acetylation could prove useful in assisting

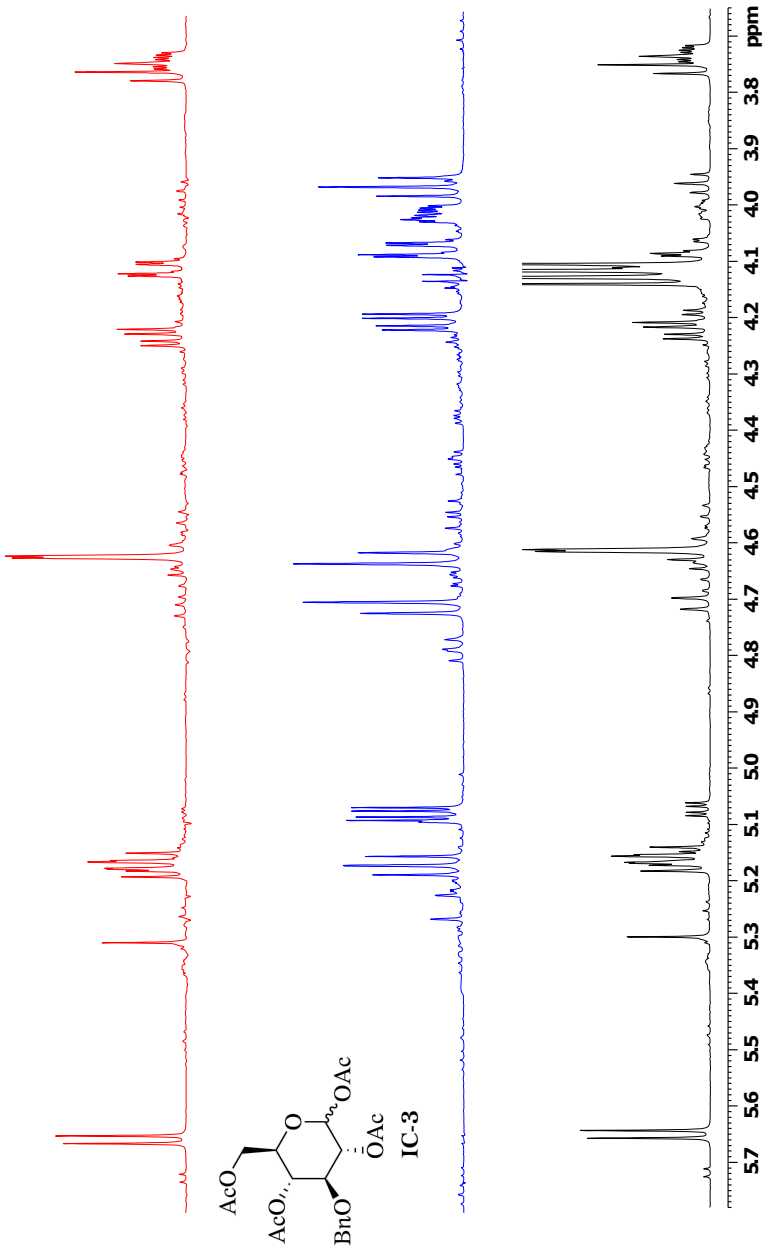

Figure 21: Unmodified spectrum containing anomeric mixture of **IC-3** (bottom, black) and difference spectra showing only the β-anomer (top, red) and α-anomer (middle, blue).

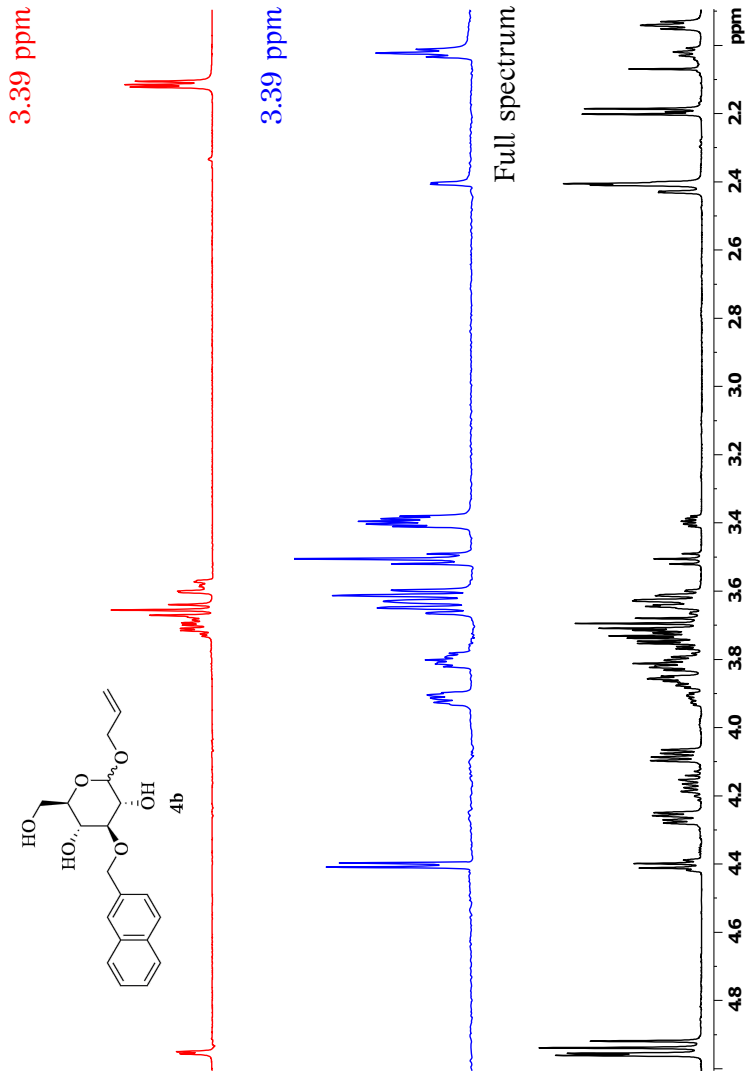

Figure 22: Selective TOCSY (α-anomer on top and β-anomer in middle) and standard ^{1}H spectrum (bottom, black) of an anomeric mixture of **4b**. The frequencies in the corners are the irradiated frequencies. Keep in mind that the positions of the bydroxyl protons are not constant.

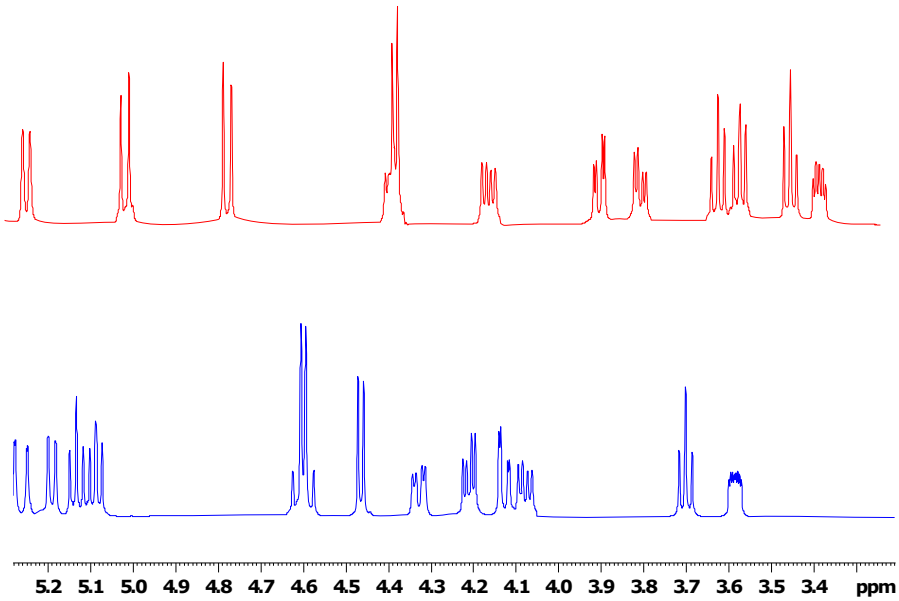

Figure 23: Comparison of acetylated (bottom) and unacetylated (top) allyl 3-*O*-benzyl-β-D-glucopyranoside.

structure elucidation of compounds, where overlap of NMR resonances pose a problem, such as with the xylopyranoside in Figure 290, in Appendix B.

Glycosylation of (**IC-5**) with glycerol acetonide was carried out (Scheme 55, but proper isolation of **LCM** proved more difficult than previously predicted, and was not completed due to time constraints. Indicators to the presence of **LCM** were found in the available NMR data. This included indications of an H-1 in β-configuration with an ether linked aglycone, glycerol moiety and an isopropylidene group. Further work was required in order to either confirm or disprove the results, however.

NMR data for various acetylated pyranosides and pyranoses are presented in Table 21 (proton shifts), Table 28 (vicinal coupling constants) and Table 29 (^{13}C shifts). Comparing **2a** to **8a**, indicated that by protecting hydroxyls with acetyl groups, the proton shift were increased by usually 0.5-

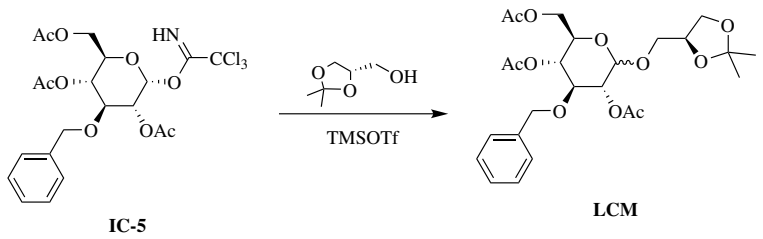

Scheme 55: Glycosylation with glycerol acetonide.

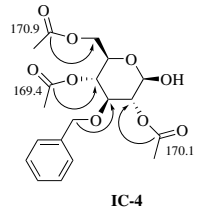

Figure 24: Coupling observed in HMBC of (**IC-4**). ^{13}C shifts of the acetyl groups are included.

1.0 ppm.

IC-4 was not described in the literature, but it was clear from the NMR spectrum that the anomeric acetyl group from **IC-3** had been removed. The key observations were the decreased shift for H-1, and the long-range coupling present in HMBC (Figure 24. Comparing **IC-4** to a similar compound (**R-1**, 2,3,4,6-tetra-*O*-acetyl-D-glucopyranose), for which spectroscopic data were available, showed a tight similarity. The only significant difference lied in the signals from around C-3, where, expectedly, higher shifts were observed for **R-1**, which has an acetyl group in 3-*O*-position.

There were no available literature spectroscopic data for **IC-5** either, but a comparison with **R-2** (*O*-(2,3,4,6-tetra-*O*-acetyl-α-D-glucopyranosyl)trichloroacetimidate) could be made. In both cases, a very high H-1 shift was observed (6.53 ppm), even higher than when an anomeric acetyl group was present (**IC-3**). Other NMR data were also consistent, only differing in the shifts around the 3-*O*-protecting group, as expected. A byproduct with the trichloroacetimidate in 4-*O*-position instead of the anomeric position was also isolated. It was

Table 27: Sugar ring proton shifts in $CDCl_3$ for various pyranoses and pyranosides, relative to TMS.

	H-1	H-2	H-3	H-4	H-5	H-6b	H-6a
				α-anomers			
2a	4.92	3.68	3.61	3.56	3.7	3.78	3.84
8a	5.11	4.88	4.01	5.09	3.94	4.07	4.2
8b	5.12	4.92	4.07	5.13	3.94	4.07	4.21
8μ	4.95	4.88	3.98	5.08	3.88	4.08	4.2
IC-3	6.32	5.07	3.96	5.16	4.01	4.07	4.2
IC-4	5.45	4.87	4.04	5.1	4.15	4.11	4.17
R-1[a]	5.44	4.88	5.44	5.08	4.24	4.14	4.21
IC-5	6.53	5.09	4.08	5.2	4.1	4.11	4.21
R-2[b]	6.56	5.13	5.57	5.18	4.22	4.13	4.28
				β-anomers			
2a	4.36	3.54	3.42	3.59	3.35	3.77	3.87
8a	4.46	5.09	3.70	5.13	3.58	4.13	4.21
8b	4.47	5.12	3.75	5.17	3.59	4.13	4.21
8μ	4.35	5.05	3.70	5.13	3.60	4.13	4.22
IC-3	5.65	5.17	3.75	5.16	3.73	4.10	4.22
IC-4	4.62	4.88	3.73	5.10	3.63	4.14	4.20
R-1[a]	4.73	4.88	5.23	5.08	3.76	4.14	4.21

[a] 2,3,4,6-Tetra-*O*-acetyl-D-glucopyranose[111] [b] *O*-(2,3,4,6-Tetra-*O*-acetyl-α-D-glucopyranosyl)trichloroacetimidate[111]

Table 28: Coupling constants in Hz for various pyranoses and pyranosides, relative to TMS in $CDCl_3$. UR unresolved.

	$J_{1,2}$	$J_{2,3}$	$J_{3,4}$	$J_{4,5}$	$J_{5,6b}$	$J_{5,6a}$
			α-anomers			
2a	3.9	9.3	8.9	9.2	3.7	4.7
8a	3.6	10.0	9.6	10.0	2.4	4.9
8b	3.7	9.8	10.0	10.1	2.4	4.8
8μ	3.7	9.8	9.5	10.1	2.4	5.0
IC-3	3.6	10.0	9.7	10.1	2.4	4.5
IC-4	3.6	9.8	9.6	9.8	10.0	4.5
R-1[a]	3.5	9.9	UR	UR	UR	UR
IC-5	3.5	10.0	9.8	9.9	2.3	4.8
R-2[b]	3.7	9.9	9.6	10.2	1.9	4.1
			β-anomers			
2a	7.8	9.1	9.2	9.4	4.9	3.6
8a	7.9	9.4	9.4	9.7	2.6	5.1
8b	7.9	9.4	9.5	10	2.6	5.1
8μ	7.9	9.2	9.4	9.9	2.5	5
IC-3	8.2	9.2	9.5	9.8	2.3	4.9
IC-4	8.2	9.2	9.5	9.8	2.2	5.2
R-1[a]	8.1	UR	9.6	UR	UR	UR

[a] 2,3,4,6-Tetra-*O*-acetyl-D-glucopyranose[111] [b] *O*-(2,3,4,6-Tetra-*O*-acetyl-α-D-glucopyranosyl)trichloroacetimidate[111]

clearly discernible from the anomeric trichloroacetimidate by HMBC, but also by having a very high H-4 shift (5.5 ppm).

2.4.6 4,6-*O*-acetals

Because of the propensity of the anthracene group (to some extent documented in this work, and in other literature[74, 112]) to take part in side reactions, special care was taken to make sure no side-reactions had occurred after introducing the 4,6-*O*-anthracenemethyl group. The propensity of the anthracene group to take part in side reactions, coupled with the unusually low proton shifts observed for the apparent phenyl group (approx. 7.0-7.1 ppm), led to the decision to confirm the structure of the 4,6-*O*-anthracene acetal protected compound (**9j**) in a conscientious manner.

The number of aromatic carbon atoms, stemming both from the anthracene and phenyl group, made it difficult to differentiate the two aromatic systems (Figure 26, top). In order to associate proton and carbon shifts, a selective HSQC experiment was executed on the aromatic region (Figure 25), as a regular HSQC experiment with reduced spectral width would produce an unusable spectrum due to folding.[113] A good improvement over the regular HSQC experiment was achieved. Now, the carbon shifts near 124.9 ppm and 128.1 ppm were unambiguously discernible. A selective HMBC experiment was also run (Figure 26). This experiment gave a radically better resolution on the carbon axis, allowing for accurate determination of coupling.

In order to assign all proton and carbon shifts, a combination of proton, COSY, selective HSQC and selective HMBC experiments were used. The results are presented in Figure 27. A conclusive determination was made as to the placement of the anthracenemethyl acetal and benzyl group, and it was determined that both aromatic systems were intact. One question remains: why are the benzyl proton shifts so unusually high? A notably high acetal proton shift at 6.91 ppm was observed. It was hypothesised that the low benzyl protons shifts could be the result of shielding from the anthracene group. An energy-minimised model of **9j**

Table 29: Carbon shifts in ppm for various pyranoses and pyranosides, relative to TMS in $CDCl_3$.

	C-1	C-2	C-3	C-4	C-5	C-6
			α-anomers			
2a	97.7	72.9	82.9	70.3	71.1	62.5
8a	95.1	73.3	77.4	69.8	67.8	62.2
8b	95.1	73.3	77.5	69.8	67.8	62.2
8μ	97.0	73.3	77.4	69.8	67.6	62.2
IC-3	89.5	71.5	77.0	69.1	70.3	61.8
IC-4	90.4	73.4	76.9	69.8	67.8	62.3
R-1[a]	90.1	71.1	69.9	68.5	67.1	61.9
IC-5	93.4	72.1	76.9	68.9	70.6	61.7
R-2[b]	92.9	69.7	69.8	67.8	70.0	61.3
			β-anomers			
2a	102.0	74.5	83.7	70.1	75.2	62.5
8a	99.8	72.5	80.1	69.6	72.1	62.3
8b	99.8	72.5	80.0	69.7	72.1	62.3
8μ	101.8	72.4	80.1	69.6	72.1	62.3
IC-3	92.0	71.6	80.0	69.1	73.0	61.8
IC-4	95.9	75.5	79.6	69.6	72.3	62.3
R-1[a]	90.1	72.0	69.9	68.4	72.2	61.9

[a] 2,3,4,6-Tetra-*O*-acetyl-D-glucopyranose[111] [b] *O*-(2,3,4,6-Tetra-*O*-acetyl-α-D-glucopyranosyl)trichloroacetimidate[111]

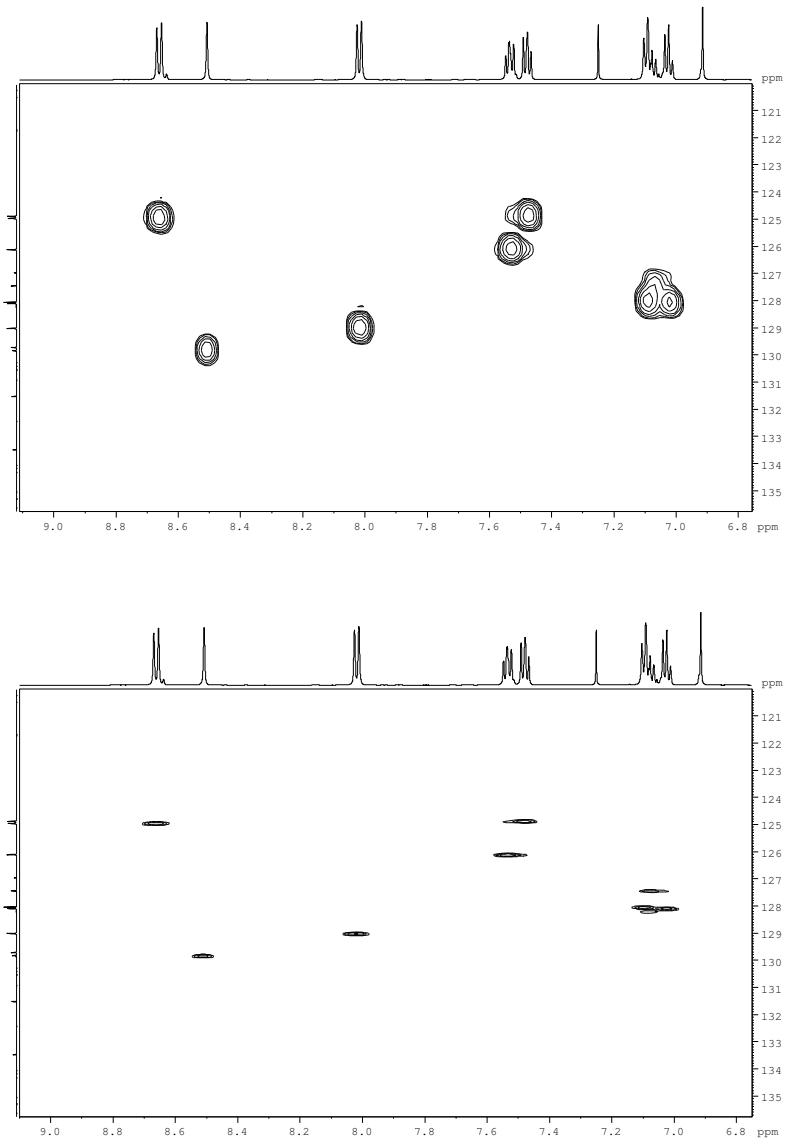

Figure 25: Comparison of HSQC (top) vs. selective HSQC (bottom) of Allyl 3-*O*-benzyl-4,6-*O*-(9'-anthracenyl)methylene-α-D-glucopyranoside (**9j**). Expansions on the F_1 axis are the same.

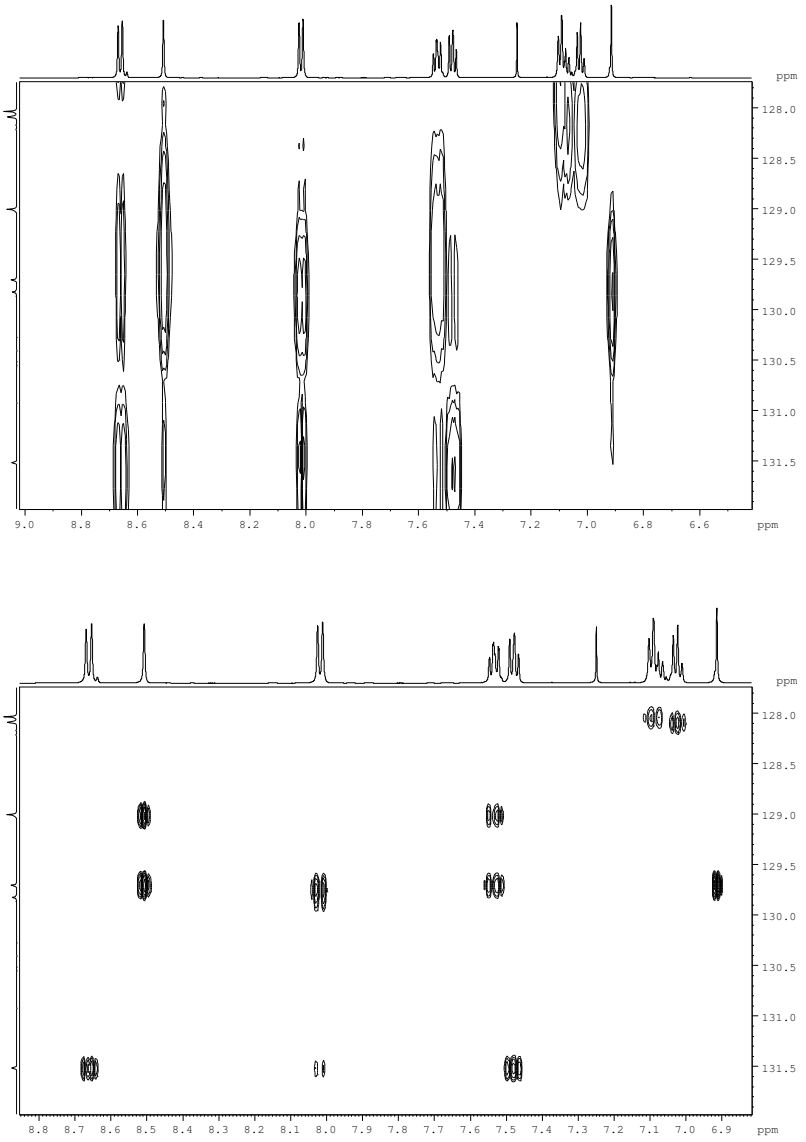

Figure 26: Comparison of HMBC (top) vs. selective HMBC (bottom) of Allyl 3-*O*-benzyl-4,6-*O*-(9'-anthracenyl)methylene-α-D-glucopyranoside (**9j**). Expansions on the F_1 axis are the same.

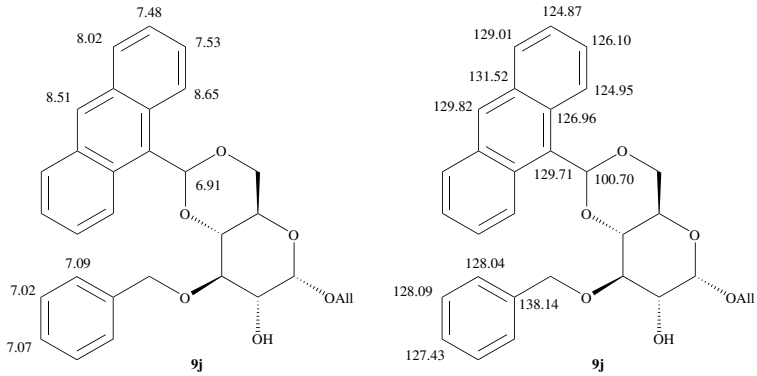

Figure 27: Assignment of proton (left) and carbon (shifts) of allyl 3-*O*-benzyl-4,6-*O*-(9'-anthracenyl)methylene-α-D-glucopyranoside (**9j**) in ppm in $CDCl_3$.

was made in "Chem3D" (Figure 28). The model did not entirely support the hypothesis that the benzyl were highly shielded by the anthracene aromatic system. In the energy-minimised model, the phenyl group was fairly distant from the anthracene group (over 6 Å), and the geometry of the shielding zone did not appear to fit either.[114] Regardless, the models from "Chem3D" might not necessarily have been all that accurate, so caution was applied before drawing any conclusions.

NMR data for allyl 3-*O*-benzyl-4,6-*O*-acetal-pyranosides and **4a** for reference are presented in Table 30 (proton shifts), Table 31 (vicinal coupling constants) and Table 32 (^{13}C shifts).

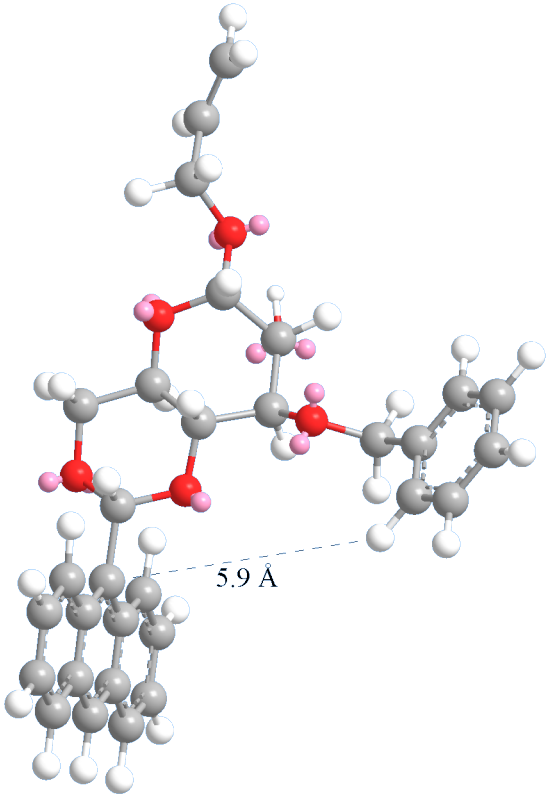

Figure 28: Energy-minimised model of allyl 3-*O*-benzyl-4,6-*O*-(9'-anthracenyl)methylene-α-D-glucopyranoside (**9j**) made in "Chem3D". Grey is carbon, white is hydrogen and red are oxygen.

Table 30: Proton shifts in ppm, for 4,6-*O*-acetal protected pyranosides, in $CDCl_3$. **4a** for reference.

	H-1	H-2	H-3	H-4	H-5	H-6b	H-6a	Bn-b	Bn-a	Ar-CH	3-*O*-Bn-H
						α-anomers					
9i	5.00	3.75	3.84	3.65	3.88	3.76	4.31	4.85	4.91	5.61	7.30-7.38
9j	5.04	3.81	3.93	3.87	4.24	3.95	4.45	4.61	4.69	6.91	7.00-7.12
9a[a]	4.96	3.73	3.85	3.64	3.88	3.74	4.28	4.80	4.96	5.57	-
4a	4.92	3.68	3.61	3.56	3.7	3.78	3.84	4.73	5.05	-	7.29-7.40
						β-anomers					
9i	4.46	3.62	3.67	3.71	3.44	3.81	4.37	4.84	4.92	5.61	7.27-7.39
9j	4.59	3.66	3.76	3.93	3.84	4.01	4.52	4.60	4.69	6.92	7.02-7.12
9a[a]	4.46	-	-	-	-	-	-	4.80	4.96	-	-
4a	4.36	3.54	3.42	3.59	3.35	3.77	3.87	4.76	5.00	-	7.29-7.40

[a] Reference value from Peer et al.[107]

Table 31: Coupling constants in Hz, for 4,6-*O*-acetal protected pyranosides, in $CDCl_3$. **4a** for reference.

	$J_{1,2}$	$J_{2,3}$	$J_{3,4}$	$J_{4,5}$	$J_{5,6b}$	$J_{5,6a}$
			α-anomers			
9i	3.9	8.9	9.2	9.3	10.4	4.9
9j	3.9	8.5	9.2	9.5	10.1	5.0
9a[a]	3.7	9.3	9.3	9.5	10.3	4.9
4a	3.9	9.3	8.9	9.2	3.7	4.7
			β-anomers			
9i	7.7	8.5	8.9	9.1	10.2	5.0
9j	7.7	8.9	9.1	9.3	10.4	4.9
4a	7.8	9.1	9.2	9.4	4.9	3.6

[a] Reference value from Peer et al.[107]

Table 32: Carbon shifts in ppm, relative to TMS, in $CDCl_3$, for 4,6-*O*-acetal protected pyranosides. **4a** for reference.

	C-1	C-2	C-3	C-4	C-5	C-6	Benzylic
				α-anomers			
9i	98.1	72.6	79.1	81.9	62.6	69.1	75.0
9j	98.1	72.4	78.5	83.3	63.0	70.1	74.5
4a	97.7	72.9	82.9	70.3	71.1	62.5	74.7
				β-anomers			
9i	102.3	74.5	80.2	81.3	66.2	68.8	74.7
9j	102.3	74.2	79.5	82.8	66.7	69.8	74.2
4a	102.0	74.5	83.7	70.1	75.2	62.5	75.0

2.4.7 Infrared spectroscopy

IR spectra of synthesised compounds are presented in Appendix B.

For the series of 3-*O*-protected isopropylidene glucofuranoses, IR spectra were, as predicted, very comparable. The substantial differences were attributed to the protecting groups. Stronger aliphatic vibrations, stemming from the plentiful methyl groups, were detected for the DTB compound (**2d**) (Figure 56). The nitro group gave some distinct peaks near 1520 cm^{-1} and 1345 cm^{-1} (Figure 84) and some fairly strong Si-O peaks could be observed at around 800 cm^{-1}.

The pattern described previously applied equally for the other series of analogues, such as the allyl 3-*O* protected furanosides and pyranosides. Some allyl 3-*O* protected pyranosides had spectra of poorer quality (e.g. Figure 274), which was due to the spectra being recorded from solid material, rather than thin film spectra. As expected, strong signals from the carbonyl in the acetylated compounds were present in the IR spectra (e.g. compare Figure 219 to 309).

Few unexpected signals were present in the IR spectra. A medium intentity peak was found at 1738-1740 cm^{-1} in the IR spectrum for 3-*O*-(*t*-Bu-diphenylsilyl)-1,2-*O*-isopropylidene-α-D-glucofuranose (**MC-4**) (Figure 212), allyl 3-*O*-(*t*-Bu-diphenylsilyl)-β-D-glucofuranoside (**3f-β**) (Figure 148), and allyl 3-*O*-(*t*-Bu-diphenylsilyl)-β-D-glucopyranoside (**4f-β**) (Figure 267). The peak was consistent with the carbonyl peak in ethyl acetate. A peak at 1430 cm^{-1} was also present, and was consistent with the acetyl C-H bend in ethyl acetate.[115]

2.4.8 Mass spectroscopy

Mass spectra are presented in Appendix B. Results from MS were generally in accordance with the expected molecular formula. For both dimethyl acetals (anthracene (Figure 402) and *p*-nitrophenyl (Figure 409)), the main peak was M-OMe, or the sodium adduct of said peak. Loss of methoxy groups from acetals is known to occur in MS.[116] Some expected fragments were observed, such as with the DTB protected

glucofuranose (**2d**), where a peak at m/z 203.18, corresponding with the (3,5-di-*t*-butyl)benzyl group, was observed.

3 Conclusion and further work

The issue of anomeric resolution in the total synthesis of **CDA** was solved through derivatisation. Both global acetylation and aromatic 4,6-*O*-acetals proved viable for separation by column chromatography, where the acetyl groups excels in their ease of preparation and the 4,6-*O*-acetals give the better separation.

Several alternatives to the benzyl group for the total synthesis project have been found. The benzyl-like ethers 2-naphthyl (NAP) and *p*-phenylbenzyl (PPB) appears to be compatible with other steps in the total synthesis. The new protecting groups allow for alternative methods of cleavage by oxidation, should catalytic hydrogenation prove problematic. PPB ethers also impart higher crystallinity than benzyl ethers, aiding purification.

An in-depth study of the mechanics of the rearrangement-glycosylation reaction of 1,2;5,6-di-*O*-isopropylidene-3-*O*-protected glucofuranoses shows the kinetic favourisation of furanosides. Significant differences between the two solvents, methanol and allyl alcohol, were discovered. An unusual, absolute selectivity for the β-anomer was discovered for allyl 3-*O*-benzyl-D-glucofuranoside. The properties of said compound could not be explained by any observations from the spectroscopic data. Other tools for conformation determination, such as X-ray crystallography could be useful if crystalline samples can be obtained.

Multiple promising methods for producing furanosides were investigated, but product isolation remains problematic, due to the large quantity of regioisomers and diastereomers present. Further optimisation of $FeCl_3$ as a promotor could result in sufficient selectivity for furanosides to make product isolation viable. Other chromatographic tools, such as ion exchange chromatography, could also be investigated.

Schmidt glycosylation of isopropylidene-protected glycerol

appears to be a viable method for introducing an enantiomerically pure glycerol aglycone for the synthesis of **CDA**. Anchimeric assistance from the 2-*O*-acetyl group could necessitate substitution with a different protecting group, such as a silyl group.

4 Experimental

4.1 General materials and methods

All chemicals were purchased from commercial vendors and used without further purification. Anhydrous solvents were collected from a *Braun* "MB SPS-800 Solvent Purification System". Solvent evaporation was performed with a rotary evaporator in a water bath at 40 or 50°C, or with a *BioChromato* "Smart Evaporator" at 50°C, using N_2-flow. Reactions were carried out in oven-dried glassware (80°C), with PTFE coated magnetic stir bars.

4.1.1 Thin-layer chromatography (TLC)

Unless otherwise stated, Silica gel on aluminium (60 Å, F_{254}, *Merck*), were used for TLC. Visualisation of aromatic compounds was achieved by UV (254 nm), whereas non-aromatic compounds were visualised by $KMnO_4$ staining.

4.1.2 High-performance liquid chromatography (HPLC)

Analytical HPLC analysis was performed using an *Agilent Technology* "1290 Infinity" instrument with a G4220B binary pump, G4226A autosampler, G1316A column compartment and G1315D diode array detector (DAD). Unless otherwise stated, a *Agilent* "Zorbax Bonus-RP", 250 x 4.6 mm, 5 µm column was used, with a *Agilent* "Zorbax Bonus-RP", 12.5 x 4.6 mm, 5 µm guard column.

For preparative HPLC, *Agilent Technology* "G1361A 1260" pump, "G2260A 1260" autosampler, "G1364B 1260" fraction collector, "G1315D 1260 Infinity" DAD VL and an *Agilent* "Zorbax Eclipse XDB-C18" 150 x 21.2 mm, 5 µm column, were used.

Agilent Technologies ChemStation for LC and CE systems (version: B.04.03 SP1[87]) software was used for automation and processing. Solvents were analytical (HPLC) grade, and the water *Milli-Q* purified. A flow of 1 mL/min for analytical and 30 mL/min for preparative and a column temperature of 25°C was used for both methods.

Method *X*: Acetonitrile:water linear gradient, starting at acetonitrile:water (20:80), and ending at pure acetonitrile at 40 min, followed by pure acetonitrile for 5 min.

Method *XX*: Isocratic elution with methanol:water (20:80) for 35 min, followed by pure methanol for 8 min.

Method *XXX*: Gradient from acetonitile:water (50:50) to pure acetonitrile over 20 min.

4.1.3 Flash chromatography

Flash chromatography was performed using silica gel (40-63 µm, 60 Å, *Merck*) or *Supelco* "VersaPak" SiO_2 and C18 cartridges. A *SciLog* "ACCU Variable Speed Metering Pump" for VersaFlash cartridges. For aromatic compounds, detection was carried out using a *Knauer* "Smartline 200", 254 nm UV detector.

4.1.4 IR spectroscopy

IR spectra were recorded as a thin film, using a *Bruker* "Alpha FTIR ECO-ATR" spectrometer with OPUS software.

4.1.5 Melting point analysis

Melting points were recorded using a *Stuart* SMP40 automatic melting point recorder.

4.1.6 MS spectroscopy

Accurate mass determination in positive and negative mode was performed on a "Synapt G2-S" Q-TOF instrument from *Waters*. Samples were ionized by the use of an ASAP probe (APCI) or ESI probe. No chromatographic separation was used previous to the mass analysis. Calculated exact mass and spectra processing was done by *Waters Software* "Masslynx V4.1 SCN871".

4.1.7 NMR spectroscopy

NMR spectra were recorded using a *Bruker* 600 MHz "Avance III" with a 5 mm cryogenic CP-TCI Z-gradient probe, operating at 600 MHz for ^{1}H-NMR and 150 MHz for ^{13}C-NMR or *Bruker* 400 MHz "Avance III HD" with a 5 mm SmartProbe Z-gradient probe. In all $CDCl_3$ spectra, chemical shifts are expressed as δ (ppm), relative to TMS, and coupling constants (*J*) are in Hertz. All spectra were processed using *Bruker* TopSpin 3.5pl7.

4.1.8 Optical rotation

Optical rotation was recorded using an *Anton Paar* "MCP 5100" polarimeter, with a 2.5 mm stainless steel sample holder, using the sodium D-line (589 nm), at 20°C.

4.2 Preparation of protecting groups

Procedures for preparing ether and acetal protecting groups employed in the carbohydrate syntheses are described below.

4.2.1 9-(Chloromethyl)anthracene (RC-1)

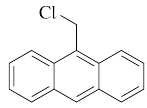

RC-1

To a suspension of 9-anthraldehyde (1.0 g, 5.0 mmol) in ethanol (40 mL), was added $NaBH_4$ (0.38 g, 10 mmol, 2 equiv) at 0°C and stirred at room temperature for 4 h. The solvent was evaporated under reduced pressure. The resulting solids were added DCM, extracted three times with brine, and dried over $MgSO_4$, prior to removal of the solvent under reduced pressure to give a yellow powder. To a solution of thionyl chloride (1.5 mL, 20 mmol, 4 equiv) in DCM (15 mL), the yellow solids were added. The reaction was stirred at room temperature for 2 h. Water was added, the layers separated and solvent evaporated under reduced pressure. Purification by flash chromatography (SiO_2, 19:1 *n*-pentane:EtOAc) gave **RC-1** as a yellow powder (0.75 g, 3.3 mmol, 66%),

mp. 135-140°C; HRMS (ASAP+) *m/z*: [M] calcd. 226.0549 for $C_{15}H_{11}Cl$, found 226.0552; IR (cm^{-1}): 3052, 1446, 1245, 884, 790, 732, 600, 511; ^{1}H-NMR (400 MHz, $CDCl_3$): 5.66 (*s*, 2H, CH_2), 7.54 (*m*, 2H, *J* = 8.2, 6.5, Ar-H) 7.65 (*m*, 2H, *J* = 8.8, 6.6, Ar-H) 8.07 (*m*, 2H, *J* = 8.4, Ar-H) 8.35 (*m*, 2H, *J* = 8.9, Ar-H) 8.53 (*s*(br), Ar-H); ^{13}C-NMR (100 MHz, $CDCl_3$): 39.00 (CH_2), 123.43, 125.25, 126.94 (Ar), 127.71 (Ar-q), 129.28, 129.32 (Ar), 130.00, 131.48 (Ar-q). NMR data matches previously reported data.[117]

4.2.2 *p*-Nitrobenzaldehyde dimethyl acetal (RC-2)

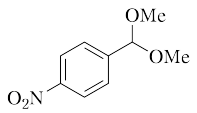

RC-2

To a solution of *p*-nitrobenzaldehyde (10 g, 67 mmol) in methanol (88 mL), was added *p*-toluenesulfonic acid (0.38 g, 2.0 mmol, 0.03 equiv) and trimethyl orthoformate (15 mL, 0.13 mol, 2 equiv). The mixture was stirred at room temperature for 2 h, before quenching with TEA and removing the solvent. The residue was added water and extracted three times with DCM, dried over $MgSO_4$ and solvent evaporated under reduced pressure, to give **RC-2** as an orange liquid (11 g, 54 mmol, 82%),

HRMS (ESI+) *m/z*: [M-OCH_3] calcd. for $C_8H_8NO_3$ 166.0504, found 166.0502; IR (cm^{-1}): 2938, 2832, 1521, 1342, 1205, 1100, 1056, 988, 854, 831, 746, 713; ^{1}H-NMR (400 MHz, $CDCl_3$): 3.36 (*s*, 6H, OCH_3), 5.50 (*s*, 1H, C<u>H</u>$(OMe)_2$), 7.66 (*m*, 2H, Ar-H), 8.25 (*m*, 2H, Ar-H); ^{13}C-NMR (100 MHz, $CDCl_3$): 52.72 (Me), 101.57 ($C(OMe)_2$), 123.45, 128.09 (Ar), 145.08, 148.02 (Ar-q). NMR data is consistent with previously reported data.[118]

4.2.3 9-Anthraldehyde dimethyl acetal (RC-3)

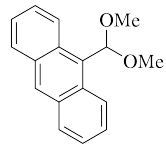

RC-3

Amberlyst-15 (0.63 g, 0.1 equiv) and trimethyl orthoformate (6.4 mL, 58 mmol, 2 equiv) was added to a suspension of 9-anthraldehyde (6.0 g, 29 mmol) in methanol (50 mL). After stirring at reflux for 6 h, DCM was added and the catalyst

was removed by filtration. The solvent was evaporated under reduced pressure and recrystallised from methanol, giving **RC-3** as yellow crystals (5.4 g, 21 mmol, 73%),

HRMS (ASAP+) *m/z*: [M-CH_3] calcd. for $C_{16}H_{13}O_2$ 237.0916, found 237.0912; IR (cm^{-1}): 2990, 2932, 2817, 1675, 1448, 1185, 1103, 1062, 969, 891, 738, 632, 552, 433; ^{1}H-NMR (400 MHz, $CDCl_3$): 3.54 (*s*, 6H, Me), 6.56 (*s*, 1H, C<u>H</u>$(OMe)_2$), 7.48 (*m*, 4H, Ar-H), 8.00 (*m*, 2H, *J* = 8.2, Ar-H), 8.47 (*s*, Ar-H), 8.70 (d, 2H, *J* = 8.3, Ar-H); ^{13}C-NMR (100 MHz, $CDCl_3$): 55.98 (OMe), 104.13 (<u>C</u>$(OMe)_2$), 124.87, 124.89, 126.02 (Ar), 128.73 (Ar-q), 129.03, 129.24 (Ar), 129.90, 131.46 (Ar-q). NMR matches previously reported data.[119]

4.3 Synthesis of 3-*O*-protected monosaccharides

4.3.1 General procedure for introducing benzyl-like ethers

NaH (60%, 3 equiv) was added to a solution of the furanoside compound in dry acetonitrile at 0°C. The mixture was stirred for 30 min while being allowed to reach room tempterature. The alkyl halide was added, and the mixture was stirred until either full conversion of the substrate monosaccharide or consumption of all alkyl halide was achieved, detected by TLC or NMR. Methanol was added in excess to quench the reaction, followed by evaporation of solvents under reduced pressure. The residue was added DCM, extracted twice times with water, the combined water phases were subsequently extracted with DCM. The combined organic phases was dried over $MgSO_4$, and the solvent evaporated under reduced pressure.

4.3.2 3-*O*-Benzyl-1,2;5,6-di-*O*-isopropylidene-α-D-glucofuranose (2a)

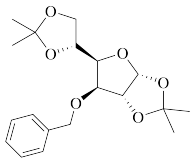

2a

General procedure 4.3.1 was used with 1,2;5,6-di-*O*-isopropylidene-α-D-glucofuranose (**1**) (1.4 g, 4.1 mmol) and benzyl bromide (0.95 mL, 8.1 mmol, 2 equiv). Full conversion of **1** was attained after 3 h. After extraction, a crude product, containing **2a** was obtained as a yellow oil (1.4 g, 3.9 mmol, 95%),

HRMS (ESI) *m/z*: [M+Na] calcd. for $C_{19}H_{26}O_6Na$ 373.1631, found 373.1627; t_R (Method *X*) 27.5 min; IR (cm^{-1}): 2986, 2930, 2859, 1454, 1372, 1252, 1213, 1070, 1020, 847, 735, 697; $[\alpha]_D^{20}$ = -26.0° (*c* 2.0, CH_2Cl_2);

^{1}H-NMR (600 MHz, $CDCl_3$): 1.31, 1.37, 1.43, 1.49 (*s*, 3H each, Me), 4.00 (*dd*, 1H, *J* = 5.9, 8.6, H-6b), 4.02 (*d*, 1H, *J* = 3.1, H-3), 4.11 (*dd*, 1H, *J* = 6.2, 8.6, H-6a), 4.15 (*dd*, 1H, *J* = 3.1, 7.7, H-4), 4.37 (*td*, 1H, *J* = 6.0, 7.7, H-5), 4.58 (*d*, 1H, *J* = 3.7, H-2), 4.66 (*ABq*, 2H, *J* = 11.8, benzylic), 5.90 (*d*, 1H, *J* = 3.7, H-1), 7.30 (*m*, 1H, *J* = 4.1, Ph-H), 7.34 (*m*, 4H, *J* = 4.4, Ph-H); ^{13}C-NMR (150 MHz, $CDCl_3$): 25.45, 26.26, 26.80, 26.86 (Me). 67.42 (C-6), 72.40 (benzylic), 72.54 (C-5), 81.35 (C-4), 81.72 (C-3), 82.69 (C-2), 105.31 (C-1) 109.00, 111.80 ($\underline{C}Me_2$), 127.66, 127.85, 128.42 (Ph), 137.67 (Ph-q). NMR corresponds with previously reported spectra.[120]

4.3.3 3-*O*-(2-Naphthyl)methyl-1,2;5,6-di-*O*-isopropylidene-α-D-glucofuranose (2b)

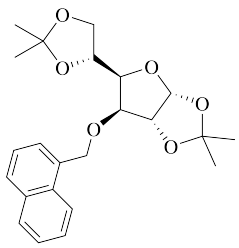

2b

General procedure 4.3.1 was used with 1,2;5,6-di-*O*-isopropylidene-α-D-glucofuranose (**1**) (3.2 g, 12 mmol) and 2-(bromomethyl)naphthalene (5.4 g, 24 mmol, 2 equiv). Full conversion of **1** was attained after 3 h. After extraction, a crude product, containing **2b** was obtained as an orange oil (4.5 g, 11 mmol, 91%),

HRMS (ESI) *m/z*: [M+Na] calcd. 423.1784 for $C_{23}H_{28}O_6Na$, found 423.1785; IR (cm^{-1}): 3055, 2986, 2933, 2893, 1455, 1372, 1214, 1165, 1074, 1021, 849, 751, 476; $[\alpha]_D^{20}$ = -24° (*c* 1.0, CH_2Cl_2);

^{1}H-NMR (600 MHz, $CDCl_3$): 1.31, 1.39, 1.43, 1.49 (*s*, 3H each, Me), 4.03 (*dd*, 1H, *J* = 5.8, 8.6, H-6b), 4.08 (*d*, 1H, *J* = 3.1, H-3), 4.14 (*dd*, 1H, *J* = 6.2, 8.5, H-6a), 4.16 (*dd*, 1H, *J* = 3.0, 7.8, H-4), 4.42 (*td*, 1H, *J* = 6.0, 7.8, H-5), 4.63 (*d*, 1H, *J* = 3.7, H-2), 4.82 (*ABq*, 2H, *J* = 12.1, Ar-C$\underline{H}_2$), 5.93 (*d*, 1H, *J* = 3.7, H-1), 7.47-7.50 (*m*, 3H, Ar-H), 7.79-7.85 (*m*, 4H, Ar-H); ^{13}C-NMR (150 MHz, $CDCl_3$): 25.54, 26.34, 26.89, 26.91 (Me), 67.55 (C-6), 72.45 (Ar-$\underline{C}H_2$), 72.54 (C-5), 81.41 (C-4), 81.60 (C-3), 82.79 (C-2), 105.31 (C-1), 109.05, 111.80 ($\underline{C}Me_2$), 125.64, 126.08, 126.29, 126.53, 127.77, 127.97, 128.24 (Ar), 133.18, 133.25, 135.15 (Ar-q). NMR matches previously reported data.[121]

4.3.4 3-*O*-(*p*-Phenyl)benzyl-1,2;5,6-di-*O*-isopropylidene-α-D-glucofuranose (2c)

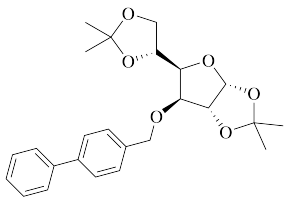

2c

General procedure 4.3.1 was used with 1,2;5,6-di-*O*-isopropylidene-α-D-glucofuranose (**1**) (3.0 g, 11 mmol) and *p*-phenylbenzyl chloride (4.7 g, 23 mmol, 2 equiv). The reaction was left overnight, resulting in conversion of all **1**. After extraction, a crude product, containing **2c** was obtained as a yellow wax (4.4 g, 10 mmol, 88%),

HRMS (ESI) *m/z*: [M+Na] calcd. 449.1940 for $C_{25}H_{30}O_6Na$, found 449.1938; t_R (Method *X*) 34.3 min; IR (cm^{-1}): 2986, 2934, 1380, 1214, 1074, 1022, 845, 761, 698; $[\alpha]_D^{20}$ = -32° (*c* 1.0, CH_2Cl_2);

^{1}H-NMR (600 MHz, $CDCl_3$): 1.32, 1.39, 1.44, 1.50 (*s*, 3H each, Me), 4.02 (*dd*, 1H, *J* = 5.8, 8.6, H-6b), 4.06 (*d*, 1H, *J* = 3.1, H-3), 4.13 (*dd*, 1H, *J* = 6.2, 8.6, H-6a), 4.16 (*dd*, 1H, *J* = 3.1, 7.8, H-4), 4.39 (*td*, 1H, *J* = 6.1, 7.7, H-5), 4.61 (*d*, 1H, *J* = 3.7, H-2), 4.70 (*ABq*, 2H, *J* = 11.8, Ar-C$\underline{H}_2$), 5.91 (*d*, 1H, *J* = 3.7, H-1), 7.35 (*m*, 1H, Ar-H), 7.43 (*m*, 4H, Ar-H), 7.58 (*m*, 4H, Ar-H); ^{13}C-NMR (150 MHz, $CDCl_3$): 25.49, 26.27, 26.82, 26.86 (Me), 67.47 (C-6), 72.14 (Ar-C$\underline{H}_2$), 72.54 (H-5), 81.37 (H-4), 81.74 (H-3), 82.73 (H-2), 105.33 (H-1), 109.03, 111.83 ($\underline{C}Me_2$), 127.10, 127.20, 127.34, 128.13, 128.79 (Ar), 136.68, 140.84, 140.86 (Ar-q). The ^{1}H-spectrum is consistent with previously reported spectrum.[122]

4.3.5 3-*O*-(3,5-Di-*tert*-butyl)benzyl-1,2;5,6-di-*O*-isopropylidene-α-D-glucofuranose (2d)

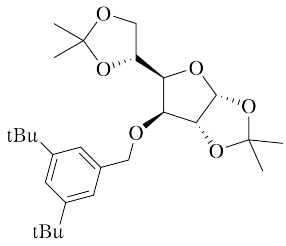

2d

General procedure 4.3.1 was used with 1,2;5,6-di-*O*-isopropylidene-α-D-glucofuranose (**1**) (0.46 g, 1.8 mmol) and 3,5-di-*tert*-butylbenzyl bromide (0.50 g, 1.8 mmol, 1 equiv). After 3 h, all alkyl bromide was reacted. The resulting residue was purified by flash chromatography (SiO_2, 9:1 *n*-pentane:Et_2O), yielding **2d** as a limpid oil (0.66 g, 1.4 mmol, 80%),

HRMS (ESI) *m/z*: [M+Na] calcd. 449.1940 for $C_{25}H_{30}O_6Na$, found 449.1938; t_R (Method *X*) 34.3 min; IR (cm^{-1}): 2955, 2869, 1601, 1457, 1371, 1249, 1212, 1072, 1020, 846, 712, 510; $[\alpha]_D^{20}$ = -24° (*c* 1.0, CH_2Cl_2);

^{1}H-NMR (600 MHz, $CDCl_3$): 1.31 (*s*, 3H, Me), 1.32 (*s*, 18H, *t*-Bu), 1.38 (*s*, 3H, Me), 1.45 (*s*, 3H, Me), 1.50 (*s*, 3H, Me), 4.04 (*d*, 2H, *J* = 3.5, H-3), 4.05 (*dd*, 2H, *J* = 5.4, 8.4, H-6b), 4.12 (*dd*, 1H, *J* = 6.3, 8.6, H-6a), 4.18 (*dd*, 1H, *J* = 3.1, 7.4, H-4), 4.41 (*td*, 1H, *J* = 6.0, 7.3, H-5), 4.60 (*d*, 1H, *J* = 3.7, H-2), 4.64 (*ABq*, 2H, *J* = 11.5, Ar-C$\underline{H}_2$), 5.89 (*d*, 1H, *J* = 3.7, H-1), 7.17 (*d*, 2H, *J* = 1.9, 2-Ar), 7.36 (*t*, 1H, *J* = 1.8, 4-Ar); ^{13}C-NMR (150 MHz, $CDCl_3$): 25.44, 26.25, 26.84, 26.87 (C$\underline{Me}_2$), 31.47, 34.83 ($\underline{C}Me_3$), 67.21 (C-6), 72.75 (C-5), 73.17 (Ar-C$\underline{H}_2$), 81.36 (C-4), 81.92 (C-3), 82.58 (C-2), 105.30 (C-1), 108.97, 111.73 ($\underline{C}Me_2$), 121.89, 121.91 (Ar), 136.74, 150.88 (Ar-q).

4.3.6 3-*O*-*p*-Nitrobenzyl-1,2;5,6-di-*O*-isopropylidene-α-D-glucofuranose (2i)

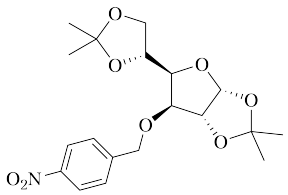

2i

To a solution of 1,2;5,6-di-*O*-isopropylidene-α-D-glucofuranose (**1**) (1.2 g, 4.5 mmol) in DCM (10 mL) was added Ag_2O (2.0 g, 8.6 mmol, 2.0 equiv) and *p*-nitrobenzyl bromide (2.7 g, 6.9 mmol, 1.5 equiv). The solution was stirred at reflux for 4 d, before removing any solids by filtration, and evaporation of the solvent under reduced pressure. Column chromatography (SiO_2, *n*-pentane:Et_2O 8:1) resulted in **2i** as a yellow oil (1.3 g, 3.2 mmol, 71%),

HRMS (ESI) *m/z*: [M+Na] calcd. 418.1478 for $C_{19}H_{25}NO_8Na$, found 418.1485; IR (cm^{-1}): 2986, 2935, 2895, 1520, 1344, 1212, 1071, 1013, 842, 738, 512; $[\alpha]_D^{20}$ = -34° (*c* 1.0, CH_2Cl_2);

^{1}H-NMR (600 MHz, $CDCl_3$): 1.33, 1.37, 1.43, 1.50 (*s*, 3H each, Me), 4.02 (*dd*, 1H, *J* = 8.6, 5.5, H-6b), 4.04 (*d*, 1H, *J* = 3.0, H-3), 4.12 (*dd*, 1H, *J* = 8.6, 3.1, H-4), 4.14 (*dd*, 1H, *J* = 8.6, 6.2, H-6a), 4.36 (*dt*, 1H, *J* = 8.5, 5.8, H-5), 4.62 (*d*, 1H, *J* = 3.7, H-2), 4.76, 4.81 (*ABq*, 2H, *J* = 13.2, Ar-CH_2), 5.92 (*d*, 1H, *J* = 3.7, H-1), 7.54 (*m*, 2H, *J* = 8.6, Ar-H), 8.21 (*m*, 2H, *J* = 8.6, Ar-H); ^{13}C-NMR (150 MHz, $CDCl_3$): 25.5, 26.2, 26.8, 26.9 (Me), 67.7 (C-6), 71.1 (Ar-$\underline{C}H_2$), 72.3 (C-5), 81.3 (C-4), 82.4 (C-3), 82.6 (C-2), 105.3 (C-1), 109.3, 112.0 ($\underline{C}Me_2$), 123.6, 127.7 (Ar), 145.2, 147.5 (Ar-q). NMR is consistent with previously reported data.[47]

4.3.7 3-*O*-(9'-Anthracenyl)methyl-1,2;5,6-di-*O*-isopropylidene-α-D-glucofuranose (2j)

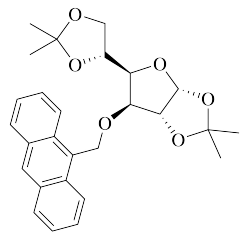

2j

General procedure 4.3.1 was used with 1,2;5,6-di-*O*-isopropylidene-α-D-glucofuranose (**1**) (0.65 g, 2.5 mmol) and 9-(chloromethyl)anthracene (**RC-1**) (0.56 g, 2.5 mmol, 1 equiv). The reaction was left to stir overnight, resulting in conversion of all 9-(chloromethyl)-anthracene. The residue was purified by flash chromatography (SiO_2, 9:1 *n*-pentane:EtOAc), yielding **2j**, as a yellow glassy substance (0.96 g, 2.1 mmol, 86%),

HRMS (ASAP+) *m/z*: [M] calcd. 450.2042 for $C_{27}H_{30}O_6$, found 450.2039; IR (cm^{-1}): 2986, 2933, 1354, 1372, 1256, 1215, 1164, 1074, 1020, 887, 847; $[\alpha]_D^{20}$ = -9° (*c* 1.0, CH_2Cl_2);

^{1}H-NMR (600 MHz, $CDCl_3$): 1.31, 1.43, 1.49, 1.50 (*s*, 3H each, Me), 4.00 (*dd*, *J* = 8.7, 5.3, H-6b) 4.07 (*dd*, *J* = 8.7, 6.3, H-6a), 4.14 (*dd*, *J* = 8.4, 3.0, H-4), 4.24 (*d*, *J* = 3.0, H-3), 4.38 (*ddd*, *J* = 8.4, 6.2, 5.4, H-5), 4.63 (*d*, *J* = 3.7, H-2), 5.59, 5.68 (*d*, 1H each, *J* = 11.2, Ar-C$\underline{H}_2$), 5.85 (*d*, *J* = 3.7, H-1), 7.47 (*m*, 2H, *J* = 8.4, 6.4, Ar-H), 7.54 (*ddd*, 2H, *J* = 8.8, 6.5, 1.3, Ar-H), 8.01 (*m*, 2H, *J* = 8.4, Ar-H), 8.45 (*m*, 3H, Ar-H); ^{13}C-NMR (150 MHz, $CDCl_3$): 25.41, 26.35, 26.90, 26.93 (Me), 65.06 (Ar-$\underline{C}H_2$), 67.62 (C-6), 72.37 (C-5), 81.58 (C-3), 81.73 (C-4), 83.57 (C-2), 105.42 (C-1), 109.17 ($\underline{C}Me_2$), 111.91 ($\underline{C}Me_2$), 124.27, 124.96, 126.29 (Ar), 127.97 (Ar-q), 128.77, 129.06 (Ar), 131.19, 131.47 (Ar-q).

4.3.8 3-*O*-(*t*-Butyl-dimethylsilyl)-1,2;5,6-di-*O*-isopropylidene-α-D-glucofuranose (2e)

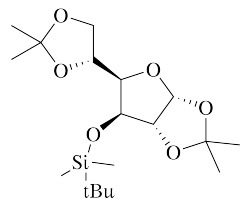

2e

To a solution of 1,2;5,6-di-*O*-isopropylidene-α-D-glucofuranose (**1**) (0.51 g, 1.9 mmol) and 2,6-lutidine (0.49 mL, 4.2 mmol, 2.2 equiv) in DCM (5 mL), was added TBDMS-OTf (0.66 mL, 2.9 mmol, 1.5 equiv) dropwise at 0 °C. The reaction was stirred at 0 °C for 5 h, before being allowed to warm to room temperature and stir for further 6 h. More DCM was added, and extracted three times with water, the organic phase dried over $MgSO_4$, and the solvent evaporated under reduced pressure. Purification by elution (Et_2O) through short pad of silica gel yielded **2e** as a limpid oil (0.54 g, 1.4 mmol, 74%),

HRMS (ESI+) *m/z*: [M+Na] calcd. 397.2022 for $C_{18}H_{34}O_6NaSi$, found 397.2027; IR (cm^{-1}): 2987, 2932, 2858, 1472, 1371, 1252, 1131, 1074, 1020, 833, 778; $[\alpha]_D^{20}$ = -16° (*c* 1.0, CH_2Cl_2);

^{1}H-NMR (600 MHz, $CDCl_3$): 0.14, 0.12 (*s*, 3H each, $SiMe_2$), 0.91 (*s*, 9H, *t*-Bu), 1.32, 1.32, 1.40, 1.50 (*s*, 3H each, CMe_2), 3.95 (*dd*, *J* = 8.5, 6.0, H-6b), 4.03 (*dd*, *J* = 8.2, 2.7, H-4), 4.11 (*dd*, *J* = 8.5, 6.1, H-6a), 4.23 (*dt*, *J* = 8.3, 6.2, H-5), 4.24 (*d*, *J* = 2.6, H-3), 4.35 (*d*, *J* = 3.6, H-2), 5.87 (*d*, *J* = 3.5, H-1); ^{13}C-NMR (150 MHz, $CDCl_3$): -5.17, -4.97 ($SiMe_2$), 18.14 ($SiCMe_3$), 25.73 ($SiCMe_3$), 25.33, 26.39, 26.78, 26.99 (CMe_2), 67.76 (C-6), 72.20 (C-5), 75.52 (C-3), 82.31 (C-4), 85.64 (C-2), 105.32 (C-1), 108.97, 111.86 (CMe_2). NMR data is consistent with previously reported data.[123]

4.3.9 1,2-*O*-Isopropylidene-5-*O*-triisopropylsilyl-α-D-xylofuranose (IC-1)

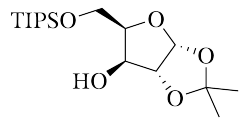

IC-1

1,2-*O*-Isopropylidene-α-D-xylofuranose (1.0 g, 5.3 mmol) and imidazole (0.98 g, 14 mmol, 2.7 equiv) was added to dry DMF (20 mL). The solution was cooled to 0°C and TIPS-Cl (1.1 g, 5.9 mmol, 1.1 equiv) was added over 0.5 h and stirred for 25 min, before being warmed to room temperature and stirred for further 16 h. A saturated solution of NH_4Cl (40 mL) was added and extracted with DCM three times. The combined organic layers were dried over $MgSO_4$ and the solvent evaporated under reduced pressure. Purification by elution (20:1 *n*-pentane:EtOAc) through a short pad of silica gel yielded **IC-1** as a limpid oil (0.65 g, 4.8 mmol, 89%),

HRMS (ASAP+) *m/z*: [M+H] calcd. 347.2254 for $C_{17}H_{35}O_5Si$, found 347.2248; IR (cm^{-1}): 2942, 2866, 1463, 1373, 1215, 1072, 1011, 881, 679, 503; $[\alpha]_D^{20}$ = -32° (*c* 1.0, CH_2Cl_2);

^{1}H-NMR (600 MHz, $CDCl_3$): 1.05-1.17 (*m*, 21H, *i*-Pr), 1.32, 1.49 (*s*, 3H each, Me), 4.13 (*m*, *J* = 6.2, 3.0, H-4), 4.22 (*ABq*, 2H, *J* = 11.5, 4.0, H-5), 4.35 (*m*, *J* = 2.6, H-3), 4.52 (*d*, *J* = 3.7, H-2), 5.97 (*d*, *J* = 3.6, H-1); ^{13}C-NMR (150 MHz, $CDCl_3$): 11.7, 17.71, 17.77, 17.82 (*i*-Pr), 26.2, 26.9 (Me), 62.9 (H-5), 78.2 (H-4), 77.2 (H-3), 85.6 (H-2), 105.0 (H-1), 111.5 ($\underline{C}Me_2$). NMR data corresponds with previously reported data.[124]

4.3.10 1,2-*O*-Isopropylidene-3-*O*-benzyl-5-*O*-triisopropylsilyl-α-D-xylofuranose (IC-2)

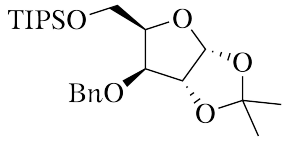

IC-2

Using benzyl bromide (1.3 mL, 11 mmol, 2 equiv), **IC-1** (1.4 g, 3.2 mmol) was benzylated according to the General procedure 4.3.1. The resulting residue was purified by column chromatography (SiO_2, *n*-pentane:Et_2O 20:1) resulted in **IC-2** as a yellow oil (1.3 g, 2.9 mmol, 92%),

HRMS (ESI+) *m/z*: [M+Na] calcd. 459.2543 for $C_{24}H_{40}O_5SiNa$, found 459.2540; IR (cm^{-1}): 2927, 2866, 1463, 1373, 1216, 1077, 1016, 883, 793, 733, 683; $[\alpha]_D^{20}$ = °34 (*c* 1.0, CH_2Cl_2);

^{1}H-NMR (600 MHz, $CDCl_3$): 1.03-1.14 (*m*, 21H, *i*-Pr), 1.31, 1.50 (*s*, 3H each, Me), 3.94 (*dd*, *J* = 5.2, 9.8, H-5b), 4.00 (*dd*, *J* = 8.1, 9.8, H-5a), 4.02 (*d*, *J* = 3.4, H-3), 4.27 (*ddd*, *J* = 3.0, 5.1, 8.1, H-4), 4.58 (*d*, *J* = 3.8, H-2), 4.62, 4.67 (*ABq*, 2H, *J* = 11.9, benzylic), 5.90 (*d*, *J* = 3.8, H-1), 7.26-7.35 (*m*, 5H, Ph-H); ^{13}C-NMR (150 MHz, $CDCl_3$): 11.9, 18.0 (*i*-Pr), 26.3, 26.9 (Me), 60.2 (C-5), 72.4 (benzylic), 81.0 (C-4), 81.4 (C-3), 82.6 (C-2), 105.0 (C-1), 111.7 ($\underline{C}Me_2$), 127.6, 127.8, 128.4 (Ph), 137.8 (Ph-q). NMR data corresponds with previously reported data.[124]

4.3.11 1,2-*O*-Isopropylidene-3-*O*-benzyl-α-D-xylofuranose (2ø)

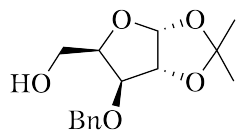

2ø

To a solution of **IC-2** (1.3 g, 2.9 mmol) in THF (11 mL), was added tetrabutylammonium fluoride (1.0 M in THF, 6.4 mL, 6.4 mmol, 1.2 equiv). The reaction was stirred for 1 h and 20 min at room temperature, before concentrating under reduced pressure. DCM was added, washed with water twice and the organic phase dried over $MgSO_4$. Purification by column chromatography (SiO_2, 9:1 *n*-pentane:EtOAc) gave **2ø** as a yellow oil (0.59 g, 2.1 mmol, 73%). Performing the last three steps, starting from 1,2-*O*-Isopropylidene-α-D-xylofuranose (2.5 g, 13 mmol), without purifying by chromatography between the steps, gave **2ø** (2.4 g, 8.6 mmol, 69%),

HRMS (ESI+) *m/z*: [M+Na] calcd. 303.1208 for $C_{15}H_{20}O_5Na$, found 303.1212; IR (cm^{-1}): 3482, 2986, 2934, 2892, 1455, 1374, 1214, 1073, 1013, 858, 739, 698; $[\alpha]_D^{20}$ = -64° (*c* 1.0, CH_2Cl_2);

^{1}H-NMR (600 MHz, $CDCl_3$): 1.33, 1.49 (*s*, 3H each, Me), 2.10 (*dd*, *J* = 8.9, 3.8, OH), 3.86 (*ddd*, *J* = 12.0, 8.8, 4.7, H-5b), 3.95 (*ddd*, *J* = 12.0, 5.2, 3.8, H-5a), 4.02 (*d*, *J* = 3.6, H-3), 4.28 (*td*, *J* = 4.9, 3.8, H-4), 4.50 (*d*, *J* = 11.9, benzylic), 4.65 (*d*, *J* = 3.8, H-2), 4.72 (*d*, *J* = 11.9, benzylic), 6.00 (*d*, *J* = 3.8, H-1), 7.30-7.39 (*m*, 5H, Ph-H); ^{13}C-NMR (150 MHz, $CDCl_3$): 26.3, 26.8 (Me), 61.0 (C-5), 71.9 (benzylic)), 80.0 (C-4), 82.5 (C-2), 82.8 (C-3), 105.1 (C-1), 111.8 ($\underline{C}Me_2$), 127.8, 128.2, 128.7 (Ph), 137.1 (Ph-q). NMR data match previously reported data.[125]

4.3.12 3-*O*-Benzyl-1,2;5,6-di-*O*-isopropylidene-α-D-allofuranose (2ð)

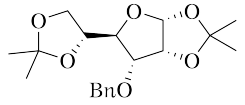

2ð

General procedure 4.3.1 was followed, benzylating 1,2:5,6-di-*O*-isopropylidene-α-D-allofuranose (0.20 g, 0.77 mmol), with benzyl bromide. Purification by column chromatography (SiO_2, 98:2 DCM:MeOH) gave **2ð** as a yellow wax (0.21 g, 0.61 mmol, 79%),

HRMS (ESI+) *m/z*: [M+Na] calcd. 303.1208 for $C_{15}H_{20}O_5Na$, found 303.1212; IR (cm^{-1}): 3482, 2986, 2934, 2892, 1455, 1374, 1214, 1073, 1013, 858, 739, 698; $[\alpha]_D^{20}$ = -64° (*c* 1.0, CH_2Cl_2);

^{1}H-NMR (600 MHz, $CDCl_3$): 1.33, 1.49 (*s*, 3H each, Me), 2.10 (*dd*, *J* = 8.9, 3.8, OH), 3.86 (*ddd*, *J* = 12.0, 8.8, 4.7, H-5b), 3.95 (*ddd*, *J* = 12.0, 5.2, 3.8, H-5a), 4.02 (*d*, *J* = 3.6, H-3), 4.28 (*td*, *J* = 4.9, 3.8, H-4), 4.50 (*d*, *J* = 11.9, benzylic), 4.65 (*d*, *J* = 3.8, H-2), 4.72 (*d*, *J* = 11.9, benzylic), 6.00 (*d*, *J* = 3.8, H-1), 7.30-7.39 (*m*, 5H, Ph-H); ^{13}C-NMR (150 MHz, $CDCl_3$): 26.3, 26.8 (Me), 61.0 (C-5), 71.9 (benzylic), 80.0 (C-4), 82.5 (C-2), 82.8 (C-3), 105.1 (C-1), 111.8 ($\underline{C}Me_2$), 127.8, 128.2, 128.7 (Ph), 137.1 (Ph-q). NMR data matches previously reported data.[125]

4.3.13 1,2-*O*-Isopropylidene-3-*O*-benzyl-α-D-glucofuranose (MC-1)

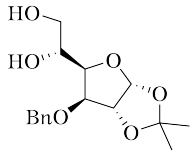

MC-1

1,2;5,6-di-*O*-isopropylidene-α-D-glucofuranose (**1**) (0.90 g, 2.6 mmol) and HCl (37%, 0.30 mL, 1.6 equiv) was added to methanol. The reaction was stirred for 70 min at room temperature, before quenching with TEA and concentrating under reduced pressure. Passing the residue through a short column (SiO_2, 3:1 *n*-pentane:EtOAc), afforded **MC-1** as a pale yellow oil (0.56 g, 1.8 mmol, 71%),

HRMS (ESI+) *m/z*: [M+Na] calcd. 333.1314 for $C_{16}H_{22}O_6Na$, found 333.1316; IR (cm^{-1}): 3451, 2925, 2854, 1455, 1375, 1255, 1216, 1165, 1076, 1020, 887, 857, 741, 682; $[\alpha]_D^{20}$ = -28° (*c* 1.0, CH_2Cl_2);

^{1}H-NMR (600 MHz, $CDCl_3$): 1.32, 1.49 (*s*, 3H each, Me), 3.69 (*dd*, *J* = 11.5, 5.7, H-6b), 3.81 (*dd*, *J* = 11.2, 3.4, H-6a), 4.03 (*m*, H-5), 4.10 (*d*, *J* = 3.3, H-3), 4.13 (*m*, *J* = 7.8, 3.3,

H-4), 4.55 (*d*, *J* = 11.8, benzylic), 4.63 (*d*, *J* = 3.9, H-2), 4.73 (*d*, *J* = 11.8, benzylic), 5.94 (*d*, *J* = 3.9, H-1), 7.31-7.39 (*m*, 5H, Ph-H); ^{13}C-NMR (150 MHz, $CDCl_3$): 26.25, 26.76 (Me), 64.42 (C-6), 69.35 (C-5), 72.12 (benzylic), 80.00 (C-4), 82.03 (C-3), 82.10 (C-2), 105.17 (C-1), 111.86 ($\underline{C}Me_2$), 127.92, 128.31, 128.77 (Ph), 137.13 (Ph-q). NMR is in accordance with previously reported data.[126]

4.3.14 1,2-*O*-Isopropylidene-3-*O*-(*p*-phenyl)benzyl-α-D-glucofuranose (MC-2)

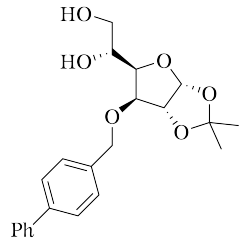

MC-2

3-*O*-(*p*-Phenyl)benzyl-1,2;5,6-di-*O*-isopropylidene-α-D-glucofuranose (**2c**) (1.7 g, 3.9 mmol) was dissolved in MeOH with HCl (37%, 0.51 mL, 1.6 equiv) and stirred for 60 min at room temperature. The solvent was evaporated under reduced pressure and purified by column chromatography to afford **MC-2** as a yellow oil (1.1 g, 2.8 mmol, 72%),

HRMS (ESI+) *m/z*: [M+Na] calcd. 409.1627 for $C_{22}H_{26}O_6Na$, found 409.1624; t_R (Method *X*) 19.7 min; IR (cm^{-1}): 3431, 2933, 1488, 1375, 1253, 1216, 1164, 1077, 1019, 855, 761, 699; $[\alpha]_D^{20}$ = -28° (*c* 1.0, CH_2Cl_2);

^{1}H-NMR (600 MHz, $CDCl_3$): 1.33, 1.50 (*s*, 3H each, Me), 2.03 (*m*, *J* = 5.5, 6-OH), 2.53 (*d*, *J* = 6.3, 5-OH), 3.72 (*ddd*, *J* = 10.8, 5.6, 5.1, H-6b), 3.84 (*ddd*, *J* = 10.2, 5.7, 3.6, H-6a), 4.07 (*m*, H-5), 4.14 (*d*, *J* = 3.3, H-3), 4.16 (*dd*, *J* = 7.6, 3.3, H-4), 4.60 (*d*, *J* = 11.8, benzylic), 4.66 (*d*, *J* = 3.8, H-2), 4.78 (*d*, *J* = 11.8, benzylic), 5.96 (*d*, *J* = 3.8, H-1), 7.35 (*m*, (*J* = 7.3), Ar-H), 7.40-7.46 (*m*, *J* = 8.3, 7.5, Ar-H), 7.59 (*m*, *J* = 8.2, 7.3, Ar-H); ^{13}C-NMR (150 MHz, $CDCl_3$): 26.27, 26.79 (Me), 64.48

(C-6), 69.39 (C-5), 71.86 (benzylic), 80.06 (C-4), 82.13 (C-2), 82.15 (C-3), 105.20 (C-1), 111.89 ($\underline{C}Me_2$), 127.13, 127.49, 128.36, 128.83 (Ar), 136.10, 140.59, 141.28 (Ar-q).

4.3.15 General procedure for introducing silyl ethers

The alcohol was added to a solution of imidazole (4.4 equiv) and the silylating agent (2.2 equiv) in DMF. The reaction was stirred at 40 °C until consumption of the alcohol, as indicated by TLC. DCM and water were added, and the layers were separated, followed by washing the aqueous phase washed with DCM and the combined organic phases washed with water. The organic phase was dried over $MgSO_4$, and the solvent evaporated under reduced pressure.

4.3.16 3-*O*-(*t*-Butyl-diphenylsilyl)-1,2;5,6-di-*O*-isopropylidene-α-D-glucofuranose (2f)

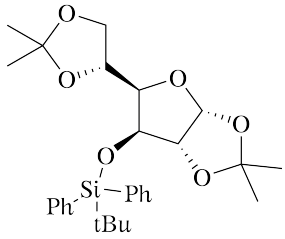

2f

According to General procedure 4.3.15 , **1** (0.50 g, 1.9 mmol) was silylated, using *t*-butyldiphenylchlorosilane (1.1 mL, 4.2 mmol, 2.2 equiv). Purification by column chromatography (SiO_2, 1:1 *n*-pentane:DCM) gave **2f** as a limpid oil (0.84 g, 1.7 mmol, 88%),

HRMS (ESI+) *m/z*: [M+Na] calcd. 521.2335 for $C_{28}H_{38}O_6NaSi$, found 521.2335; t_R (Method *XX*) 41.9 min; IR (cm^{-1}): 3050, 2933, 2859, 1371, 1214, 1112, 1071, 1017, 823, 739, 700, 619, 504; $[\alpha]_D^{20}$ = +32° (*c* 1.0, CH_2Cl_2);

^{1}H-NMR (600 MHz, $CDCl_3$): 1.08 (*s*, 3H, C$\underline{Me_2}$) 1.09 (*s*, 9H, *t*-Bu), 1.33, 1.39, 1.42 (*s*, 3H each, C$\underline{Me_2}$), 4.00 (*dd*, *J* = 8.5, 6.0, H-6b), 4.03 (*dd*, *J* = 8.4, 2.8, H-4), 4.06 (*d*, *J* = 3.5, H-2), 4.17 (*dd*, *J* = 8.4, 6.3, H-6a), 4.43 (*d*, *J* = 2.5, H-3), 4.46 (*dt*, *J* = 8.3, 6.1, H-5), 5.80 (*d*, *J* = 3.5, H-1), 7.35-7.47 (*m*, 6H, Ph-H), 7.70 (*m*, 2H, *J* = 8.0, Ph-H), 7.76 (*m*, 2H, *J* = 8.0, Ph-H); ^{13}C-NMR (150 MHz, $CDCl_3$): 19.42 (C$\underline{Me_3}$), 25.30, 26.00, 26.80, 26.81 (C$\underline{Me_2}$), 26.87 (C$\underline{Me_3}$), 67.90 (C-6) 72.18 (C-5), 76.52 (C-3), 82.56 (C-4), 84.49 (C-2), 105.01 (C-1), 109.05, 111.59 (C$\underline{Me_2}$), 127.66, 127.79, 129.94 (Ph), 132.50, 134.02 (Ph-q), 135.75, 136.06 (Ph).

4.3.17 3-*O*-(Triisopropylsilyl)-1,2;5,6-di-*O*-isopropylidene-α-D-glucofuranose (2g)

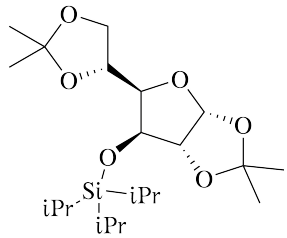

2g

According to the General procedure 4.3.15, **1** (0.50 g, 1.9 mmol) was silylated, using triisopropylsilyl chloride (0.90 mL, 4.2 mmol, 2.2 equiv). Purification by column chromatography (SiO_2, 20:1 *n*-pentane:EtOAc) gave **2g** as a limpid oil (0.43 g, 1.0 mmol, 54%),

HRMS (ESI+) *m/z*: [M+Na] calcd. 439.2492 for $C_{21}H_{40}O_6NaSi$, found 439.2501; IR (cm^{-1}): 3050, 2933, 2859, 1317, 1214, 1112, 1071, 1017, 848, 823, 739, 700, 610, 504, 487; $[\alpha]_D^{20}$ = -20° (*c* 1.0, CH_2Cl_2);

^{1}H-NMR (600 MHz, $CDCl_3$): 1.07-1.16 (*m*, 21H, SiC$\underline{H}$Me$_2$), 1.31 (*s*, 6H, C$\underline{Me_2}$), 1.40 (*s*, 3H, C$\underline{Me_2}$), 1.50 (*s*, 3H, C$\underline{Me_2}$), 3.96 (*dd*, *J* = 8.5, 6.2, H-6b), 4.03 (*dd*, *J* = 8.1, 2.6, H-4), 4.11

(*dd*, *J* = 8.5, 6.3, H-6a), 4.32 (*dt*, *J* = 8.1, 6.3, H-5), 4.41 (*d*, *J* = 2.7, H-3), 4.42 (*d*, *J* = 3.7, H-2), 5.87 (*d*, *J* = 3.5, H-1); ^{13}C-NMR (150 MHz, $CDCl_3$): 12.49 ($Si\underline{C}HMe_2$) 18.00 ($SiCH\underline{Me_2}$), 25.28, 26.35, 26.74, 26.96 ($C\underline{Me_2}$), 67.75 (C-6), 72.01 (C-5), 76.06 (C-3), 82.54 (C-4), 85.64 (C-2), 105.11 (C-1), 109.00, 111.82 ($\underline{C}Me_2$).

4.4 Glycosylation of 3-*O*-protected monosaccharides

4.4.1 General procedure for Fischer glycosylation

HCl (37%, 1.6 equiv) was added to the alcohol, with the 3-*O*-protected furanoside (0.26 M). After refluxing for 30 min to 1 h, the reaction was quenched with Et_3N (3.2 equiv) and concentrated under reduced pressure.

4.4.2 General procedure for deacetylation

The acetylated sugar was added to MeOH with NaOMe (0.2 M), and stirred at room temperature until completion, as indicated by TLC. Amberlyst-15 was added until neutral pH was achieved. The solvent was evaporated under reduced pressure.

4.4.3 Allyl 3-*O*-benzyl-2,4,6-tri-*O*-acetyl-α,β-D-glucopyranoside (8a)

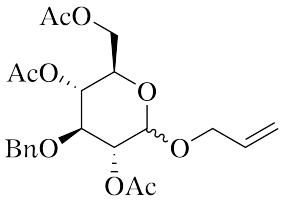

8a

3-*O*-Benzyl-1,2;5,6-di-*O*-isopropylidene-α-D-glucofuranose (**2a**) (1.1 g, 3.0 mmol) was glucosylated with allyl alcohol, according to the General procedure 4.4.1. The resulting residue,

was added to pyridine-acetic anhydride (12 mL, 1:1 V:V), and stirred overnight. After concentration under reduced pressure, water and DCM were added, the layers separated, and solvent removed. Purification by column chromatography (SiO_2, 8:1 → 4:1 *n*-pentane:EtOAc) gave **8a** (1.0 g, 2.4 mmol, 79%, 73:27 α:β). Partial anomeric separation yielded:

α-anomer: pale yellow oil (0.64 g, 1.5 mmol, 49%), HRMS (ESI+) *m/z*: [M+Na] calcd. 459.1631 for $C_{22}H_{28}O_9Na$, found 459.1629; IR (cm^{-1}): 2923, 1743, 1367, 1221, 1036, 930, 742, 699; $[\alpha]_D^{20}$ = +76° (*c* 1.0, CH_2Cl_2); ^{1}H-NMR (600 MHz, $CDCl_3$): 1.94, 2.06, 2.09 (*s*, 3H each, Me), 3.94 (*ddd*, *J* = 10.2, 4.8, 2.4, H-5), 4.01 (*m*, *J* = 9.7, H-3), 4.02 (*m*, *J* = 13.1, 6.2, 1.3, allylic), 4.07 (*dd*, *J* = 12.3, 2.4, H-6b), 4.18 (*m*, *J* = 13.2, 5.3, 1.4, allylic), 4.20 (*dd*, *J* = 12.4, 4.9, H-6a), 4.61, 4.72 (*d*, 1H each, *J* = 11.8, benzylic), 4.88 (*dd*, *J* = 10.0, 3.8, H-2), 5.09 (*dd*, *J* = 10.1, 9.4, H-4), 5.11 (*d*, *J* = 3.6, H-1), 5.24 (*m*, *J* = 10.4, 2.7, 1.2, CH=C$\underline{H}_2$), 5.31 (*m*, *J* = 17.1, 3.2, 1.6, CH=C$\underline{H}_2$), 5.89 (*m*, *J* = 17.2, 10.4, 6.1, 5.2, C$\underline{H}$=CH_2), 7.23-7.34 (*m*, 5H, Ph-H); ^{13}C-NMR (150 MHz, $CDCl_3$): 20.74, 20.76, 20.86 (Me), 62.19 (C-6), 67.81 (C-5), 68.67 (allylic), 69.76 (C-4), 73.25 (C-2), 74.94 (benzylic), 77.42 (C-3), 95.08 (C-1), 118.12 (CH=$\underline{C}H_2$), 127.49, 127.70, 128.41 (Ph), 133.27 ($\underline{C}$H=CH_2), 138.22 (Ph-q), 169.46, 170.07, 170.78 (CO).

β-anomer: yellow wax (0.30 g, 0.69 mmol, 23%), HRMS (ESI+) *m/z*: [M+Na] calcd. 459.1631 for $C_{22}H_{28}O_9Na$, found 459.1628; IR (cm^{-1}): 2956, 2883, 1743, 1371, 1219, 1070, 1039, 926, 741, 700; $[\alpha]_D^{20}$ = -20° (*c* 1.0, CH_2Cl_2); ^{1}H-NMR (600 MHz, $CDCl_3$): 1.97, 2.02, 2.08 (*s*, 3H each, Me), 3.58 (*ddd*, *J* = 9.9, 5.1, 2.6, H-5), 3.70 (*t*, *J* = 9.3, H-3), 4.08 (*m*, *J* = 13.3, 6.1, 1.3, allylic), 4.13 (*dd*, *J* = 12.2, 2.6, H-6b), 4.21 (*dd*, *J* = 12.2, 5.1, H-6a), 4.33 (*m*, *J* = 13.3, 4.8, 1.5, allylic), 4.46 (*d*, *J* = 7.9, H-1), 4.60 (*ABq*, 2H, *J* = 11.7, benzylic), 5.09 (*dd*, *J* = 9.4, 7.9, H-2), 5.13 (*t*, *J* = 9.6, H-4), 5.19 (*m*, *J* = 10.4, 1.4, CH=C$\underline{H}_2$), 5.27 (*m*, *J* = 17.2, 3.3, 1.6, CH=C$\underline{H}_2$), 5.85 (*m*, *J* = 17.0, 10.8, 6.1, 4.8, C$\underline{H}$=CH_2), 7.20-7.36 (*m*, 5H, Ph-H); ^{13}C-NMR (150 MHz, $CDCl_3$): 20.78, 20.80, 20.87 (Me), 62.32 (C-6), 69.62 (C-4), 69.76 (allylic), 72.07 (C-5), 72.48 (C-2), 73.70 (benzylic), 80.07 (C-3), 99.80 (C-1), 117.45 (CH=$\underline{C}H_2$), 127.81, 127.85, 128.45 (Ph), 133.53 ($\underline{C}$H=CH_2), 137.79 (Ph-q), 169.23, 169.36, 170.84

(CO). NMR of both anomers is consistent with previously data.[127]

4.4.4 Allyl 3-*O*-benzyl-α,β-D-glucopyranoside (4a)

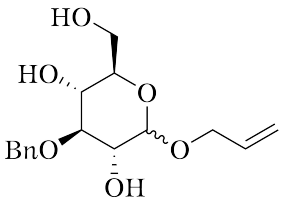

4a

Both anomers of the acetylated sugar (**8a**) (α-anomer: 0.51 g, 1.2 mmol, β-anomer: 0.10 g, 0.32 mmol), were deacetylated General procedure 4.4.2. Purification of the resulting residue was achieved by column chromatography (SiO_2, 1:1 *n*-pentane: EtOAc), yielding both anomers of **4a**:

α-anomer: white crystals (0.31 g, 1.0 mmol, 86%), mp. 89-95°C; HRMS (ESI+) *m/z*: [M+Na] calcd. 333.1314 for $C_{16}H_{22}O_6Na$, found 333.1314; t_R (Method *X*) 8.0 min; IR (cm^{-1}): 3414, 2923, 1455, 1407, 1349, 1261, 1114, 1080, 1028, 928, 740, 966; $[\alpha]_D^{20}$ = +98° (*c* 1.0, CH_2Cl_2); ^{1}H-NMR (600 MHz, $CDCl_3$): 1.89 (*dd*, *J* = 7.3, 5.6, 6-OH), 2.12 (*d*, *J* = 9.7, 2-OH), 2.30 (*d*, *J* = 2.6, 4-OH), 3.56 (*td*, *J* = 9.0, 2.5, H-4), 3.61 (pseudo-*t*, *J* = 8.9, H-3), 3.68 (*dd*, *J* = 9.5, 3.8, H-2), 3.70 (*m*, *J* = 9.4, 4.1, H-5), 3.78 (*ddd*, *J* = 11.9, 7.2, 4.7, H-6b), 3.84 (*ddd*, *J* = 11.7, 5.5, 3.7, H-6a), 4.05 (*m*, *J* = 12.7, 6.3, 1.2, allylic), 4.24 (*m*, *J* = 12.7 5.4, 1.4, allylic), 4.73 (*d*, *J* = 11.4, benzylic), 4.92 (*d*, *J* = 3.9, H-1), 5.05 (*d*, *J* = 11.6, benzylic), 5.25 (*m*, *J* = 11.6, CH=C$\underline{H}_2$), 5.32 (*m*, *J* = 17.2, 2.9, 1.6, CH=C$\underline{H}_2$), 5.93 (*m*, *J* = 17.1, 10.4, 6.2, 5.4, C$\underline{H}$=CH_2), 7.28-7.40 (*m*, 5H, Ph-H); ^{13}C-NMR (150 MHz, $CDCl_3$): 62.59 (C-6), 68.69 (allylic), 70.26 (C-4), 71.13 (C-5), 72.92 (C-2), 74.97 (benzylic), 82.92 (C-3), 97.74 (C-1), 118.22 (CH=$\underline{C}H_2$), 127.94, 128.00, 128.67, 128.73 (Ph), 133.42 ($\underline{C}$H=CH_2), 138.55 (Ph-q).

β-anomer: colourless oil (0.10 g, 0.32 mmol, 88%), HRMS (ESI+) *m/z*: [M+Na] calcd. 333.1314 for $C_{16}H_{22}O_6Na$, found

333.1315; t_R (Method *X*) 7.9 min; IR (cm^{-1}): 3407, 2922, 2877, 1454, 1406, 1358, 1207, 1160, 1105, 1071, 1029, 928, 737, 699, 603; $[\alpha]_D^{20}$ = -28° (*c* 1.0, CH_2Cl_2); ^{1}H-NMR (600 MHz, $CDCl_3$): 3.35 (*ddd*, *J* = 9.5, 4.9, 3.6, H-5), 3.42 (pseudo-*t*, *J* = 9.0, H-3), 3.54 (*dd*, *J* = 9.1, 7.8, H-2), 3.59 (pseudo-*t*, *J* = 9.3, H-4), 3.77 (*dd*, *J* = 11.8, 4.8, H-6b), 3.87 (*dd*, *J* = 11.9, 3.5, H-6a), 4.13 (*m*, *J* = 12.7, 6.3, 1.3, allylic), 4.36 (*d*, *J* = 7.8, H-1), 4.36 (*m*, *J* = 12.5, 4.4, 1.4, allylic), 4.76, 5.00 (*d*, 1H each, *J* = 11.6, benzylic), 5.23 (*m*, *J* = 10.4, 2.5, 1.2, CH=C$\underline{H}_2$), 5.32 (*m*, *J* = 17.2, 2.9, 1.4, CH=C$\underline{H}_2$), 5.93 (*m*, *J* = 17.1, 10.6, 6.4, 5.6, C$\underline{H}$=CH_2), 7.28-7.39 (*m*, 5H, Ph-H); ^{13}C-NMR (150 MHz, $CDCl_3$): 62.53 (C-6), 70.14 (C-4), 70.60 (allylic), 74.47 (C-2), 74.74 (benzylic), 75.23 (C-5), 83.68 (C-3), 101.99 (C-1), 118.20 (CH=$\underline{C}H_2$), 128.03, 128.67 (Ph), 133.64 ($\underline{C}$H=CH_2), 138.49 (Ph-q). ^{13}C shift of C-1 for both anomers matches literature data.[128]

4.4.5 Allyl 3-*O*-(2-naphthyl)methyl-2,4,6-tri-*O*-acetyl-α,β-D-glucopyranoside (8b)

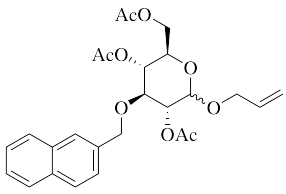

8b

3-*O*-(2-Naphthyl)methyl-1,2;5,6-di-*O*-isopropylidene-α-D-glucofuranose (**2b**) (0.48 g, 1.2 mmol) was glucosylated with allyl alcohol (4.6 mL) according to the General procedure 4.4.1. The resulting residue, was added to pyridine-acetic anhydride (5.0 mL, 1:1 V:V), and stirred overnight. After concentration under reduced pressure, water and DCM were added, the layers separated, and solvent removed. Purification by column chromatography (SiO_2, 3:1 *n*-pentane:EtOAc) afforded **8b** (0.46 g, 0.94 mmol, 78%, 73:27 α:β). Partial anomeric separation yielded:

α-anomer: yellow oil (0.22 g, 0.45 mmol, 38%), HRMS (ESI+) *m/z*: [M+Na] calcd. 509.1788 for $C_{26}H_{30}O_9Na$, found 509.1788; IR (cm^{-1}): 2925, 1745, 168, 1223, 1081, 1038; $[\alpha]_D^{20}$ = +58° (*c* 1.0, CH_2Cl_2); ^{1}H-NMR (600 MHz, $CDCl_3$): 1.88, 2.04, 2.09 (*s*, 3H each, Me), 3.94 (*ddd*, *J* = 10.2, 4.8, 2.4, H-5), 4.03 (*m*, *J* = 13.1, 6.2, 1.3, allylic), 4.07 (*dd*, *J* = 12.3, 2.4, H-6a), 4.07 (*t*, *J* = 9.6, H-3), 4.18 (*m*, *J* = 13.1, 6.2, 1.3, allylic), 4.21 (*dd*, *J* = 12.3, 4.8, H-6b), 4.78, 4.88 (*d*, 1H each, *J* = 12.1, benzylic), 4.92 (*dd*, *J* = 10.0, 3.7, H-2), 5.12 (*d*, *J* = 3.7, H-1), 5.13 (*dd*, *J* = 10.1, 9.4, H-4), 5.23 (*m*, *J* = 10.4, 2.6, 1.2, CH=C$\underline{H}_2$), 5.31 (*m*, *J* = 17.1, 3.1, 1.6, CH=C$\underline{H}_2$), 5.89 (*m*, *J* = 17.0, 10.6, 6.3, 5.3, C$\underline{H}$=CH_2), 7.36 (*dd*, *J* = 8.4, 1.6, Ar-H), 7.44-7.50 (*m*, 2H, Ar-H), 7.71 (*s*(br), Ar-H), 7.79-7.83 (*m*, 3H, Ar-H); ^{13}C-NMR (150 MHz, $CDCl_3$): 20.76, 20.77, 20.88 (Me), 62.18 (C-6), 67.83 (C-5), 68.68 (allylic), 69.78 (C-4), 73.29 (C-2), 74.99 (benzylic), 77.48 (C-3), 95.09 (C-1), 118.15 (CH=$\underline{C}H_2$), 125.51, 125.96, 126.11, 126.20, 127.66, 127.88, 128.13 (Ar), 132.92 (Ar-q), 133.24 ($\underline{C}$H=CH_2), 133.26, 135.69 (Ar-q), 170.78, 170.08, 169.49 (CO).

β-anomer: yellow oil (0.13 g, 0.28 mmol, 13%), HRMS (ESI+) *m/z*: [M+Na] calcd. 509.1788 for $C_{26}H_{30}O_9Na$, found 509.1787; IR (cm^{-1}): 2926, 1754, 1370, 1221, 1040; $[\alpha]_D^{20}$ = +10° (*c* 1.0, CH_2Cl_2); ^{1}H-NMR (600 MHz, $CDCl_3$): 1.94, 1.98, 2.09 (*s*, 3H each, Me), 3.59 (*ddd*, *J* = 9.9, 5.1, 2.6, H-5), 3.75 (*t*, *J* = 9.3, H-3), 4.08 (*m*, *J* = 13.3, 6.2, 1.3, allylic), 4.13 (*dd*, *J* = 12.2, 2.6, H-6a), 4.21 (*dd*, *J* = 12.2, 5.1, H-6b), 4.33 (*m*, *J* = 13.3, 4.8, 1.6, allylic), 4.47 (*d*, *J* = 7.9, H-1), 4.77 (*ABq*, *J* = 11.8, benzylic), 5.12 (*dd*, *J* = 9.4, 7.9, H-2), 5.17 (*dd*, *J* = 10.0, 9.2, H-4), 5.19 (*m*, *J* = 10.5, 2.9, 1.4, CH=C$\underline{H}_2$), 5.26 (*m*, *J* = 17.3, 3.3, 1.6, CH=C$\underline{H}_2$), 5.85 (*m*, C$\underline{H}$=CH_2), 7.35 (*dd*, *J* = 8.5, 1.6, Ar-H), 7.48 (*m*, Ar-H), 7.69 (*s*(br), Ar-H), 7.81 (*m*, *J* = 8.2, 7.5, Ar-H); ^{13}C-NMR (150 MHz, $CDCl_3$): 20.73, 20.79, 20.88 (Me), 62.31 (C-6), 69.66 (C-4), 69.76 (allylic), 72.06 (C-5), 72.53 (C-2), 73.77 (benzylic), 80.00 (C-3), 99.78 (C-1), 117.44 (CH=$\underline{C}H_2$), 125.74, 126.04, 126.22, 126.53, 127.67, 127.89, 128.20 (Ar), 132.98, 133.08 (Ar-q), 133.50 ($\underline{C}$H=CH_2), 135.23 (Ar-q), 169.23, 169.36, 170.82 (CO).

4.4.6 Allyl 3-*O*-(2-naphthyl)methyl-α,β-D-glucopyranoside (4b)

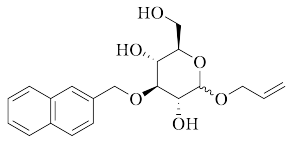

4b

Both anomers of the acetylated sugar (**8b**) (α-anomer: 0.17 g, 0.36 mmol, β-anomer: 0.10 g, 0.21 mmol), were deacetylated according to the General procedure 4.4.2. Purification of the resulting residue, was performed by passing through a pad of SiO_2 (EtOAc), affording both anomers of **4b**:

α-anomer: white solids (0.11 g, 0.31 mmol, 86%), mp. 96-99°C; HRMS (ESI+) *m/z*: [M+Na] calcd. 383.1471 for $C_{20}H_{24}O_6Na$, found 383.1470; t_R (Method *X*) 14.6 min; IR (cm^{-1}): 3382, 3055, 2923, 1347, 1124, 1084, 1031, 930, 856, 819, 748, 476; $[\alpha]_D^{20}$ = +85° (*c* 1.0, CH_2Cl_2); ^{1}H-NMR (600 MHz, $CDCl_3$): 1.92 (*dd*, *J* = 7.0, 6.8, 6-OH), 2.17 (*d*, *J* = 9.6, 2-OH), 2.38 (*m*, *J* = 2.5, 4-OH), 3.61 (*ddd*, *J* = 9.1, 6.1, 2.2, H-4), 3.67 (*t*, *J* = 8.9, H-3), 3.70 (*m*, *J* = 9.1, 5.2, 4.3, H-5), 3.73 (*td*, *J* = 9.3, 3.9, H-2), 3.78 (*ddd*, *J* = 7.1, 4.7, H-6b), 3.84 (*ddd*, *J* = 11.7, 5.3, 3.7, H-6a), 4.06 (*m*, *J* = 12.8, 6.3, 1.3, allylic), 4.24 (*m*, *J* = 12.8, 5.4, 1.4, allylic), 4.90 (*t*, *J* = 11.8, benzylic), 4.93 (*d*, *J* = 3.8, H-1), 5.21 (*d*, *J* = 11.7, benzylic), 5.25 (*m*, *J* = 10.4, 2.4, 1.1, CH=C$\underline{H}_2$), 5.32 (*m*, *J* = 17.2, 3.0, 1.5, CH=C$\underline{H}_2$), 5.93 (*m*, *J* = 17.1, 10.2, 6.4, 5.5, C$\underline{H}$=CH_2), 7.54-7.52 (*m*, 3H, Ar-H), 7.81-7.87 (*m*, 4H, Ar-H); ^{13}C-NMR (150 MHz, $CDCl_3$): 62.56 (C-6), 68.69 (allylic), 70.28 (C-4), 71.14 (C-5), 72.97 (C-2), 75.04 (benzylic), 82.88 (C-3), 97.73 (C-1), 118.26 (CH=$\underline{C}H_2$), 125.81, 126.05, 126.25, 126.70, 127.95, 128.52 (Ar), 133.07 (Ar-q), 133.41 ($\underline{C}$H=CH_2), 135.83 (Ar-q).

β-anomer: yellow wax (65 mg, 0.18 mmol, 87%), HRMS (ESI+) *m/z*: [M+Na] calcd. 383.1471 for $C_{20}H_{24}O_6Na$, found 383.1468; t_R (Method *X*) 14.6 min; IR (cm^{-1}): 3419, 2923, 2855, 1458, 1366, 1238, 1106, 1076, 1038, 820, 754, 476; $[\alpha]_D^{20}$ = -26° (*c* 1.0, CH_2Cl_2); ^{1}H-NMR (600 MHz, $CDCl_3$): 3.36 (*ddd*, *J* = 9.6, 5.0, 3.6, H-5), 3.48 (pseudo-*t*, *J* = 9.0, H-3), 3.58 (*dd*,

J = 9.2, 7.8, H-2), 3.63 (pseudo-*t*, *J* = 9.3, H-4), 3.78 (*dd*, *J* = 11.8, 5.0, H-6b), 3.88 (*dd*, *J* = 12.0, 3.6, H-6a), 4.14 (*m*, *J* = 12.7, 6.3, allylic), 4.37 (*m*, *J* = 12.6, allylic), 4.37 (*d*, *J* = 7.7, H-1), 4.93, 5.17 (*d*, 1H each, *J* = 11.8, benzylic), 5.24 (*m*, *J* = 10.4, CH=C$\underline{H}_2$), 5.32 (*m*, *J* = 17.2, CH=C$\underline{H}_2$), 5.94 (*m*, *J* = 17.1, 10.9, C$\underline{H}$=CH$_2$), 7.45-7.54 (*m*, 3H, Ar-H), 7.80-7.88 (*m*, 4H, Ar-H); ^{13}C-NMR (150 MHz, $CDCl_3$): 62.63 (C-6), 70.27 (C-4), 70.63 (allylic), 74.61 (C-2), 74.78 (benzylic), 75.23 (C-5), 83.54 (C-3), 102.01 (C-1), 118.22 (CH=$\underline{C}$H$_2$), 125.82, 126.08, 126.27, 126.33, 126.89, 127.77, 127.96, 128.56 (Ar), 133.09, 133.33 (Ar-q), 133.62 ($\underline{C}$H=CH$_2$), 135.85 (Ar-q).

4.4.7 Allyl 3-*O*-(*p*-phenyl)benzyl-D-glucopyranoside (4c)

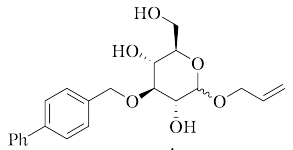

4c

3-*O*-(*p*-Phenyl)benzyl-1,2;5,6-di-*O*-isopropylidene-α-D-glucofuranose (**2c**) (1.0 g, 2.4 mmol) was glucosylated with allyl alcohol (9.1 mL) according to the General proceude 4.4.1. Column chromatography (SiO_2, 1:2 *n*-pentane:EtOAc) gave an anomeric mixture of **4c** as white solids (0.49 g, 1.3 mmol, 54%, 73:27 α:β), mp. 98-104°C; HRMS (ESI+) *m/z*: [M+Na] calcd. 409.1627 for $C_{22}H_{26}O_6Na$, found 409.1624; t_R (Method *X*) 17.8 min; IR (cm^{-1}): 3301, 2919, 2886, 1487, 1396, 1356, 1217, 1034, 923, 824, 759, 696, 518;

^{1}H-NMR (600 MHz, $CDCl_3$): α-anomer: 1.94 (*t*, *J* = 6.3, 6-OH), 2.17 (*d*, *J* = 9.6, 2-OH), 2.41 (*d*, *J* = 2.5, 4-OH), 3.65 (pseudo-*t*, *J* = 9.0, H-3), 3.59 (*td*, *J* = 9.2, 2.2, H-4), 3.70 (*td*, *J* = 9.5, 4.0, H-2), 3.71 (*td*, *J* = 9.7, 3.2, H-5), 3.80 (*ddd*, *J* = 11.6, 7.0, 4.6, H-6b), 3.85 (*ddd*, *J* = 11.7, 4.8, 4.0, H-6a), 4.06 (*m*, *J* = 12.8, 6.3, 1.2, allylic), 4.25 (*m*, *J* = 12.8, 5.4, 1.4, allylic), 4.78 (*d*, *J* = 11.4, benzylic), 4.93 (*d*, *J* = 3.8, H-1), 5.09 (*d*, *J* = 11.6, benzylic), 5.25 (*m*, *J* = 10.4, 2.5, 1.2, CH=C$\underline{H}_2$), 5.33 (*m*, *J* = 17.2, 3.1, 1.5, CH=C$\underline{H}_2$), 5.94 (*m*, *J* = 17.3, 10.5, C$\underline{H}$=CH$_2$),

7.35 (*m*, *J* = 7.3, Ar-H), 7.44 (*m*, *J* = 7.9, Ar-H), 7.59 (*m*, *J* = 8.2, Ar-H); β-anomer: 2.02 (*t*, *J* = 6.7, 6-OH), 2.40 (*d*, *J* = 2.2, 2-OH), 3.39 (*ddd*, *J* = 9.5, 5.2, 3.8, H-5), 3.46 (pseudo-*t*, *J* = 9.0, H-3), 3.57 (*m*, *J* = 8.1, 1.8, H-2), 3.64 (*td*, *J* = 9.2, 2.4, H-4), 3.82 (*ddd*, *J* = 12.0, 6.6, 5.7, H-6b), 3.91 (*ddd*, *J* = 11.7, 5.5, 3.8, H-6a), 4.15 (*m*, *J* = 12.6, 6.3, 1.3, allylic), 4.39 (*m*, *J* = 12.6, 5.4, 1.4, allylic), 4.39 (*d*, *J* = 7.7, H-1), 4.80 (*d*, *J* = 11.3, benzylic), 5.07 (*d*, *J* = 11.6, benzylic), 5.25 (*m*, *J* = 10.4, 2.5, 1.2, CH=C$\underline{H}_2$), 5.33 (*m*, *J* = 17.2, 3.1, 1.5, CH=C$\underline{H}_2$), 5.94 (*m*, *J* = 17.3, 10.5, C$\underline{H}$=CH_2), 7.35 (*m*, *J* = 7.3, Ar-H), 7.44 (*m*, *J* = 7.9, Ar-H), 7.59 (*m*, *J* = 8.2, Ar-H);

^{13}C-NMR (150 MHz, $CDCl_3$): α-anomer: 62.57 (C-6), 68.70 (allylic), 70.28 (C-4), 71.15 (C-5), 72.95 (C-3, C-2) 74.71 (benzylic), 82.99 (C-3), 97.74 (C-1), 118.26 (CH=$\underline{C}H_2$), 127.13, 127.41, 128.41, 128.79 (Ar), 133.42 ($\underline{C}$H=CH_2), 137.52, 140.80, 140.94 (Ar-q); β-anomer: 62.71 (C-6), 70.33 (C-4), 70.64 (allylic), 74.46 (benzylic), 74.62 (C-2), 75.21 (C-5), 83.69 (C-3), 102.00 (C-1), 118.26 (CH=$\underline{C}H_2$), 127.13, 127.43, 128.47, 128.79 (Ar), 133.60 ($\underline{C}$H=CH_2), 137.44, 140.77, 140.99 (Ar-q).

4.4.8 Allyl 3-*O*-(3,5-di-*tert*-butyl)benzyl-D-glucopyranoside (4d)

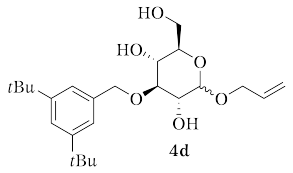

4d

According to the General procedure 4.4.1, 3-*O*-(3,5-di-*tert*-butyl)benzyl-1,2;5,6-di-*O*-isopropylidene-α-D-glucofuranose (**2d**) (0.45 g, 1.0 mmol) was glycosylated with allyl alcohol (3.8 mL). Purification by column chromatography (SiO_2, 1:1 *n*-pentane:EtOAc) afforded an anomeric mixture of **4d** as a limpid oil (0.12 g, 0.48 mmol, 49%, 81:19 α:β), HRMS (ESI+) *m*/*z*: [M+Na] calcd. 445.2566 for $C_{24}H_{38}O_6Na$, found 445.2566; t_R (Method *X*) 25.6 min; IR (cm^{-1}): 2953, 2925, 2868, 1600, 1477, 1460, 1393, 1363, 1249, 1202, 1081, 1032, 926, 895, 873, 714, 608, 528;

^{1}H-NMR (600 MHz, $CDCl_3$): α-anomer: 1.33 (*s*, 18H, *t*-Bu), 1.93 (*t*, *J* = 6.4, 6-OH), 2.13 (*d*, *J* = 9.5, 2-OH), 2.35 (*d*, *J* = 2.3, 4-OH), 3.56 (*ddd*, *J* = 9.4, 9.1, 2.0, H-4), 3.63 (pseudo-*t*, *J* = 9.0, H-3), 3.70 (*td*, *J* = 9.7, 3.0, H-2), 3.70 (*m*, H-5), 3.78 (*ddd*, *J* = 11.7, 7.0, 4.7, H-6b), 3.84 (*ddd*, *J* = 11.7, 5.0, 3.9, H-6a), 4.05 (*m*, *J* = 12.7, 6.2, 1.3, allylic), 4.24 (*m*, *J* = 12.7, 5.3, 1.4, allylic), 4.70 (*d*, *J* = 11.2, benzylic), 4.93 (*d*, *J* = 3.8, H-1), 5.03 (*d*, *J* = 11.2, benzylic), 5.24 (*m*, *J* = 10.4, 1.3, CH=C$\underline{H}_2$), 5.32 (*m*, *J* = 17.2, 1.5, CH=C$\underline{H}_2$), 5.94 (*m*, C$\underline{H}$=CH_2), 7.21 (*m*, *J* = 1.8, Ar-H), 7.38 (*m*, *J* = 1.8, Ar-H); β-anomer: 1.33 (*s*, 18H, *t*-Bu), 2.01 (*t*, *J* = 6.6, 6-OH), 2.34 (*d*, *J* = 2.4, 4-OH), 2.38 (*d*, *J* = 2.1, 2-OH), 3.38 (*ddd*, *J* = 9.7, 5.1, 3.6, H-5), 3.43 (pseudo-*t*, *J* = 9.0, H-3), 3.58 (*td*, *J* = 8.7, 2.2, H-4), 3.58 (*td*, *J* = 8.2, 2.0, H-2), 3.78 (*ddd*, *J* = 11.7, 7.0, 4.7, H-6b), 3.90 (*ddd*, *J* = 11.8, 5.7, 3.7, H-6a), 4.15 (*m*, *J* = 12.5, 6.3, 1.3, allylic), 4.38 (*m*, *J* = 12.6, 5.4, 1.4, allylic), 4.38 (*d*, *J* = 7.8, H-1), 4.71, 5.01 (*d*, 1H each, *J* = 11.5, benzylic), 5.24 (*m*, *J* = 10.4, 1.3, CH=C$\underline{H}_2$), 5.33 (*m*, *J* = 17.2, 1.5, CH=C$\underline{H}_2$), 5.94 (*m*, C$\underline{H}$=CH_2), 7.21 (*m*, *J* = 1.8, Ar-H), 7.38 (*m*, *J* = 1.8, Ar-H);

^{13}C-NMR (150 MHz, $CDCl_3$): α-anomer: 31.45 (*t*-Bu), 62.64 (C-6), 68.65 (allylic), 70.25 (C-4), 71.21 (C-5), 72.92 (C-2), 75.76 (benzylic), 82.91 (C-3), 97.80 (C-1), 118.13 (CH=$\underline{C}H_2$), 122.14, 122.31 (Ar), 133.45 ($\underline{C}$H=CH_2), 137.60, 151.21 (Ar-q); β-anomer: 31.45 (*t*-Bu), 62.77 (C-6), 70.31 (C-4), 70.61 (allylic), 74.53 (C-2), 75.26 (C-5), 75.56 (benzylic), 83.97 (C-3), 102.03 (C-1), 118.20 (CH=$\underline{C}H_2$), 122.17, 122.24 (Ar), 133.66 ($\underline{C}$H=CH_2), 137.60, 151.25 (Ar-q).

4.4.9 Allyl 3-*O*-*p*-nitrobenzyl-D-glucopyranoside (4i)

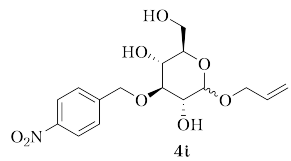

4i

3-*O*-*p*-Nitrobenzyl-1,2;5,6-di-*O*-isopropylidene-α-D-glucofuranose (**2i**) (0.52 g, 1.3 mmol) was glucosylated with allyl alcohol (5.1 mL), according to General procedure 4.4.1. After con-

centrating under reduced pressure, crystallisation from acetone gave an anomeric mixture of **4i** as white solis (0.32 g, 0.91 mmol, 69%, 76:24 α:β),

mp. 160-163°C; HRMS (ESI+) *m/z*: [M+Na] calcd. 378.1165 for $C_{16}H_{21}NO_8Na$, found 378.1164; t_R (Method *X*) 10.4 min; IR (cm^{-1}): 3443, 3378, 2918, 1602, 1503, 1454, 1348, 1120, 1086, 1023, 843, 711, 528, 439;

^{1}H-NMR (600 MHz, $CDCl_3$): α-anomer: 1.89 (*dd*, *J* = 7.1, 5.6, 6-OH), 2.13 (*d*, *J* = 10.0, 2-OH), 2.43 (*d*, *J* = 2.8, 4-OH), 3.63 (pseudo-*t*, *J* = 8.8, H-3), 3.67 (*m*, *J* = 8.7, 2.8, H-4), 3.70 (*dd*, *J* = 10.2, 4.1, H-2), 3.71 (*dd*, *J* = 9.0, 4.2, H-5), 3.80-3.89 (*m*, *J* = 11.3, 8.8, 6.9, 5.1, 4.2, H-6b, H-6a), 4.06 (*m*, *J* = 12.6, 6.4, 1.2, allylic), 4.25 (*m*, *J* = 12.7, 5.5, 1.4, allylic), 4.90 (*d*, *J* = 13.0, benzylic), 4.93 (*d*, *J* = 3.8, H-1), 5.16 (*d*, *J* = 12.8, benzylic), 5.25 (*m*, *J* = 10.3, 2.7, 1.3, CH=C$\underline{H}_2$), 5.33 (*m*, *J* = 17.2, 3.1, 1.7, CH=C$\underline{H}_2$), 5.93 (*m*, C$\underline{H}$=CH_2), 7.55 (*m*, 2H, *J* = 8.8, m-Ar-H), 8.21 (*m*, 2H, *J* = 8.5, o-Ar-H); β-anomer: 2.22 (*t*, *J* = 7.6, 6-OH), 2.38 (*d*, *J* = 2.1, 2-OH), 2.46 (*d*, *J* = 3.0, 4-OH), 3.40 (*ddd*, *J* = 9.5, 4.7, 3.8, H-5), 3.47 (pseudo-*t*, 9.0, H-3), 3.56 (*ddd*, *J* = 9.2, 7.9, 2.0, H-2) 3.68 (*m*, *J* = 9.8, 2.6, H-4), 3.92 (*ddd*, *J* = 10.6, 5.6, 3.8, H-6b), 3.74 (*m*, H-6a), 4.14 (*m*, *J* = 12.6, 6.4, 1.3, allylic), 4.38 (*d*, *J* = 7.9, H-1), 4.39 (*m*, *J* = 12.5, 5.4, 1.3, allylic), 4.90, 5.14 (*d*, 1H each, *J* = 12.8, benzylic), 5.25 (*m*, *J* = 10.3, 2.7, 1.3, CH=C$\underline{H}_2$), 5.33 (*m*, *J* = 17.2, 3.1, 1.7, CH=C$\underline{H}_2$), 5.93 (*m*, C$\underline{H}$=CH_2), 7.55 (*m*, 2H, *J* = 8.8, m-Ar-H), 8.21 (*m*, 2H, *J* = 8.5, o-Ar-H);

^{13}C-NMR (150 MHz, $CDCl_3$): α-anomer: 62.42 (C-6), 68.77 (allylic), 70.30 (C-4), 71.03 (C-5), 72.85 (C-2), 73.51 (benzylic), 83.47 (C-3), 97.63 (C-1), 118.44 (CH=$\underline{C}H_2$) 123.69, 127.81 (Ar), 133.28 ($\underline{C}$H=CH_2), 146.15 (Ar-q); β-anomer: 62.57 (C-6), 70.36 (C-4), 73.30 (benzylic), 70.65 (allylic), 74.58 (C-2), 75.10 (C-5), 84.02 (C-3), 101.85 (C-1), 118.44 (CH=$\underline{C}H_2$), 123.69, 127.90 (Ar), 133.28 ($\underline{C}$H=CH_2), 147.38 (Ar-q).

4.4.10 Methyl 3-*O*-benzyl-2,4,6-tri-*O*-acetyl-α,β-D-glucopyranoside (8μ)

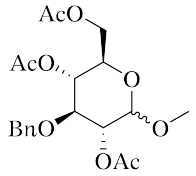

8μ

General procedure 4.4.1 was followed for 3-*O*-benzyl-1,2;5,6-di-*O*-isopropylidene-α-D-glucofuranose (**2a**) (0.49 g, 1.4 mmol), with methanol (5.4 mL). After concentrating under reduced pressure, pyridine-acetic anhydride (6.0 mL, 1:1 V:V), was added, and stirred overnight at room temperature. The reaction was concentrated under reduced pressure, and water and DCM were added, before separating the layers, and drying over $MgSO_4$. Column chromatography (SiO_2, 3:1 *n*-pentane:EtOAc) afforded **8μ** (0.46 g, 1.1 mmol, 80%, 62:38 α:β). Partial anomeric separation yielded:

α-anomer: colourless oil (0.20 g, 0.48 mmol, 35%), HRMS (ESI+) *m/z*: [M+Na] calcd. 433.1475 for $C_{20}H_{26}O_9Na$, found 433.1473; IR (cm^{-1}): 2940, 1743, 1455, 1370, 1224, 1130, 1037, 743, 700; $[\alpha]_D^{20}$ = +52° (*c* 1.0, CH_2Cl_2); ^{1}H-NMR (600 MHz, $CDCl_3$): 1.94, 2.06, 2.09 (*s*, 3H each, Me), 3.40 (*s*, 3H, OMe), 3.88 (*ddd*, *J* = 10.2, 4.9, 2.3, H-5), 3.98 (pseudo-*t*, *J* = 9.6, H-3), 4.08 (*dd*, *J* = 12.3, 2.4, H-6b), 4.20 (*dd*, *J* = 12.3, 5.0, H-6a), 4.60, 4.70 (*d*, 1H each, *J* = 11.9, benzylic), 4.88 (*dd*, *J* = 10.0, 3.7, H-2), 4.95 (*d*, *J* = 3.7, H-1), 5.08 (*dd*, *J* = 10.1, 9.4, H-4), 7.22-7.38 (*m*, 5H, Ph-H); ^{13}C-NMR (150 MHz, $CDCl_3$): 20.73, 20.75, 20.89, (CO<u>Me</u>), 55.35 (OMe), 62.23 (C-6), 67.59 (C-5), 69.80 (C-4), 73.25 (C-2), 74.95 (benzylic), 77.38 (C-3), 96.99 (C-1), 127.54, 127.72, 128.41 (Ph), 138.18 (Ph-q), 169.44, 170.06, 170.74 (CO). NMR matches previously reported data.[106]

β-anomer: white wax (0.19 g, 0.38 mmol, 27%), HRMS (ESI+) *m/z*: [M+Na] calcd. 433.1475 for $C_{20}H_{26}O_9Na$, found 433.1471; IR (cm^{-1}): 2924, 2853, 1745, 1454, 1372, 1220, 1038; $[\alpha]_D^{20}$ = -8° (*c* 1.0, CH_2Cl_2); ^{1}H-NMR (600 MHz, $CDCl_3$): 1.98, 2.02, 2.08 (*s*, 3H each, Me), 3.49 (*s*, 3H, OMe), 3.60 (*ddd*, *J* =

9.9, 5.0, 2.6, H-5), 3.70 (pseudo-*t*, *J* = 9.3, H-3), 4.13 (*dd*, *J* = 12.3, 2.5, H-6b), 4.22 (*dd*, *J* = 12.2, 5.0, H-6a), 4.35 (*d*, *J* = 7.9, H-1), 4.60 (*ABq*, 1H each, *J* = 11.3, benzylic), 5.05 (*dd*, *J* = 9.1, 8.1, H-2), 5.13 (pseudo-*t*, *J* = 9.6, H-4), 7.20-7.36 (*m*, 5H, Ph-H); ^{13}C-NMR (150 MHz, $CDCl_3$): 20.76, 20.78, 20.90 (CO<u>Me</u>), 56.74 (OMe), 62.30 (C-6), 69.62 (C-4), 72.07 (C-5), 72.40 (C-2), 73.75 (benzylic), 80.09 (C-3), 101.81 (C-1), 127.79, 127.84, 128.45 (Ph), 137.77 (Ph-q), 169.29, 169.33, 170.81 (CO). NMR for both anomers matches data previously reported.[129]

4.4.11 Methyl 3-*O*-benzyl-α,β-D-glucopyranoside (4μ)

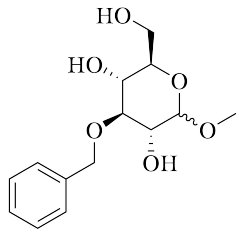

4μ

Both anomers of the acetylated sugar (**8μ**) (α-anomer: 0.11 g, 0.27 mmol, β-anomer: 94 mg, 0.19 mmol), were deacetylated, following the General procedure 4.4.2. The crude product was passed through a short column (SiO_2, 1:2 *n*-pentane:EtOAc), yielding both anomers of **4μ**:

α-anomer: white crystals (62 mg, 0.22 mmol, 81%), mp. 90-93°C; HRMS (ESI+) *m/z*: [M+Na] calcd. 307.1158 for $C_{14}H_{20}O_6Na$, found 307.1161; t_R (Method *X*) 5.2 min; IR (cm^{-1}): 3411, 2924, 2854, 1454, 1362, 1192, 1149, 1119, 1078, 1035, 739, 700; $[\alpha]_D^{20}$ = +96° (*c* 1.0, CH_2Cl_2); ^{1}H-NMR (600 MHz, $CDCl_3$): 1.91 (*dd*, *J* = 7.0, 5.8, 6-OH), 2.14 (*d*, *J* = 9.3, 2-OH), 2.30 (*d*, *J* = 2.4, 4-OH), 3.45 (*s*, 3H, OMe), 3.55 (*td*, *J* = 9.0, 2.3, H-4), 3.59 (pseudo-*t*, *J* = 8.8, H-3), 3.64 (*dt*, *J* = 9.3, 4.2, H-5), 3.68 (*td*, *J* = 9.2, 3.9, H-2), 3.79 (*ddd*, *J* = 11.8, 7.1, 4.7, H-6b), 3.90 (*ddd*, *J* = 11.7, 5.5, 3.7, H-6a), 4.73 (*d*, *J* = 11.6, benzylic), 4.76 (*d*, *J* = 3.9, H-1), 5.03 (*d*, *J* = 11.6, benzylic), 7.28-7.40 (*m*, 5H, Ph-H); ^{13}C-NMR (150 MHz, $CDCl_3$): 55.38 (OMe), 62.62 (C-6), 70.31 (C-4), 70.94 (C-5), 72.96 (C-2), 74.98 (benzylic),

82.81 (C-3), 99.62 (C-1), 127.98, 128.03, 128.70 (Ph), 138.55 (Ph-q).

β-anomer: white solids (42 mg, 0.15 mmol, 77%), mp. 100-105°C; HRMS (ESI+) *m/z*: [M+Na] calcd. 307.1158 for $C_{14}H_{20}O_6Na$, found 307.1154; t_R (Method *X*) 5.1 min; IR (cm^{-1}): 3406, 2924, 2854, 1354, 1377, 1360, 1212, 1106, 1078, 1038, 739, 700, 615; $[\alpha]_D^{20}$ = -2° (*c* 1.0, CH_2Cl_2); ^{1}H-NMR (600 MHz, $CDCl_3$): 1.99 (*m*, *J* = 6.3, 6-OH), 2.33 (*d*, *J* = 1.8, 4-OH), 2.35 (*d*, *J* = 1.8, 2-OH), 3.38 (*m*, *J* = 9.6, 5.0, 3.7, H-5), 3.42 (pseudo-*t*, *J* = 9.0, H-3), 3.50 (*ddd*, *J* = 9.2, 7.8, 1.5, H-2), 3.57 (*s*, 3H, OMe), 3.60 (*m*, *J* = 9.2, H-4), 3.79 (*ddd*, *J* = 11.6, 6.4, 5.1, H-6b), 3.91 (*dt*, *J* = 11.6, 4.1, H-6a), 4.24 (*d*, *J* = 7.7, H-1), 4.76, 5.01 (*d*, 1H each, *J* = 11.7, benzylic), 7.29-7.40 (*m*, 5H, Ph-H); ^{13}C-NMR (150 MHz, $CDCl_3$): 57.42 (OMe), 62.70 (C-6), 70.34 (C-4), 74.60 (C-2), 74.74 (benzylic), 75.19 (C-5), 83.64 (C-3), 103.96 (C-1), 128.03, 128.07, 128.72 (Ph), 138.47 (Ph-q). NMR for both anomers matches data previously reported.[129]

4.4.12 Allyl 3-*O*-benzyl-α-D-xylopyranoside (4ø)

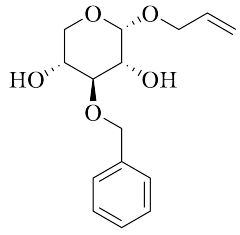

4ø

1,2-*O*-Isopropylidene-3-*O*-benzyl-α-D-xylofuranose (**2ø**) (0.59 g, 2.1 mmol) was glycosylated, according to the General procedure 4.4.1, using allyl alochol (8.1 mL). Crystallisation from ethanol-water gave **4ø** as white needles (0.31 g, 0.66 mmol, 31%),

mp. 90-93°C; HRMS (ESI+) *m/z*: [M+Na] calcd. 303.1208 for $C_{15}H_{20}O_5Na$, found 303.1208; t_R (Method *X*) 11.9 min; IR (cm^{-1}): 3436, 3311, 2933, 2867, 1454, 1353, 1141, 1097, 1035, 945, 921, 762, 742, 701, 535; $[\alpha]_D^{20}$ = +72° (*c* 1.0, CH_2Cl_2);

^{1}H-NMR (600 MHz, $CDCl_3$): 2.25 (*d*, *J* = 7.8, OH-2), 2.50 (*d*, *J* = 4.1, OH-4), 3.67 (*m*, 5H, H-2, H-3, H-4, H-5a, H-5b), 4.06 (*m*, *J* = 12.7, 6.3, 1.3, allylic), 4.28 (*m*, *J* = 12.7, 5.3, 1.4, allylic), 4.71, 4.95 (*d*, 1H each, *J* = 11.5, benzylic), 4.83 (*d*, *J* = 3.2, H-1), 5.24 (*m*, *J* = 10.4, 1.2, CH=C$\underline{H}_2$), 5.32 (*m*, *J* = 17.2, 1.5, term-all), 5.93 (*dddd*, *J* = 17.1, 10.5, 6.4, 5.4, C$\underline{H}$=CH_2), 7.29-7.39 (*m*, 5H, Ph-H); ^{13}C-NMR (150 MHz, $CDCl_3$): 62.89 (C-5), 68.75 (C-6), 68.81 (C-4), 72.11 (C-2), 74.43 (benzylic), 81.71 (C-3), 97.68 (C-1), 118.04 (CH=$\underline{C}H_2$), 127.91, 127.99, 128.63 (Ph), 133.57 ($\underline{C}$H=CH_2), 138.38 (Ph-q). NMR is consistent with previously reported data.[130]

4.4.13 Allyl 3-*O*-benzyl-β-D-allopyranoside (4ð) and allyl 3-*O*-benzyl-β-D-allofuranoside (3ð)

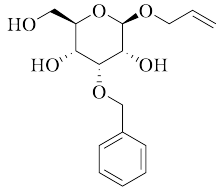

4ð

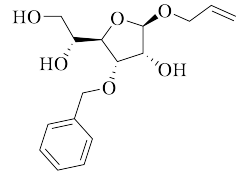

3ð

3-*O*-Benzyl-1,2;5,6-di-*O*-isopropylidene-α-D-allofuranose (**2ð**) (0.20 g, 0.8 mmol) was glucosylated with allyl alcohol (2.9 mL), following General procedure 4.4.1. Purification by column chromatography (SiO_2, 3:7 *n*-pentane:EtOAc) gave **3ð** and **4ð**:

β-Allopyranoside (**4ð**): white wax (46 mg, 0.15 mmol, 19%), HRMS (ESI+) *m/z*: [M+Na] calcd. 333.1314 for $C_{16}H_{22}O_6Na$, found 333.1312; t_R (Method *X*) 9.9 min; IR (cm^{-1}): 3420, 2923, 2855, 1455, 1398, 1347, 1211, 1154, 1088, 1032, 926, 733, 699; $[\alpha]_D^{20}$ = -8° (*c* 1.0, CH_2Cl_2); ^{1}H-NMR (600 MHz, $CDCl_3$): 2.00 (*t*, *J* = 6.6, 6-OH), 2.30 (*d*, *J* = 10.1, 4-OH), 2.41 (*d*, *J* = 4.1, 2-OH), 3.56 (*ddd*, *J* = 7.7, 3.0, 3.9, H-2), 3.62 (*dt*, *J* = 9.7, 3.2, H-4), 3.67 (*ddd*, *J* = 9.5, 5.0, 3.3, H-5), 3.75 (*ddd*, *J* = 11.9, 6.9, 5.0, H-6b), 3.87 (*ddd*, *J* = 11.8, 6.0, 3.4, H-6a), 4.12 (pseudo-*t*, *J* = 3.0, H-3), 4.14 (*tdd*, *J* = 12.6, 6.1, 1.3, allylic), 4.38 (*m*, *J* = 12.6, 5.6, 1.4, allylic), 4.69, 5.07 (*d*, 1H each, 11.5, benzylic), 4.76 (*d*, *J* = 7.8, H-1), 5.23 (*m*, *J* =

10.4, 1.3, CH=C$\underline{H}_2$), 5.32 (*m*, *J* = 17.2, 1.6, CH=C$\underline{H}_2$), 5.95 (*m*, *J* = 12.3, 5.7, 7.0, C$\underline{H}$=CH$_2$), 7.30-7.40 (*m*, 5H, Ph-H); ^{13}C-NMR (150 MHz, $CDCl_3$): 62.94 (C-6), 67.99 (C-4), 70.55 (allylic), 72.70 (C-2), 74.87 (C-5), 75.38 (benzylic), 78.24 (C-3), 99.98 (C-1), 117.98 (all-ter), 127.91, 128.06, 128.66 (Ph), 133.80 (C$\underline{H}$=CH$_2$). 138.25 (Ph-q).

β-Allofuranoside (**3ð**): white solids (55 mg, 0.18 mmol, 23%), mp. 80-84°C; HRMS (ESI+) *m/z*: [M+Na] calcd. 333.1314 for $C_{16}H_{22}O_6Na$, found 333.1315; t_R (Method *X*) 9.6 min; IR (cm^{-1}): 3421, 2927, 1455, 1407, 1345, 1260, 1208, 1112, 1084, 1042, 1027, 936, 738, 700; $[\alpha]_D^{20}$ = -36° (*c* 1.0, CH_2Cl_2); ^{1}H-NMR (600 MHz, $CDCl_3$): 1.94 (*dd*, *J* = 7.1, 5.5, OH-6), 2.59 (*d*, *J* = 3.3, OH-5), 2.69 (*d*, *J* = 3.2, OH-2), 3.67 (*ddd*, *J* = 11.2, 5.9, 5.6, H-6b), 3.71 (*ddd*, *J* = 11.2, 7.2, 4.3, H-6a), 3.87 (*m*, *J* = 9.8, 3.5, 6.1, H-5), 4.03 (*m*, *J* = 12.8, 6.0, allylic), 4.08 (*dd*, *J* = 3.5, 4.5, H-2), 4.11 (*dd*, *J* = 6.1, 4.6, H-4), 4.19 (*m*, *J* = 12.8, 5.4, allylic), 4.38 (*dd*, *J* = 6.0, 5.0, H-3), 4.61 (*ABq*, 2H, *J* = 11.3, benzylic), 5.01 (*s*, H-1), 5.22 (*m*, *J* = 10.3, CH=C$\underline{H}_2$), 5.29 (*m*, *J* = 16.2, CH=C$\underline{H}_2$), 5.89 (*m*, *J* = 17.0, 10.6, 5.2, C$\underline{H}$=CH$_2$), 5.33-7.40 (*m*, 5H, Ph-H); ^{13}C-NMR (150 MHz, $CDCl_3$): 63.30 (C-6) 69.19 (allylic), 72.01 (C-5), 73.18 (benzylic), 73.47 (C-2), 78.24 (C-3), 82.69 (C-4), 107.12 (C-1), 118.09 (CH=C$\underline{H}_2$), 128.26, 128.56, 128.67, 128.79 (Ph), 133.44 (C$\underline{H}$=CH$_2$), 136.72 (Ph-q). NMR is consistent with with available literature data for both anomers.[131]

4.4.14 Allyl 3-*O*-benzyl-β-D-glucofuranoside (3a-β)

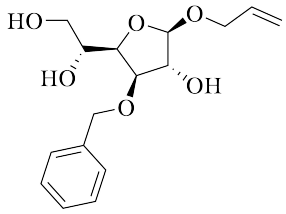

3a

HCl (69 µL, 37%, 1.6 equiv) was added to allyl alcohol (2.0 mL), with the 3-*O*-Benzyl-1,2;5,6-di-*O*-isopropylidene-α-D-glucofu-

ranose (**2a**) (0.18 g, 0.53 mmol). The reaction was stirred at room temperature for 16 h, before the reaction was quenched with Et_3N (3.2 equiv) and concentrated under reduced pressure. Purification by column chromatography (SiO_2, 2:1 *n*-pentane:EtOAc) yielded **3a-β** as a white wax (23 mg, 75 μmol, 14%),

HRMS (ESI) *m/z*: [M+Na] calcd. 333.1314 for $C_{16}H_{22}O_6Na$, found 333.1316; t_R (Method *X*) 10.4 min; IR (cm^{-1}): 3367, 2923, 1455, 1356, 1029, 927, 740, 699; $[\alpha]_D^{20}$ = -71° (*c* 1.0, CH_2Cl_2);

^{1}H-NMR (600 MHz, $CDCl_3$): 1.68, 2.21, 3.15 (*s*(br), 1H each, OH), 3.70 (*dd*, *J* = 11.5, 5.5, H-6b), 3.82 (*dd*, *J* = 11.4, 3.3, H-6a), 3.98 (*m*, *J* = 12.9, 6.1, 1.4, allylic), 4.03 (*ddd*, *J* = 8.8, 5.6, 3.4, H-5), 4.17 (*dd*, *J* = 6.6, 3.0, H-3), 4.21 (*m*, *J* = 12.9, 5.1, 1.4, allylic), 4.25 (*dd*, *J* = 8.9, 6.5, H-4), 4.35 (*m*, *J* = 2.7, 2.0, H-2), 4.59, 4.79 (*d*, 1H each, *J* = 11.7, benzylic), 4.92 (*d*, *J* = 1.8, H-1), 5.19 (*m*, *J* = 10.4, 1.4, CH=C$\underline{H}_2$), 5.29 (*m*, *J* = 17.2, 1.6, CH=C$\underline{H}_2$), 5.80 (*m*, *J* = 16.9, 10.6, 5.2, C$\underline{H}$=CH_2), 7.30-7.39 (*m*, 5H, Ph-H); ^{13}C-NMR (150 MHz, $CDCl_3$): 64.06 (C-6), 68.88 (allylic), 71.03 (C-5), 72.45 (benzylic), 79.19 (C-2), 79.27 (C-4), 84.46 (C-3), 107.49 (C-1), 117.44 (CH=$\underline{C}H_2$), 127.85, 128.25, 128.73 (Ph), 133.80 ($\underline{C}$H=CH_2), 137.16 (Ph-q).

4.4.15 1,2,4,6-Tetra-*O*-acetyl-3-*O*-benzyl-D-glucopyranose (IC-3)

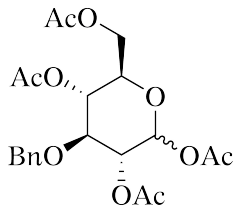

IC-3

3-*O*-Benzyl-1,2;5,6-di-*O*-isopropylidene-α-D-glucofuranose (**2a**) (0.79 g, 2.2 mmol) was glucosylated in water (8.6 mL), following the General procedure 4.4.1. The resulting residue was added to pyridine-acetic anhydride (9.0 mL, 1:1 V:V), and

stirred overnight at room temperature. After concentration under reduced pressure, water and DCM were added, the layers separated, and solvent removed. Column chromatography (SiO_2, 3:1 *n*-pentane:EtOAc) resulted in an anomeric mixture of **IC-3** as a yellow oil (0.79 g, 1.8 mmol, 80%, 30:70 α:β),

HRMS (ESI+) *m/z*: [M+Na] calcd. 461.1424 for $C_{21}H_{26}O_{10}Na$, found 461.1418; t_R (Method *X*) 23.4 min (β), 23.8 min (α); IR (cm^{-1}): 2919, 2850, 1746, 1455, 1368, 1215, 1058, 1038, 908, 738, 700, 601;

^{1}H-NMR (600 MHz, $CDCl_3$): α-anomer: 1.97, 1.99, 2.09, 2.17 (*s*, 3H each, Me), 3.96 (pseudo-*t*, *J* = 9.7, H-3), 4.01 (*ddd*, *J* = 10.2, 4.4, 2.4, H-5), 4.07 (*dd*, *J* = 12.3, 2.4, H-6b), 4.20 (*dd*, *J* = 12.5, 4.5, H-6a), 4.62, 4.71 (*d*, 1H each, *J* = 11.9, benzylic), 5.07 (*dd*, *J* = 10.0, 3.7, H-2), 5.16 (*dd*, *J* = 10.1, 9.6, H-4), 6.32 (*d*, *J* = 3.6, H-1), 7.23-7.36 (*m*, 5H, Ph-H); β-anomer: 1.98, 1.98, 2.08, 2.10 (*s*, 3H each, Me), 3.73 (*ddd*, *J* = 9.9, 4.9, 2.3, H-5), 3.75 (pseudo-*t*, *J* = 9.3, H-3), 4.10 (*dd*, *J* = 12.3, 2.3, H-6b), 4.22 (*dd*, *J* = 12.5, 4.9, H-6a), 4.61 (*ABq*, *J* = 10.9, benzylic), 5.16 (pseudo-*t*, *J* = 9.6, H-4), 5.17 (*dd*, *J* = 9.2, 8.2, H-2), 5.65 (*d*, *J* = 8.2, H-1); 7.22-7.36 (*m*, 5H, Ph-H);

^{13}C-NMR (150 MHz, $CDCl_3$): α-anomer: 20.90, 20.59, 20.73, 20.71 (Me), 61.80 (C-6), 69.05 (C-4), 70.28 (C-5), 71.52 (C-2), 74.77 (benzylic), 77.01 (C-3), 89.52 (C-1), 127.63, 127.84, 127.89, 128.50, 128.63 (Ph), 137.56 (Ph-q), 168.76, 169.24, 169.57, 170.79 (CO). β-anomer: 20.59, 20.71, 20.73, 20.90 (Me), 61.80 (C-6), 69.05 (C-4), 71.55 (C-2), 73.03 (C-5), 74.19 (benzylic), 79.98 (C-3), 92.00 (C-1), 127.51, 127.80, 127.96, 128.46, 128.51 (Ph), 137.94 (Ph-q), 169.07, 169.26, 169.28, 170.74 (CO). NMR is consistent with previously reported data for both anomers.[132]

4.4.16 3-*O*-Benzyl-2,4,6-tri-*O*-acetyl-D-glucopyranose (IC-4)

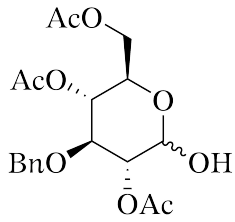

IC-4

1,2,4,6-Tetra-*O*-acetyl-3-*O*-benzyl-D-glucopyranose (**IC-3**) (0.21 g, 0.47 mmol) was dissolved in THF (2.3 mL, 0.2 M). Benzylamine (0.26 mL, 2.3 mmol, 5 equiv) was added dropwise, and the reaction stirred at room temperature for 3.5 h. The solvent was evaporated under reduced pressure, dissolved in Et_2O, extracted three times with NH_4Cl (sat.), and the solvent evaporated under reduced pressure. Purification by column chromatography (SiO_2, 2:1 → 1:1 *n*-pentane:EtOAc) afforded an anomeric mixture of **IC-4** as a yellow wax (39 mg, 0.10 mmol, 21%, 75:25 α:β),

HRMS (ESI+) *m/z*: [M+Na] calcd. 419.1318 for $C_{19}H_{24}O_9Na$, found 419.1314; t_R (Method *X*): 17.6 min (β-anomer), 18.7 min (α-anomer); IR (cm^{-1}): 3433, 3031, 2954, 2927, 1743, 1368, 1225, 1151, 1036, 984, 746, 699, 601;

^{1}H-NMR (600 MHz, $CDCl_3$): α-anomer: 1.95, 2.06, 2.09 (*s*, 3H each, Me), 4.04 (pseudo-*t*, *J* = 9.6, H-3), 4.11 (*dd*, *J* = 12.0, 10.0, H-6b), 4.15 (*m*, H-5), 4.17 (*dd*, *J* = 12.0, 4.5, H-6a), 4.62, 4.71 (*d*, 1H each, *J* = 11.7, benzylic), 4.87 (*dd*, *J* = 10.0, 3.6, H-2), 5.10 (pseudo-*t*, *J* = 9.6, H-4), 5.45 (*d*, *J* = 3.6, H-1), 7.22-7.35 (*m*, 5H, Ph-H); β-anomer: 1.97, 2.06, 2.09 (*s*, 3H each, Me), 3.63 (*ddd*, *J* = 10.1, 5.2, 2.4, H-5), 3.73 (pseudo-*t*, *J* = 9.4, H-3), 4.14 (*m*, *J* = 12.7, 2.2, H-6b), 4.20 (*dd*, *J* = 12.4, 5.2, H-6a), 4.61 (*d*, *J* = 11.7, benzylic), 4.62 (*d*, *J* = 8.2, H-1), 4.66 (*d*, *J* = 11.8, benzylic), 4.88 (*dd*, *J* = 9.2, 8.3, H-2), 5.10 (pseudo-*t*, *J* = 9.6, H-4), 7.22-7.35 (*m*, 5H, Ph-H);

^{13}C-NMR (150 MHz, $CDCl_3$): α-anomer: 20.76, 20.80, 20.88 (Me), 62.27 (C-6), 67.79 (C-5), 69.77 (C-4), 73.41 (C-2), 74.94

(benzylic), 76.86 (C-3), 90.37 (C-1), 127.58, 127.76, 128.44 (Ph), 138.14 (Ph-q), 169.52, 170.12, 170.93 (CO); β-anomer: 20.76, 20.80, 20.88 (Me), 62.27 (C-6), 69.64 (C-4), 72.32 (C-5), 74.52 (benzylic), 75.46 (C-2), 79.58 (C-3), 95.89 (C-1), 127.71, 127.95, 128.50 (Ph), 137.70 (Ph-q), 169.42, 170.89, 171.32 (CO).

4.4.17 *O*-(3-*O*-Benzyl-2,4,6-tri-*O*-acetyl-α-D-glucopyranosyl)trichloroacetimidate (IC-5)

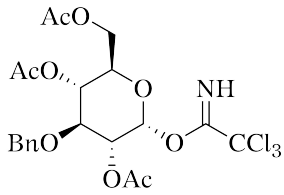

IC-5

3-*O*-Benzyl-2,4,6-tri-*O*-acetyl-D-glucopyranose (**6**) (39 mg, 99 μmol) was added to dry DCM (0.8 mL, 0.12 M), with 3 Å molecular sieve under inert atmosphere and cooled to 0°C. DBU (7 μL, 45 μmol, 0.46 equiv) and CCl_3CN (7 μL, 0.73 mmol, 7.4 equiv) were added dropwise, and stirred at 0°C for 4 h. The solvent was evaporated under reduced pressure and the residue was purified by column chromatography (SiO_2, 8:1 → 6:1) to afford **IC-5** as a yellow wax (0.23 g, 42 μmol, 42%),

^{1}H-NMR (400 MHz, $CDCl_3$): 1.98, 1.99, 2.07 (*s*, 3H each, Me), 4.08 (*pseudo-t*, *J* = 9.8, H-3), 4.10 (*m*, H-5), 4.11 (*dd*, *J* = 12.5, 2.3, H-6b), 4.21 (*dd*, *J* = 12.5, 4.8, H-6a), 4.65, 4.72 (*ABq*, 1H each, *J* = 12.0, benzylic), 5.09 (*dd*, *J* = 10.0, 3.6, H-2), 5.20 (*pseudo-t*, *J* = 9.9, H-4), 6.53 (*d*, *J* = 3.5, H-1), 7.22-7.37 (*m*, 5H, Ph-H), 8.65 (*s*, NH); ^{13}C-NMR (100 MHz, $CDCl_3$): 20.58, 20.72, 20.75 (Me), 61.69 (C-6), 68.90 (C-4), 70.59 (C-5), 72.10 (C-2), 74.91 (benzylic), 76.60 (C-3), 93.41 (C-1), 127.78, 127.91, 128.46 (Ph), 137.79 (Ph-q), 160.68 (C=NH) 169.35, 169.80, 170.70 (C=O).

4.5 Acetal protection of 1,3-diols

4.5.1 Allyl 3-*O*-benzyl-4,6-*O*-(*p*-nitrobenzylidene)-α,β-D-glucopyranoside (9i)

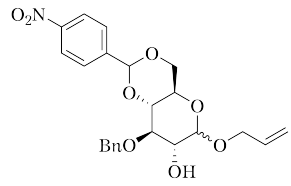

9i

Allyl 3-*O*-benzyl-D-glucopyranoside (**4a**) (0.29 g, 0.93 mmol) was dissolved in MeCN (2.3 mL). *p*-Nitrobenzaldehyde dimethyl acetal (**RC-2**) (0.27 g, 1.4 mmol, 1.5 equiv) and *p*-toluenesulfonic acid (18 mg, 93 μmol, 0.1 equiv) were added. The reaction was stirred overnight at room temperature, the solvent removed under under reduced pressure. DCM was added, and extracted three times with brine. Purification by column chromatography (SiO_2, 4:1 *n*-pentane:EtOAc) afforded anomeric separation of **9i**:

α-anomer: white solids (0.21 g, 0.47 mmol, 51%), mp. 169-171°C; HRMS (ESI+) *m/z*: [M+Na] calcd. 466.1478 for $C_{23}H_{25}NO_8Na$, found 466.1480; IR (cm^{-1}): 3419, 3087, 3034, 2917, 2870, 1526, 1347, 1076, 1027, 855, 833, 697; $[\alpha]_D^{20}$ = +55° (*c* 1.0, CH_2Cl_2); ^{1}H-NMR (600 MHz, $CDCl_3$): 2.49 (*d*, *J* = 8.4, 2-OH), 3.65 (pseudo-*t*, *J* = 9.4, H-4), 3.75 (*td*, *J* = 8.7, 4.1, H-2), 3.76 (pseudo-*t*, *J* = 10.4, H-6b), 3.84 (pseudo-*t*, *J* = 9.1, H-3), 3.88 (*td*, *J* = 9.9, 4.7, H-5), 4.08 (*m*, *J* = 12.8, 6.4, allylic), 4.24 (*m*, *J* = 12.8, 5.4, allylic), 4.31 (*dd*, *J* = 10.3, 4.9, H-6a), 4.85, 4.91 (*ABq*, 1H each, *J* = 11.7, benzylic), 4.96 (*d*, *J* = 3.9, H-1), 5.26 (*m*, *J* = 10.4, CH=C$\underline{H}_2$), 5.33 (*m*, *J* = 17.2, CH=C$\underline{H}_2$), 5.61 (*s*, Ar-C$\underline{H}$), 5.94 (*m*, *J* = 17.1, 3.0, 1.4, C$\underline{H}$=CH_2), 7.29 (*m*, Ph-H), 7.33 (*m*, 2H, Ph-H), 7.38 (*m*, 2H, Ph-H), 7.63 (*m*, 2H, *J* = 8.6, Ar-H), 8.23 (*m*, 2H, *J* = 8.8, Ar-H); ^{13}C-NMR (150 MHz, $CDCl_3$): 62.62 (C-5), 68.92 (allylic), 69.05 (C-6), 72.61 (C-2), 74.96 (benzylic), 79.13 (C-3), 81.86 (C-4), 98.07 (C-1), 99.78 (Ar-$\underline{C}$H), 118.41 (CH=$\underline{C}H_2$), 123.46, 127.25 (Ar), 127.82, 128.44 (Ph), 133.29 ($\underline{C}$H=CH_2), 138.43 (Ph-q), 143.72, 148.31 (Ar-q).

β-anomer: white solids (0.10 g, 0.23 mmol, 25%), mp. 161-163°C; HRMS (ESI+) *m/z*: [M+Na] calcd. 466.1478 for $C_{23}H_{25}NO_8Na$, found 466.1478; IR (cm^{-1}): 3467, 3082, 3030, 2981, 2876, 1737, 1609, 1523, 1347, 1175, 1098, 1073, 1015, 929, 855, 836, 748, 699; $[\alpha]_D^{20}$ = -28° (*c* 1.0, CH_2Cl_2); ^{1}H-NMR (600 MHz, $CDCl_3$): 2.46 (*d*, *J* = 2.3, 2-OH), 3.44 (*ddd*, *J* = 9.9, 9.2, 5.0, H-5), 3.62 (*m*, *J* = 8.1, 2.2, H-2), 3.67 (pseudo-*t*, *J* = 8.8, H-3), 3.71 (pseudo-*t*, *J* = 9.0, H-4), 3.81 (pseudo-*t*, *J* = 10.4, H-6b), 4.16 (*m*, *J* = 12.6, 6.4, 1.2, allylic), 4.37 (*dd*, *J* = 10.6, 5.0, H-6a), 4.38 (*m*, *J* = 12.6, 5.3, 1.4, allylic), 4.46 (*d*, *J* = 7.7, H-1), 4.84, 4.92 (*ABq*, 2H, *J* = 11.8, benzylic), 5.24 (*m*, *J* = 10.4, CH=C$\underline{H}_2$), 5.37 (*m*, *J* = 17.2, 3.0, 1.5, CH=C$\underline{H}_2$), 5.61 (*s*, Ar-C$\underline{H}$), 5.94 (*m*, *J* = 17.1, 10.6, 6.4, 5.4, C$\underline{H}$=CH_2), 7.27-7.39 (*m*, 5H, Ph-H), 7.62 (*m*, 2H, Ar-H), 8.23 (*m*, 2H, Ar-H); ^{13}C-NMR (150 MHz, $CDCl_3$): 66.24 (C-5), 68.79 (C-6), 70.64 (allylic), 74.50 (C-2), 74.73 (benzylic), 80.24 (C-3), 81.30 (C-4), 99.78 (Ar-$\underline{C}$H), 102.30 (C-1), 118.30 (CH=$\underline{C}H_2$), 123.45, 127.24 (Ar), 127.89, 128.48 (Ph), 133.43 ($\underline{C}$H=CH_2), 138.26 (Ph-q), 143.61, 148.30 (Ar-q).

4.5.2 Allyl 3-*O*-benzyl-4,6-*O*-(9'-anthracenyl)methylene-α,β-D-glucopyranoside (9j)

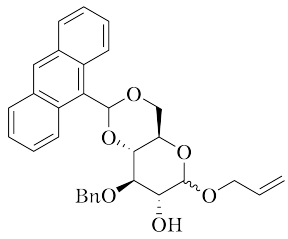

9j

Allyl 3-*O*-benzyl-D-glucopyranoside (**4a**) (0.99 g, 3.2 mmol) was dissolved in MeCN (8.1 mL) with 9-anthraldehyde dimethyl acetal (1.2 g, 4.8 mmol, 1.5 equiv) and TsOH (61 mg, 0.32 mmol, 0.1 equiv). After stirring at 50°C for 5 h, the solvent under reduced pressure, the residue was purified by column chromatography (SiO_2, 9:1 → 6:1 toluene:EtOAc), to give partial anomeric separation. Both anomers were purified by column

chromatography (C18-SiO_2, 1:1 → 9:1 MeCN:H_2O), affording **9j** (0.46 g, 0.92 mmol, 34%), HRMS (ESI+) *m/z*: [M+H] calcd. 499.2121 for $C_{31}H_{31}O_6$, found 499.2120; Partial anomeric separation gave:

α-anomer: yellow solids (80 mg, 0.16 mmol, 14%), mp. 95-99°C; t_R (Method *X*) 34.6 min; IR (cm^{-1}): 3472, 3059, 3031, 2925, 2868, 1454, 1261, 1159, 1107, 1088, 1041, 993, 968, 921, 892, 732, 699, 630; $[\alpha]_D^{20}$ = +88° (*c* 1.0, CH_2Cl_2); ^{1}H-NMR (600 MHz, $CDCl_3$): 2.29 (*d*, *J* = 7.8, 2-OH), 3.81 (*m*, *J* = 8.0, 4.0, H-2), 3.87 (pseudo-*t*, *J* = 9.3, H-4), 3.93 (pseudo-*t*, *J* = 9.2, H-3), 3.95 (*dd*, *J* = 10.5, H-6b), 4.16 (*m*, *J* = 12.9, 6.3, allylic), 4.24 (*td*, *J* = 9.9, 5.0, H-5), 4.36 (*m*, *J* = 12.9, 5.3, allylic), 4.45 (*dd*, *J* = 10.5, 5.0, H-6a), 4.61, 4.69 (*d*, 1H each, *J* = 11.7, benzylic), 5.04 (*d*, *J* = 3.9, H-1), 5.32 (*m*, *J* = 10.4, CH=C$\underline{H}_2$), 5.40 (*m*, *J* = 17.2, CH=C$\underline{H}_2$), 6.02 (*m*, *J* = 17.2, 11.0, C$\underline{H}$=CH_2), 6.91 (*s*, Ar-C$\underline{H}$), 7.00-7.12 (*m*, 5H, Ph-H), 7.48 (*m*, 2H, *J* = 8.0, Anthracene-H), 7.53 (*m*, 2H, *J* = 8.9, 6.6, Anthracene-H), 8.02 (*d*, 2H, *J* = 8.4, 6.6, Anthracene-H), 8.51 (*s*, Anthracene-H), 8.65 (*d*, 2H, *J* = 9.2, Anthracene-H); ^{13}C-NMR (150 MHz, $CDCl_3$): 63.02 (C-5), 69.07 (allylic), 70.05 (C-6), 72.38 (C-2), 74.46 (benzylic), 78.48 (C-3), 83.31 (C-4), 98.13 (C-1), 100.70 (Ar-$\underline{C}$H), 118.46 (CH=$\underline{C}H_2$), 124.87 (Anthracene), 124.95 (Anthracene), 126.10 (Anthracene), 126.96 (Anthracene-q), 127.43 (Ph), 128.04 (Ph), 128.09 (Ph), 129.01 (Anthracene), 129.71 (Anthracene-q), 129.82 (Anthracene), 131.52 (Anthracene-q), 133.48 (C$\underline{H}$=CH_2), 138.14 (Ph-q).

β-anomer: yellows solids (9.4 mg, 19 μmol, 1.7%), mp. 94-105°C; t_R (Method *X*) 34.6 min; IR (cm^{-1}): 3440, 3031, 2924, 1730, 1461, 1261, 1175, 1089, 1019, 934, 735, 699; $[\alpha]_D^{20}$ = -24° (*c* 1.0, CH_2Cl_2); ^{1}H-NMR (600 MHz, $CDCl_3$): 3.66 (*dd*, *J* = 8.6, 8.0, H-2), 3.76 (pseudo-*t*, *J* = 9.0, H-3), 3.84 (*td*, *J* = 9.6, 4.9, H-5), 3.93 (pseudo-*t*, *J* = 9.2, H-4), 4.01 (pseudo-*t*, *J* = 10.3, H-6b), 4.21 (*m*, *J* = 12.7, 6.3, allylic), 4.42 (*m*, *J* = 12.7, 5.3, allylic), 4.52 (*dd*, *J* = 10.6, 4.9, H-6a), 4.59 (*d*, *J* = 7.7, H-1), 4.60, 4.69 (*d*, 1H each, *J* = 11.8, benzylic), 5.27 (*m*, *J* = 10.5, CH=C$\underline{H}_2$), 5.37 (*m*, *J* = 17.1, CH=C$\underline{H}_2$), 5.98 (*m*, *J* = 17.1, 10.7, 6.2, 5.4, C$\underline{H}$=CH_2), 6.92 (*s*, Ar-C$\underline{H}$), 7.02-7.12 (*m*, 5H, Ph-H), 7.48 (*m*, 2H, *J* = 8.5, 6.7, Anthracene-H), 7.53 (*m*, 2H, *J* = 8.7, 6.6, Anthracene-H), 8.03 (*m*, 2H, *J* = 8.5, Anthracene-H),

8.51 (*s*, Anthracene-H), 8.64 (*d*, 2H, *J* = 8.8, Anthracene-H); ^{13}C-NMR (150 MHz, $CDCl_3$): 66.70 (C-5), 69.81 (C-6), 70.60 (allylic), 74.17 (C-2), 74.21 (benzylic), 79.52 (C-3), 82.77 (C-4), 100.55 (Ar-$\underline{C}$H), 102.29 (C-1), 118.33 (CH=$\underline{C}H_2$), 124.90 (Ph), 124.94 (Anthracene), 126.12 (Ph), 126.93 (Anthracene-q), 127.61 (Ph), 128.19 (Anthracene-q), 128.24 (Ph), 129.05 (Anthracene), 129.70 (Anthracene-q), 129.88 (Anthracene), 131.54 (Anthracene-q), 133.57 (C$\underline{H}$=CH_2), 137.90 (Ph-q).

References

(1) Diefenbach, W. C.; Meneely Jr, J. K. *Yale J. Biol. Med.* **1949**, *21*, 421.

(2) McDonald, F. E.; Reddy, K. S. *Angew. Chem. Int. Ed.* **2001**, *40*, 3653–3655.

(3) Petitou, M.; van Boeckel, C. A. *Angew. Chem. Int. Ed.* **2004**, *43*, 3118–3133.

(4) Kim, C. U.; Lew, W.; Williams, M. A.; Liu, H.; Zhang, L.; Swaminathan, S.; Bischofberger, N.; Chen, M. S.; Mendel, D. B.; Tai, C. Y., et al. *J. Am. Chem. Soc.* **1997**, *119*, 681–690.

(5) Zhang, J.; Li, C.; Yu, G.; Guan, H. *Marine drugs* **2014**, *12*, 3634–3659.

(6) Loya, S.; Reshef, V.; Mizrachi, E.; Silberstein, C.; Rachamim, Y.; Carmeli, S.; Hizi, A. *J. Nat. Prod.* **1998**, *61*, 891–895.

(7) Bukhari, S. M.; Feuerherm, A. J.; Tunset, H. M.; Isaksen, S. M.; Sæther, M.; Thvedt, T. H. K.; Gonzalez, S. V.; Schmid, R.; Brunsvik, A.; Fuglseth, E. *J. Serb. Chem. Soc.* **2016**, *81*, 1–12.

(8) Miljkovic, M., *Carbohydrates: Synthesis, Mechanisms, and Stereoelectronic Effects*, 1st ed.; Springer-Verlag New York: 2009.

(9) Tobie, W. *Ind. Eng. Chem. Anal. Ed.* **1942**, *14*, 405–406.

(10) Tollens, B. *Ber. Dtsch. Chem. Ges.* **1883**, *16*, 921–924.

(11) Kamerling, J. P., *Comprehensive Glycoscience, Four-Volume Set: From Chemistry to Systems Biology*, 1st ed.; Elsevier Science: 2007.

(12) Lemieux, R. U. In *Molecular Rearrangements*; Wiley Interscience: 1963, p 709.

(13) Dubrunfaut, A. *Compt. Rend* **1856**, *42*, 228–233.

(14) Lowry, T. M. *J. chem. Soc. Trans.* **1899**, *75*, 211–244.

(15) Lowry, T. *J. Chem. Soc* **1904**, *85*, 1551–70.

(16) Edward, J. *Chem. Ind. (London)* **1955**, *3*, 1102–1104.

(17) Chu, N. J., Ph.D. Thesis, Ottawa, Canada: Department of Chemistry, University of Ottawa, 1959.

(18) Juaristi, E.; Cuevas, G. *Tetrahedron* **1992**, *48*, 5019–5087.

(19) Ouedraogo, A.; Lessard, J. *Can. J. Chem.* **1991**, *69*, 474–480.

(20) Reeves, R. E. *JACS* **1949**, *71*, 212–214.

(21) Tvaroŝka, I.; Bleha, T. In *Advances in Carbohydrate Chemistry and Biochemistry*; Elsevier: 1989; Vol. 47, pp 45–123.

(22) Lowry, T. M. *J. Chem. Soc* **1927**, 2554–2565.

(23) Isbell, H. S.; Pigman, W. In *Advances in Carbohydrate Chemistry and Biochemistry*; Elsevier: 1969; Vol. 24, pp 13–65.

(24) Swain, C. G.; Brown Jr, J. F. *J. Am. Chem. Soc.* **1952**, *74*, 2538–2543.

(25) Rittenberg, D.; Graff, C. *J. Am. Chem. Soc.* **1958**, *80*, 3370–3372.

(26) Los, J.; Simpson, L.; Wiesner, K. *J. Am. Chem. Soc.* **1956**, *78*, 1564–1568.

(27) Bohé, L.; Crich, D. *C. R. Chim.* **2011**, *14*, 3–16.

(28) Boons, G.-J.; Hale, K. J., *Organic Synthesis with Carbohydrates*, 1st; Post-Graduate Chemistry Series; Blackwell Publishing: 2000.

(29) Garegg, P.; Konradsson, P.; Kvarnstrom, I.; Norberg, T.; Svensson, S.; Wigilius, B. *Acta Chem. Scand. B* **1985**, *39*.

(30) Toshima, K.; Tatsuta, K. *Chem. Rev.* **1993**, *93*, 1503–1531.

(31) Codee, J. D.; Litjens, R. E.; van den Bos, L. J.; Overkleeft, H. S.; van der Marel, G. A. *Chem. Soc. Rev.* **2005**, *34*, 769–782.

(32) Fukase, K.; Hasuoka, A.; Kinoshita, I.; Aoki, Y.; Kusumoto, S. *Tetrahedron* **1995**, *51*, 4923–4932.

(33) Schmidt, R. R. *Angew. Chem. Int. Ed.* **1986**, *25*, 212–235.

(34) Nicolaou, K.; Hummel, C.; Pitsinos, E.; Nakada, M.; Smith, A.; Shibayama, K.; Saimoto, H. *J. Am. Chem. Soc.* **1992**, *114*, 10082–10084.

(35) Yang, F.; He, H.; Du, Y.; Lú, M. *Carbohydr. Res.* **2002**, *337*, 1165–1169.

(36) Adero, P. O.; Amarasekara, H.; Wen, P.; Bohé, L.; Crich, D. *Chem. Rev.* **2018**, *118*, 8242–8284.

(37) Lu, S.-R.; Lai, Y.-H.; Chen, J.-H.; Liu, C.-Y.; Mong, K.-K. T. *Angew. Chem. Int. Ed.* **2011**, *50*, 7315–7320.

(38) Mukaiyama, T.; Katsurada, M.; Takashima, T. *Chem. Lett.* **1991**, *20*, 985–988.

(39) Boeing, G. *Systems* **2016**, *4*, 37.

(40) Chatterjee, S.; Moon, S.; Hentschel, F.; Gilmore, K.; Seeberger, P. H. *J. Am. Chem. Soc.* **2018**, *140*, 11942–11953.

(41) Wuts, P. G.; Greene, T. W., *Greene's protective groups in organic synthesis*; John Wiley & Sons: 2006.

(42) Smith, A. B.; Zhu, W.; Shirakami, S.; Sfouggatakis, C.; Doughty, V. A.; Bennett, C. S.; Sakamoto, Y. *Org. Lett.* **2003**, *5*, 761–764.

(43) Boeckman Jr, R. K.; Clark, T. J.; Shook, B. C. *Helv. Chim. Acta* **2002**, *85*, 4532–4560.

(44) Evans, D. A.; Carter, P. H.; Carreira, E. M.; Prunet, J. A.; Charette, A. B.; Lautens, M. *Angew. Chem. Int. Ed.* **1998**, *37*, 2354–2359.

(45) Lipták, A.; Borbás, A.; Bajza, I., *Protecting Group Manipulations in Carbohydrate Synthesis*, 2007, pp 203–259.

(46) Wardrop, D. J.; Landrie, C. L. In; Wiley Online Library: 2001.

(47) Kakitsubata, Y.; Aramaki, R.; Nishioka, K.; Wakao, M.; Suda, Y. *Tetrahedron Lett.* **2016**, *57*, 1154–1157.

(48) Liu, X.; Seeberger, P. H. *Chem. Commun.* **2004**, 1708–1709.

(49) Lehrfeld, J. *J. Org. Chem.* **1967**, *32*, 2544–2546.

(50) Karimi, B.; Zamani, A.; Zareyee, D. *Tetrahedron Lett.* **2004**, *45*, 9139–9141.

(51) Sakagami, M.; Hamana, H. *Tetrahedron Lett.* **2000**, *41*, 5547–5551.

(52) Grice, P.; Ley, S. V.; Pietruszka, J.; Osborn, H. M.; Priepke, H. W.; Warriner, S. L. *Chem.–Eur. J.* **1997**, *3*, 431–440.

(53) Ritter, T.; Zarotti, P.; Carreira, E. M. *Org. Lett.* **2004**, *6*, 4371–4374.

(54) Esmurziev, A.; Sundby, E.; Hoff, B. H. *Eur. J. Org. Chem.* **2009**, *2009*, 1592–1597.

(55) Hanashima, S.; Mizushina, Y.; Yamazaki, T.; Ohta, K.; Takahashi, S.; Sahara, H.; Sakaguchi, K.; Sugawara, F. *Bioorg. Med. Chem.* **2001**, *9*, 367–376.

(56) Moitessier, N.; Chrétien, F.; Chapleur, Y. *Tetrahedron: Asymmetry* **1997**, *8*, 2889–2892.

(57) Jakab, Z.; Mándi, A.; Borbás, A.; Bényei, A.; Komáromi, I.; Lázár, L.; Antus, S.; Lipták, A. *Carbohydr. Res.* **2009**, *344*, 2444–2453.

(58) Ito, S.; Hayashi, A.; Komai, H.; Yamaguchi, H.; Kubota, Y.; Asami, M. *Tetrahedron* **2011**, *67*, 2081–2089.

(59) Ellervik, U. *Tetrahedron Lett.* **2003**, *44*, 2279–2281.

(60) Xia, J.; Abbas, S. A.; Locke, R. D.; Piskorz, C. F.; Alderfer, J. L.; Matta, K. L. *Tetrahedron Lett.* **2000**, *41*, 169–173.

(61) Sharma, G. et al. *Tetrahedron Lett.* **2001**, *42*, 5571–5573.

(62) Savela, R.; Leino, R. *Synthesis* **2015**, *47*, 1749–1760.

(63) Zhao, C.; Sojdak, C. A.; Myint, W.; Seidel, D. *J. Am. Chem. Soc.* **2017**, *139*, 10224–10227.

(64) Bajwa, J. S.; Jiang, X.; Slade, J.; Prasad, K.; Repič, O.; Blacklock, T. J. *Tetrahedron Lett.* **2002**, *43*, 6709–6713.

(65) Urgaonkar, S.; Verkade, J. G. *Org. Lett.* **2005**, *7*, 3319–3322.

(66) Iwanami, K.; Yano, K.; Oriyama, T. *Synthesis* **2005**, *2005*, 2669–2672.

(67) Chandrasekhar, S.; Chandrashekar, G.; Babu, B. N.; Vijeender, K.; Reddy, K. V. *Tetrahedron Lett.* **2004**, *45*, 5497–5499.

(68) Evans, P. A.; Cui, J.; Gharpure, S. J.; Hinkle, R. J. *J. Am. Chem. Soc.* **2003**, *125*, 11456–11457.

(69) Sassaman, M. B.; Kotian, K. D.; Prakash, G. S.; Olah, G. A. *J. Org. Chem.* **1987**, *52*, 4314–4319.

(70) Yang, W.-C.; Lu, X.-A.; Kulkarni, S. S.; Hung, S.-C. *Tetrahedron Lett.* **2003**, *44*, 7837–7840.

(71) Storer, R. I.; Aciro, C.; Jones, L. H. *Chem. Soc. Rev.* **2011**, *40*, 2330–2346.

(72) Xu, B.; Liu, X.; Haubrich, J.; Friend, C. M. *Nat. Chem.* **2010**, *2*, 61.

(73) Wang, C.-C.; Lee, J.-C.; Luo, S.-Y.; Fan, H.-F.; Pai, C.-L.; Yang, W.-C.; Lu, L.-D.; Hung, S.-C. *Angew. Chem. Int. Ed.* **2002**, *41*, 2360–2362.

(74) Kulkarni, S. S.; Liu, Y.-H.; Hung, S.-C. *J. Org. Chem.* **2005**, *70*, 2808–2811.

(75) Bartkovitz, D. J.; Chu, X.-J.; Vu, B. T.; Zhao, C.; Fishlock, D. Substituted pyrrolidine-2-carboxamides., US Patent 8,993,614, 2015.

(76) Verhart, C. G.; Fransen, C. T.; Zwanenburg, B.; Chittenden, G. J. *Recl. Trav. Chim. Pays-Bas* **1996**, *115*, 133–139.

(77) Shi, Z.; Sun, L.; Li, C. *J. Agric. Food. Chem.* **2014**, *62*, 3287–3292.

(78) Szarek, W. A.; Zamojski, A.; Tiwari, K. N.; Ison, E. R. *Tetrahedron Lett.* **1986**, *27*, 3827–3830.

(79) Bishop, C.; Cooper, F. *Can. J. Chem.* **1962**, *40*, 224–232.

(80) Ferrières, V.; Bertho, J.-N.; Plusquellec, D. *Tetrahedron Lett.* **1995**, *36*, 2749–2752.

(81) Chapat, J.-F.; Finiels, A.; Joffre, J.; Moreau, C. *J. Catal.* **1999**, *185*, 445–453.

(82) Lee, D.-S.; Perlin, A. S. *Carbohydr. Res.* **1984**, *125*, 265–282.

(83) Solomons, T. W. G.; Fryhle, C. B.; Snyder, S. A., *Organic Chemistry*, 11th ed.; Wiley: 2014.

(84) Nervik, S. Total synthesis of 1-*O*-(3-*O*-linolenoyl-6-deoxy-6-sulfo-α-D-glucopyranosyl)glycerol., Unpublished work, n.d.

(85) Polanki, I. K.; Kurma, S. H.; Bhattacharya, A. K. *J. Carbohydr. Chem.* **2015**, *34*, 196–205.

(86) Carey, F. A.; Sundberg, R. J., *Advanced organic chemistry, part B: Reactions and synthesis*, 5th; Springer: 2007.

(87) Prasad, J. S.; Vu, T.; Totleben, M. J.; Crispino, G. A.; Kacsur, D. J.; Swaminathan, S.; Thornton, J. E.; Fritz, A.; Singh, A. K. *Org. Process Res. Dev.* **2003**, *7*, 821–827.

(88) Kolb, H. C.; VanNieuwenhze, M. S.; Sharpless, K. B. *Chem. Rev.* **1994**, *94*, 2483–2547.

(89) Sharpless, K. B.; Amberg, W.; Bennani, Y. L.; Crispino, G. A.; Hartung, J.; Jeong, K. S.; Kwong, H. L.; Morikawa, K.; Wang, Z. M. *J. Org. Chem.* **1992**, *57*, 2768–2771.

(90) Coombs, J. R.; Morken, J. P. *Angew. Chem. Int. Ed.* **2016**, *55*, 2636–2649.

(91) Crispino, G. A.; Jeong, K. S.; Kolb, H. C.; Wang, Z. M.; Xu, D.; Sharpless, K. B. *J. Org. Chem.* **1993**, *58*, 3785–3786.

(92) Heravi, M. M.; Zadsirjan, V.; Esfandyari, M.; Lashaki, T. B. *Tetrahedron: Asymmetry* **2017**, *28*, 987–1043.

(93) Hanashima, S.; Mizushina, Y.; Yamazaki, T.; Ohta, K.; Takahashi, S.; Koshino, H.; Sahara, H.; Sakaguchi, K.; Sugawara, F. *Tetrahedron Lett.* **2000**, *41*, 4403–4407.

(94) Sun, Y.; Zhang, J.; Li, C.; Guan, H.; Yu, G. *Carbohydr. Res.* **2012**, *355*, 6–12.

(95) Lafont, D.; Carrière, F.; Ferrato, F.; Boullanger, P. *Carbohydr. Res.* **2006**, *341*, 695–704.

(96) Gordon, D. M.; Danishefsky, S. J. *J. Am. Chem. Soc.* **1992**, *114*, 659–663.

(97) Cai, T. B.; Lu, D.; Tang, X.; Zhang, Y.; Landerholm, M.; Wang, P. G. *J. Org. Chem.* **2005**, *70*, 3518–3524.

(98) Kværnø, L.; Ritter, T.; Werder, M.; Hauser, H.; Carreira, E. M. *Angew. Chem. Int. Ed.* **2004**, *43*, 4653–4656.

(99) Knerr, L.; Pannecoucke, X.; Luu, B. *Tetrahedron Lett.* **1998**, *39*, 273–274.

(100) Andersen, S. M.; Heuckendorff, M.; Jensen, H. H. *Org. Lett.* **2015**, *17*, 944–947.

(101) Ghosh, N. *Synlett* **2004**, *2004*, 574–575.

(102) Watanabe, K.; Itoh, K.; Araki, Y.; Ishido, Y. *Carbohydr. Res.* **1986**, *154*, 165–176.

(103) Cumpstey, I. *Org. Biomol. Chem.* **2012**, *10*, 2503–2508.

(104) Ghorai, S.; Mukhopadhyay, R.; Kundu, A. P.; Bhattacharjya, A. *Tetrahedron* **2005**, *61*, 2999–3012.

(105) Finan, P.; Warren, C. *J. Chem. Soc.* **1962**, 3089–3092.

(106) Klemer, A.; Bieber, M.; Wilbers, H. *Liebigs Ann. Chem.* **1983**, *1983*, 1416–1421.

(107) Peer, A.; Vasella, A. *Helv. Chim. Acta* **1999**, *82*, 1044–1065.

(108) Pecul, M. *Chem. Phys. Lett.* **2006**, *418*, 1–10.

(109) Wolfe, S.; Pinto, B. M.; Varma, V.; Leung, R. Y. *Can. J. Chem.* **1990**, *68*, 1051–1062.

(110) Arévalo, J. M.; Simons, C. *J. Carbohydr. Chem.* **1999**.

(111) Neumaier, J. M.; Madani, A.; Klein, T.; Ziegler, T. *Beilstein J. Org. Chem.* **2019**, *15*, 558–566.

(112) Ciganek, E. *J. Org. Chem.* **1980**, *45*, 1497–1505.

(113) Gaillet, C.; Lequart, C.; Debeire, P.; Nuzillard, J.-M. *J. Magn. Reson.* **1999**, *139*, 454–459.

(114) Martin, N.; Allen Iii, N.; Moore, K.; Vo, L. *J. Mol. Struct. THEOCHEM* **1998**, *454*, 161–166.

(115) Nolin, B.; Jones, R. N. *Can. J. Chem.* **1956**, *34*, 1392–1404.

(116) Blanc-Muesser, M.; Defaye, J.; Foltz, R. L.; Horton, D. *Org. Mass Spectrom.* **1980**, *15*, 317–325.

(117) Bentley, M. D.; Dewar, M. J. *J. Org. Chem.* **1970**, *35*, 2707–2710.

(118) Bruck, D.; Rabinovitz, M. *J. Chem. Soc., Perkin Trans. 2* **1975**, 1656–1661.

(119) Yamamoto, G. *Bull. Chem. Soc. Jpn.* **1992**, *65*, 1967–1975.

(120) Elsaidi, H. R.; Paszkiewicz, E.; Bundle, D. R. *Carbohydr. Res.* **2015**, *408*, 96–106.

(121) Csuk, R.; Doerr, P. *Tetrahedron* **1994**, *50*, 9983–9988.

(122) Shen, Z.; Sheng, L.; Zhang, X.; Mo, W.; Hu, B.; Sun, N.; Hu, X. *Tetrahedron Lett.* **2013**, *54*, 1579–1583.

(123) Gracza, T.; Szolcsányi, P. *Molecules* **2000**, *5*, 1386–1398.

(124) Streicher, H.; Meisch, J.; Bohner, C. *Tetrahedron* **2001**, *57*, 8851–8859.

(125) Fleet, G. W.; Witty, D. R. *Tetrahedron: Asymmetry* **1990**, *1*, 119–136.

(126) Kapeller, D. C.; Hammerschmidt, F. *Tetrahedron* **2010**, *66*, 591–598.

(127) Dussouy, C.; Bultel, L.; Saguez, J.; Cherqui, A.; Khelifa, M.; Grand, E.; Giordanengo, P.; Kovensky, J. *Chem.–Eur. J.* **2012**, *18*, 10021–10028.

(128) Fukase, K.; Matsumoto, T.; Ito, N.; Yoshimura, T.; Kotani, S.; Kusumoto, S. *Bull. Chem. Soc. Jpn.* **1992**, *65*, 2643–2654.

(129) Rao, V. S.; Perlin, A. S. *Can. J. Chem.* **1983**, *61*, 2688–2694.

(130) Moitessier, N.; Dufour, S.; Chrétien, F.; Thiery, J. P.; Maigret, B.; Chapleur, Y. *Bioorg. Med. Chem.* **2001**, *9*, 511–523.

(131) Ohnuma, T.; Hoshi, H. Epipodophyllotoxin glycosides., US Patent 4,997,931, 1991.

(132) Utamura, T.; Kuromatsu, K.; Suwa, K.; Koizumi, K.; Shingu, T. *Chem. Pharm. Bull. (Tokyo)* **1986**, *34*, 2341–2353.

Appendix A Experimental data

A.1 Intermediates and byproducts isolated from the glycosylation reactions

A.1.1 General procedure for isolating glycosylation intermediates

To a solution of HCl (37%, 1.6 equiv) in the alcohol was added the 3-*O*-protected furanoside (0.26 M). The reaction was stirred at room temperature for 1 h to 24 h, followed by quenching with Et_3N (3.2 equiv) and concentrating under reduced pressure.

A.1.2 Allyl 3-*O*-benzyl-α-D-glucofuranoside (3a-α)

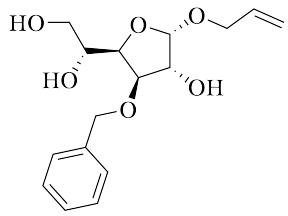

3a

Preparative HPLC (Method *X*) of the residue resulting from applying General procedure 4.4.1 on **2a** in allyl alcohol, yielded **3a-α**,

HRMS (ESI+) *m/z*: [M+Na] calcd. 333.1314 for $C_{16}H_{22}O_6Na$, found 333.1317; IR (cm^{-1}): 3413, 3065, 3031, 2924, 1724, 1455, 1261, 1119, 1089, 1024, 931, 802, 738, 699; $[\alpha]_D^{20}$ = +68° (*c* 0.5, CH_2Cl_2); ^{1}H-NMR (400 MHz, $CDCl_3$): 2.05 (*t*, *J* = 6.3, 6-OH), 2.74 (*d*, *J* = 8.3, 2-OH), 3.11 (*d*, *J* = 4.4, 5-OH), 3.66 (*m*, *J* = 11.5, 5.8, H-6b), 3.79 (*ddd*, *J* = 11.4, 6.6, 3.5, H-6a), 3.93 (*m*, *J* = 5.7, 3.8, 7.9, H-5), 4.08 (*ddt*, *J* = 12.8, 6.2, 1.3, allylic), 4.17 (*m*, *J* = 6.7, H-4), 4.19 (*m*, H-3), 4.29 (*m*, *J* = 4.7, H-2), 4.28 (*m*, allylic), 4.60, 4.88 (*d*, 1H each, *J* = 11.7, benzylic), 5.11 (*d*, *J* = 4.6, H-1), 5.22 (*m*, *J* = 10.3, CH=C$\underline{H}_2$), 5.29 (*m*, *J* = 17.4, CH=C$\underline{H}_2$), 5.90 (*m*, *J* = 17.0, 10.4, C$\underline{H}$=CH_2),

7.30-7.40 (*m*, 5H, Ph-H); ^{13}C-NMR (100 MHz, $CDCl_3$): 64.07 (C-6), 69.05 (allylic), 70.79 (C-5), 71.80 (benzylic), 76.90 (C-4), 77.55 (C-2), 84.32 (C-3), 99.93 (C-1), 117.96 (CH=$\underline{C}H_2$), 127.92, 128.22, 128.73 (Ph), 133.56 ($\underline{C}H=CH_2$), 137.13 (Ph-q).

A.1.3 Allyl 3-*O*-(*p*-phenyl)benzyl-α,β-D-glucofuranoside (3c)

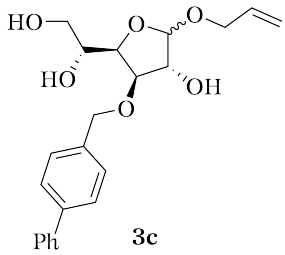

3c

Preparative HPLC (Method *X*) of the residue resulting from applying General procedure A.1.1 on **2c** in allyl alcohol, yielded anomeric separation of **3c** (56:44 α : β),

α-anomer: HRMS (ESI+) *m/z*: [M+Na] calcd. 409.1627 for $C_{22}H_{26}O_6Na$, found 409.1629; IR (cm^{-1}): 3405, 2927, 1488, 1451, 1410, 1215, 1077, 1043, 1008, 939, 826, 761, 698; $[\alpha]_D^{20}$ = +80° (*c* 0.5, CH_2Cl_2); ^{1}H-NMR (600 MHz, $CDCl_3$): 1.90 (*d*, *J* = 4.3, 2-OH), 2.07 (*t*, *J* = 6.2, 6-OH), 3.14 (*d*, *J* = 3.3, 5-OH), 3.72 (*dt*, *J* = 11.3, 5.6, H-6b), 3.84 (*ddd*, *J* = 11.3, 6.2, 3.4, H-6a), 4.00 (*m*, *J* = 12.9, 6.1, 1.3, allylic), 4.07 (*ddt*, *J* = 8.8, 5.6, 3.2, H-5), 4.22 (*dd*, *J* = 6.5, 3.2, H-3), 4.24 (*m*, *J* = 12.9, 5.0, 1.4, allylic), 4.28 (*dd*, *J* = 8.8, 6.6, H-4), 4.40 (*m*, H-2), 4.65, 4.84 (*d*, *J* = 11.8, 1H each, benzylic), 4.94 (*d*, *J* = 1.8, H-1), 5.21 (*m*, *J* = 10.4, 2.6, 1.3, CH=C$\underline{H}_2$), 5.31 (*m*, *J* = 17.2, 3.2, 1.5, CH=C$\underline{H}_2$), 5.91 (*m*, *J* = 17.0, 10.7, 6.1, 5.1, C$\underline{H}$=CH_2), 7.36 (*m*, (*J* = 7.4), Ar-H), 7.40-7.47 (*m*, (*J* = 8.3, 7.8), Ar-H), 7.59 (*m*, (*J* = 8.2, 7.6), Ar-H); ^{13}C-NMR (150 MHz, $CDCl_3$): 64.17 (C-6), 68.96 (allylic), 71.09 (C-5), 72.26 (benzylic), 79.26 (C-4), 79.49 (C-2), 84.59 (C-3), 107.44 (C-1), 117.53 (CH=$\underline{C}H_2$), 127.12, 127.49 128.33, 128.82 (Ar), 133.76 ($\underline{C}H=CH_2$), 136.04, 140.59, 141.28 (Ar-q).

β-anomer: HRMS (ESI+) *m/z*: [M+Na] calcd. 409.1627 for $C_{22}H_{26}O_6Na$, found 409.1621; IR (cm^{-1}): 3427, 2925, 1488, 1410, 1261, 1120, 1088, 1031, 933, 824, 760, 698; $[\alpha]_D^{20}$ = -104° (*c* 1.0, CH_2Cl_2); ^{1}H-NMR (600 MHz, $CDCl_3$): 2.04 (*t*, *J* = 6.2, 6-OH), 2.75 (*d*, *J* = 8.3, 2-OH), 3.14 (*d*, *J* = 4.4, 5-OH), 3.68 (*dt*, *J* = 11.3, 5.6, H-6b), 3.81 (*ddd*, *J* = 11.3, 6.4, 3.6, H-6a), 3.96 (*ddt*, *J* = 8.0, 5.6, 4.0, H-5), 4.09 (*m*, *J* = 12.8, 6.2, 1.3, allylic), 4.19 (*dd*, *J* = 7.8, 6.6, H-4), 4.23 (*dd*, *J* = 6.4, 4.1, H-3), 4.29 (*m*, *J* = 12.8, 5.3, 1.4, allylic), 4.32 (*dd*, *J* = 8.4, 4.2, H-2), 4.65, 4.92 (*d*, 1H each, *J* = 11.7, benzylic), 5.12 (*d*, *J* = 4.6, H-1), 5.23 (*m*, *J* = 10.4, 2.5, 1.2, CH=C$\underline{H}_2$), 5.29 (*m*, *J* = 17.2, 3.1, 1.5, CH=C$\underline{H}_2$), 5.91 (*dddd*, *J* = 17.1, 10.6, 6.3, 5.4, C$\underline{H}$=CH_2), 7.35 (*m*, (*J* = 7.0), Ar-H), 7.39-7.46 (*m*, (*J* = 8.0, 7.7), Ar-H), 7.59 (*m*, (*J* = 8.2, 7.4), Ar-H); ^{13}C-NMR (150 MHz, $CDCl_3$): 64.10 (C-6), 69.07 (allylic), 70.82 (C-5), 71.54 (benzylic), 76.93 (C-4), 77.59 (C-2), 84.39 (C-3), 99.94 (C-1), 117.97 (CH=$\underline{C}H_2$), 127.14, 127.47, 128.39, 128.83 (Ar), 133.58 ($\underline{C}$H=CH_2), 136.11, 140.66, 141.21 (Ar-q).

A.1.4 Methyl 3-*O*-benzyl-α,β-D-glucofuranoside (3μ)

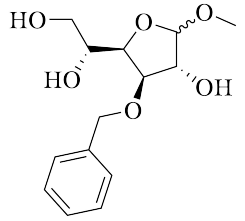

3μ

Preparative HPLC (Method *X*) of the residue resulting from applying General procedure A.1.1 on **2a** in methanol, yielded anomeric separation of **3μ** (56:44 α : β),

α-anomer: HRMS (ESI+) *m/z*: [M+Na] calcd. 307.1158 for $C_{14}H_{20}O_6Na$, found 307.1153; IR (cm^{-1}): 3385, 2928, 1454, 1197, 1109, 1080, 1042, 981, 739, 699; $[\alpha]_D^{20}$ = +76° (*c* 0.5, CH_2Cl_2); ^{1}H-NMR (600 MHz, $CDCl_3$): 1.84 (*d*, *J* = 4.9, 2-OH), 2.07 (*t*, *J* = 6.3, 6-OH), 3.06 (*d*, *J* = 3.4, 5-OH), 3.40 (*s*, 3H, OMe), 3.71 (*dt*, *J* = 11.6, 5.4, H-6b), 3.84 (*ddd*, *J* = 11.4, 6.2,

3.2, H-6a), 4.02 (*ddt*, *J* = 9.0, 5.6, 3.4, H-5), 4.17 (*dd*, *J* = 6.5, 2.9, H-3), 4.24 (*dd*, *J* = 8.9, 6.6, H-4), 4.31 (*m*, H-2), 4.59 (*d*, *J* = 11.8, benzylic), 4.79 (*s*(br), H-1), 4.80 (*d*, *J* = 11.5, benzylic), 7.30-7.40 (*m*, 5H, Ph-H); ^{13}C-NMR (150 MHz, $CDCl_3$): 55.90 (OMe), 64.22 (C-6), 71.03 (C-5), 72.61 (benzylic), 79.33 (C-4), 79.43 (C-2), 84.44 (C-3), 109.61 (C-1), 127.96, 128.38, 128.81 (Ph), 137.03 (Ph-q).

β-anomer: HRMS (ESI+) *m*/*z*: [M+Na] calcd. 307.1158 for $C_{14}H_{20}O_6Na$, found 307.1153; IR (cm^{-1}): 3408, 2928, 1454, 1402, 1206, 1121, 1090, 1039, 903, 738, 699; $[\alpha]_D^{20}$ = -112° (*c* 0.5, CH_2Cl_2); ^{1}H-NMR (600 MHz, $CDCl_3$): 2.08 (*t*, *J* = 5.7, 6-OH), 2.70 (*d*, *J* = 8.2, 2-OH), 3.12 (*d*, *J* = 4.3, 5-OH), 3.46 (*s*, 3H, OMe), 3.67 (*dt*, *J* = 11.3, 5.1, H-6b), 3.79 (*ddd*, *J* = 11.2, 5.1, 3.5, H-6a), 3.94 (*ddt*, *J* = 7.7, 5.6, 3.8, H-5), 4.14 (*dd*, *J* = 7.7, 6.5, H-4), 4.17 (*dd*, *J* = 6.4, 4.0, H-3), 4.28 (*dt*, *J* = 8.1, 4.3, H-2), 4.60, 4.88 (*d*, 1H each, *J* = 11.6, benzylic), 4.95 (*d*, *J* = 4.7, H-1), 7.30-7.40 (*m*, 5H, Ph-H); ^{13}C-NMR (150 MHz, $CDCl_3$): 55.64 (OMe), 64.06 (C-6), 70.81 (C-5), 71.79 (benzylic), 76.80 (C-4), 77.50 (C-2), 84.27 (C-3), 101.68 (C-1), 127.92, 128.21, 128.72 (Ph), 137.13 (Ph-q). NMR of both anomers is consistent with previously reported data.[110]

A.1.5 Allyl 3-*O*-(*t*-butyl-diphenylsilyl)-α,β-D-glucofuranoside (3f)

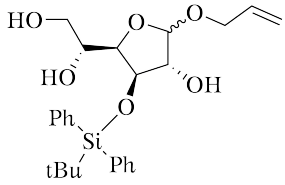

3f

Preparative HPLC (Method *XXX*) of the residue resulting from applying General procedure A.1.1 on **2f** with allyl alcohol, yielded separation of **3f-β** and what appears to be **3f-α** (see discussion on spectroscopic data in Section 2.4) (53:47 α : β),

α-anomer: HRMS (ESI+) *m/z*: [M+Na] calcd. 481.2022 for $C_{25}H_{34}O_6NaSi$, found 481.2020; t_R (Method *X*) 28.2 min; ^{1}H-NMR (400 MHz, $CDCl_3$): 1.13 (*m*, 9H, *t*-Bu), 3.72 (*dd*, *J* = 10.2, 5.7, H-6a), 3.84 (*m*, *J* = 10.4, H-6b), 3.99 (*m*, H-5), 4.06 (*dd*, *J* = 3.8, 4.2, H-2), 4.07 (*m*, H-4), 4.09 (*m*, *J* = 12.9, 6.0, 1.3, allylic), 4.28 (*m*, *J* = 13.1, 5.2, 1.3, allylic), 4.48 (*dd*, *J* = 4.1, 3.1, H-3), 5.16 (*d*, *J* = 4.2, H-1), 5.20 (*m*, *J* = 10.5, CH=C$\underline{H}_2$), 5.25 (*m*, *J* = 17.1, CH=C$\underline{H}_2$), 5.88 (*m*, *J* = 17.2, 10.5, C$\underline{H}$=CH_2), 7.40-7.52 (*m*, 6H, Ph-H), 7.68-7.76 (*m*, 4H, Ph-H); ^{13}C-NMR (100 MHz, $CDCl_3$): 19.40 ($\underline{C}Me_3$), 27.02 ($C\underline{Me}_3$), 64.53 (C-6), 69.47 (allylic), 69.57 (C-5), 77.43 (C-4), 78.96 (C-3), 79.62 (C-2), 100.52 (C-1), 117.68 (CH=$\underline{C}H_2$), 127.92, 128.04, 130.22, 130.28 (Ph), 133.65 ($\underline{C}$H=CH_2), 135.78, 135.82 (Ph).

β-anomer: HRMS (ESI+) *m/z*: [M+Na] calcd. 481.2022 for $C_{25}H_{34}O_6SiNa$, found 481.2024; t_R (Method *X*) 28.0 min; IR (cm^{-1}): 3396, 3073, 2931, 2858, 1739, 1427, 1364, 1111, 1034, 940, 822, 740, 703, 613, 508; $[\alpha]_D^{20}$ = -112° (*c* 1.0, CH_2Cl_2); ^{1}H-NMR (400 MHz, $CDCl_3$): 1.10 (*s*, 9H, *t*-Bu), 0.91 (*d*, *J* = 4.1, 2-OH), 2.12 (*t*, *J* = 6.4, 6-OH), 3.13 (*d*, *J* = 3.0, 4-OH), 3.79 (*dt*, *J* = 11.1, 5.6, H-6b), 3.87 (*ddd*, *J* = 11.4, 6.8, 3.0, H-6a), 3.94 (*m*, *J* = 12.8, 5.9, allylic), 4.08 (*m*, *J* = 3.8, 2.1, H-2), 4.20 (*m*, *J* = 8.9, 5.7, H-4), 4.20 (*m*, allylic), 4.21 (*m*, H-5), 4.43 (*dd*, *J* = 5.5, 3.9, H-3), 4.74 (*d*, *J* = 2.0, H-1), 5.19 (*m*, *J* = 10.6, CH=C$\underline{H}_2$), 5.28 (*m*, *J* = 17.3, CH=C$\underline{H}_2$), 5.89 (*m*, *J* = 17.2, 10.0, C$\underline{H}$=CH_2), 7.40-7.52 (*m*, 6H, Ph-H), 7.71 (*m*, *J* = 8.2, Ph-H), 7.77 (*m*, *J* = 8.0, Ph-H); ^{13}C-NMR (100 MHz, $CDCl_3$): 19.24 ($\underline{C}Me_3$), 26.98 ($C\underline{Me}_3$), 64.25 (C-6), 69.21 (allylic), 70.94 (C-5), 80.28 (C-4), 80.35 (C-3), 81.90 (C-2), 107.34 (C-1), 117.41 (CH=$\underline{C}H_2$), 128.24, 130.49, 130.58 (Ph), 131.81, 133.14 (Ph-q), 133.82 ($\underline{C}$H=CH_2), 135.72, 135.86 (Ph).

A.1.6 Allyl 3-*O*-(*t*-butyl-diphenylsilyl)-α,β-D-glucopyranoside (4f)

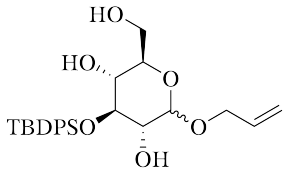

4f

Preparative HPLC (Method *XXX*) of the residue resulting from applying General procedure A.1.1 on **2f** in allyl alcohol, yielded anomeric separation of **4f** (52:48 α : β),

α-anomer: HRMS (ESI+) *m/z*: [M+Na] calcd. 481.2022 for $C_{25}H_{34}O_6NaSi$, found 481.2025; t_R (Method *XX*) 29.0 min; ^{1}H-NMR (400 MHz, $CDCl_3$): 1.09 (*m*, 9H, *t*-Bu), 1.99 (*d*, *J* = 2.9, 4-OH), 3.50 (*dt*, *J* = 9.7, 3.9, H-5), 3.58 (*td*, *J* = 9.5, 3.9, H-2), 3.64 (*td*, *J* = 9.1, 1.7, H-4), 3.72-3.78 (*m*, 2H, H-6), 3.77 (*t*, *J* = 8.8, H-3), 3.90 (*m*, *J* = 13.2, 5.8, 1.5, allylic), 4.10 (*m*, *J* = 13.4, 4.9, 1.6, allylic), 4.83 (*d*, *J* = 3.9, H-1), 5.08 (*m*, *J* = 7.8, CH=C$\underline{H}_2$), 5.06-5.13 (*m*, 2H, CH=C$\underline{H}_2$), 5.77 (*m*, C$\underline{H}$=CH_2), 7.36-7.47 (*m*, Ph-H), 7.70 (*m*, *J* = 7.9, Ph-H), 7.75 (*m*, *J* = 7.9, Ph-H); ^{13}C-NMR (100 MHz, $CDCl_3$): 19.67 ($\underline{C}Me_3$), 27.07 ($C\underline{Me}_3$), 62.43 (C-6), 68.13 (allylic), 70.95 (C-5), 71.57 (C-4), 72.63 (C-2), 77.22 (C-3), 97.65 (C-1), 117.10 (CH=$\underline{C}H_2$), 127.74, 128.02, 129.90, 129.94 (Ph), 133.12 (Ph-q), 133.34 ($\underline{C}$H=CH_2), 134.17 (Ph-q), 135.61, 136.05 (Ph).

β-anomer: HRMS (ESI+) *m/z*: [M+Na] calcd. 481.2022 for $C_{25}H_{34}O_6SiNa$, found 481.2020; t_R (Method *X*) 28.6 min; IR (cm^{-1}): 3449, 3072, 2930, 2857, 1738, 1427, 1363, 1110, 1073, 1034, 824, 741, 703, 612, 510, 489; $[\alpha]_D^{20}$ = -52° (*c* 1.0, CH_2Cl_2); ^{1}H-NMR (400 MHz, $CDCl_3$): 1.07 (*s*, 9H, *t*-Bu), 1.96 (*d*, *J* = 3.2, 4-OH), 1.99 (*dd*, *J* = 7.5, 6.1, 6-OH), 2.09 (*d*, *J* = 2.8, 2-OH), 3.20 (*ddd*, *J* = 9.2, 4.8, 3.6, H-5), 3.50 (*td*, *J* = 8.2, 2.8, H-2), 3.59 (*t*, *J* = 8.5, H-3), 3.65 (*td*, *J* = 8.6, 3.2, H-4), 3.73 (*ddd*, *J* = 11.9, 7.4, 4.8, H-6b), 3.83 (*ddd*, *J* = 11.8, 5.9, 3.5, H-6a), 4.07 (*m*, *J* = 12.3, 6.2, 1.3, allylic), 4.22 (*d*, *J* = 7.7, H-1), 4.32 (*m*, *J* = 12.6, 5.5, 1.4, allylic), 5.19 (*m*, *J* = 10.3, CH=C$\underline{H}_2$), 5.28 (*m*, *J* = 17.2, CH=C$\underline{H}_2$), 5.89 (*m*, *J* = 17.1,

10.3, C<u>H</u>=CH_2), 7.35-7.50 (*m*, 6H, Ph-H), 7.68-7.78 (*m*, 4H, Ph-H); ^{13}C-NMR (100 MHz, $CDCl_3$): 19.64 (<u>C</u>Me_3), 27.03 (C<u>Me</u>$_3$), 62.53 (C-6), 70.64 (allylic), 71.61 (C-4), 74.31 (C-2), 74.75 (C-5), 79.08 (C-3), 101.81 (C-1), 118.04 (CH=<u>C</u>H_2), 127.85, 128.04, 129.95, 130.02 (Ph), 133.08 (Ph-q), 133.69 (<u>C</u>H=CH_2), 135.68 (Ph), 135.92 (Ph-q).

A.1.7 Allyl 3-*O*-benzyl-5,6-*O*-isopropylidene-β-D-glucofuranoside (MC-3)

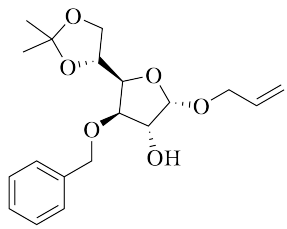

MC-3

Purification by column chromatography (SiO_2, 6:1 *n*-pentane: EtOAc) of the residue resulting from applying General procedure A.1.1 on **2a** in allyl alcohol, gave **MC-3**,

HRMS (ESI+) *m/z*: [M+Na] calcd. 373.1627 for $C_{19}H_{26}O_6Na$, found 373.1622; t_R (Method *X*) 22.4 min; ^{1}H-NMR (600 MHz, $CDCl_3$): 1.37, 1.44 (*s*, 3H each, Me), 1.76 (*d*, *J* = 4.7, 2-OH), 3.95 (*dd*, *J* = 5.1, 2.1, H-3), 4.00 (*m*, *J* = 13.0, 6.2, 1.3, allylic), 4.04 (*dd*, *J* = 8.6, 6.2, H-6b), 4.07 (*dd*, *J* = 8.6, 6.2, H-6a), 4.25 (*m*, *J* = 13.0, 5.0, 1.6, allylic), 4.27 (*m*, *J* = 3.9, 2.0, H-2), 4.38 (*dd*, *J* = 6.2, 5.2, H-4), 4.41 (*dd*, *J* = 12.4, 6.2, H-5), 4.64 (*ABq*, 2H, *J* = 11.9, benzylic), 4.95 (*d*, *J* = 1.3, H-1), 5.19 (*m*, *J* = 10.4, 1.4, CH=C<u>H</u>$_2$), 5.30 (*m*, *J* = 17.2, 1.6, CH=C<u>H</u>$_2$), 5.91 (*dddd*, *J* = 17.1, 10.5, 5.0, 6.1, C<u>H</u>=CH_2), 7.27-7.38 (*m*, Ph-H); ^{13}C-NMR (150 MHz, $CDCl_3$): 25.50, 26.67 (Me), 66.87 (C-6), 68.91 (allylic), 72.25 (benzylic), 74.12 (C-5), 79.26 (C-2), 81.94 (C-4), 83.06 (C-3), 107.56 (C-1), 108.82 (<u>C</u>Me_2), 117.30 (CH=<u>C</u>H_2), 127.66, 127.70, 128.34 (Ph), 133.98 (<u>C</u>H=CH_2), 137.96 (Ph-q).

A.1.8 1,2-*O*-Isopropylidene-3-*O*-(*t*-butyl-diphenylsilyl)-α-D-glucofuranose (MC-4)

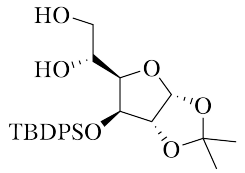

MC-4

Preparative HPLC (Method *XXX*) of the residue resulting from applying General procedure A.1.1 on **2f** in allyl alcohol, **MC-4**,

HRMS (ESI+) *m/z*: [M+Na] calcd. 481.2022 for $C_{25}H_{34}O_6NaSi$, found 481.2017; t_R (Method *XX*) 31.1 min; IR (cm^{-1}): 3456, 2932, 2858, 1738, 1428, 1374, 1216, 111, 1076, 1016, 824, 737, 703, 612, 508; $[\alpha]_D^{20}$ = -19° (*c* 1.0, CH_2Cl_2); ^{1}H-NMR (600 MHz, $CDCl_3$): 1.10 (*s*, 9H, *t*-Bu), 1.14, 1.40 (*s*, 3H each, CMe_2), 1.92 (*m*, *J* = 5.8, 5-OH), 2.06 (*pseudo-t*, *J* = 6.1, 6-OH), 3.73 (*m*, *J* = 11.3, 5.1, H-6b), 3.83 (*m*, *J* = 11.0, 6.5, 2.8), H-6a), 4.01 (*m*, 2H, H-5, H-4), 4.28 (*d*, *J* = 3.6, H-2), 4.48 (*m*, *J* = 1.3, H-3), 5.84 (*d*, *J* = 3.7, H-1), 7.39-7.50 (*m*, 6H, Ph-H), 7.68 (*m*, *J* = 7.9, Ph-H), 7.73 (*m*, *J* = 8.0, Ph-H); ^{13}C-NMR (150 MHz, $CDCl_3$): 19.49 ($\underline{C}Me_3$), 26.09, 26.71 ($C\underline{Me}_2$), 26.98 ($C\underline{Me}_3$), 64.68 (C-6), 68.57 (C-5), 77.23 (C-3), 81.32 (C-4), 84.46 (C-2), 104.85 (C-1), 111.71 ($\underline{C}Me_2$), 128.00, 128.06, 130.23, 130.29 (Ph), 132.40, 133.58 (Ph-q), 135.67, 135.78 (Ph).

A.2 Other byproducts

A.2.1 *N*-Benzyl-3-*O*-benzyl-4,6-di-*O*-acetyl-β-D-glucopyranosylamine

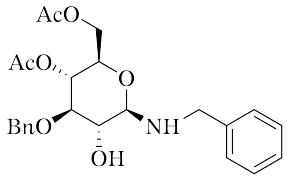

In the deacetylation of the anomeric acetyl group of **5** (Experimental section 4.4.16), *N*-Benzyl-3-*O*-benzyl-4,6-di-*O*-acetyl-β-D-glucopyranosylamine (80 mg, 0.18 mmol, 39%) was isolated as white solids,

HRMS (ASAP+) *m/z*: [M+H] calcd. 444.2022 for $C_{24}H_{30}NO_7$, found 444.2019; t_R (Method *X*) 24.4 min; ^{1}H-NMR (600 MHz, $CDCl_3$): 1.95, 2.09 (*s*, 3H each, Me), 3.41 (pseudo-*t*, *J* = 8.8, H-2), 3.52 (pseudo-*t*, *J* = 9.0, H-3), 3.52 (*m*, *J* = 7.0, 3.0, H-5), 3.88 (*d*, *J* = 12.6, *N*-benzylic), 3.90 (*d*, *J* = 8.4, H-1), 4.07 (*dd*, *J* = 12.2, 2.3, H-6b), 4.10 (*d*, *J* = 13.1, *N*-benzylic), 4.26 (*dd*, *J* = 12.2, 5.1, H-6a), 4.68, 4.87 (*d*, 1H each, *J* = 11.8, 3-*O*-benzylic), 5.02 (pseudo-*t*, *J* = 9.7, H-4), 7.26-7.35 (*m*, Ar-H); ^{13}C-NMR (150 MHz, $CDCl_3$): 20.83 (2x Me), 49.39 (*N*-benzylic), 62.68 (C-6), 69.62 (C-4), 73.35 (C-5), 74.24 (3-*O*-benzylic), 74.61 (C-2), 82.17 (C-3), 89.70 (C-1), 127.35, 127.64, 127.78, 128.30, 128.37, 128.55, 128.65 (Ar), 138.46, 139.22 (Ar-q), 169.69, 170.84 (CO).

A.2.2 3-*O*-Benzyl-4-*O*-trichloroacetimidate-1,2,6-tri-*O*-acetyl-α, β-D-glucopyranose

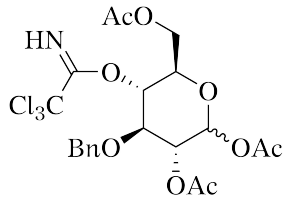

Isolated in small quantities from the reaction described in Section 4.4.17, starting from **IC-3** (Discussed further in Section 2.3.1).

α-anomer: ^{1}H-NMR (600 MHz, $CDCl_3$): 1.95, 2.08, 2.20 (*s*, 3H each, OAc), 4.13 (*pseudo-t*, *J* = 9.7, H-3), 4.15-4.20 (*m*, 2H, H-6b, H-5), 4.28 (*m*, *J* = 12.8, 4.8, H-6a), 4.67, 4.79 (*d*, 1H each, *J* = 11.3, benzylic), 5.13 (*dd*, *J* = 10.0, 3.7, H-2), 5.53 (*pseudo-t*, *J* = 9.6, H-4), 6.33 (*d*, *J* = 3.7, H-1), 7.20-7.32 (*m*, Ph-H), 8.63 (*s*, NH); ^{13}C-NMR (150 MHz, $CDCl_3$): 20.50, 20.81, 20.95 (OAc), 61.86 (C-6), 70.35 (C-5), 71.30 (C-2), 73.73 (C-4), 75.10 (benzylic), 77.40 (C-3), 89.44 (C-1),

90.91 (CCl3), 127.34, 127.74, 128.35, 128.42 (Ph), 137.90 (Ph-q), 161.60 (CNH), 168.80, 169.59, 170.70 (C=O).

β-anomer: ^{1}H-NMR (600 MHz, $CDCl_3$): 1.93, 2.08, 2.10 (*s*, 3H each, Me), 3.94 (*ddd*, *J* = 9.5, 5.3, 2.4, H-5), 3.95 (*pseudo-t*, *J* = 9.1, H-3), 4.21 (*dd*, *J* = 12.4, 2.3, H-6b), 4.29 (*dd*, *J* = 12.4, 5.1, H-6a), 4.61, 4.78 (*d*, 1H each, *J* = 11.3, benzylic), 5.22 (*pseudo-t*, *J* = 8.7, H-2), 5.50 (*pseudo-t*, *J* = 9.4, H-4), 5.71 (*d*, *J* = 8.2, H-1), 7.20-7.34 (*m*, 5H, Ph-H), 8.62 (*s*, NH); ^{13}C-NMR (150 MHz, $CDCl_3$): 20.65, 20.85, 20.89 (Me), 61.99 (C-6), 71.35 (C-2), 73.12 (C-5), 73.90 (C-4), 74.57 (benzylic), 80.22 (C-3), 90.85 (CCl3), 91.98 (C-1), 127.64, 127.85, 128.42 (Ph), 137.59 (Ph-q), 161.52 ((C)NH), 169.13, 169.21, 170.64 (CO).

Appendix B Spectroscopic data

B.1 Spectroscopic data for compound 2a

Elemental Composition Report **Page 1**

Single Mass Analysis
Tolerance = 5.0 PPM / DBE: min = -2.0, max = 50.0
Element prediction: Off
Number of isotope peaks used for i-FIT = 2

Monoisotopic Mass, Even Electron Ions
550 formula(e) evaluated with 2 results within limits (all results (up to 1000) for each mass)
Elements Used:
C: 0-100 H: 0-150 N: 0-5 O: 0-10 Na: 0-1

2018_651 36 (0.670) AM2 (Ar,35000.0,0.00,0.00); Cm (33:37)
1: TOF MS ES+

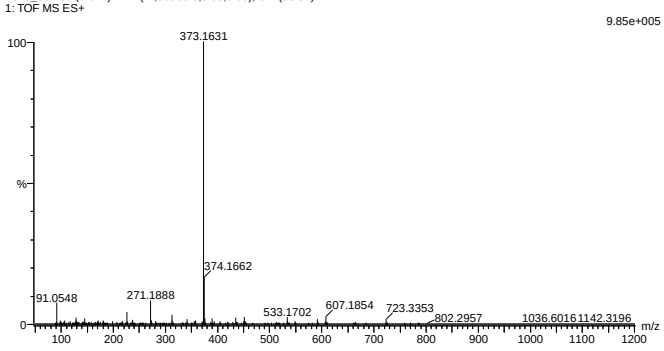

Minimum:				-2.0				
Maximum:		5.0	5.0	50.0				
Mass	Calc. Mass	mDa	PPM	DBE	i-FIT	Norm	Conf(%)	Formula
373.1631	373.1627	0.4	1.1	6.5	720.6	0.159	85.31	C19 H26 O6 Na
	373.1640	-0.9	-2.4	11.5	722.3	1.918	14.69	C20 H22 N4 O2 Na

Figure 29: HRMS (ESI+) of **2a**.

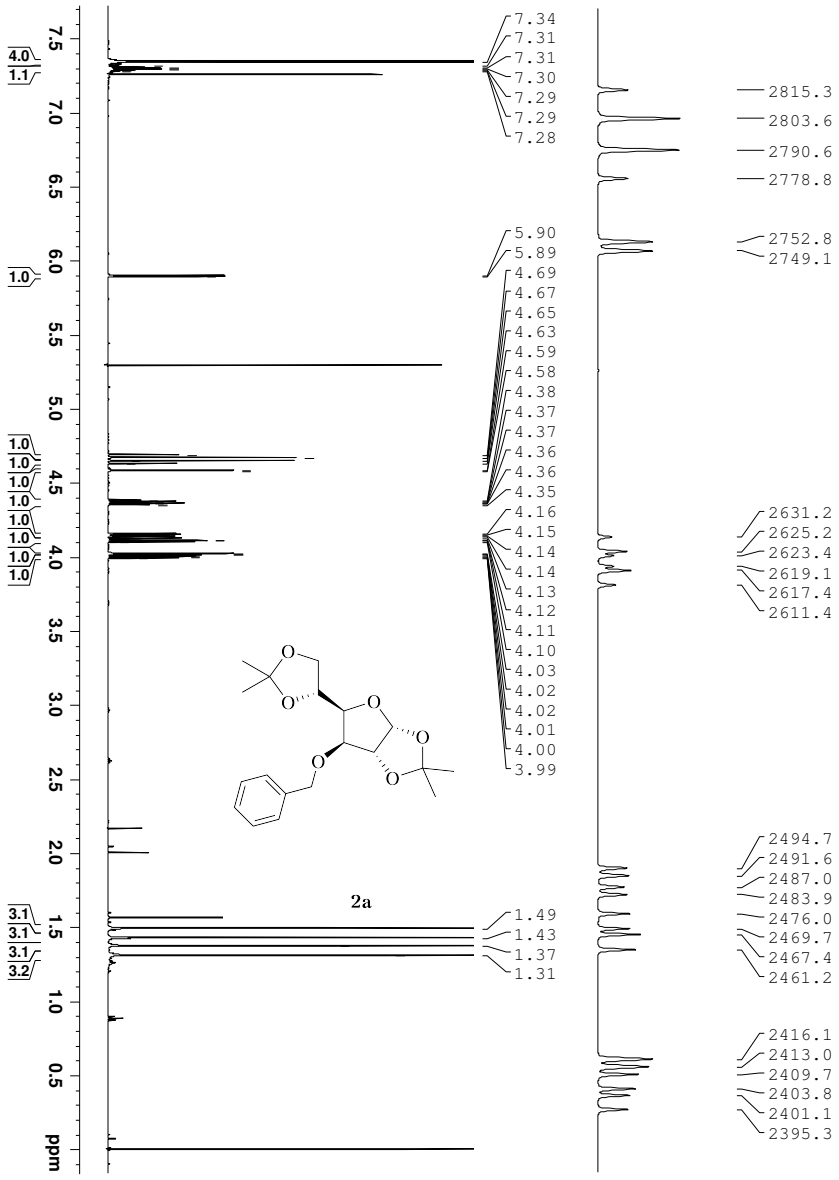

Figure 30: ^{1}H NMR spectrum of **2a**.

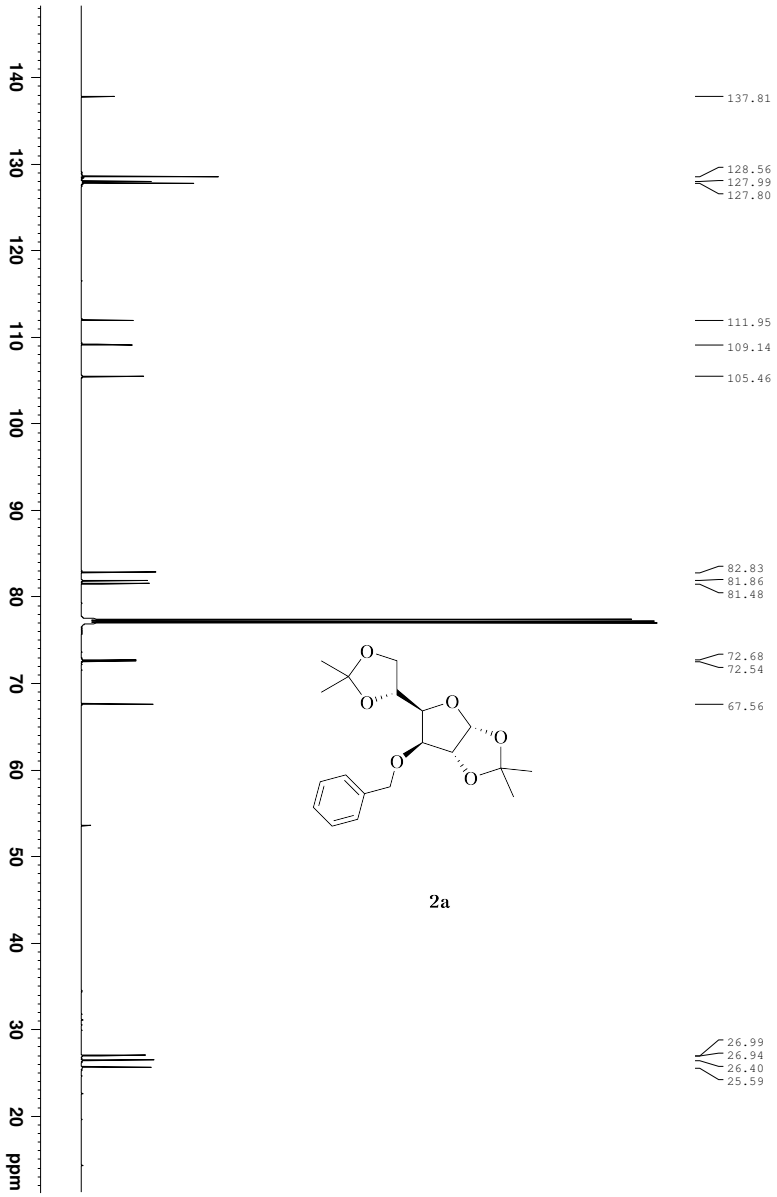

Figure 31: ^{13}C NMR spectrum of **2a**.

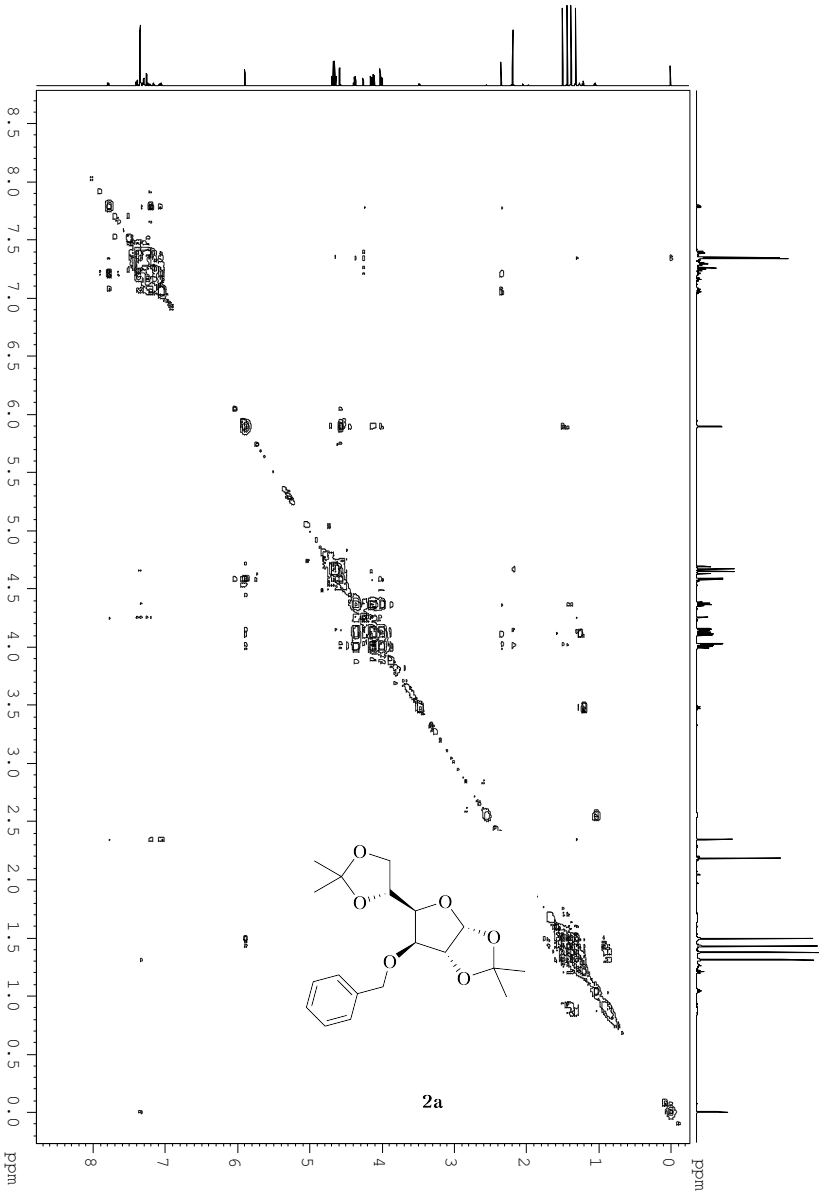

Figure 32: COSY spectrum of **2a**.

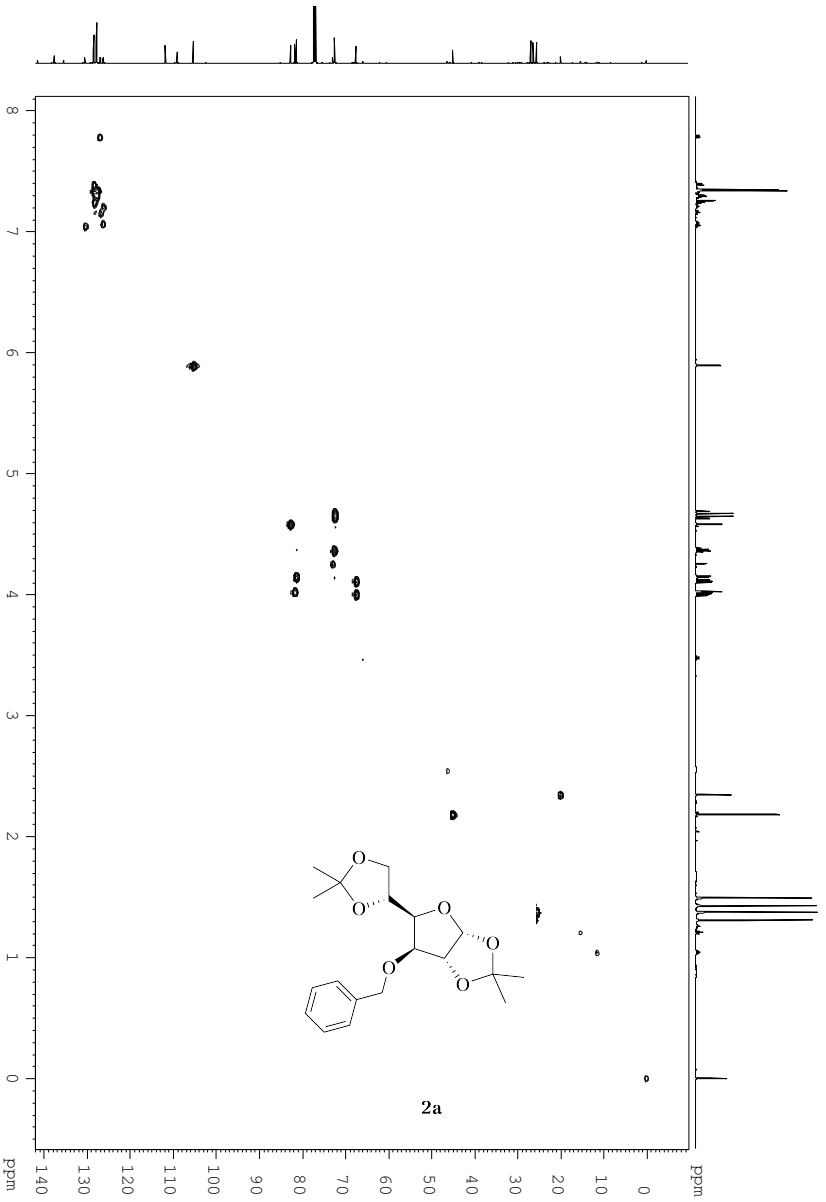

Figure 33: HSQC spectrum of **2a**.

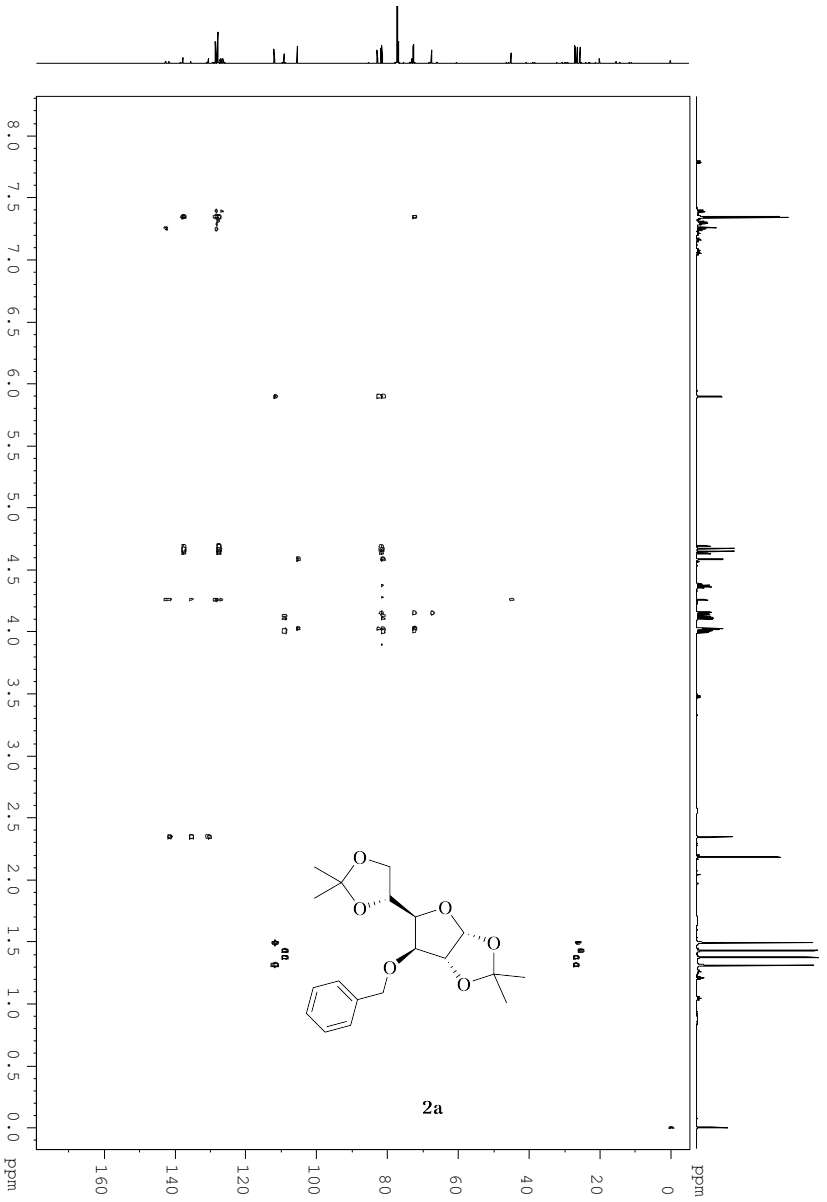

Figure 34: HMBC spectrum of **2a**.

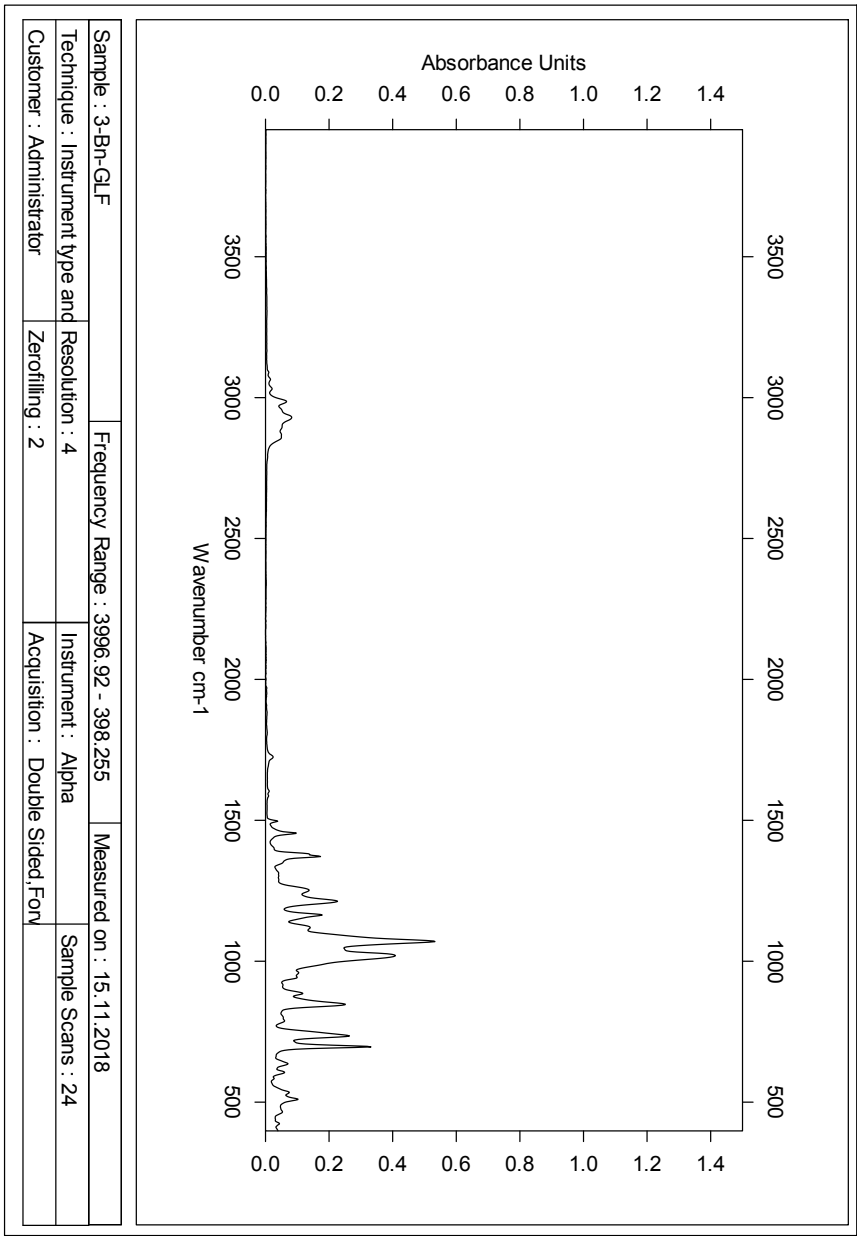

Figure 35: IR spectrum of **2a**.

B.2 Spectroscopic data for compound 2b

Elemental Composition Report **Page 1**

Single Mass Analysis
Tolerance = 2.0 PPM / DBE: min = -2.0, max = 50.0
Element prediction: Off
Number of isotope peaks used for i-FIT = 2

Monoisotopic Mass, Even Electron Ions
173 formula(e) evaluated with 1 results within limits (all results (up to 1000) for each mass)
Elements Used:
C: 0-100 H: 0-150 O: 0-20 Na: 0-1
2018-613esi 229 (2.128) AM2 (Ar,35000.0,0.00,0.00); Cm (226:234)
1: TOF MS ES+

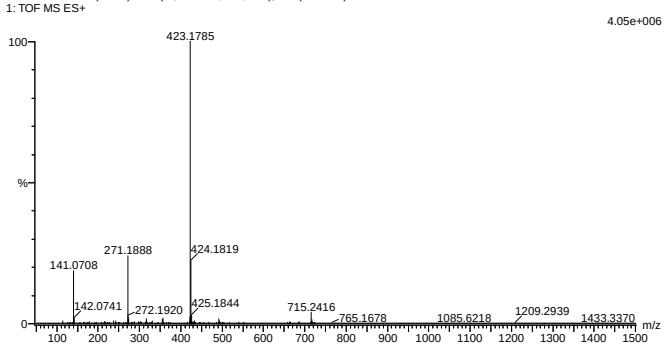

Minimum:				-2.0				
Maximum:		5.0	2.0	50.0				
Mass	Calc. Mass	mDa	PPM	DBE	i-FIT	Norm	Conf(%)	Formula
423.1785	423.1784	0.1	0.2	9.5	848.8	n/a	n/a	C23 H28 O6 Na

Figure 36: HRMS (ESI+) of **2b**.

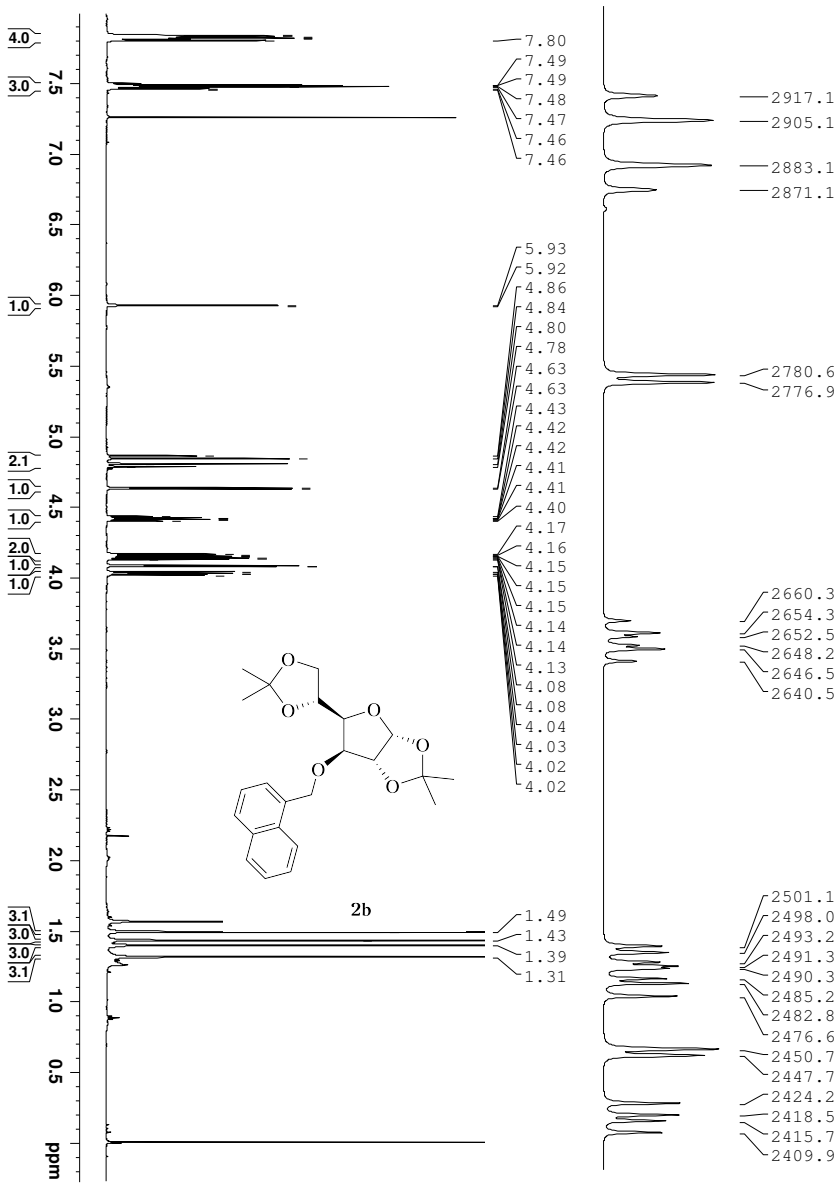

Figure 37: ^{1}H NMR spectrum of **2b**.

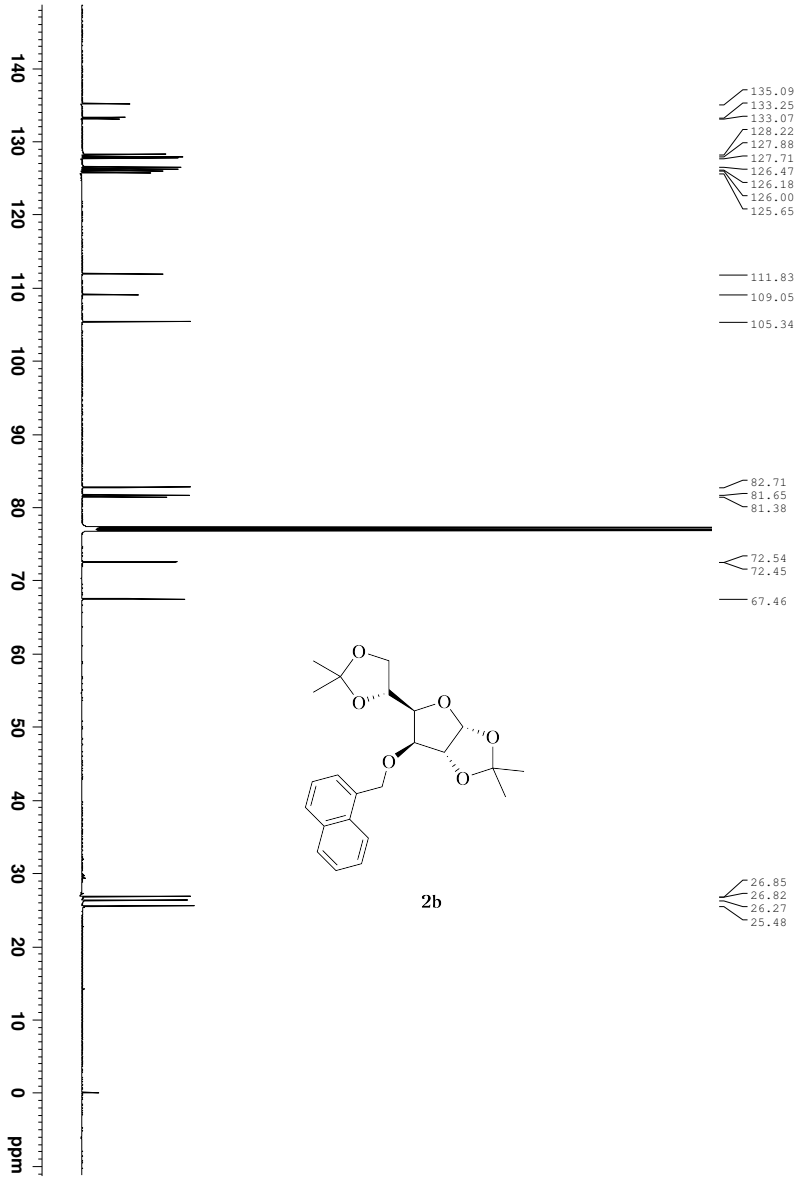

Figure 38: ^{13}C NMR spectrum of **2b**.

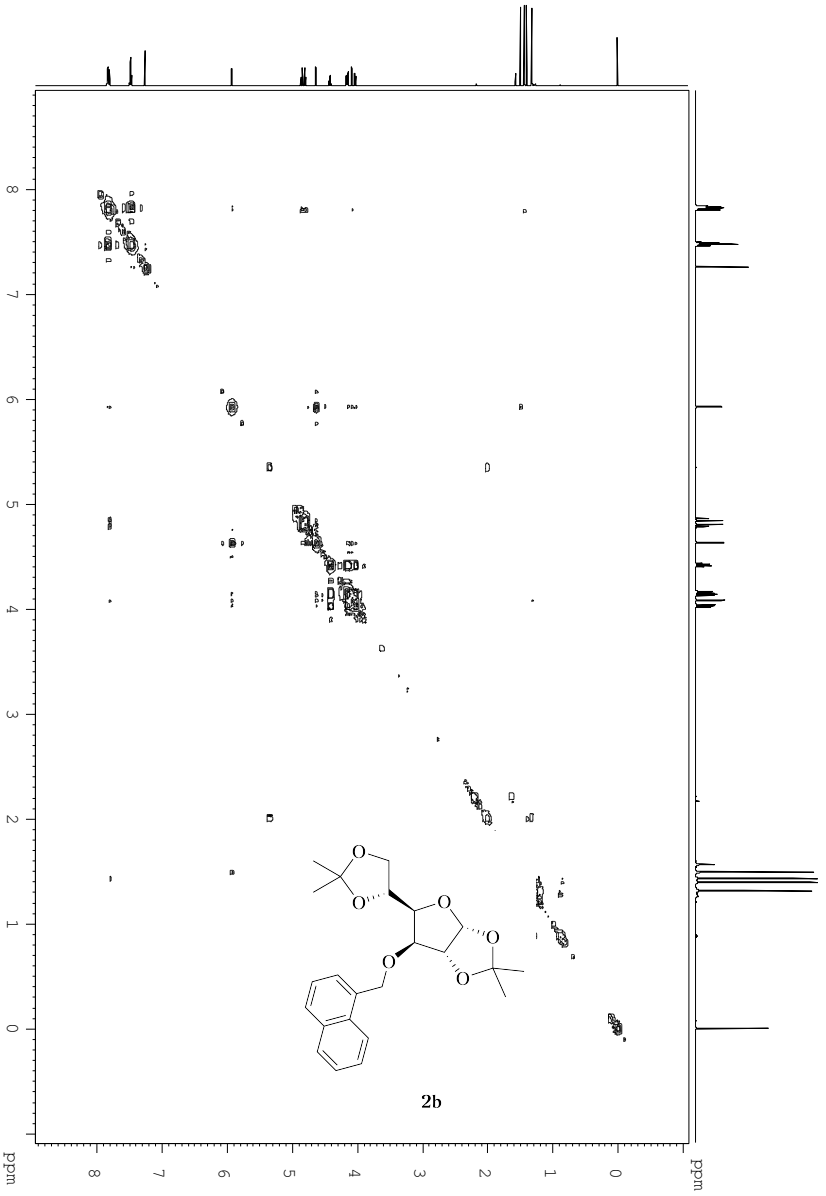

Figure 39: COSY spectrum of **2b**.

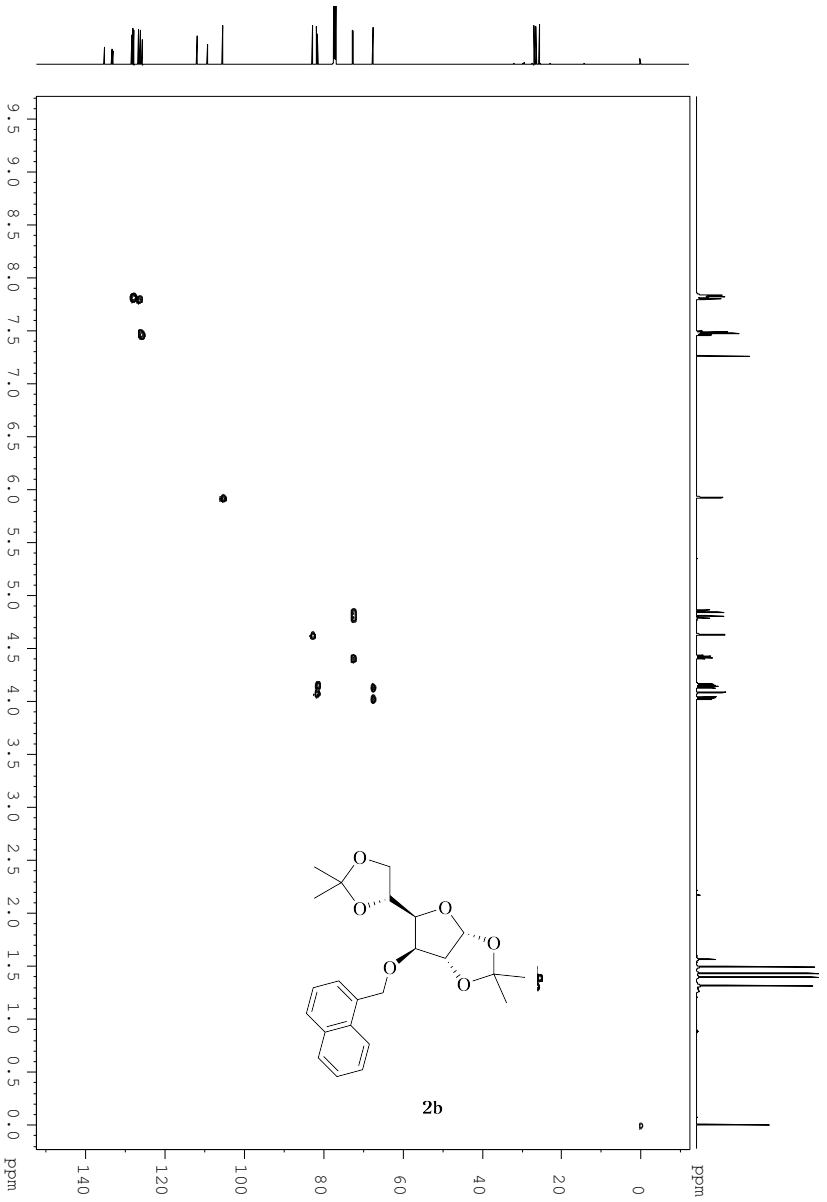

Figure 40: HSQC spectrum of **2b**.

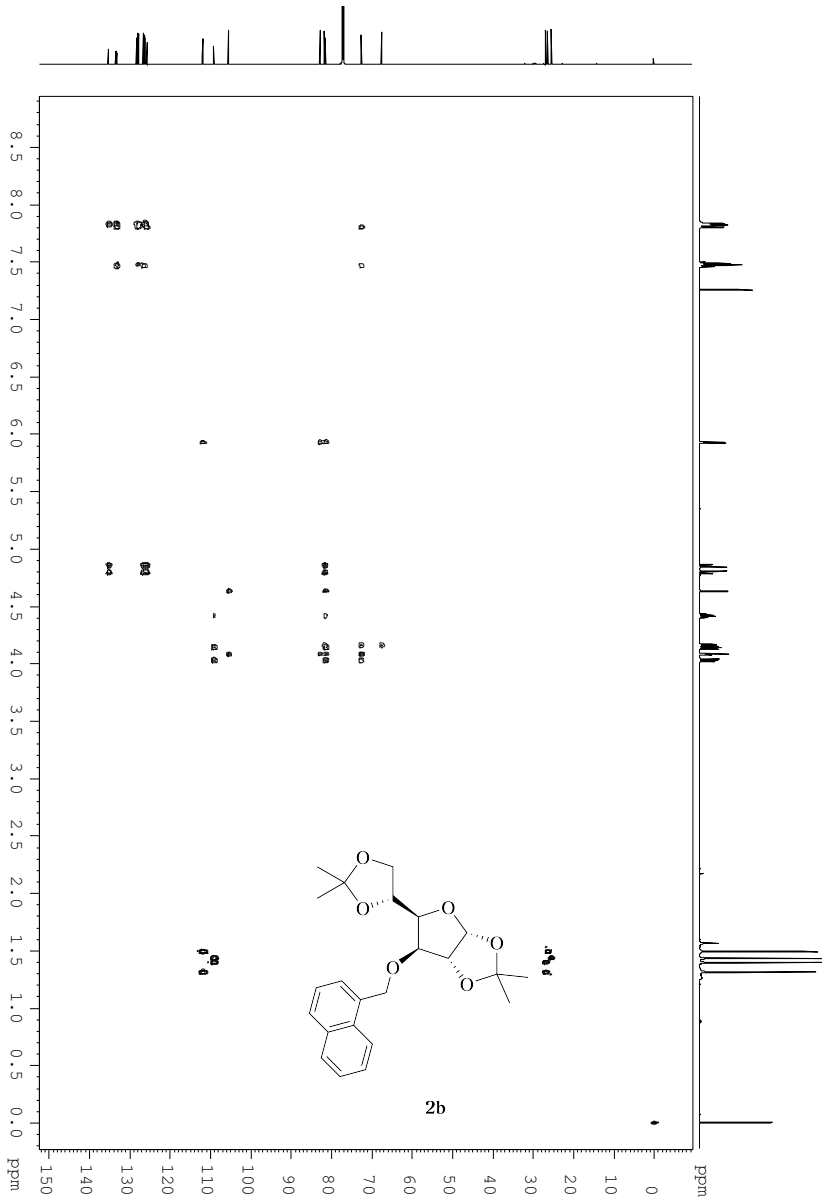

Figure 41: HMBC spectrum of **2b**.

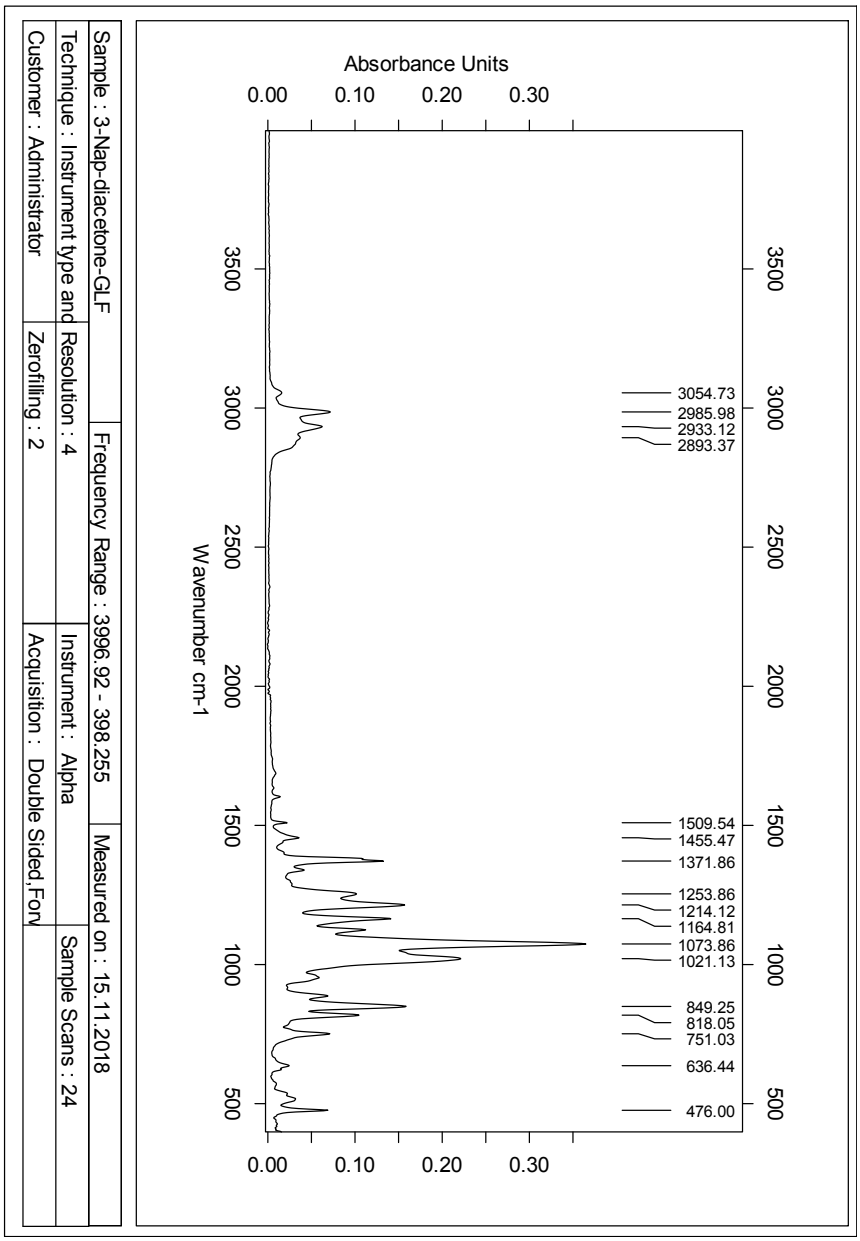

Figure 42: IR spectrum of **2b**.

B.3 Spectroscopic data for compound 2c

Elemental Composition Report **Page 1**

Single Mass Analysis
Tolerance = 2.0 PPM / DBE: min = -2.0, max = 50.0
Element prediction: Off
Number of isotope peaks used for i-FIT = 3

Monoisotopic Mass, Even Electron Ions
116 formula(e) evaluated with 1 results within limits (all results (up to 1000) for each mass)
Elements Used:
C: 0-100 H: 0-150 O: 0-10 Na: 0-1
2018-730esi2 117 (1.100) AM2 (Ar,35000.0,0.00,0.00); Cm (117:123)
1: TOF MS ES+

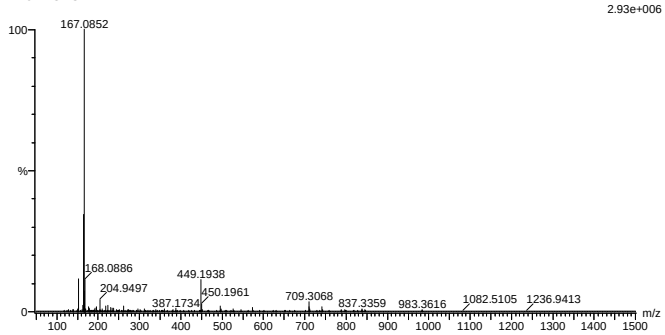

Minimum:				-2.0				
Maximum:		5.0	2.0	50.0				
Mass	Calc. Mass	mDa	PPM	DBE	i-FIT	Norm	Conf(%)	Formula
449.1938	449.1940	-0.2	-0.4	10.5	963.3	n/a	n/a	C25 H30 O6 Na

Figure 43: HRMS (ESI+) of **2c**.

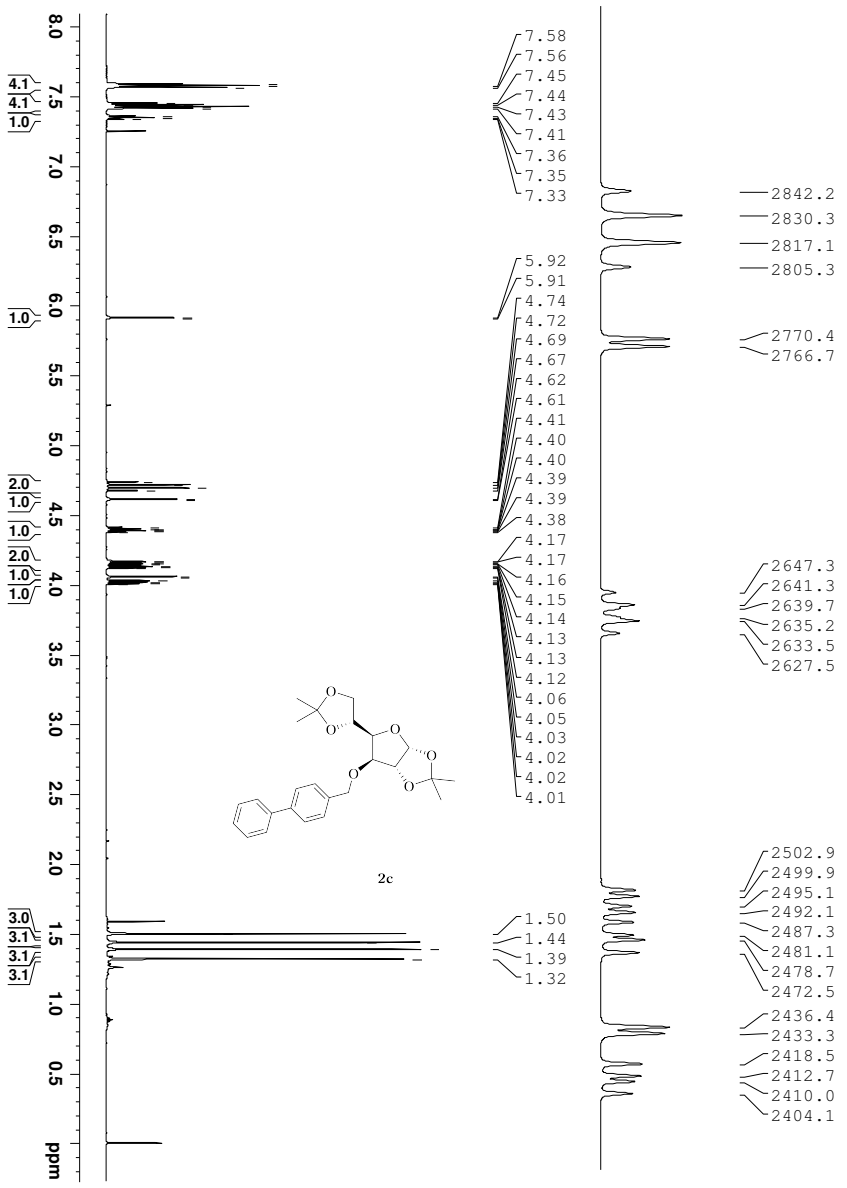

Figure 44: ^{1}H NMR spectrum of **2c**.

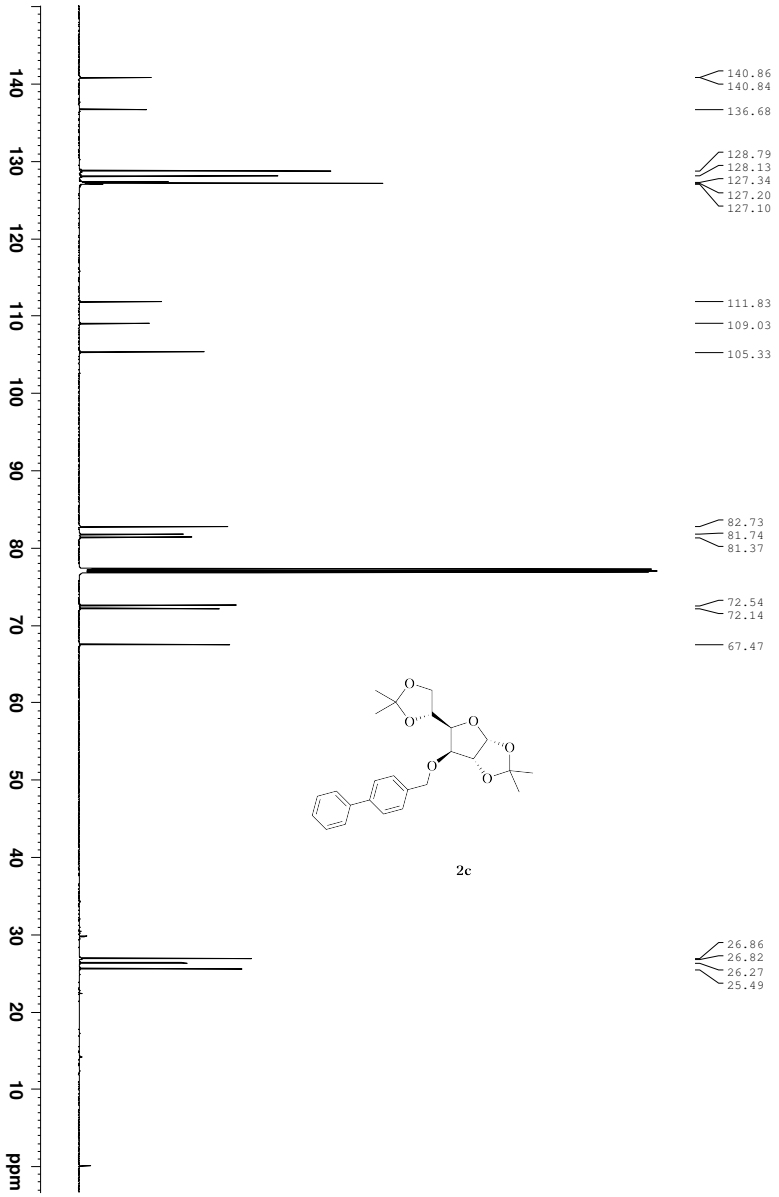

Figure 45: ^{13}C NMR spectrum of **2c**.

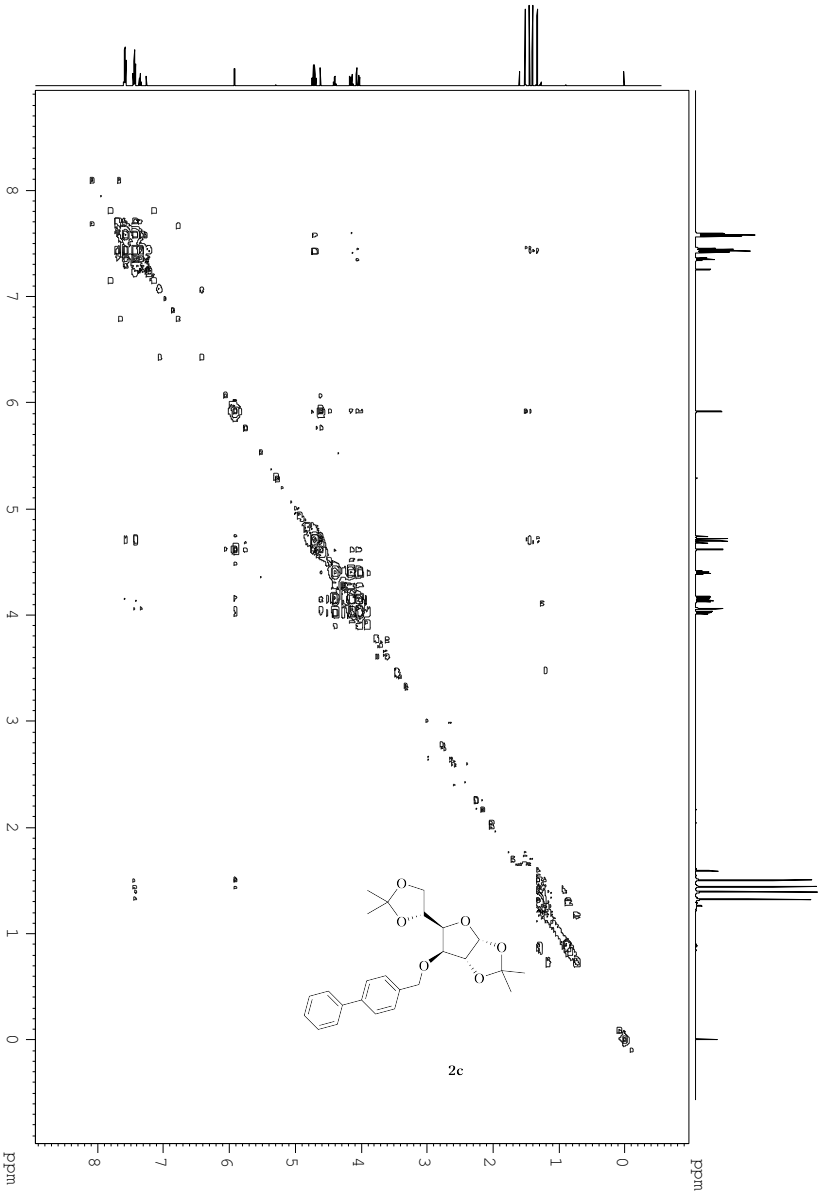

Figure 46: COSY spectrum of **2c**.

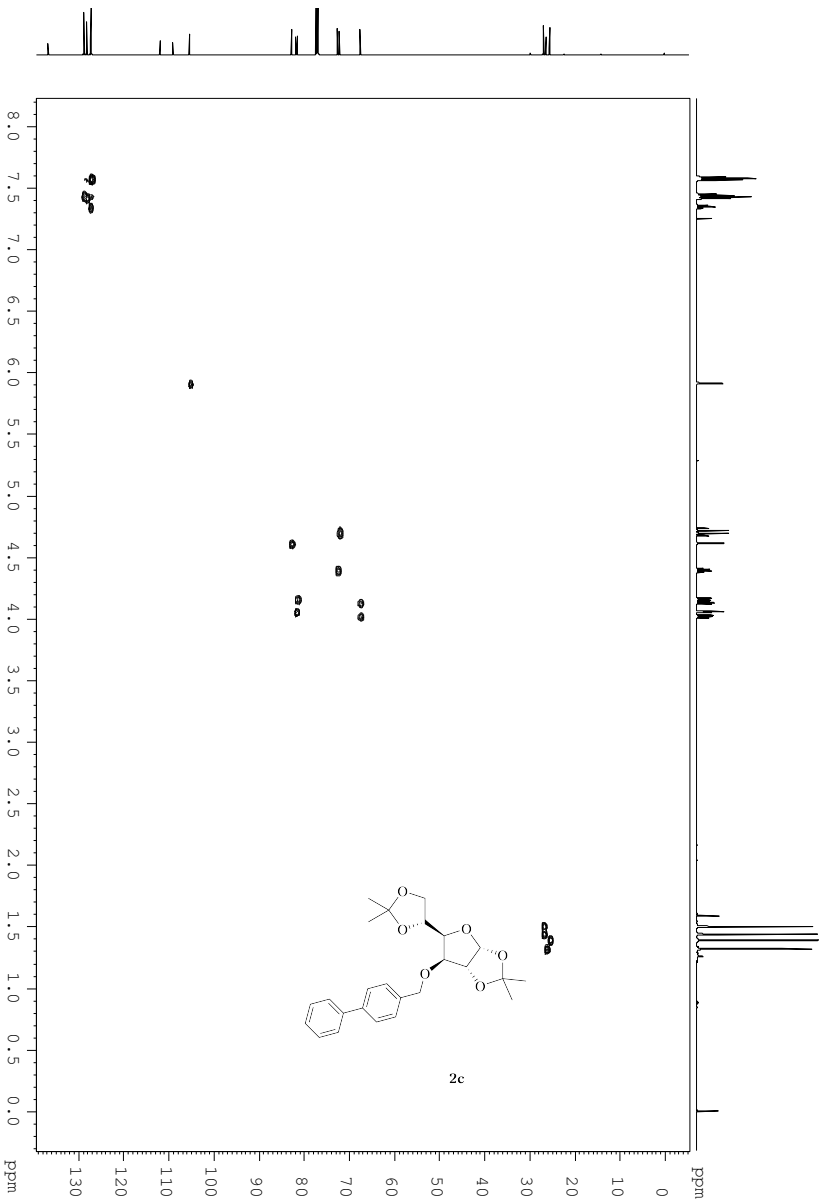

Figure 47: HSQC spectrum of **2c**.

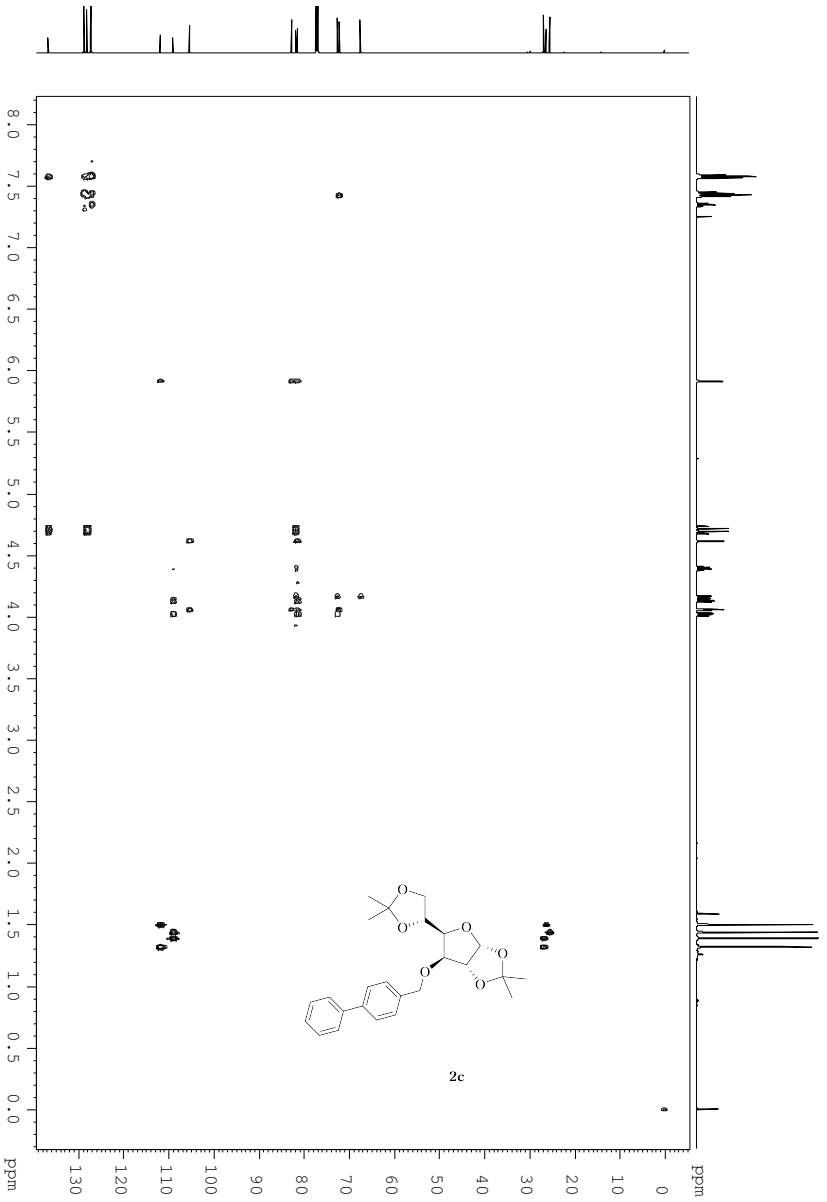

Figure 48: HMBC spectrum of **2c**.

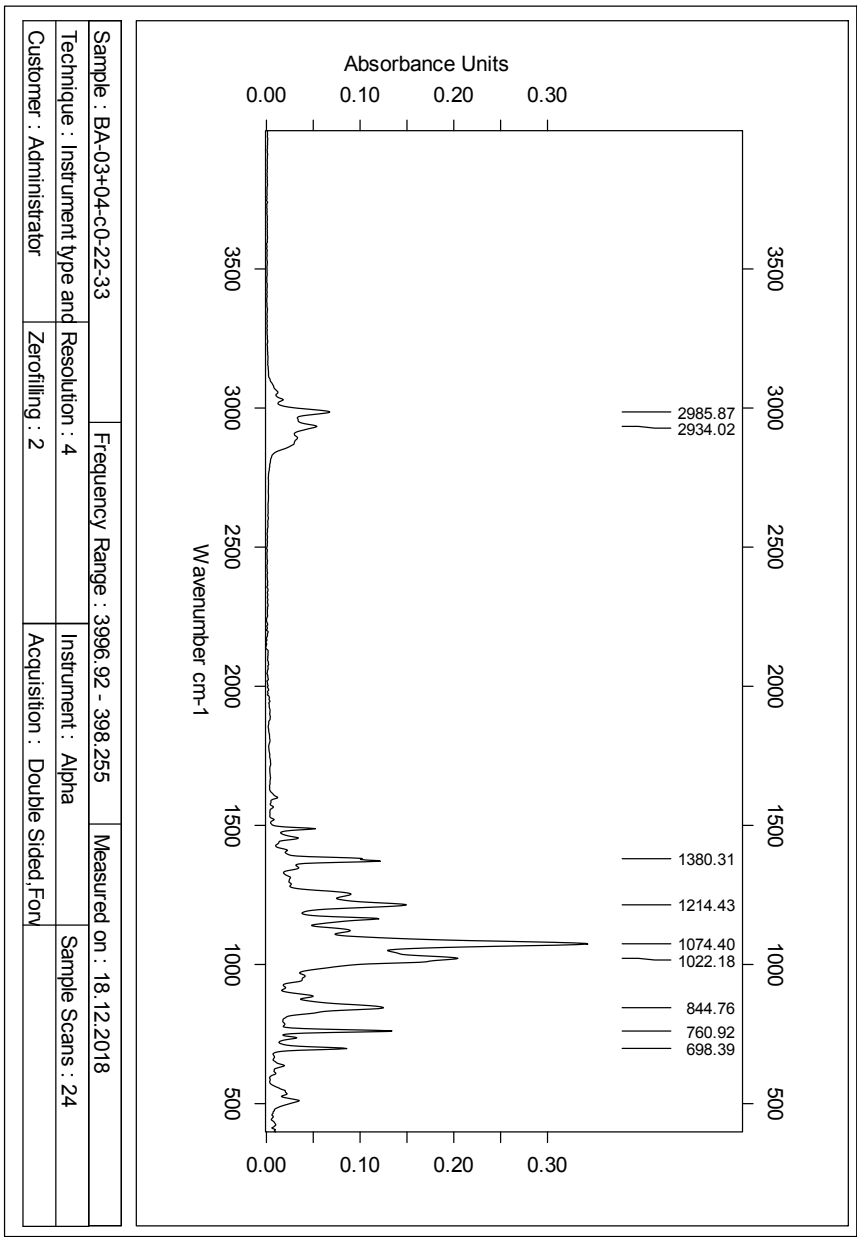

Figure 49: IR spectrum of **2c**.

B.4 Spectroscopic data for compound 2d

Elemental Composition Report **Page 1**

Single Mass Analysis
Tolerance = 2.0 PPM / DBE: min = -2.0, max = 50.0
Element prediction: Off
Number of isotope peaks used for i-FIT = 3

Monoisotopic Mass, Even Electron Ions
1271 formula(e) evaluated with 3 results within limits (all results (up to 1000) for each mass)
Elements Used:
C: 0-100 H: 0-150 N: 0-10 O: 0-10 Na: 0-1
2018-720esi 5 (0.071) AM2 (Ar,35000.0,0.00,0.00); Cm (5:14)
1: TOF MS ES+

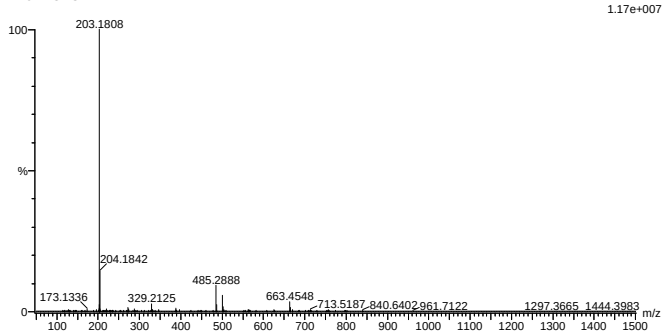

Minimum:				-2.0				
Maximum:		5.0	2.0	50.0				
Mass	Calc. Mass	mDa	PPM	DBE	i-FIT	Norm	Conf(%)	Formula
485.2888	485.2890	-0.2	-0.4	15.5	1011.5	2.479	8.38	C26 H33 N10
	485.2892	-0.4	-0.8	11.5	1009.5	0.485	61.54	C28 H38 N4 O2 Na
	485.2879	0.9	1.9	6.5	1010.2	1.201	30.08	C27 H42 O6 Na

Figure 50: HRMS (ESI+) of **2d**.

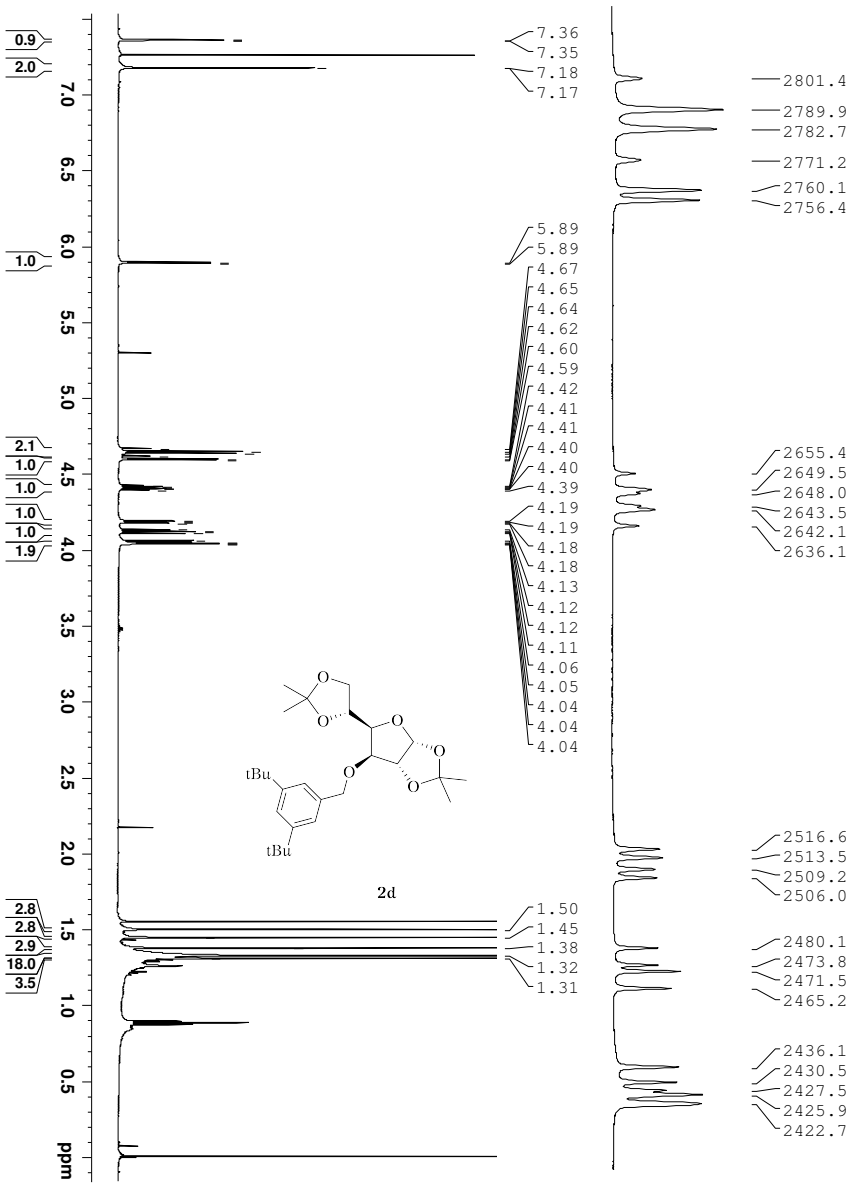

Figure 51: ^{1}H NMR spectrum of **2d**.

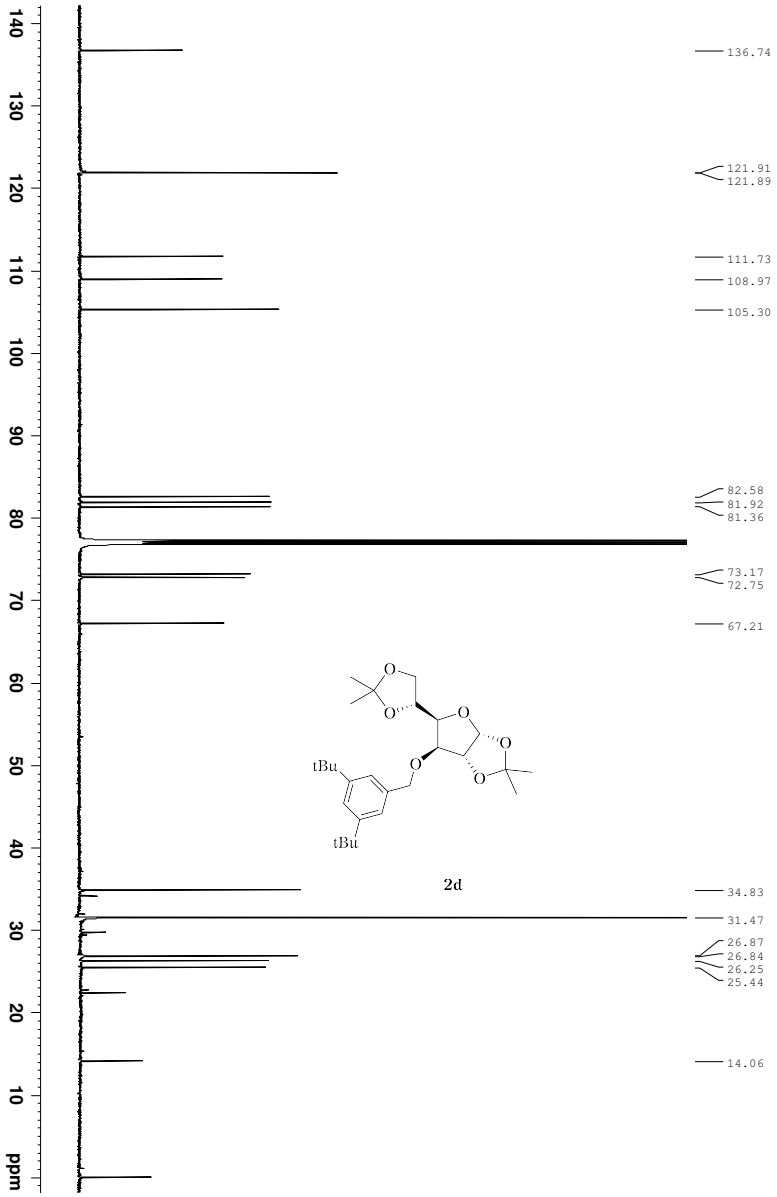

Figure 52: ^{13}C NMR spectrum of **2d**.

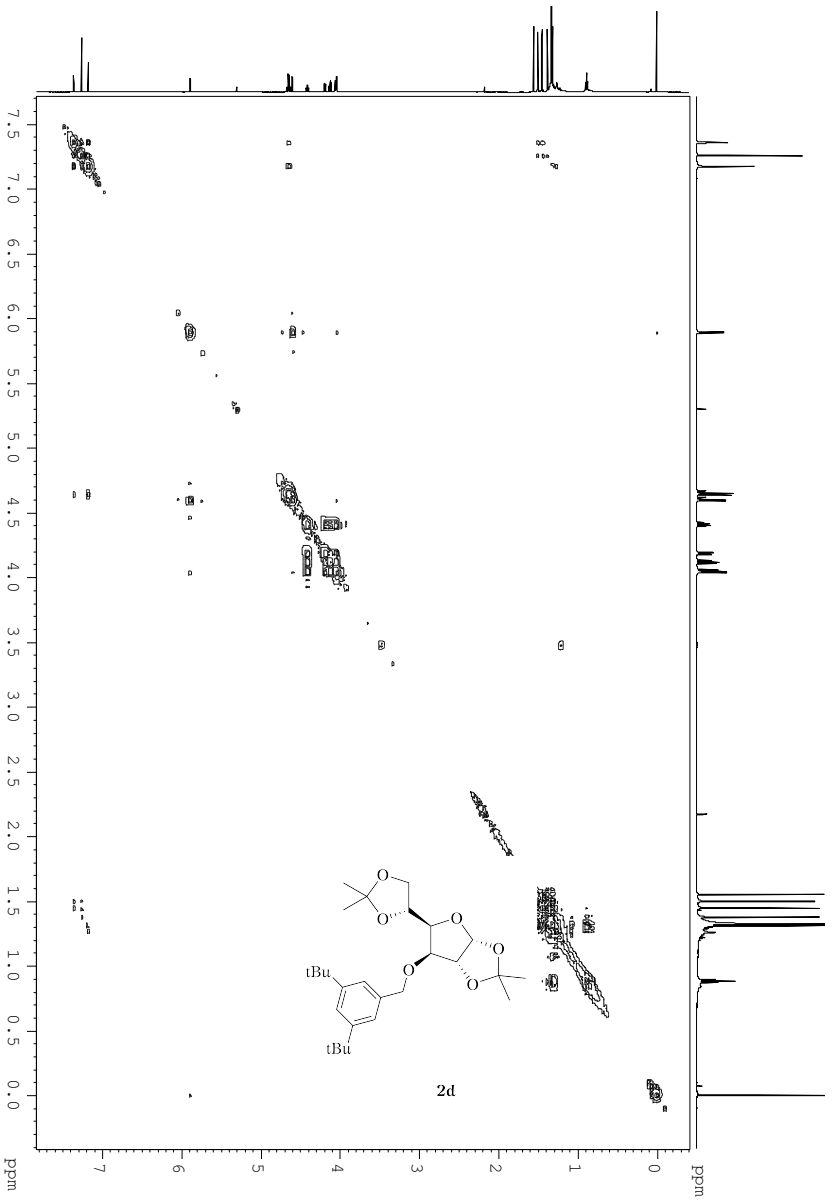

Figure 53: COSY spectrum of **2d**.

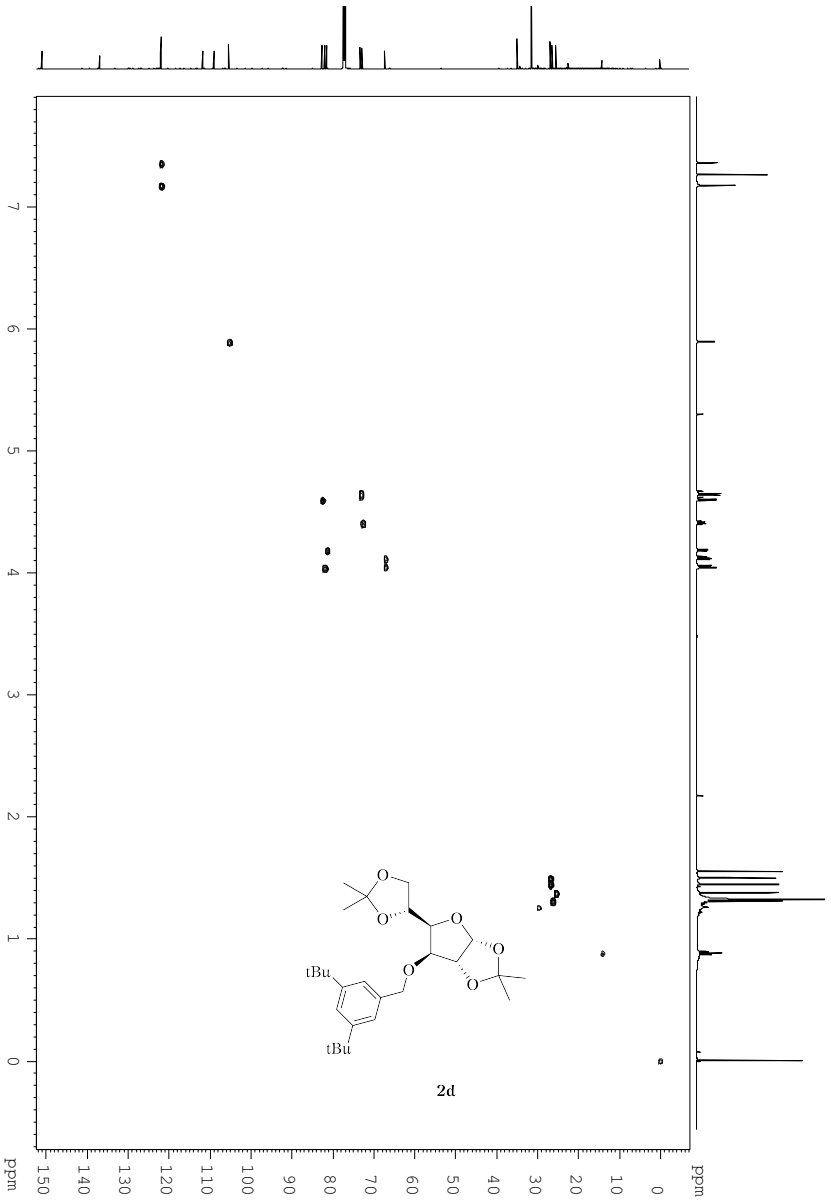

Figure 54: HSQC spectrum of **2d**.

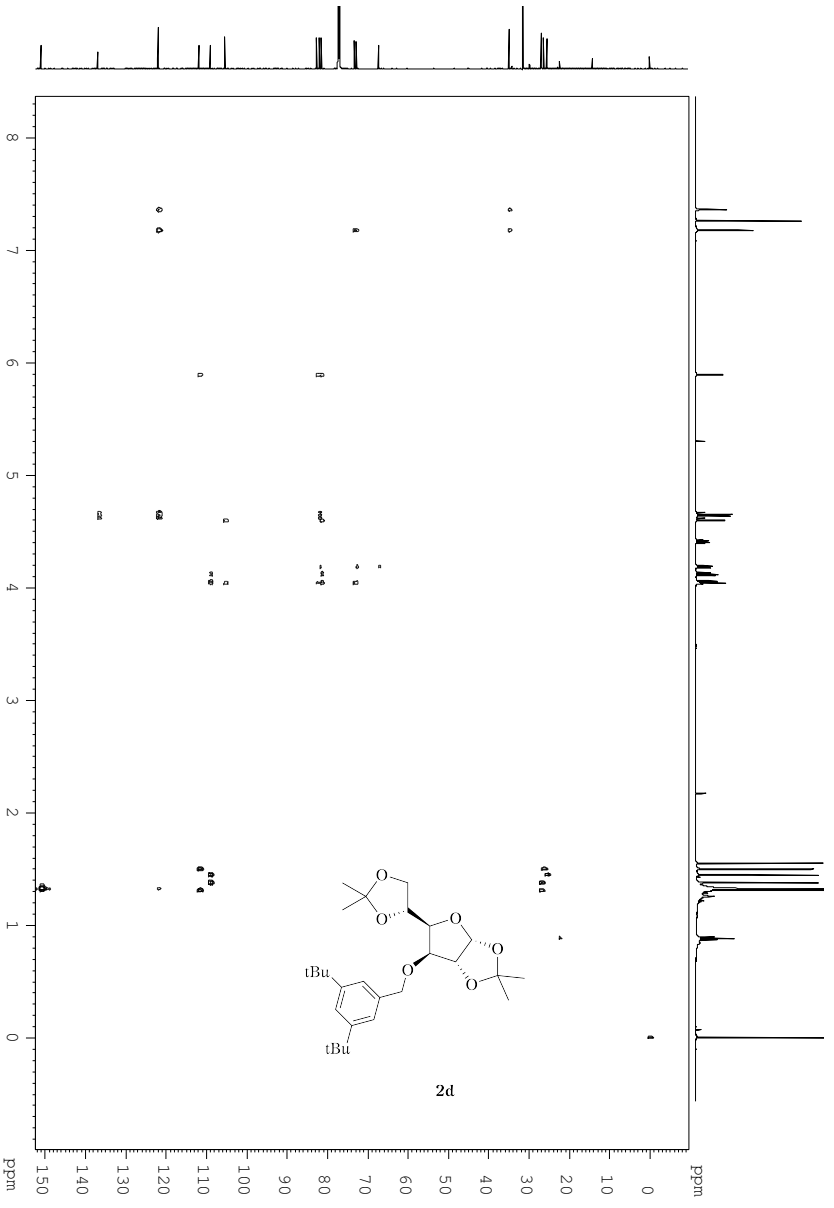

Figure 55: HMBC spectrum of **2d**.

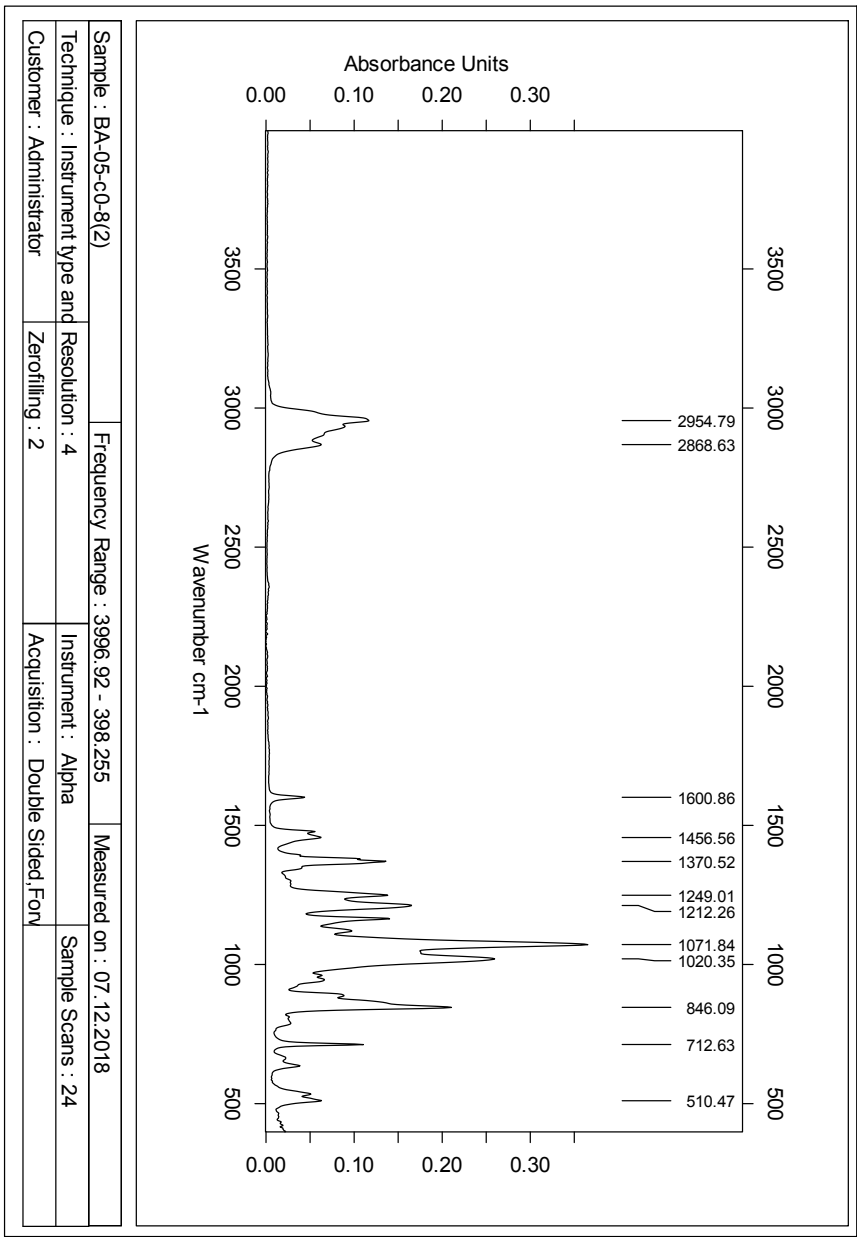

Figure 56: IR spectrum of **2d**.

B.5 Spectroscopic data for compound 2e

Elemental Composition Report **Page 1**

Single Mass Analysis
Tolerance = 2.0 PPM / DBE: min = -2.0, max = 50.0
Element prediction: Off
Number of isotope peaks used for i-FIT = 3

Monoisotopic Mass, Even Electron Ions
293 formula(e) evaluated with 2 results within limits (all results (up to 1000) for each mass)
Elements Used:
C: 0-100 H: 0-150 O: 0-10 Na: 0-1 Si: 0-2

2019-49 19 (0.203) AM2 (Ar,35000.0,0.00,0.00); Cm (19:32)
1: TOF MS ES+

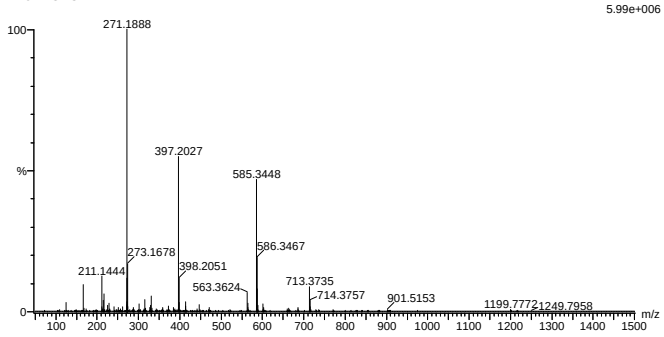

Minimum:				-2.0				
Maximum:		5.0	2.0	50.0				
Mass	Calc. Mass	mDa	PPM	DBE	i-FIT	Norm	Conf(%)	Formula
397.2027	397.2022	0.5	1.3	2.5	1374.9	0.001	99.93	C18 H34 O6 Na Si
	397.2019	0.8	2.0	9.5	1382.2	7.277	0.07	C23 H33 O2 Si2

Figure 57: HRMS (ESI+) of **2e**.

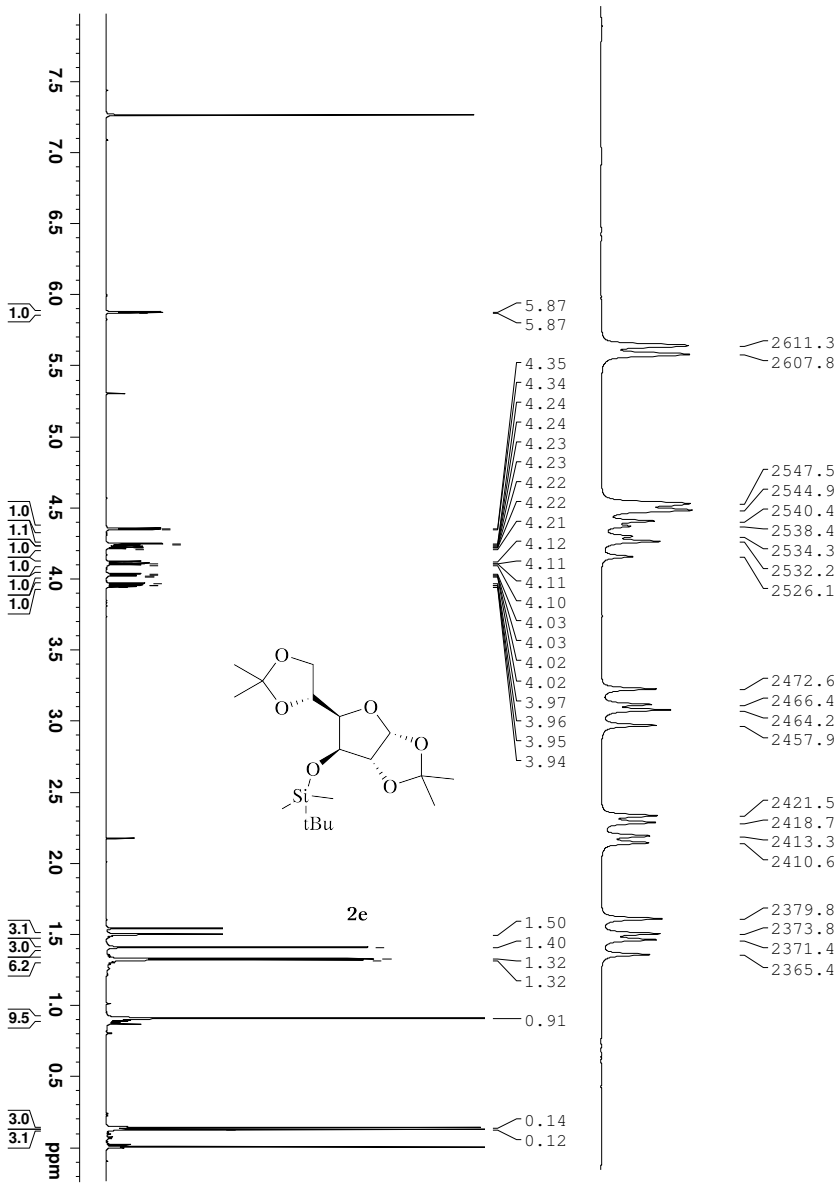

Figure 58: ^{1}H NMR spectrum of **2e**.

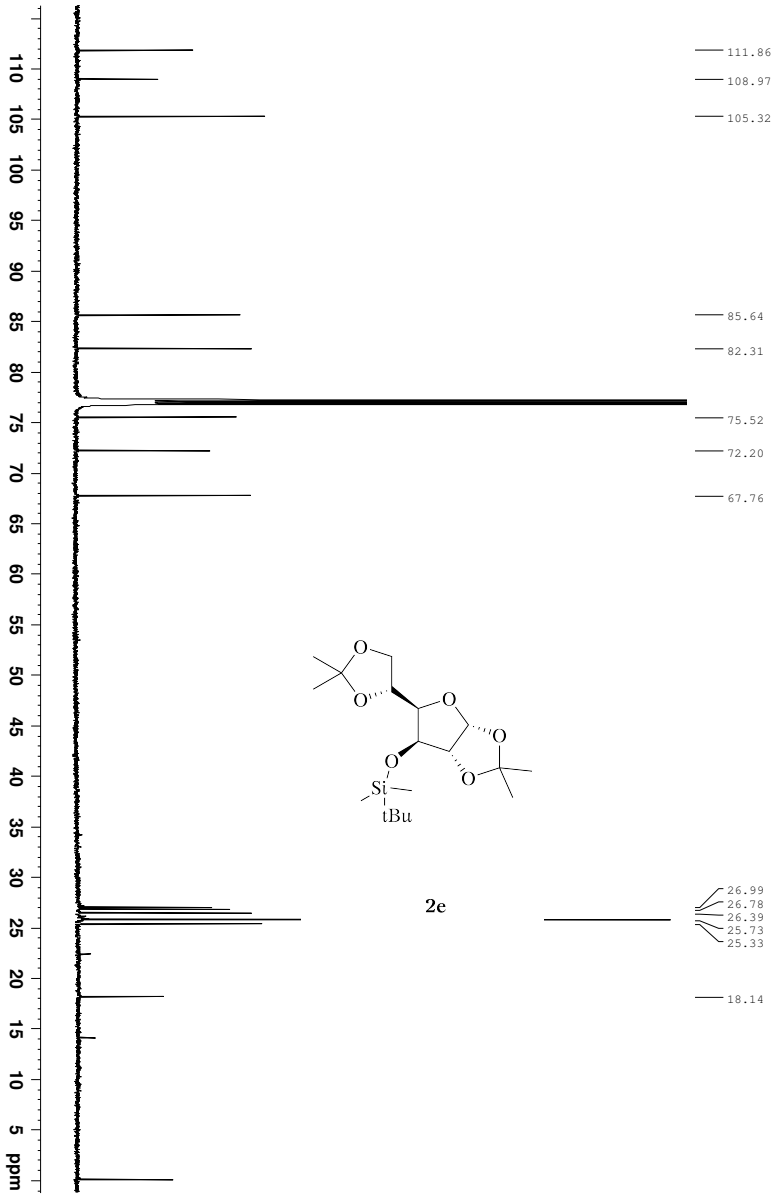

Figure 59: ^{13}C NMR spectrum of **2e**.

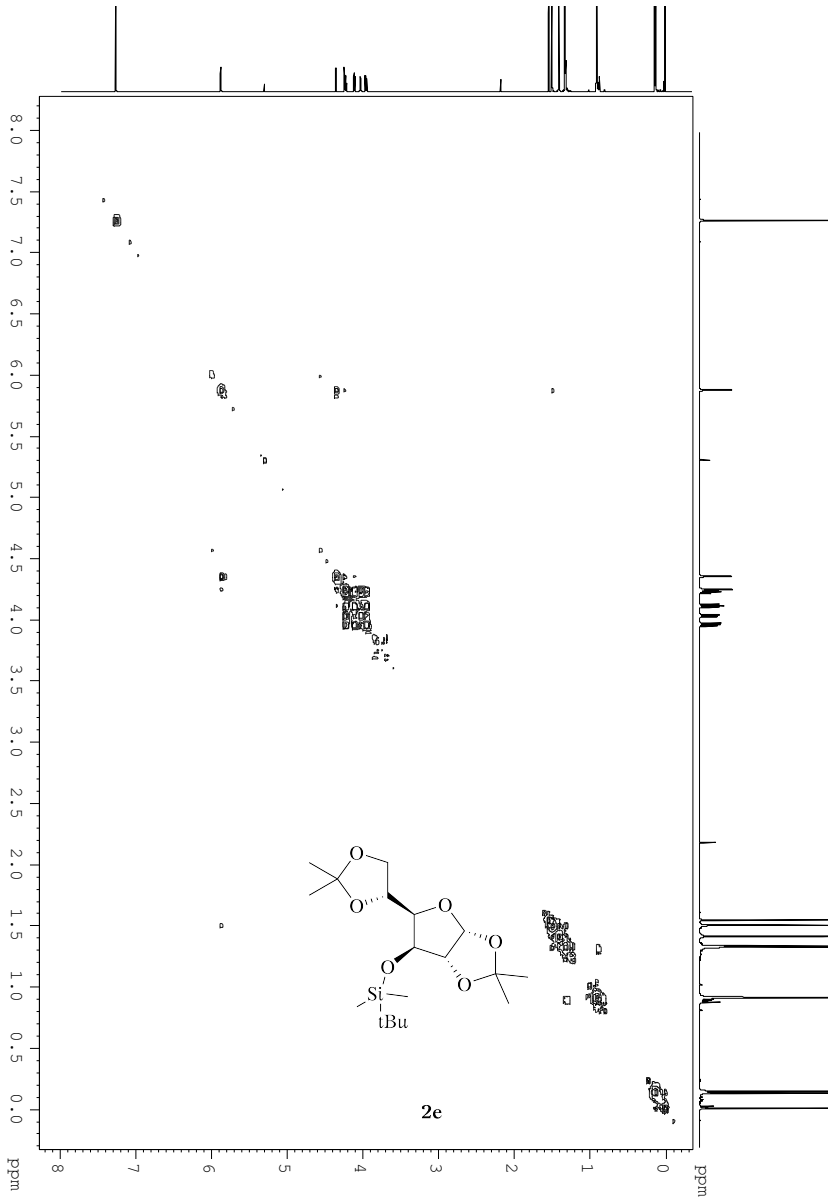

Figure 60: COSY spectrum of **2e**.

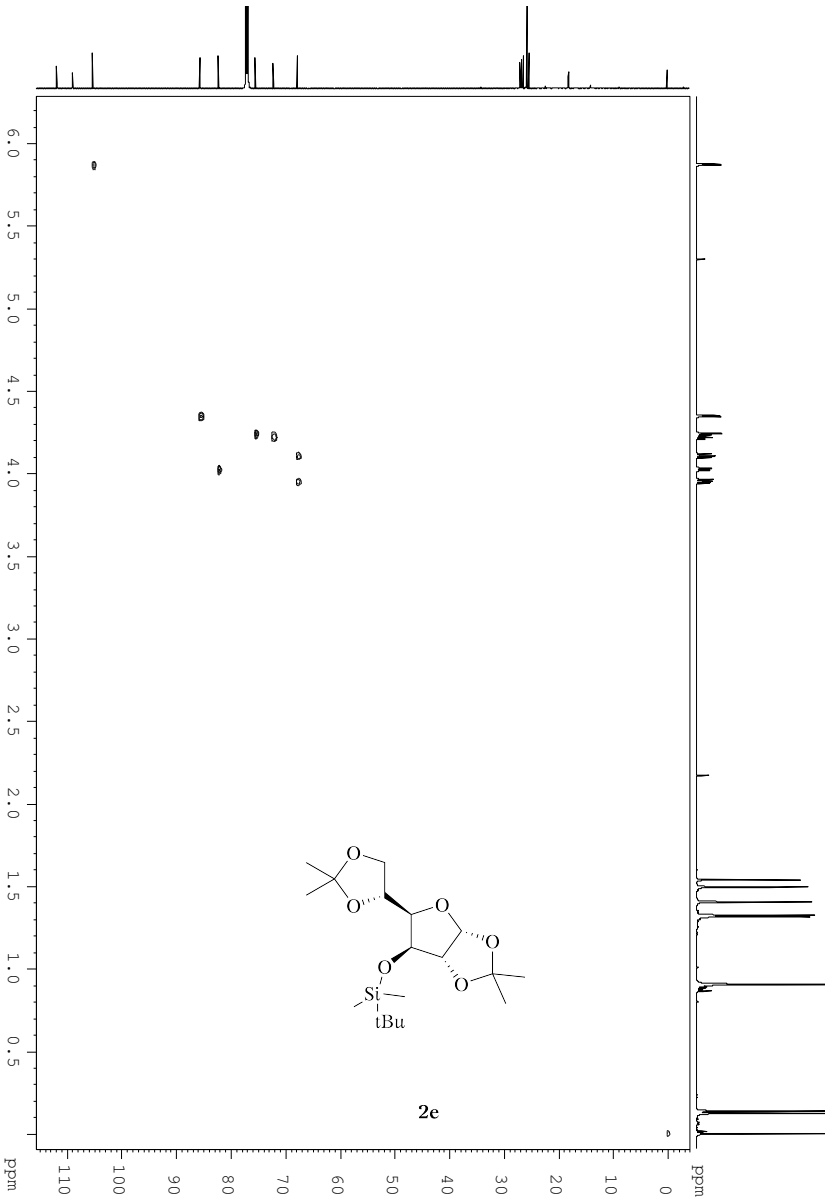

Figure 61: HSQC spectrum of **2e**.

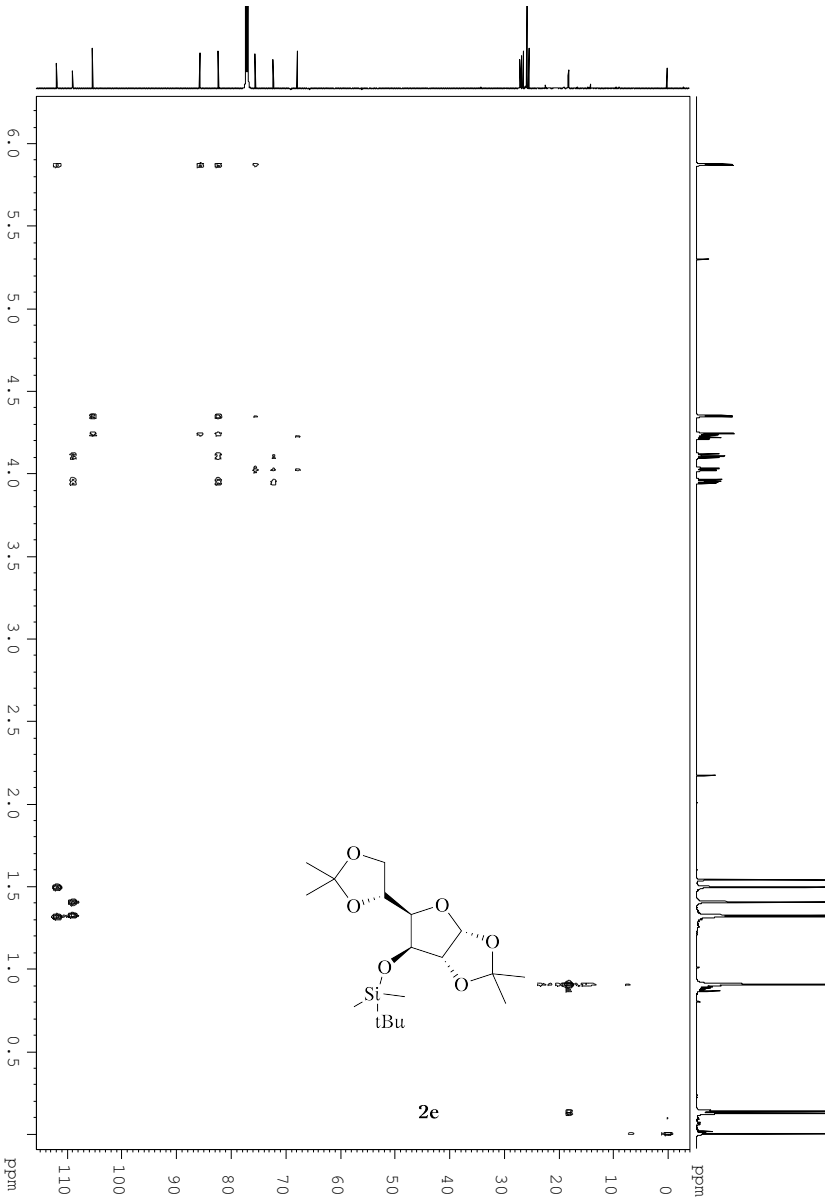

Figure 62: HMBC spectrum of **2e**.

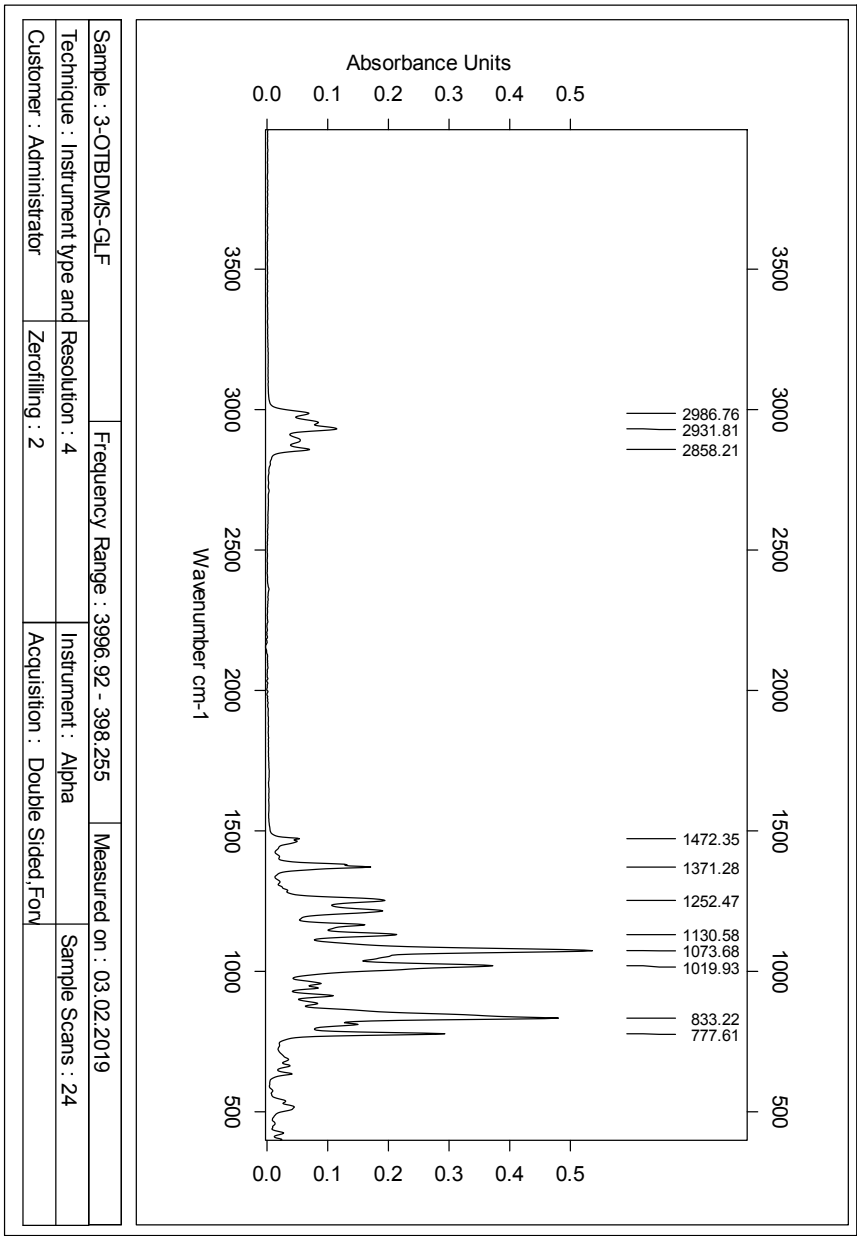

Figure 63: IR spectrum of **2e**.

B.6 Spectroscopic data for compound 2f

Elemental Composition Report **Page 1**

Single Mass Analysis
Tolerance = 2.1 PPM / DBE: min = -50.0, max = 50.0
Element prediction: Off
Number of isotope peaks used for i-FIT = 3

Monoisotopic Mass, Even Electron Ions
822 formula(e) evaluated with 3 results within limits (all results (up to 1000) for each mass)
Elements Used:
C: 0-100 H: 0-150 O: 0-10 Na: 0-1 Si: 0-2
2019_538 33 (0.619) AM2 (Ar,35000.0,0.00,0.00); Cm (31:33)
1: TOF MS ES+

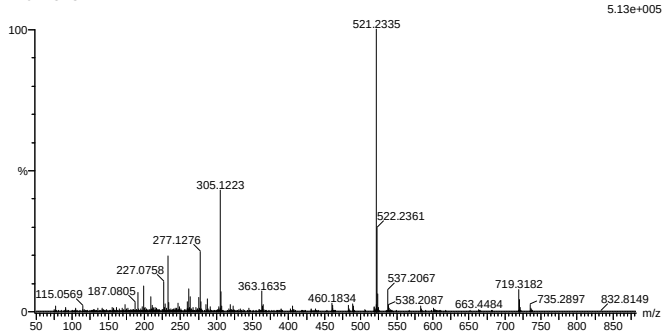

Minimum:				-50.0				
Maximum:		5.0	2.1	50.0				
Mass	Calc. Mass	mDa	PPM	DBE	i-FIT	Norm	Conf(%)	Formula
521.2335	521.2335	0.0	0.0	10.5	869.6	0.027	97.34	C28 H38 O6 Na Si
	521.2332	0.3	0.6	17.5	873.5	3.947	1.93	C33 H37 O2 Si2
	521.2328	0.7	1.3	18.5	874.5	4.915	0.73	C34 H33 O5

Figure 64: HRMS (ESI+) of **2f**.

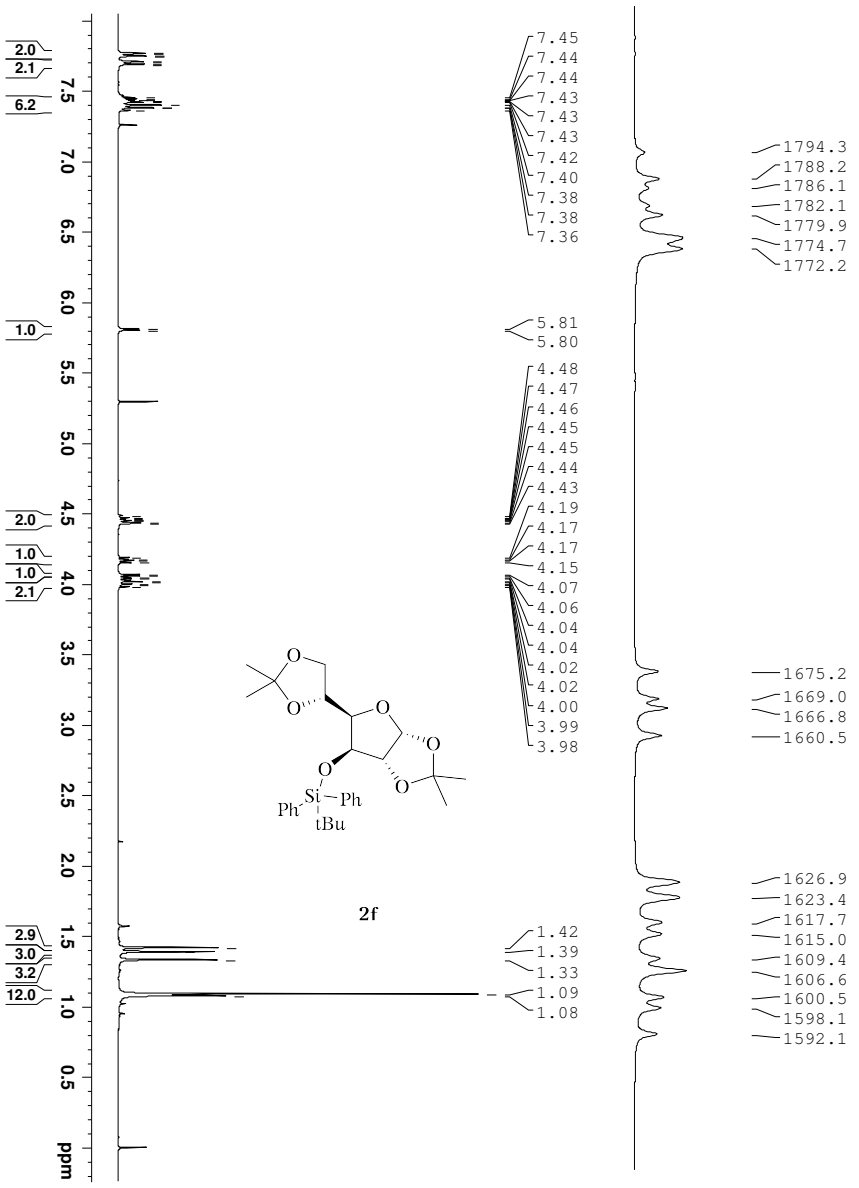

Figure 65: ^{1}H NMR (400 MHz) spectrum of **2f**.

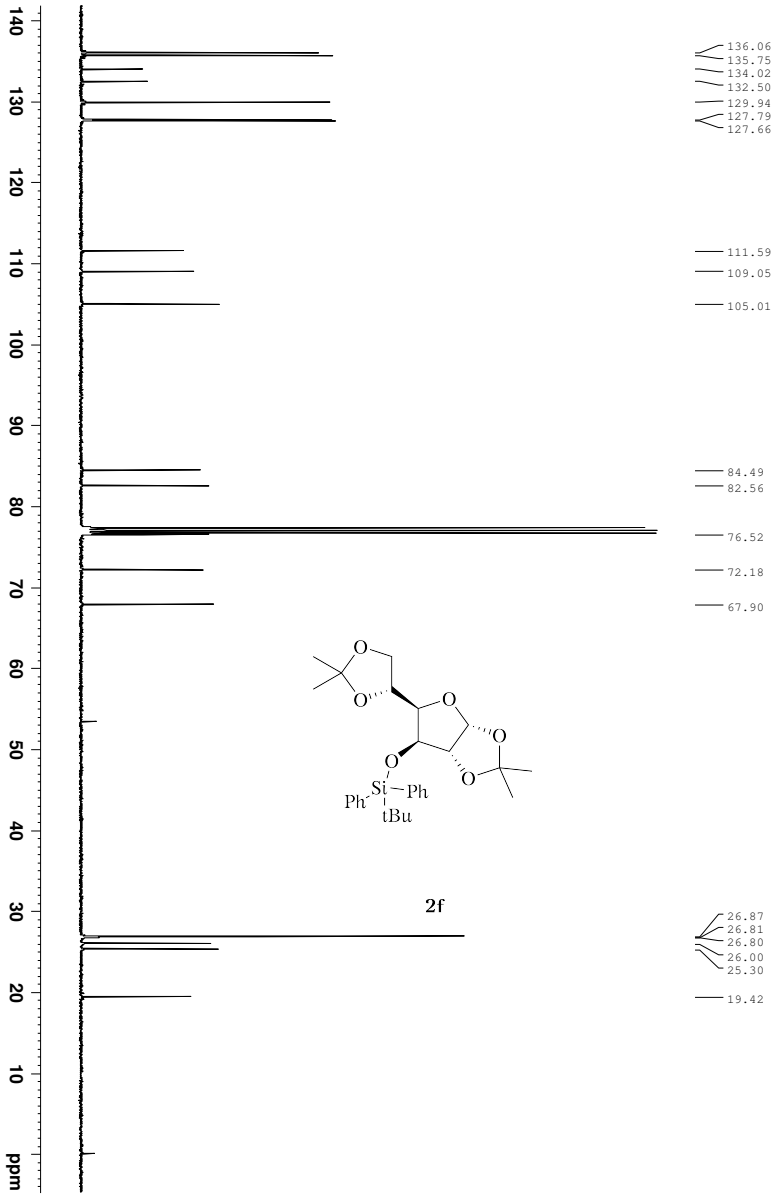

Figure 66: ^{13}C NMR (100 MHz) spectrum of **2f**.

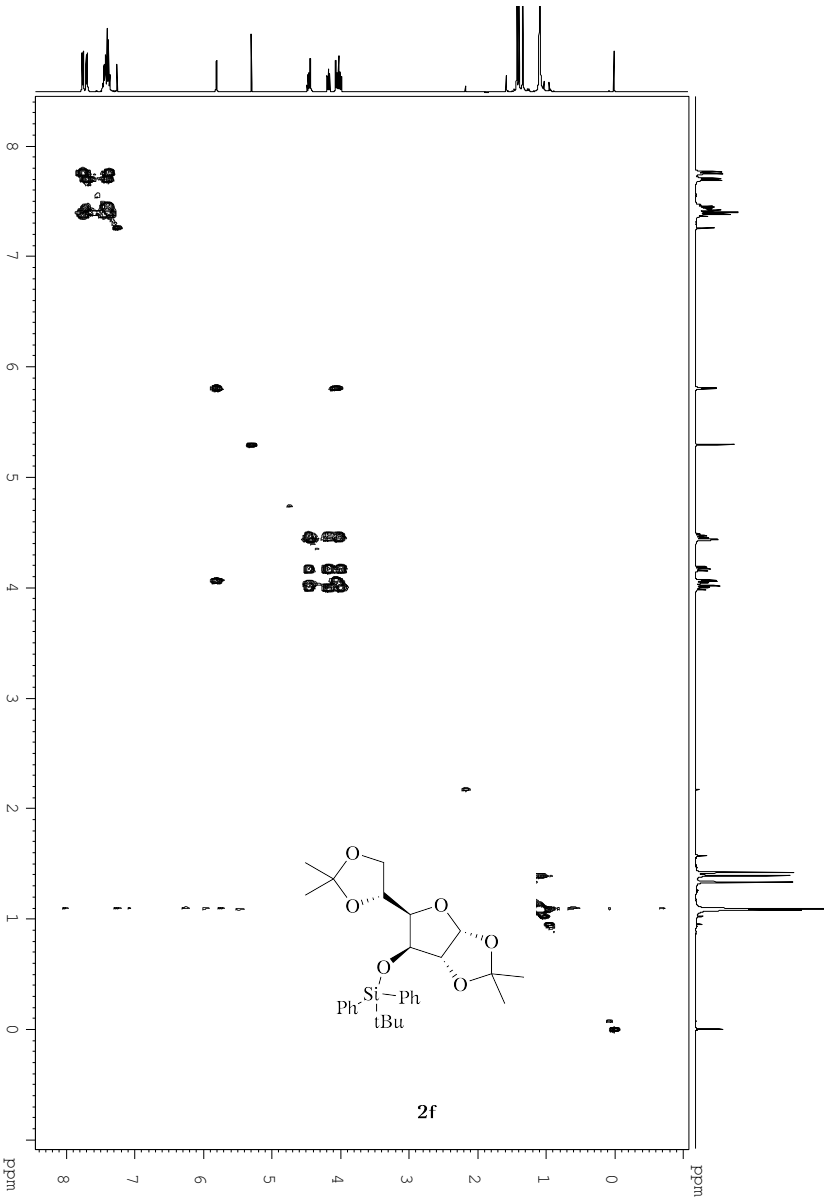

Figure 67: COSY (400 MHz) spectrum of **2f**.

l

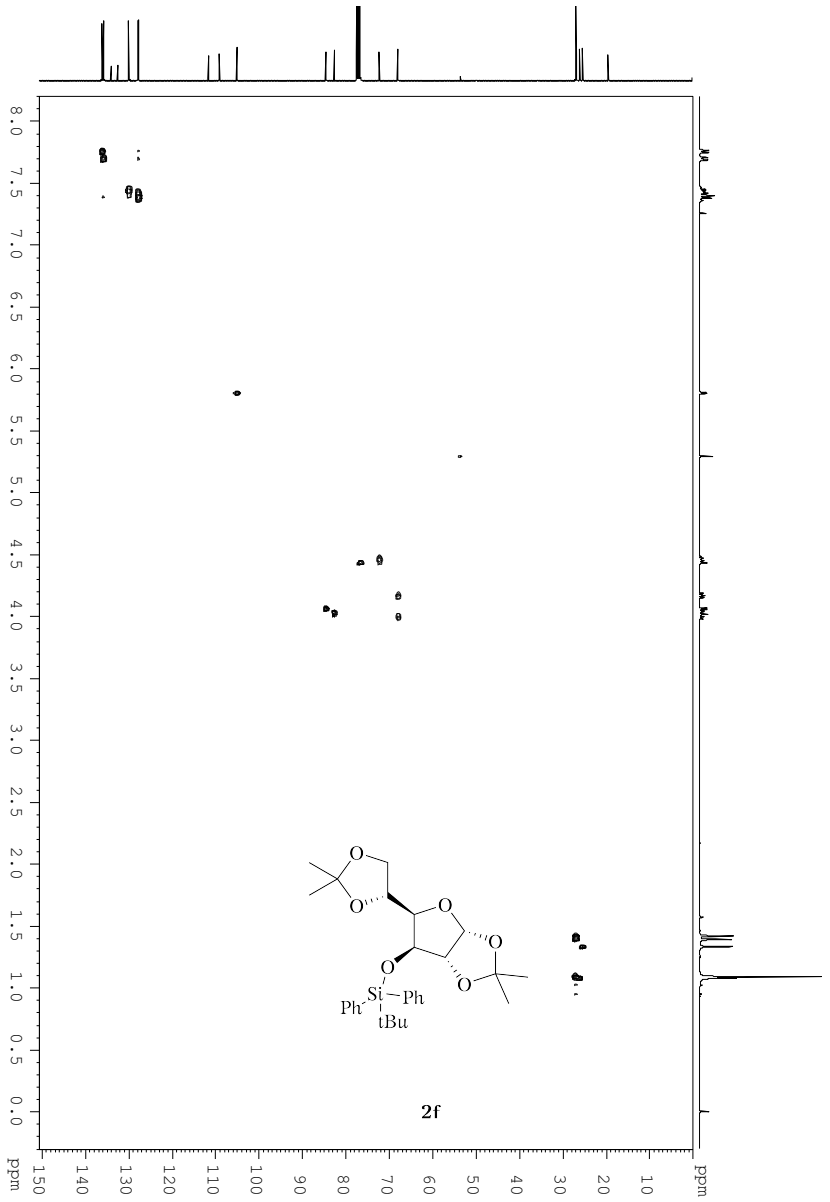

Figure 68: HSQC (400 MHz) spectrum of **2f**.

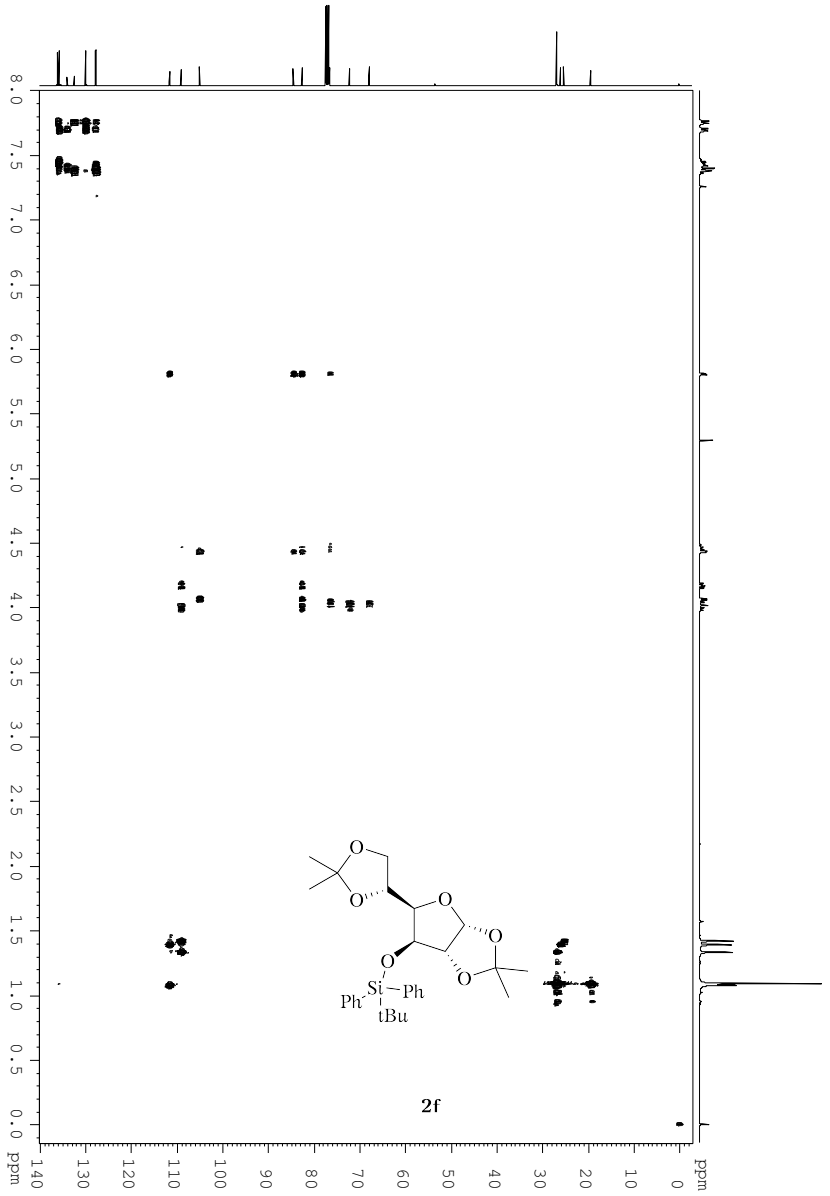

Figure 69: HMBC (400 MHz) spectrum of **2f**.

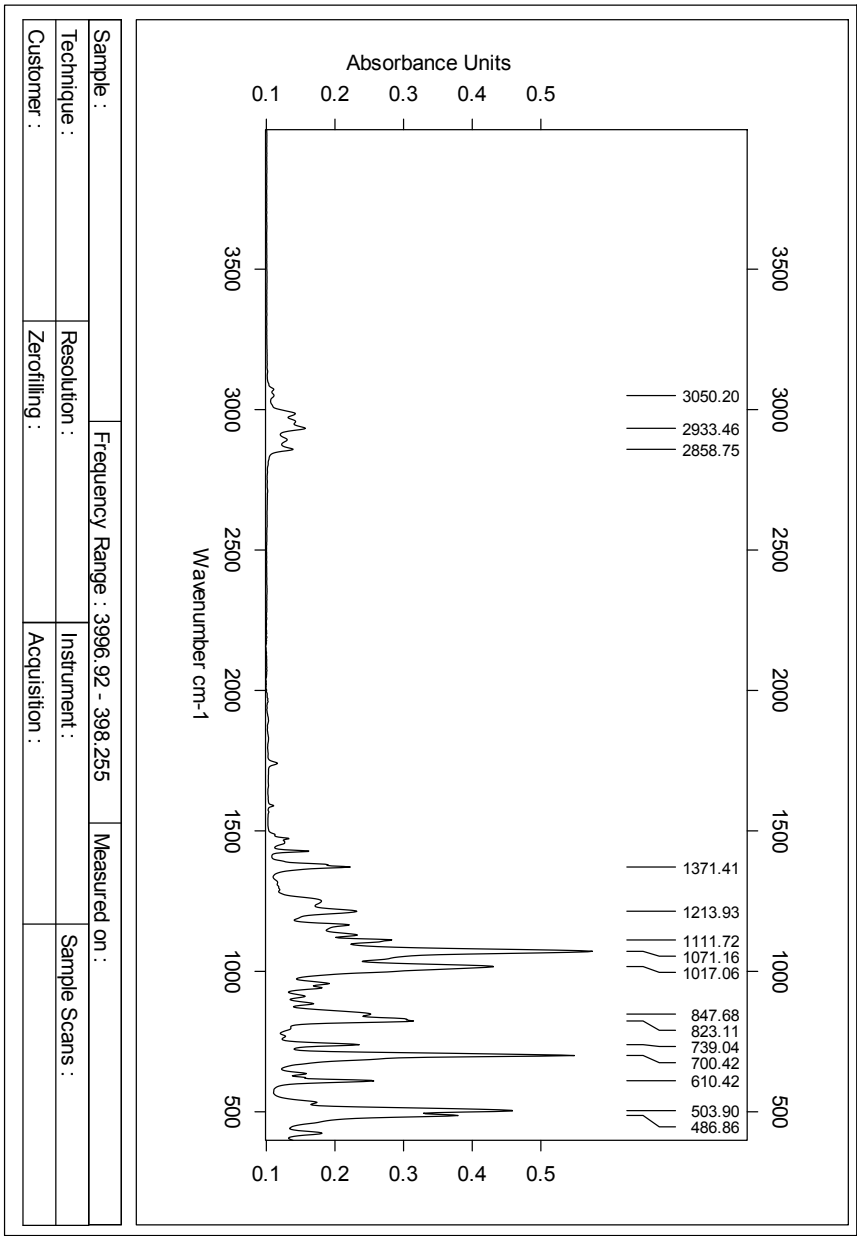

Figure 70: IR spectrum of **2f**.

B.7 Spectroscopic data for compound 2g

Elemental Composition Report **Page 1**

Single Mass Analysis
Tolerance = 2.1 PPM / DBE: min = -50.0, max = 50.0
Element prediction: Off
Number of isotope peaks used for i-FIT = 3

Monoisotopic Mass, Even Electron Ions
789 formula(e) evaluated with 1 results within limits (all results (up to 1000) for each mass)
Elements Used:
C: 0-100 H: 0-150 O: 0-10 Na: 0-1 Si: 0-2

2019_537 34 (0.636) AM2 (Ar,35000.0,0.00,0.00)
1: TOF MS ES+

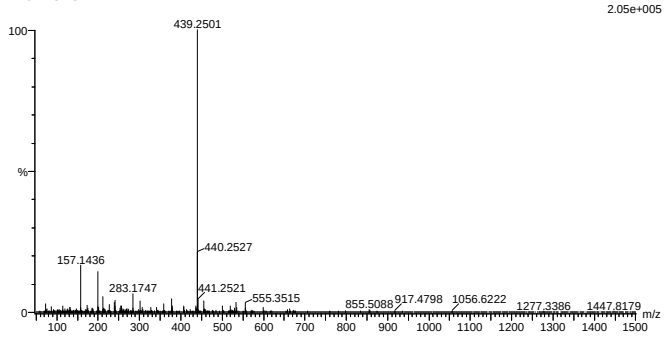

Minimum:				-50.0				
Maximum:		5.0	2.1	50.0				
Mass	Calc. Mass	mDa	PPM	DBE	i-FIT	Norm	Conf(%)	Formula
439.2501	439.2492	0.9	2.0	2.5	696.3	n/a	n/a	C21 H40 O6 Na Si

Figure 71: HRMS (ESI+) of **2g**.

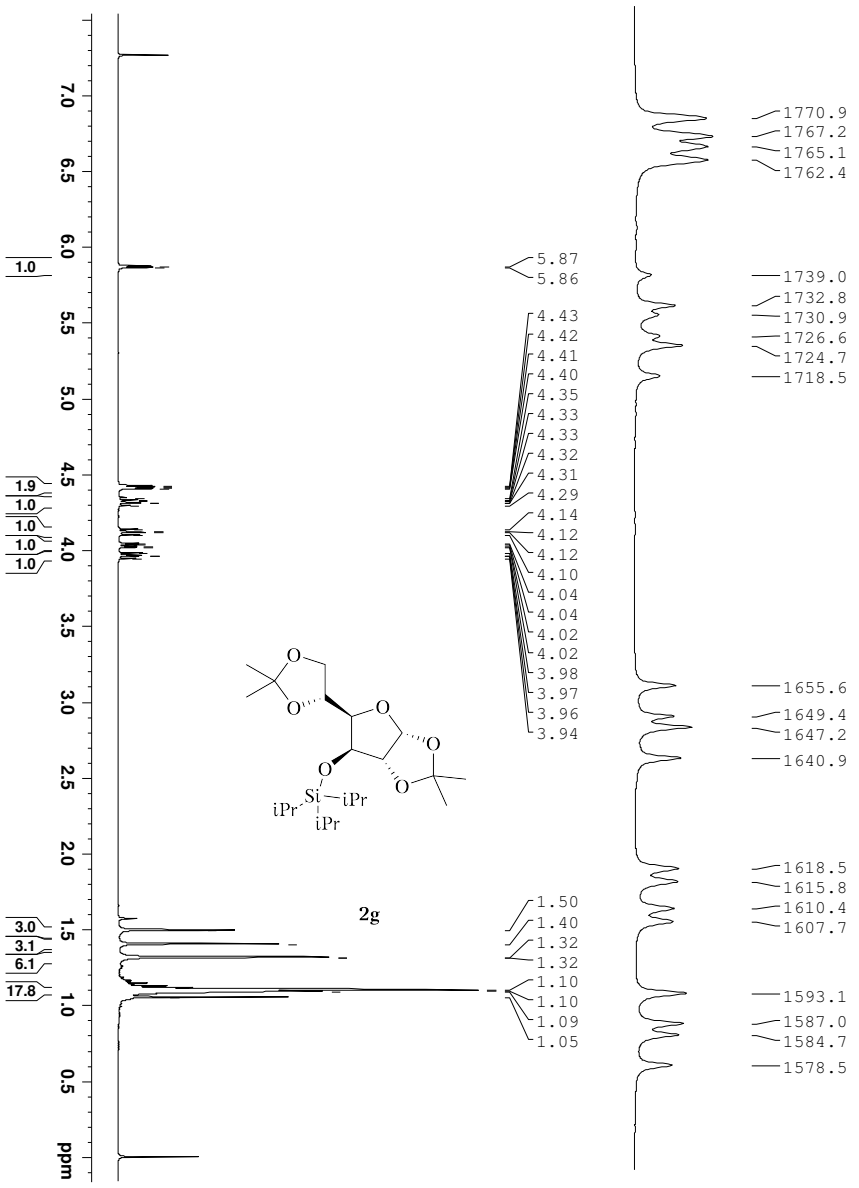

Figure 72: ^{1}H NMR (400 MHz) spectrum of **2g**.

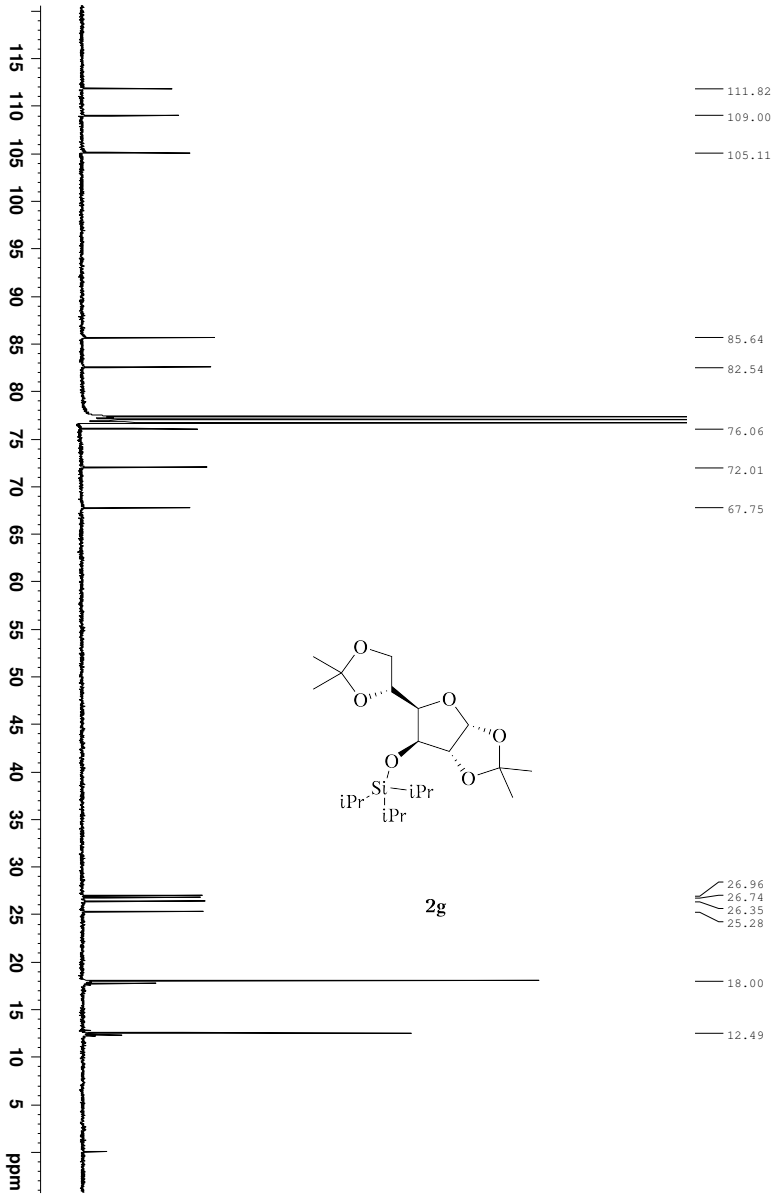

Figure 73: ^{13}C NMR (100 MHz) spectrum of **2g**.

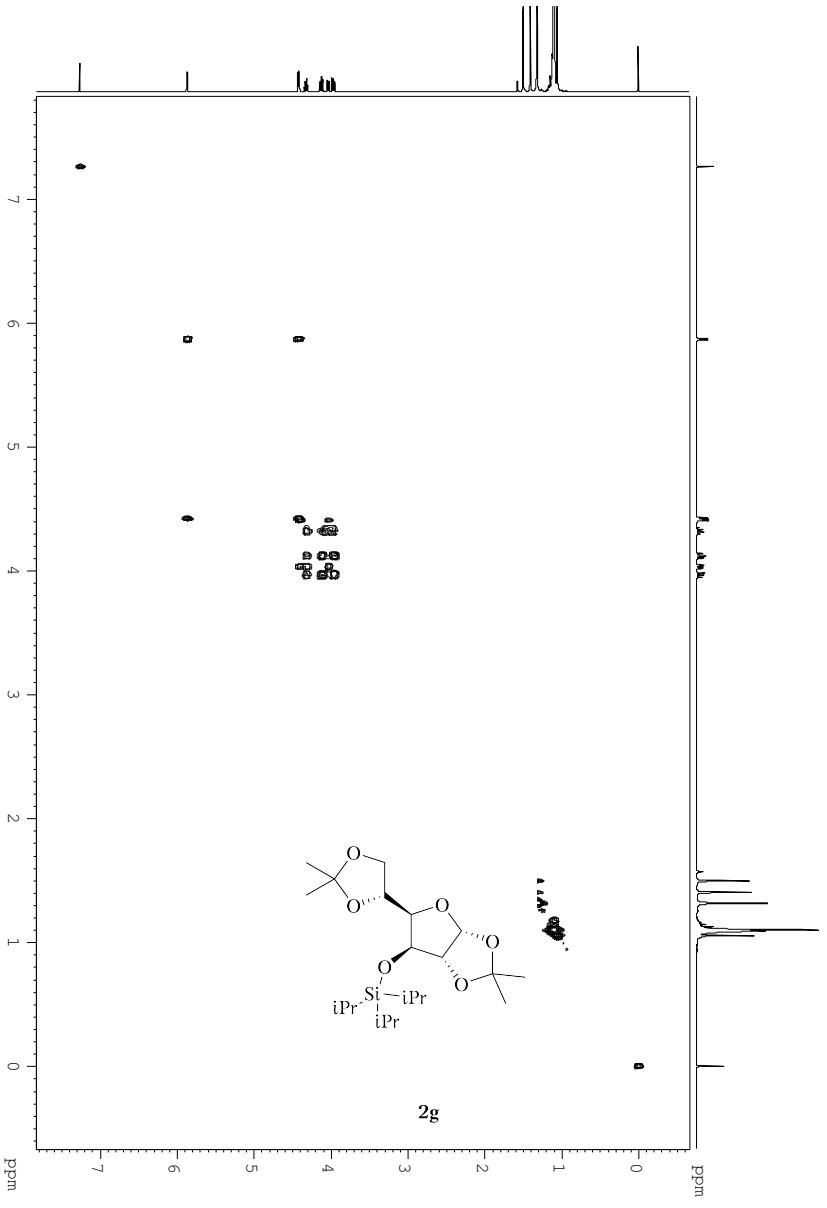

Figure 74: COSY (400 MHz) spectrum of **2g**.

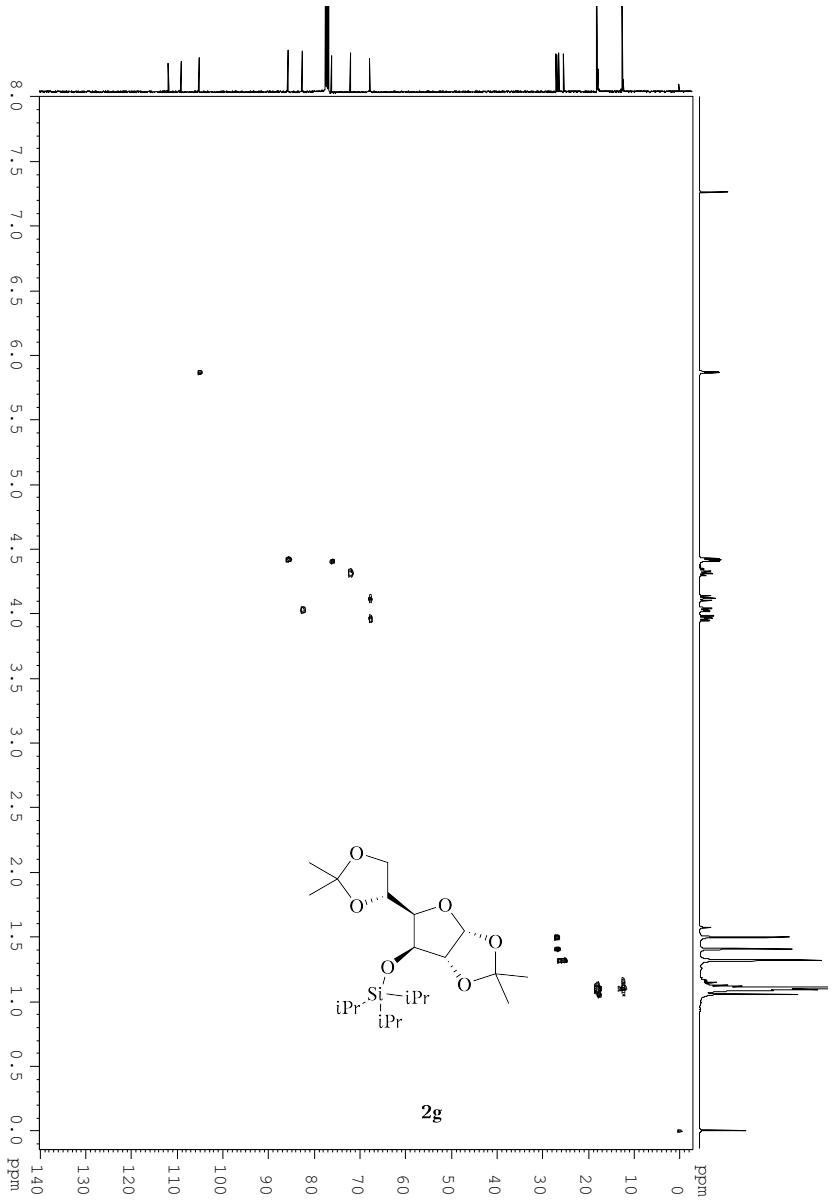

Figure 75: HSQC (400 MHz) spectrum of **2g**.

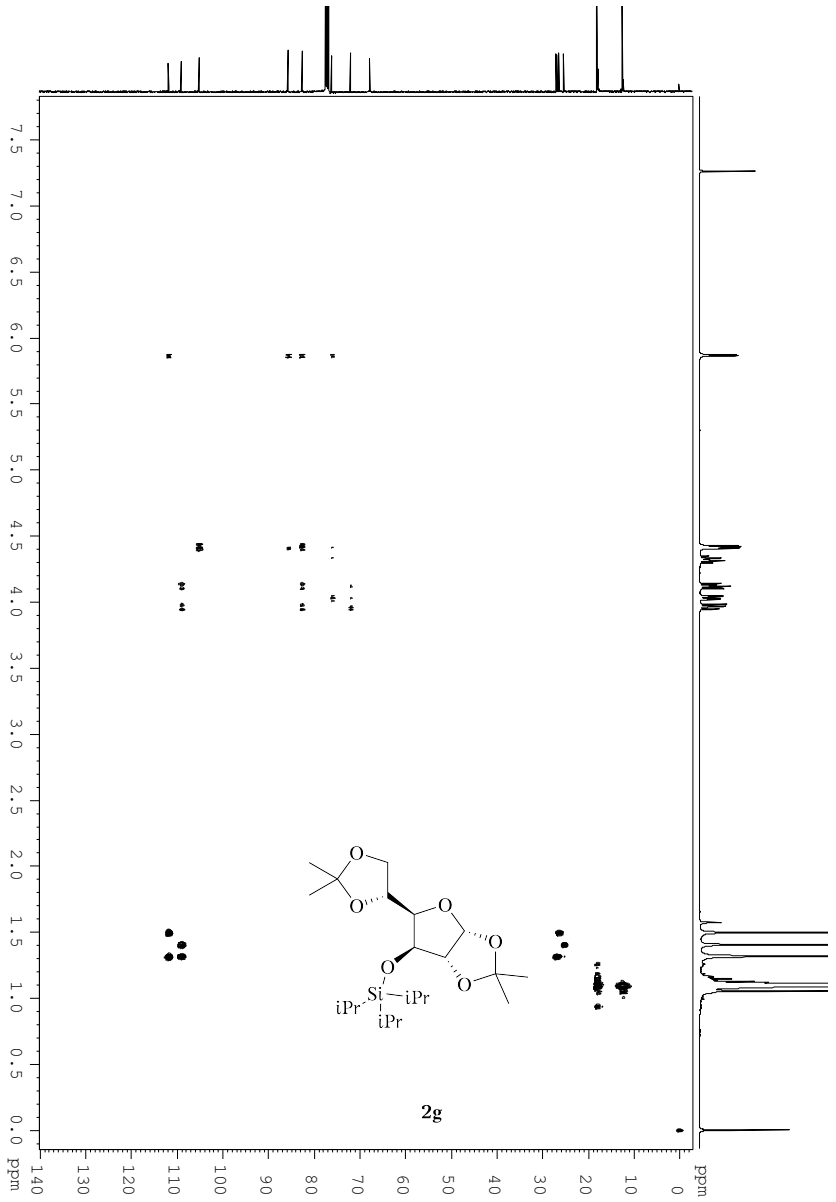

Figure 76: HMBC (400 MHz) spectrum of **2g**.

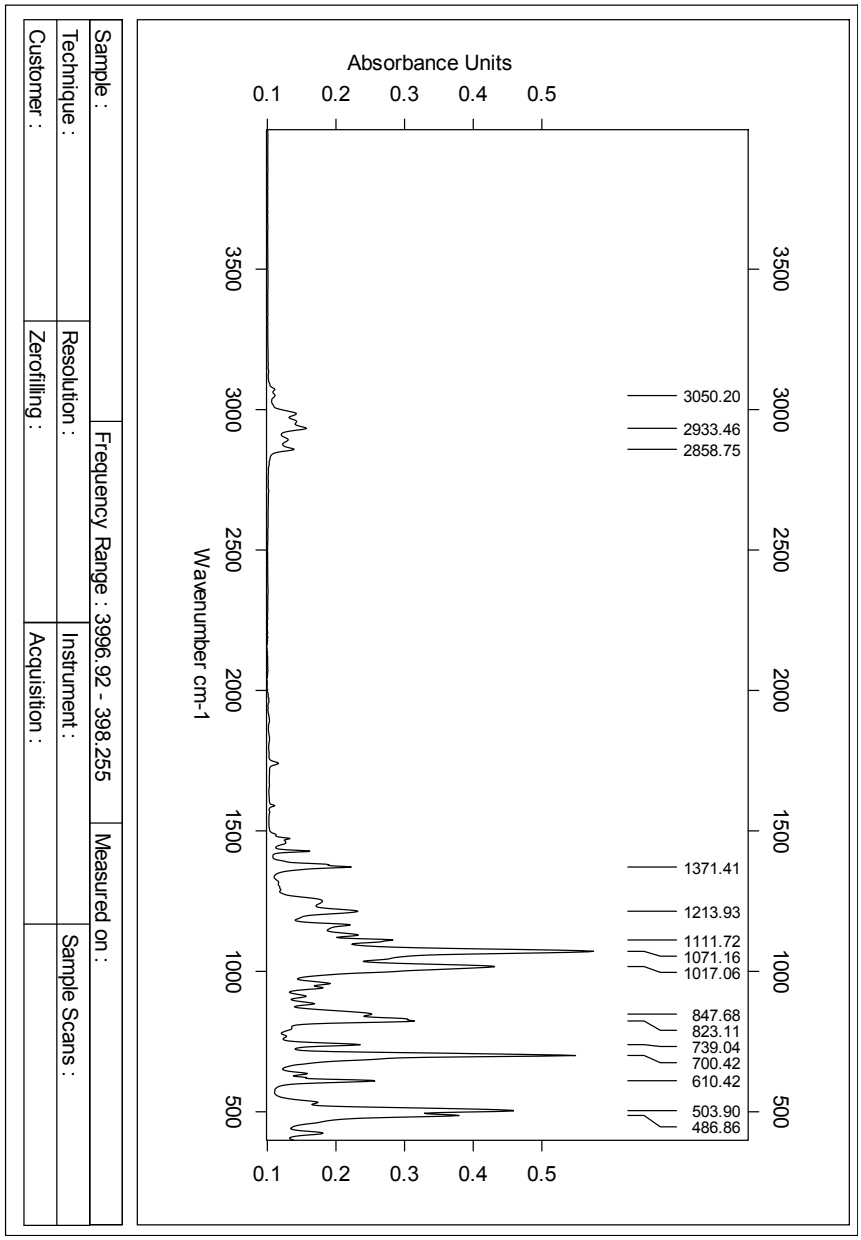

Figure 77: IR spectrum of **2g**.

B.8 Spectroscopic data for compound 2i

Elemental Composition Report **Page 1**

Single Mass Analysis
Tolerance = 5.0 PPM / DBE: min = -2.0, max = 50.0
Element prediction: Off
Number of isotope peaks used for i-FIT = 3

Monoisotopic Mass, Even Electron Ions
1080 formula(e) evaluated with 5 results within limits (all results (up to 1000) for each mass)
Elements Used:
C: 0-100 H: 0-150 N: 0-10 O: 0-10 Na: 0-1
2019-39esi 139 (1.300) AM2 (Ar,35000.0,0.00,0.00); Cm (135:139)
1: TOF MS ES+

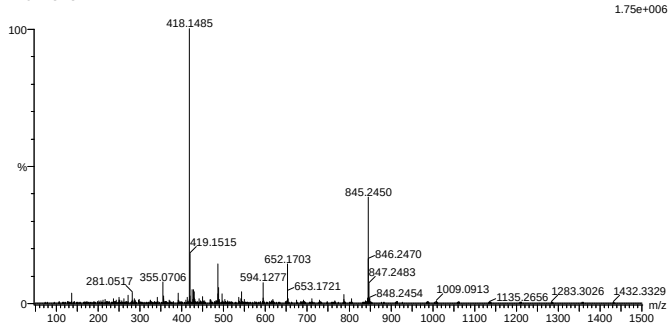

Minimum:				-2.0				
Maximum:		5.0	5.0	50.0				
Mass	Calc. Mass	mDa	PPM	DBE	i-FIT	Norm	Conf(%)	Formula
418.1485	418.1478	0.7	1.7	7.5	1197.4	1.688	18.49	C19 H25 N O8 Na
	418.1502	-1.7	-4.1	10.5	1200.8	5.027	0.66	C21 H24 N O8
	418.1491	-0.6	-1.4	12.5	1198.9	3.162	4.23	C20 H21 N5 O4 Na
	418.1475	1.0	2.4	11.5	1196.0	0.274	76.04	C17 H20 N7 O6
	418.1505	-2.0	-4.8	17.5	1200.9	5.149	0.58	C21 H17 N9 Na

Figure 78: HRMS (ESI+) of **2i**.

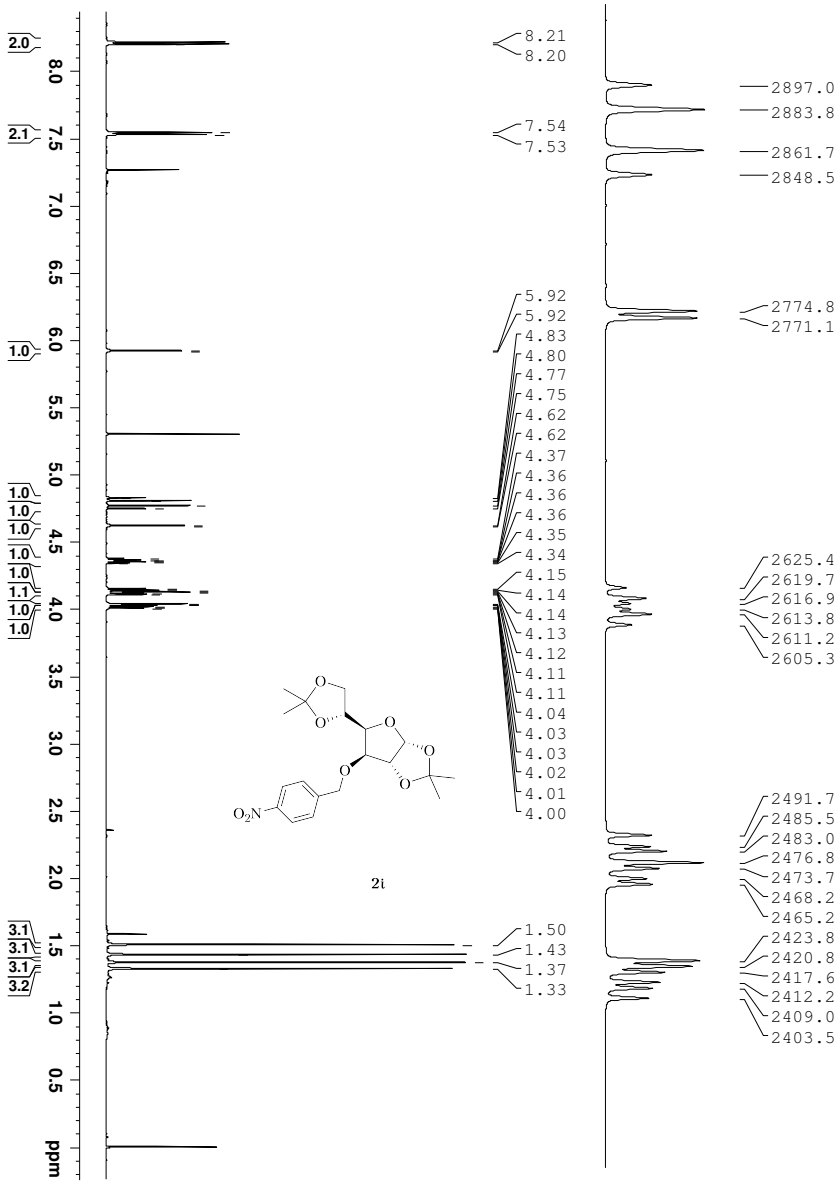

Figure 79: ^{1}H NMR spectrum of **2i**.

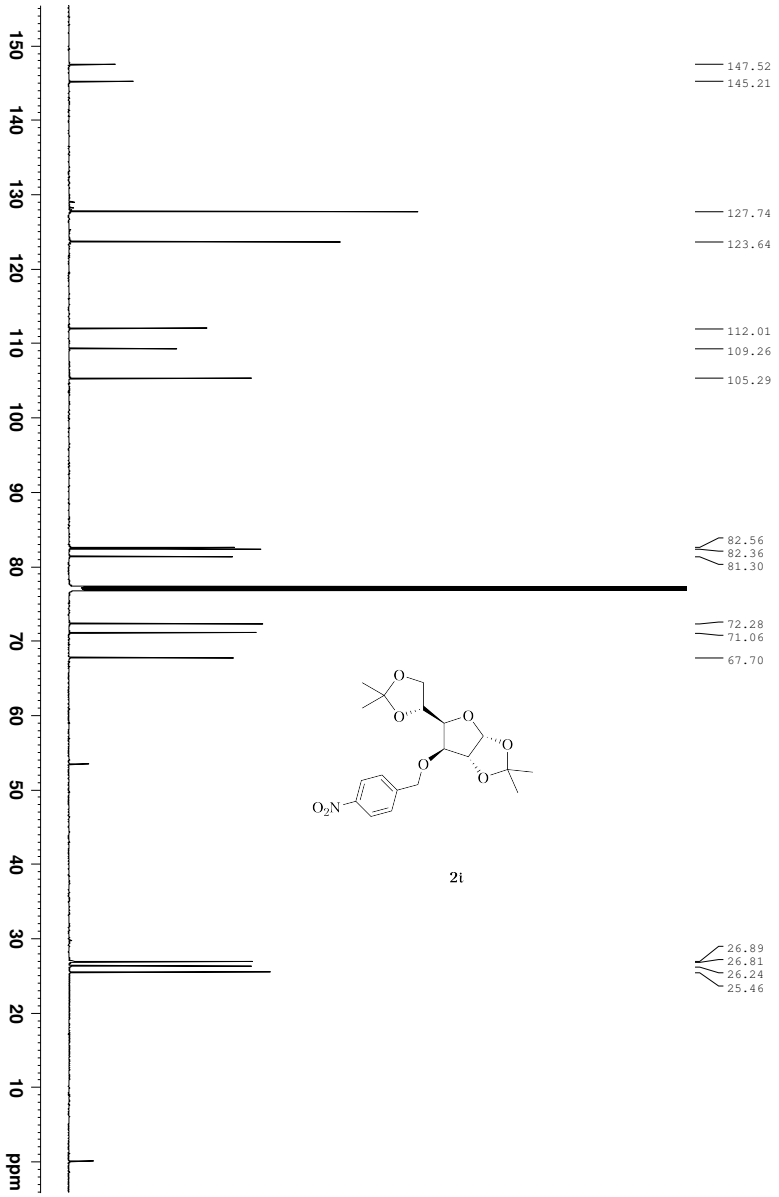

Figure 80: ^{13}C NMR spectrum of **2i**.

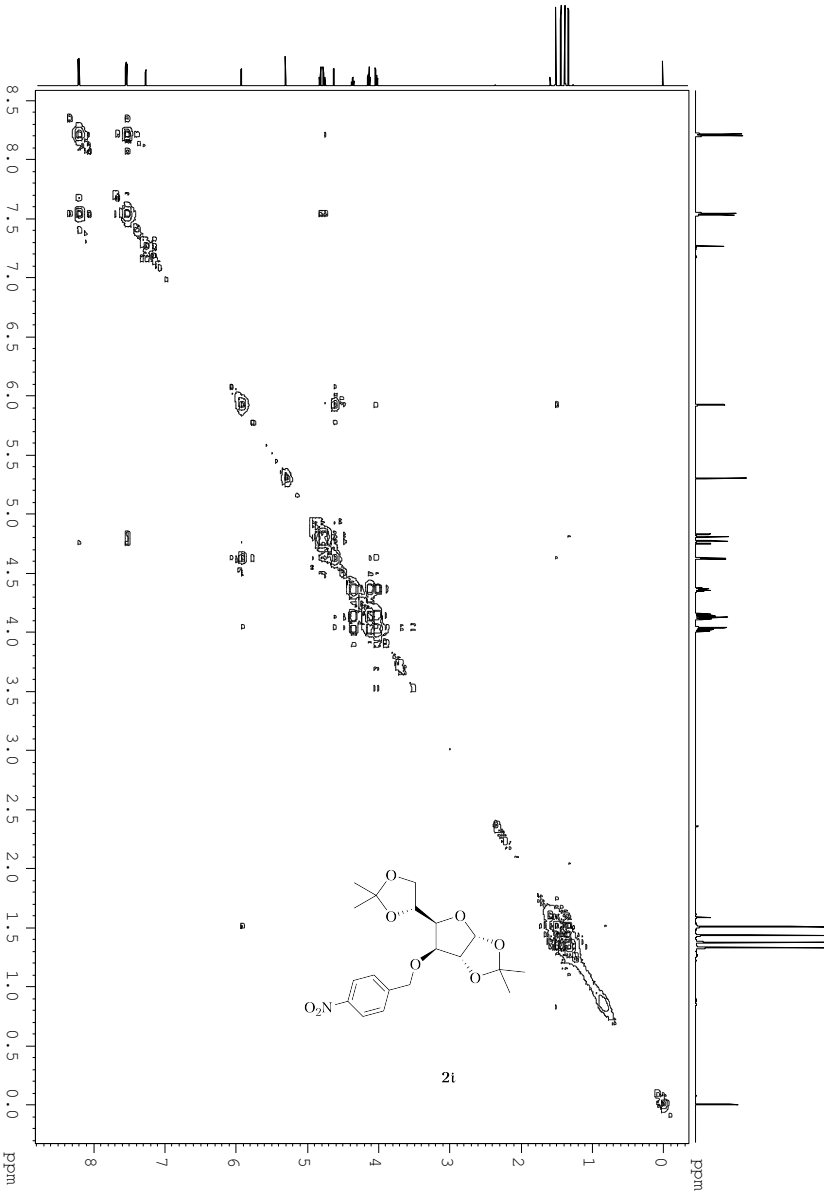

Figure 81: COSY spectrum of **2i**.

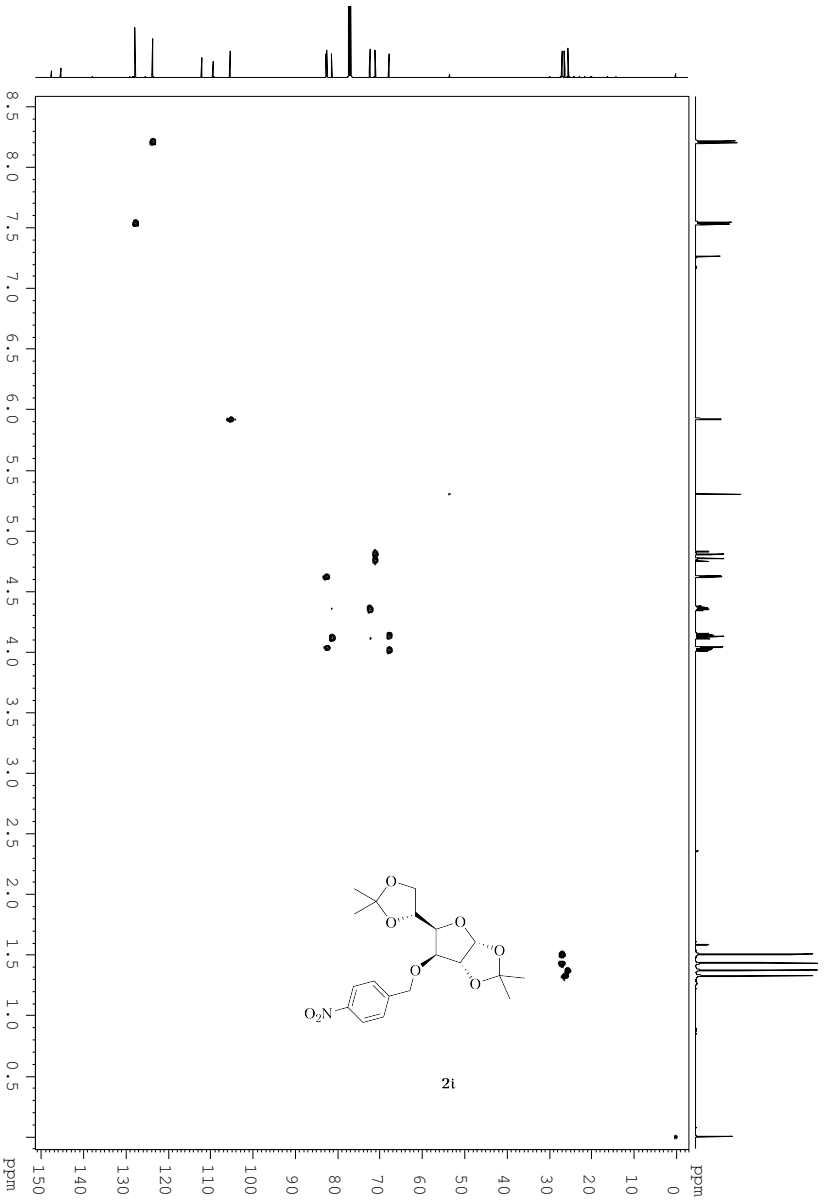

Figure 82: HSQC spectrum of **2i**.

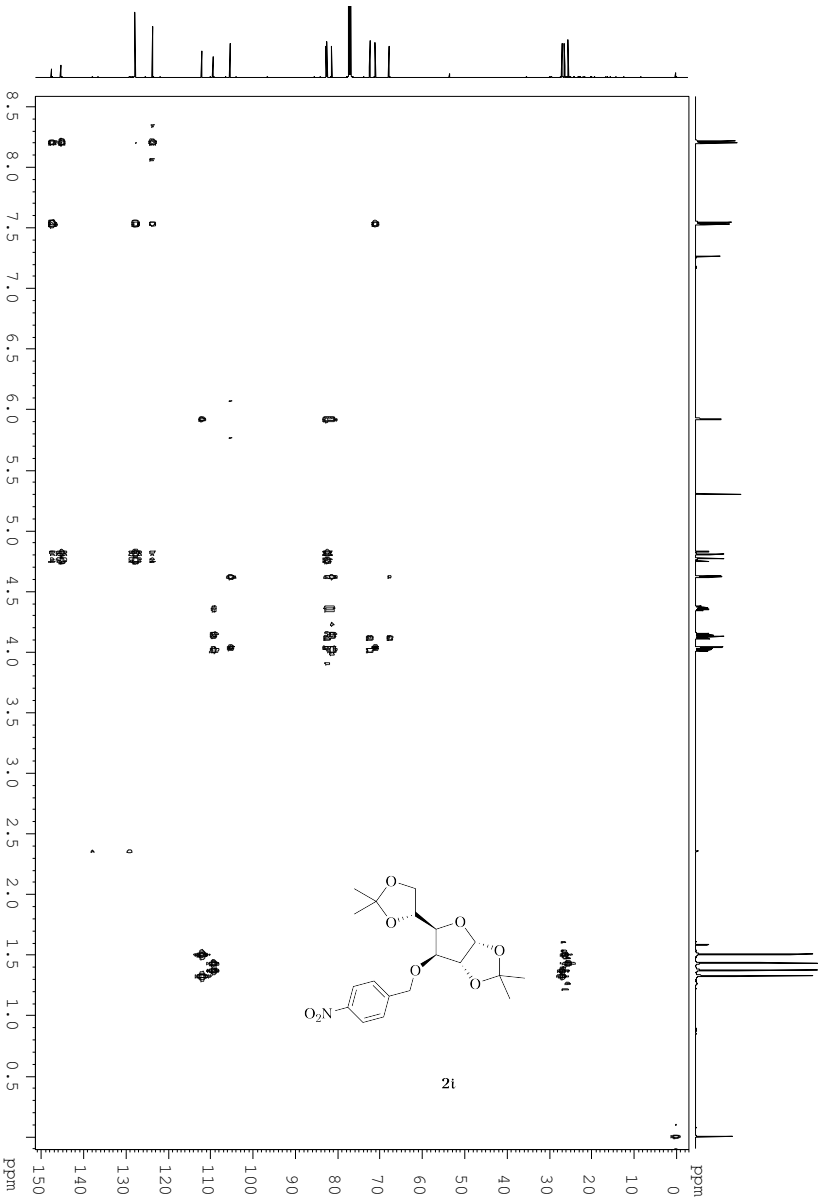

Figure 83: HMBC spectrum of **2i**.

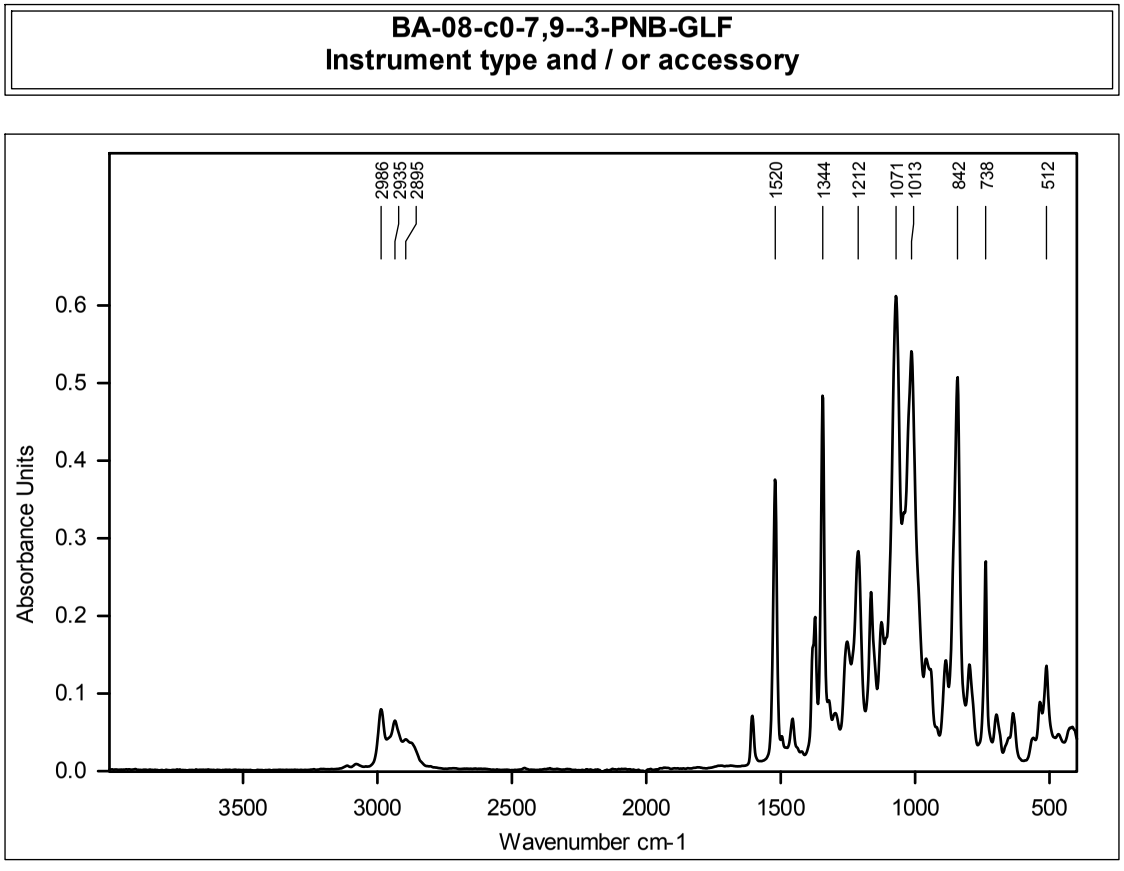

Figure 84: IR spectrum of **2i**.

B.9 Spectroscopic data for compound 2j

Elemental Composition Report **Page 1**

Single Mass Analysis
Tolerance = 2.0 PPM / DBE: min = -50.0, max = 50.0
Element prediction: Off
Number of isotope peaks used for i-FIT = 3

Monoisotopic Mass, Odd Electron Ions
1787 formula(e) evaluated with 3 results within limits (all results (up to 1000) for each mass)
Elements Used:
C: 0-100 H: 0-150 N: 0-6 O: 0-6 Si: 0-2
2019-214 73 (1.449) AM2 (Ar,35000.0,0.00,0.00); Cm (70:75)
1: TOF MS ASAP+

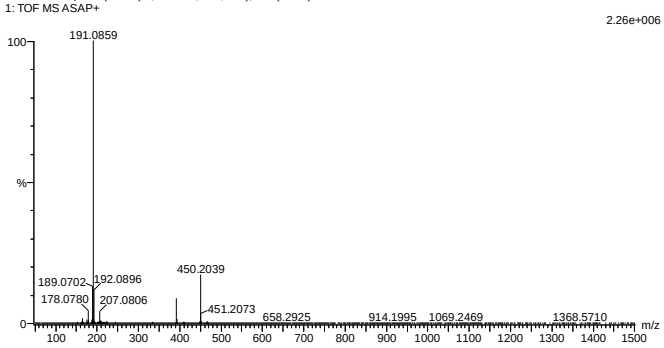

Minimum:				-50.0				
Maximum:		5.0	2.0	50.0				
Mass	Calc. Mass	mDa	PPM	DBE	i-FIT	Norm	Conf(%)	Formula
450.2039	450.2042	-0.3	-0.7	13.0	915.1	0.001	99.95	C27 H30 O6
	450.2046	-0.7	-1.6	12.0	925.1	9.995	0.00	C26 H34 O3 Si2
	450.2047	-0.8	-1.8	9.0	922.8	7.660	0.05	C19 H30 N6 O5 Si

Figure 85: HRMS (ASAP+) [M] of **2j**.

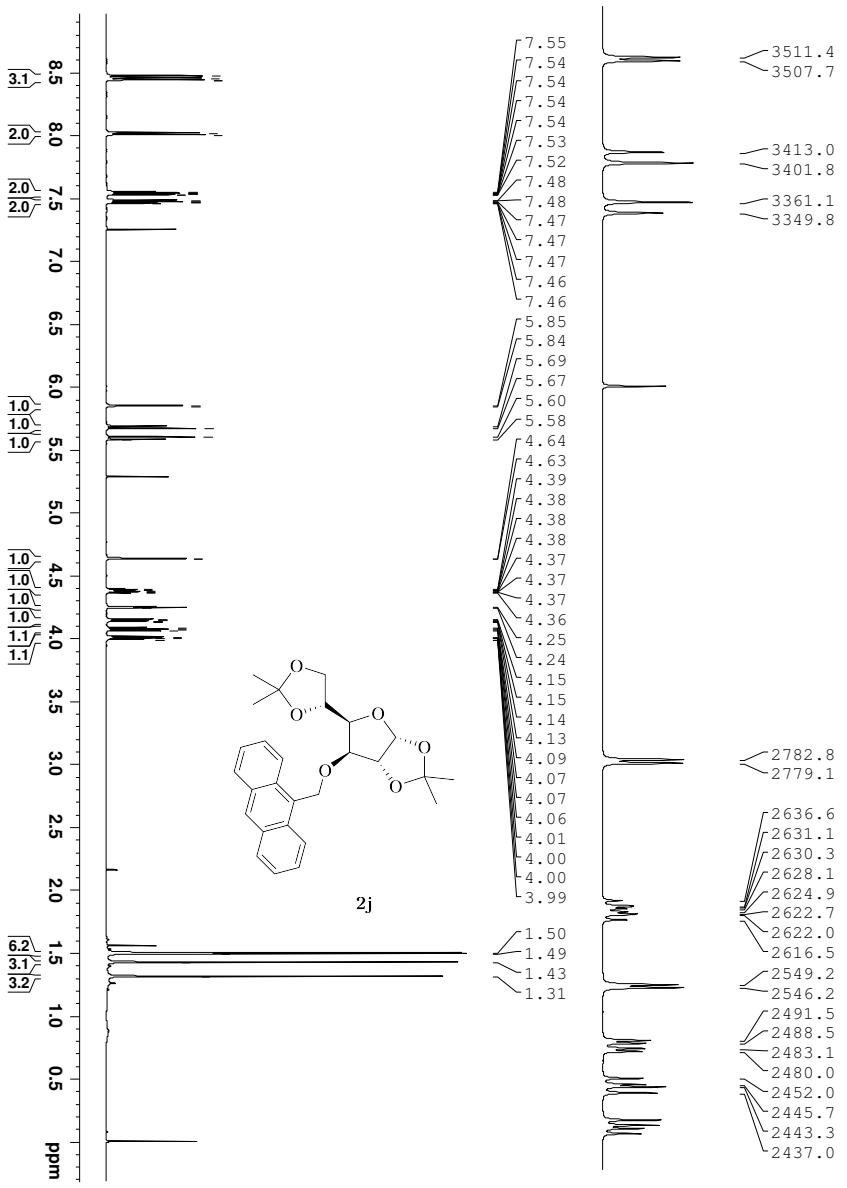

Figure 86: ^{1}H NMR spectrum of **2j**.

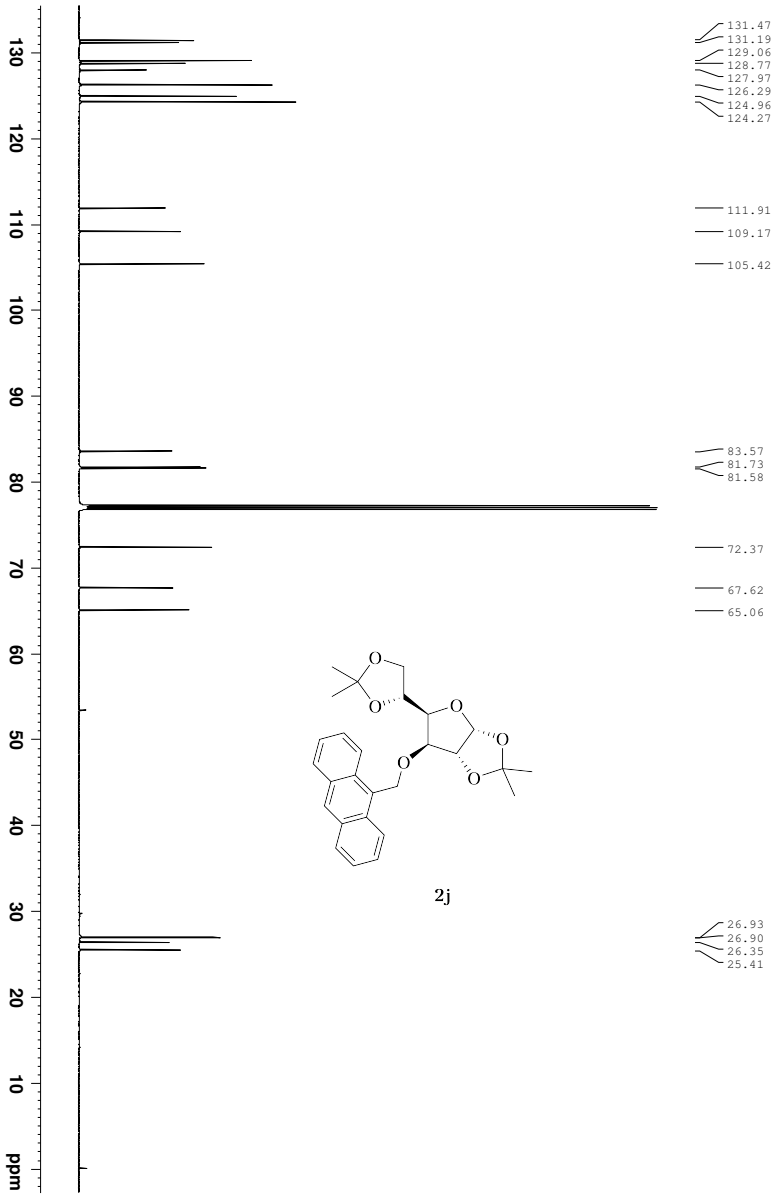

Figure 87: ^{13}C NMR spectrum of **2j**.

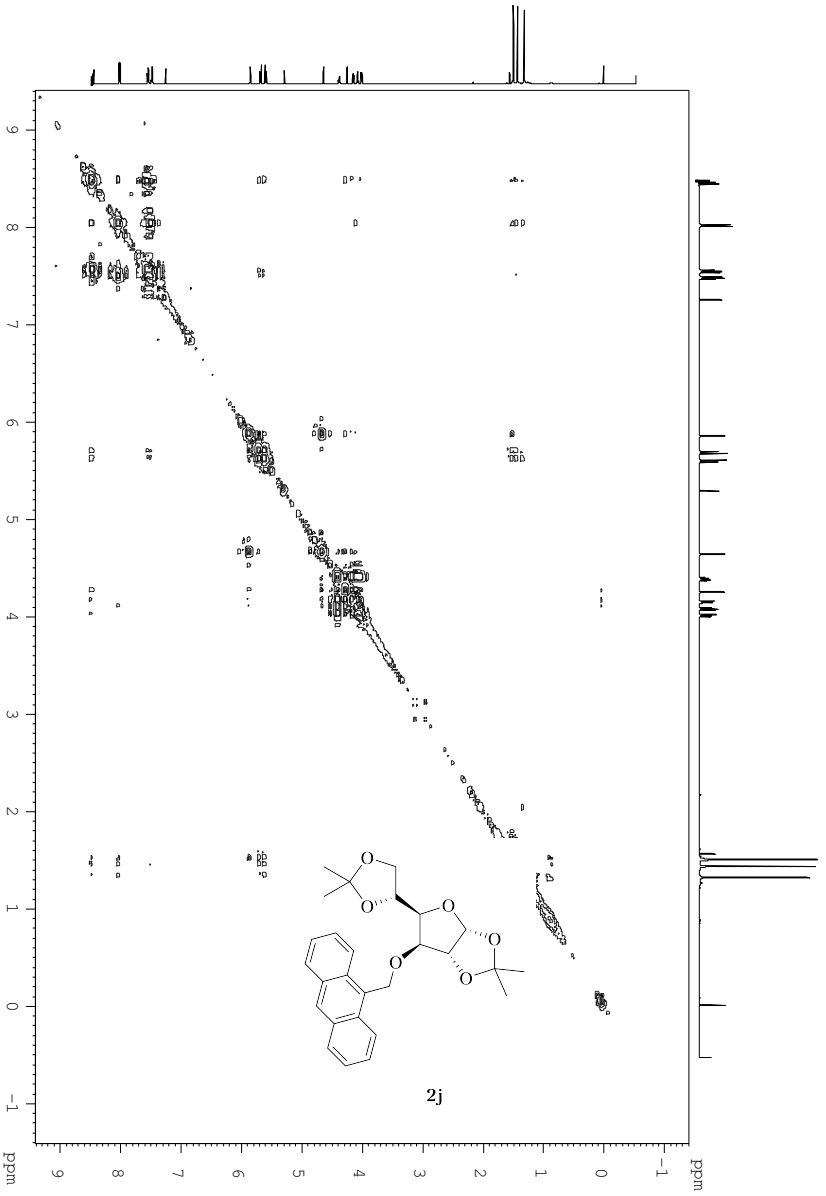

Figure 88: COSY spectrum of **2j**.

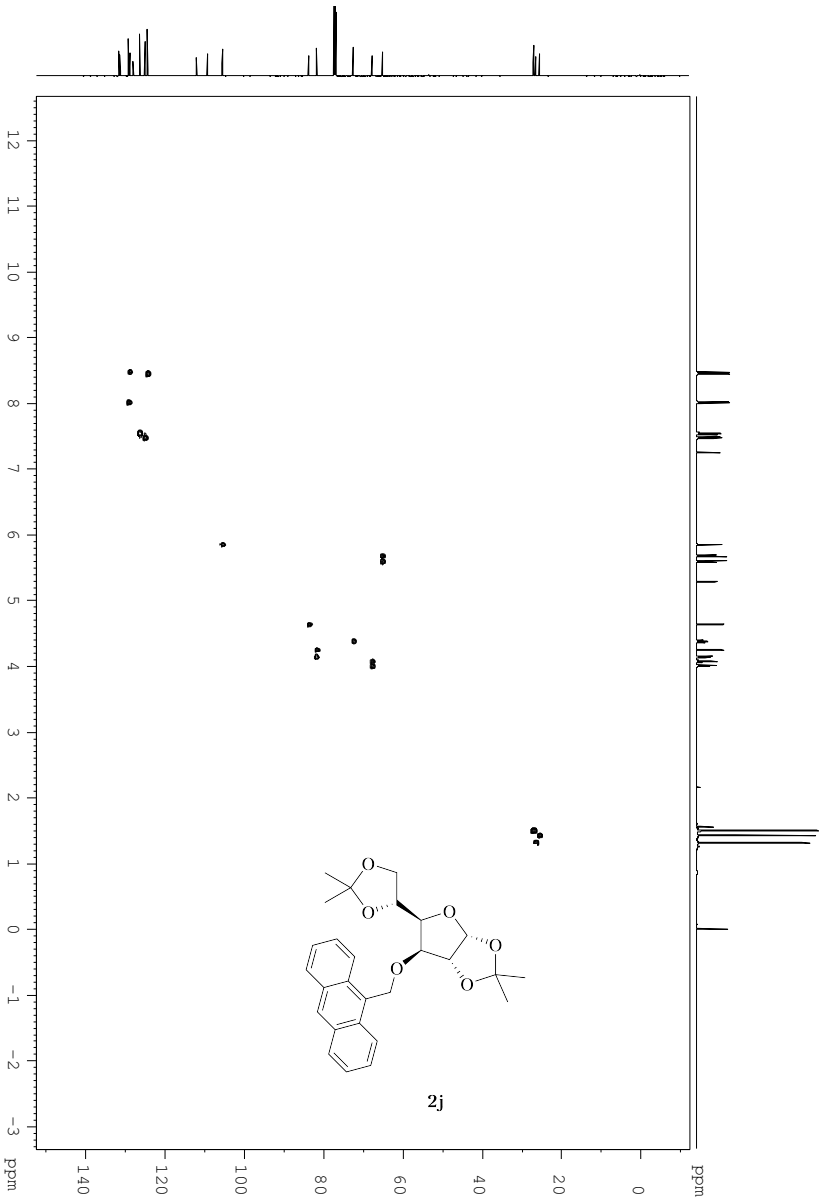

Figure 89: HSQC spectrum of **2j**.

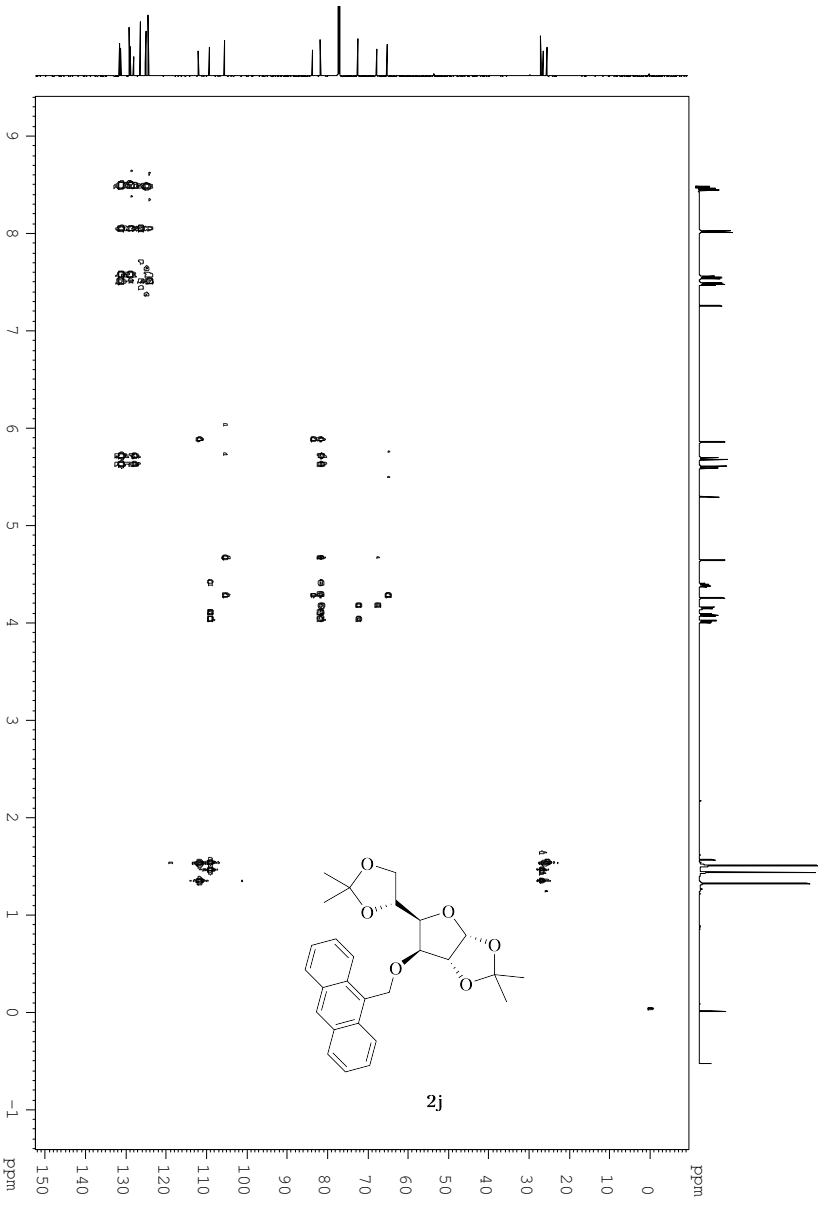

Figure 90: HMBC spectrum of **2j**.

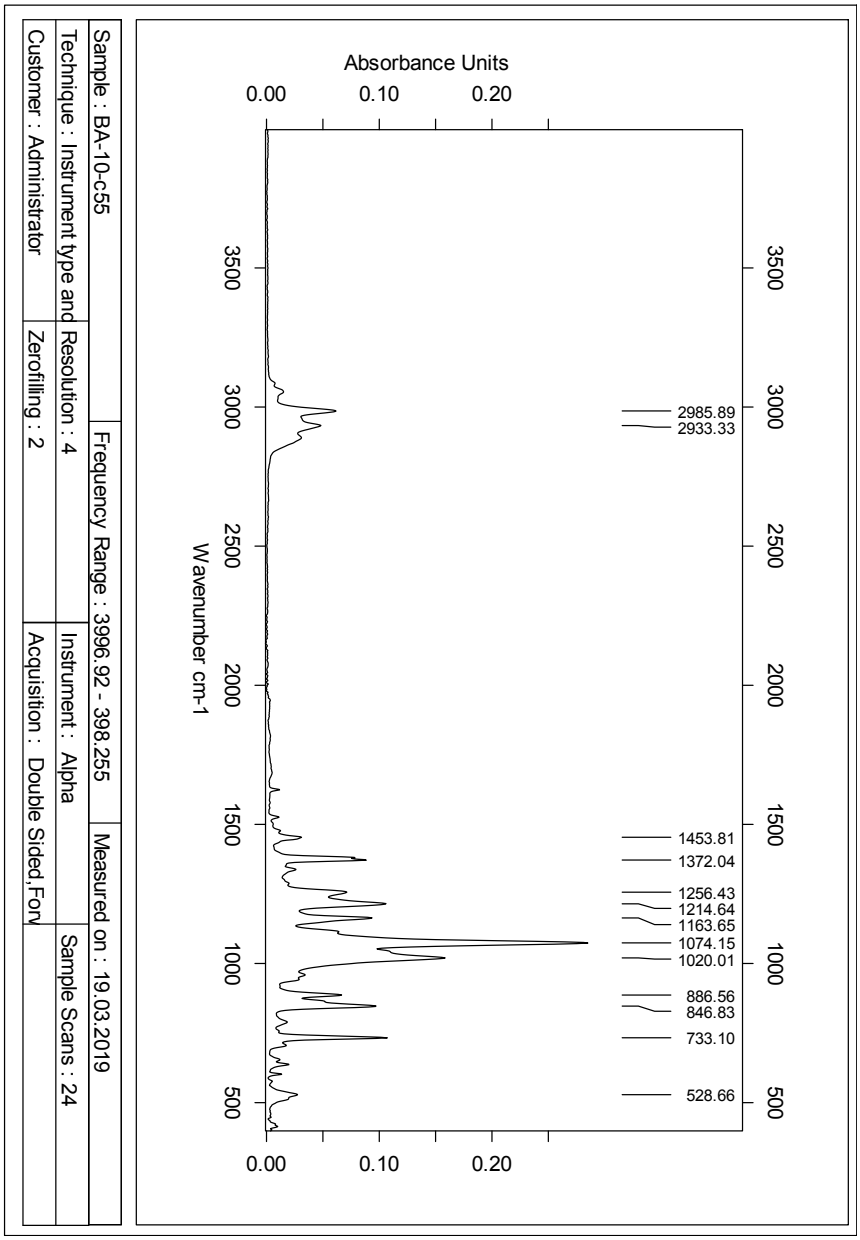

Figure 91: IR spectrum of **2j**.

B.10 Spectroscopic data for compound 2ð

Elemental Composition Report **Page 1**

Single Mass Analysis
Tolerance = 2.0 PPM / DBE: min = -2.0, max = 50.0
Element prediction: Off
Number of isotope peaks used for i-FIT = 3

Monoisotopic Mass, Even Electron Ions
96 formula(e) evaluated with 1 results within limits (all results (up to 1000) for each mass)
Elements Used:
C: 0-100 H: 0-150 O: 0-10 Na: 0-1
2019-48b 78 (0.743) AM2 (Ar,35000.0,0.00,0.00); Cm (71:87)
1: TOF MS ES+

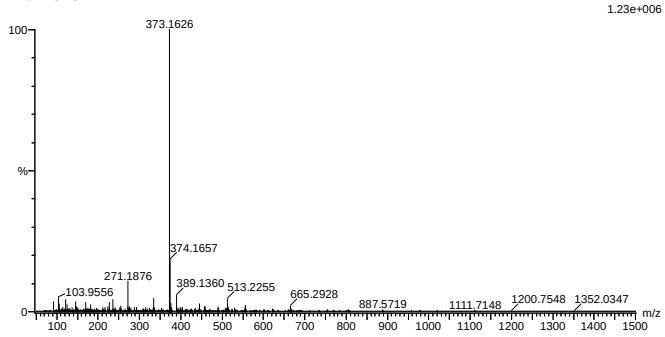

Minimum:				-2.0				
Maximum:		5.0	2.0	50.0				
Mass	Calc. Mass	mDa	PPM	DBE	i-FIT	Norm	Conf(%)	Formula
373.1626	373.1627	-0.1	-0.3	6.5	1203.4	n/a	n/a	C19 H26 O6 Na

Figure 92: HRMS (ESI+) of **2ð**.

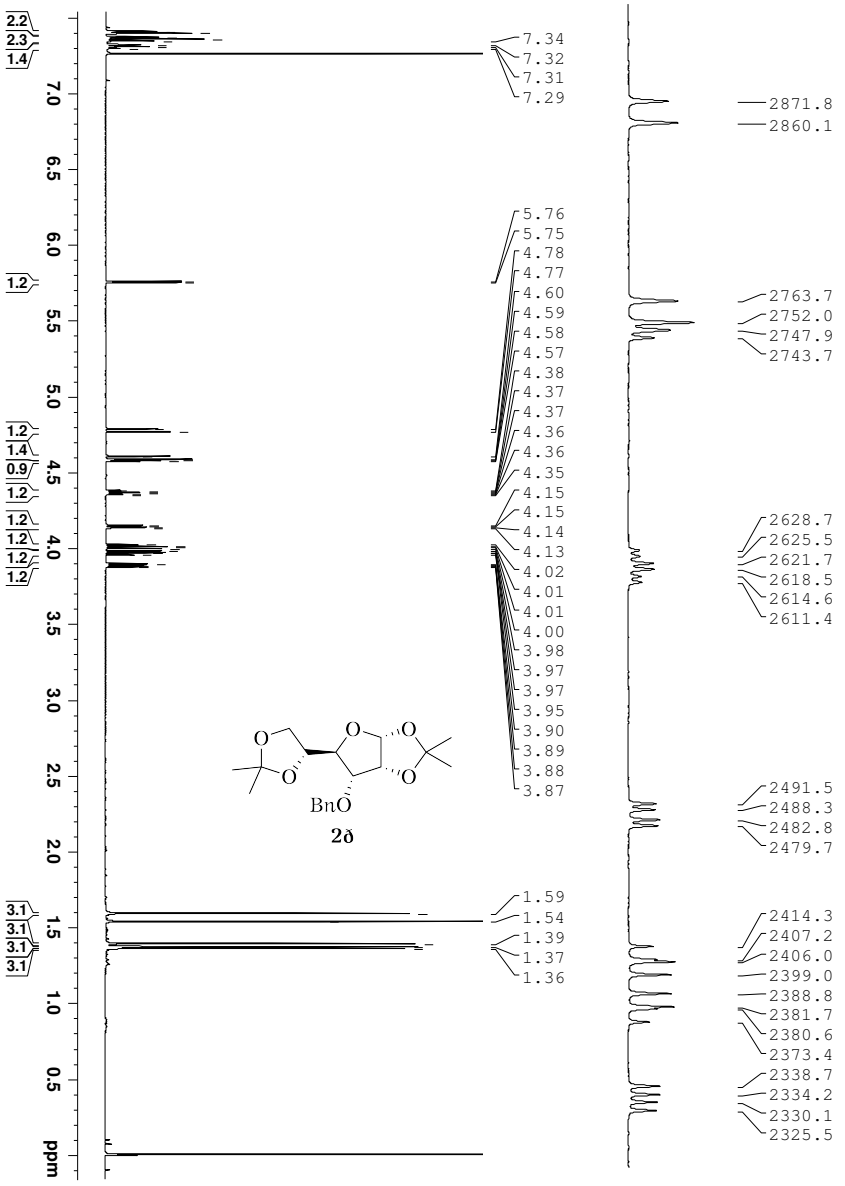

Figure 93: ^{1}H NMR spectrum of **2ð**.

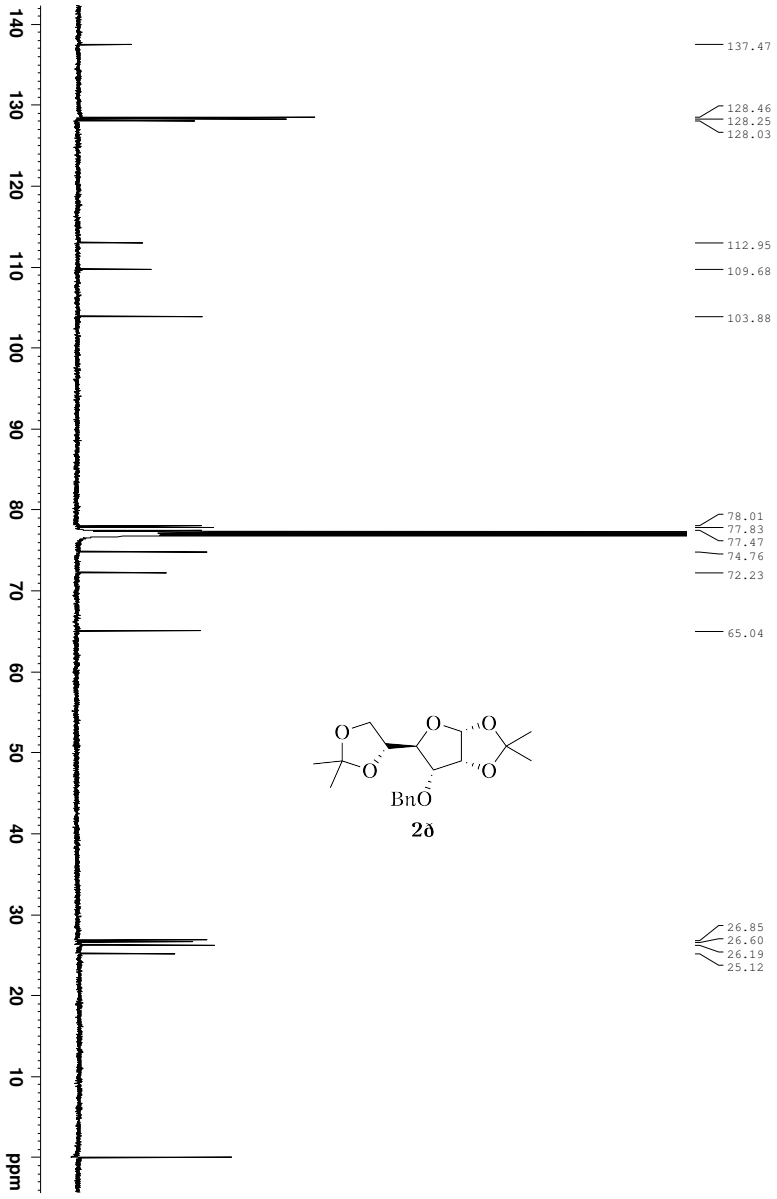

Figure 94: ^{13}C NMR spectrum of **2ð**.

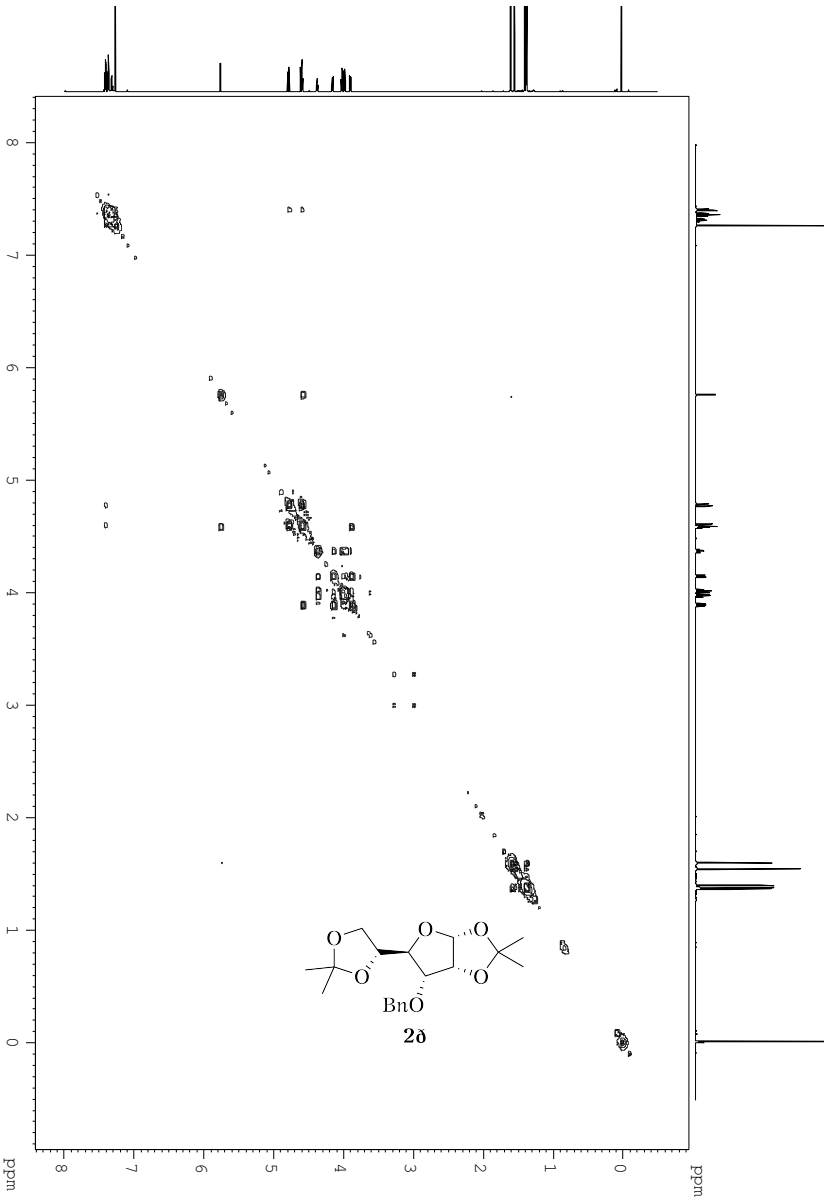

Figure 95: COSY spectrum of **2ð**.

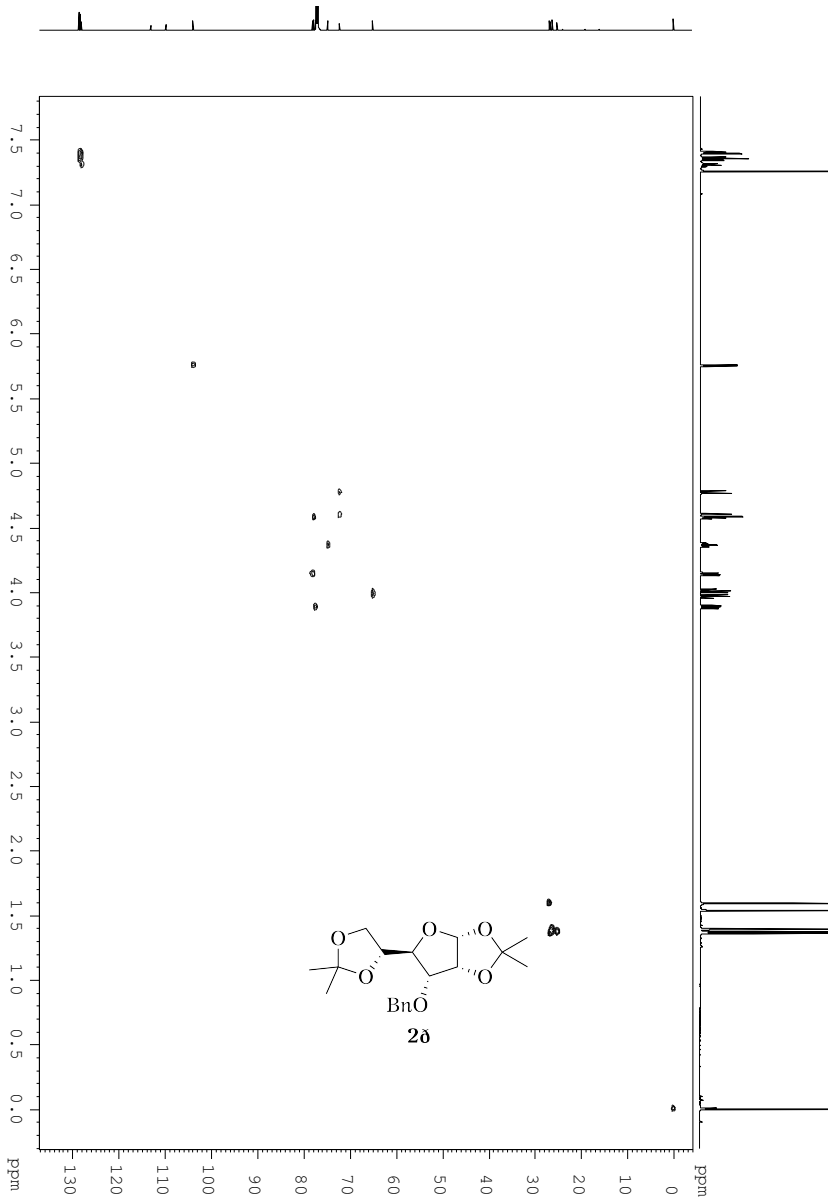

Figure 96: HSQC spectrum of **2ð**.

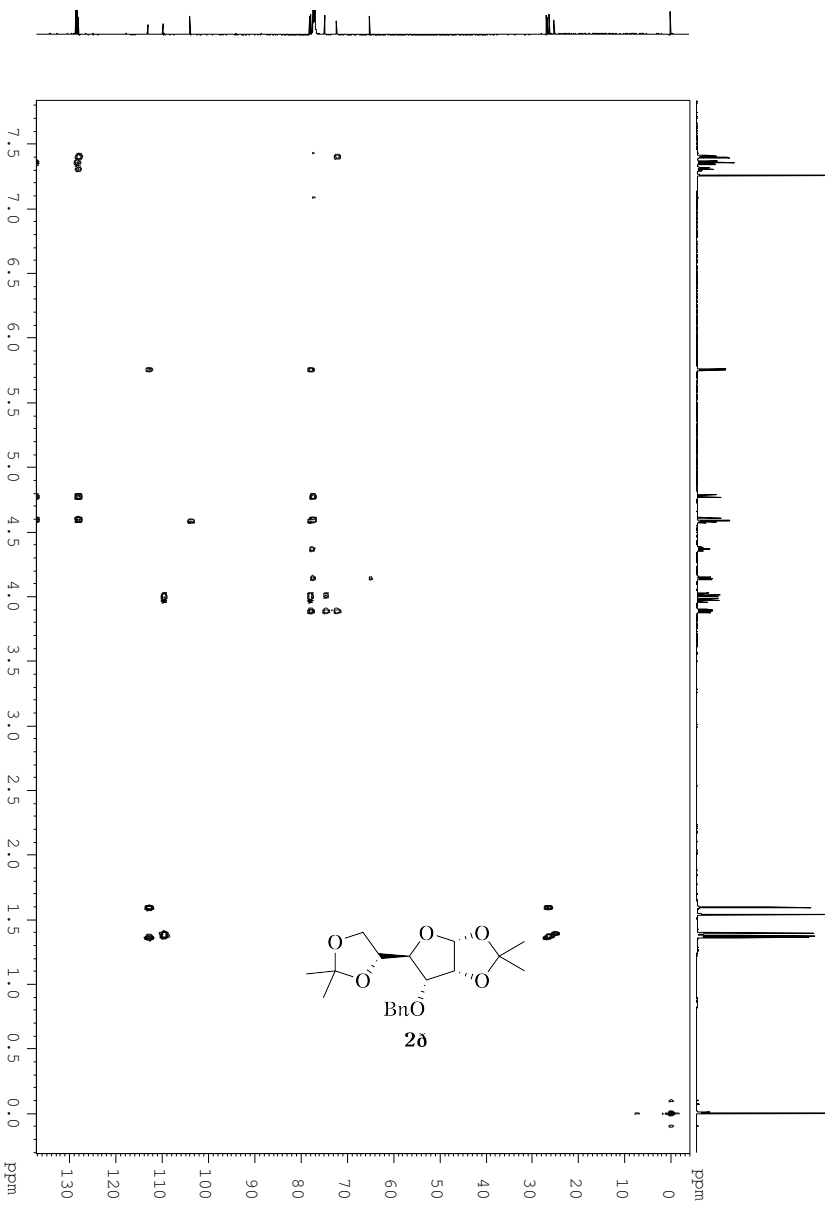

2ð

Figure 97: HMBC spectrum of **2ð**.

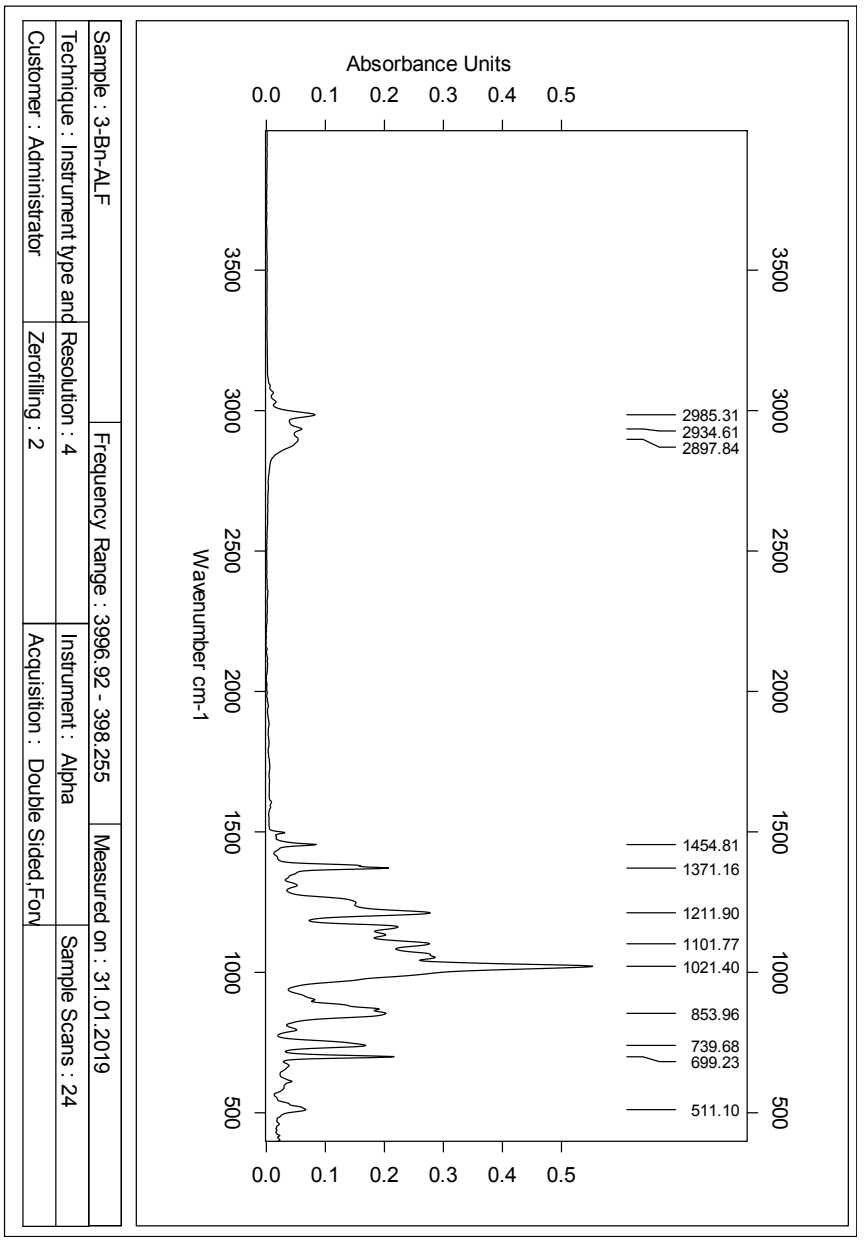

Figure 98: IR spectrum of **2ð**.

B.11 Spectroscopic data for compound 2ø

Elemental Composition Report **Page 1**

Single Mass Analysis
Tolerance = 2.0 PPM / DBE: min = -2.0, max = 50.0
Element prediction: Off
Number of isotope peaks used for i-FIT = 3

Monoisotopic Mass, Even Electron Ions
274 formula(e) evaluated with 2 results within limits (all results (up to 1000) for each mass)
Elements Used:
C: 0-100 H: 0-150 O: 0-10 Na: 0-1 Si: 0-2 Au: 0-2

2019-44 69 (0.654) AM2 (Ar,35000.0,0.00,0.00); Cm (66:71)
1: TOF MS ES+

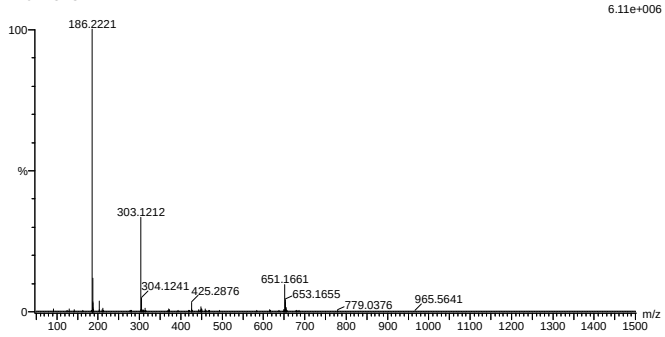

Minimum:				-2.0				
Maximum:		5.0	2.0	50.0				
Mass	Calc. Mass	mDa	PPM	DBE	i-FIT	Norm	Conf(%)	Formula
303.1212	303.1213	-0.1	-0.3	4.5	1493.9	14.605	0.00	C14 H24 O2 Na Si2
	303.1208	0.4	1.3	5.5	1479.3	0.000	100.00	C15 H20 O5 Na

Figure 99: HRMS (ESI+) of **2ø**.

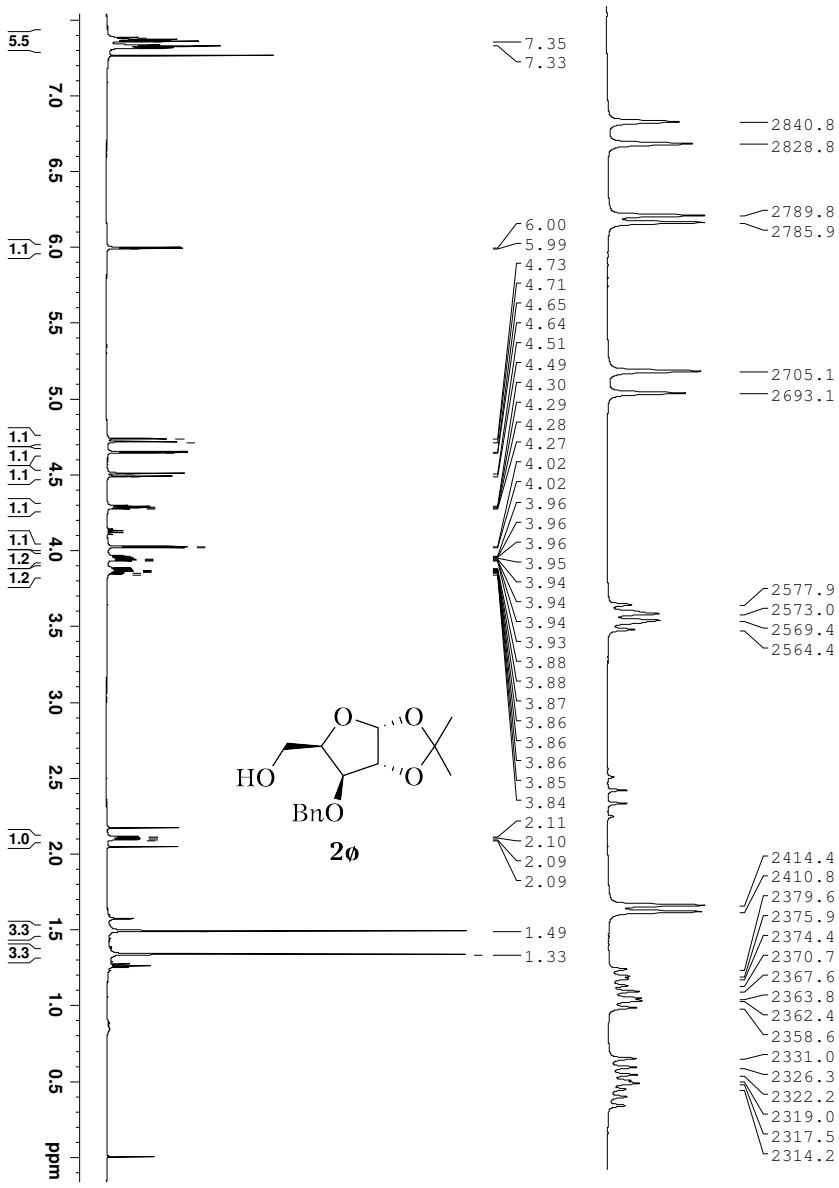

Figure 100: ^{1}H NMR spectrum of **2ø**.

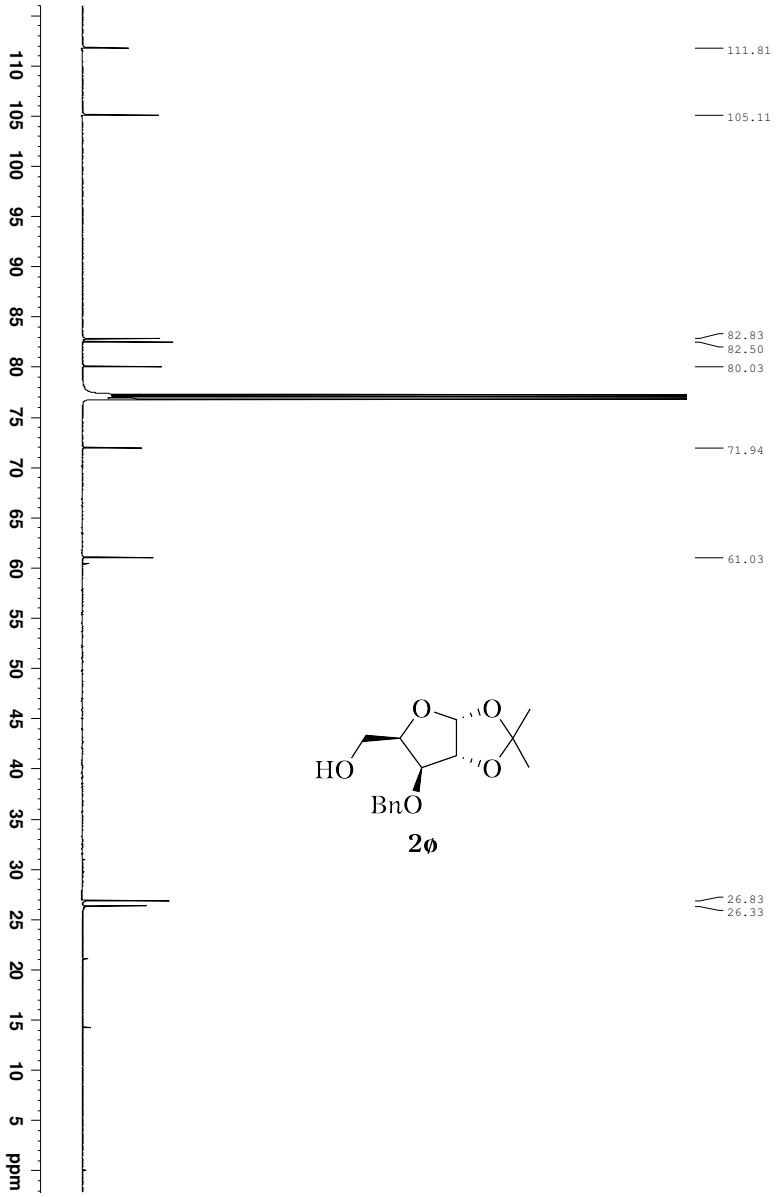

2ø

Figure 101: ^{13}C NMR spectrum of **2ø**.

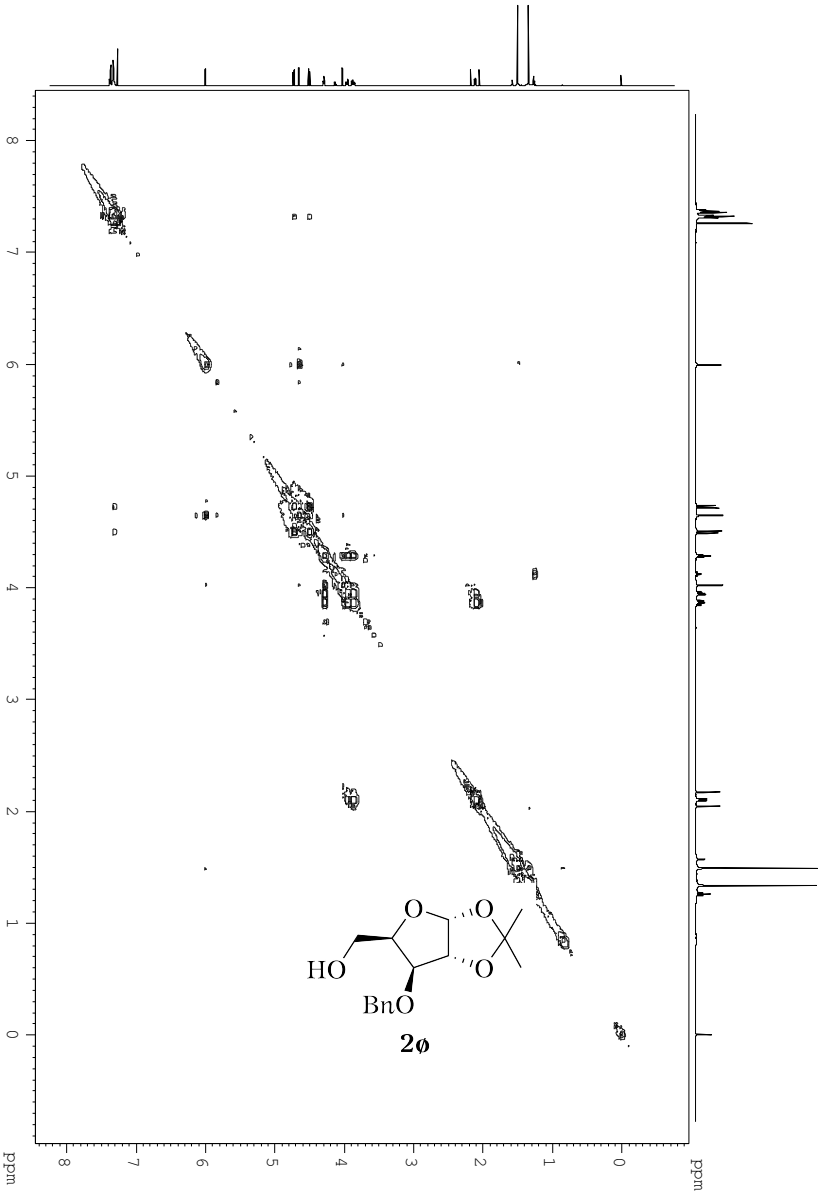

Figure 102: COSY spectrum of **2ø**.

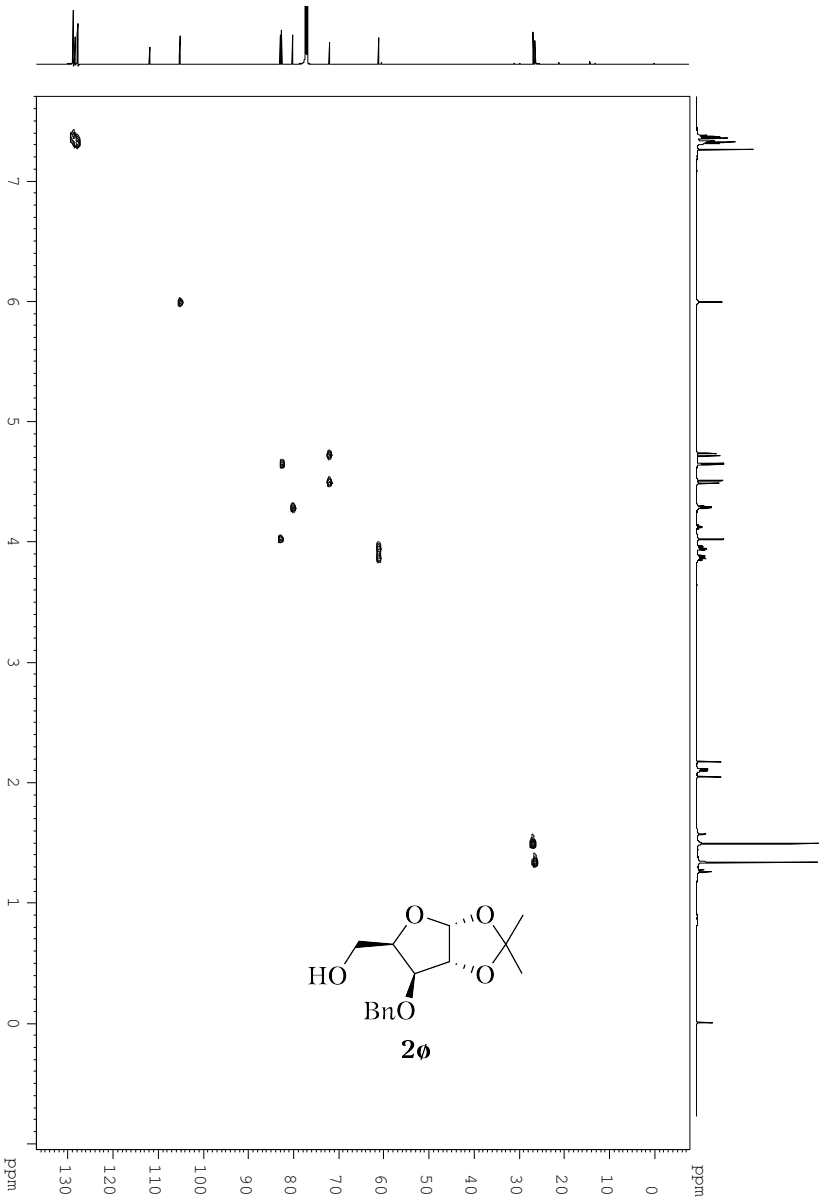

Figure 103: HSQC spectrum of **2ø**.

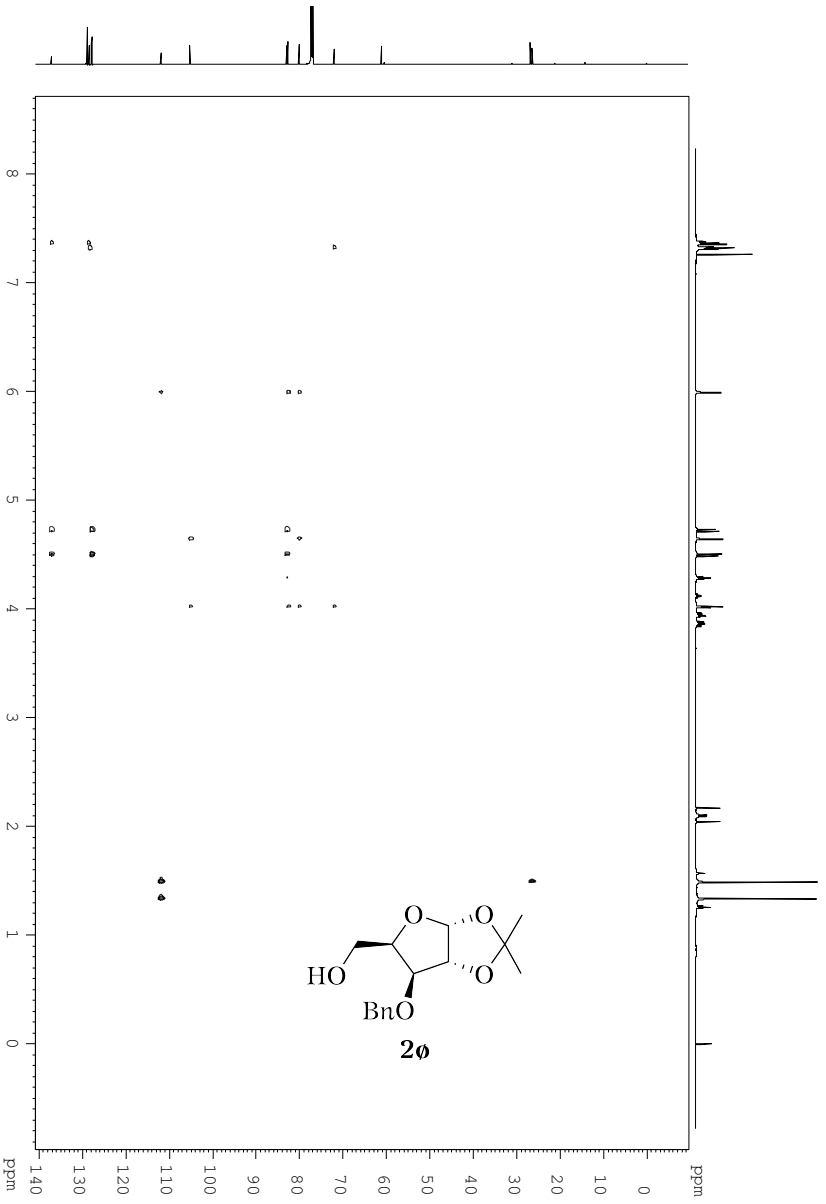

Figure 104: HMBC spectrum of **2ø**.

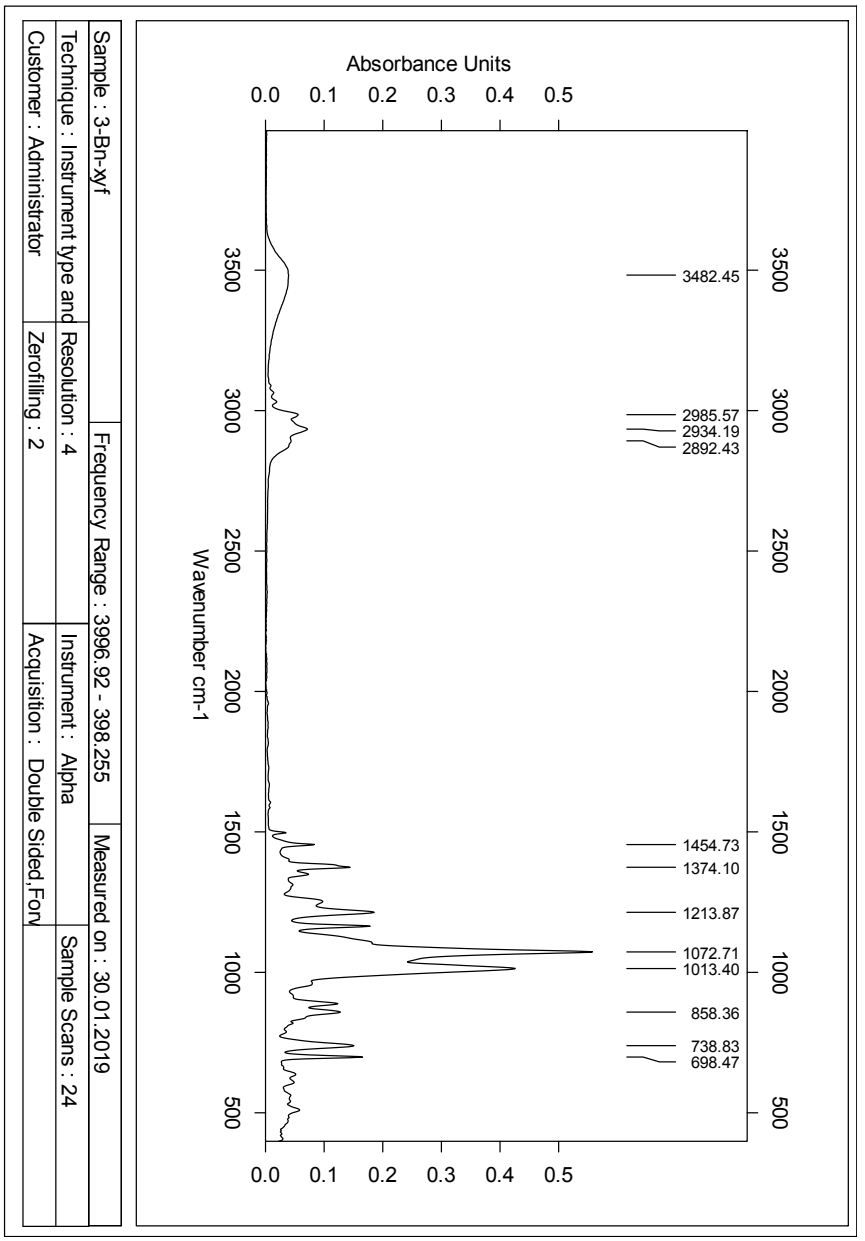

Figure 105: IR spectrum of **2ø**.

B.12 Spectroscopic data for compound 3a-α

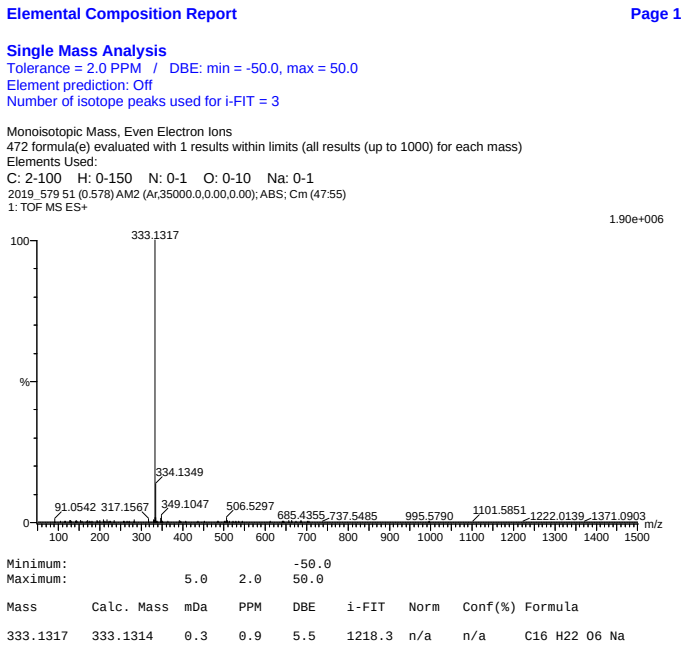

Elemental Composition Report **Page 1**

Single Mass Analysis
Tolerance = 2.0 PPM / DBE: min = -50.0, max = 50.0
Element prediction: Off
Number of isotope peaks used for i-FIT = 3

Monoisotopic Mass, Even Electron Ions
472 formula(e) evaluated with 1 results within limits (all results (up to 1000) for each mass)
Elements Used:
C: 2-100 H: 0-150 N: 0-1 O: 0-10 Na: 0-1
2019_579 51 (0.578) AM2 (Ar,35000.0,0.00,0.00); ABS; Cm (47:55)
1: TOF MS ES+
1.90e+006

Minimum:				-50.0				
Maximum:		5.0	2.0	50.0				
Mass	Calc. Mass	mDa	PPM	DBE	i-FIT	Norm	Conf(%)	Formula
333.1317	333.1314	0.3	0.9	5.5	1218.3	n/a	n/a	C16 H22 O6 Na

Figure 106: HRMS (ESI+) of **3a-α**.

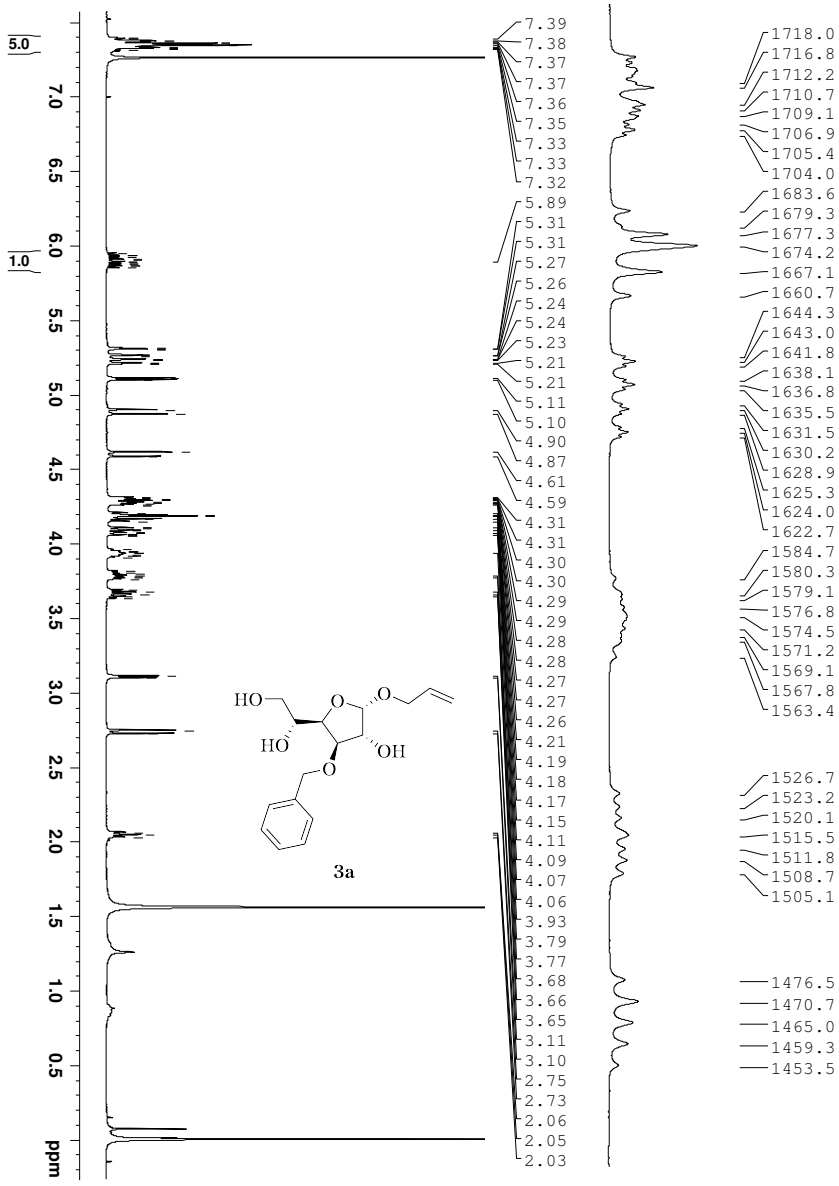

Figure 107: ^{1}H NMR (400 MHz) spectrum of **3a-α**.

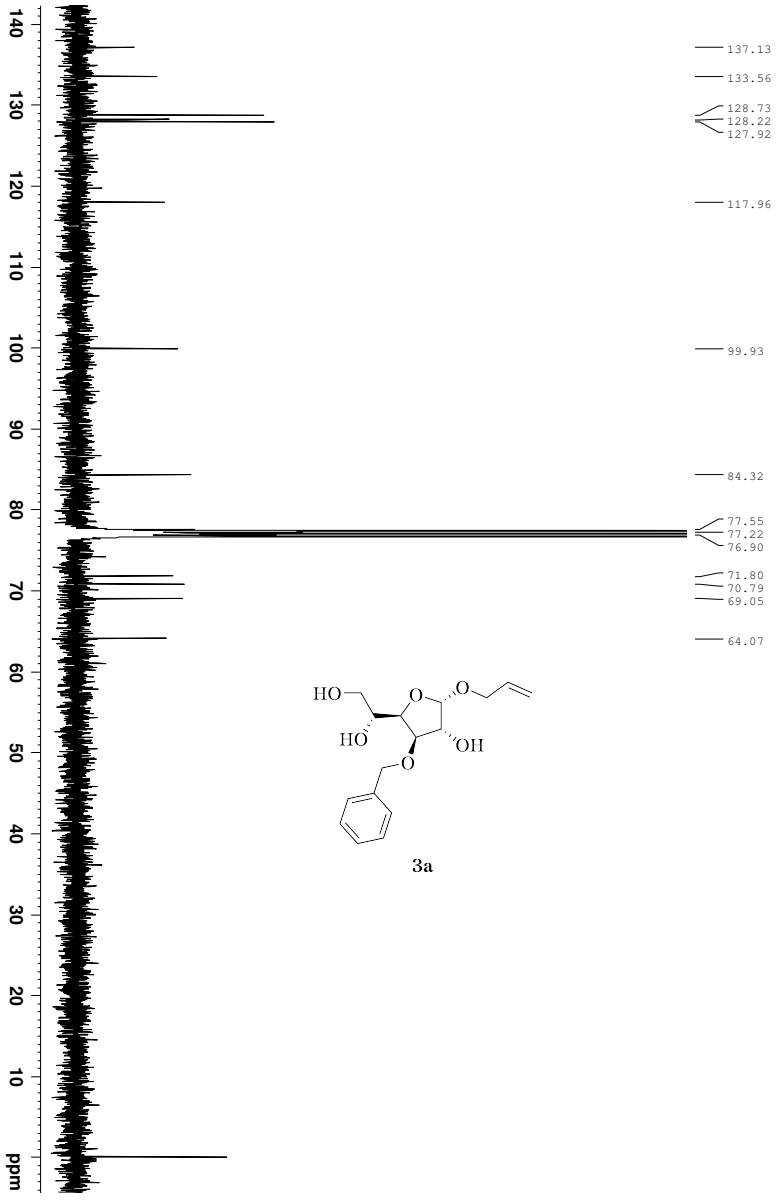

Figure 108: ^{13}C NMR (100 MHz) spectrum of **3a-α**.

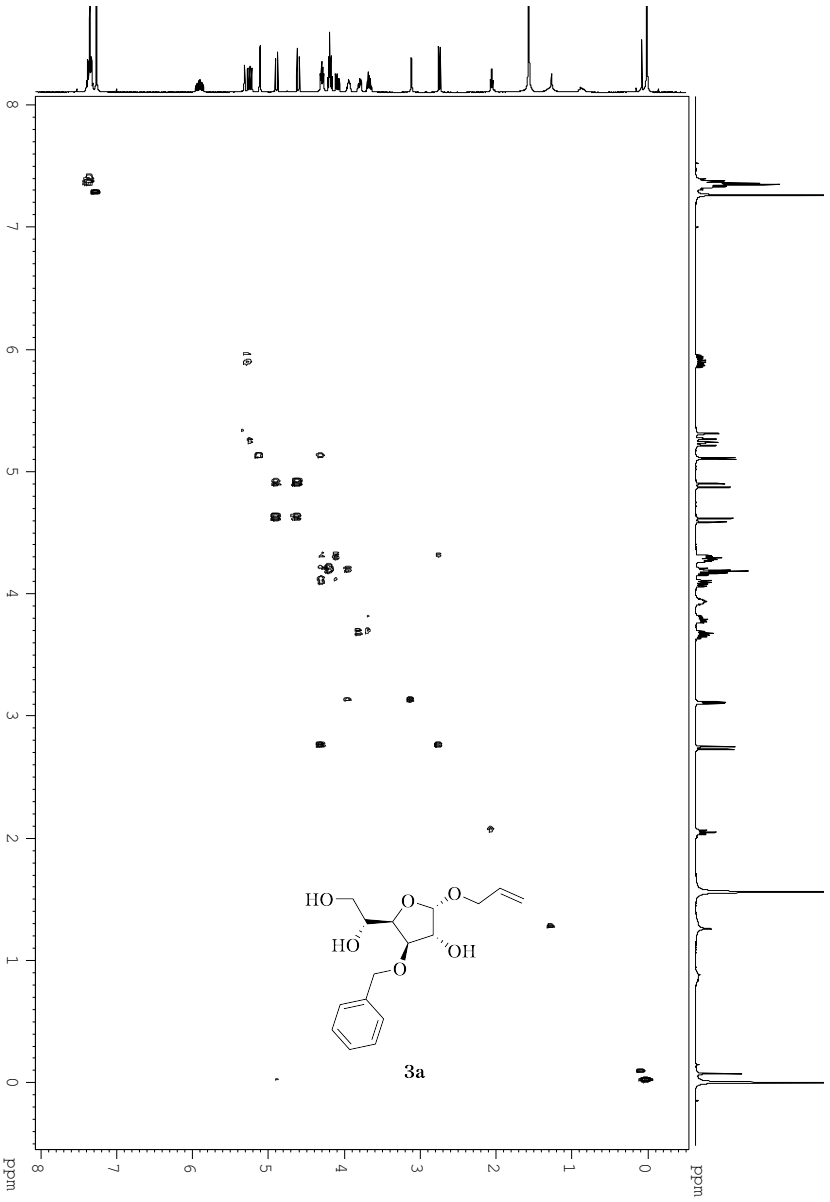

Figure 109: COSY (400 MHz) spectrum of **3a-α**.

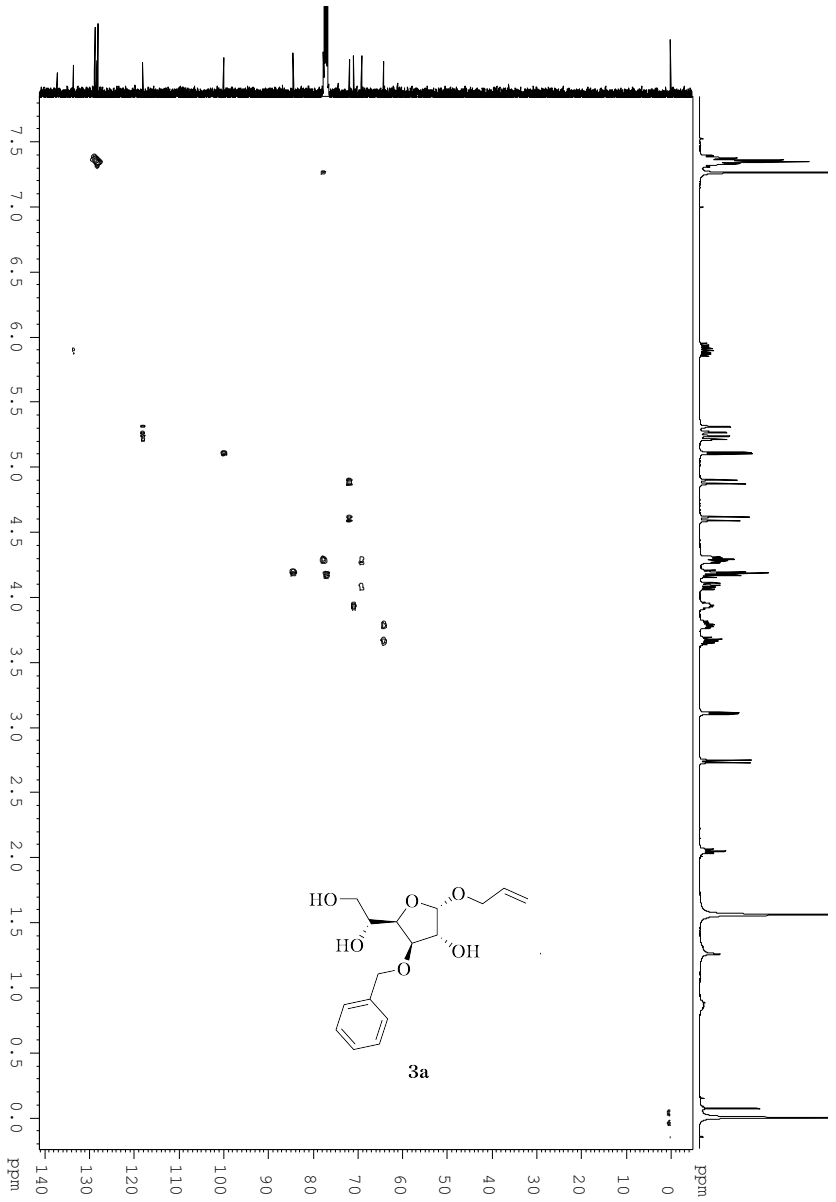

Figure 110: HSQC (400 MHz) spectrum of **3a-α**.

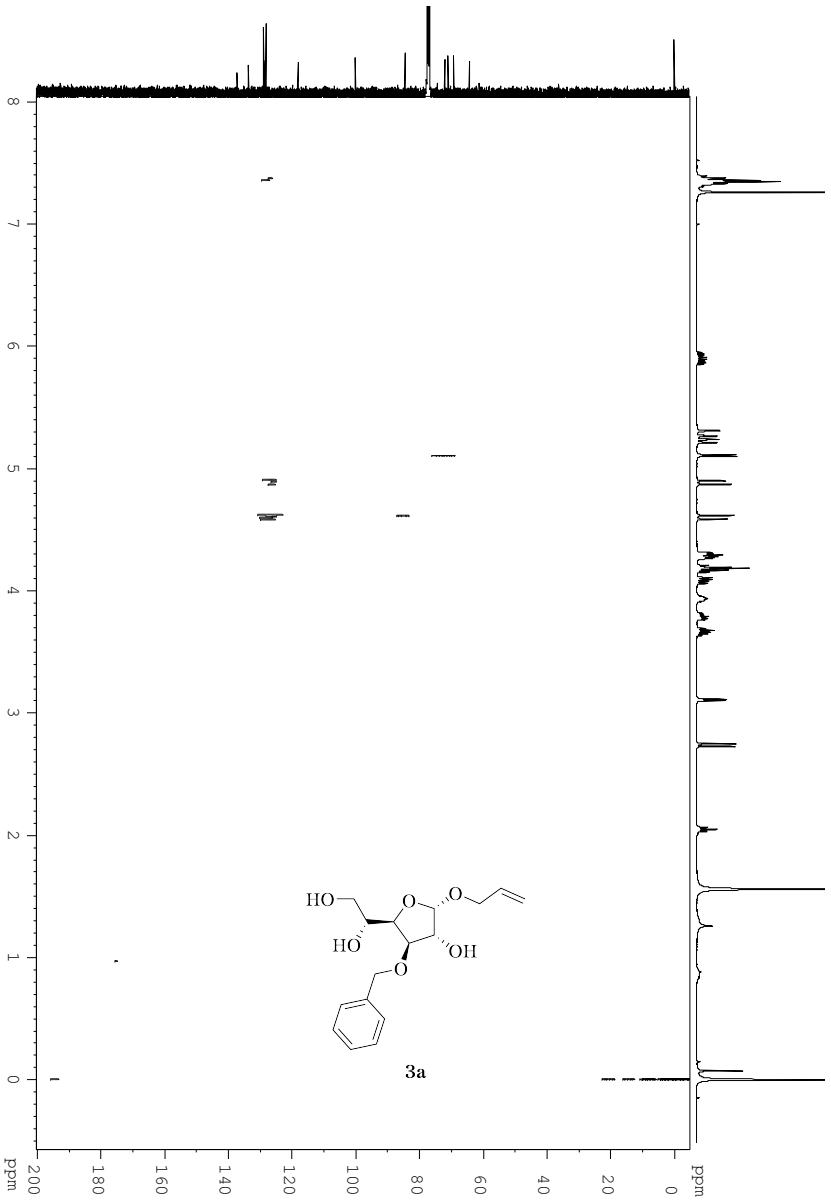

Figure 111: HMBC (400 MHz) spectrum of **3a-α**.

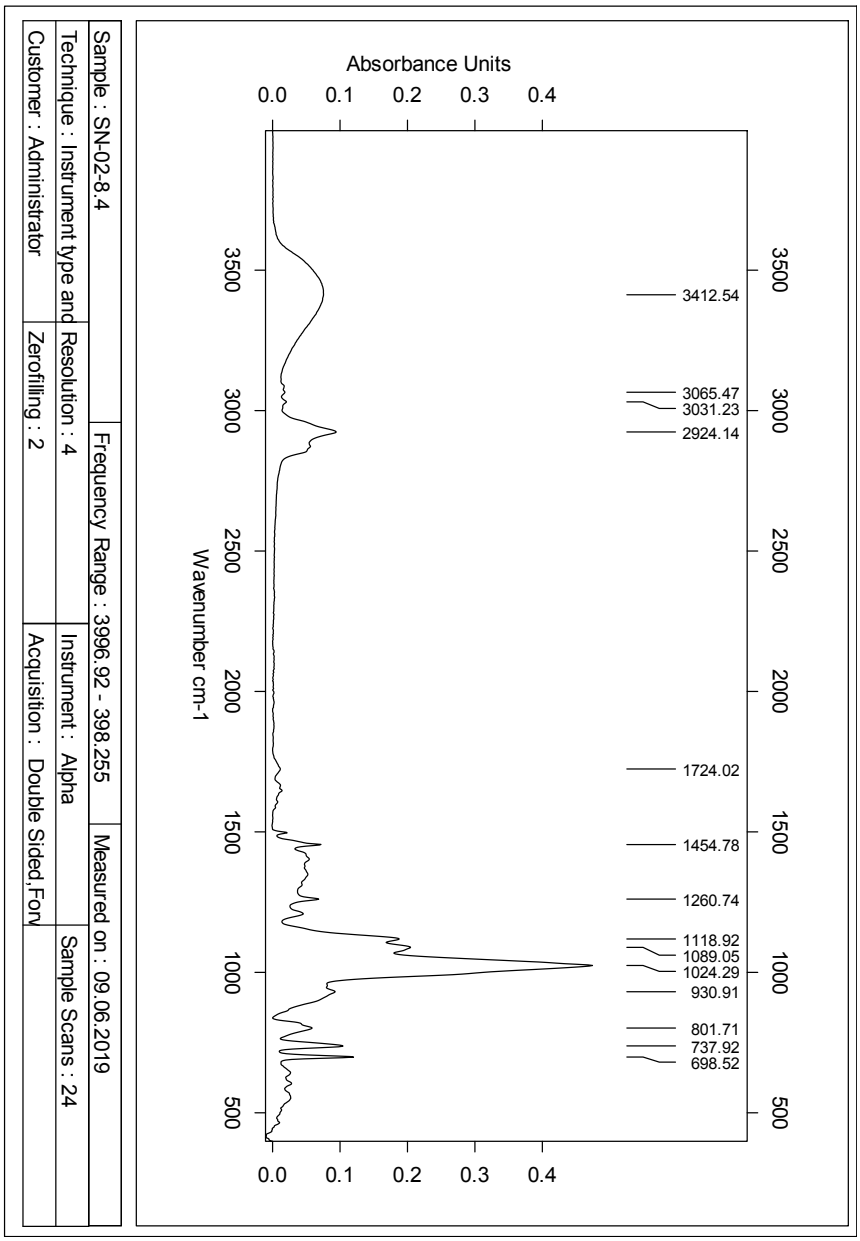

Figure 112: IR spectrum of **3a-α**.

B.13 Spectroscopic data for compound 3a-β

Elemental Composition Report **Page 1**

Single Mass Analysis
Tolerance = 2.0 PPM / DBE: min = -2.0, max = 50.0
Element prediction: Off
Number of isotope peaks used for i-FIT = 2

Monoisotopic Mass, Even Electron Ions
150 formula(e) evaluated with 1 results within limits (all results (up to 1000) for each mass)
Elements Used:
C: 0-100 H: 0-150 O: 0-20 Na: 0-1 Au: 0-2

2018_551 74 (0.708) AM2 (Ar,35000.0,0.00,0.00); Cm (74:81)
1: TOF MS ES+

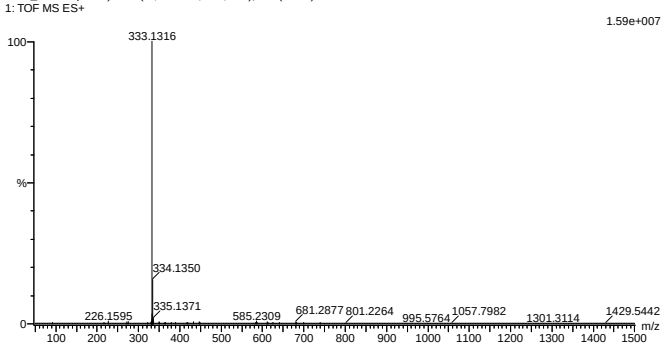

Minimum:				-2.0				
Maximum:		5.0	2.0	50.0				
Mass	Calc. Mass	mDa	PPM	DBE	i-FIT	Norm	Conf(%)	Formula
333.1316	333.1314	0.2	0.6	5.5	1091.3	n/a	n/a	C16 H22 O6 Na

Figure 113: HRMS (ESI+) of **3a-β**.

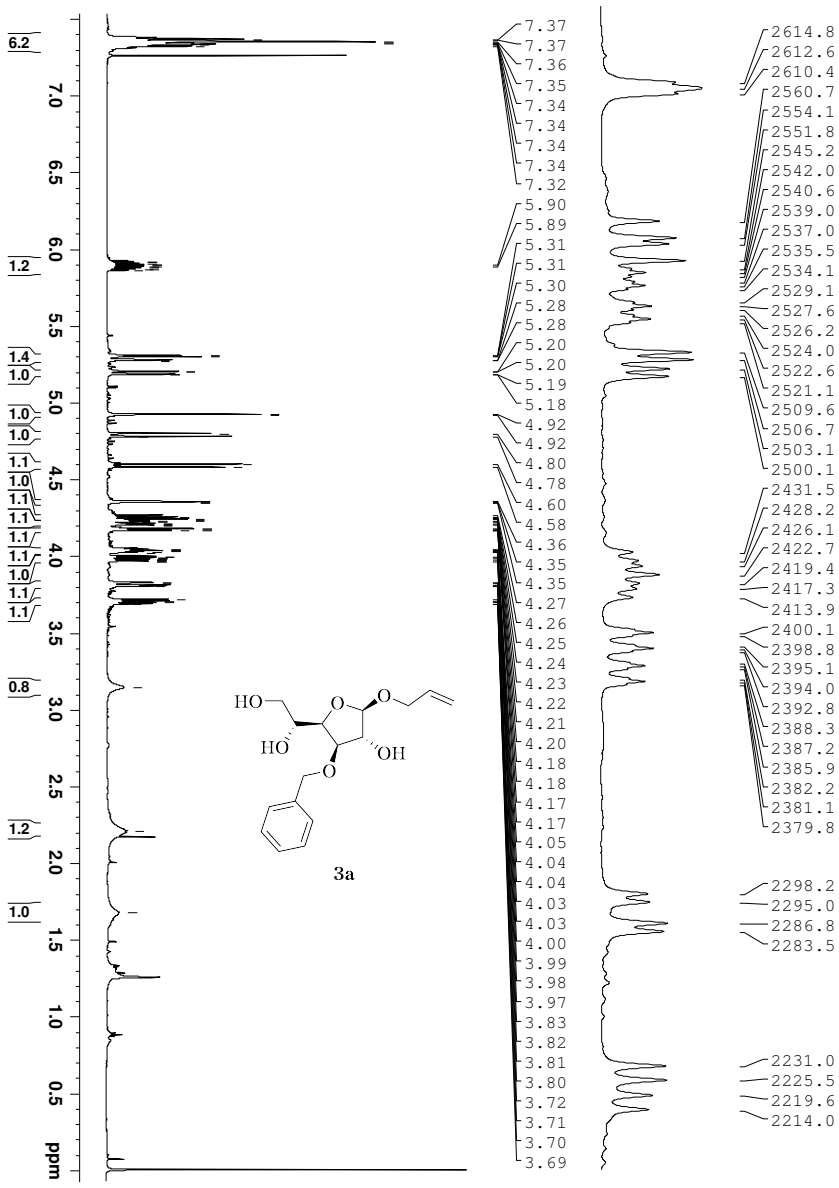

Figure 114: ^{1}H NMR spectrum of **3a-β**.

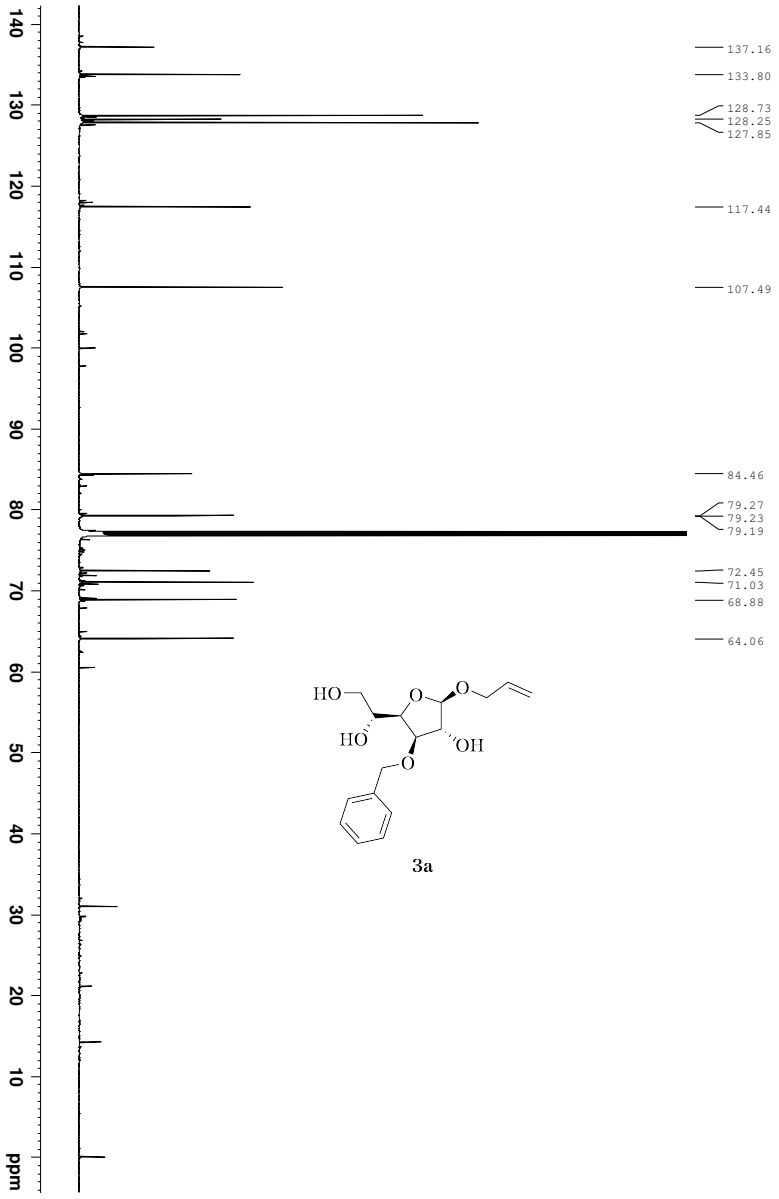

Figure 115: ^{13}C NMR spectrum of **3a-β**.

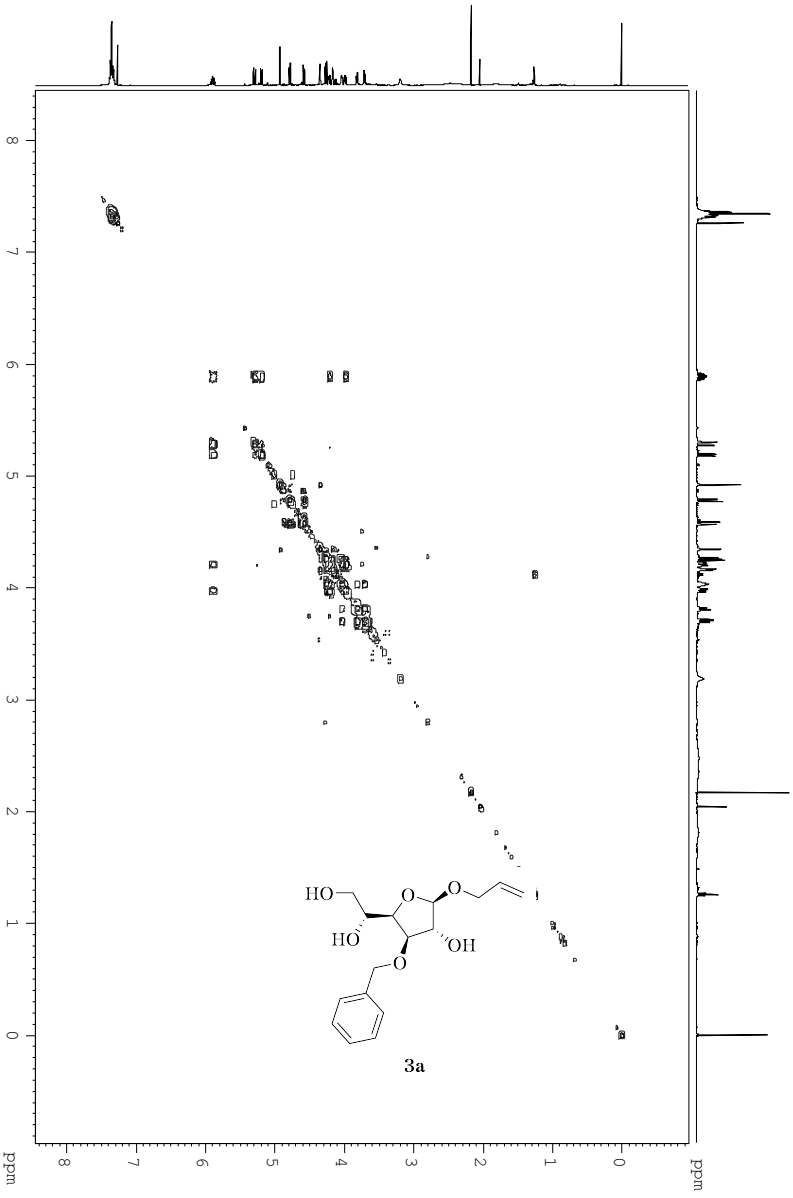

Figure 116: COSY spectrum of **3a-β**.

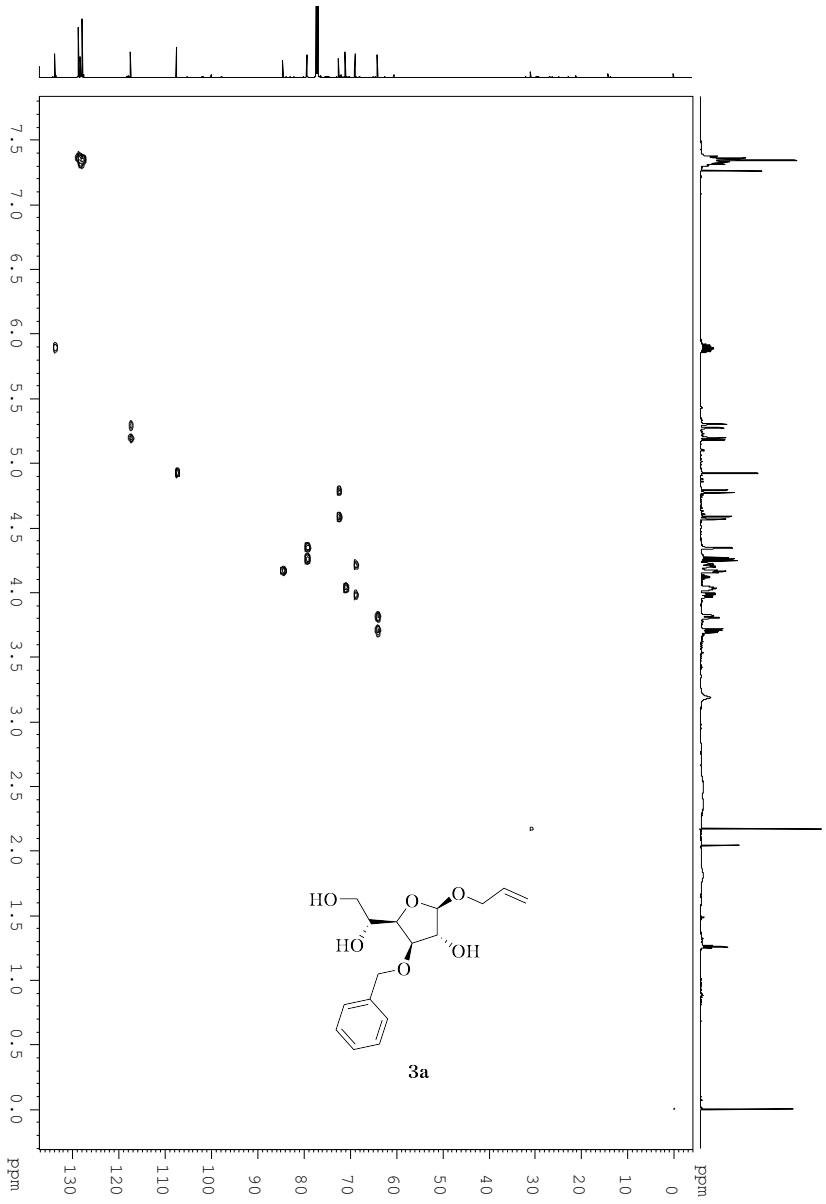

Figure 117: HSQC spectrum of **3a-β**.

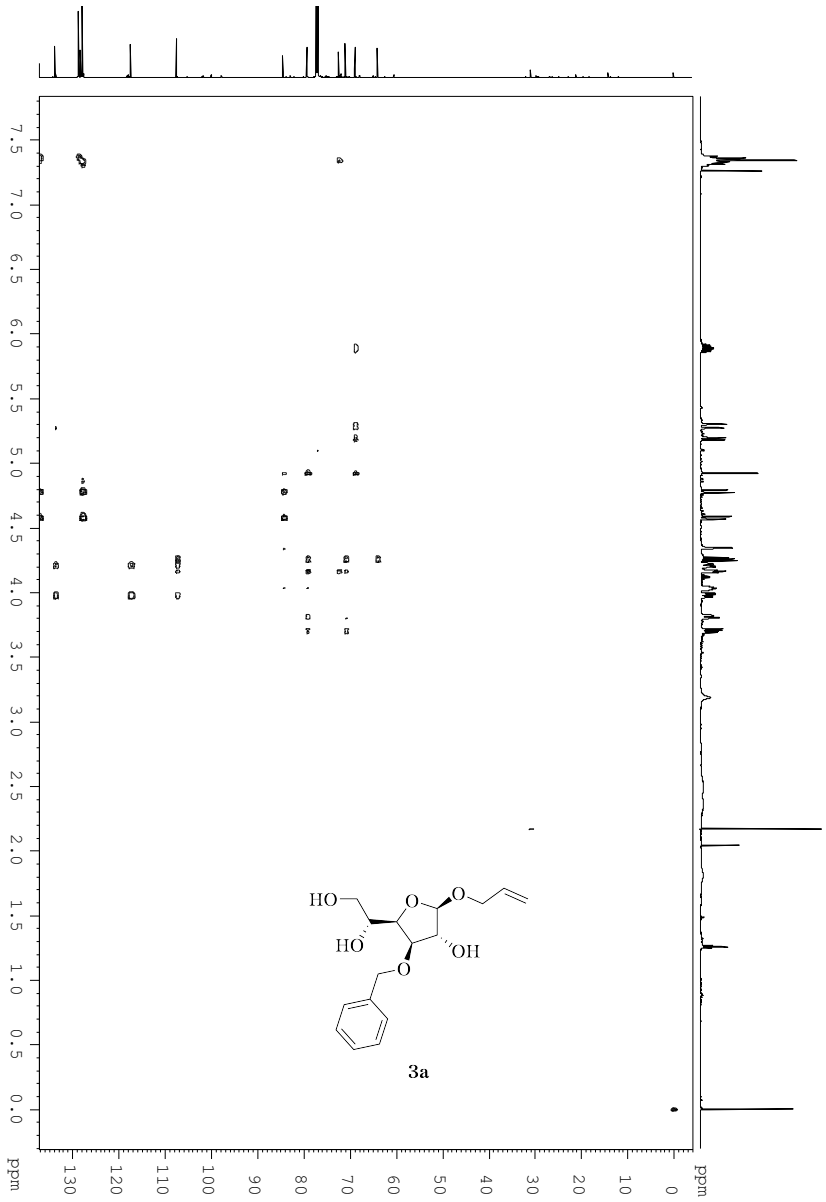

Figure 118: HMBC spectrum of **3a-β**.

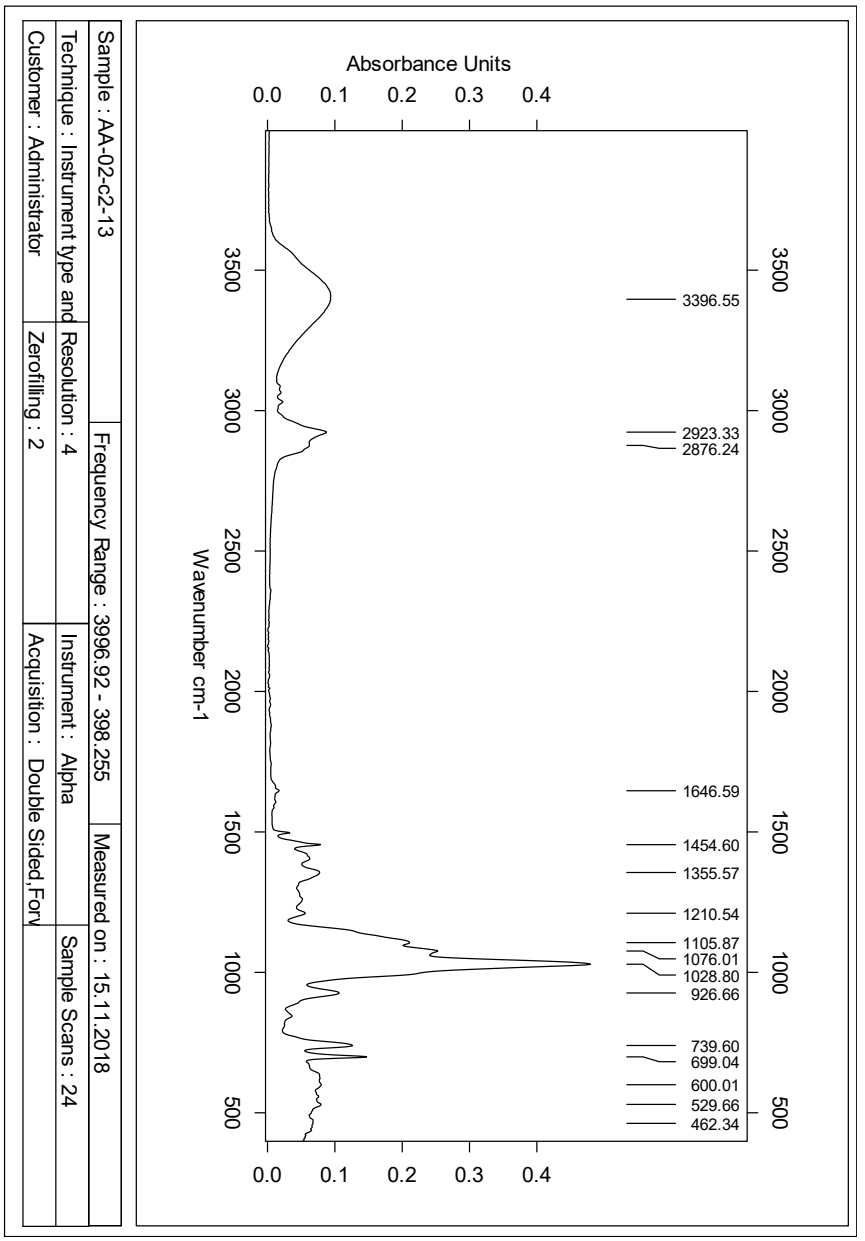

Figure 119: IR spectrum of **3a-β**.

B.14 Spectroscopic data for compound 3c-α

Elemental Composition Report **Page 1**

Single Mass Analysis
Tolerance = 3.0 PPM / DBE: min = -50.0, max = 50.0
Element prediction: Off
Number of isotope peaks used for i-FIT = 3

Monoisotopic Mass, Even Electron Ions
256 formula(e) evaluated with 1 results within limits (all results (up to 1000) for each mass)
Elements Used:
C: 0-100 H: 0-150 O: 0-10 Na: 0-1
svg_20190403_2019_257 18 (0.339) AM2 (Ar,35000.0,0.00,0.00); Cm (17:18)
1: TOF MS ES+

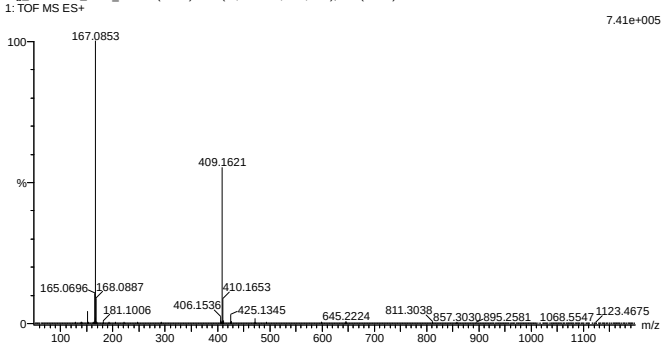

Minimum:				-50.0				
Maximum:		5.0	3.0	50.0				
Mass	Calc. Mass	mDa	PPM	DBE	i-FIT	Norm	Conf(%)	Formula
409.1621	409.1627	-0.6	-1.5	9.5	852.0	n/a	n/a	C22 H26 O6 Na

Figure 120: HRMS (ESI+) of **3c-α**.

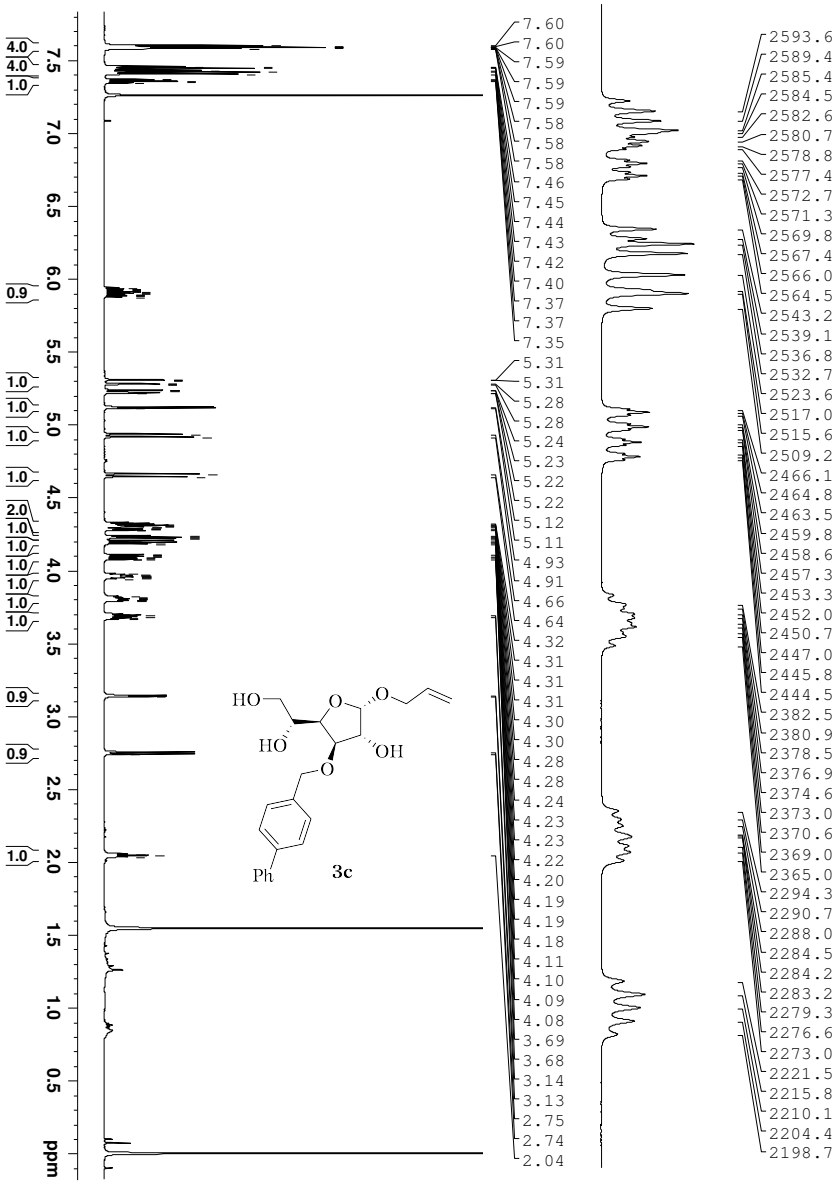

Figure 121: ^{1}H NMR spectrum of **3c-α**.

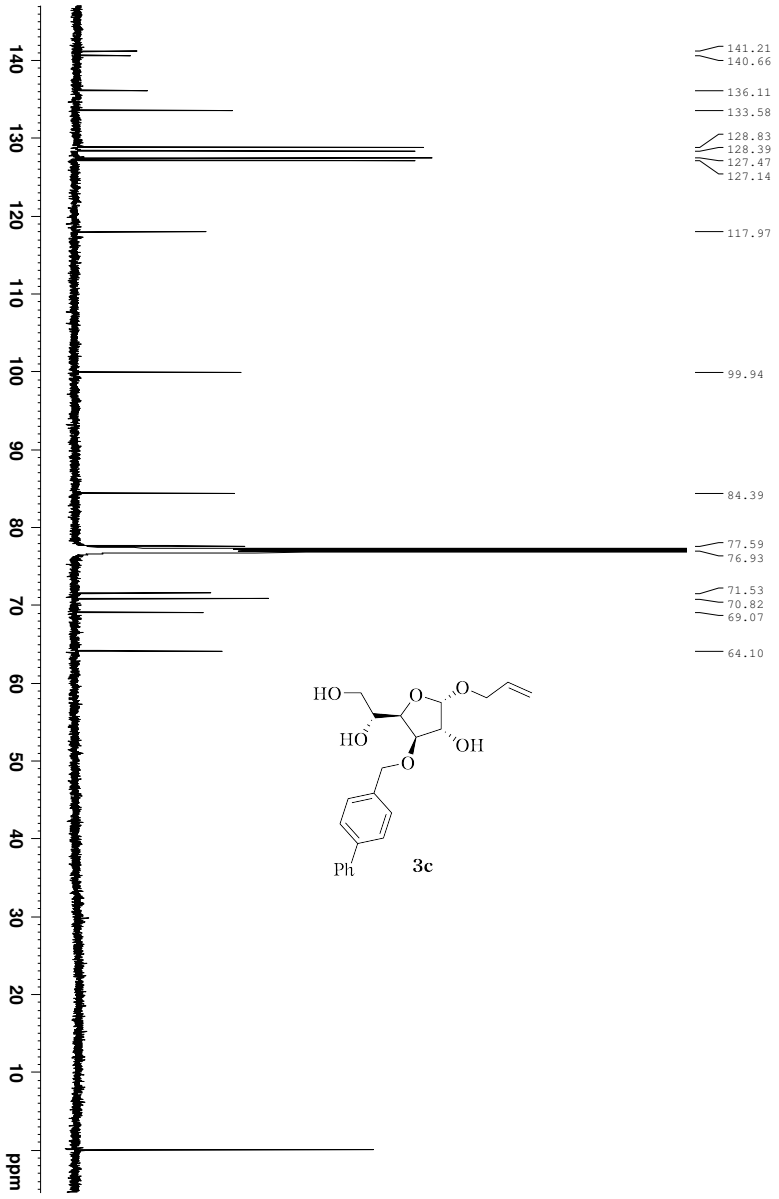

Figure 122: ^{13}C NMR spectrum of **3c-α**.

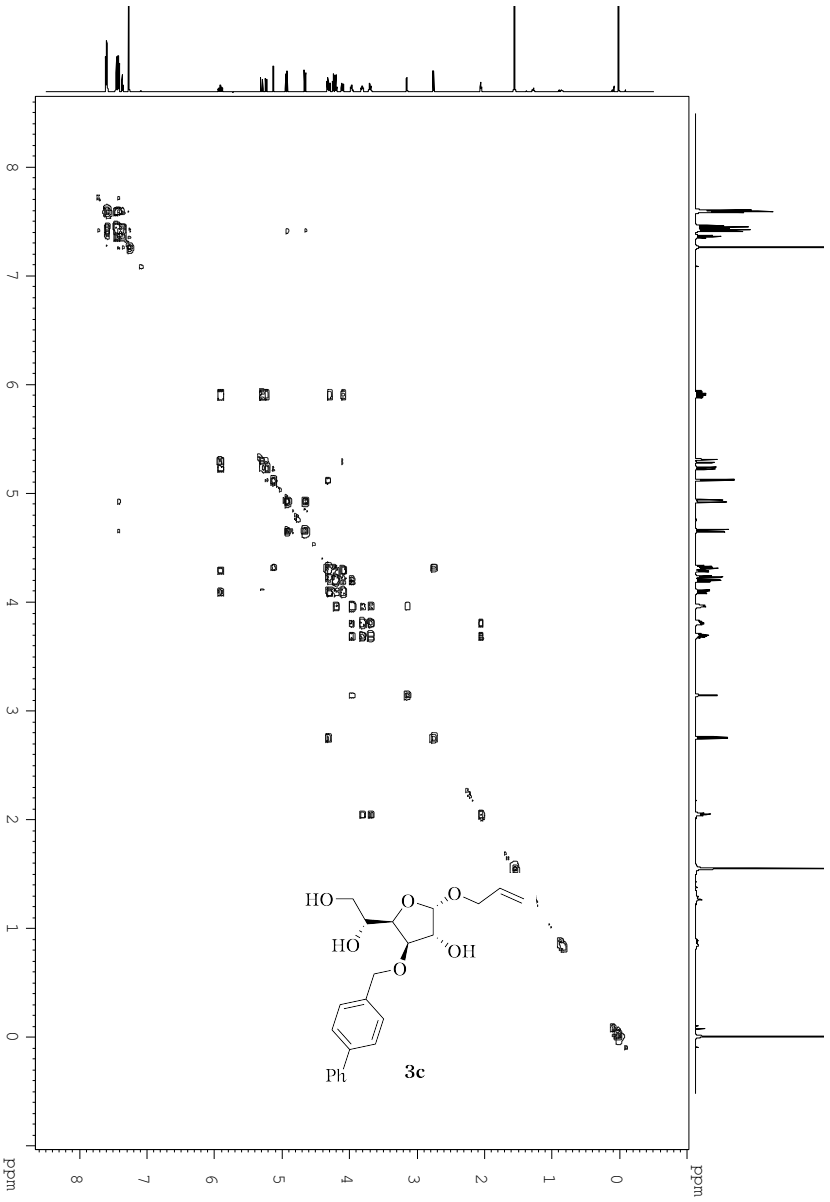

Figure 123: COSY spectrum of **3c-α**.

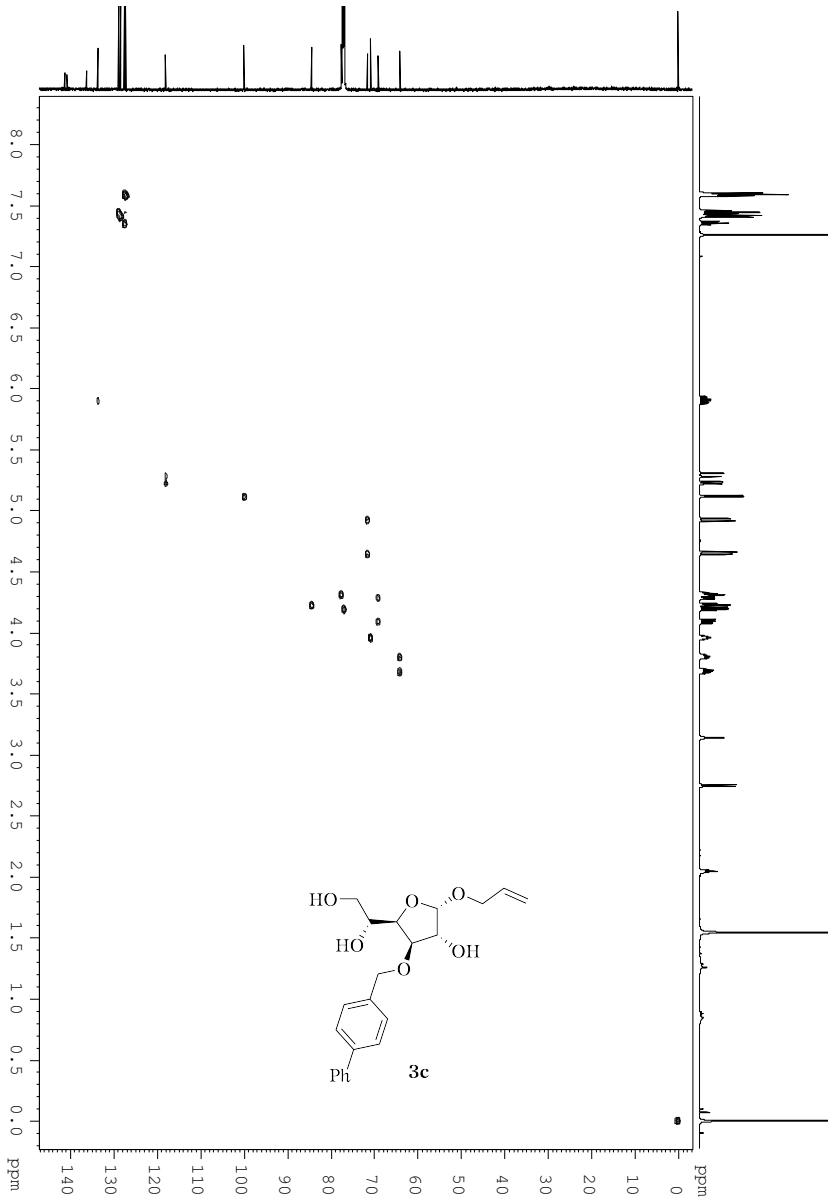

Figure 124: HSQC spectrum of **3c-α**.

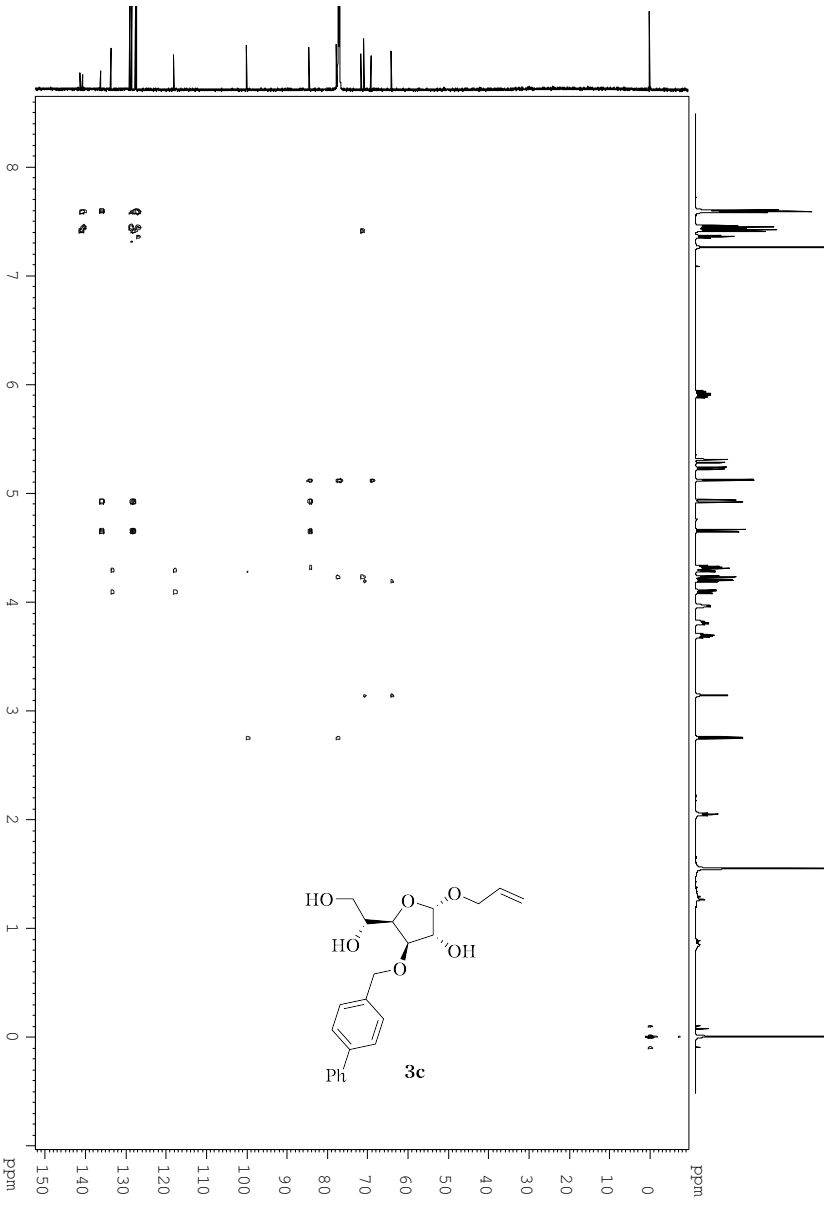

Figure 125: HMBC spectrum of **3c-α**.

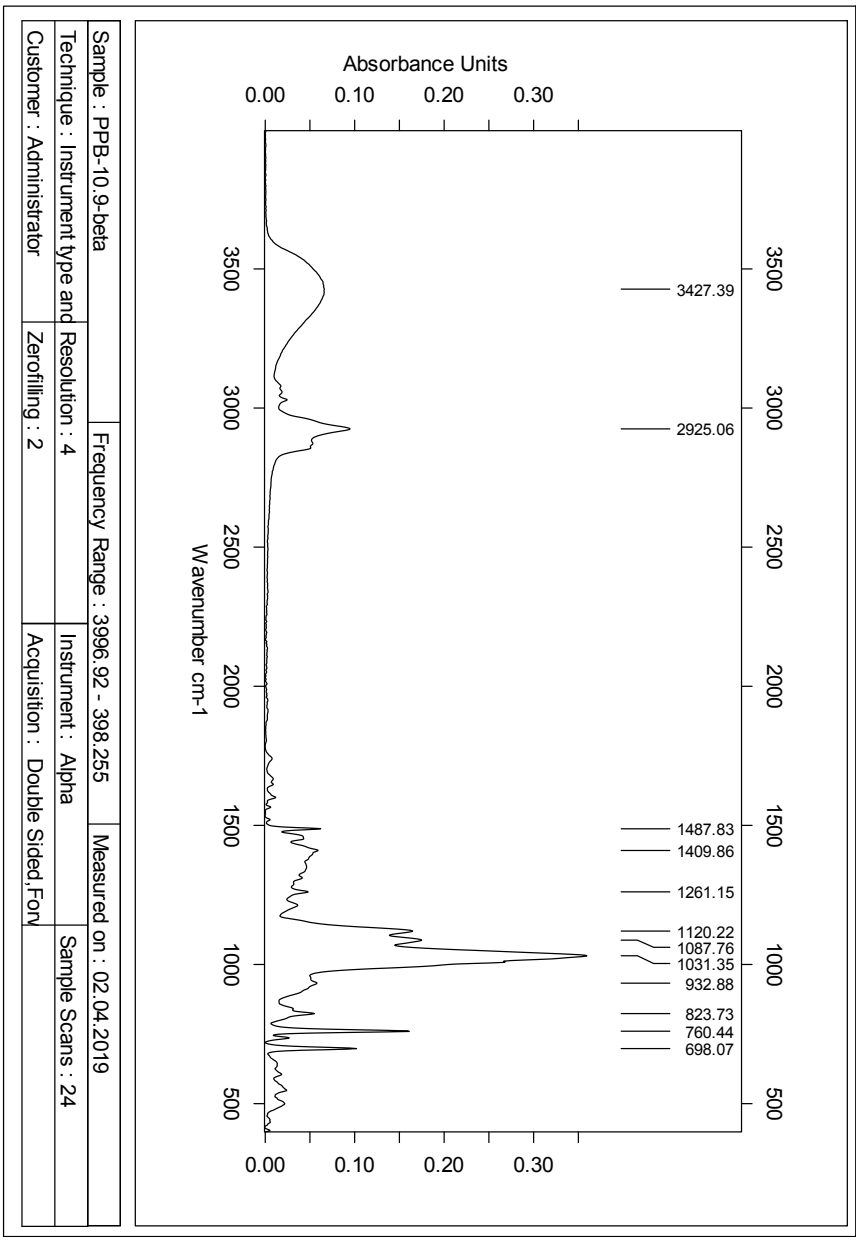

Figure 126: IR spectrum of **3c-α**.

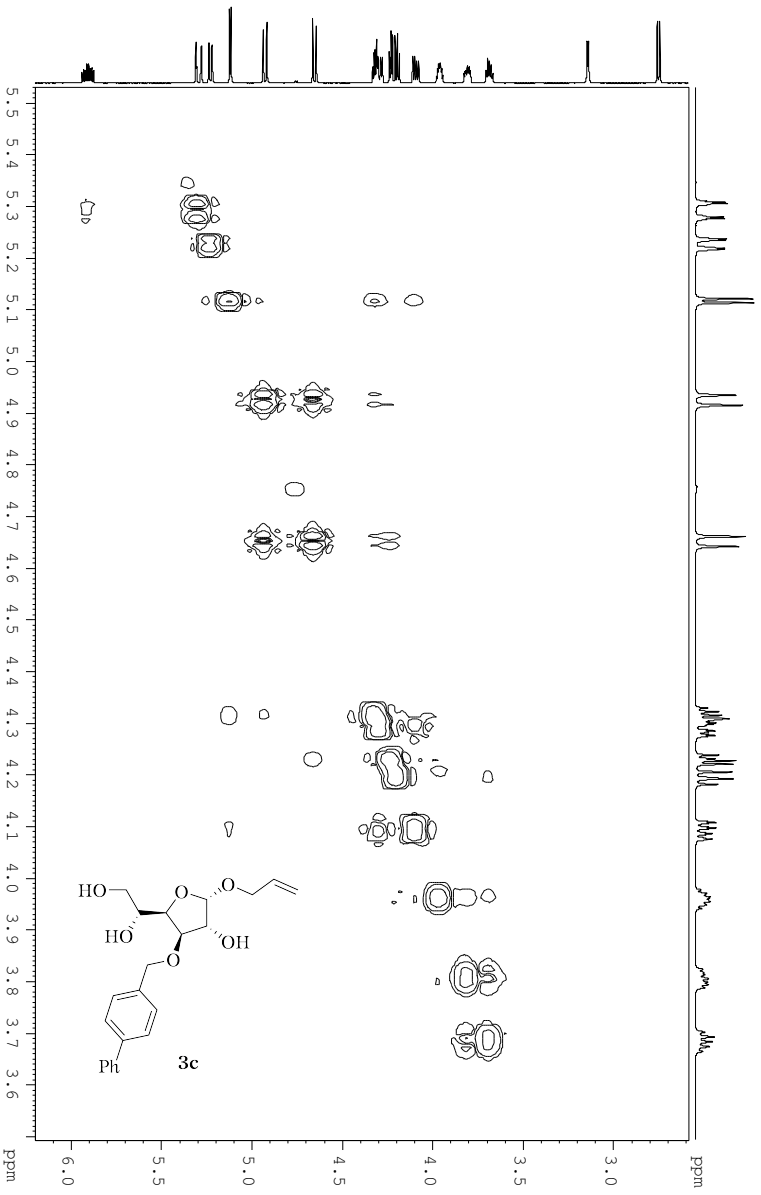

Figure 127: NOESY spectrum of **3c-α**.

B.15 Spectroscopic data for compound 3c-β

Elemental Composition Report **Page 1**

Single Mass Analysis
Tolerance = 3.0 PPM / DBE: min = -50.0, max = 50.0
Element prediction: Off
Number of isotope peaks used for i-FIT = 3

Monoisotopic Mass, Even Electron Ions
256 formula(e) evaluated with 1 results within limits (all results (up to 1000) for each mass)
Elements Used:
C: 0-100 H: 0-150 O: 0-10 Na: 0-1
svg_20190403_2019_254 32 (0.602) AM2 (Ar,35000.0,0.00,0.00); Cm (29:32)
1: TOF MS ES+

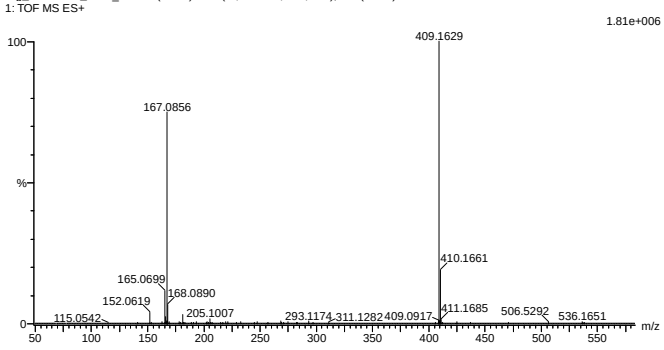

Minimum:				-50.0				
Maximum:		5.0	3.0	50.0				
Mass	Calc. Mass	mDa	PPM	DBE	i-FIT	Norm	Conf(%)	Formula
409.1629	409.1627	0.2	0.5	9.5	1017.5	n/a	n/a	C22 H26 O6 Na

Figure 128: HRMS (ESI+) of **3c-β**.

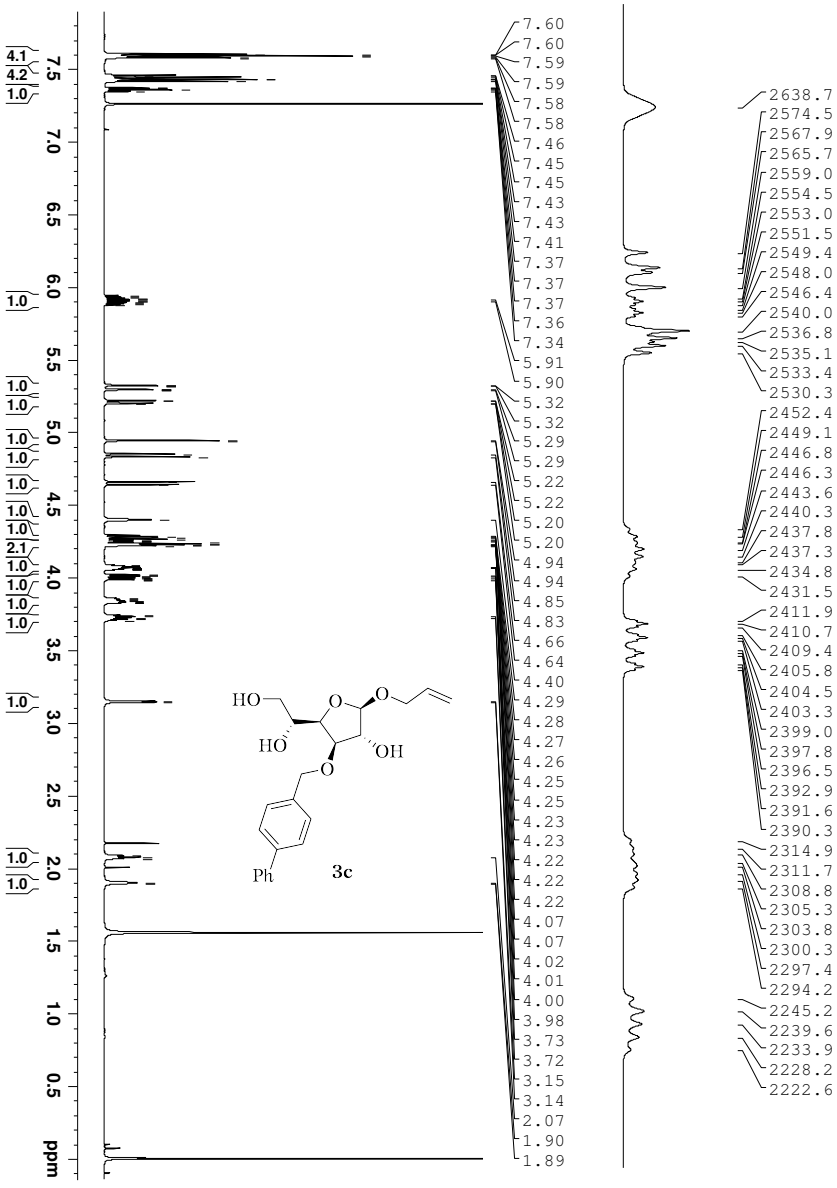

Figure 129: ^{1}H NMR spectrum of **3c-β**.

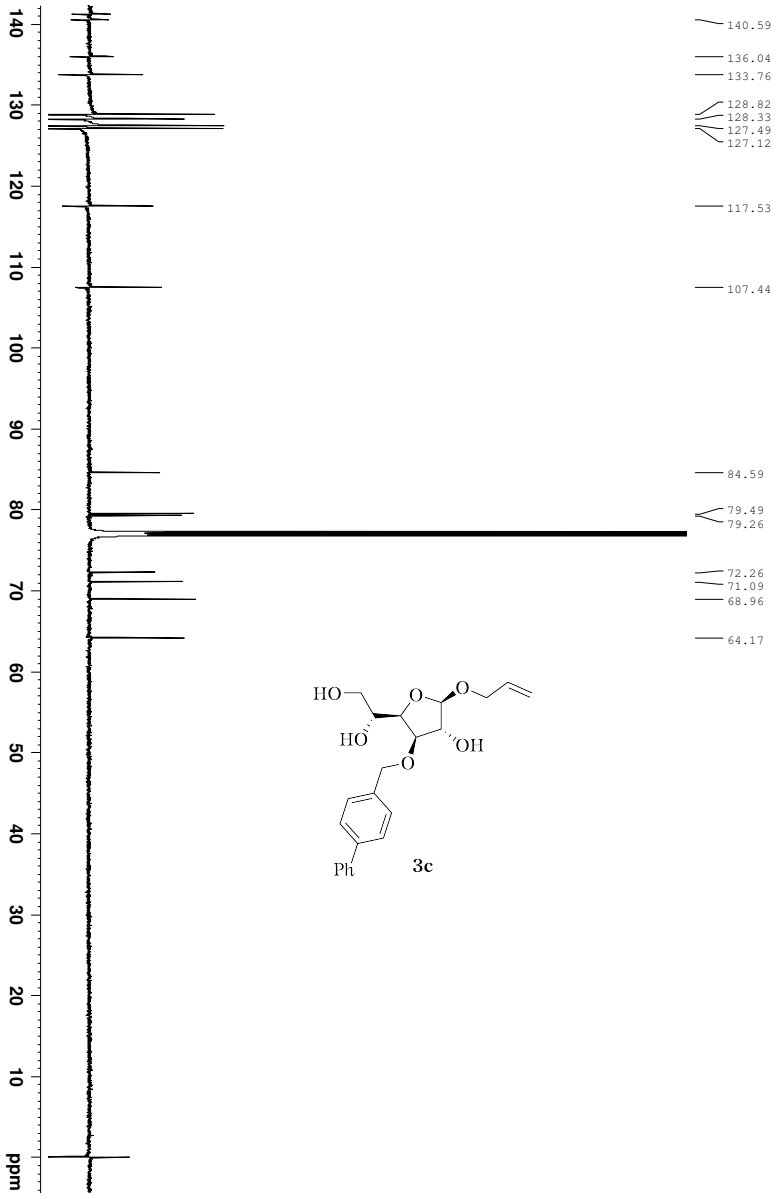

Figure 130: ^{13}C NMR spectrum of **3c-β**.

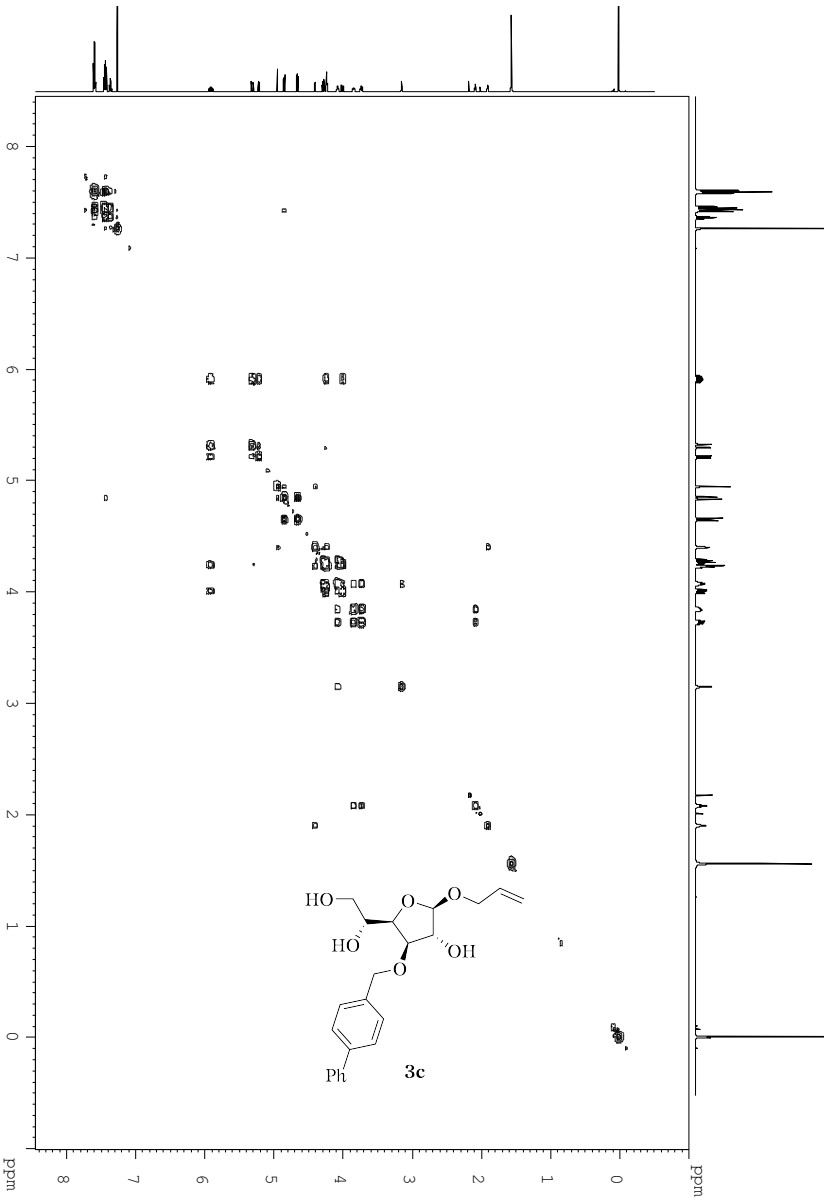

Figure 131: COSY spectrum of **3c-β**.

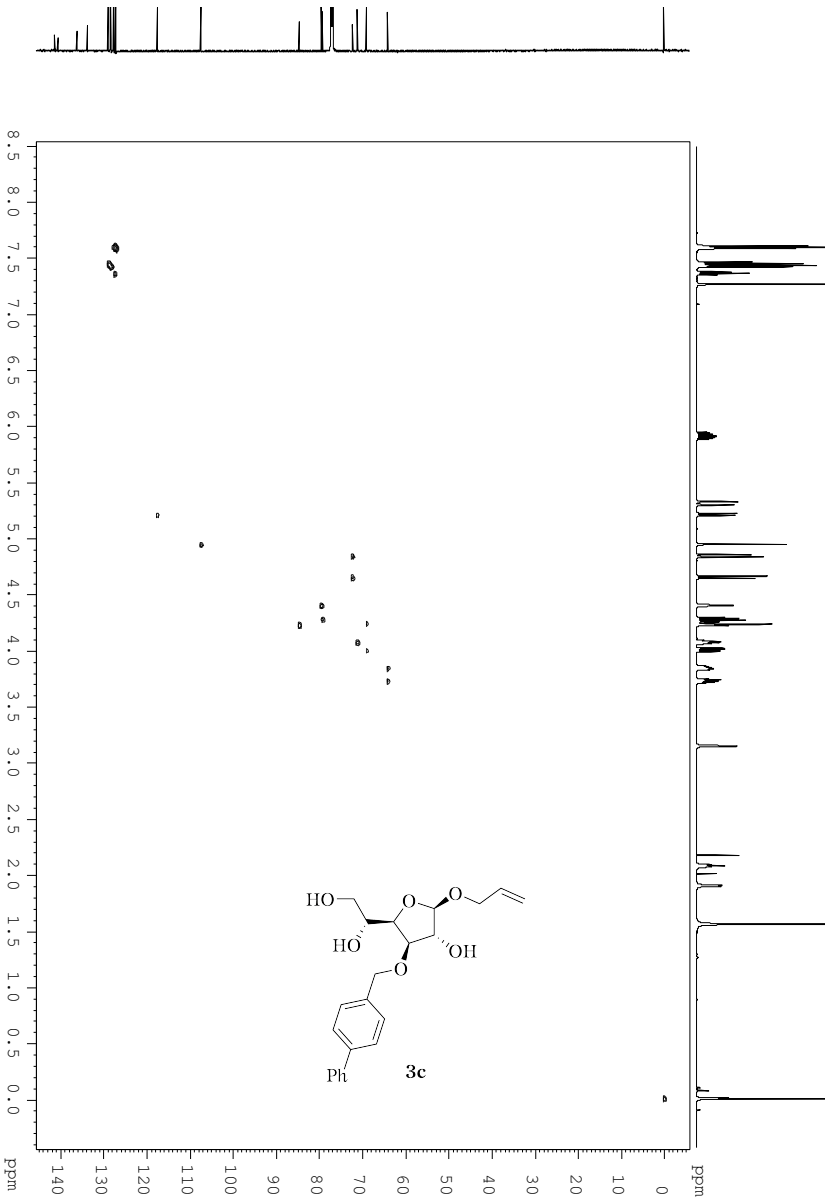

Figure 132: HSQC spectrum of **3c-β**.

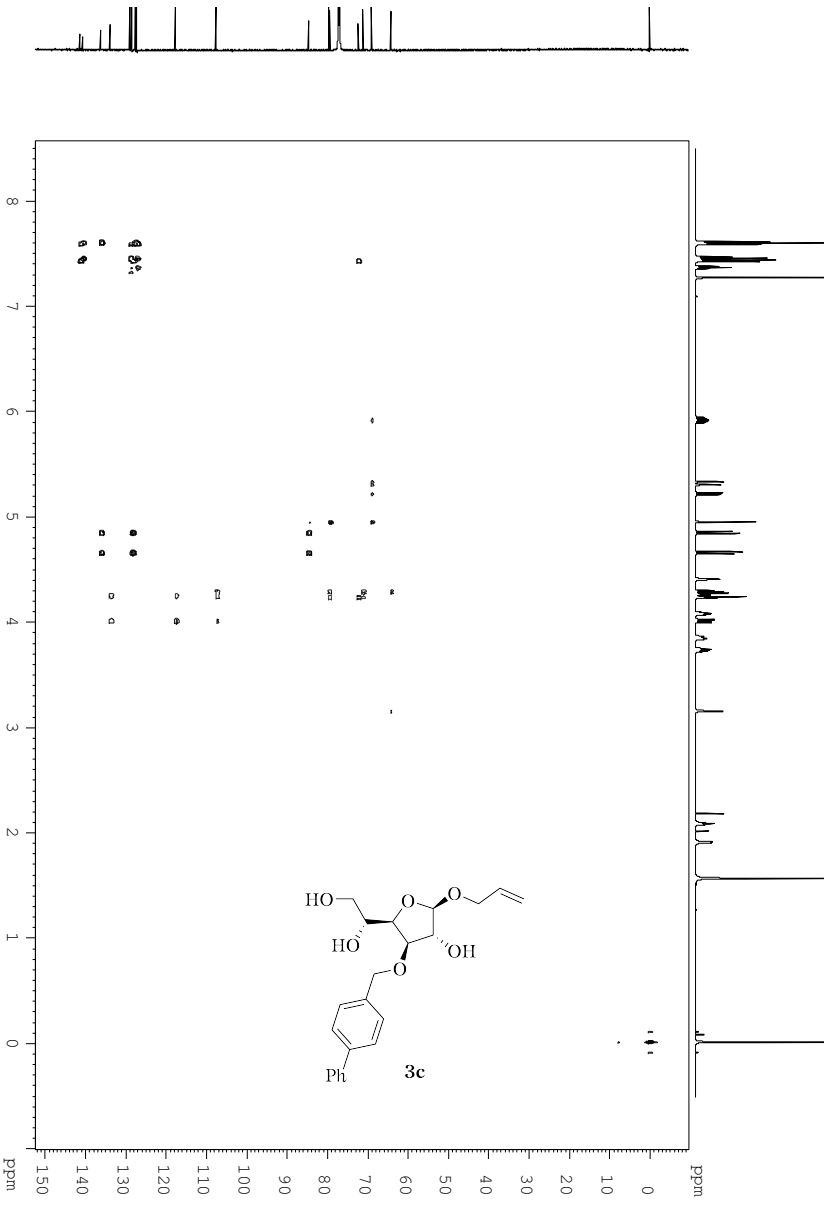

Figure 133: HMBC spectrum of **3c-β**.

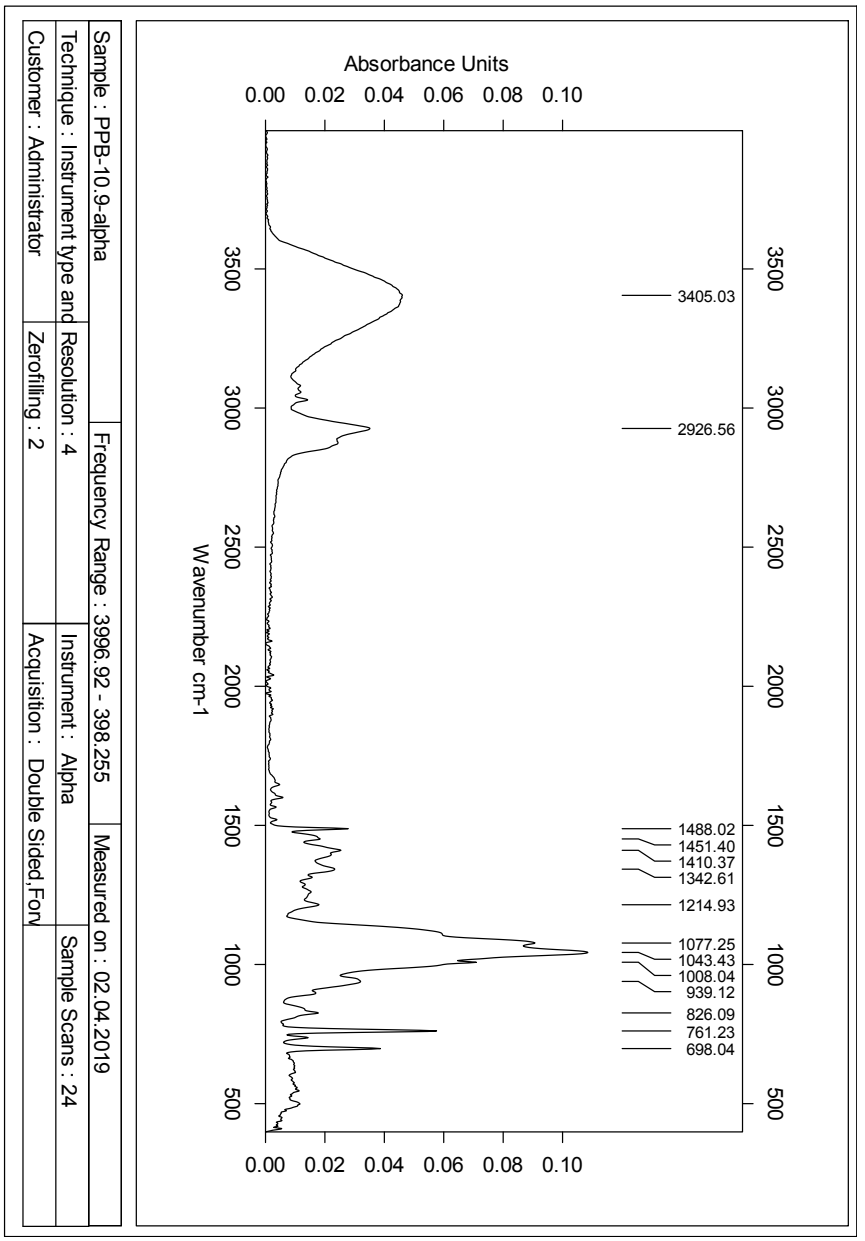

Figure 134: IR spectrum of **3c-β**.

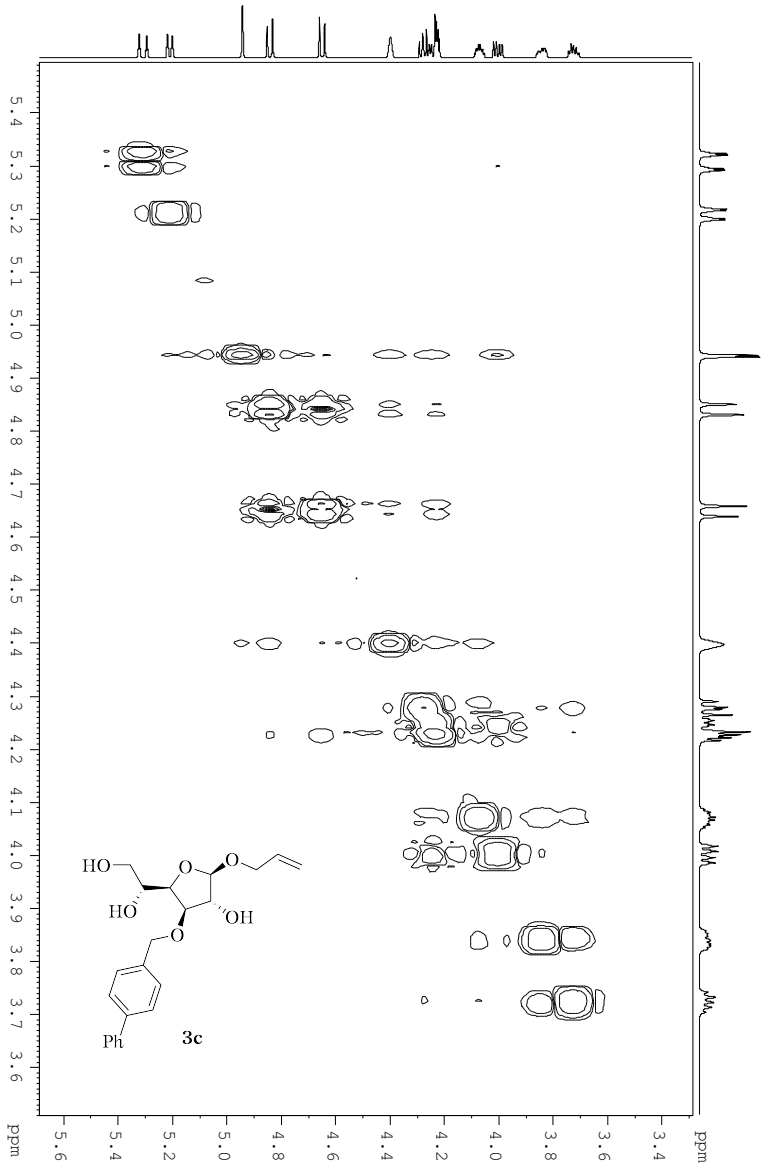

Figure 135: NOESY spectrum of **3c-β**.

B.16 Spectroscopic data for compound 3f-α

Elemental Composition Report **Page 1**

Single Mass Analysis
Tolerance = 2.0 PPM / DBE: min = -50.0, max = 50.0
Element prediction: Off
Number of isotope peaks used for i-FIT = 3

Monoisotopic Mass, Even Electron Ions
803 formula(e) evaluated with 3 results within limits (all results (up to 1000) for each mass)
Elements Used:
C: 2-100 H: 0-150 O: 0-10 Na: 0-1 Si: 0-2
2019_581 51 (0.577) AM2 (Ar,35000.0,0.00,0.00); ABS; Cm (46:60)
1: TOF MS ES+

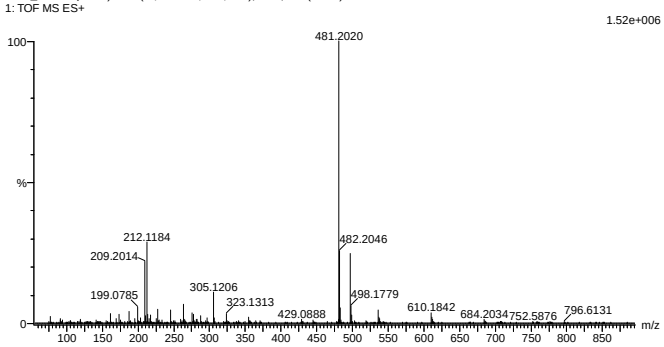

Minimum:				-50.0				
Maximum:		5.0	2.0	50.0				
Mass	Calc. Mass	mDa	PPM	DBE	i-FIT	Norm	Conf(%)	Formula
481.2020	481.2019	0.1	0.2	16.5	1044.6	2.180	11.30	C30 H33 O2 Si2
	481.2022	-0.2	-0.4	9.5	1042.5	0.125	88.22	C25 H34 O6 Na Si
	481.2015	0.5	1.0	17.5	1047.7	5.336	0.48	C31 H29 O5

Figure 136: HRMS (ESI+) of **3f-α**.

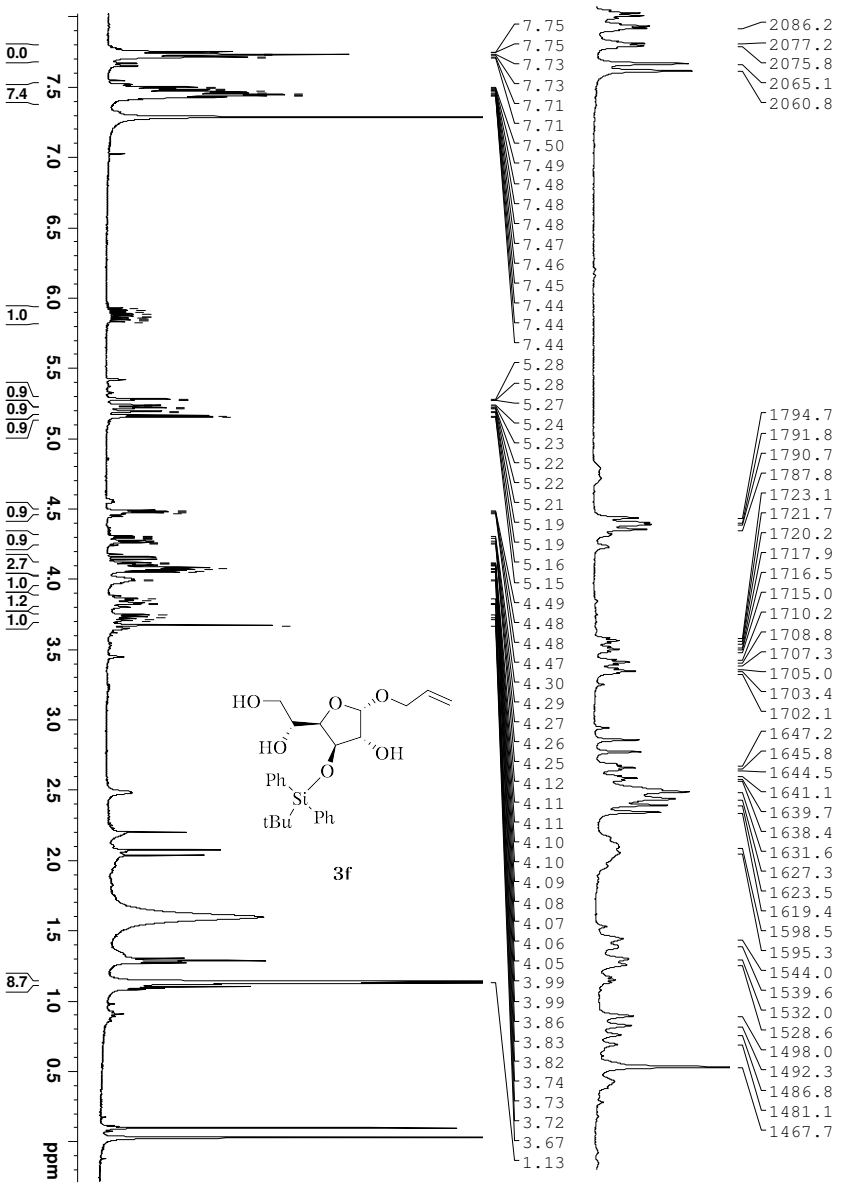

Figure 137: ^{1}H NMR (400 MHz) spectrum of **3f-α**.

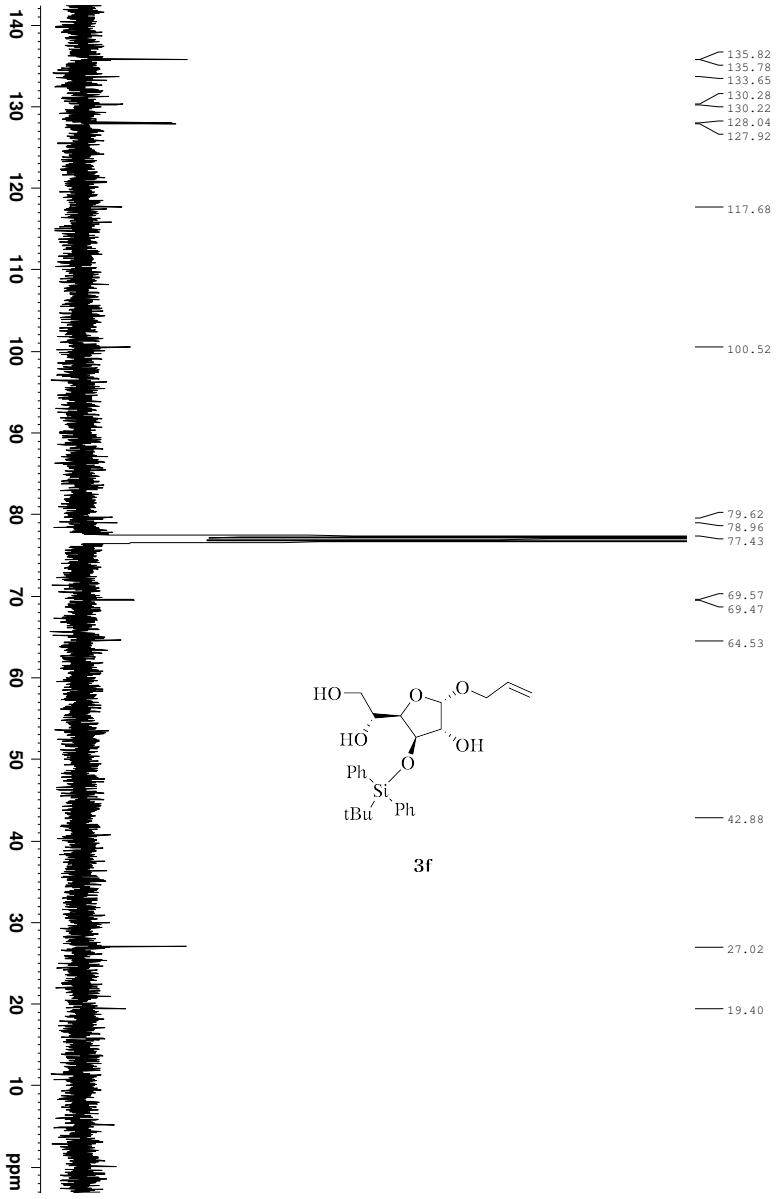

3f

Figure 138: ^{13}C NMR (100 MHz) spectrum of **3f-α**.

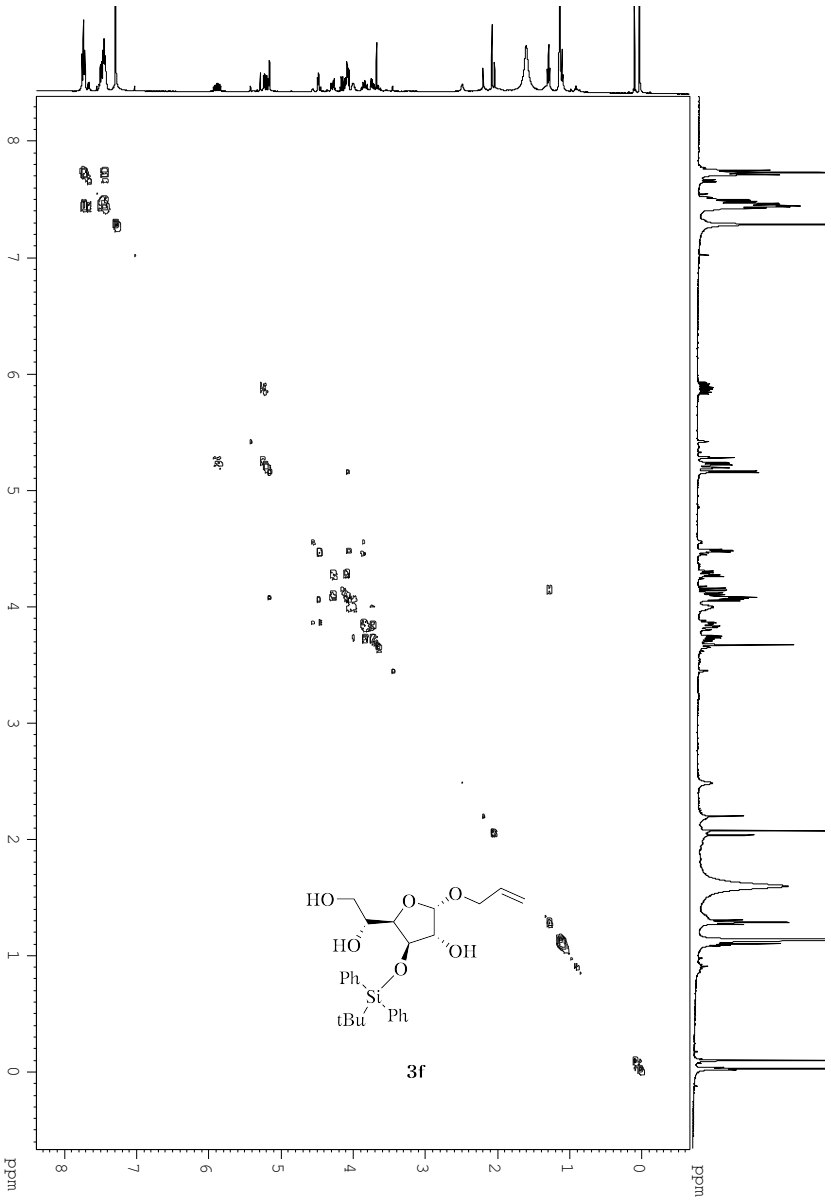

Figure 139: COSY (400 MHz) spectrum of **3f-α**.

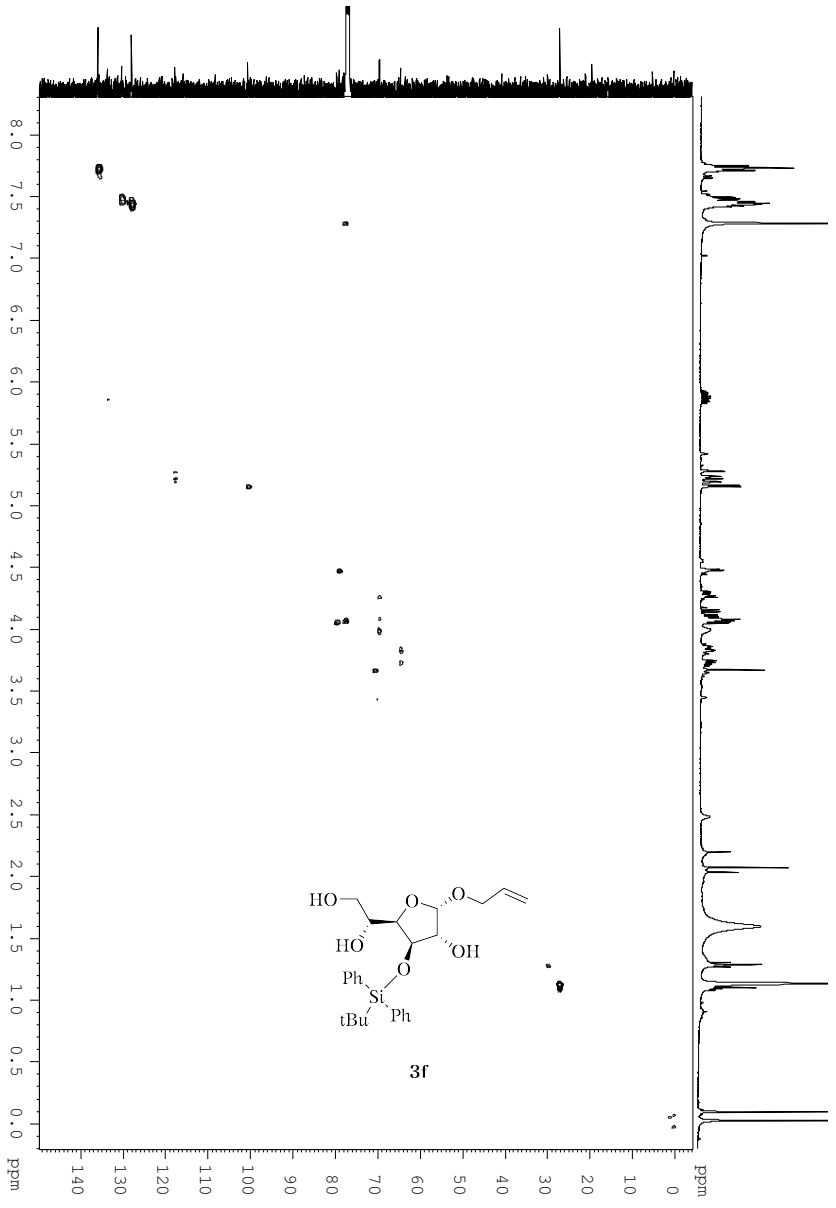

Figure 140: HSQC (400 MHz) spectrum of **3f-α**.

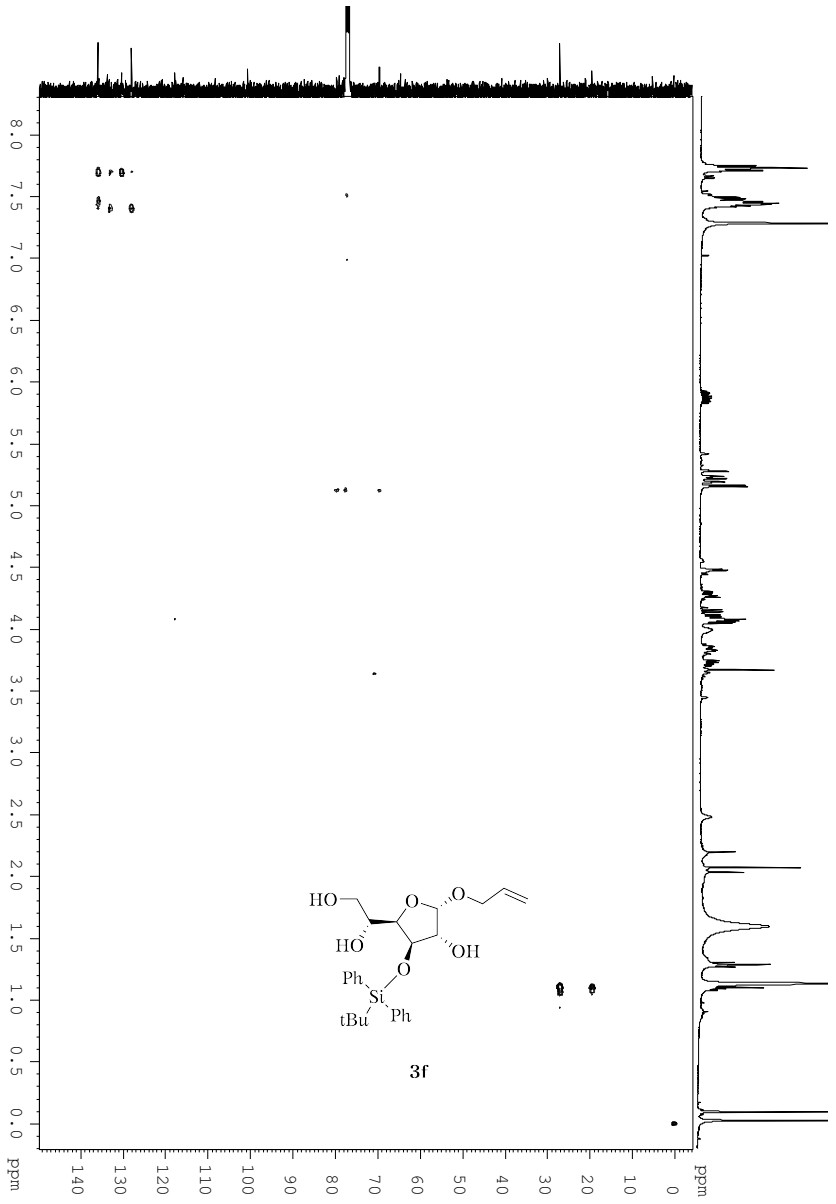

Figure 141: HMBC (400 MHz) spectrum of **3f-α**.

B.17 Spectroscopic data for compound 3f-β

Elemental Composition Report **Page 1**

Single Mass Analysis
Tolerance = 5.0 PPM / DBE: min = -50.0, max = 50.0
Element prediction: Off
Number of isotope peaks used for i-FIT = 3

Monoisotopic Mass, Even Electron Ions
803 formula(e) evaluated with 4 results within limits (all results (up to 1000) for each mass)
Elements Used:
C: 2-100 H: 0-150 O: 0-10 Si: 0-2 Na: 0-1

2019_575 59 (0.661) AM2 (Ar,35000.0,0.00,0.00); ABS; Cm (59:63)
1: TOF MS ES+

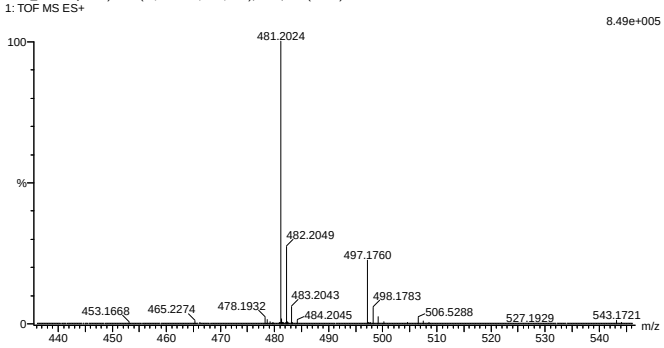

Minimum:				-50.0				
Maximum:		5.0	5.0	50.0				
Mass	Calc. Mass	mDa	PPM	DBE	i-FIT	Norm	Conf(%)	Formula
481.2024	481.2022	0.2	0.4	9.5	974.4	0.054	94.71	C25 H34 O6 Si Na
	481.2019	0.5	1.0	16.5	977.7	3.369	3.44	C30 H33 O2 Si2
	481.2015	0.9	1.9	17.5	979.7	5.417	0.44	C31 H29 O5
	481.2046	-2.2	-4.6	12.5	978.6	4.268	1.40	C27 H33 O6 Si

Figure 142: HRMS (ESI+) of **3f-β**.

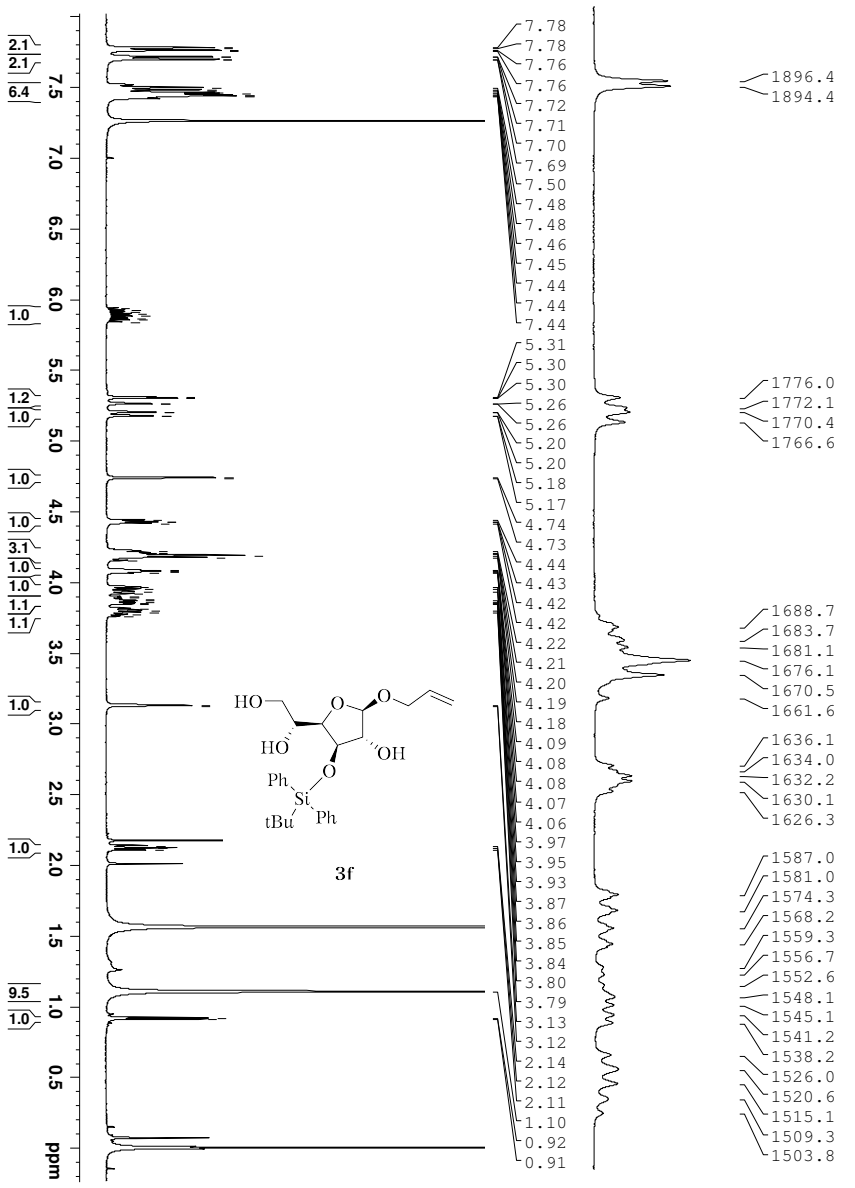

Figure 143: ^{1}H NMR (400 MHz) spectrum of **3f-β**.

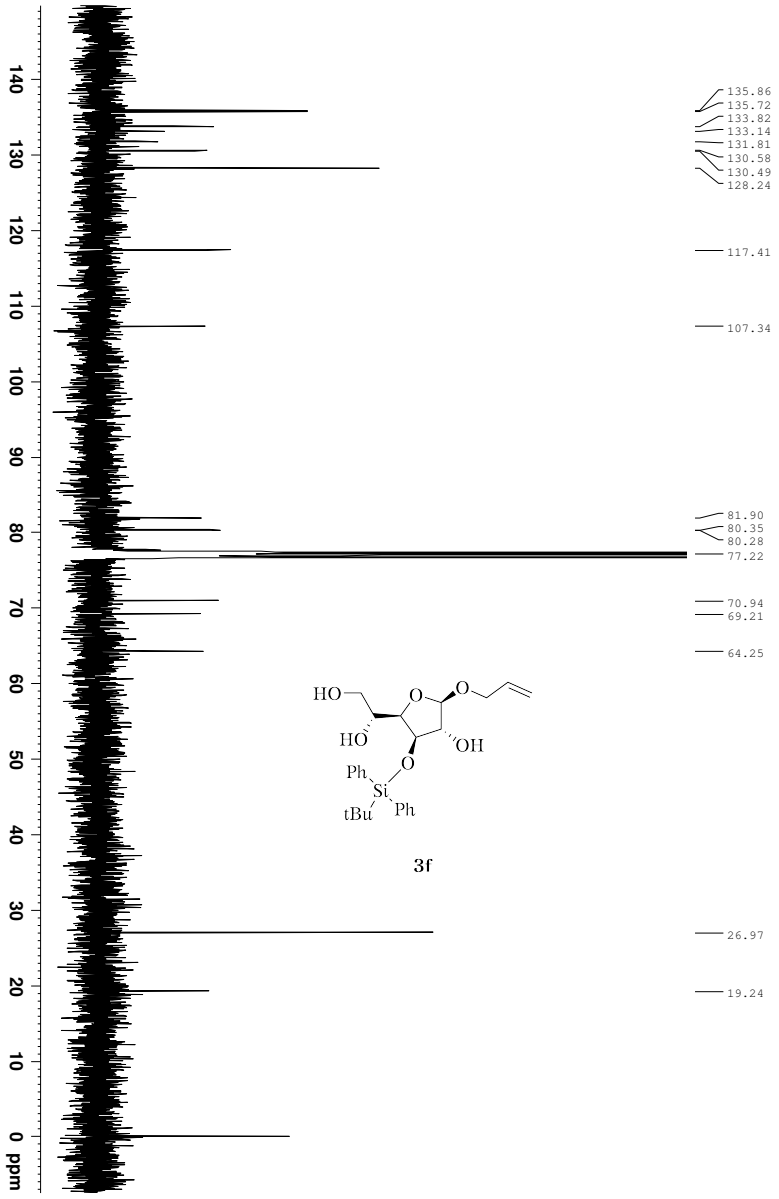

Figure 144: ^{13}C NMR (100 MHz) spectrum of **3f-β**.

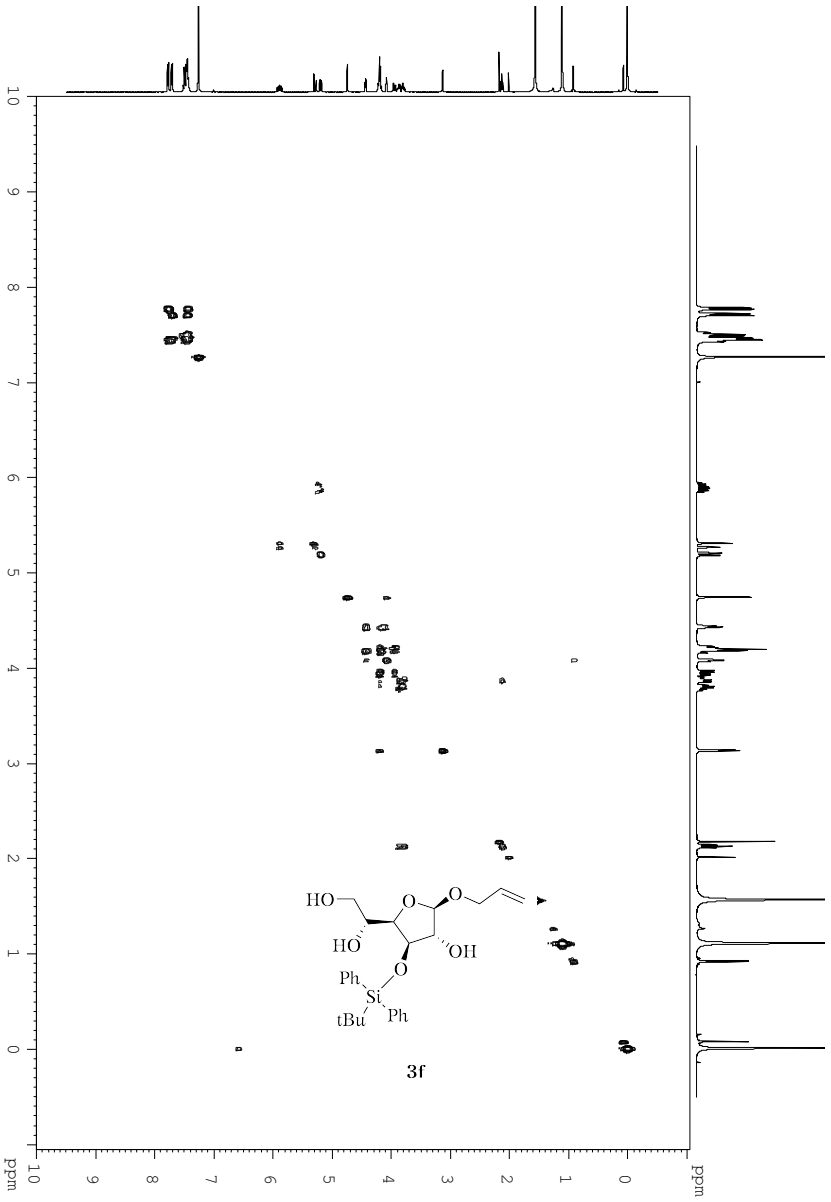

Figure 145: COSY (400 MHz) spectrum of **3f-β**.

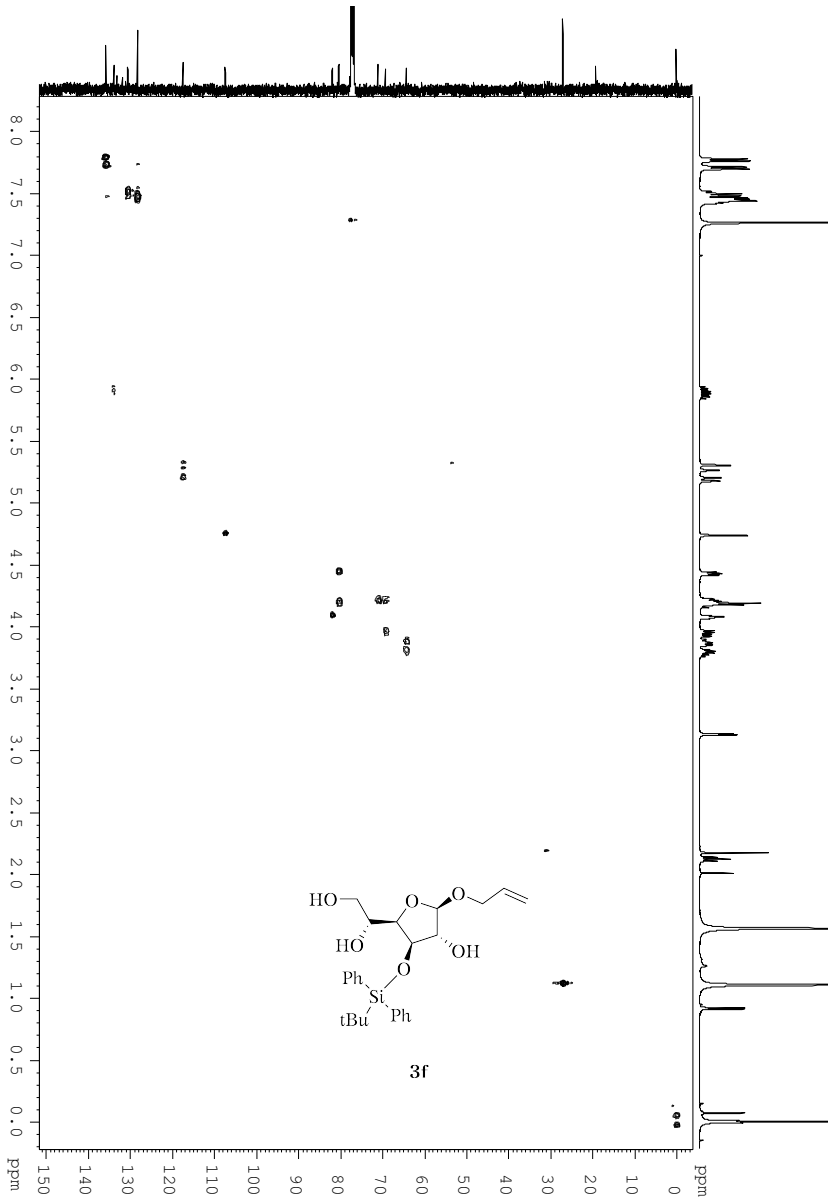

Figure 146: HSQC (400 MHz) spectrum of **3f-β**.

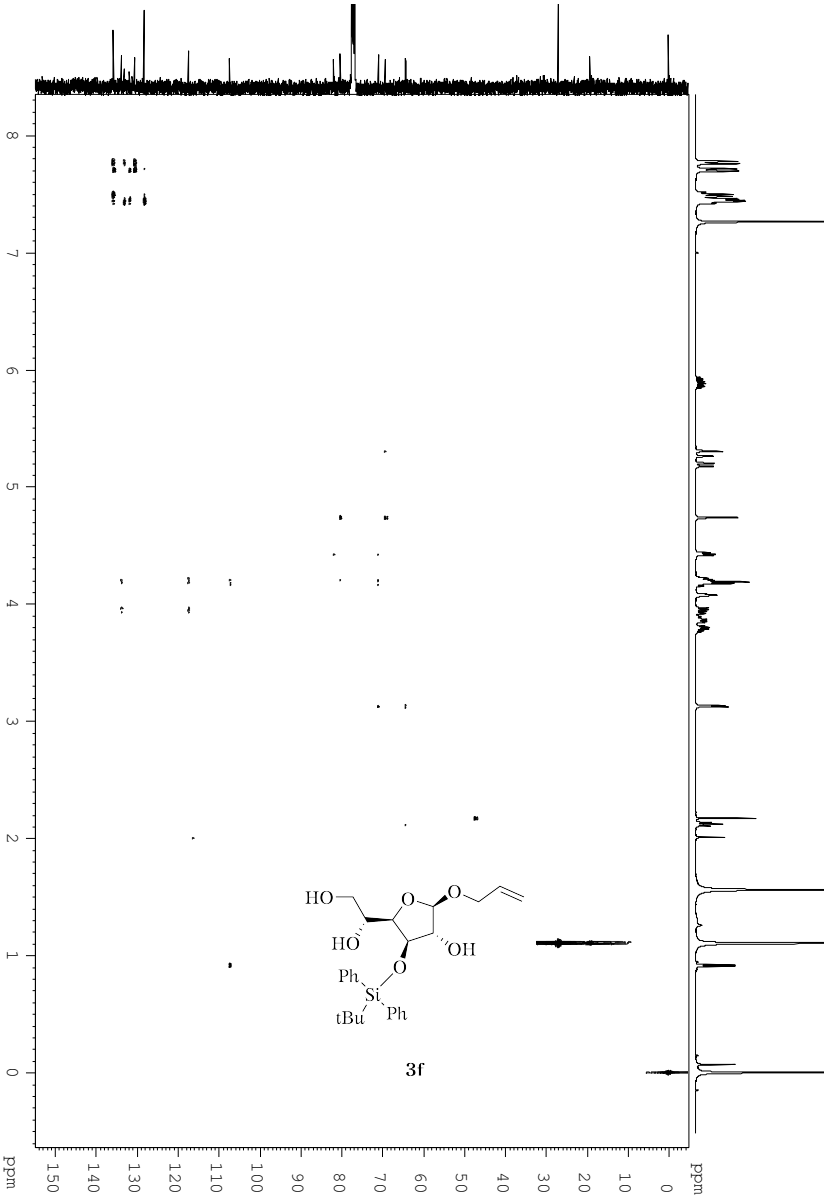

Figure 147: HMBC (400 MHz) spectrum of **3f-β**.

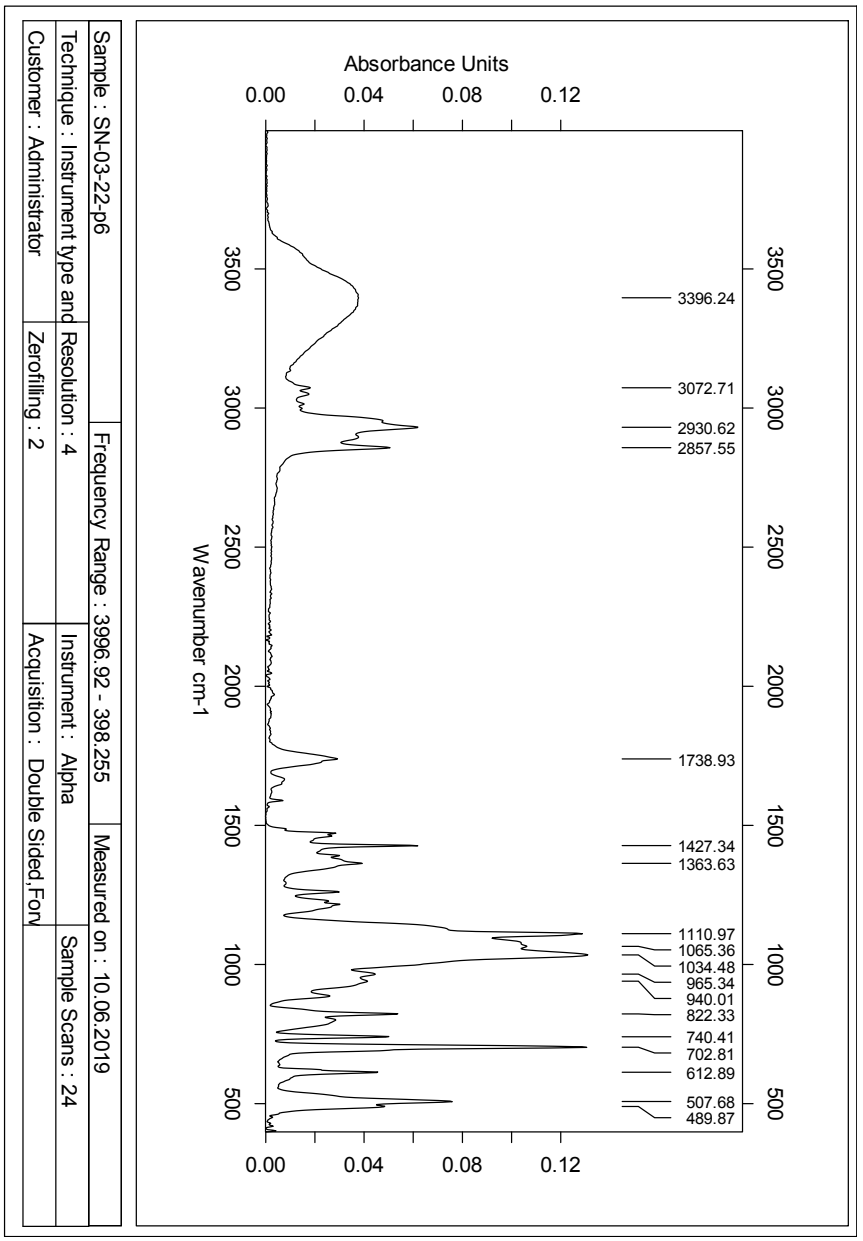

Figure 148: IR spectrum of **3f-β**.

B.18 Spectroscopic data for compound 3μ-α

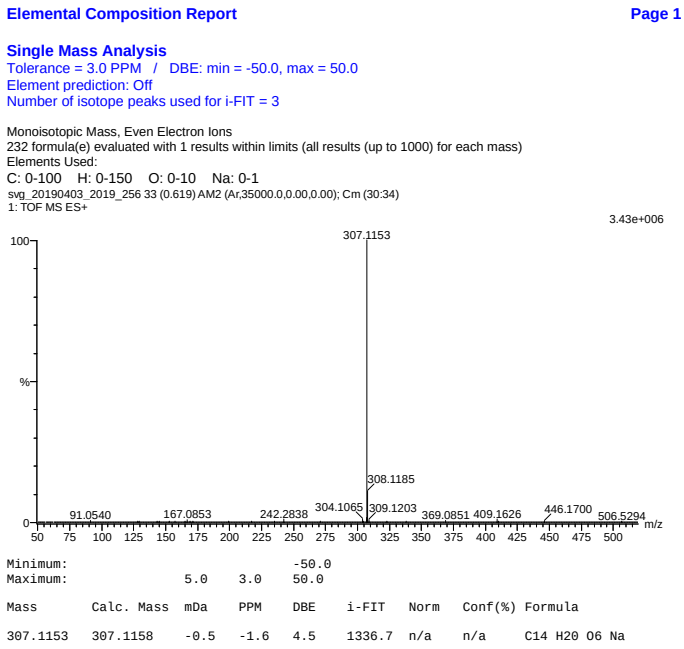

Elemental Composition Report **Page 1**

Single Mass Analysis
Tolerance = 3.0 PPM / DBE: min = -50.0, max = 50.0
Element prediction: Off
Number of isotope peaks used for i-FIT = 3

Monoisotopic Mass, Even Electron Ions
232 formula(e) evaluated with 1 results within limits (all results (up to 1000) for each mass)
Elements Used:
C: 0-100 H: 0-150 O: 0-10 Na: 0-1
svg_20190403_2019_256 33 (0.619) AM2 (Ar,35000.0,0.00,0.00); Cm (30:34)
1: TOF MS ES+
3.43e+006

Minimum:				-50.0				
Maximum:		5.0	3.0	50.0				
Mass	Calc. Mass	mDa	PPM	DBE	i-FIT	Norm	Conf(%)	Formula
307.1153	307.1158	-0.5	-1.6	4.5	1336.7	n/a	n/a	C14 H20 O6 Na

Figure 149: HRMS (ESI+) of **3μ-α**.

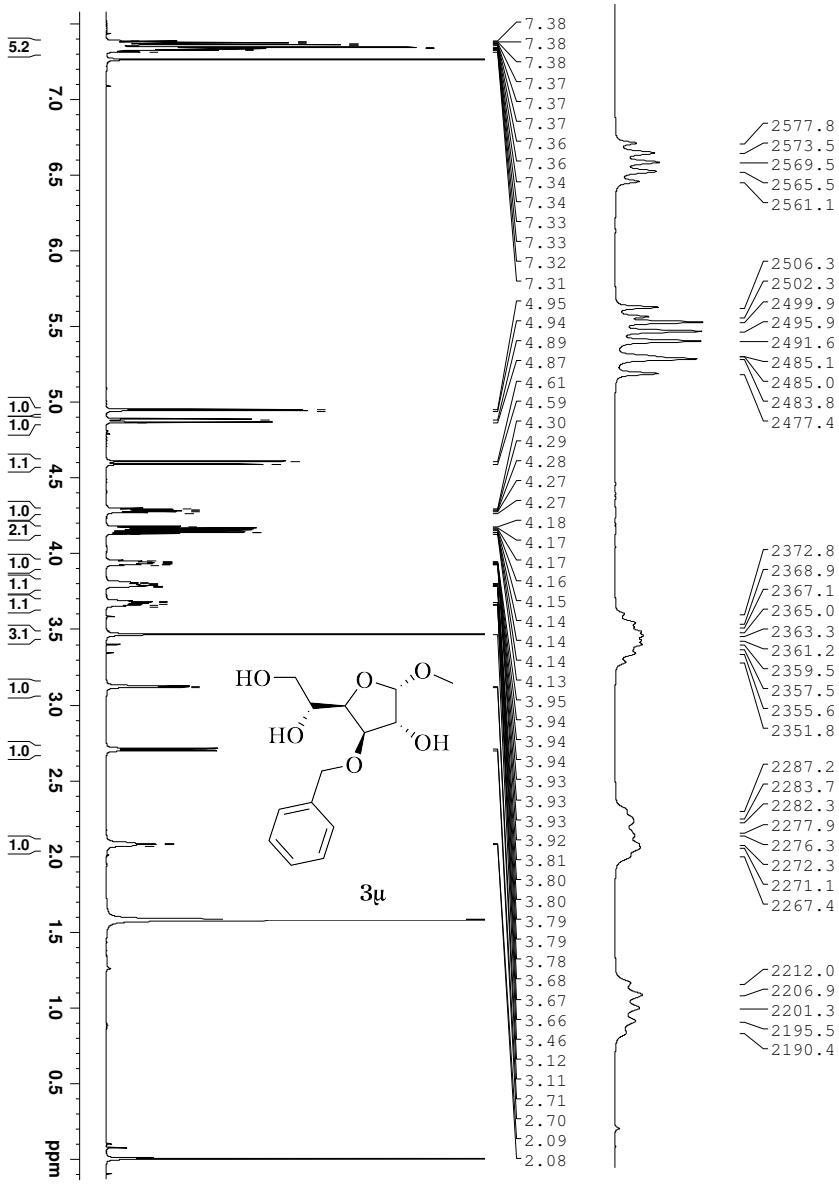

Figure 150: ^{1}H NMR spectrum of **3μ-α**.

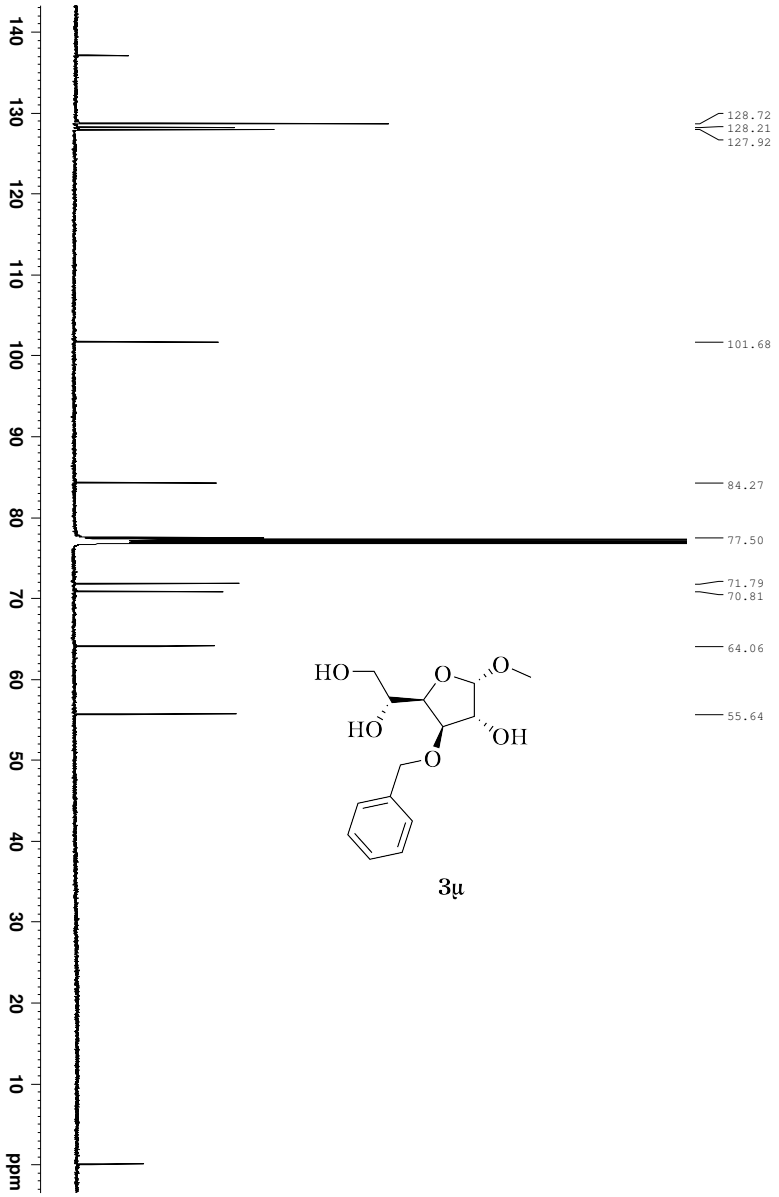

3μ

Figure 151: ^{13}C NMR spectrum of **3μ-α**.

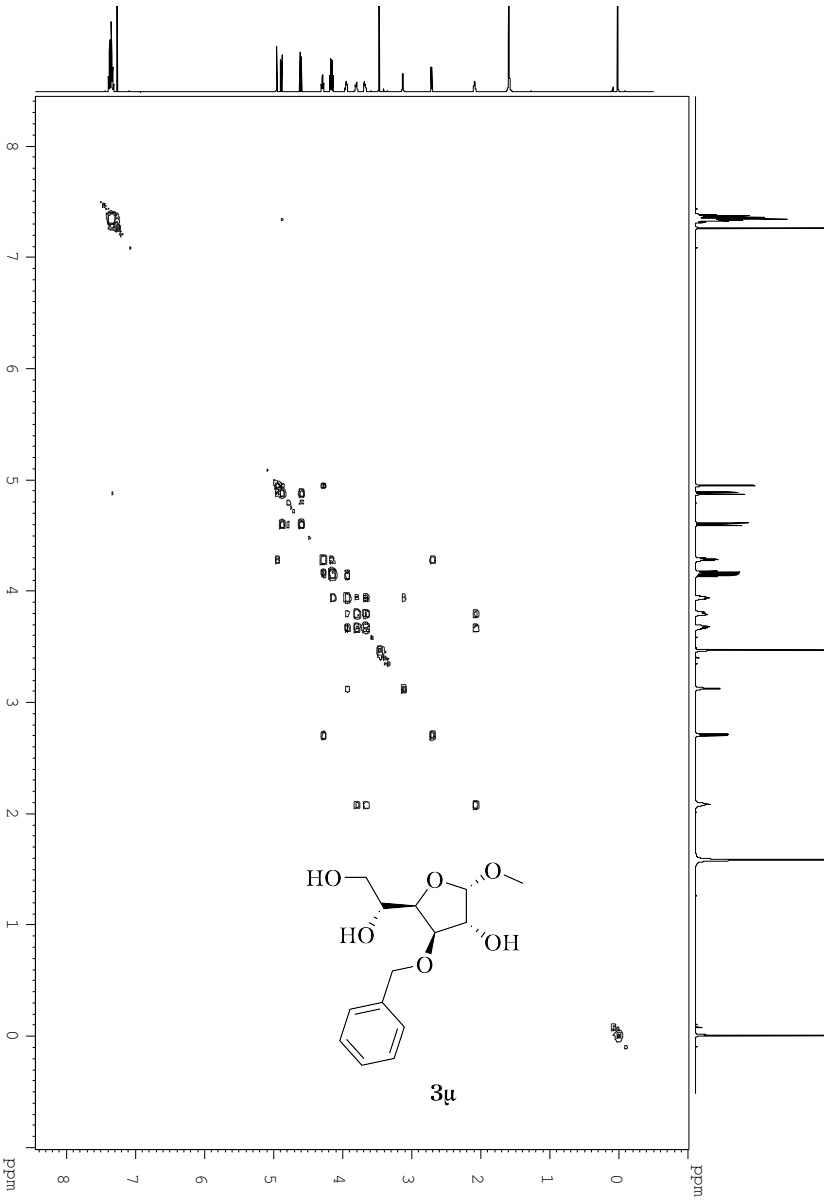

Figure 152: COSY spectrum of **3μ-α**.

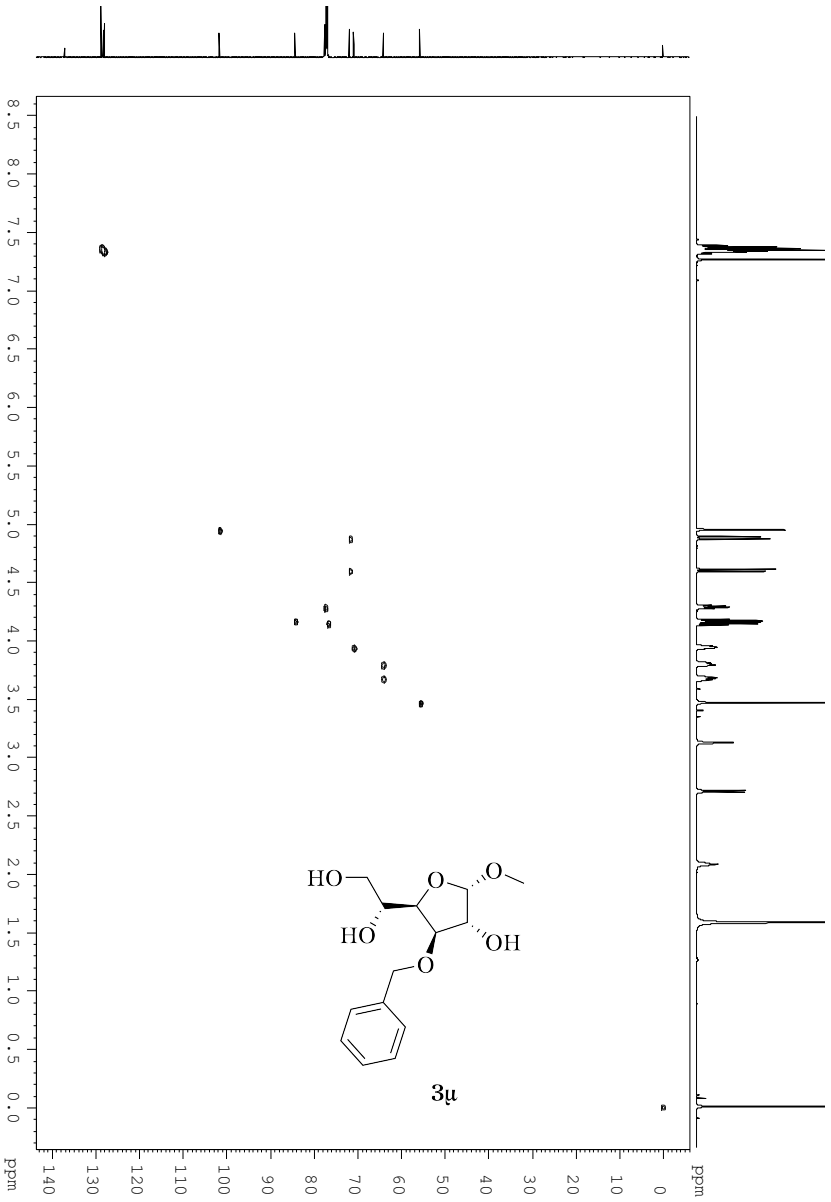

Figure 153: HSQC spectrum of **3μ-α**.

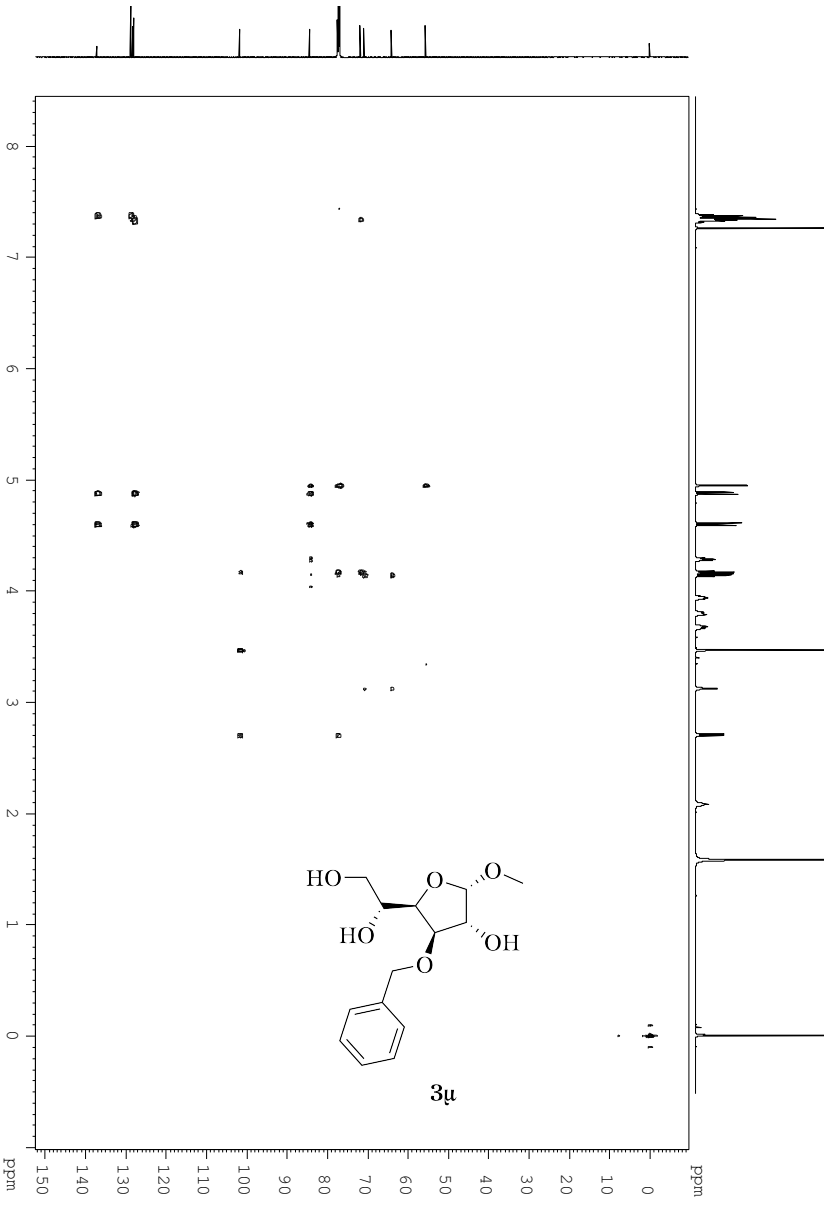

Figure 154: HMBC spectrum of **3μ-α**.

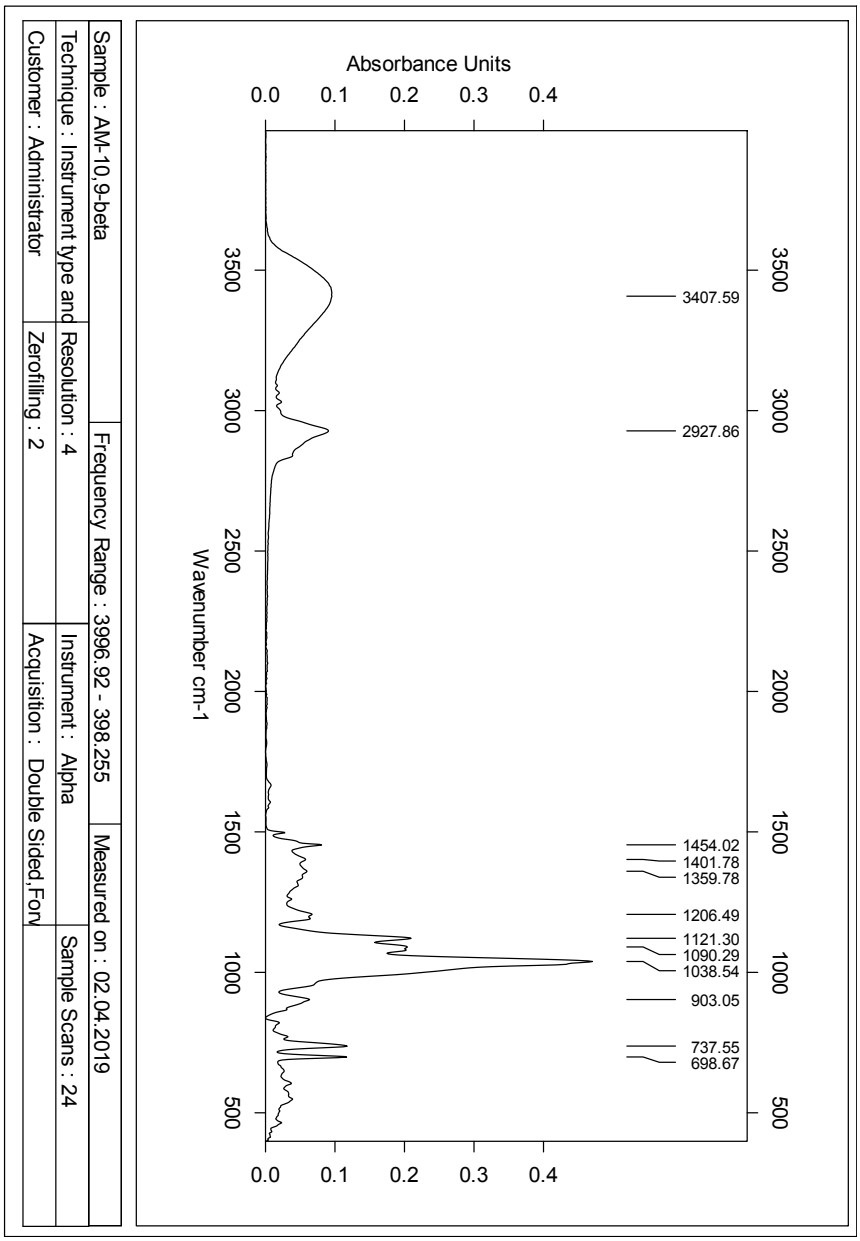

Figure 155: IR spectrum of **3μ-α**.

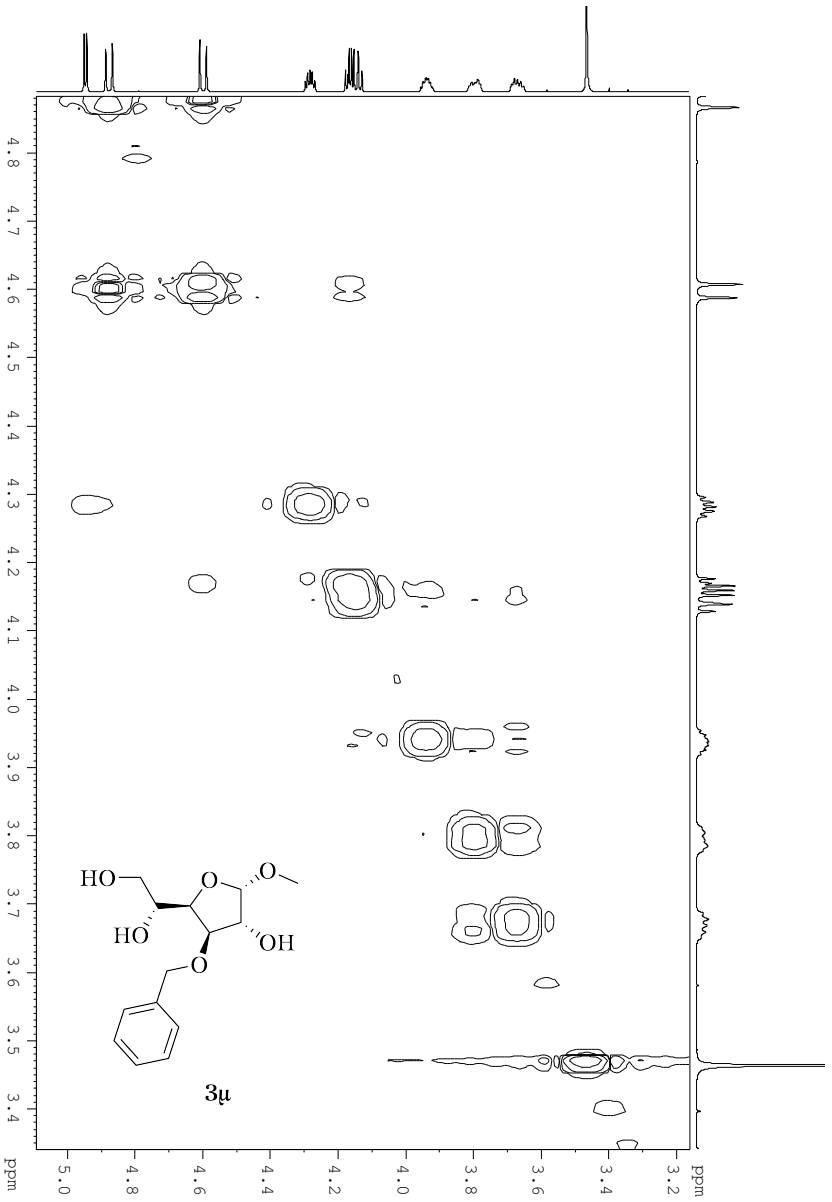

Figure 156: NOESY spectrum of **3μ-α**.

B.19 Spectroscopic data for compound 3μ-β

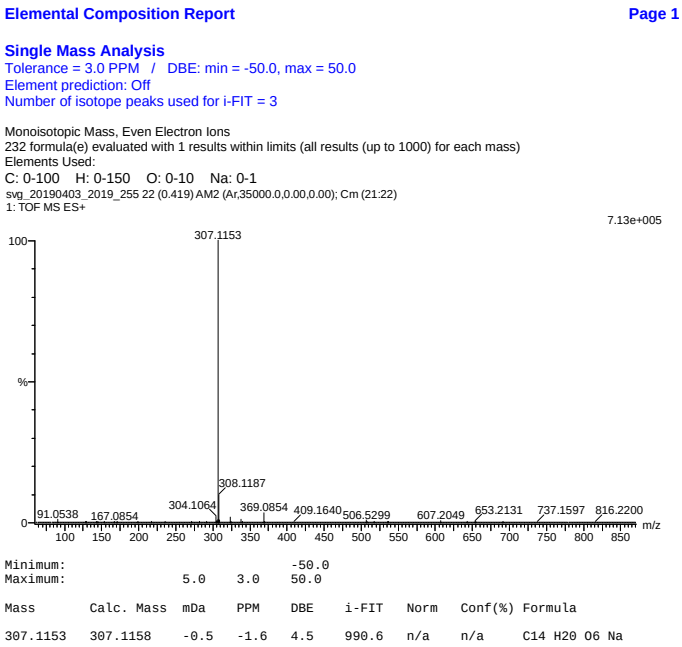

Figure 157: HRMS (ESI+) of **3μ-β**.

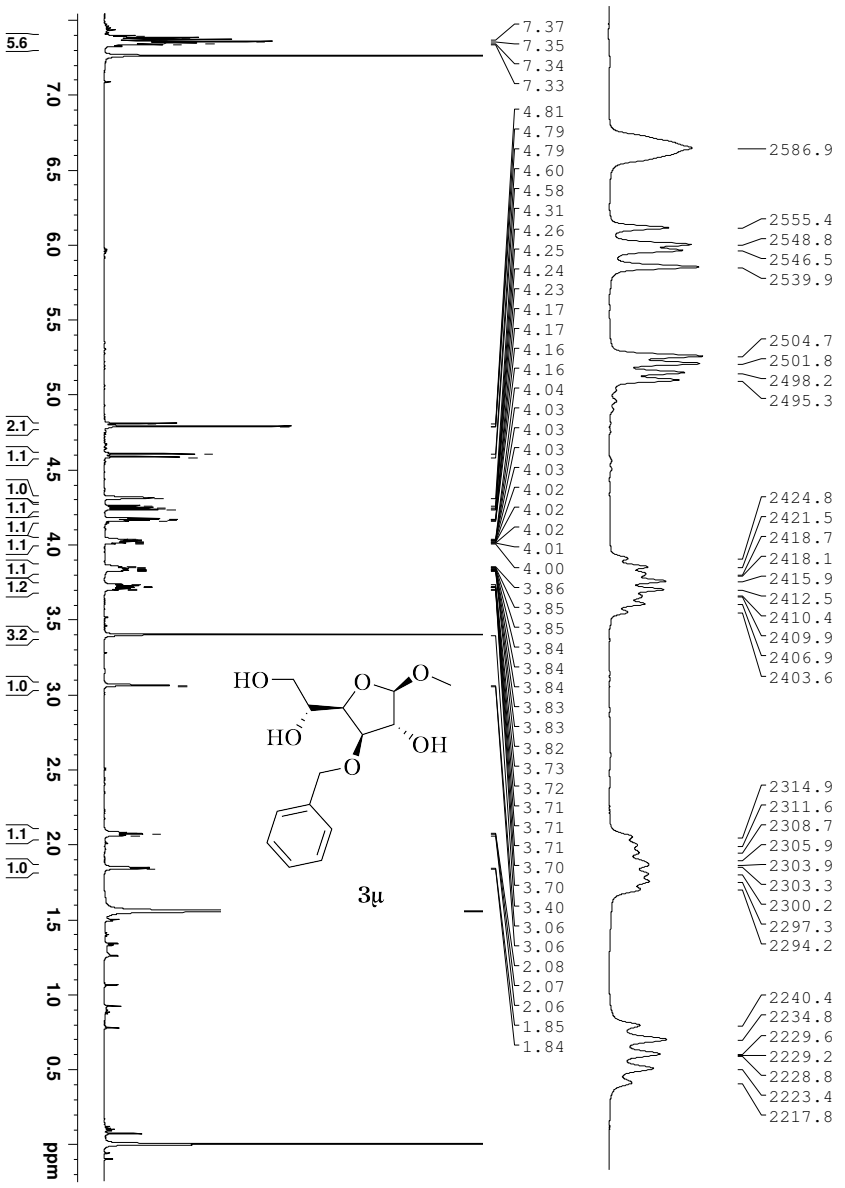

Figure 158: ^{1}H NMR spectrum of **3μ-β**.

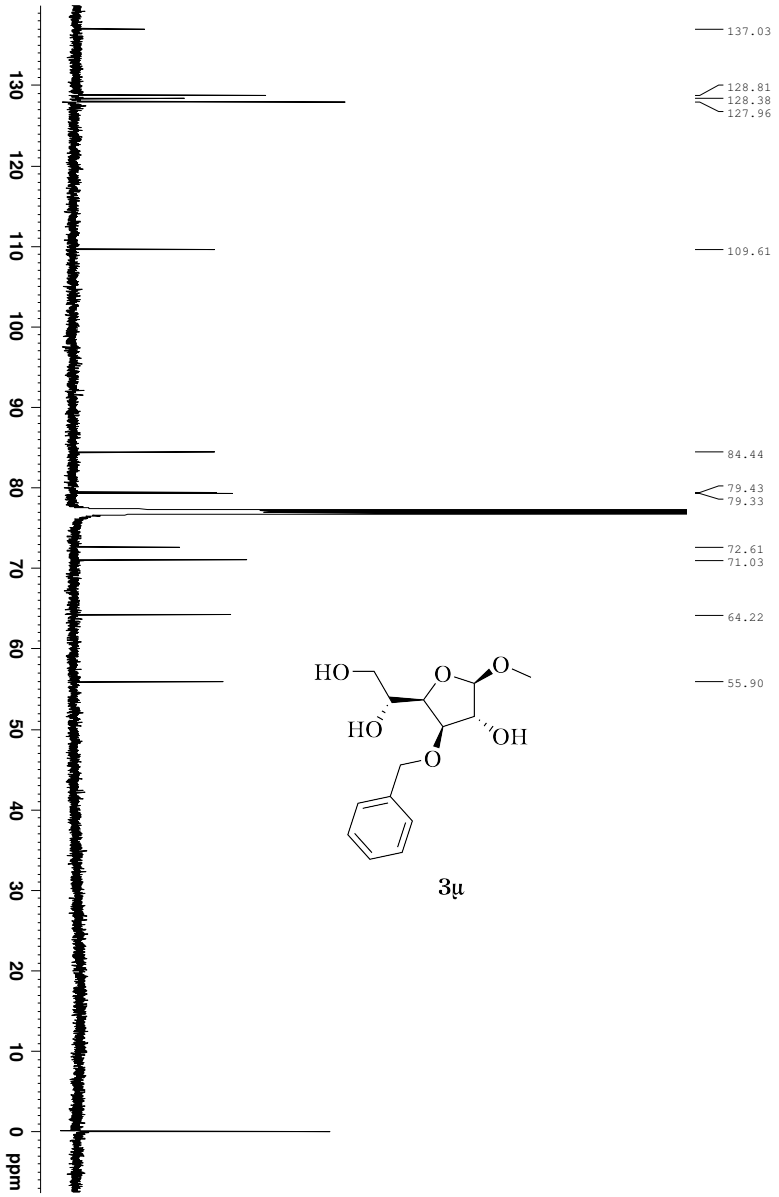

Figure 159: ^{13}C NMR spectrum of **3μ-β**.

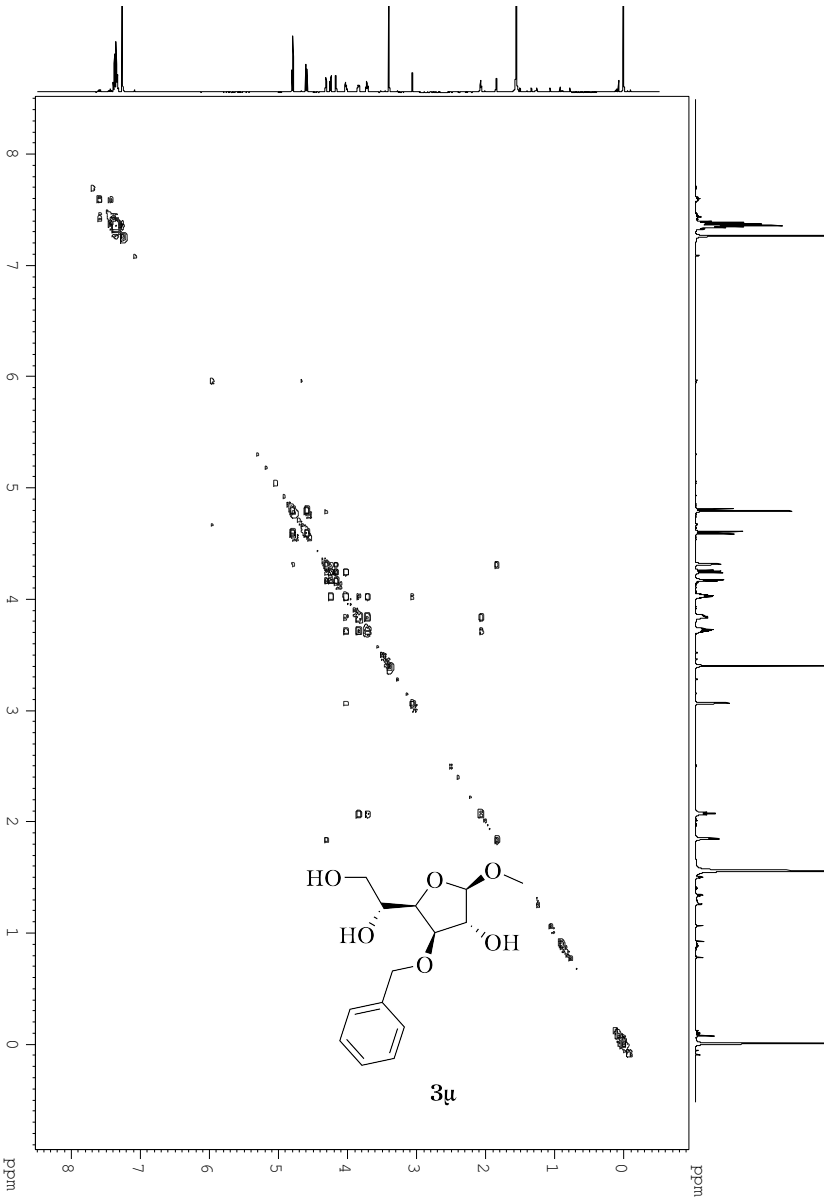

Figure 160: COSY spectrum of **3μ-β**.

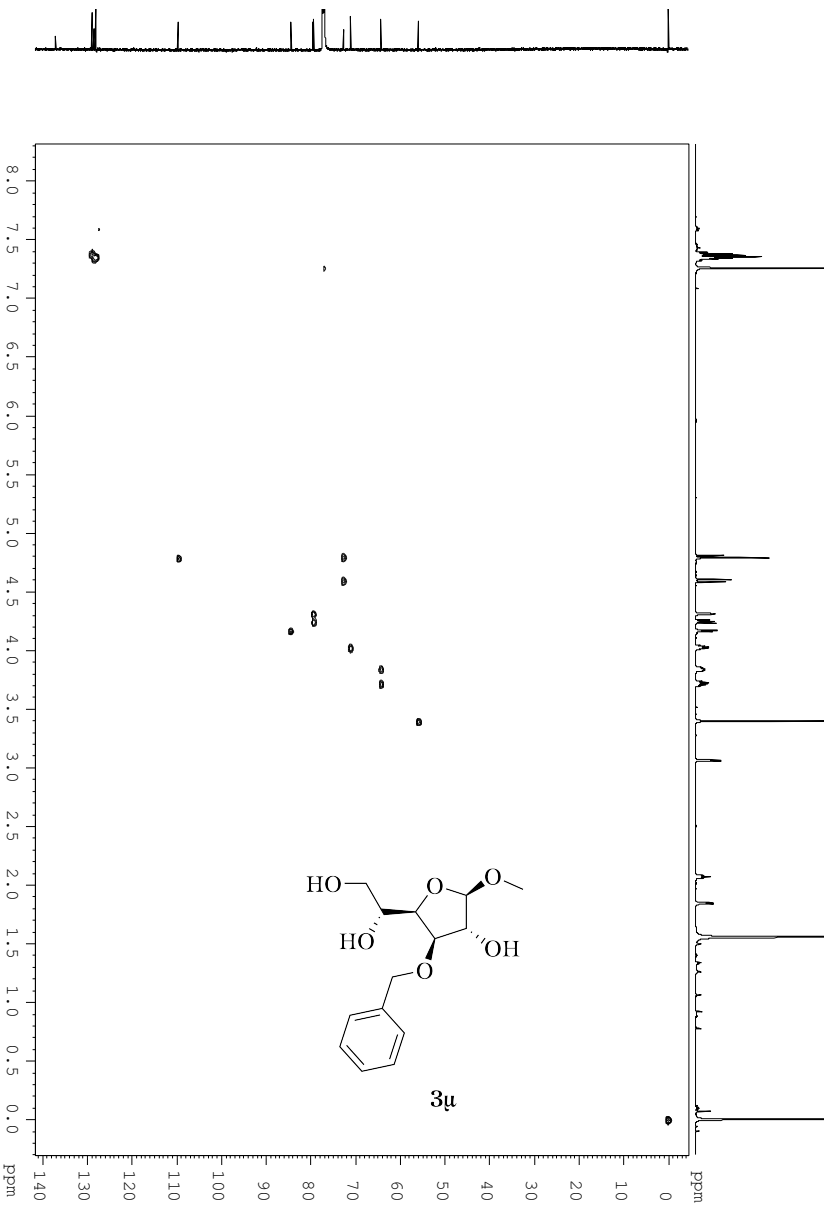

Figure 161: HSQC spectrum of **3μ-β**.

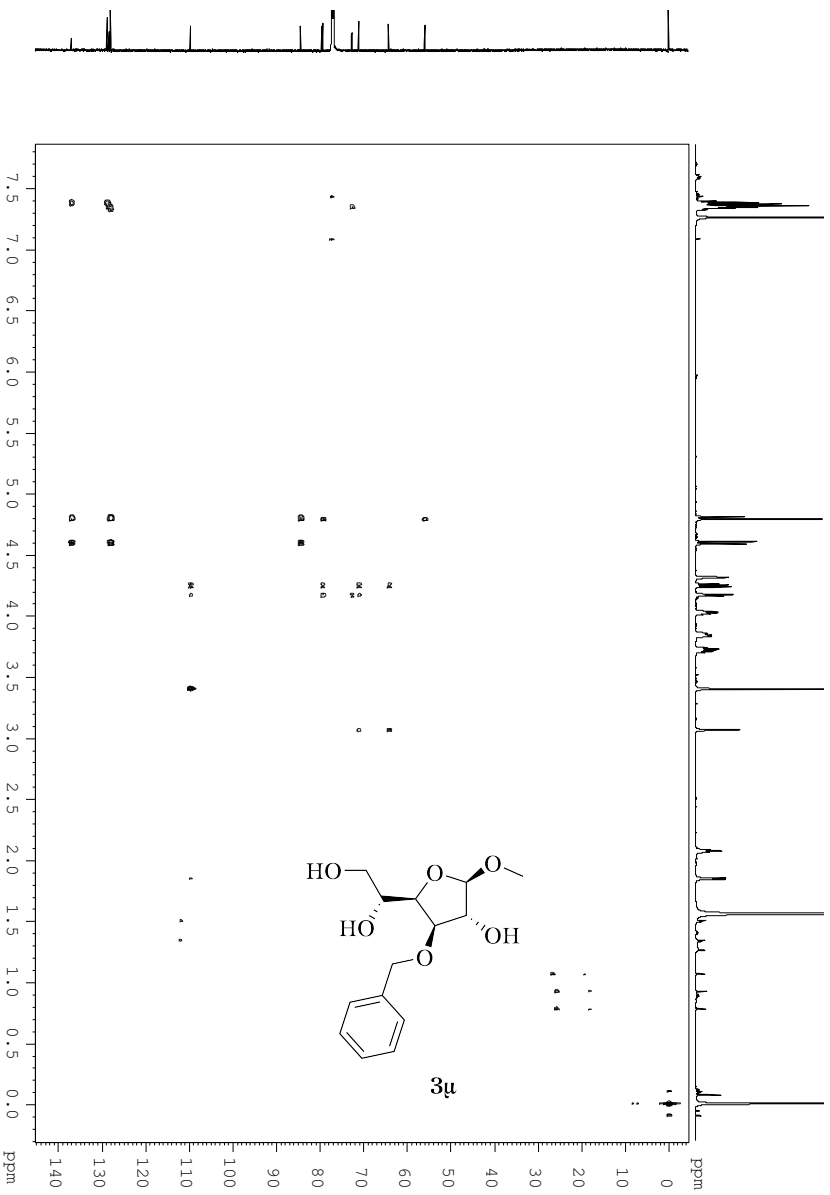

Figure 162: HMBC spectrum of **3μ-β**.

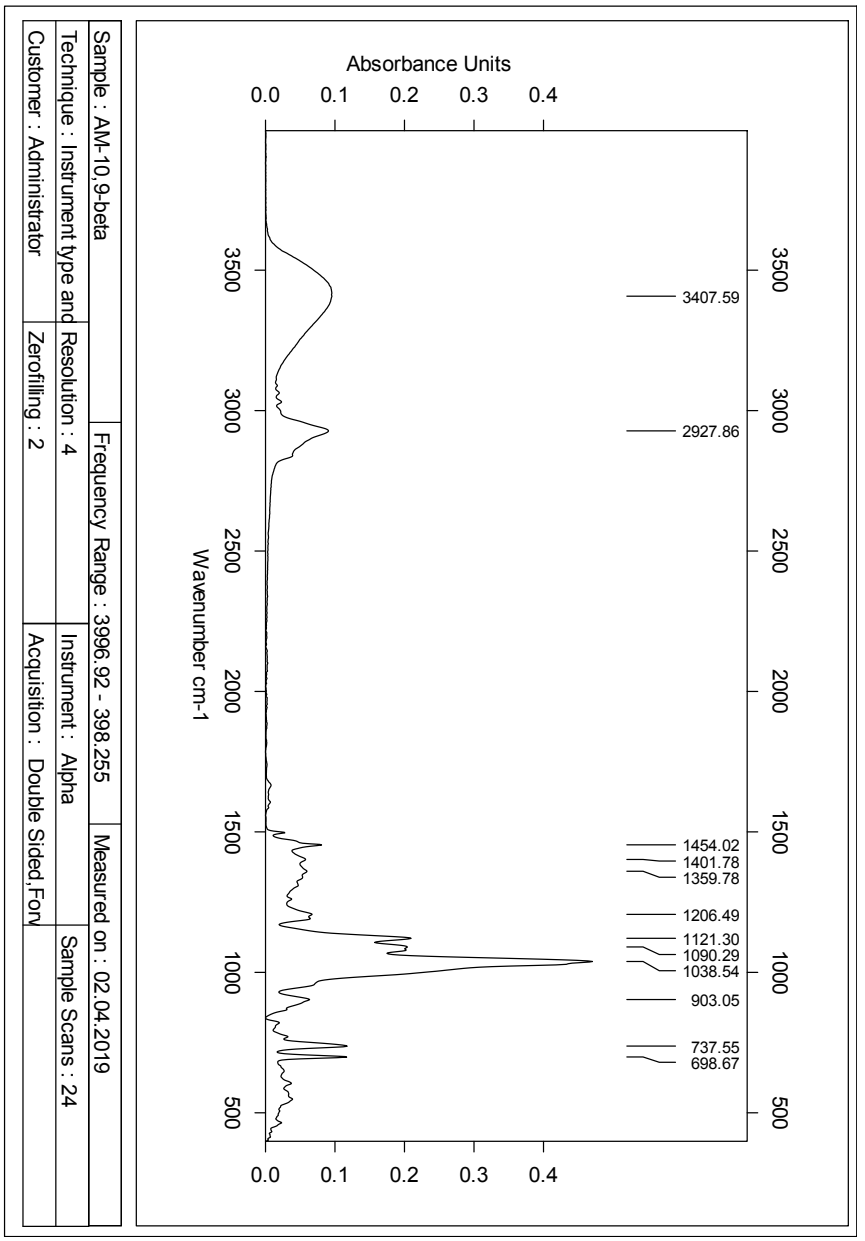

Figure 163: IR spectrum of **3μ-β**.

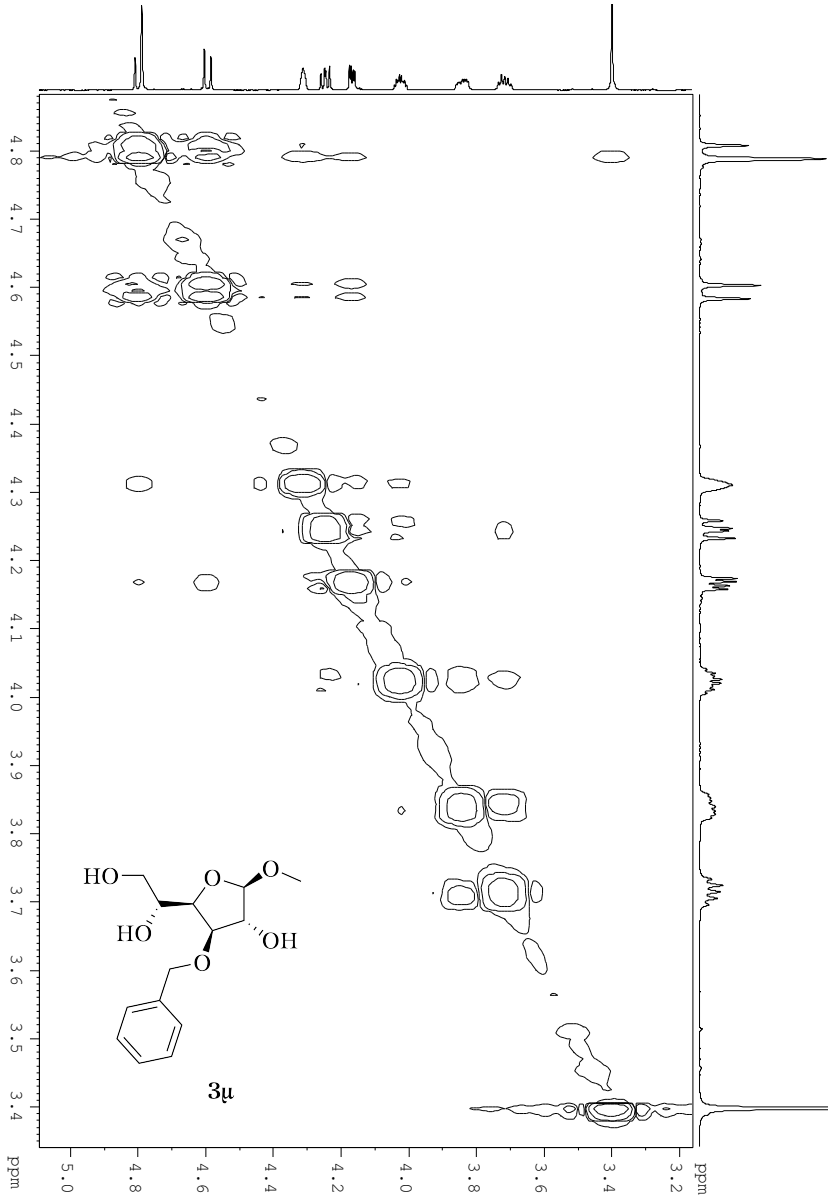

Figure 164: NOESY spectrum of **3μ-β**.

B.20 Spectroscopic data for compound 3ð

Elemental Composition Report **Page 1**

Single Mass Analysis
Tolerance = 2.0 PPM / DBE: min = -2.0, max = 50.0
Element prediction: Off
Number of isotope peaks used for i-FIT = 3

Monoisotopic Mass, Even Electron Ions
834 formula(e) evaluated with 2 results within limits (all results (up to 1000) for each mass)
Elements Used:
C: 0-100 H: 0-150 N: 0-10 O: 0-10 Na: 0-1

2019-115 207 (1.929) AM2 (Ar,35000.0,0.00,0.00); Cm (204:228)
1: TOF MS ES+

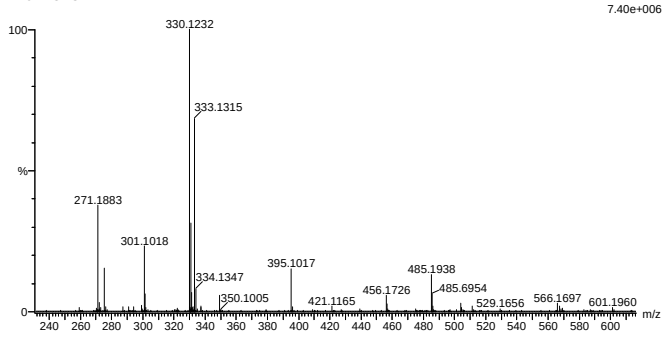

Minimum:				-2.0				
Maximum:		5.0	2.0	50.0				
Mass	Calc. Mass	mDa	PPM	DBE	i-FIT	Norm	Conf(%)	Formula
333.1315	333.1314	0.1	0.3	5.5	1438.2	0.106	89.98	C16 H22 O6 Na
	333.1311	0.4	1.2	9.5	1440.4	2.301	10.02	C14 H17 N6 O4

Figure 165: HRMS (ESI+) of **3ð**.

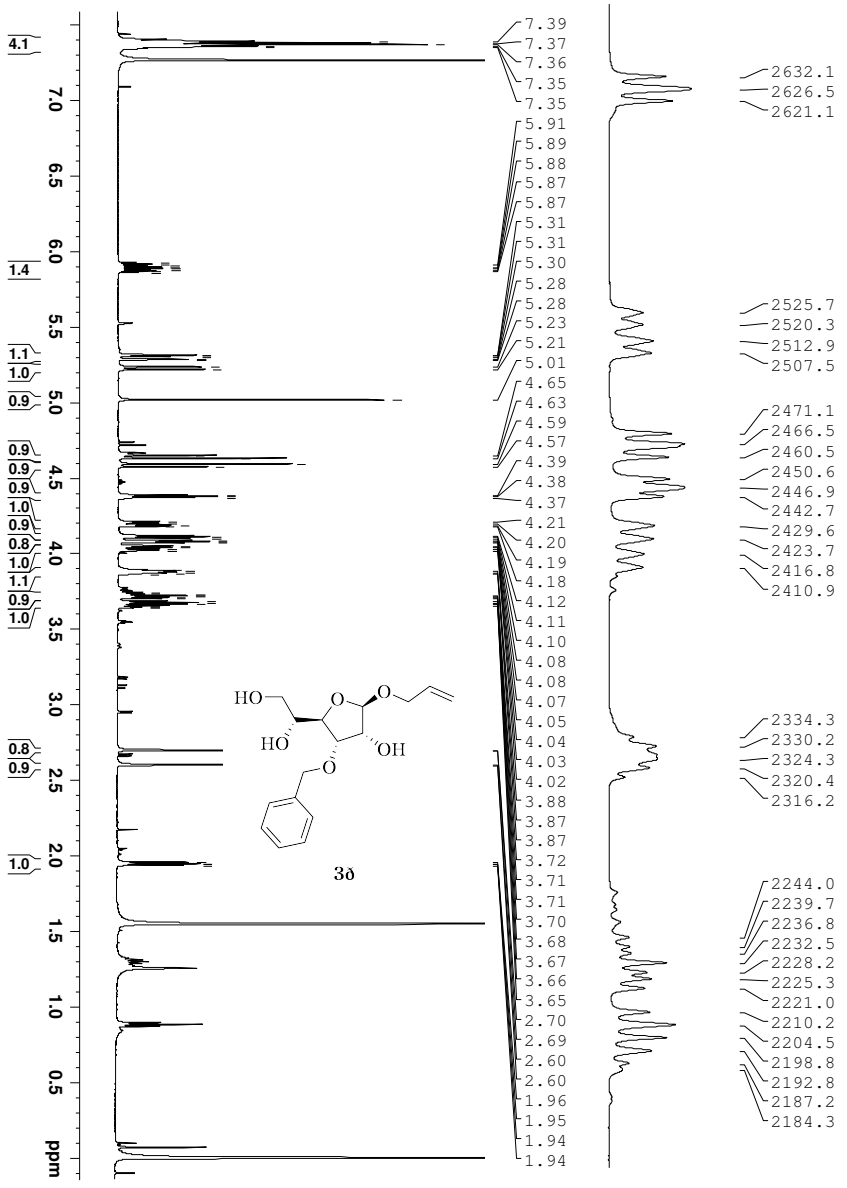

Figure 166: ^{1}H NMR spectrum of **3ð**.

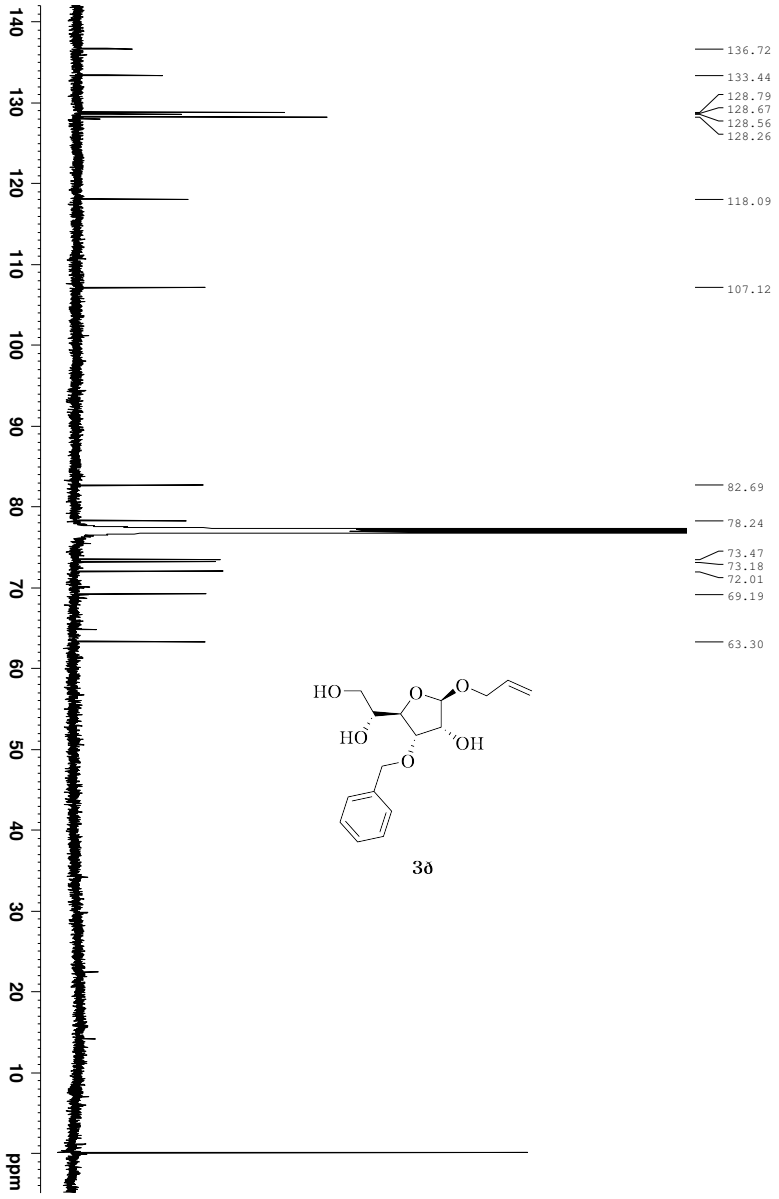

Figure 167: ^{13}C NMR spectrum of **3ð**.

cl

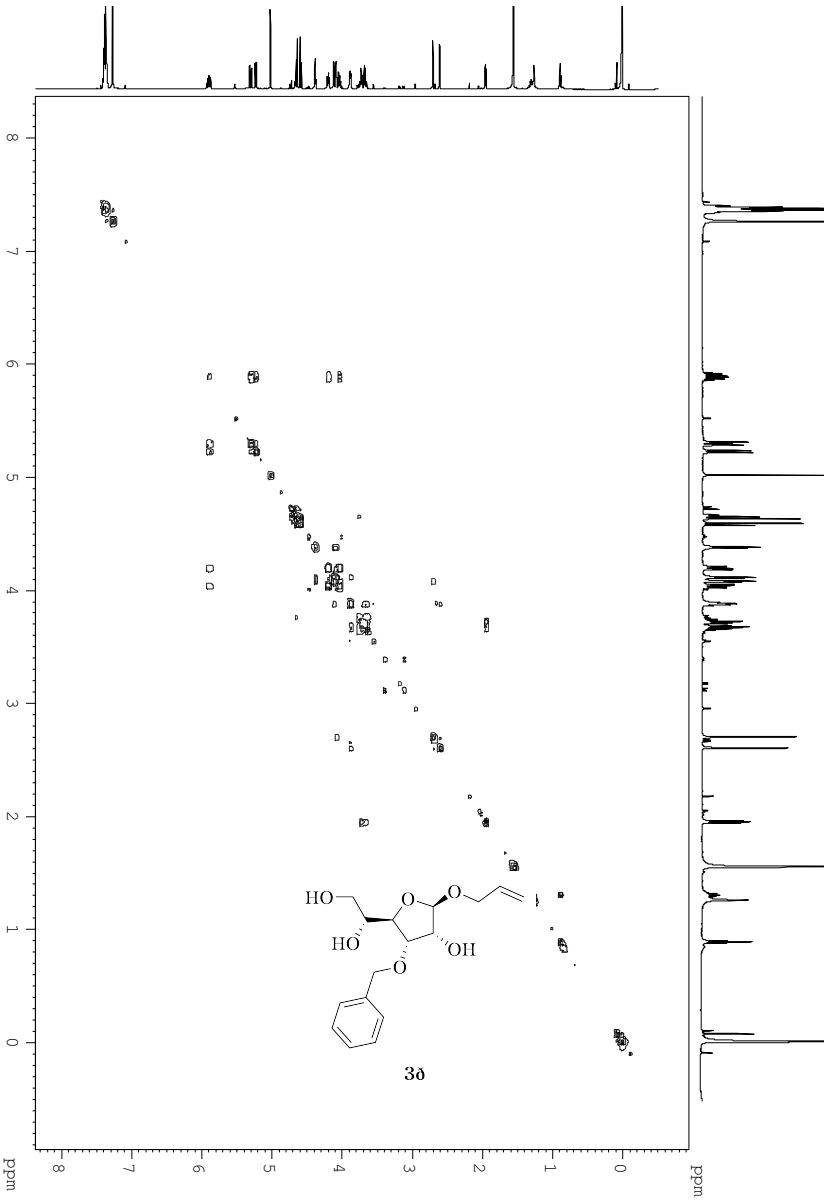

Figure 168: COSY spectrum of **3ð**.

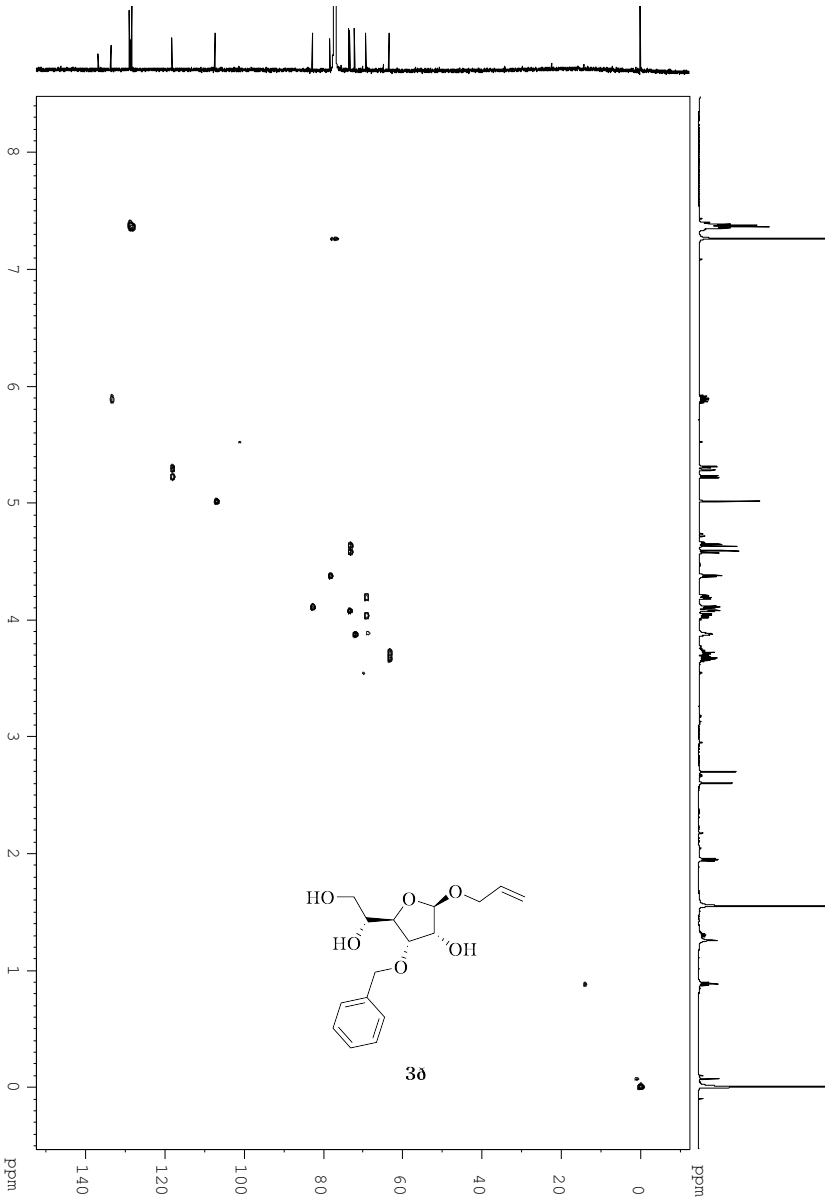

Figure 169: HSQC spectrum of **3ð**.

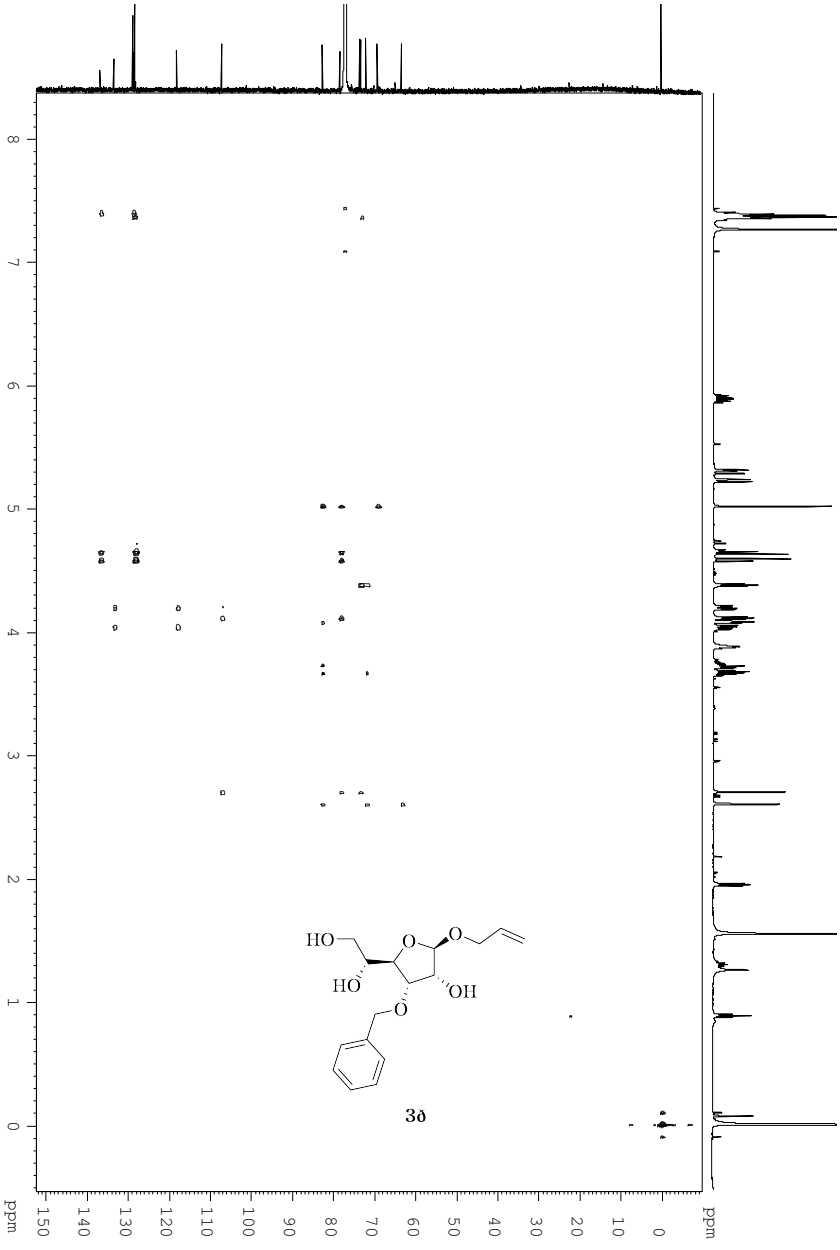

Figure 170: HMBC spectrum of **3ð**.

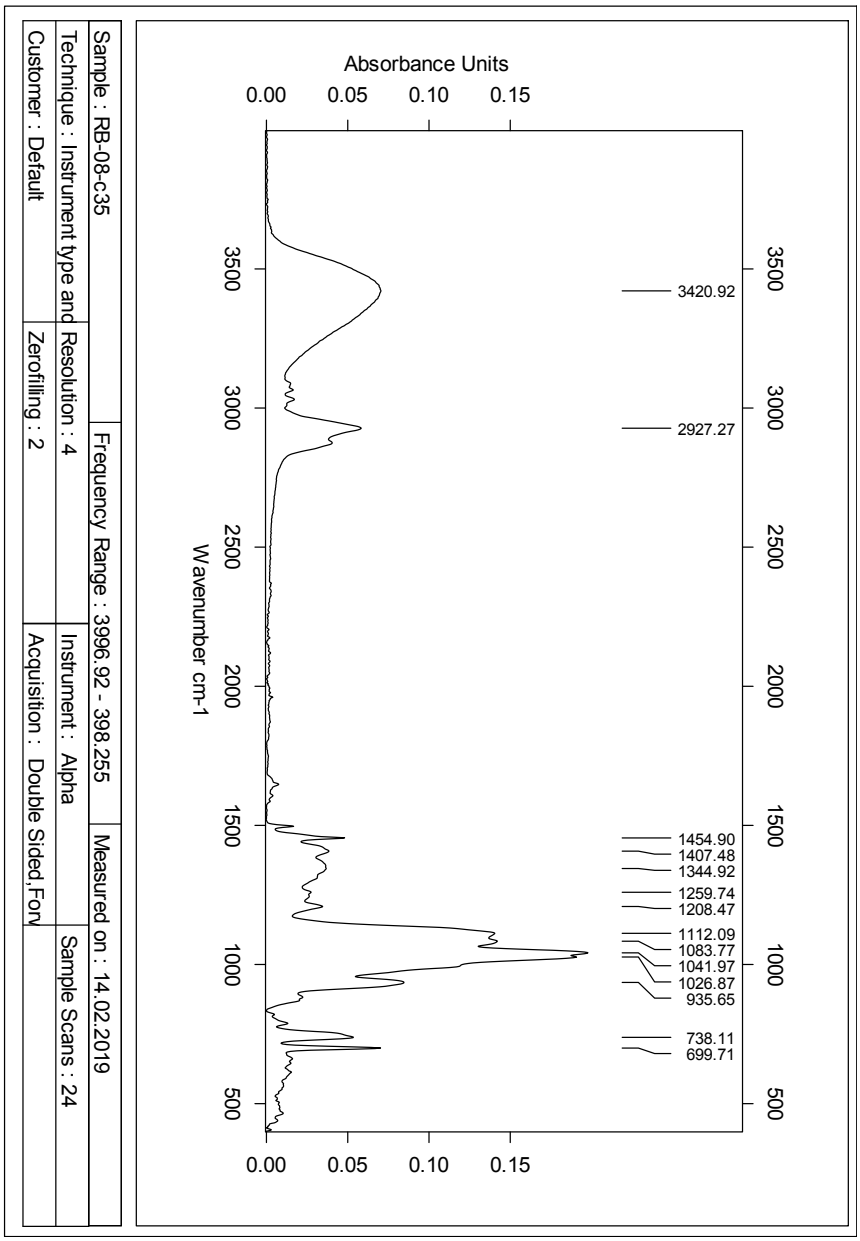

Figure 171: IR spectrum of **3ð**.

B.21 Spectroscopic data for compound IC-1

Elemental Composition Report **Page 1**

Single Mass Analysis
Tolerance = 2.0 PPM / DBE: min = -2.0, max = 50.0
Element prediction: Off
Number of isotope peaks used for i-FIT = 3

Monoisotopic Mass, Even Electron Ions
139 formula(e) evaluated with 1 results within limits (all results (up to 1000) for each mass)
Elements Used:
C: 0-100 H: 0-150 O: 0-10 Si: 0-2

2019-30 82 (1.621) AM2 (Ar,35000.0,0.00,0.00); Cm (82:93)
1: TOF MS ASAP+

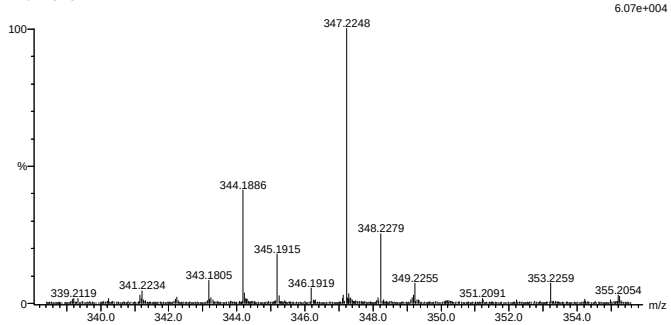

Mass	Calc. Mass	mDa	PPM	DBE	i-FIT	Norm	Conf(%)	Formula
Minimum:				-2.0				
Maximum:		5.0	2.0	50.0				
347.2248	347.2254	-0.6	-1.7	1.5	953.1	n/a	n/a	C17 H35 O5 Si

Figure 172: HRMS (ASAP+) [M+H] of **IC-1**.

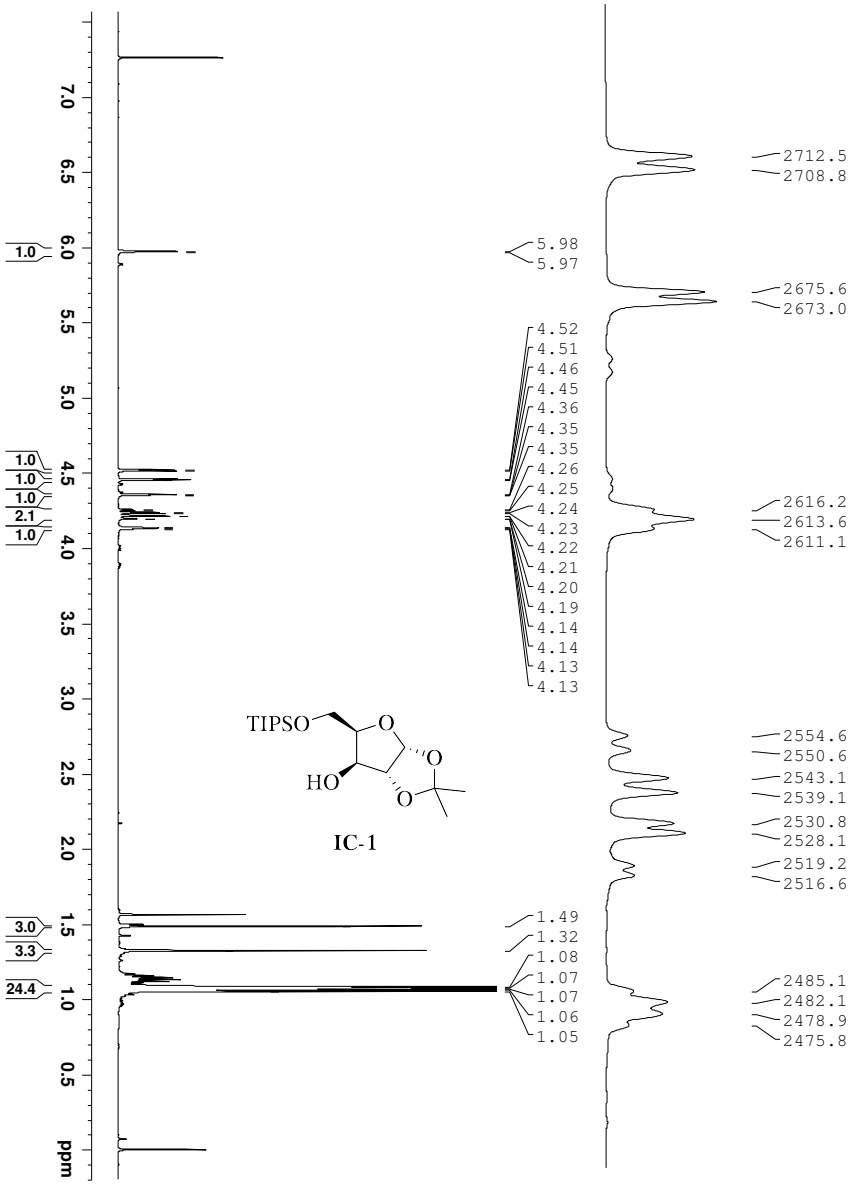

Figure 173: ^{1}H NMR spectrum of **IC-1**.

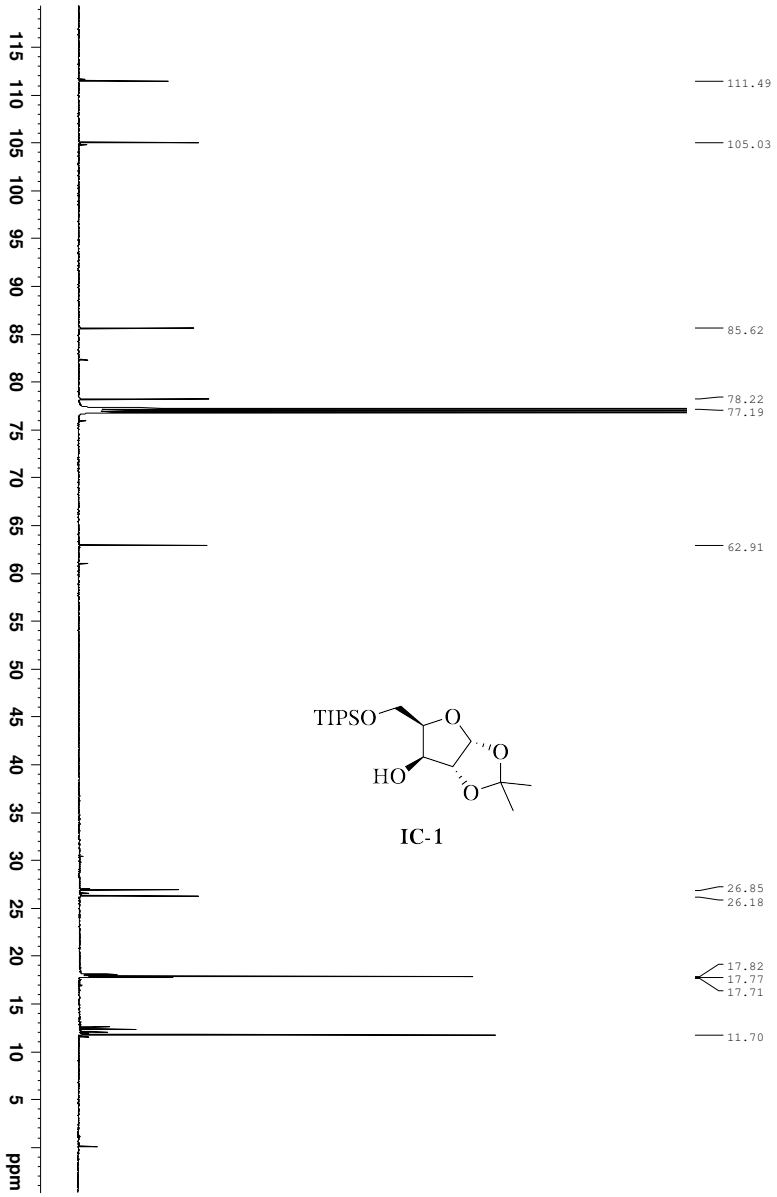

Figure 174: ^{13}C NMR spectrum of **IC-1**.

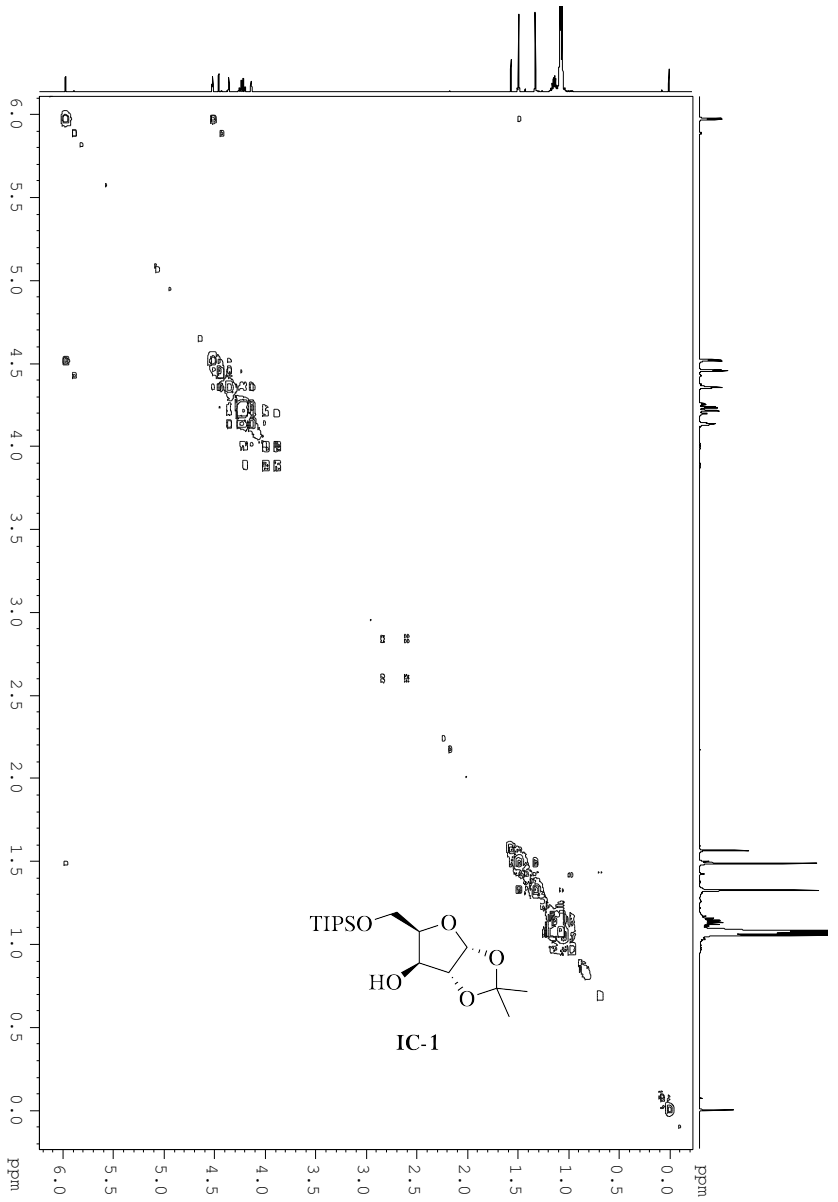

Figure 175: COSY spectrum of **IC-1**.

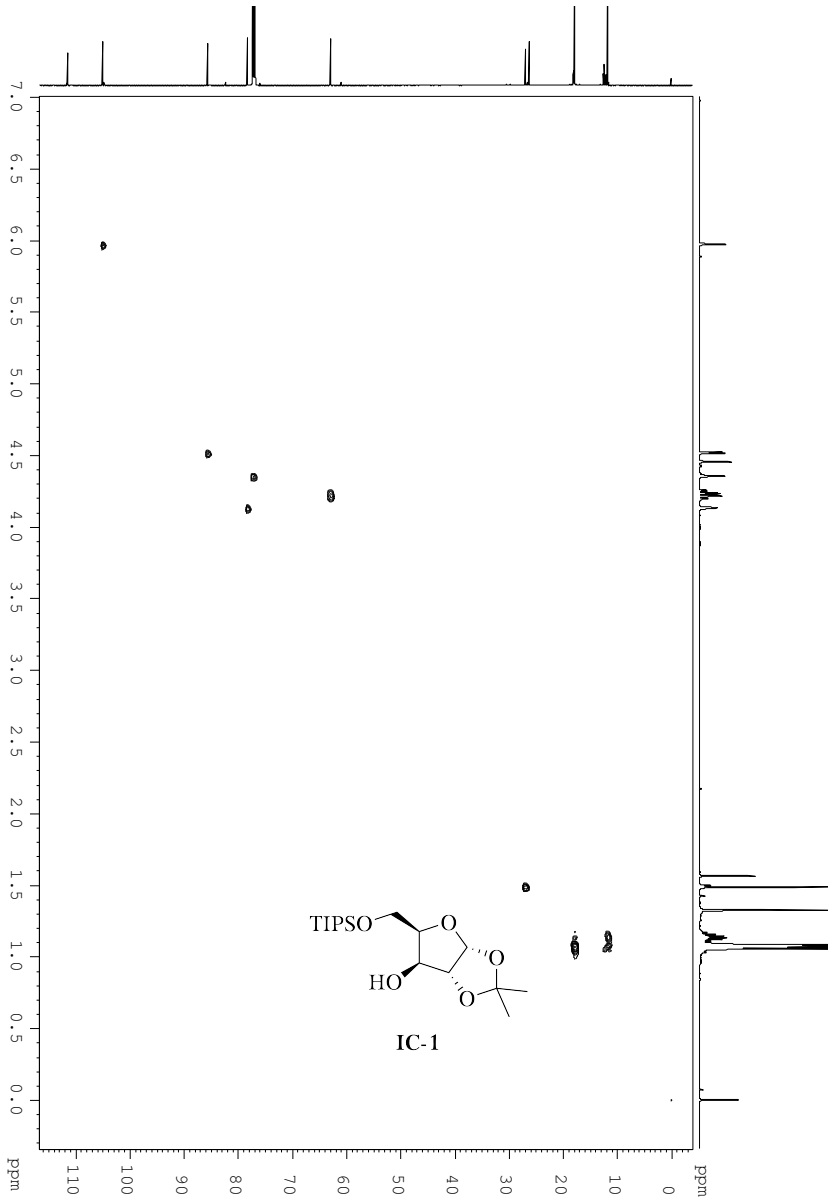

Figure 176: HSQC spectrum of **IC-1**.

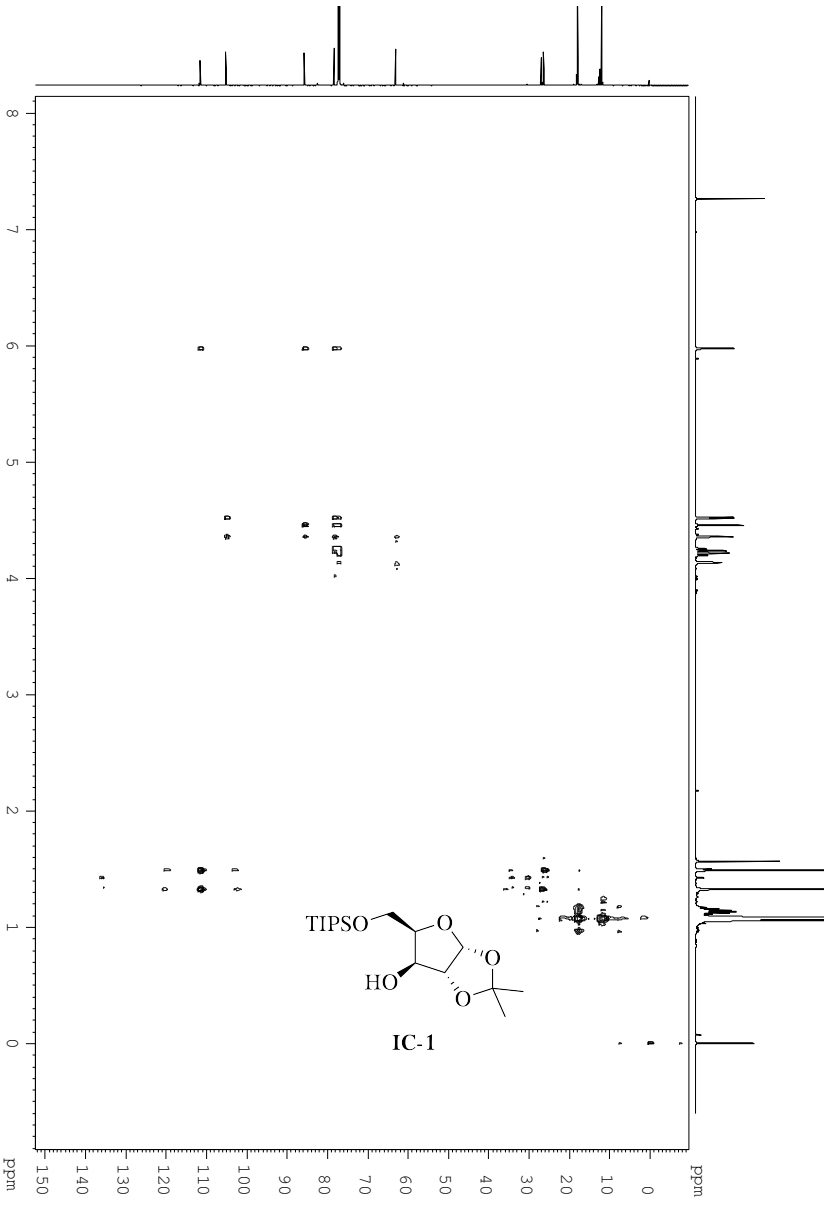

Figure 177: HMBC spectrum of **IC-1**.

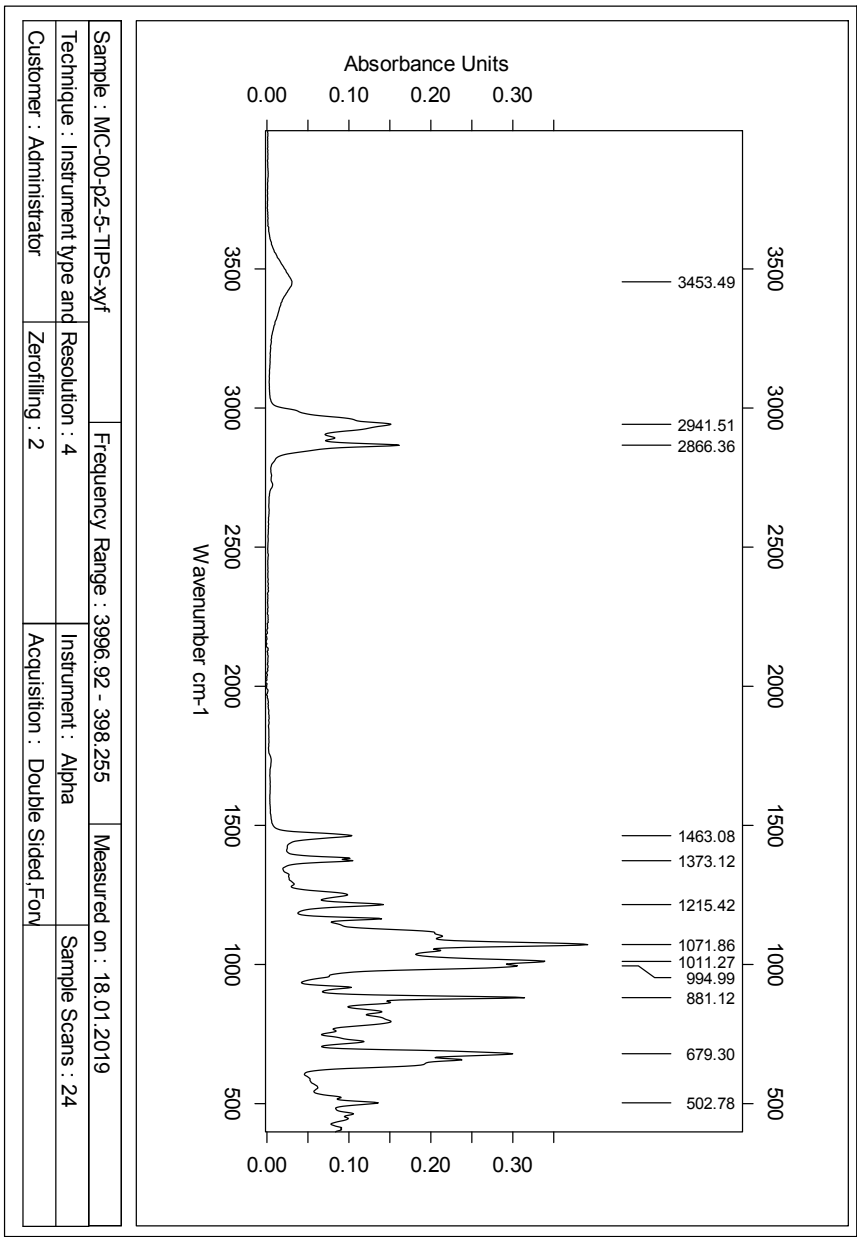

Figure 178: IR spectrum of **IC-1**.

B.22 Spectroscopic data for compound IC-2

Elemental Composition Report **Page 1**

Single Mass Analysis
Tolerance = 5.0 PPM / DBE: min = -2.0, max = 50.0
Element prediction: Off
Number of isotope peaks used for i-FIT = 3

Monoisotopic Mass, Even Electron Ions
561 formula(e) evaluated with 4 results within limits (all results (up to 1000) for each mass)
Elements Used:
C: 0-100 H: 0-150 O: 0-10 Si: 0-2 Au: 0-2 Na: 0-1

2019-40 9 (0.105) AM2 (Ar,35000.0,0.00,0.00)
1: TOF MS ES+

1.55e+006

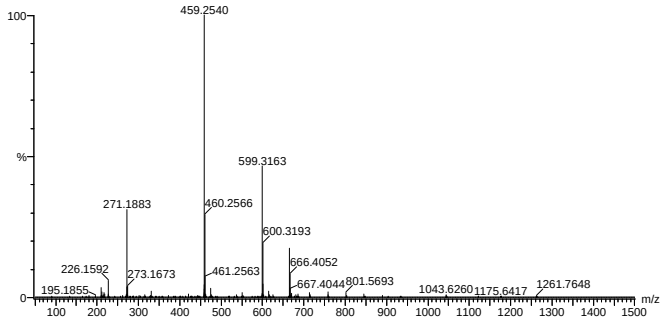

Minimum:				-2.0				
Maximum:		5.0	5.0	50.0				
Mass	Calc. Mass	mDa	PPM	DBE	i-FIT	Norm	Conf(%)	Formula
459.2540	459.2539	0.1	0.2	12.5	1165.8	6.532	0.15	C29 H39 O Si2
	459.2537	0.3	0.7	-1.5	1171.4	12.160	0.00	C16 H38 O2 Au
	459.2543	-0.3	-0.7	5.5	1159.2	0.002	99.77	C24 H40 O5 Si Na
	459.2535	0.5	1.1	13.5	1166.3	7.121	0.08	C30 H35 O4

Figure 179: HRMS (ESI+) of **IC-2**.

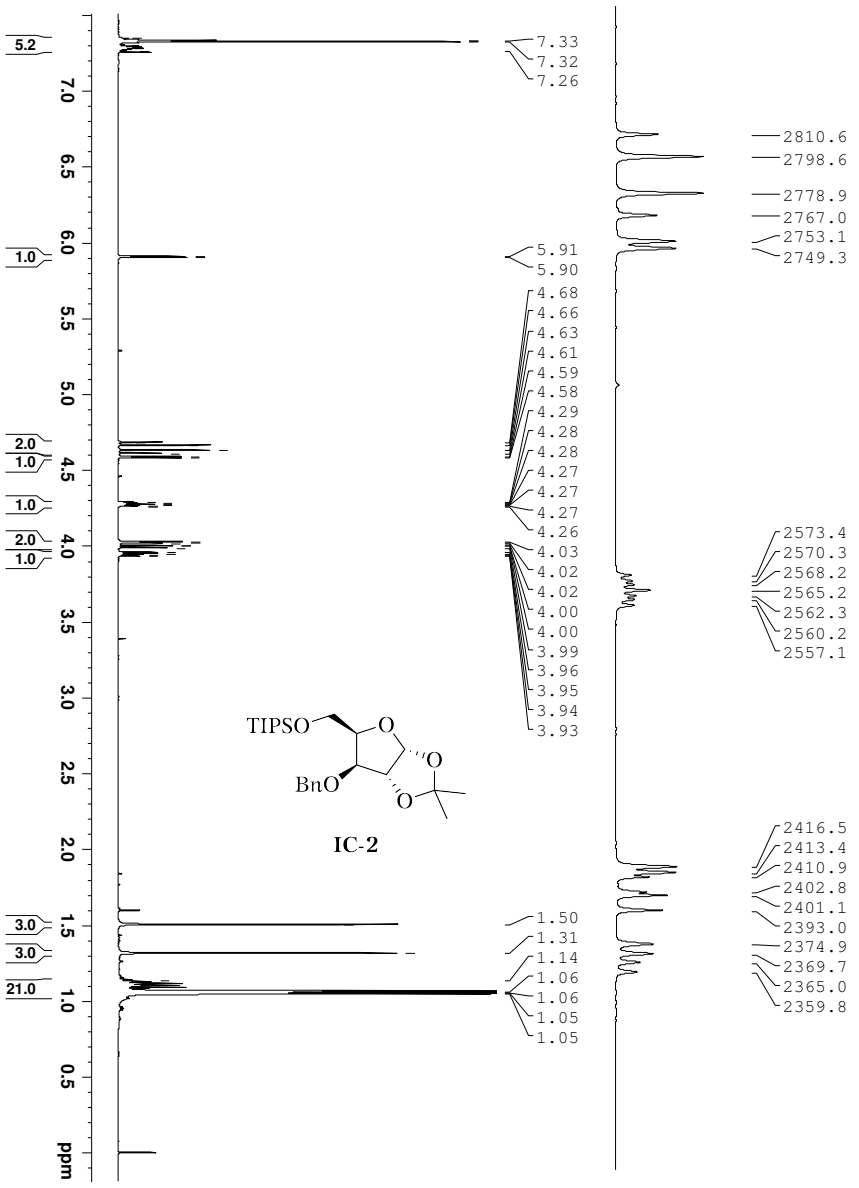

IC-2

Figure 180: ^{1}H NMR spectrum of **IC-2**.

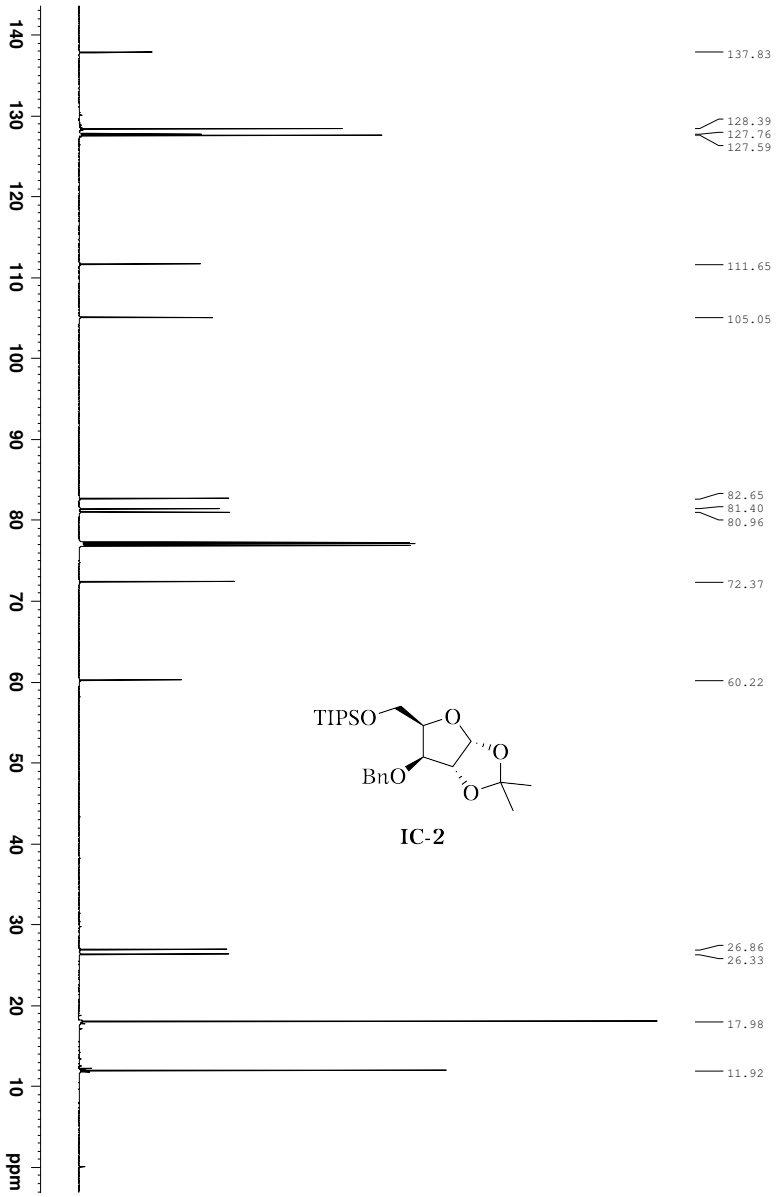

IC-2

Figure 181: ^{13}C NMR spectrum of **IC-2**.

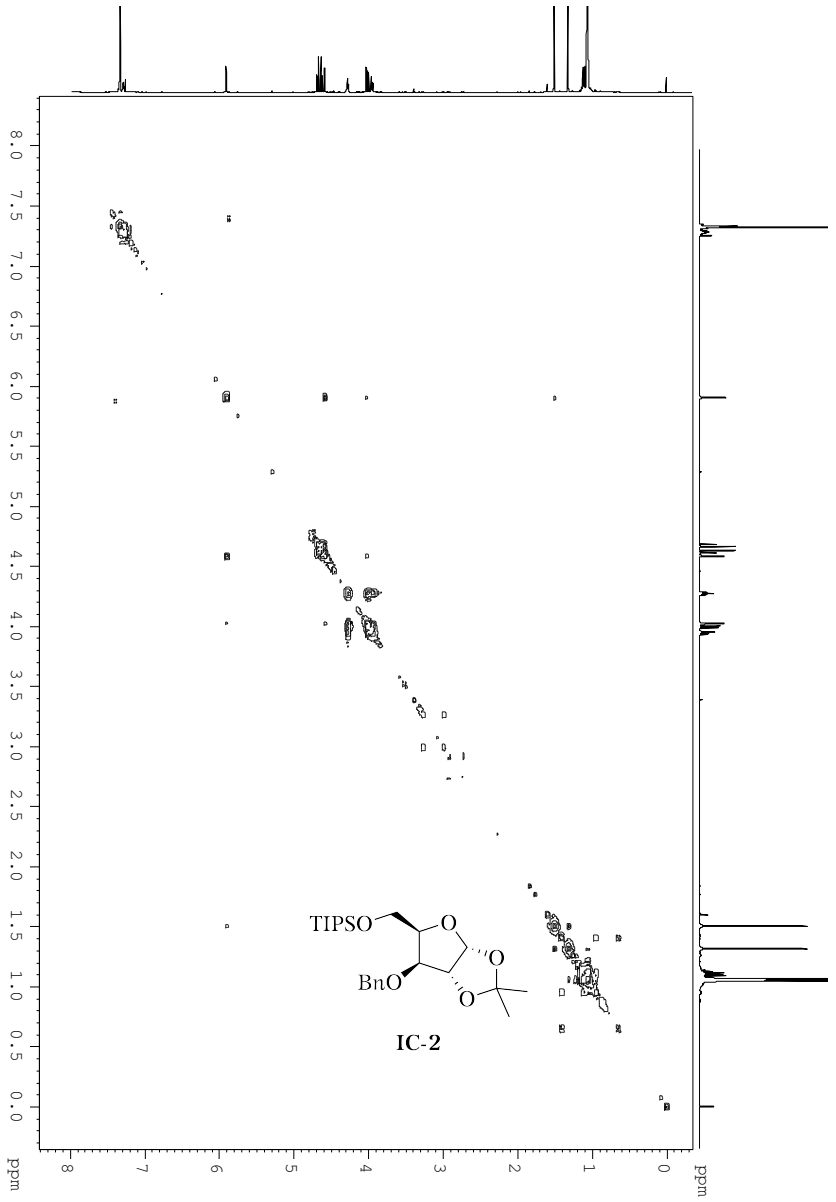

Figure 182: COSY spectrum of **IC-2**.

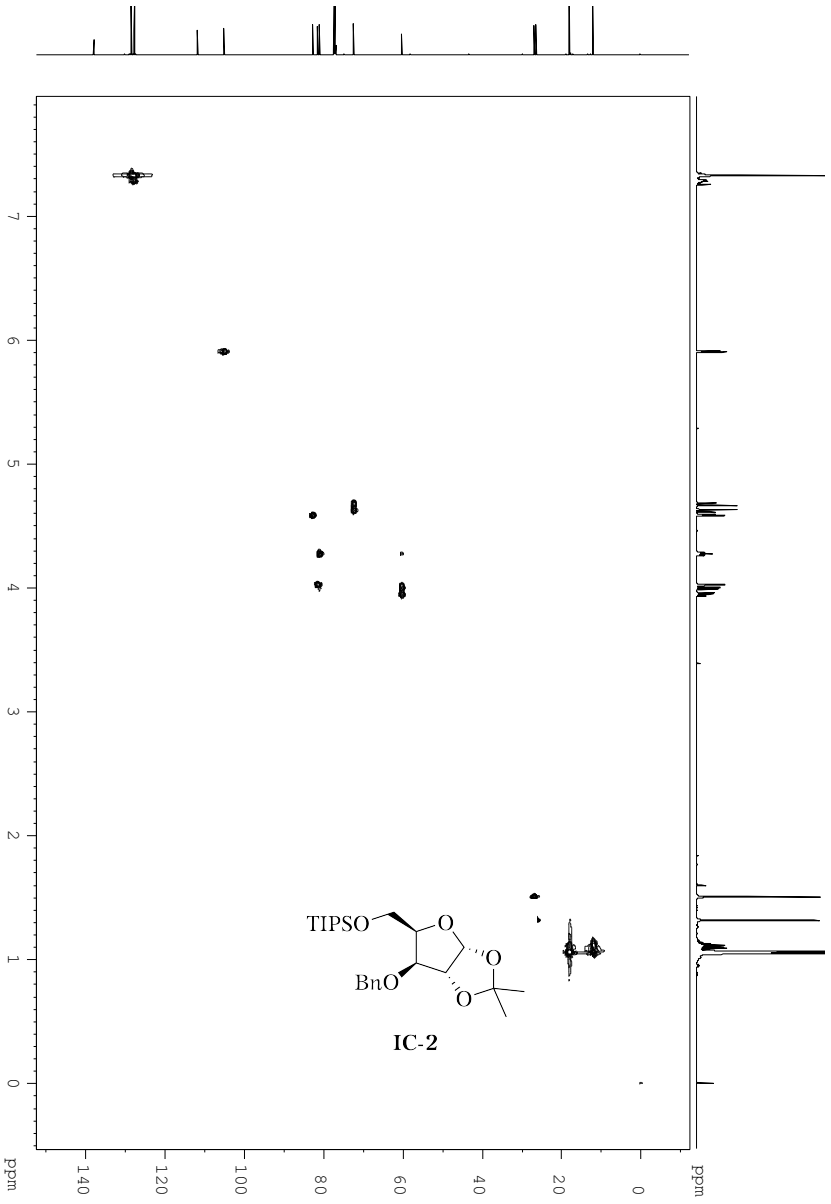

Figure 183: HSQC spectrum of **IC-2**.

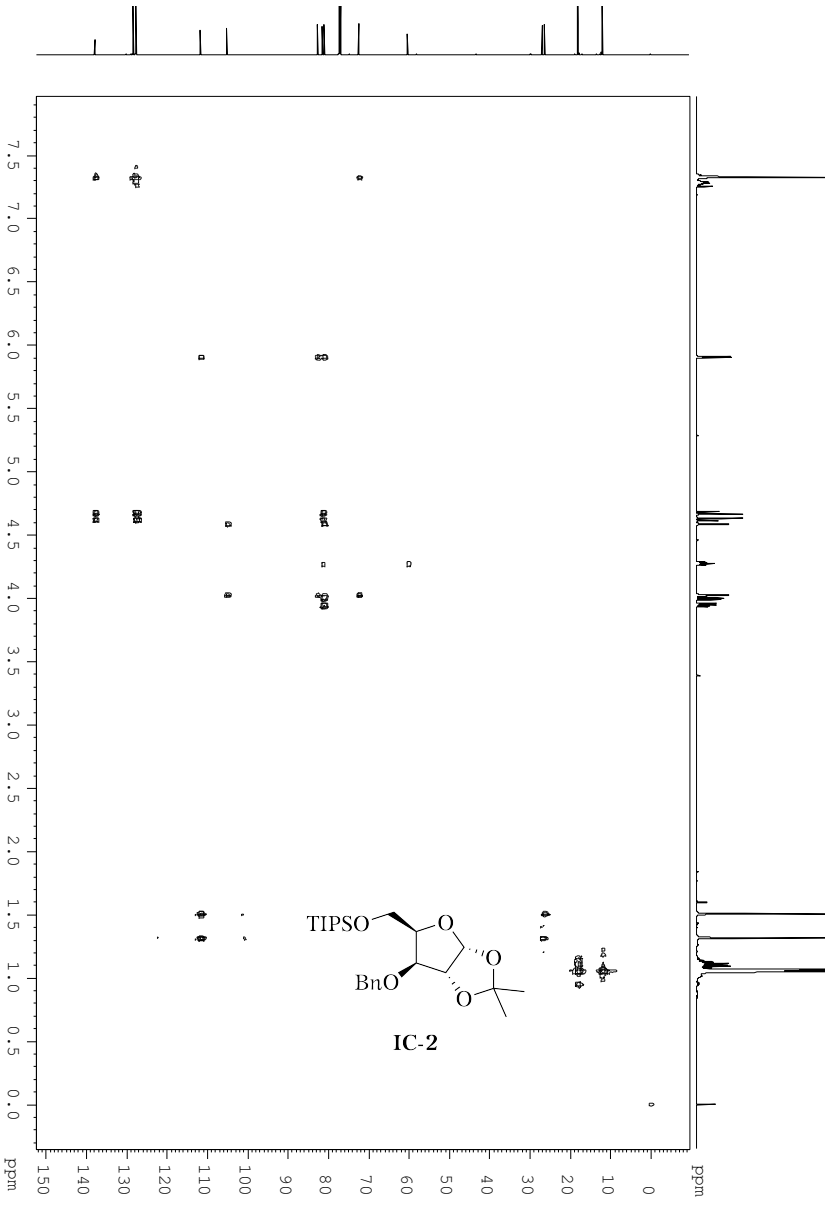

Figure 184: HMBC spectrum of **IC-2**.

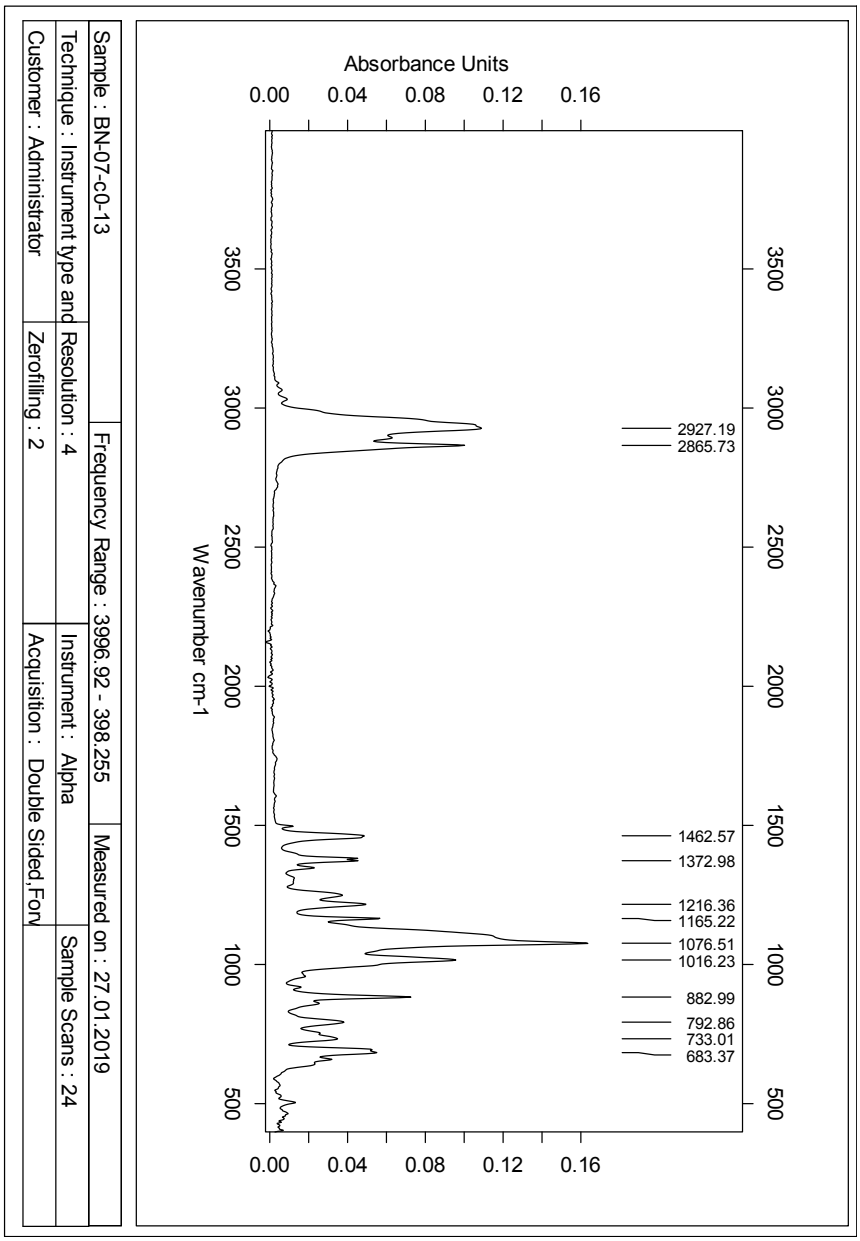

Figure 185: IR spectrum of **IC-2**.

B.23 Spectroscopic data for compound MC-1

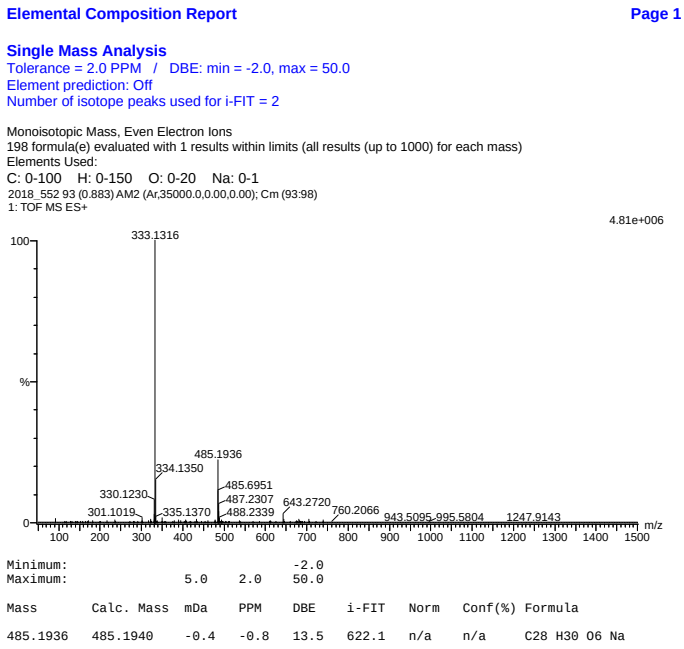

Figure 186: HRMS (ESI+) of **MC-1**.

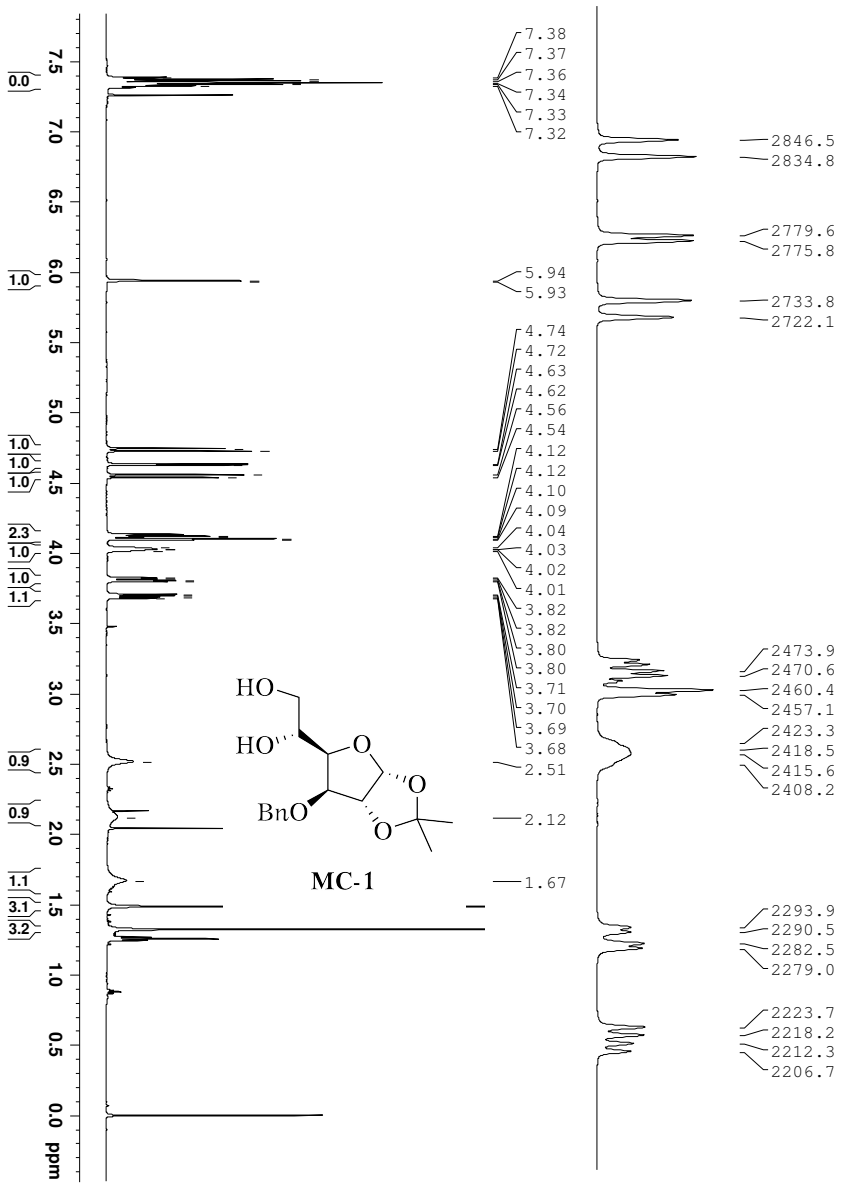

Figure 187: ^{1}H NMR spectrum of **MC-1**.

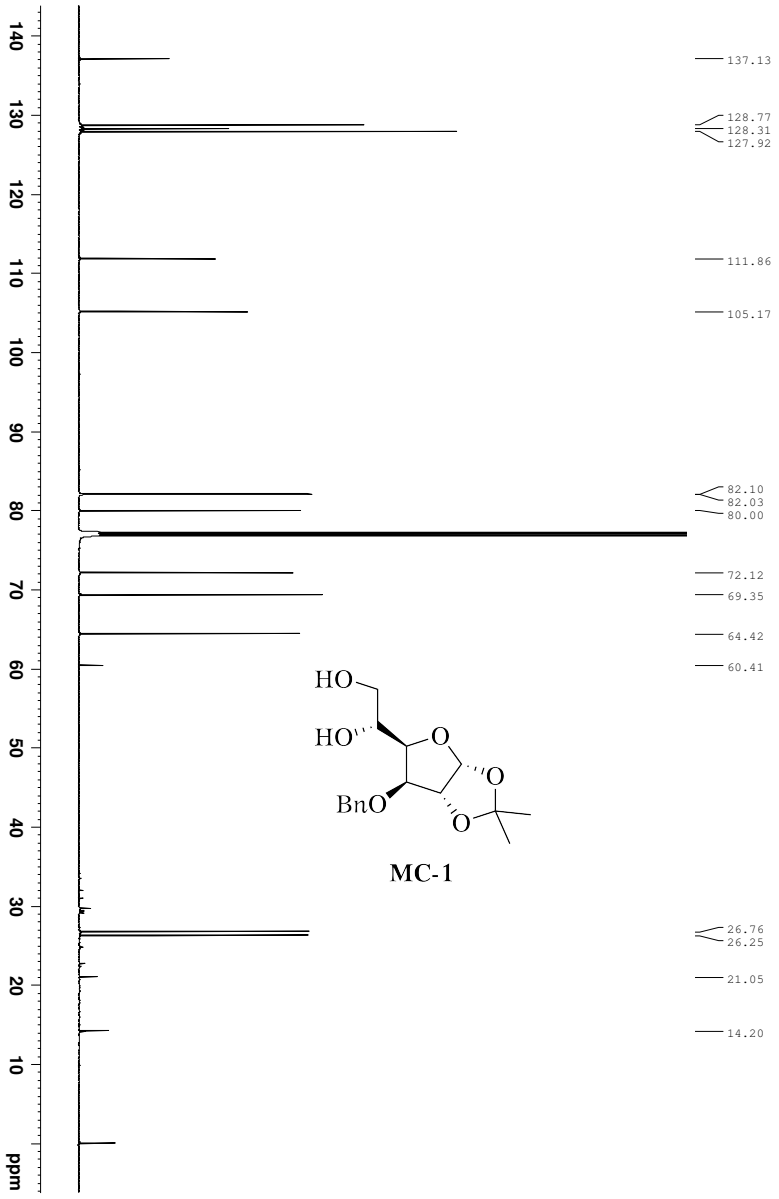

Figure 188: ^{13}C NMR spectrum of **MC-1**.

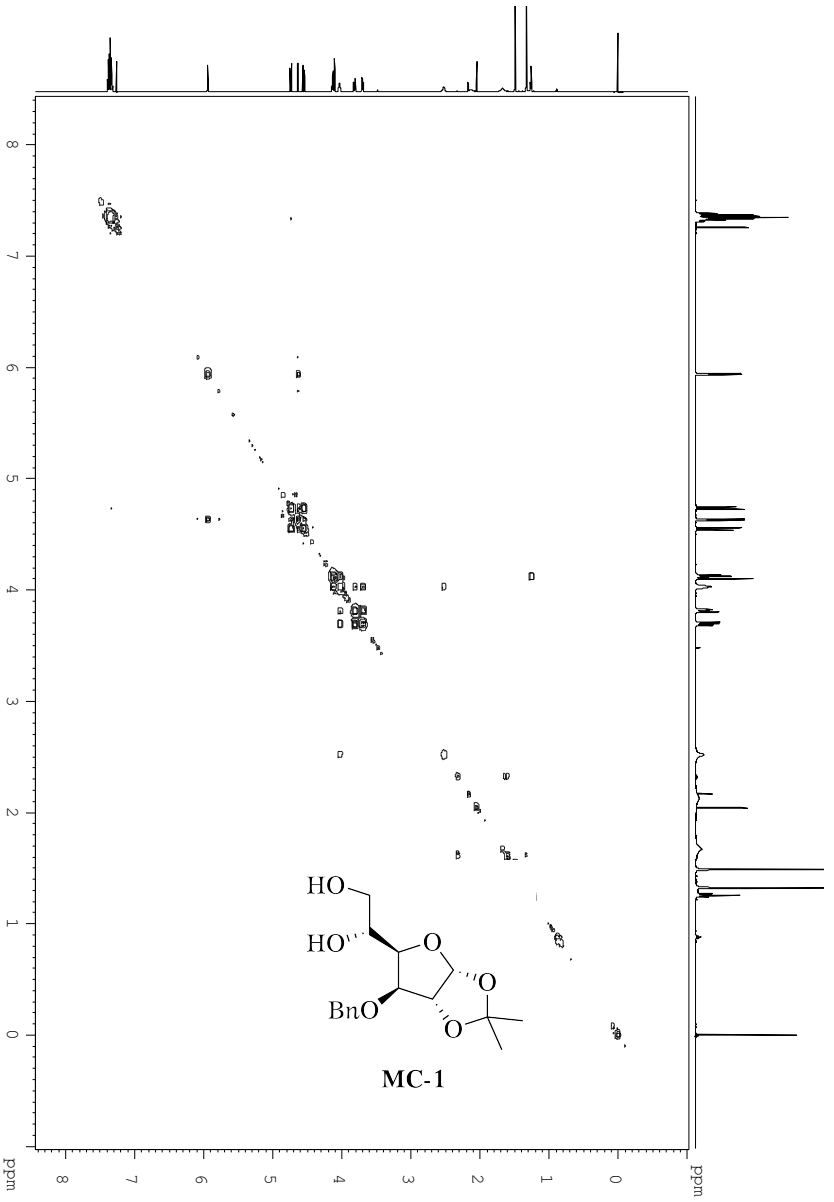

Figure 189: COSY spectrum of **MC-1**.

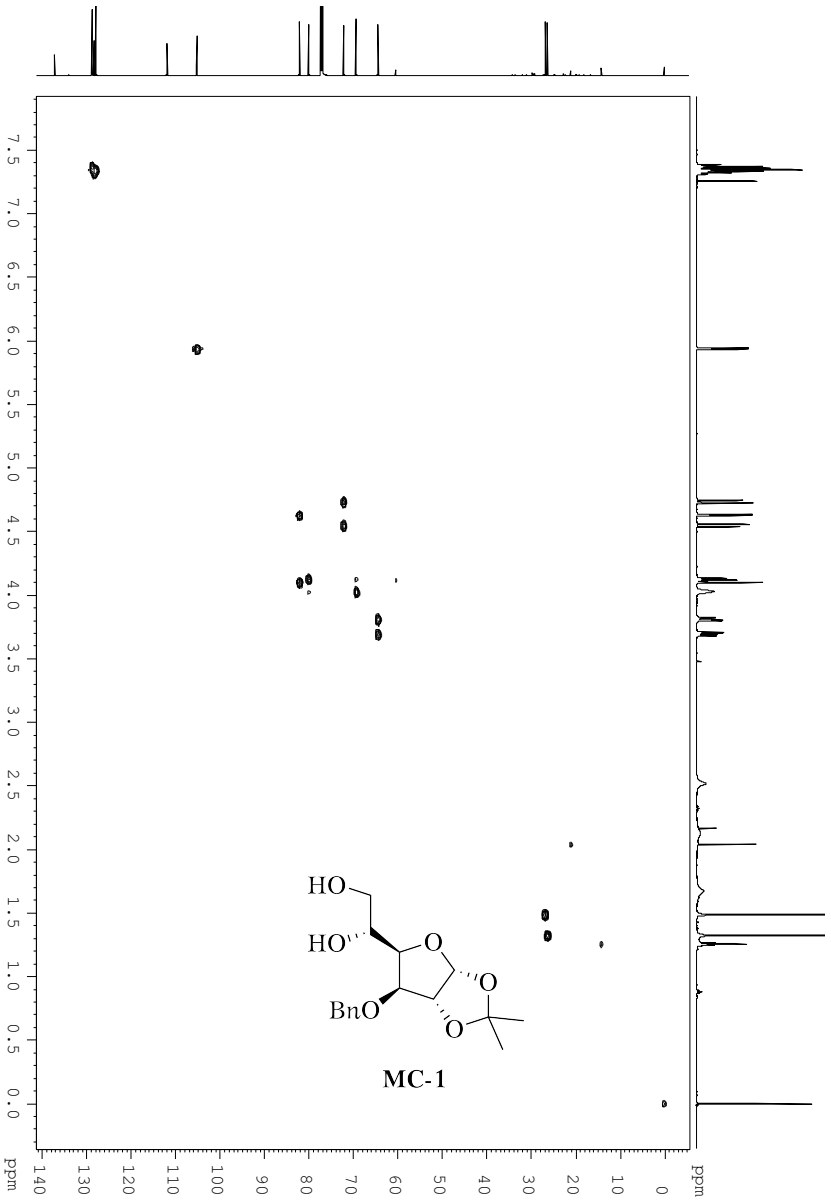

Figure 190: HSQC spectrum of **MC-1**.

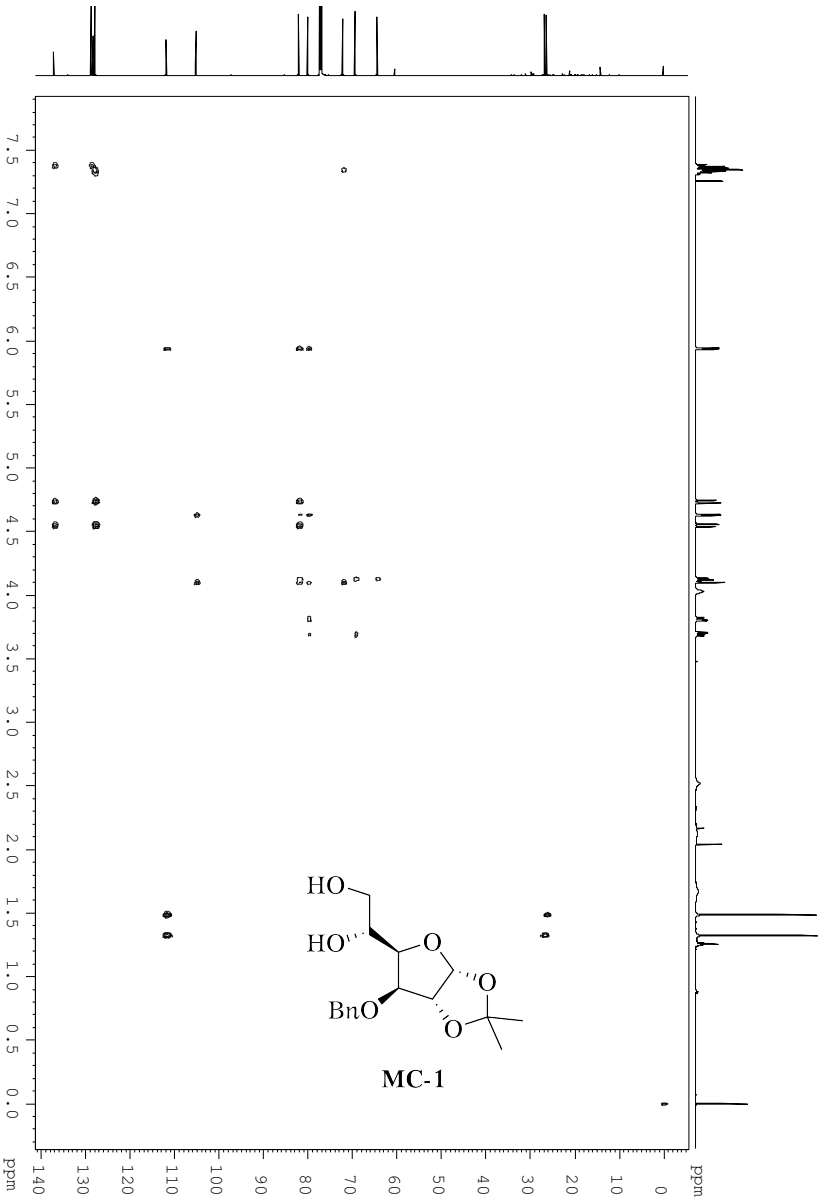

Figure 191: HMBC spectrum of **MC-1**.

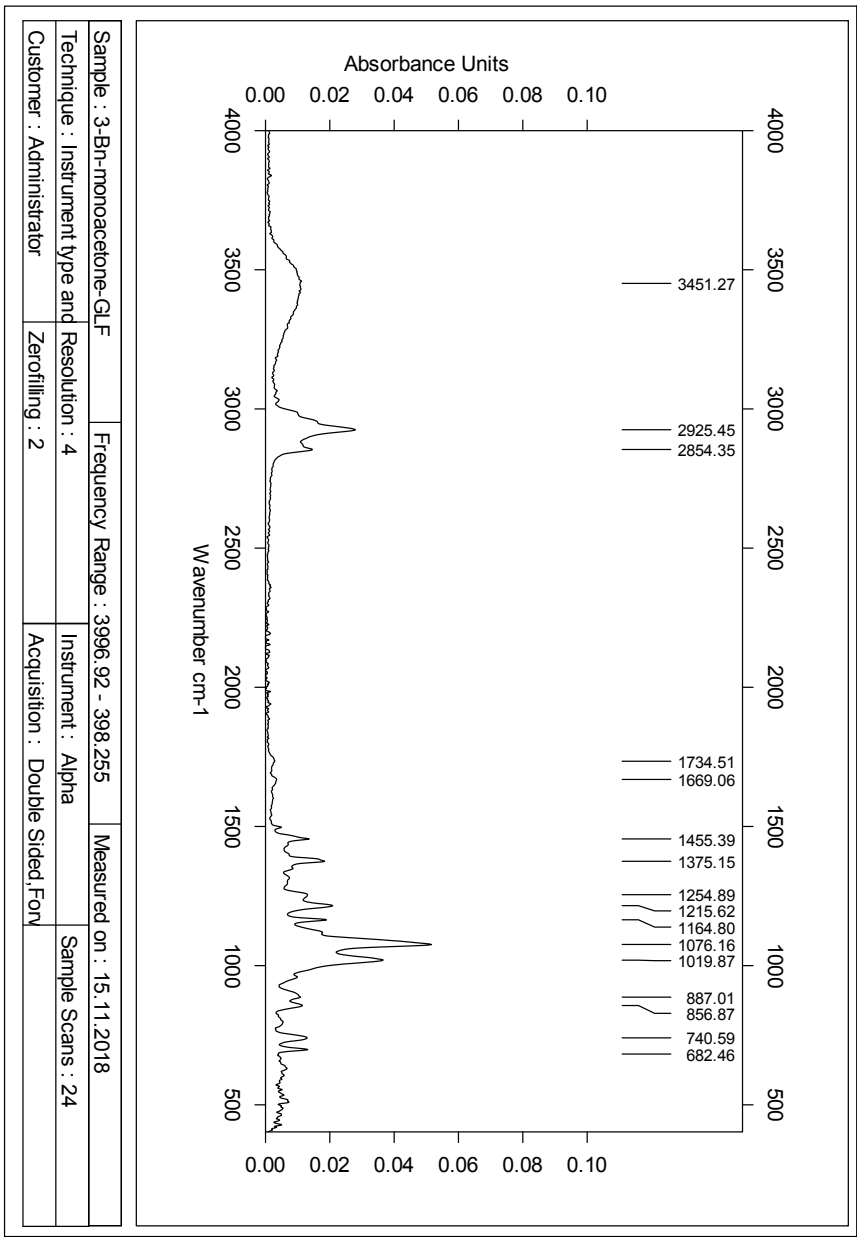

Figure 192: IR spectrum of **MC-1**.

B.24 Spectroscopic data for compound MC-2

Elemental Composition Report **Page 1**

Single Mass Analysis
Tolerance = 3.0 PPM / DBE: min = -50.0, max = 50.0
Element prediction: Off
Number of isotope peaks used for i-FIT = 3

Monoisotopic Mass, Even Electron Ions
256 formula(e) evaluated with 1 results within limits (all results (up to 1000) for each mass)
Elements Used:
C: 0-100 H: 0-150 O: 0-10 Na: 0-1
svg_20190403_2019_253 15 (0.288) AM2 (Ar,35000.0,0.00,0.00); Cm (13:15)
1: TOF MS ES+

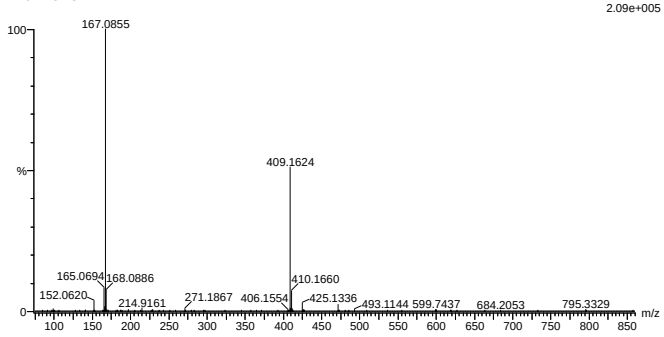

Minimum:				-50.0				
Maximum:		5.0	3.0	50.0				
Mass	Calc. Mass	mDa	PPM	DBE	i-FIT	Norm	Conf(%)	Formula
409.1624	409.1627	-0.3	-0.7	9.5	616.4	n/a	n/a	C22 H26 O6 Na

Figure 193: HRMS (ESI+) of **MC-2**.

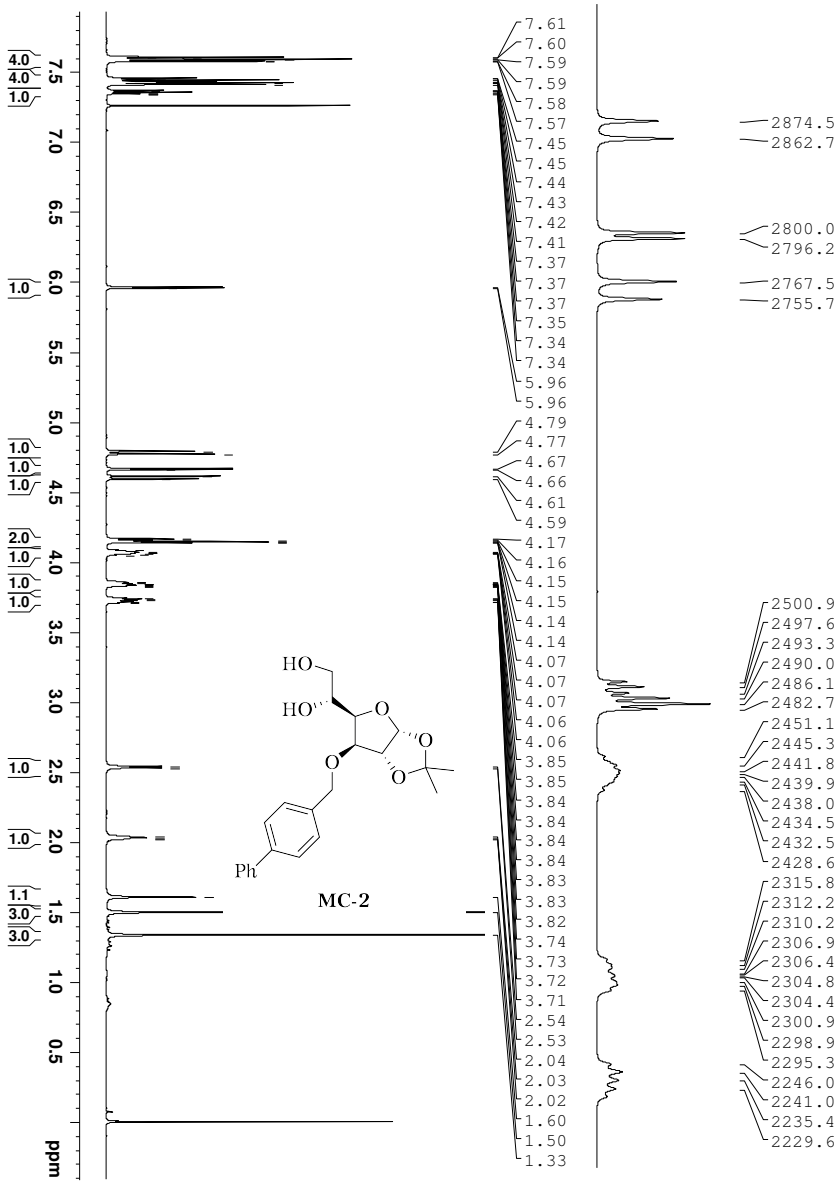

Figure 194: ^{1}H NMR spectrum of **MC-2**.

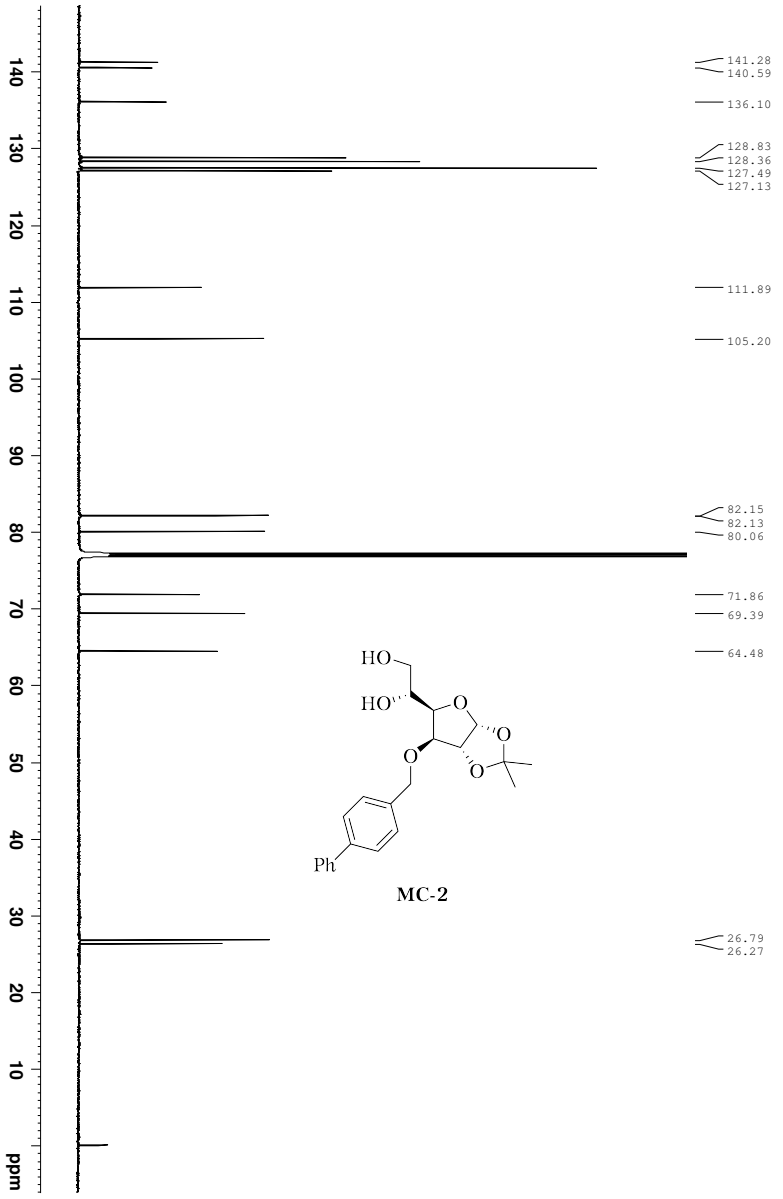

Figure 195: ^{13}C NMR spectrum of **MC-2**.

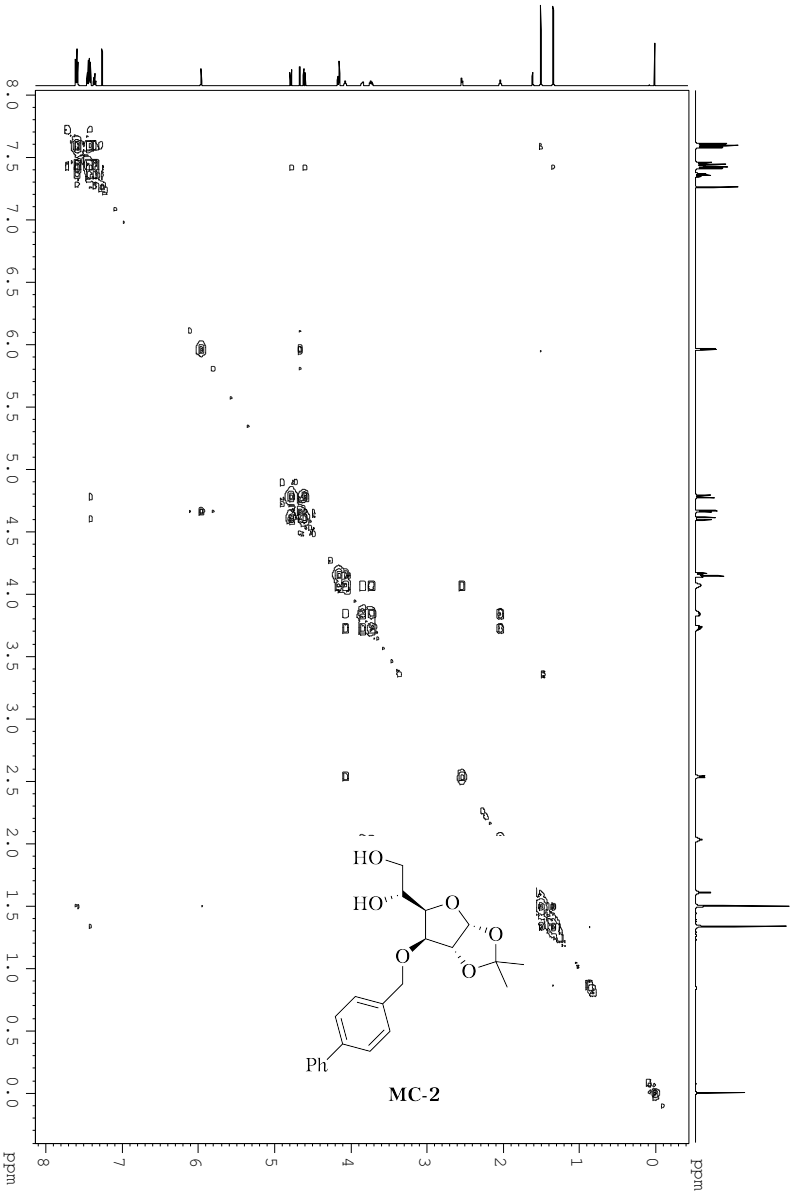

Figure 196: COSY spectrum of **MC-2**.

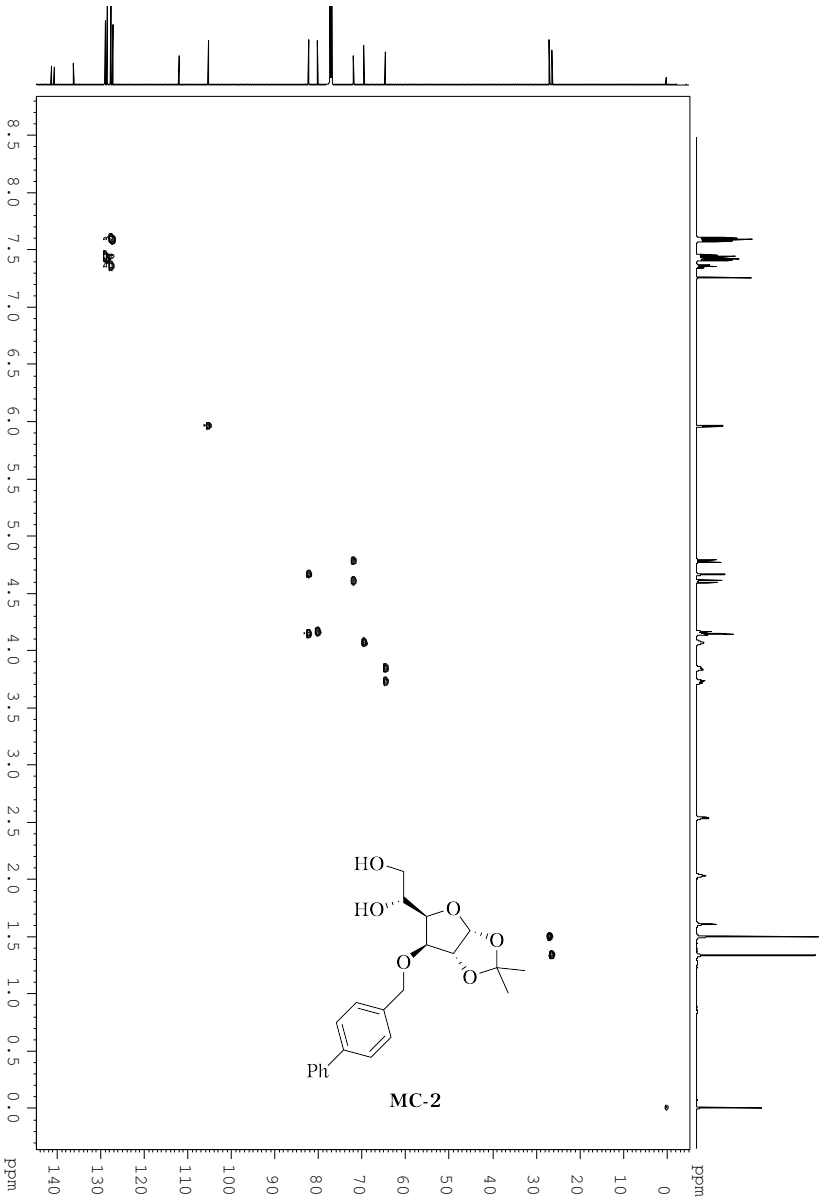

Figure 197: HSQC spectrum of **MC-2**.

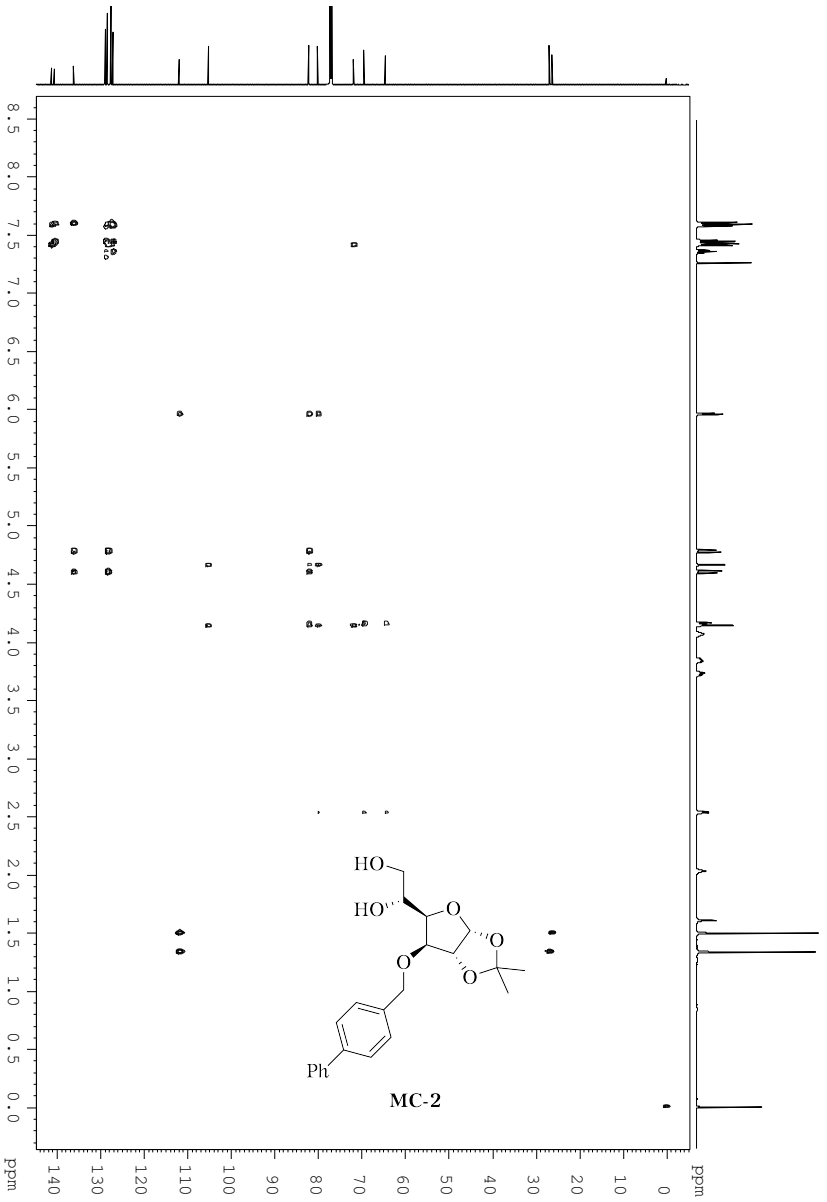

Figure 198: HMBC spectrum of **MC-2**.

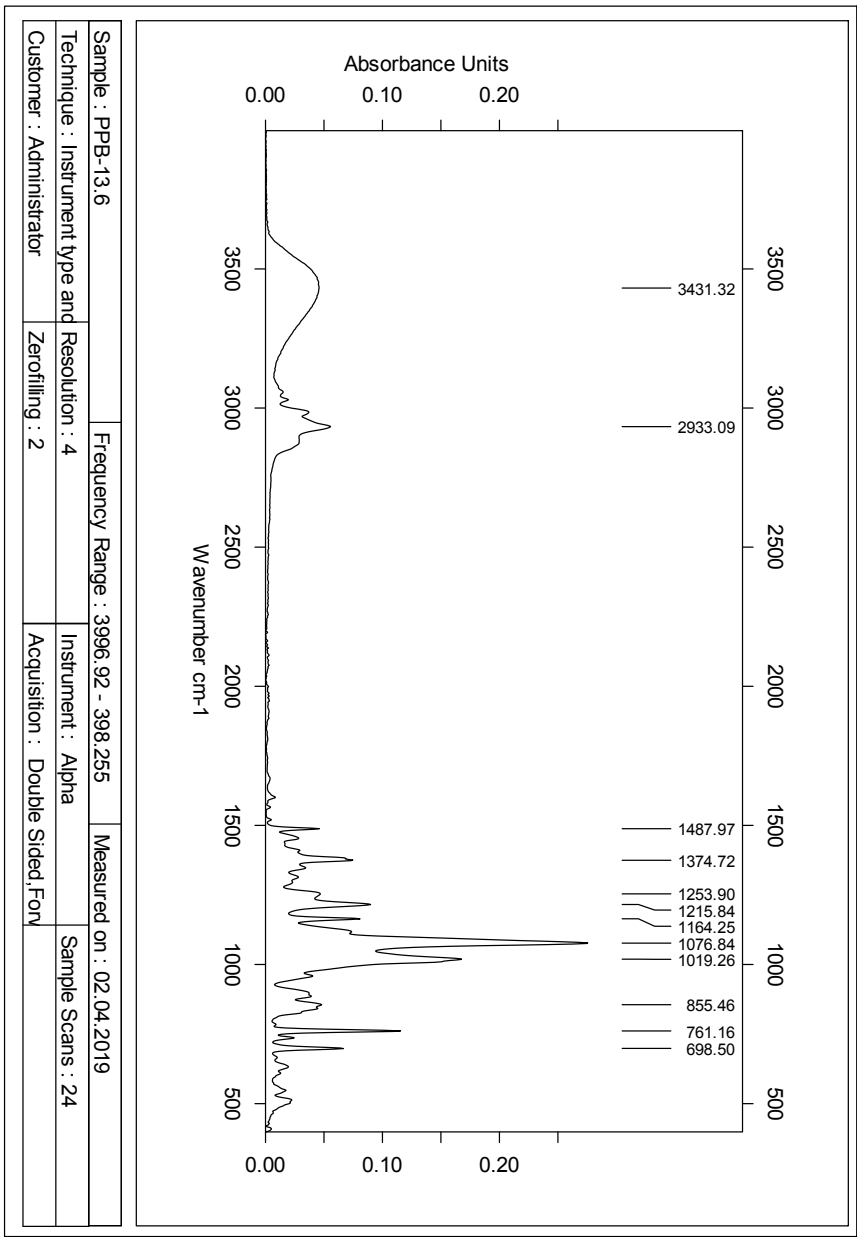

Figure 199: IR spectrum of **MC-2**.

B.25 Spectroscopic data for compound MC-3

Elemental Composition Report **Page 1**

Single Mass Analysis
Tolerance = 2.0 PPM / DBE: min = -50.0, max = 50.0
Element prediction: Off
Number of isotope peaks used for i-FIT = 3

Monoisotopic Mass, Even Electron Ions
2578 formula(e) evaluated with 2 results within limits (all results (up to 1000) for each mass)
Elements Used:
C: 0-100 H: 0-150 N: 0-10 O: 0-10 Na: 0-1
2019-524 76 (1.414) AM2 (Ar,35000.0,0.00,0.00); Cm (53:77)
1: TOF MS ES+

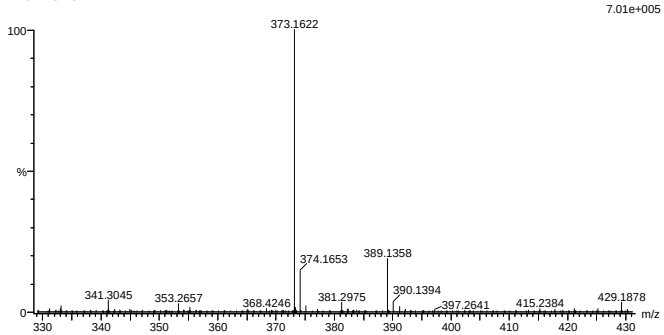

Minimum:				-50.0				
Maximum:		5.0	2.0	50.0				
Mass	Calc. Mass	mDa	PPM	DBE	i-FIT	Norm	Conf(%)	Formula
373.1622	373.1627	-0.5	-1.3	6.5	1087.5	2.034	13.08	C19 H26 O6 Na
	373.1624	-0.2	-0.5	10.5	1085.6	0.140	86.92	C17 H21 N6 O4

Figure 200: HRMS (ESI+) of **MC-3**.

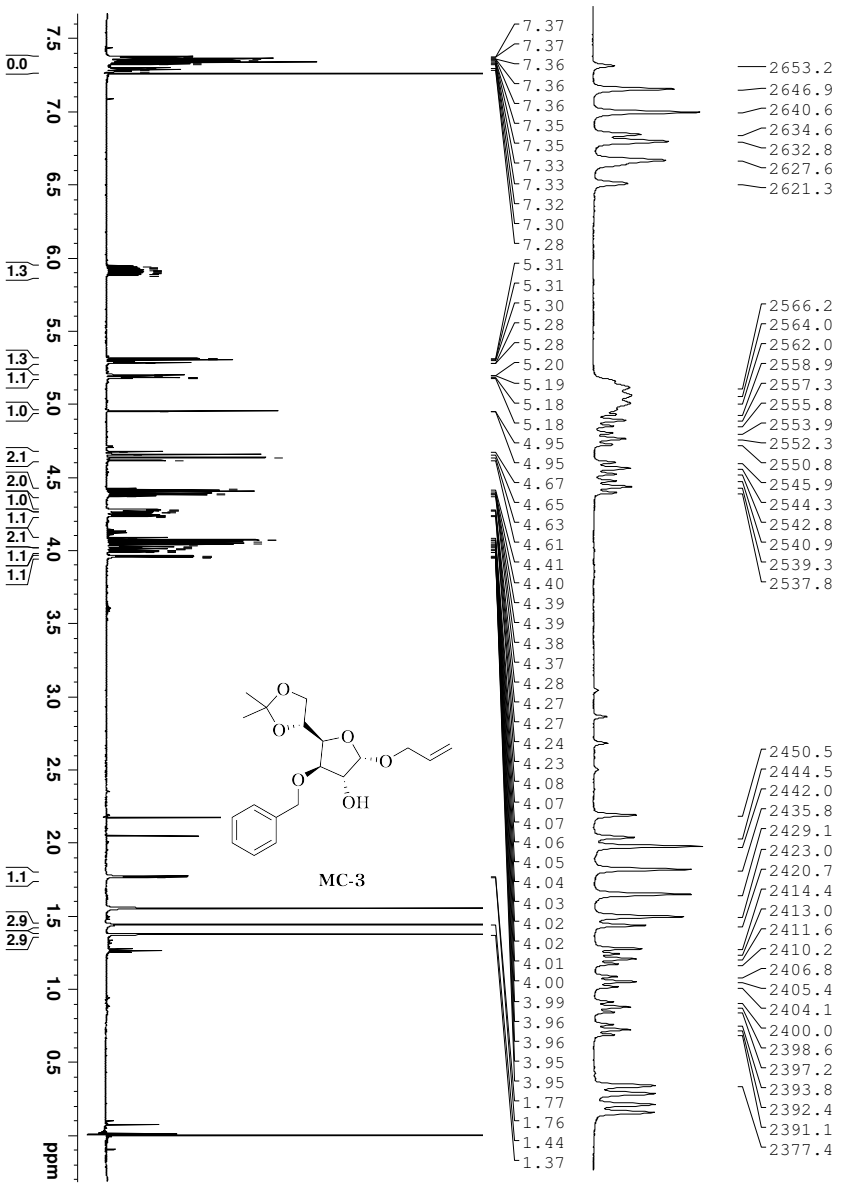

Figure 201: ^{1}H NMR spectrum of **MC-3**.

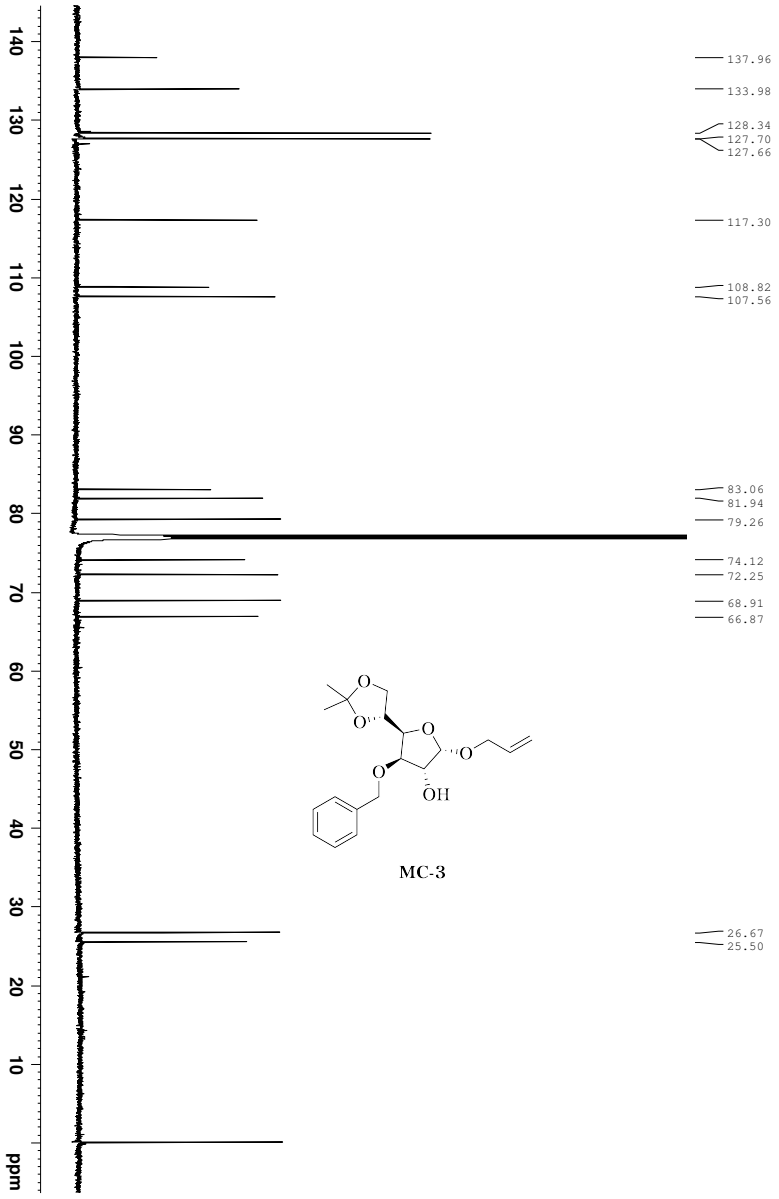

Figure 202: ^{13}C NMR spectrum of **MC-3**.

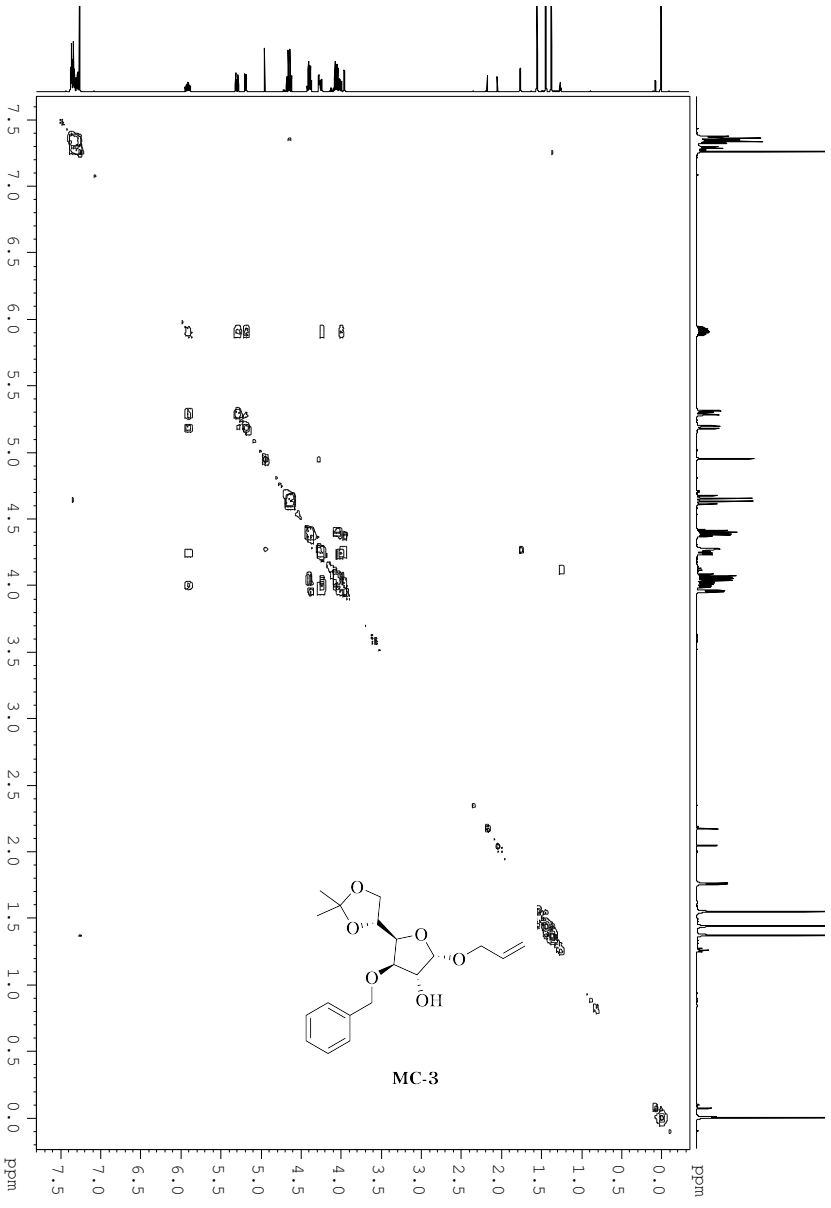

Figure 203: COSY spectrum of **MC-3**.

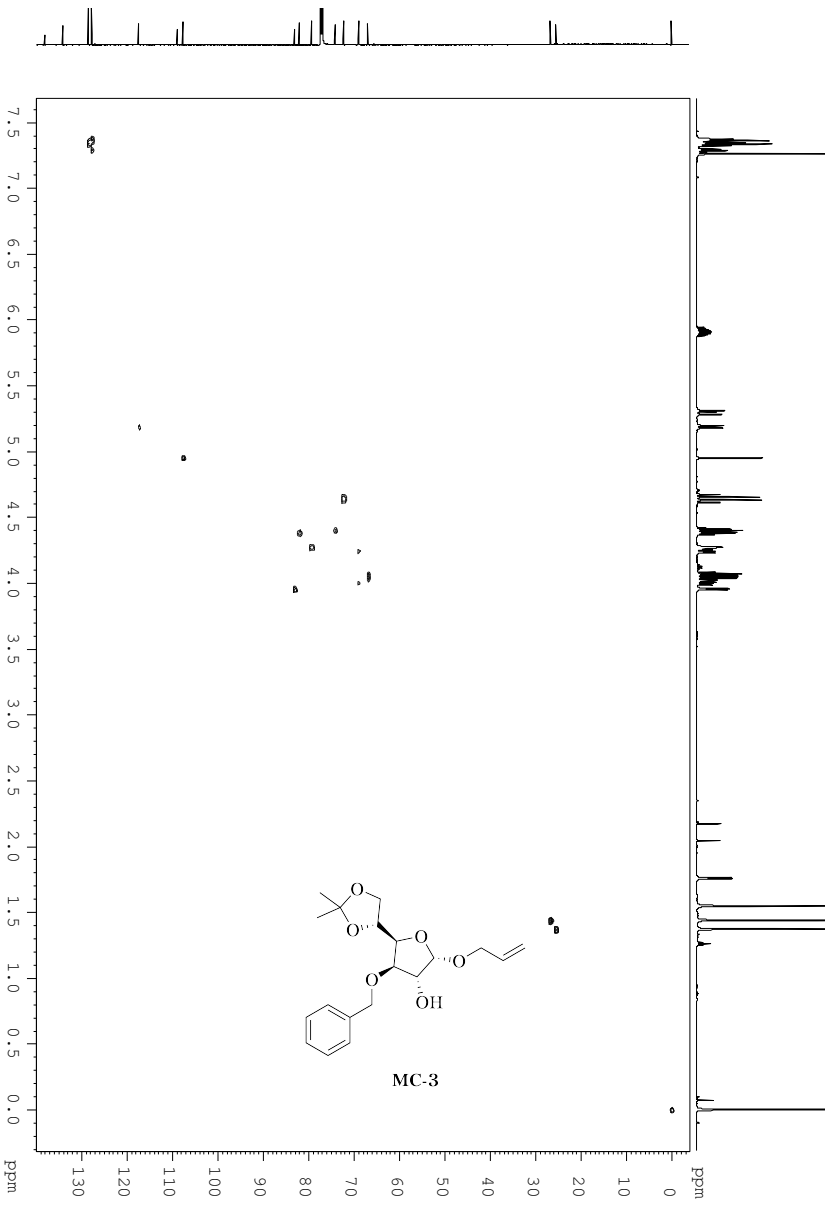

Figure 204: HSQC spectrum of **MC-3**.

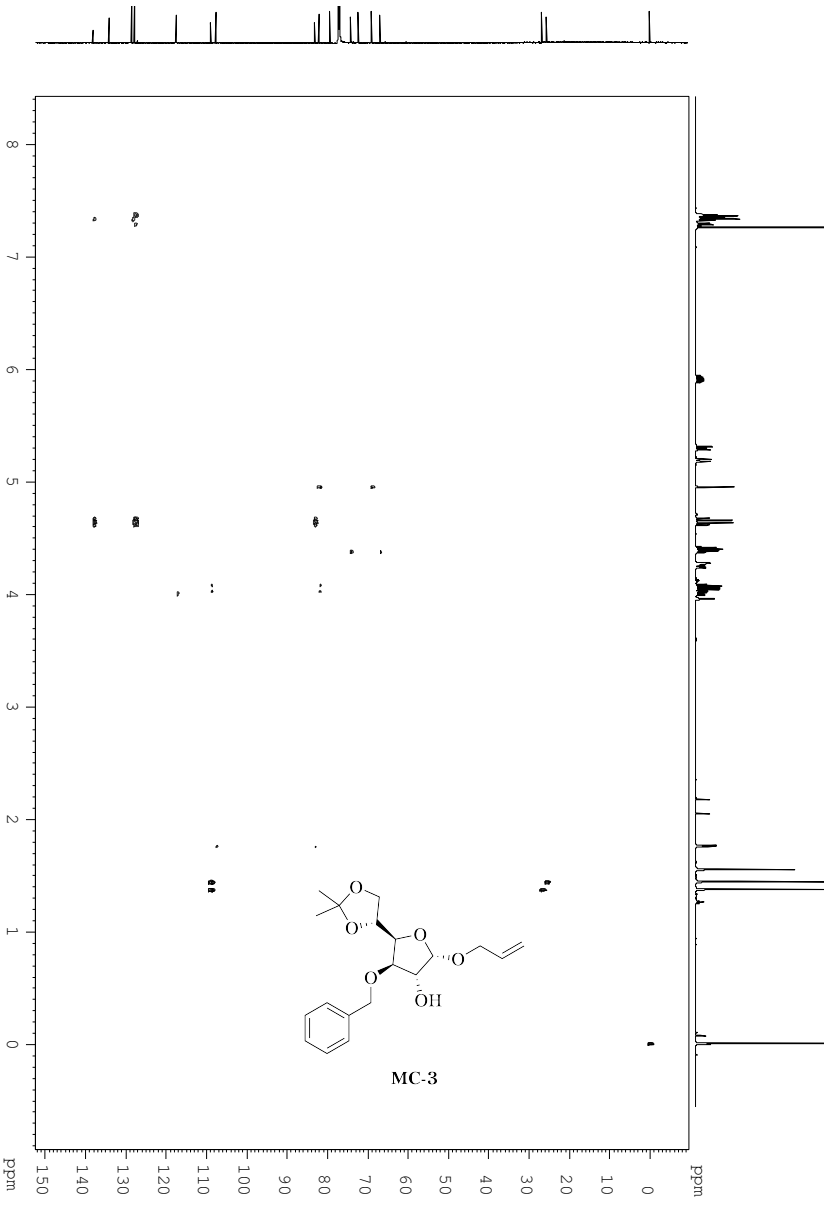

Figure 205: HMBC spectrum of **MC-3**.

B.26 Spectroscopic data for compound MC-4

Elemental Composition Report **Page 1**

Single Mass Analysis
Tolerance = 2.0 PPM / DBE: min = -50.0, max = 50.0
Element prediction: Off
Number of isotope peaks used for i-FIT = 3

Monoisotopic Mass, Even Electron Ions
803 formula(e) evaluated with 3 results within limits (all results (up to 1000) for each mass)
Elements Used:
C: 2-100 H: 0-150 O: 0-10 Na: 0-1 Si: 0-2
2019_577 27 (0.310) AM2 (Ar,35000.0,0.00,0.00); ABS; Cm (19:27)
1: TOF MS ES+

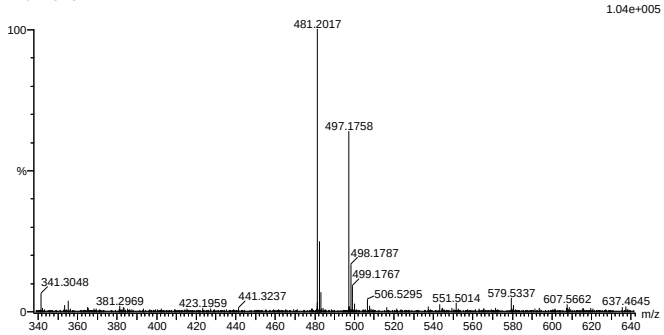

Minimum:				-50.0				
Maximum:		5.0	2.0	50.0				
Mass	Calc. Mass	mDa	PPM	DBE	i-FIT	Norm	Conf(%)	Formula
481.2017	481.2019	-0.2	-0.4	16.5	747.5	2.157	11.57	C30 H33 O2 Si2
	481.2015	0.2	0.4	17.5	751.4	6.096	0.23	C31 H29 O5
	481.2022	-0.5	-1.0	9.5	745.4	0.126	88.20	C25 H34 O6 Na Si

Figure 206: HRMS (ESI+) of **MC-4**.

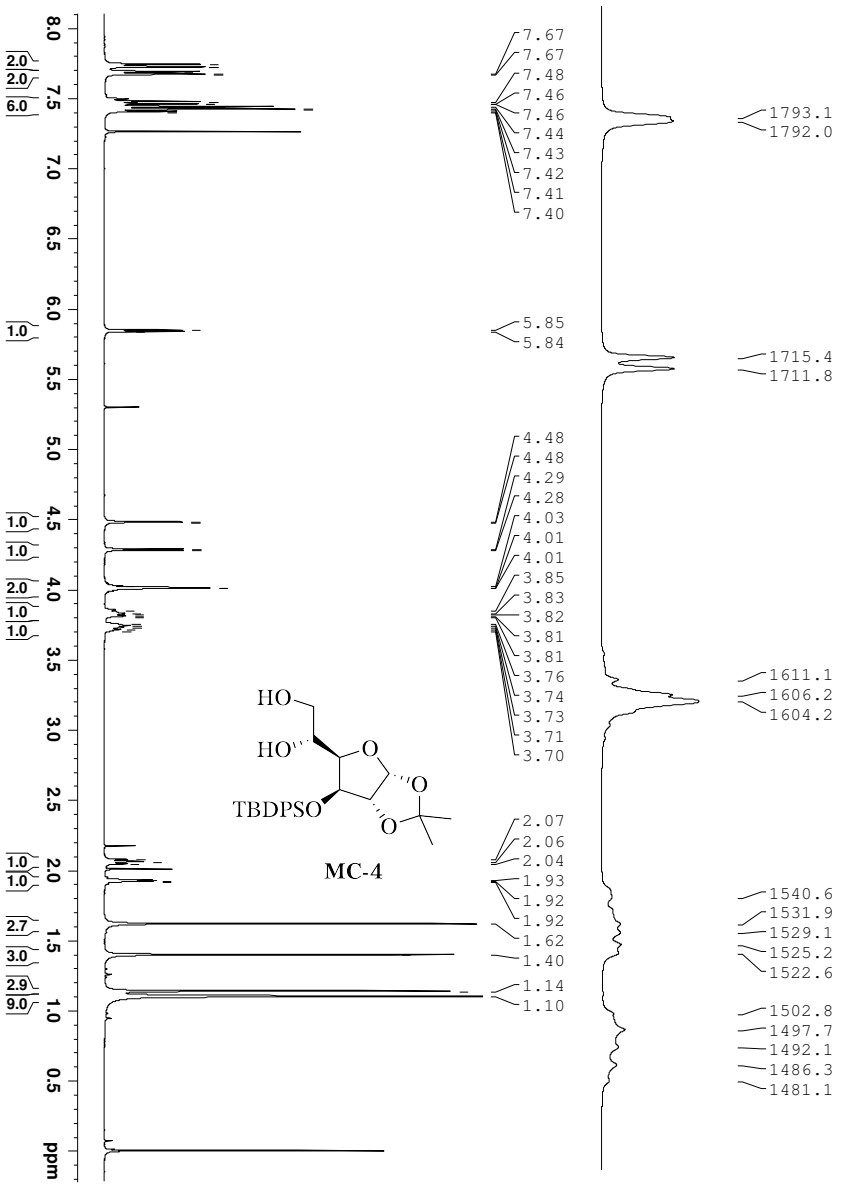

Figure 207: ^{1}H NMR (400 MHz) spectrum of **MC-4**.

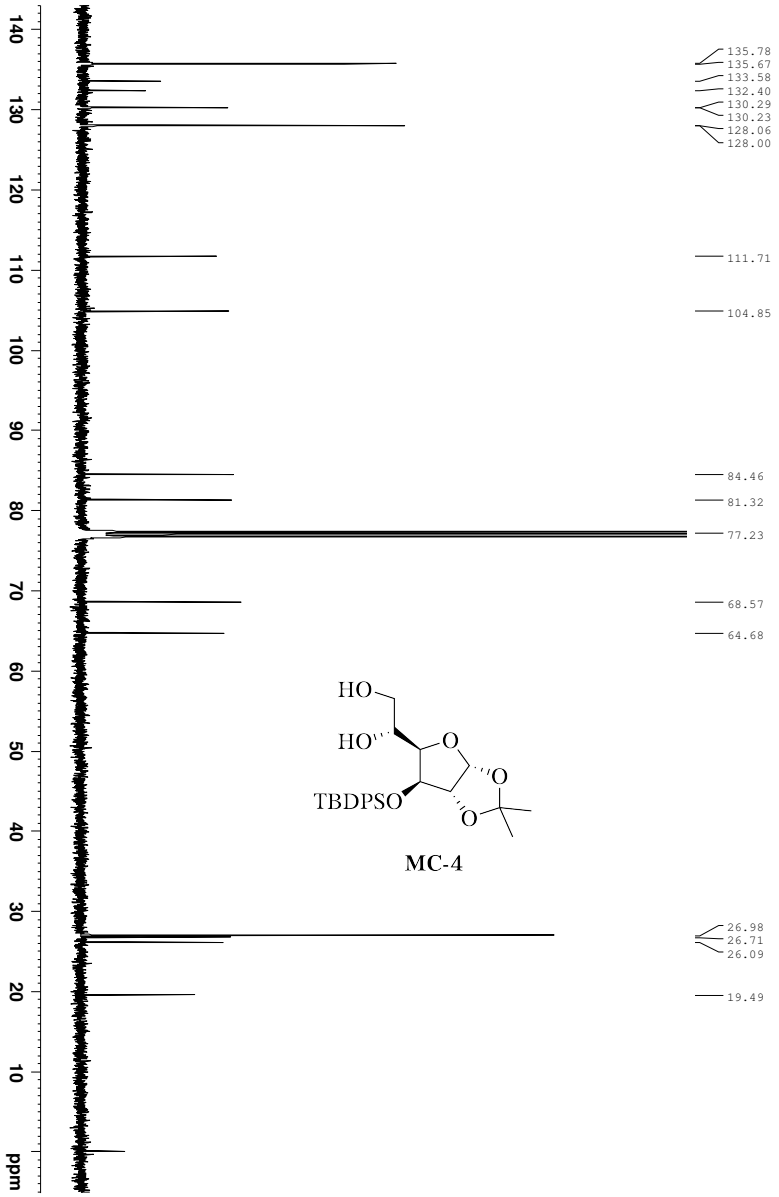

Figure 208: ^{13}C NMR (100 MHz) spectrum of **MC-4**.

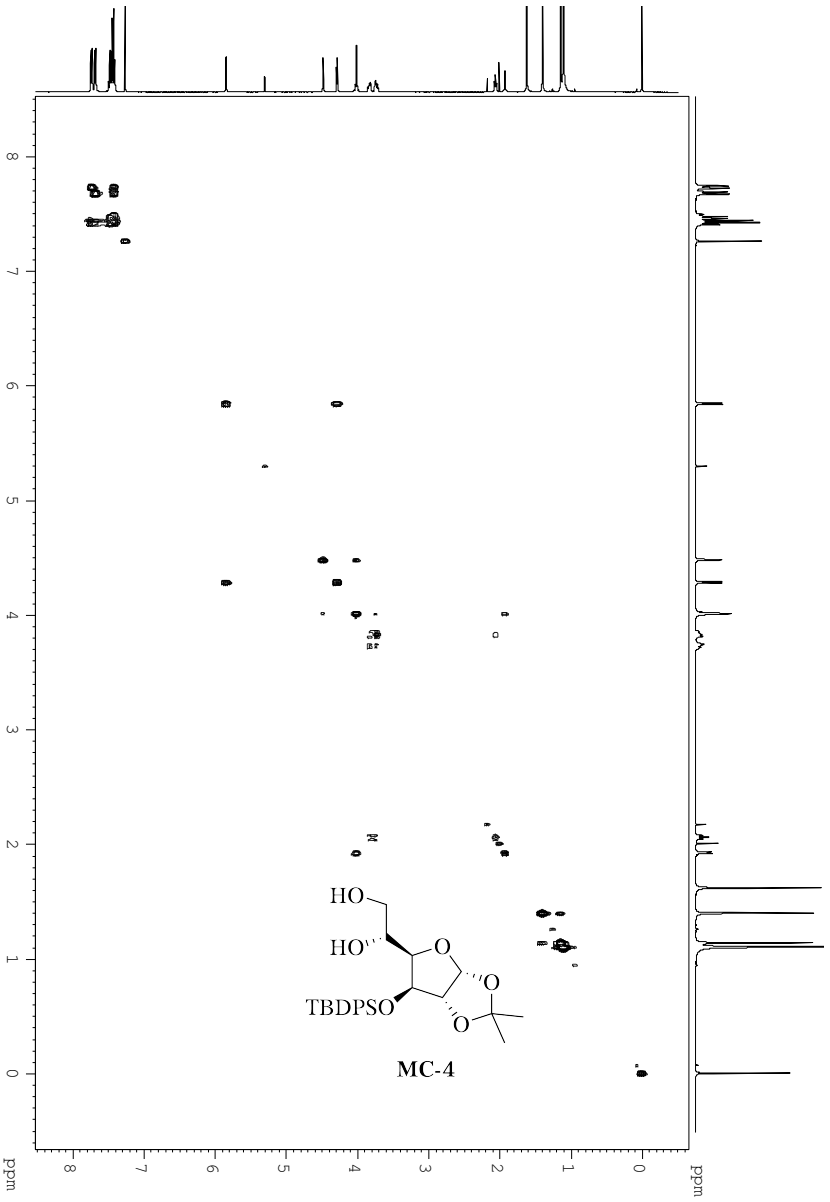

Figure 209: COSY (400 MHz) spectrum of **MC-4**.

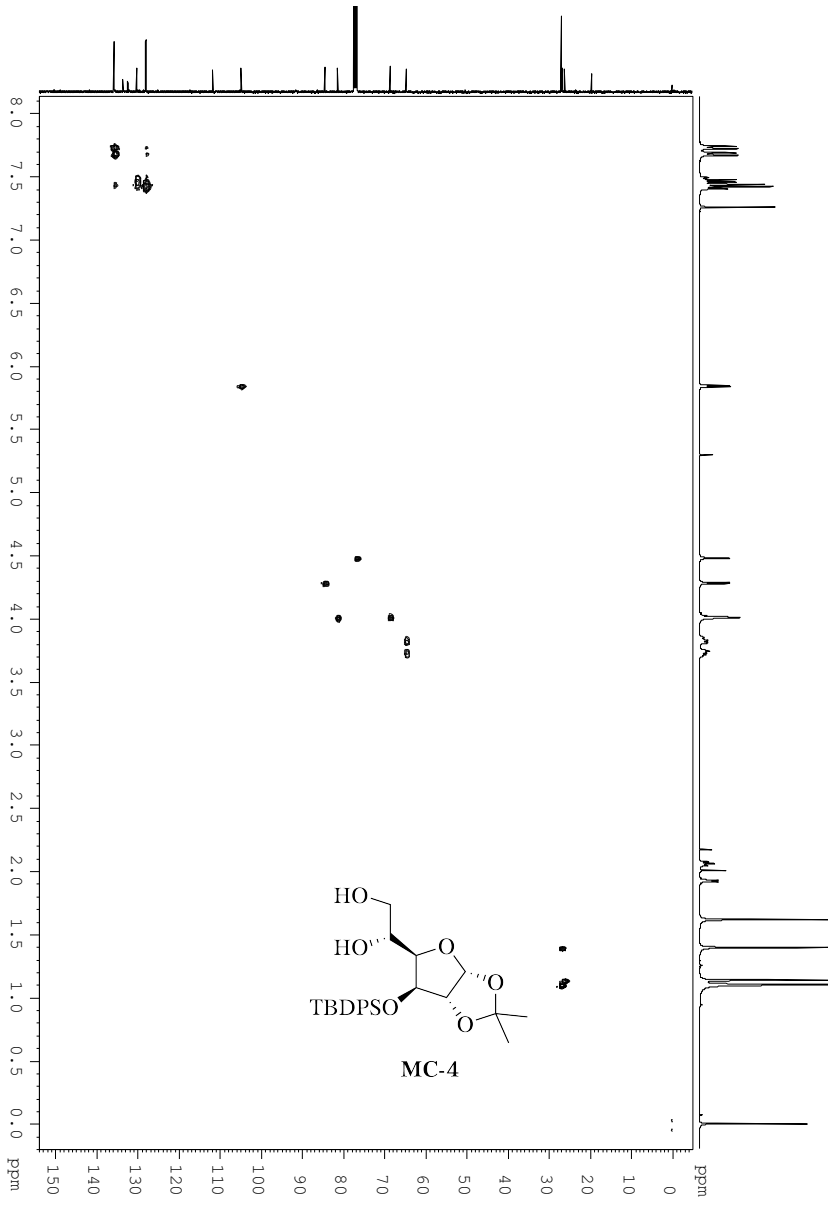

Figure 210: HSQC (400 MHz) spectrum of **MC-4**.

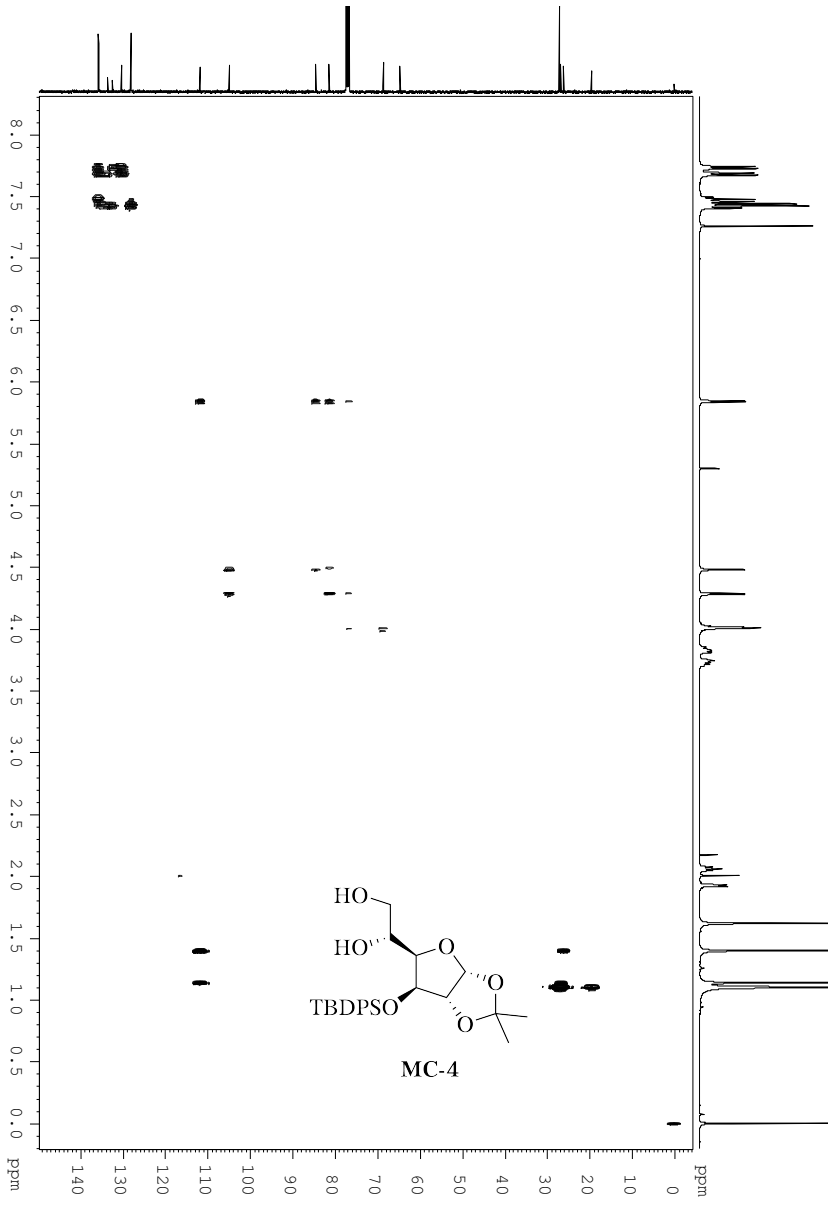

Figure 211: HMBC (400 MHz) spectrum of **MC-4**.

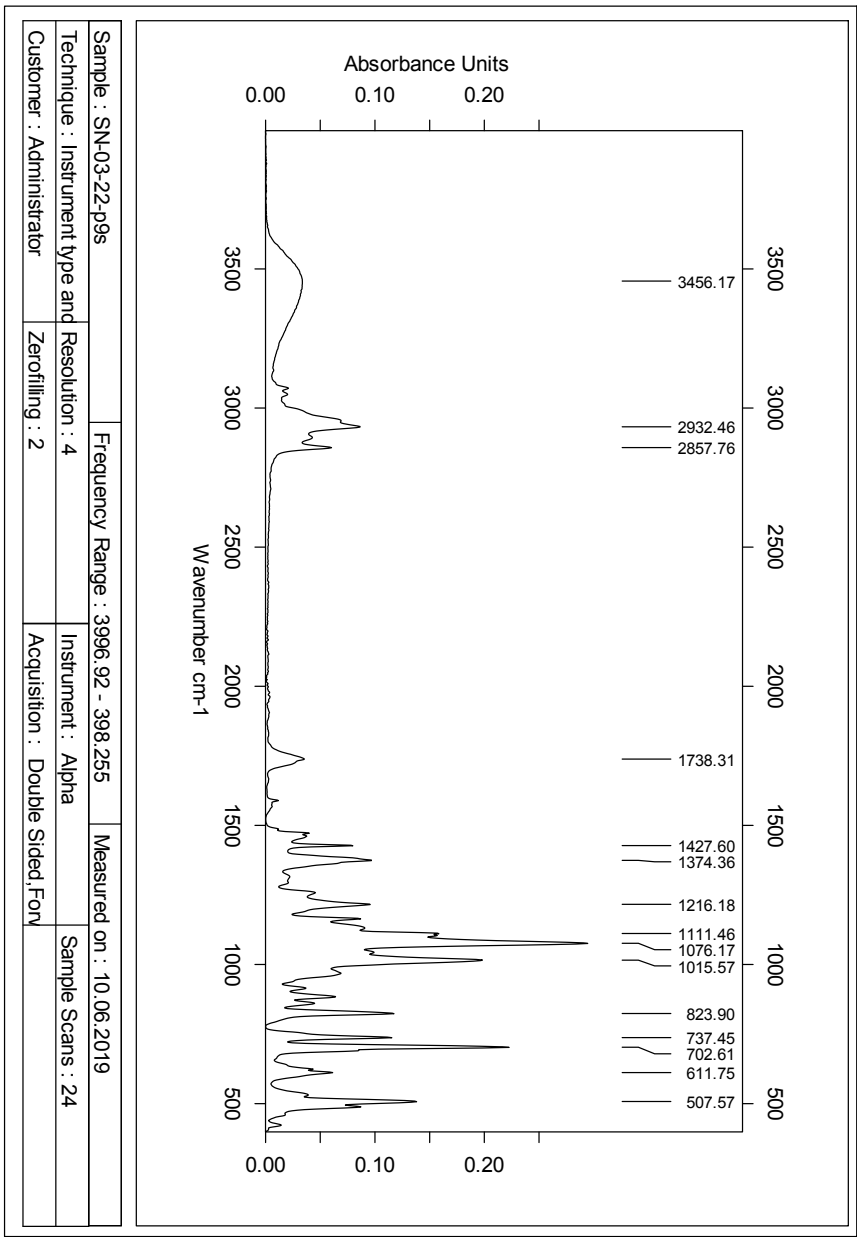

Figure 212: IR spectrum of **MC-4**.

B.27 Spectroscopic data for compound 4a-α

Elemental Composition Report **Page 1**

Single Mass Analysis
Tolerance = 2.0 PPM / DBE: min = -50.0, max = 50.0
Element prediction: Off
Number of isotope peaks used for i-FIT = 3

Monoisotopic Mass, Even Electron Ions
1390 formula(e) evaluated with 1 results within limits (all results (up to 1000) for each mass)
Elements Used:
C: 0-100 H: 0-150 N: 0-5 O: 0-10 Na: 0-1

2019_299_fia 31 (0.360) AM2 (Ar,35000.0,0.00,0.00); Cm (26:31)
1: TOF MS ES+

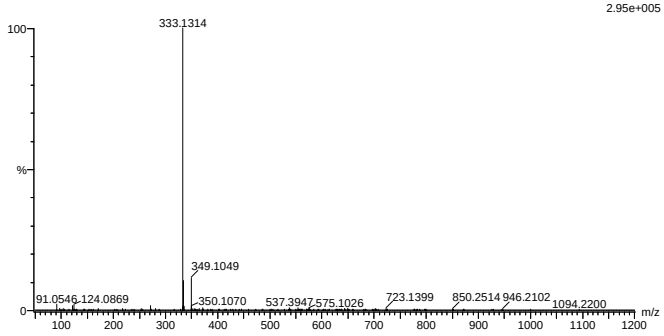

Minimum:				-50.0				
Maximum:		5.0	2.0	50.0				
Mass	Calc. Mass	mDa	PPM	DBE	i-FIT	Norm	Conf(%)	Formula
333.1314	333.1314	0.0	0.0	5.5	836.7	n/a	n/a	C16 H22 O6 Na

Figure 213: HRMS (ESI+) of **4a-α**.

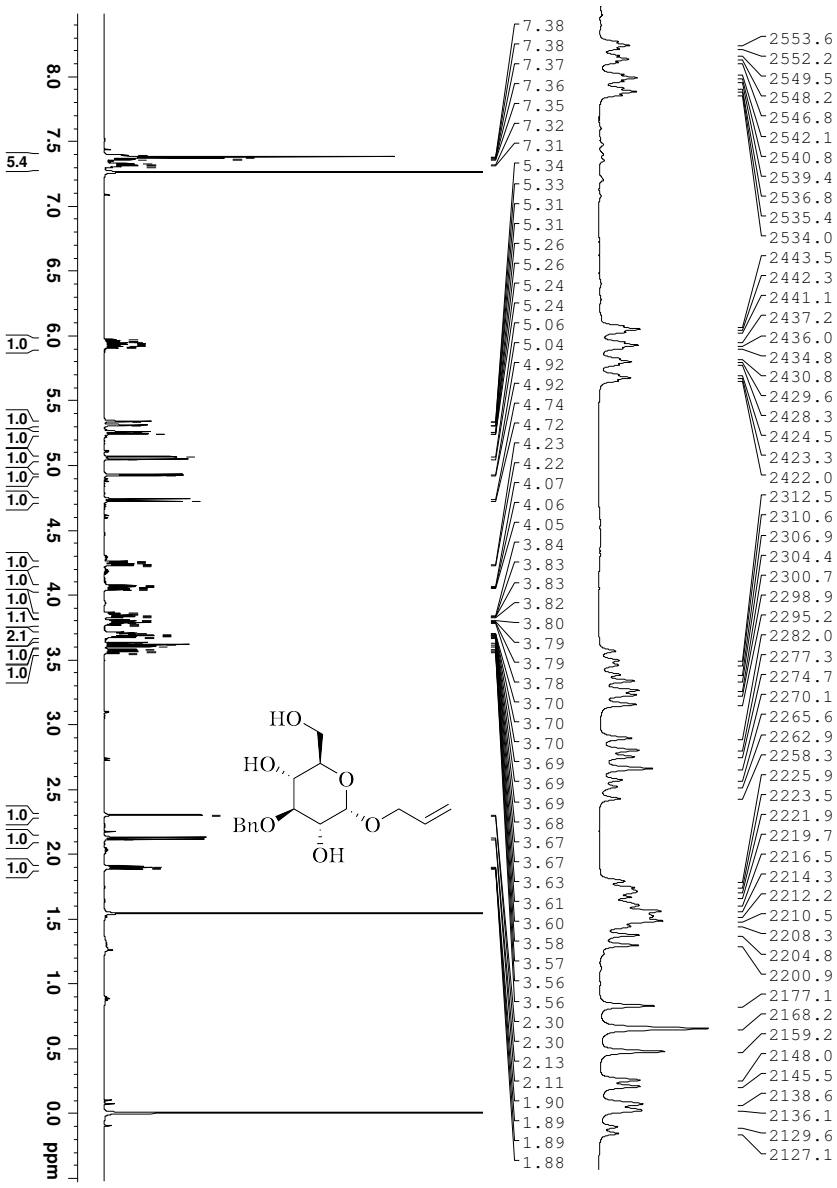

Figure 214: ^{1}H NMR spectrum of **4a-α**.

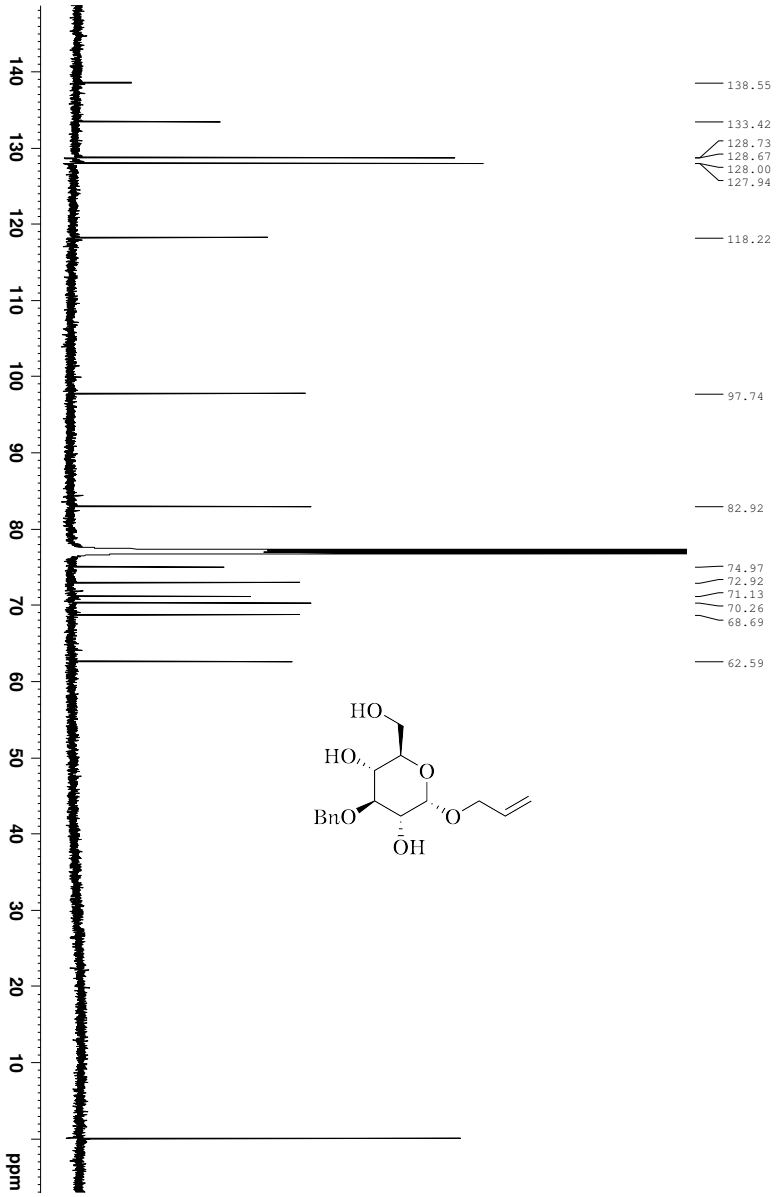

Figure 215: ^{13}C NMR spectrum of **4a-α**.

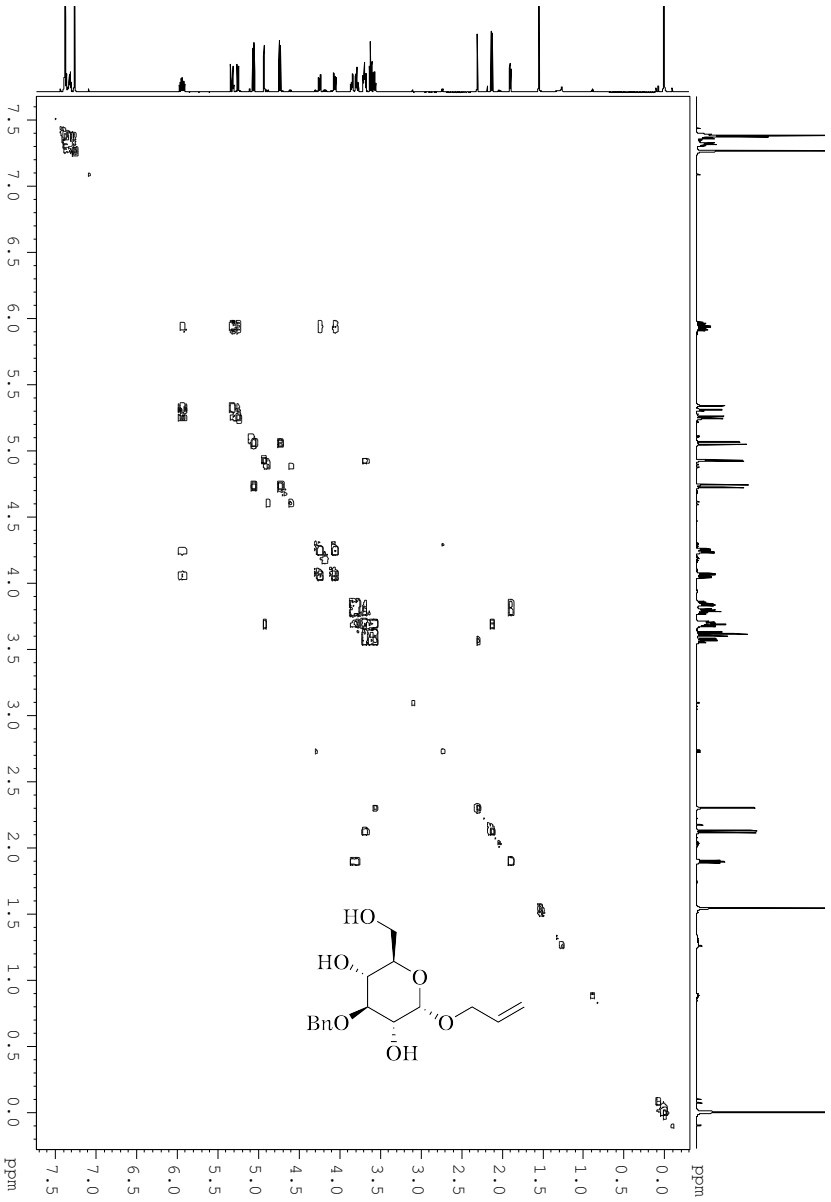

Figure 216: COSY spectrum of **4a-α**.

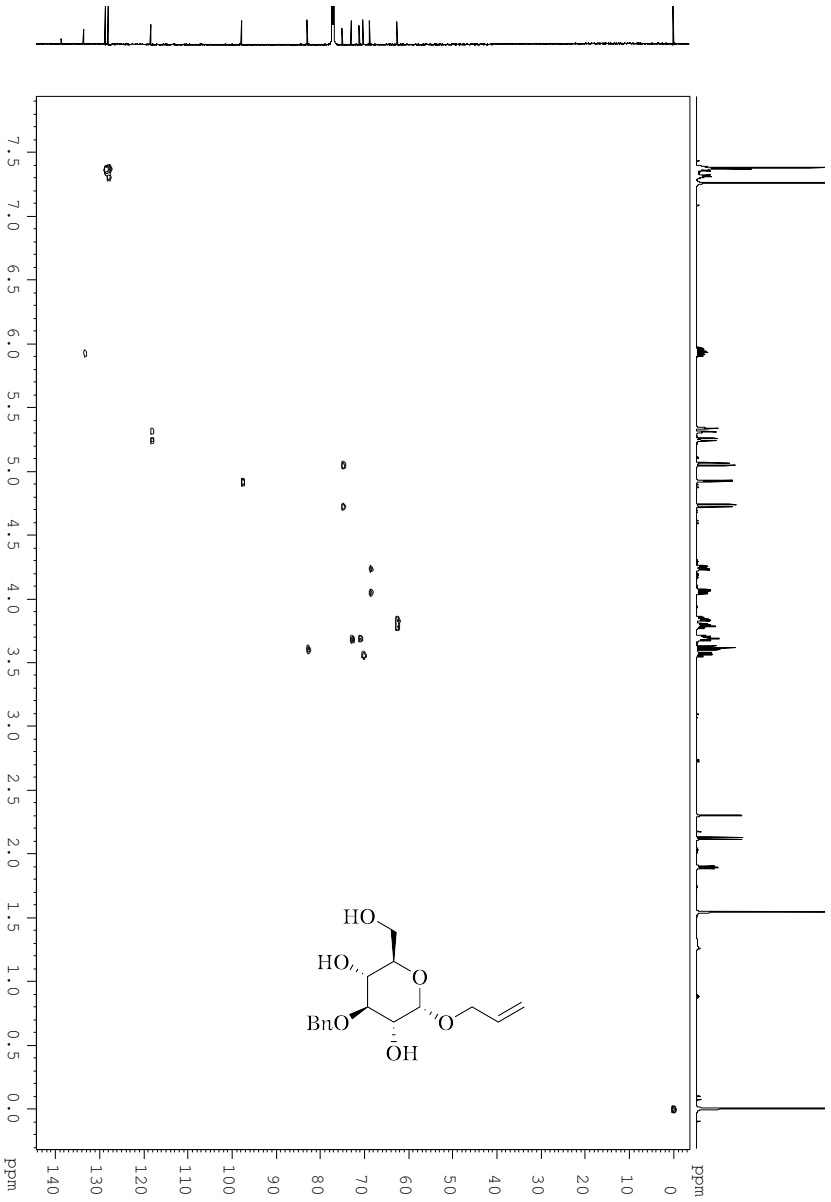

Figure 217: HSQC spectrum of **4a-α**.

cc

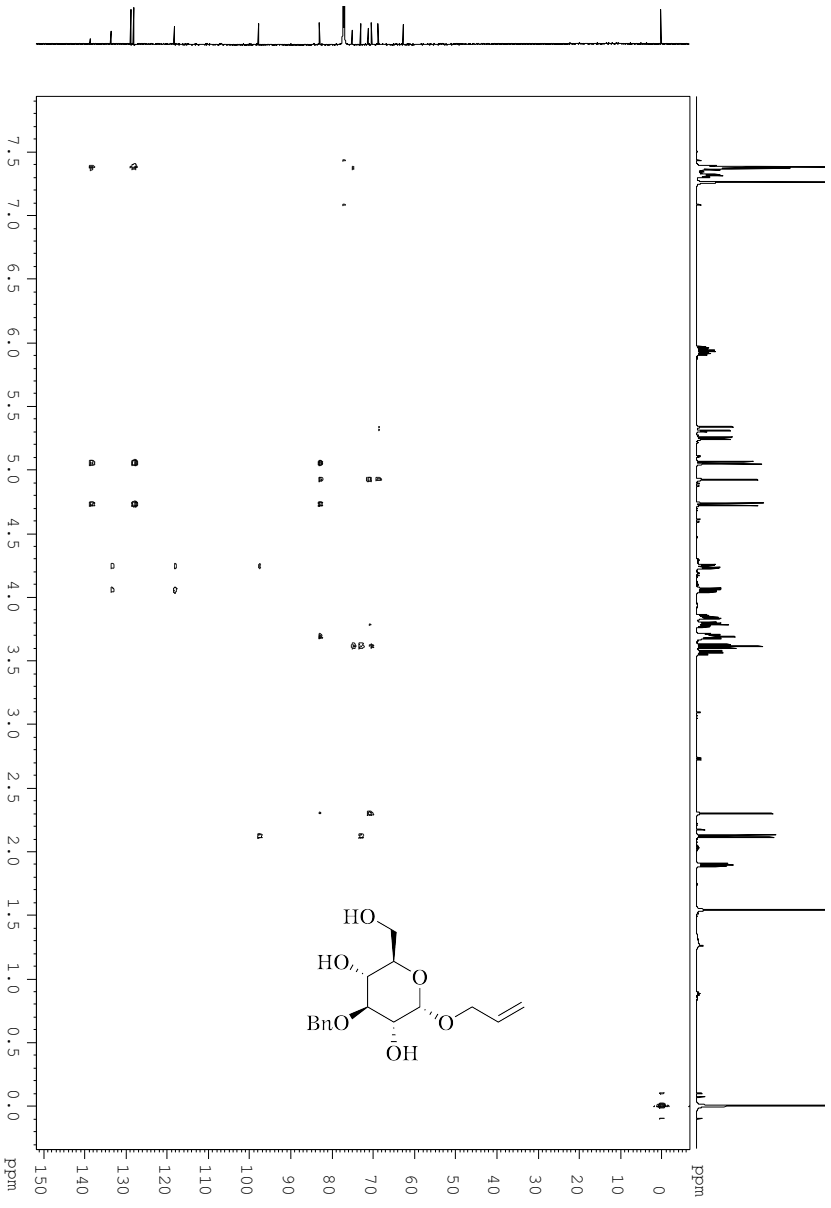

Figure 218: HMBC spectrum of **4a-α**.

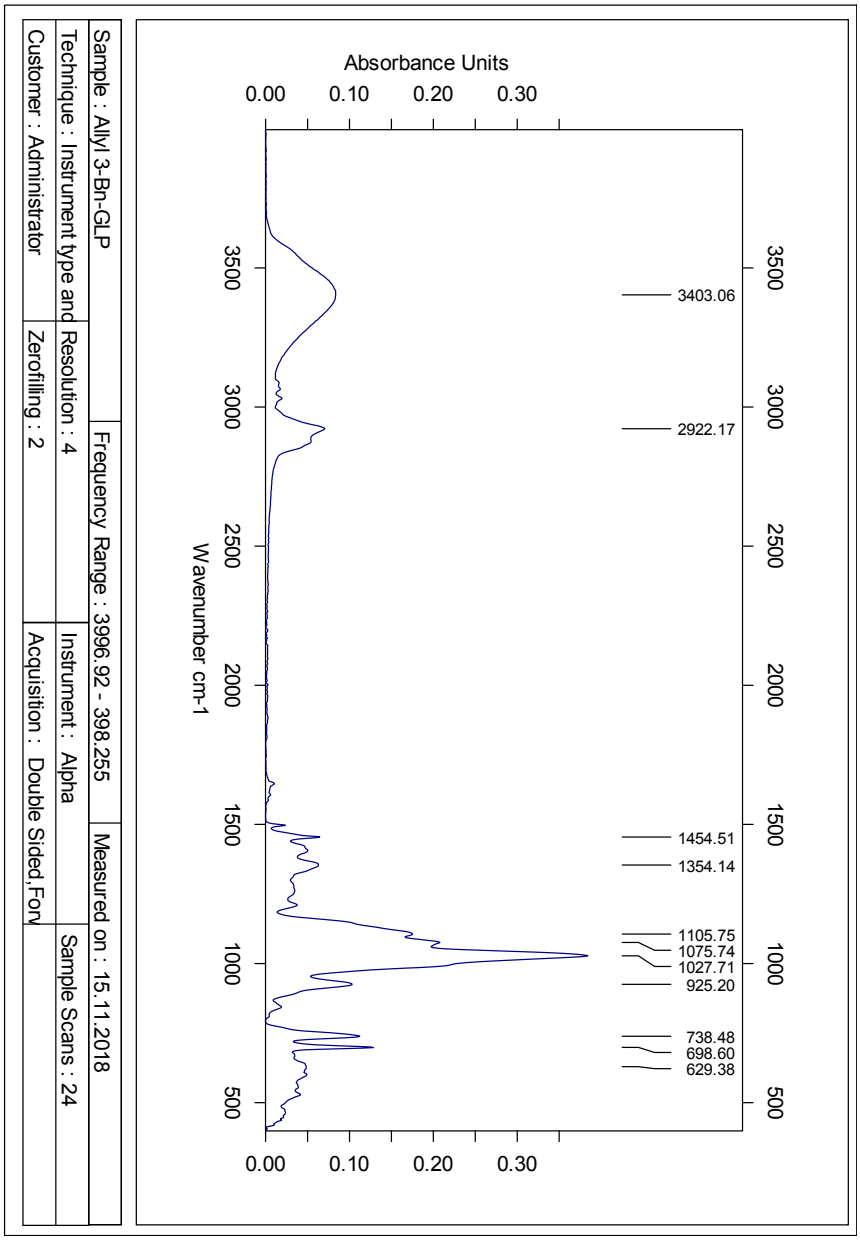

Figure 219: IR spectrum of **4a-α**.

B.28 Spectroscopic data for compound 4a-β

Elemental Composition Report **Page 1**

Single Mass Analysis
Tolerance = 2.0 PPM / DBE: min = -50.0, max = 50.0
Element prediction: Off
Number of isotope peaks used for i-FIT = 3

Monoisotopic Mass, Even Electron Ions
1390 formula(e) evaluated with 1 results within limits (all results (up to 1000) for each mass)
Elements Used:
C: 0-100 H: 0-150 N: 0-5 O: 0-10 Na: 0-1
2019_300_fia 52 (0.588) AM2 (Ar,35000.0,0.00,0.00); Cm (43:52)
1: TOF MS ES+

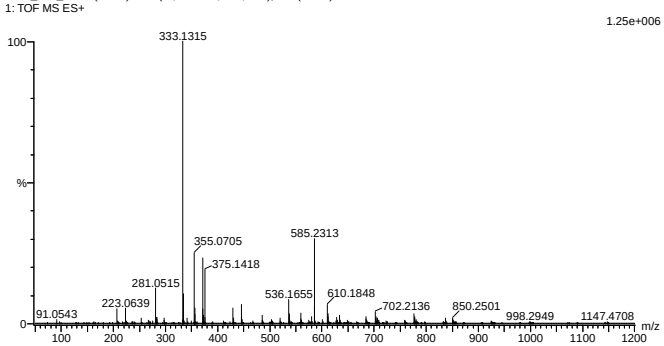

Minimum:		5.0	2.0	-50.0				
Maximum:				50.0				
Mass	Calc. Mass	mDa	PPM	DBE	i-FIT	Norm	Conf(%)	Formula
333.1315	333.1314	0.1	0.3	5.5	1079.2	n/a	n/a	C16 H22 O6 Na

Figure 220: HRMS (ESI+) of **4a-β**.

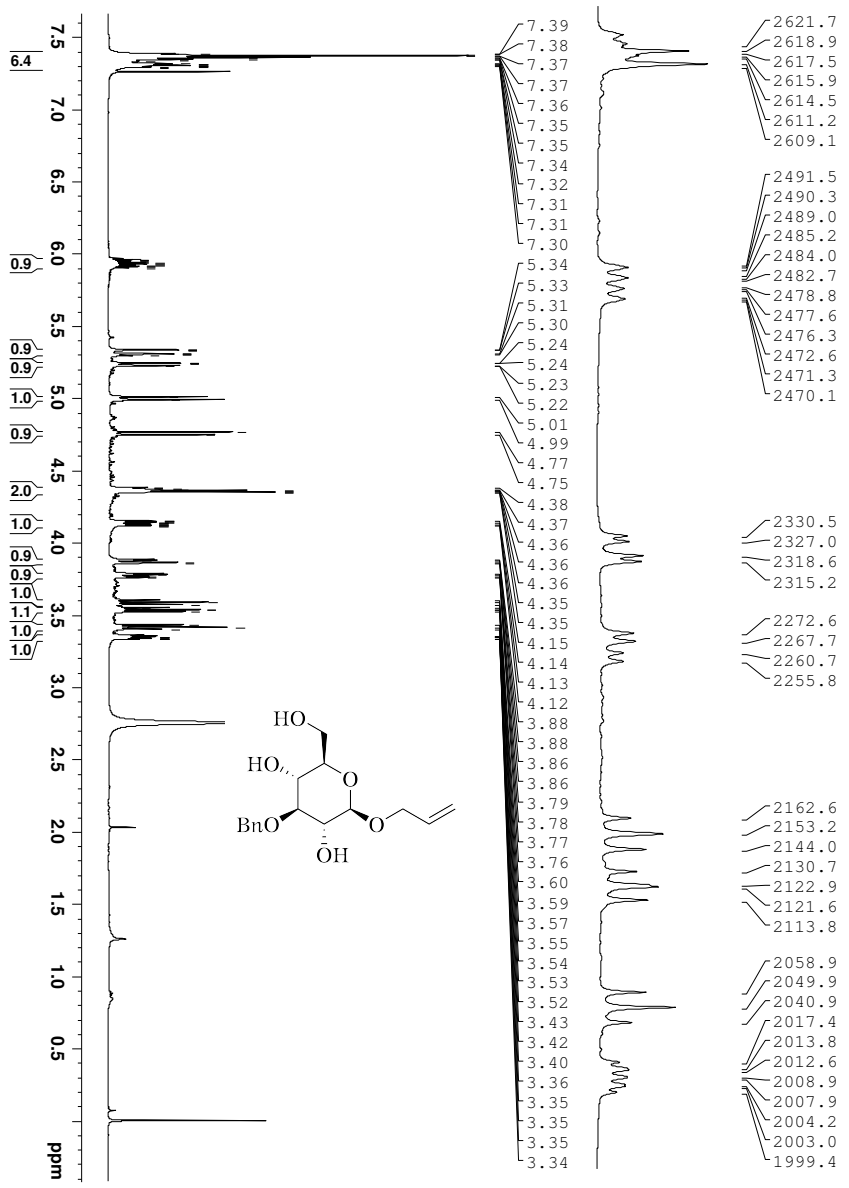

Figure 221: ^{1}H NMR spectrum of **4a-β**.

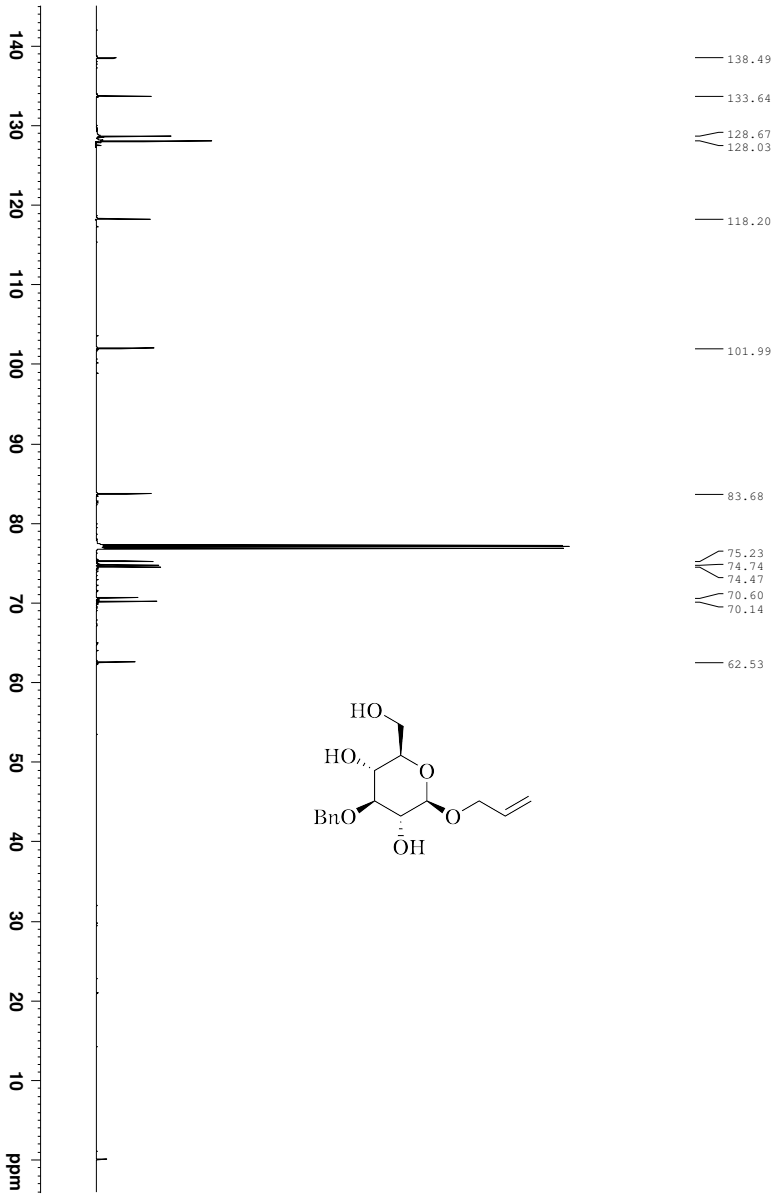

Figure 222: ^{13}C NMR spectrum of **4a-β**.

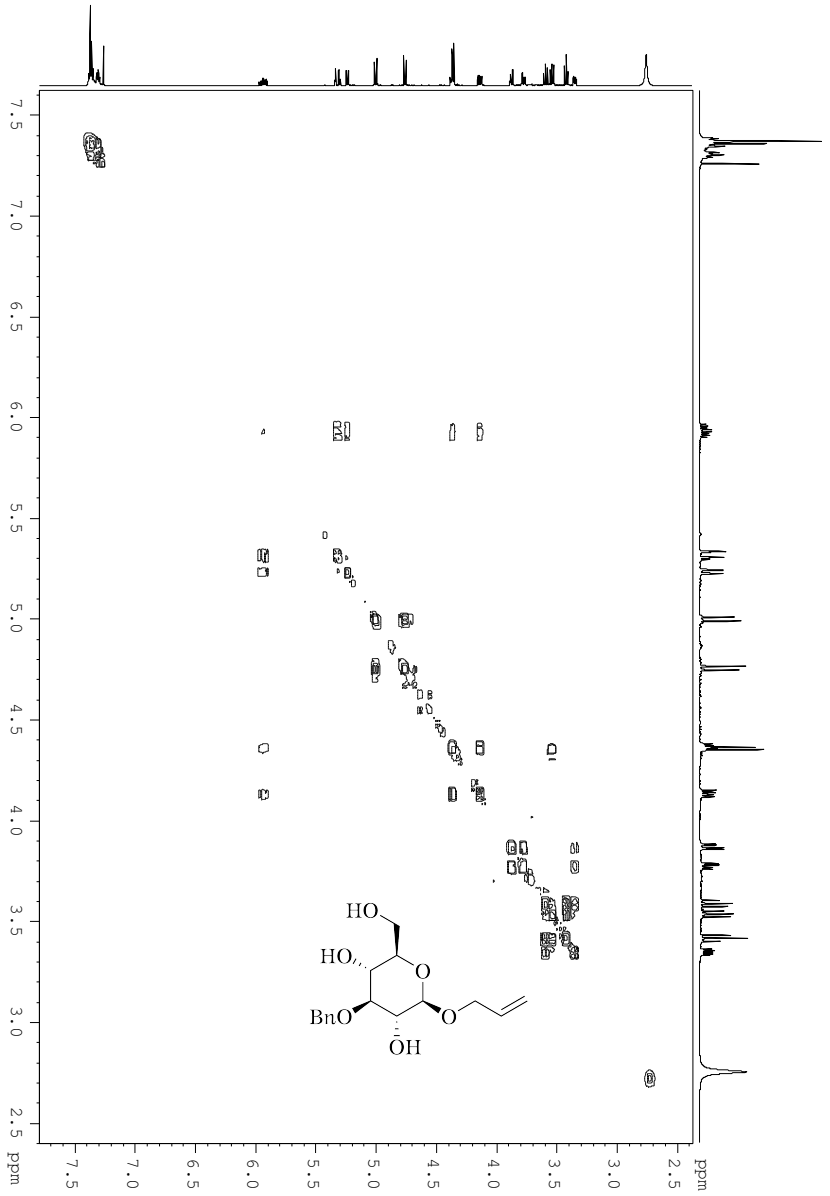

Figure 223: COSY spectrum of **4a-β**.

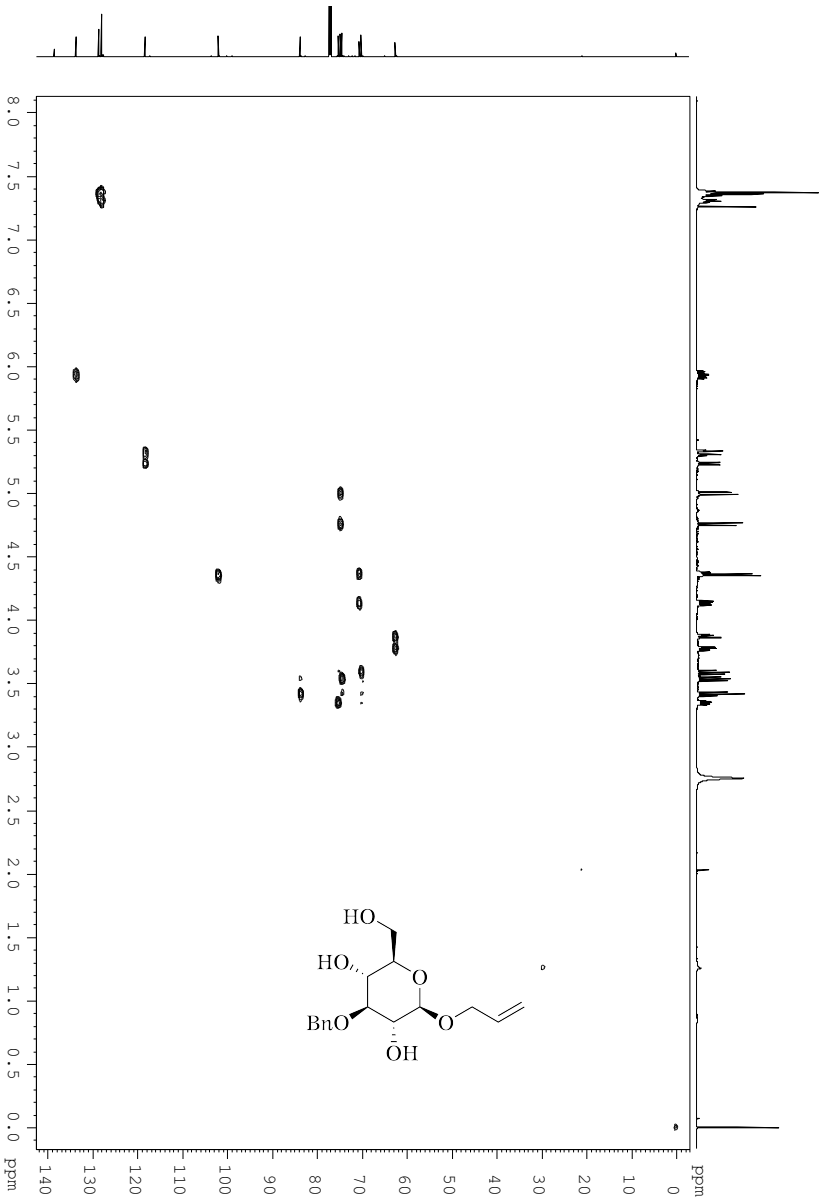

Figure 224: HSQC spectrum of **4a-β**.

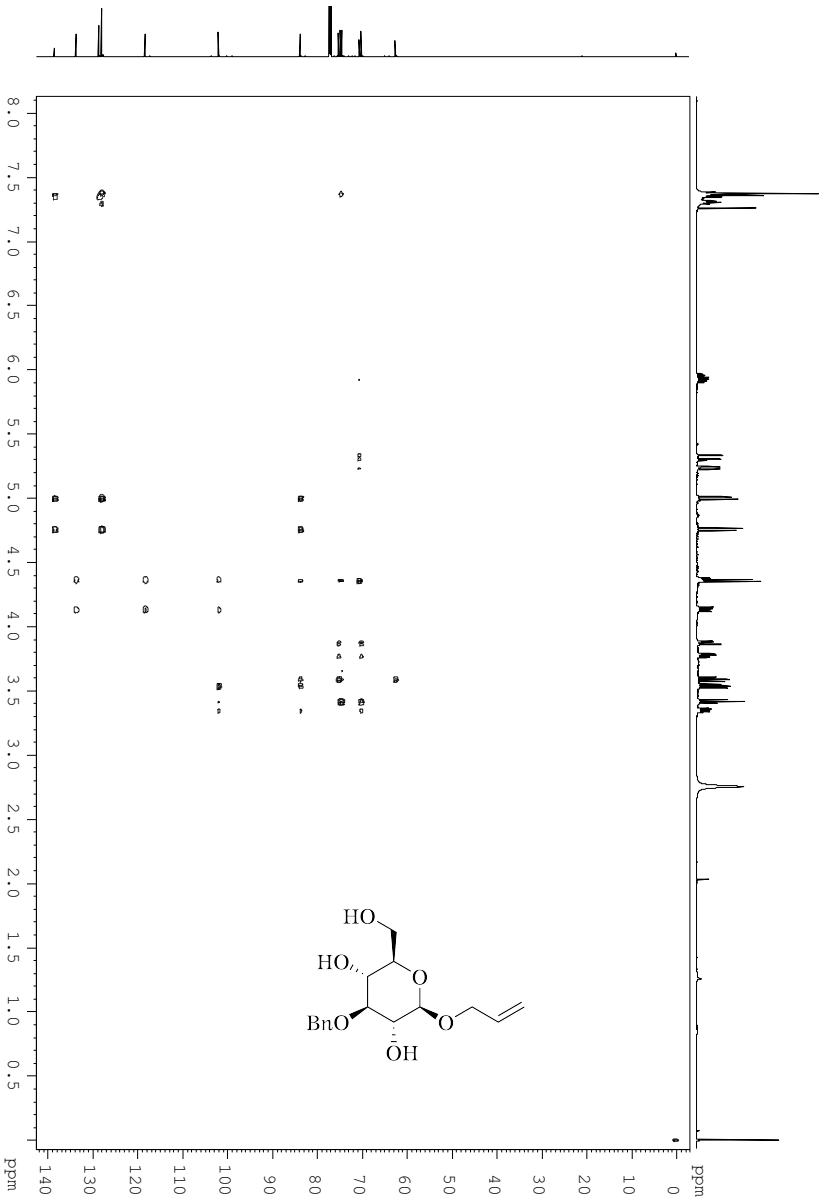

Figure 225: HMBC spectrum of **4a-β**.

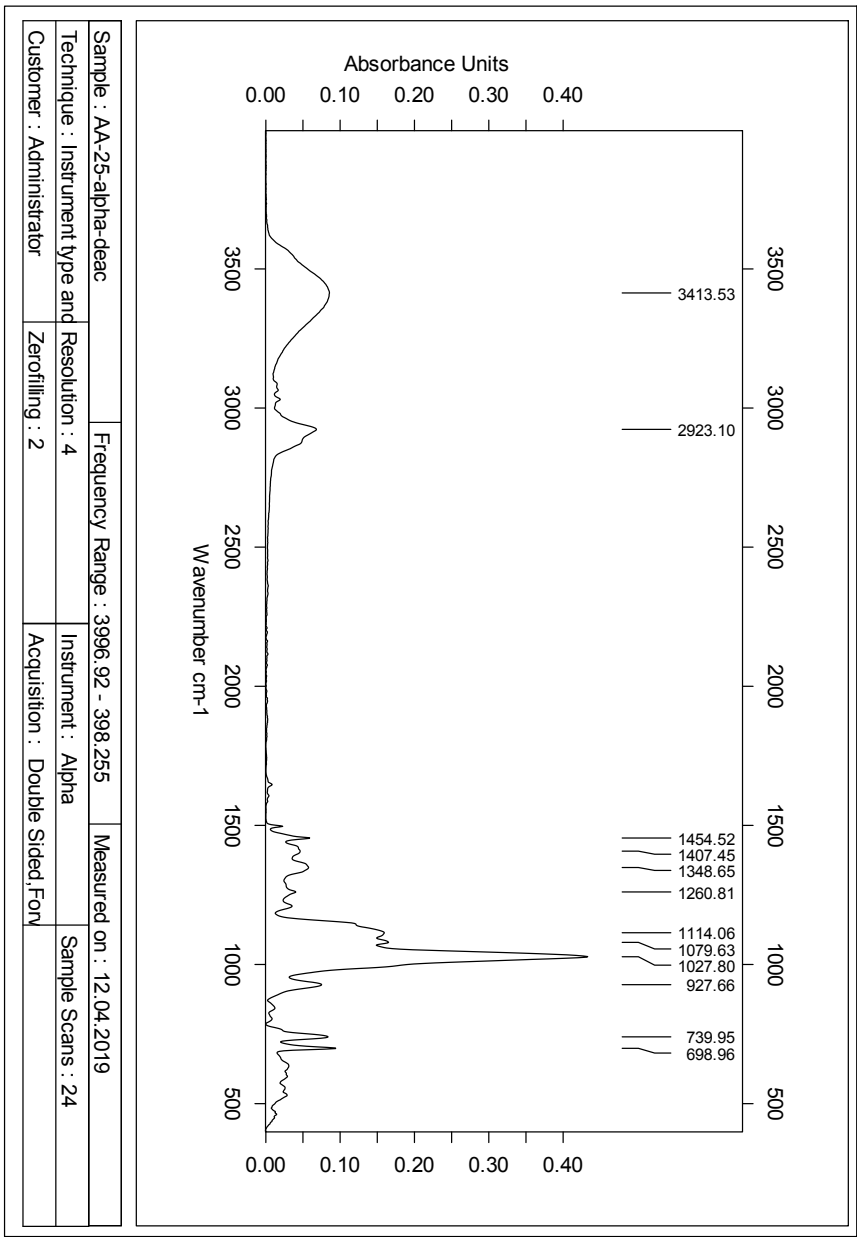

Figure 226: IR spectrum of **4a-β**.

B.29 Spectroscopic data for compound 4b-α

Elemental Composition Report **Page 1**

Single Mass Analysis
Tolerance = 2.0 PPM / DBE: min = -50.0, max = 50.0
Element prediction: Off
Number of isotope peaks used for i-FIT = 3

Monoisotopic Mass, Even Electron Ions
2623 formula(e) evaluated with 2 results within limits (all results (up to 1000) for each mass)
Elements Used:
C: 0-100 H: 0-150 N: 0-10 O: 0-10 Na: 0-1
2019_521 21 (0.403) AM2 (Ar,35000.0,0.00,0.00); Cm (15:21)
1: TOF MS ES+

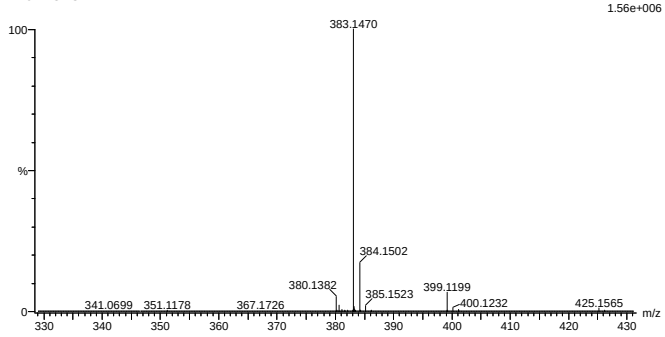

Minimum:				-50.0				
Maximum:		5.0	2.0	50.0				
Mass	Calc. Mass	mDa	PPM	DBE	i-FIT	Norm	Conf(%)	Formula
383.1470	383.1471	-0.1	-0.3	8.5	1149.2	1.114	32.82	C20 H24 O6 Na
	383.1468	0.2	0.5	12.5	1148.5	0.398	67.18	C18 H19 N6 O4

Figure 227: HRMS (ESI+) of **4b-α**.

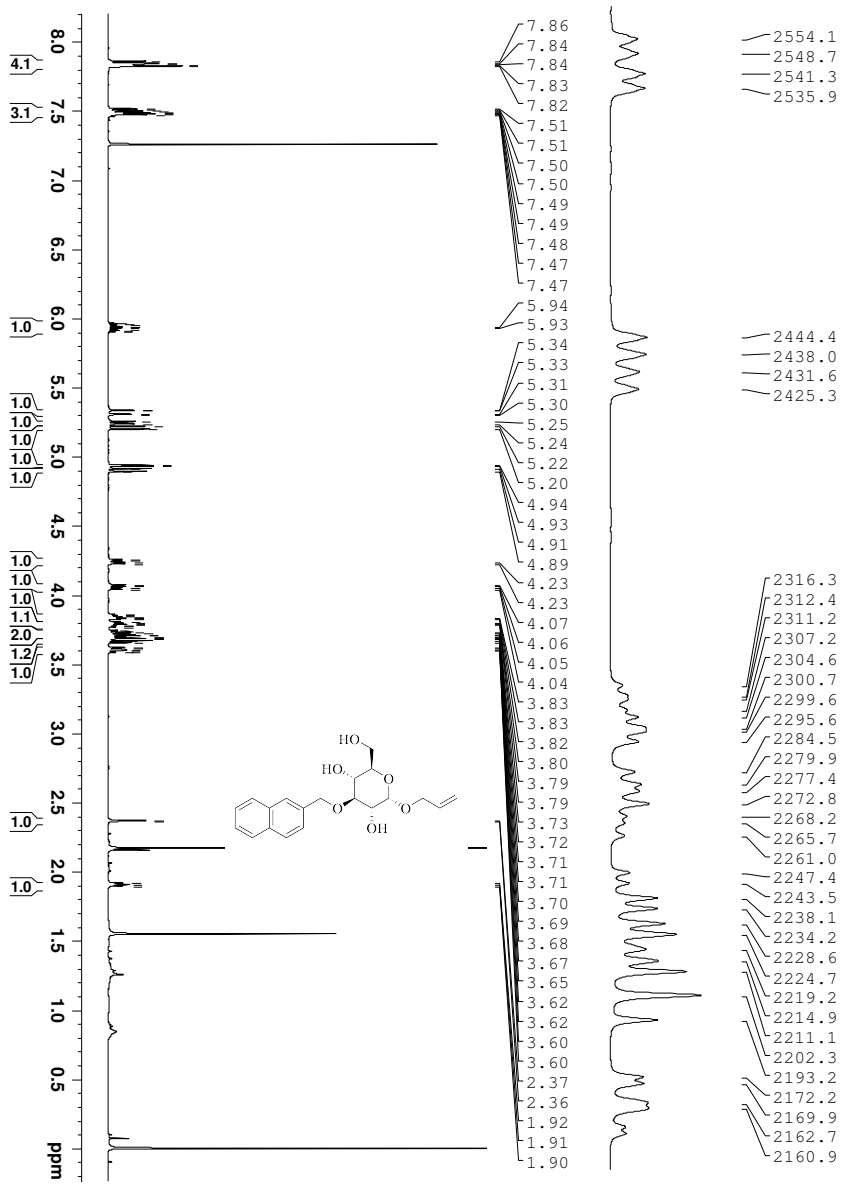

Figure 228: ^{1}H NMR spectrum of **4b-α**.

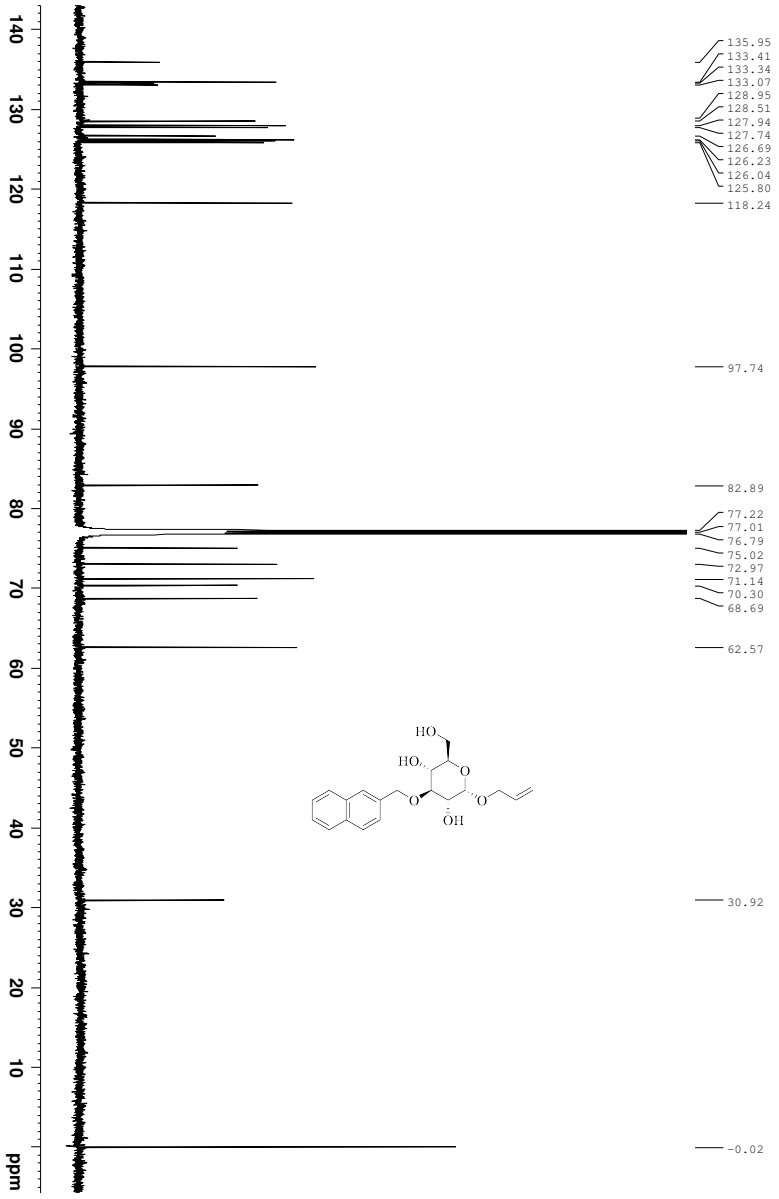

Figure 229: ^{13}C NMR spectrum of **4b-α**.

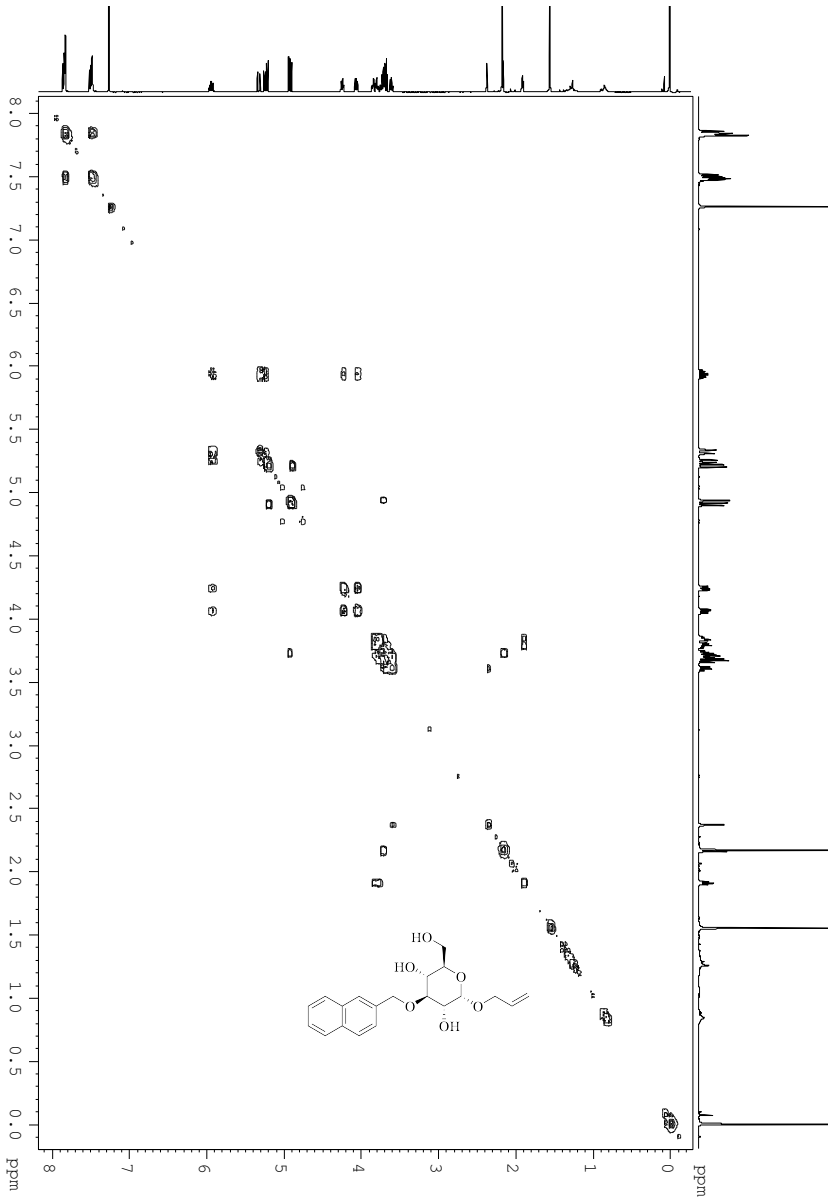

Figure 230: COSY spectrum of **4b-α**.

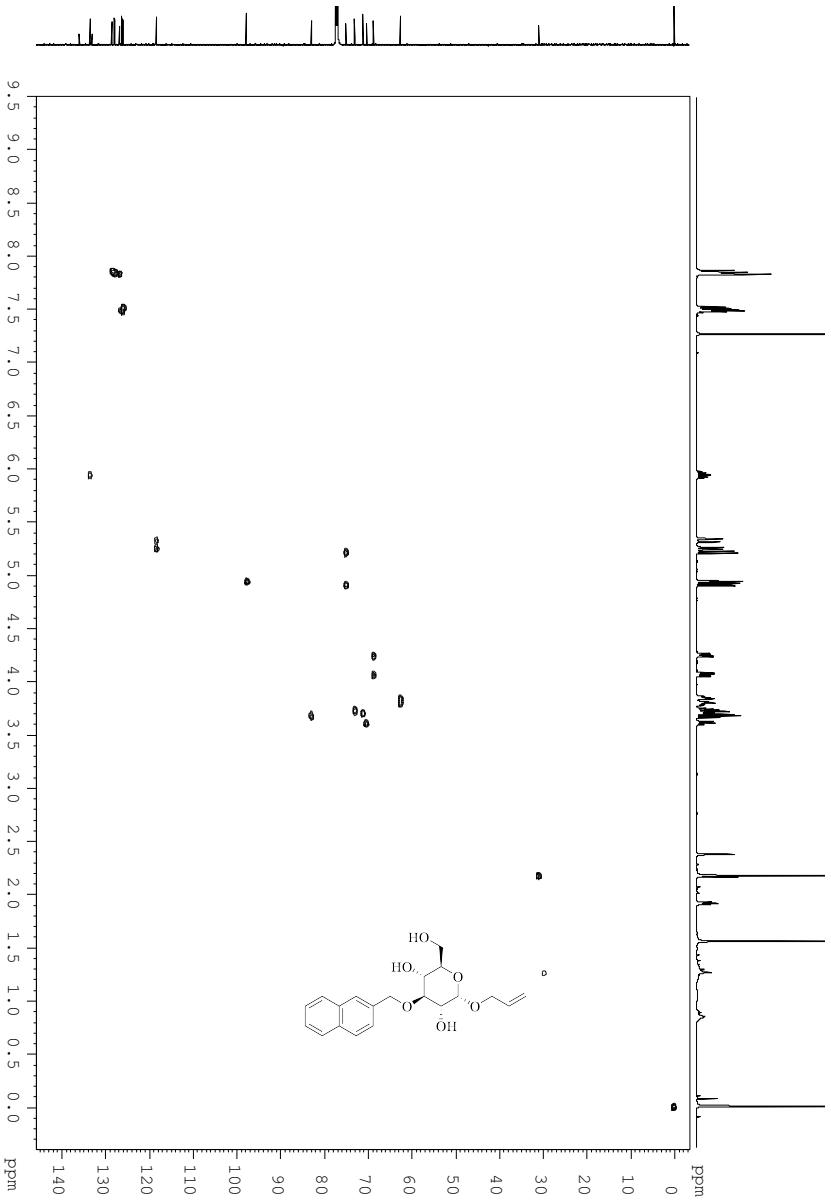

Figure 231: HSQC spectrum of **4b-α**.

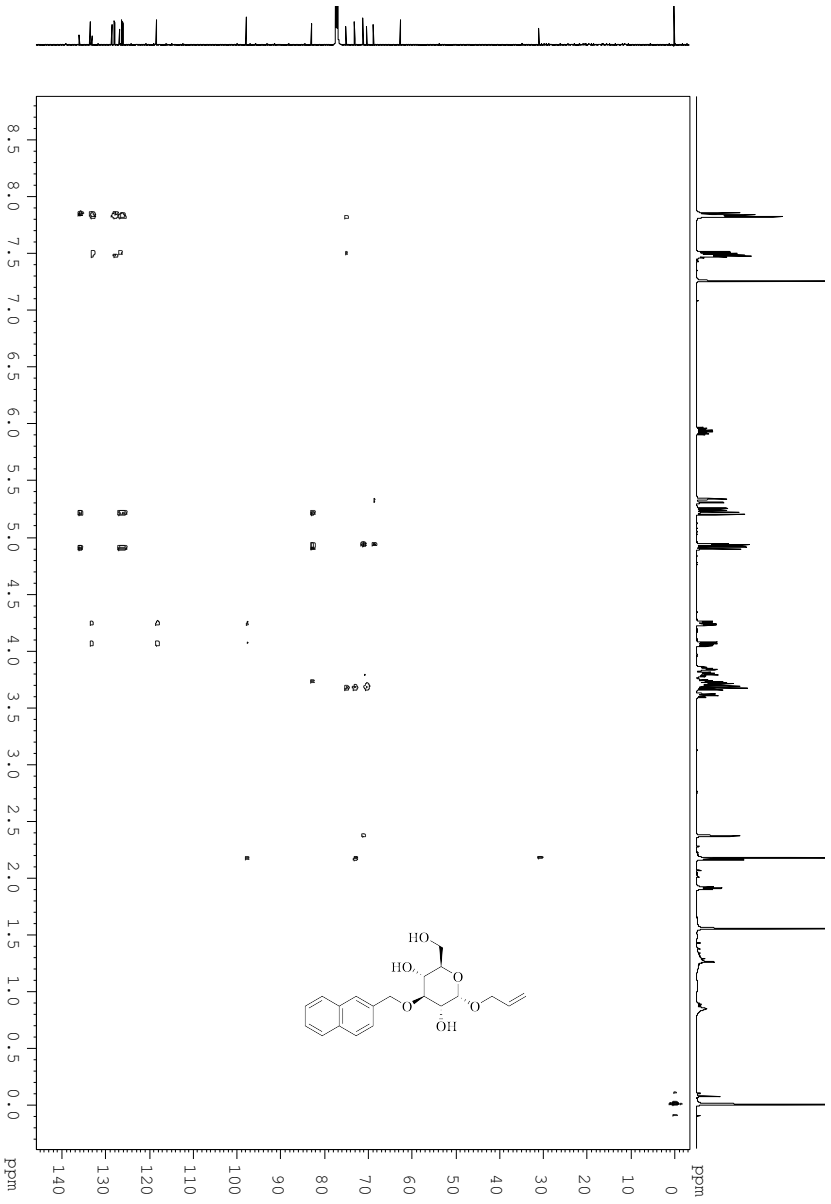

Figure 232: HMBC spectrum of **4b-α**.

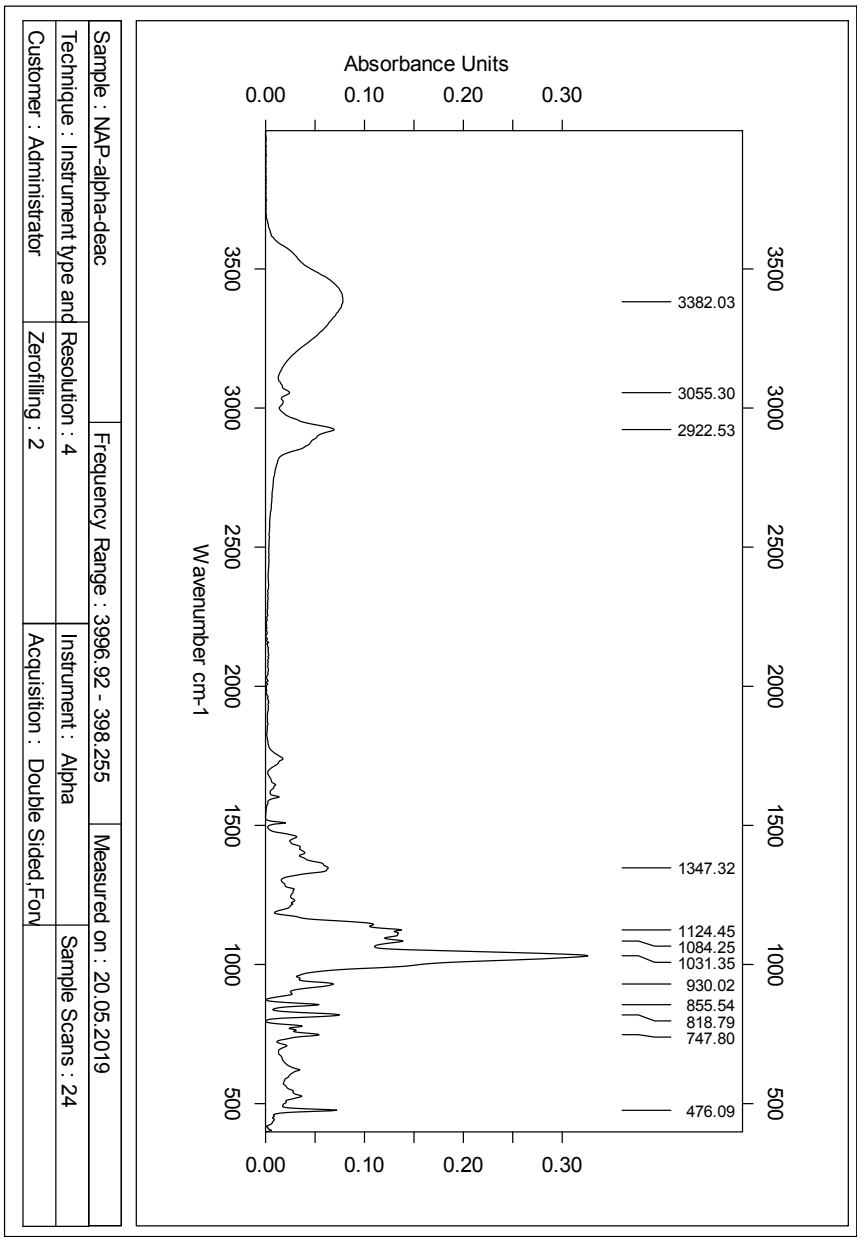

Figure 233: IR spectrum of **4b-α**.

B.30 Spectroscopic data for compound 4b-β

Elemental Composition Report **Page 1**

Single Mass Analysis
Tolerance = 5.0 PPM / DBE: min = -2.0, max = 50.0
Element prediction: Off
Number of isotope peaks used for i-FIT = 3

Monoisotopic Mass, Even Electron Ions
102 formula(e) evaluated with 1 results within limits (all results (up to 1000) for each mass)
Elements Used:
C: 0-100 H: 0-150 O: 0-10 Na: 0-1

svg_20190211_83 43 (0.802) AM2 (Ar,35000.0,0.00,0.00); Cm (43:45)
1: TOF MS ES+

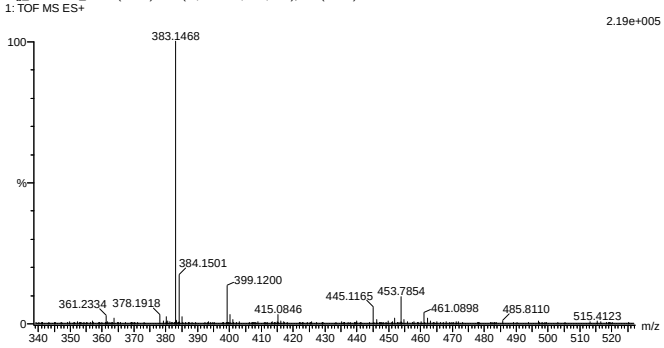

Minimum:				-2.0				
Maximum:		5.0	5.0	50.0				
Mass	Calc. Mass	mDa	PPM	DBE	i-FIT	Norm	Conf(%)	Formula
383.1468	383.1471	-0.3	-0.8	8.5	870.9	n/a	n/a	C20 H24 O6 Na

Figure 234: HRMS (ESI+) of **4b-β**.

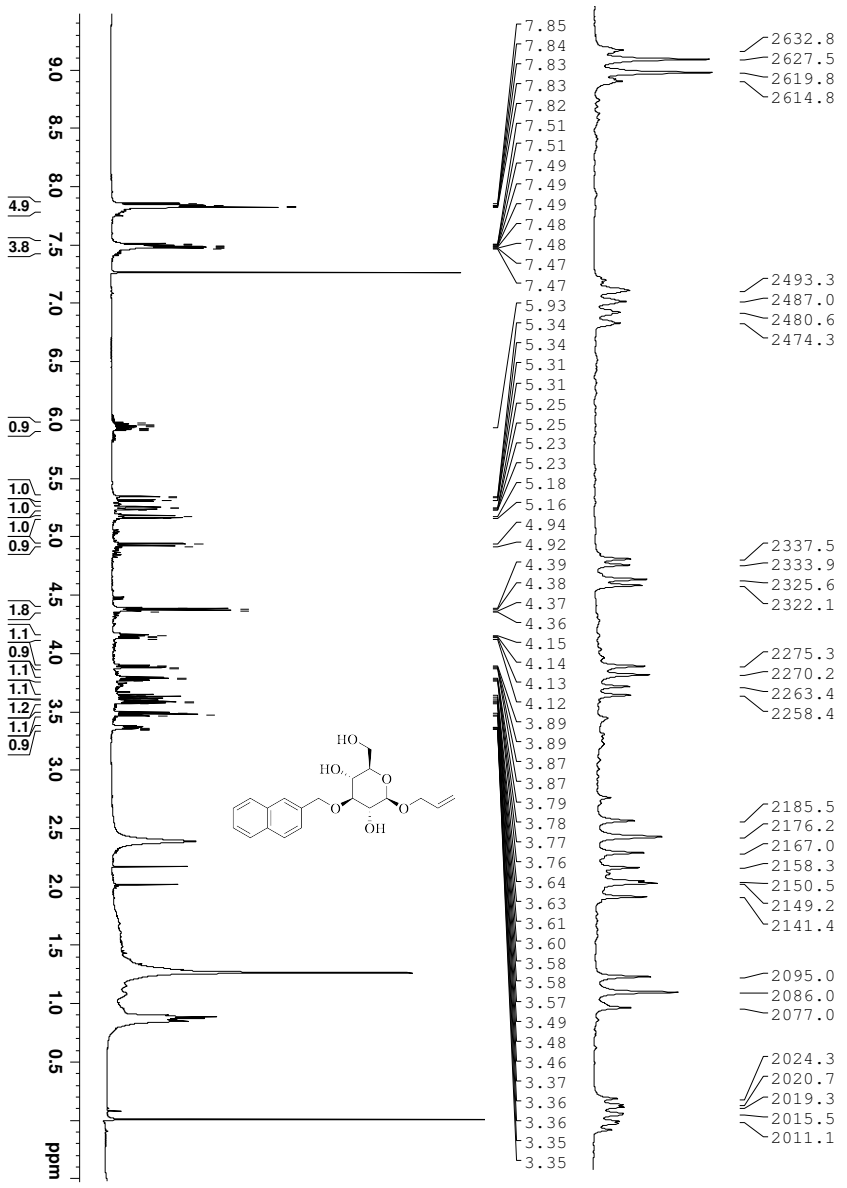

Figure 235: ^{1}H NMR spectrum of **4b-β**.

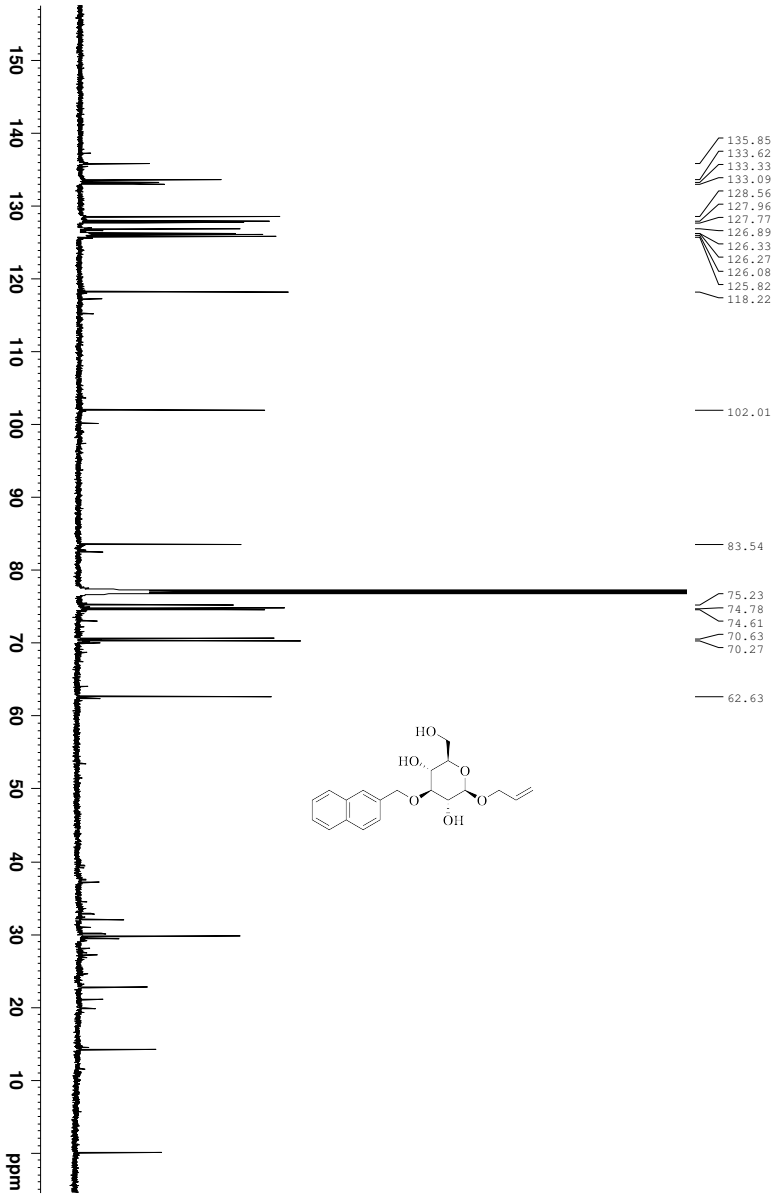

Figure 236: ^{13}C NMR spectrum of **4b-β**.

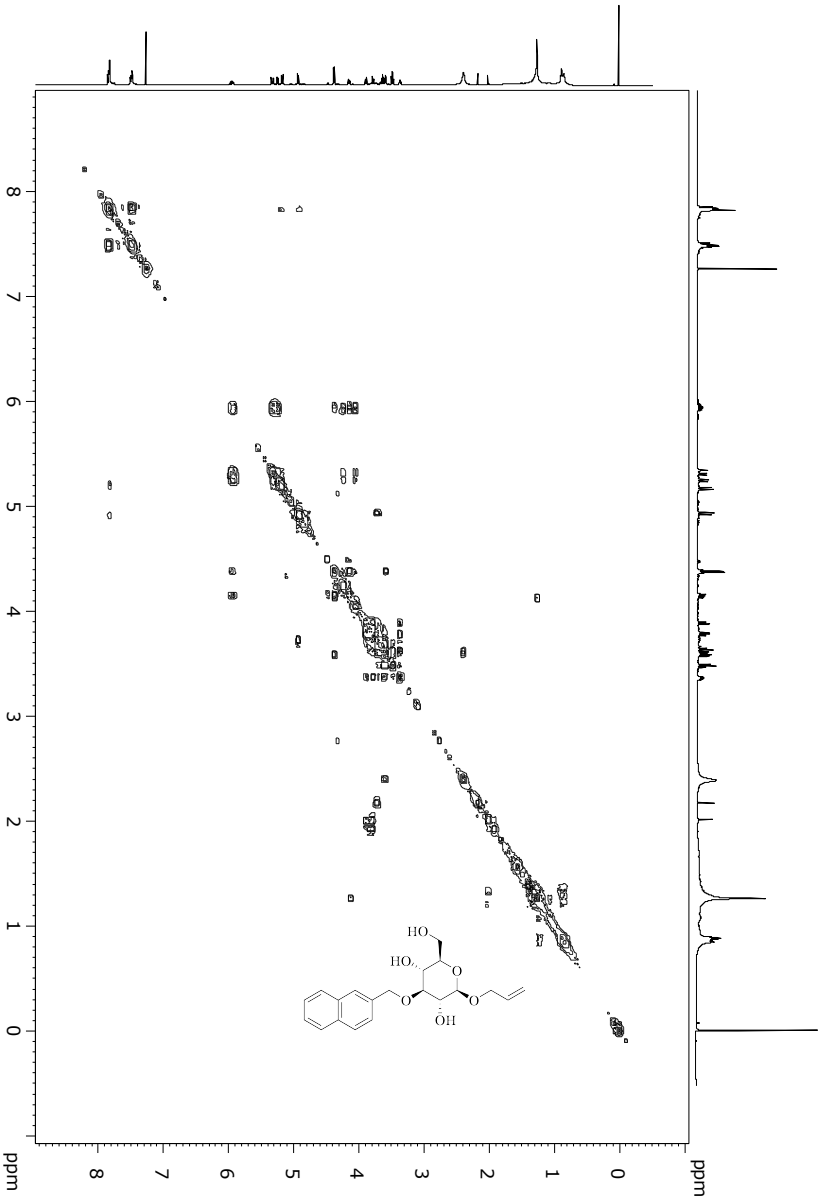

Figure 237: COSY spectrum of **4b-β**.

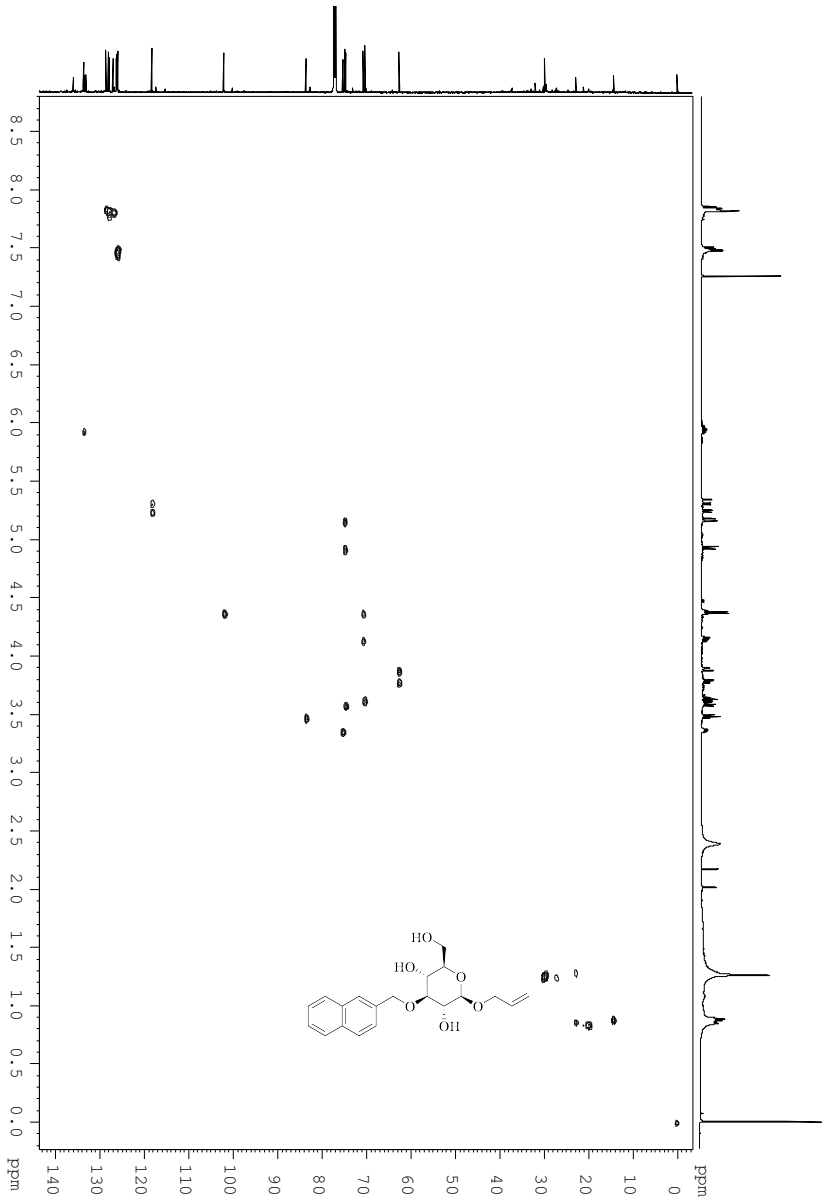

Figure 238: HSQC spectrum of **4b-β**.

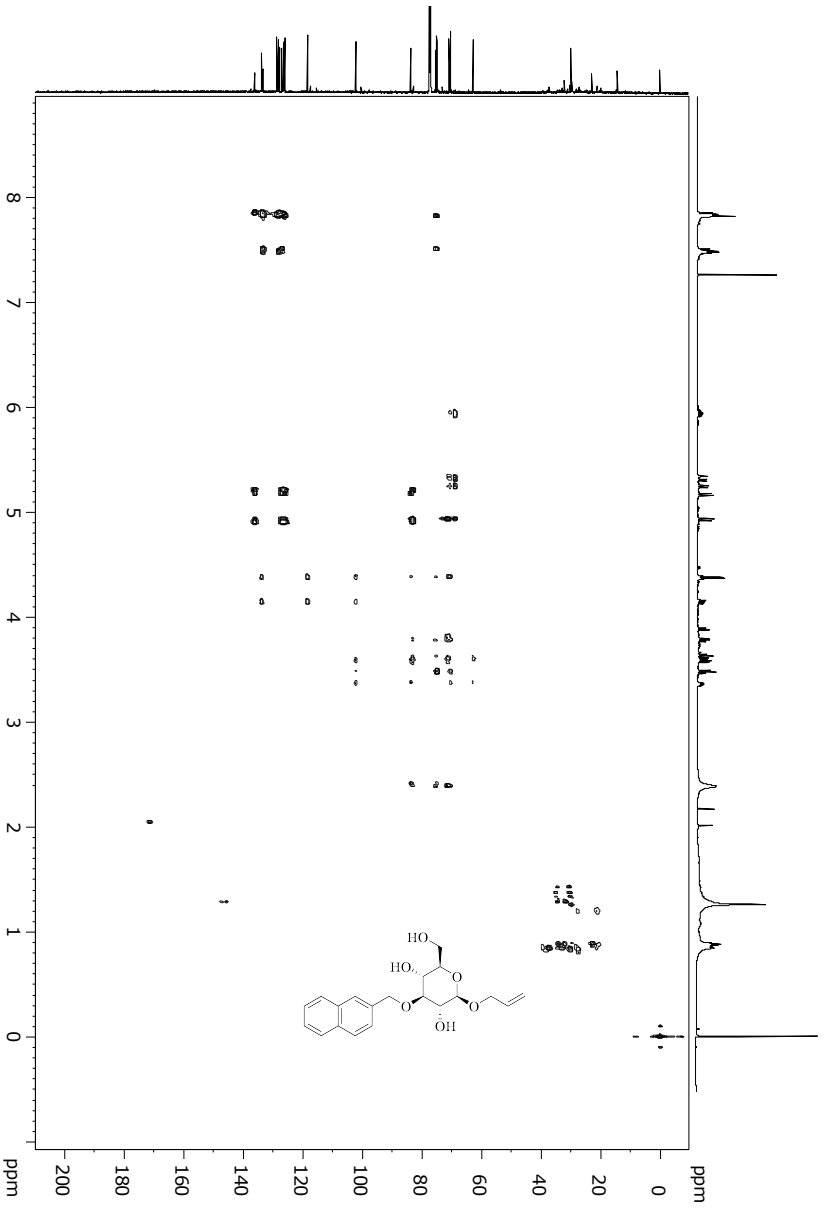

Figure 239: HMBC spectrum of **4b-β**.

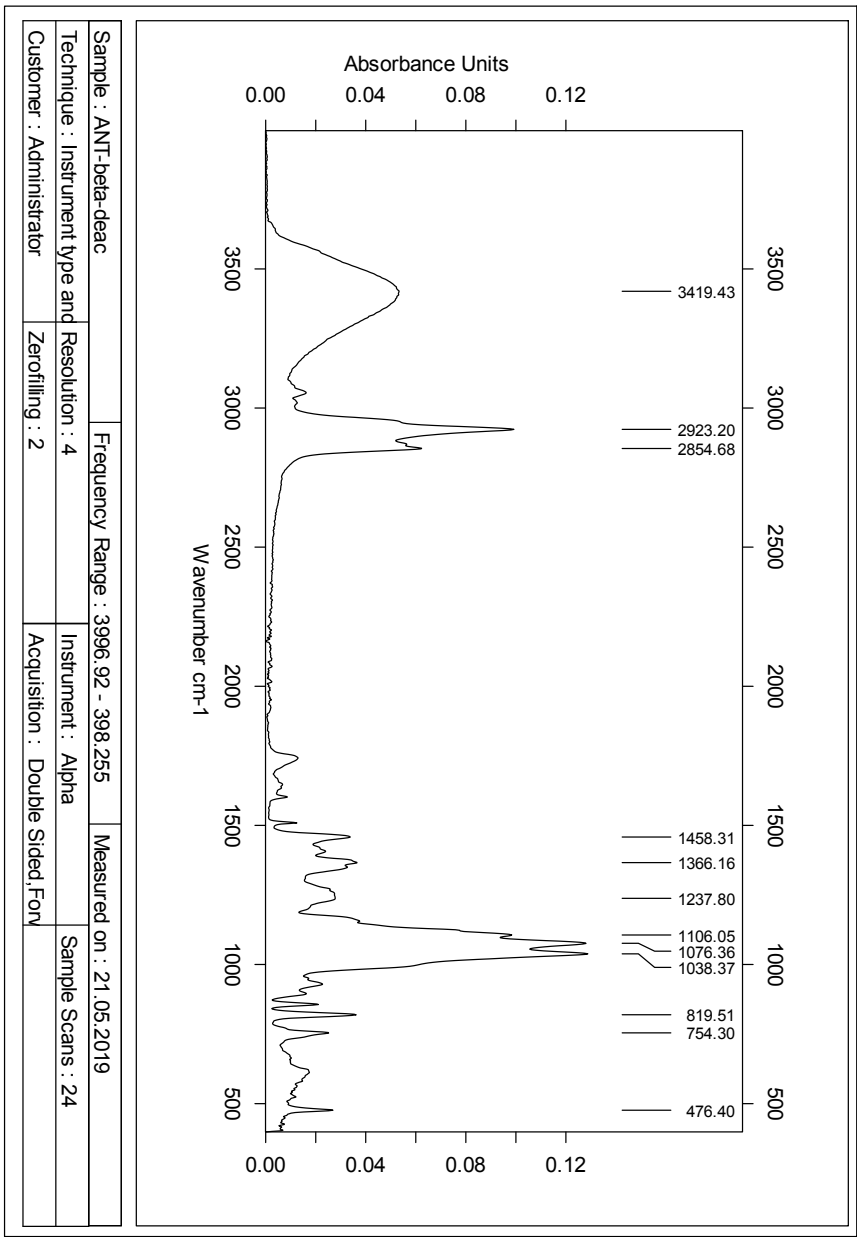

Figure 240: IR spectrum of **4b-β**.

B.31 Spectroscopic data for compound 4c

Elemental Composition Report **Page 1**

Single Mass Analysis
Tolerance = 2.0 PPM / DBE: min = -2.0, max = 50.0
Element prediction: Off
Number of isotope peaks used for i-FIT = 3

Monoisotopic Mass, Even Electron Ions
1053 formula(e) evaluated with 2 results within limits (all results (up to 1000) for each mass)
Elements Used:
C: 0-100 H: 0-150 N: 0-10 O: 0-10 Na: 0-1

svg_20190214_89 48 (0.899) AM2 (Ar,35000.0,0.00,0.00); Cm (48:66)
1: TOF MS ES+

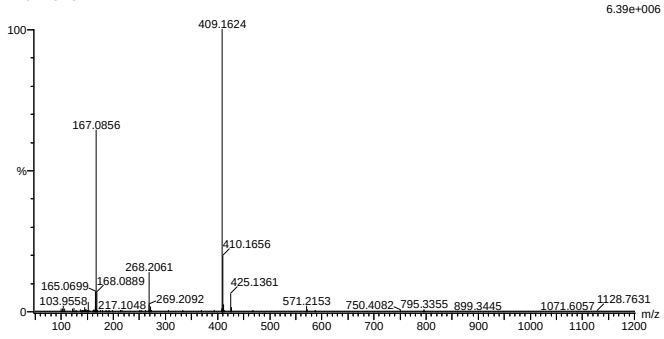

Minimum:				-2.0				
Maximum:		5.0	2.0	50.0				
Mass	**Calc. Mass**	**mDa**	**PPM**	**DBE**	**i-FIT**	**Norm**	**Conf(%)**	**Formula**
409.1624	409.1624	0.0	0.0	13.5	1271.4	0.297	74.28	C20 H21 N6 O4
	409.1627	-0.3	-0.7	9.5	1272.5	1.358	25.72	C22 H26 O6 Na

Figure 241: HRMS (ESI+) of anomeric mixture of **4c**.

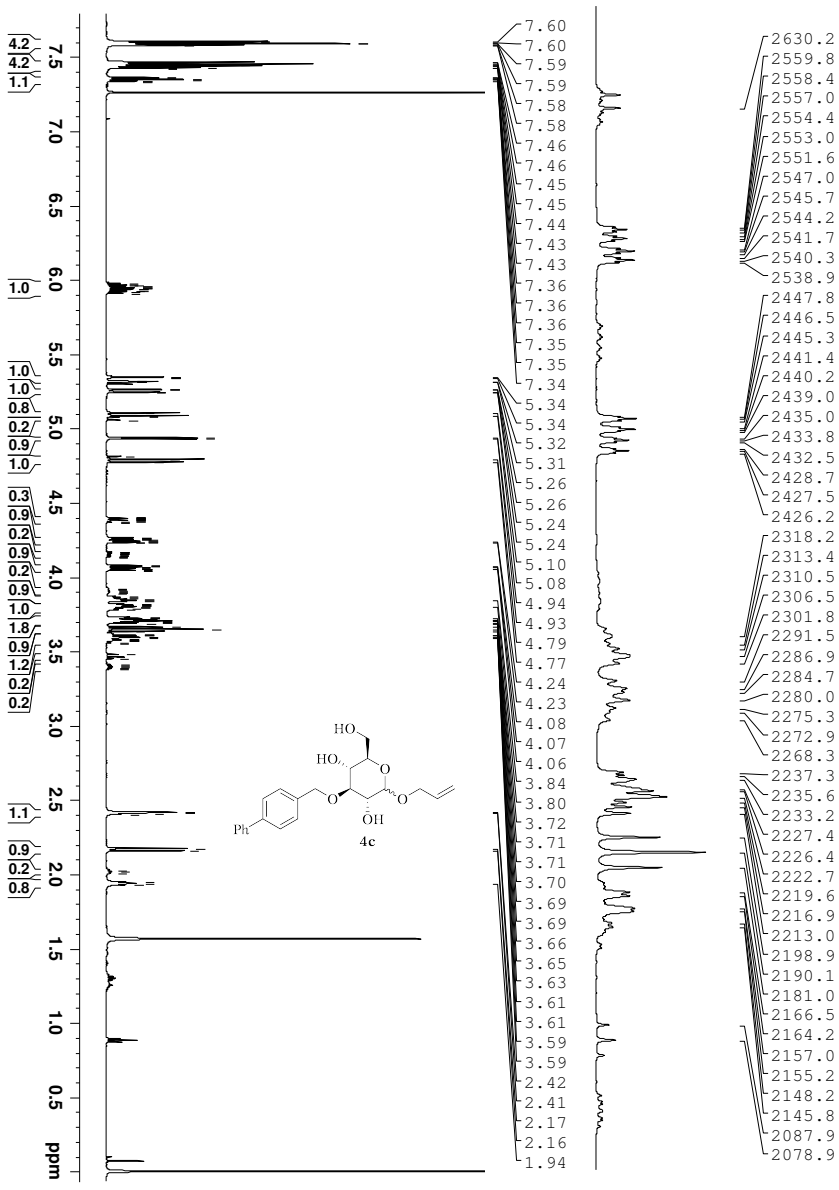

Figure 242: ^{1}H NMR spectrum of anomeric mixture of **4c**.

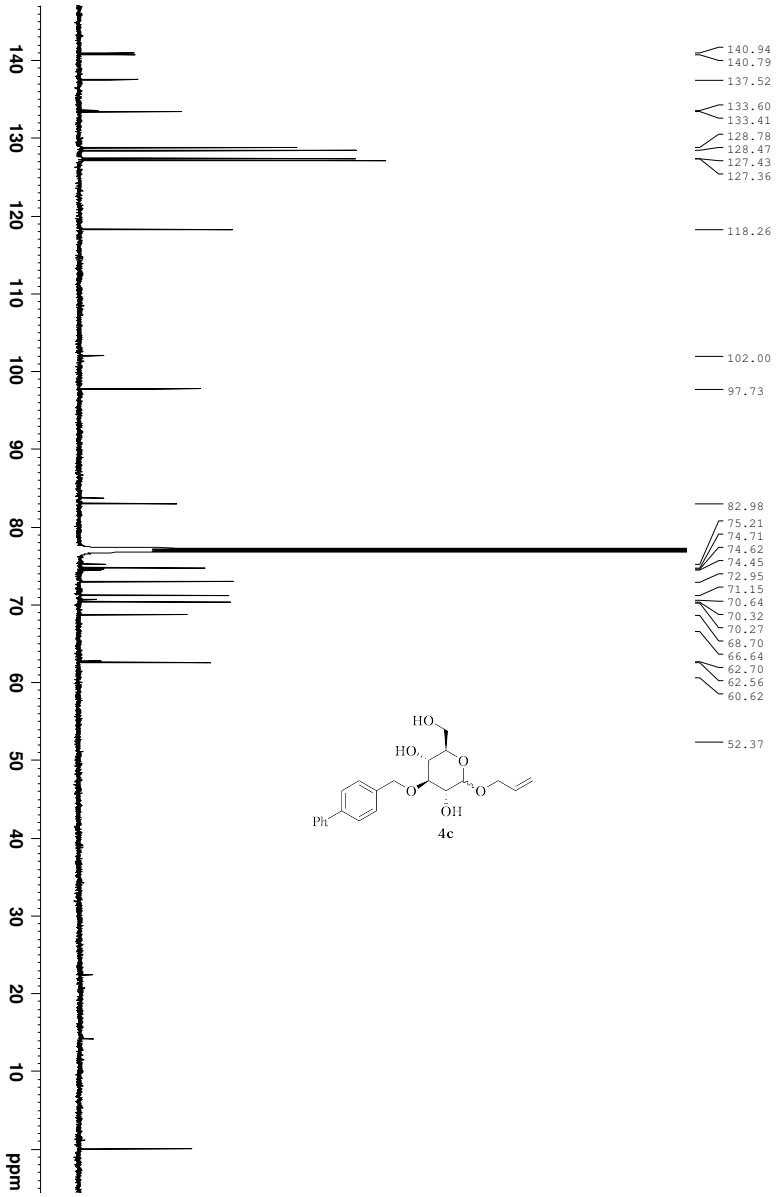

Figure 243: ^{13}C NMR spectrum of anomeric mixture of **4c**.

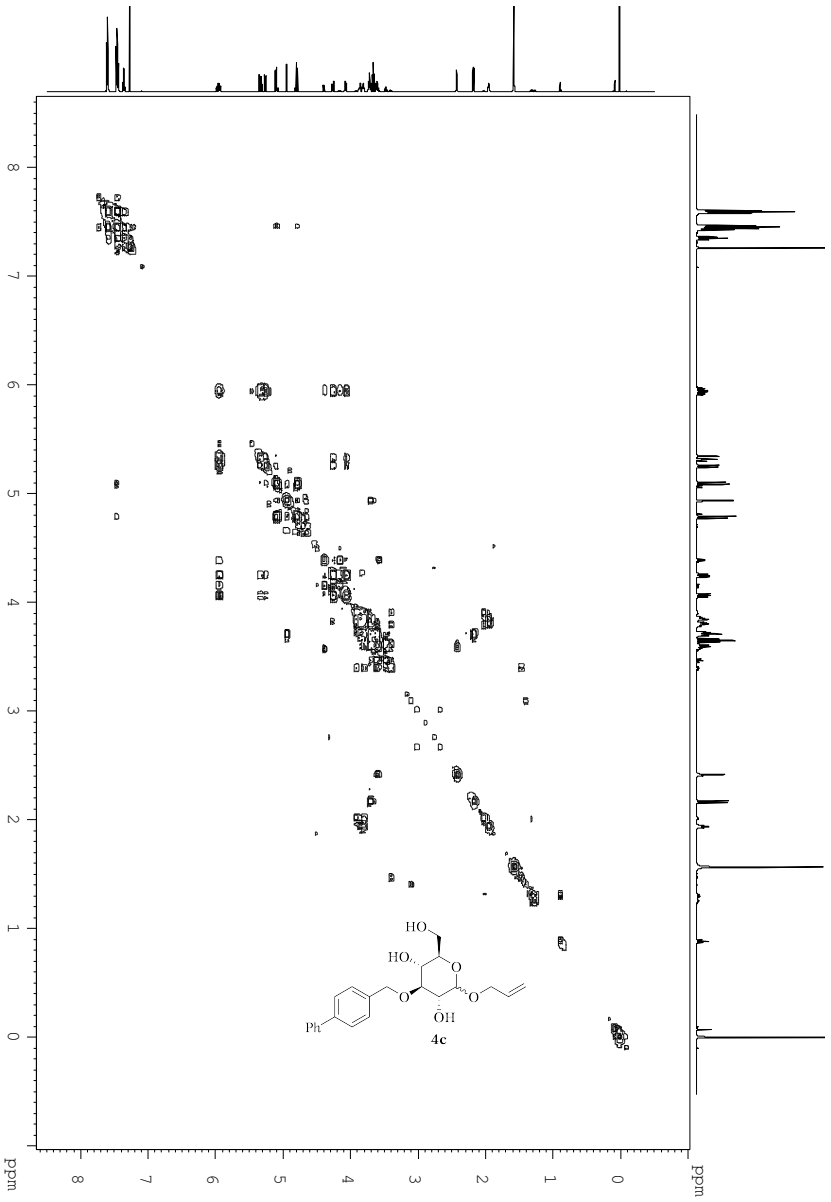

Figure 244: COSY spectrum of anomeric mixture of **4c**.

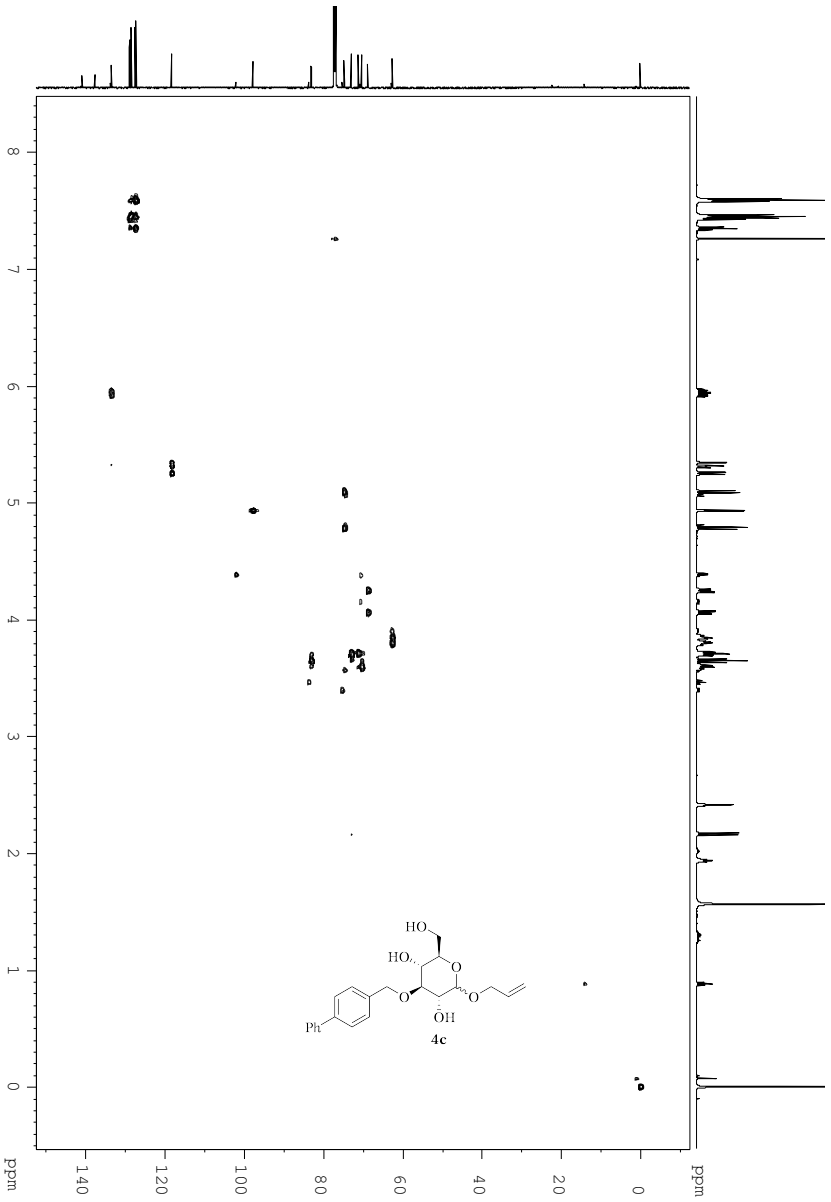

Figure 245: HSQC spectrum of anomeric mixture of **4c**.

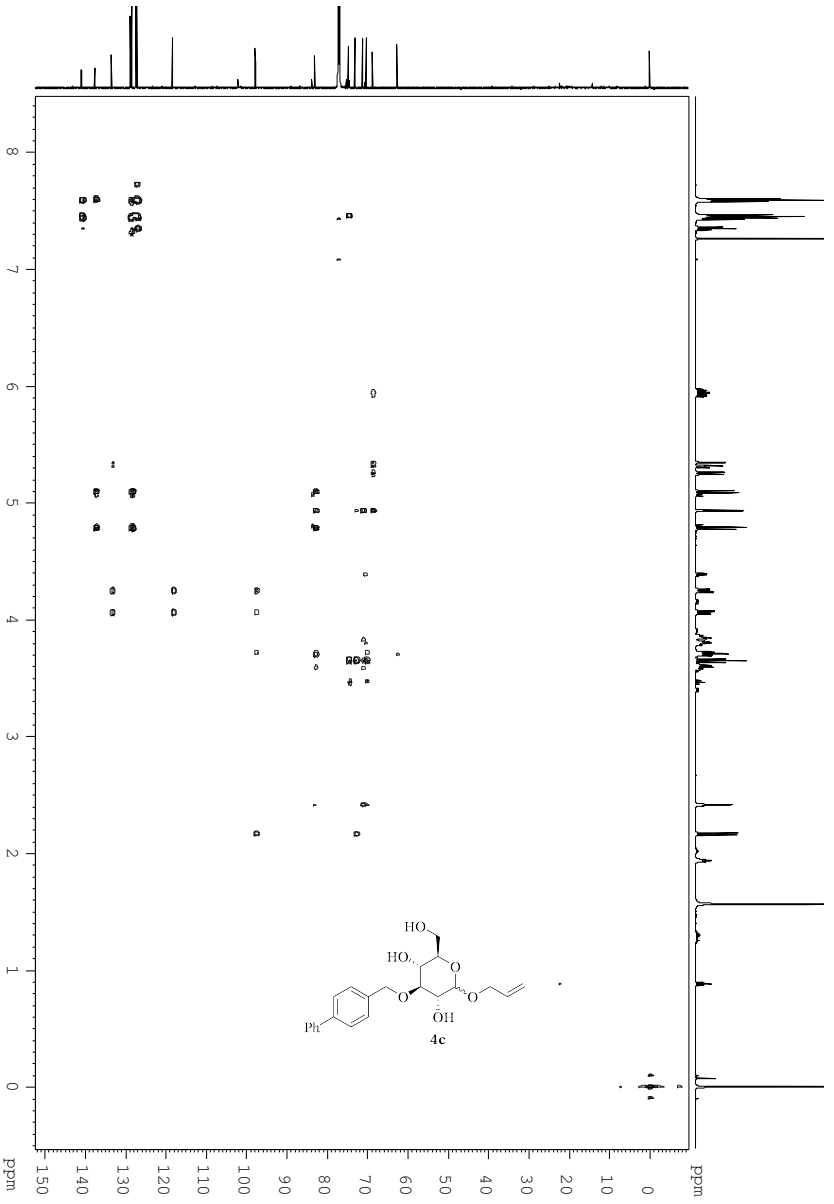

Figure 246: HMBC spectrum of anomeric mixture of **4c**.

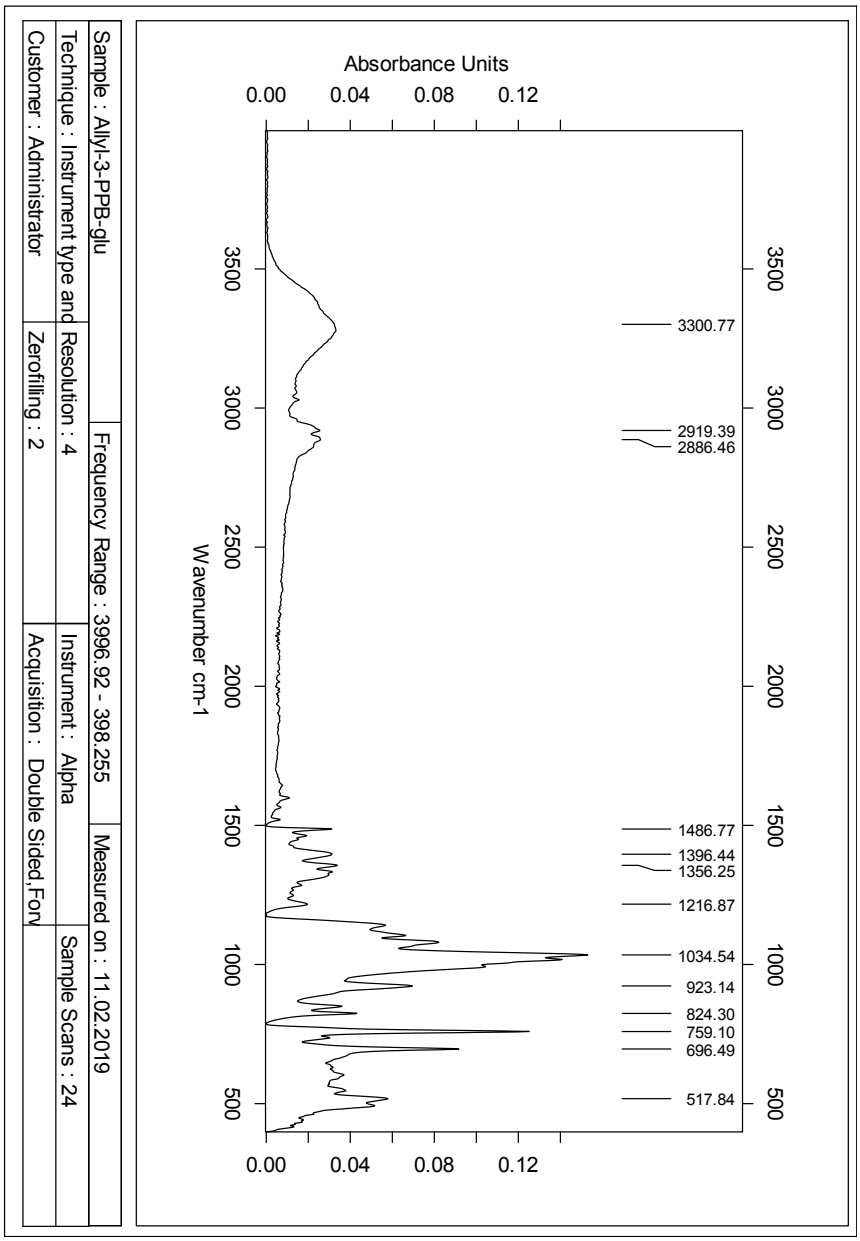

Figure 247: IR spectrum of anomeric mixture of **4c**.

B.32 Spectroscopic data for compound 4d

Elemental Composition Report **Page 1**

Single Mass Analysis
Tolerance = 2.0 PPM / DBE: min = -2.0, max = 50.0
Element prediction: Off
Number of isotope peaks used for i-FIT = 3

Monoisotopic Mass, Even Electron Ions
1156 formula(e) evaluated with 2 results within limits (all results (up to 1000) for each mass)
Elements Used:
C: 0-100 H: 0-150 N: 0-10 O: 0-10 Na: 0-1

svg_20190214_95 33 (0.620) AM2 (Ar,35000.0,0.00,0.00)
1: TOF MS ES+

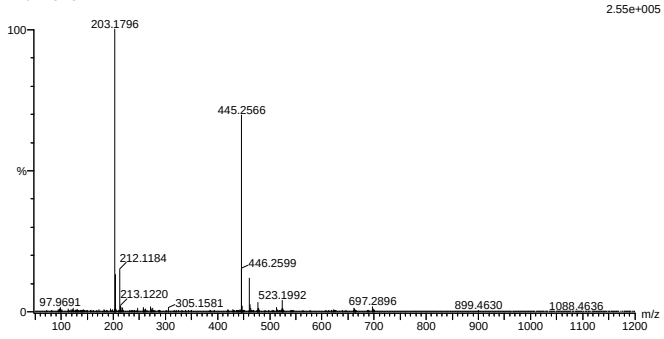

Minimum:				-2.0				
Maximum:		5.0	2.0	50.0				
Mass	Calc. Mass	mDa	PPM	DBE	i-FIT	Norm	Conf(%)	Formula
445.2566	445.2566	0.0	0.0	5.5	708.3	0.151	85.95	C24 H38 O6 Na
	445.2563	0.3	0.7	9.5	710.1	1.963	14.05	C22 H33 N6 O4

Figure 248: HRMS (ESI+) of anomeric mixture of **4d**.

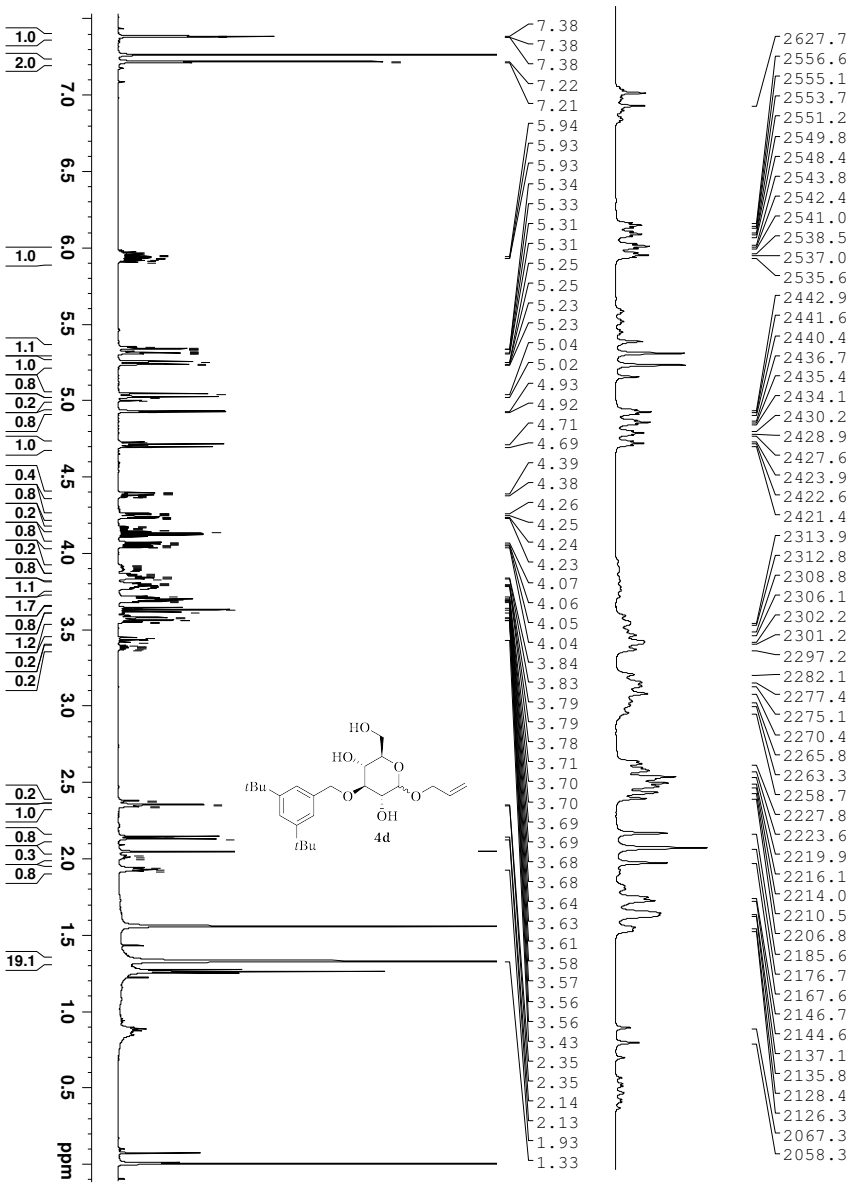

Figure 249: ^{1}H NMR spectrum of anomeric mixture of **4d**.

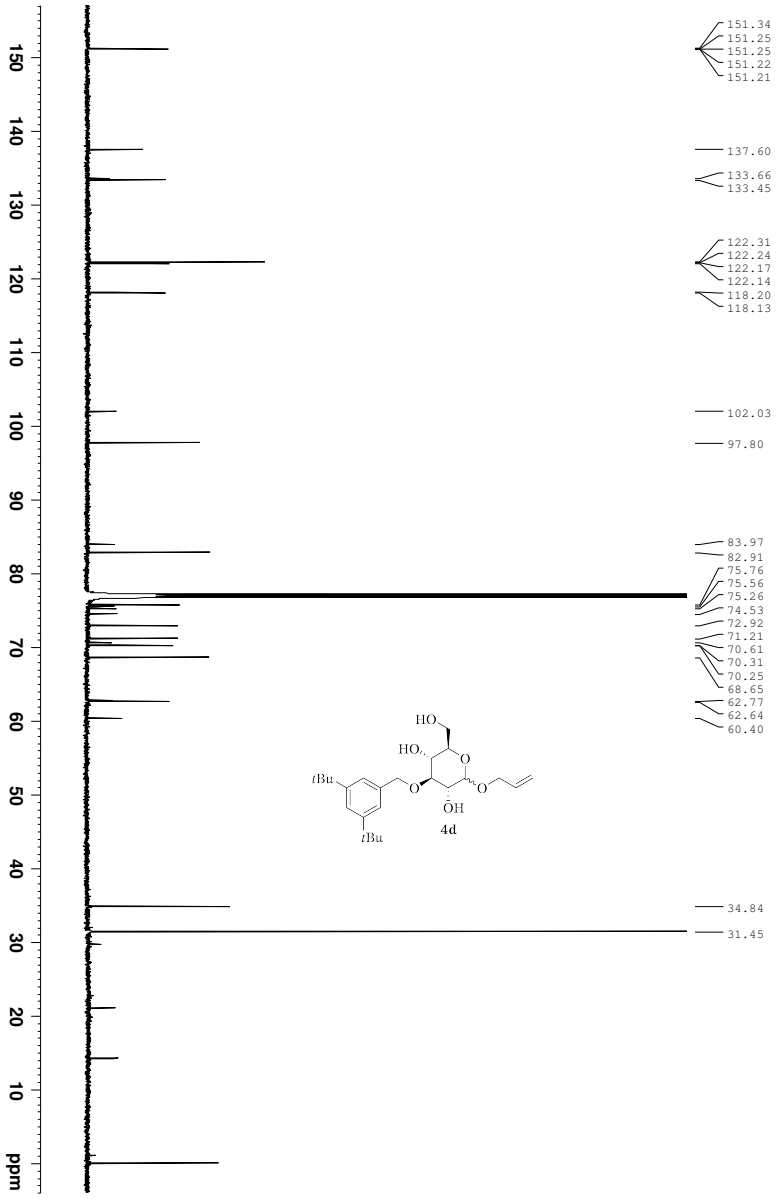

Figure 250: ^{13}C NMR spectrum of anomeric mixture of **4d**.

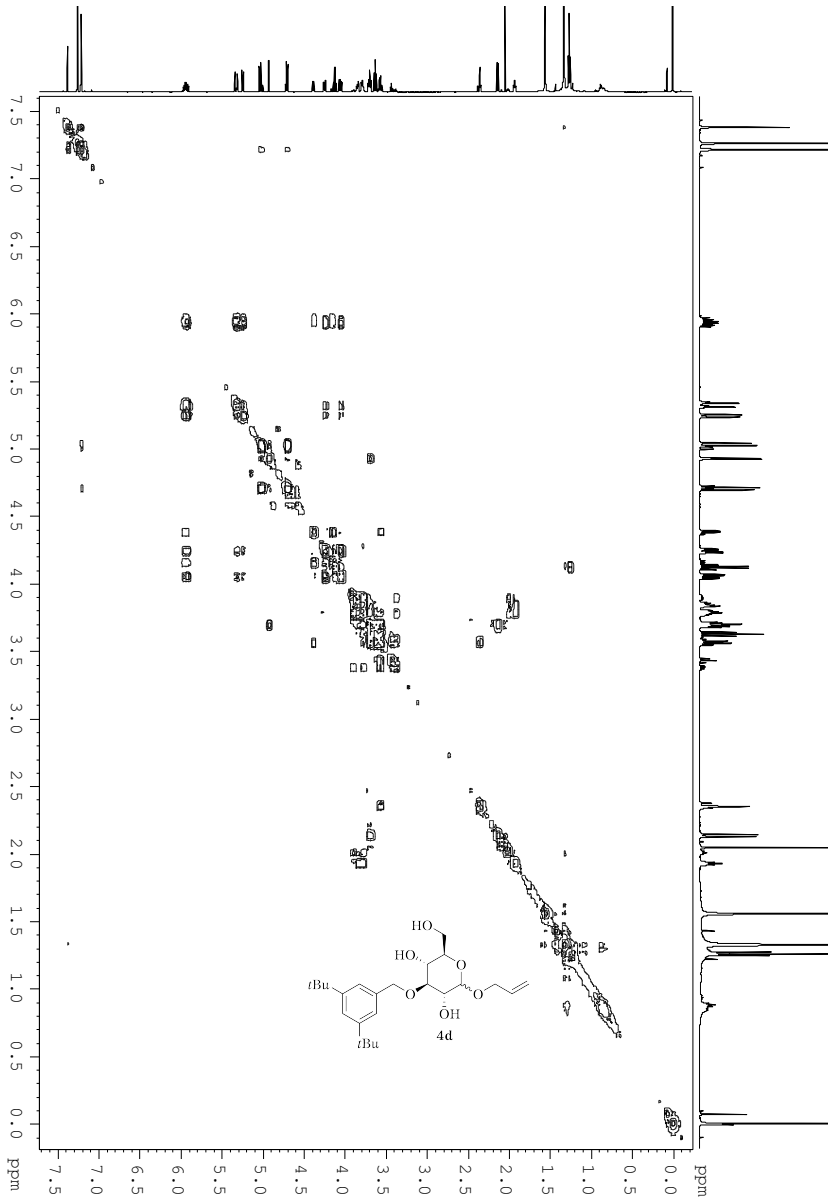

Figure 251: COSY spectrum of anomeric mixture of **4d**.

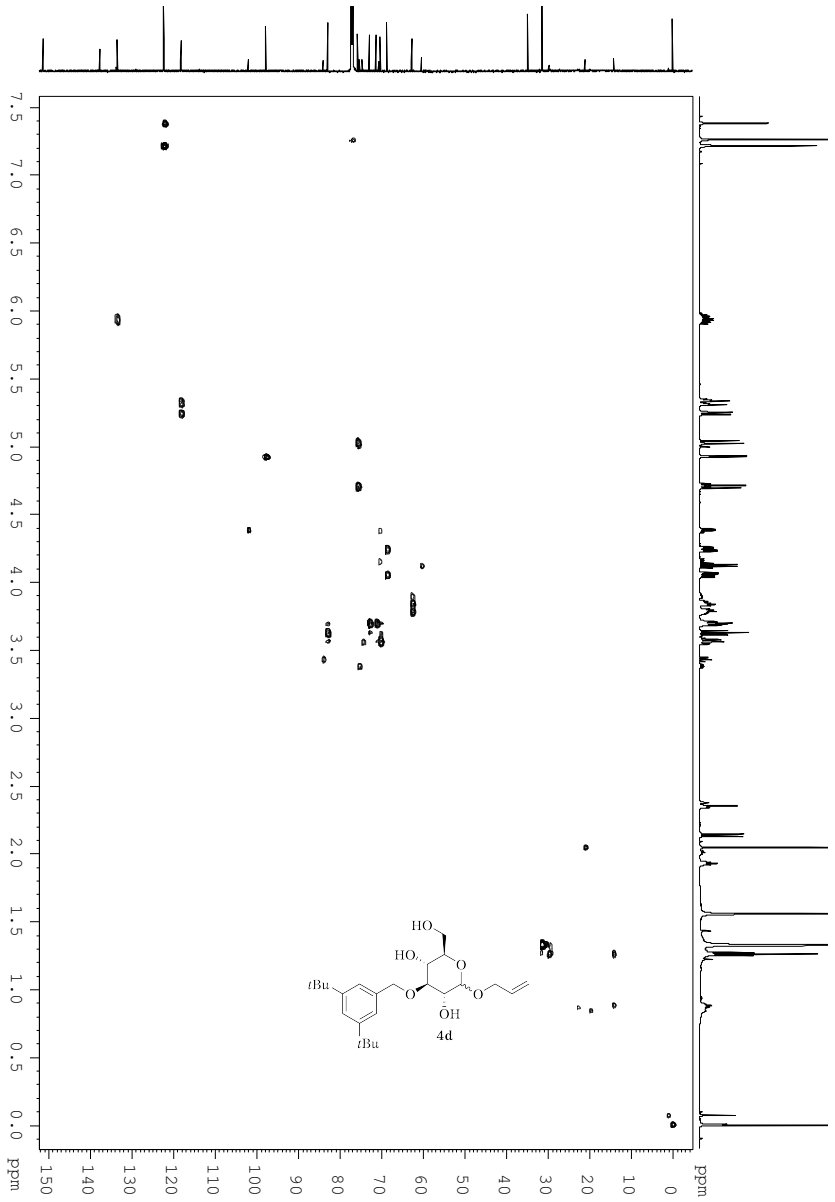

Figure 252: HSQC spectrum of anomeric mixture of **4d**.

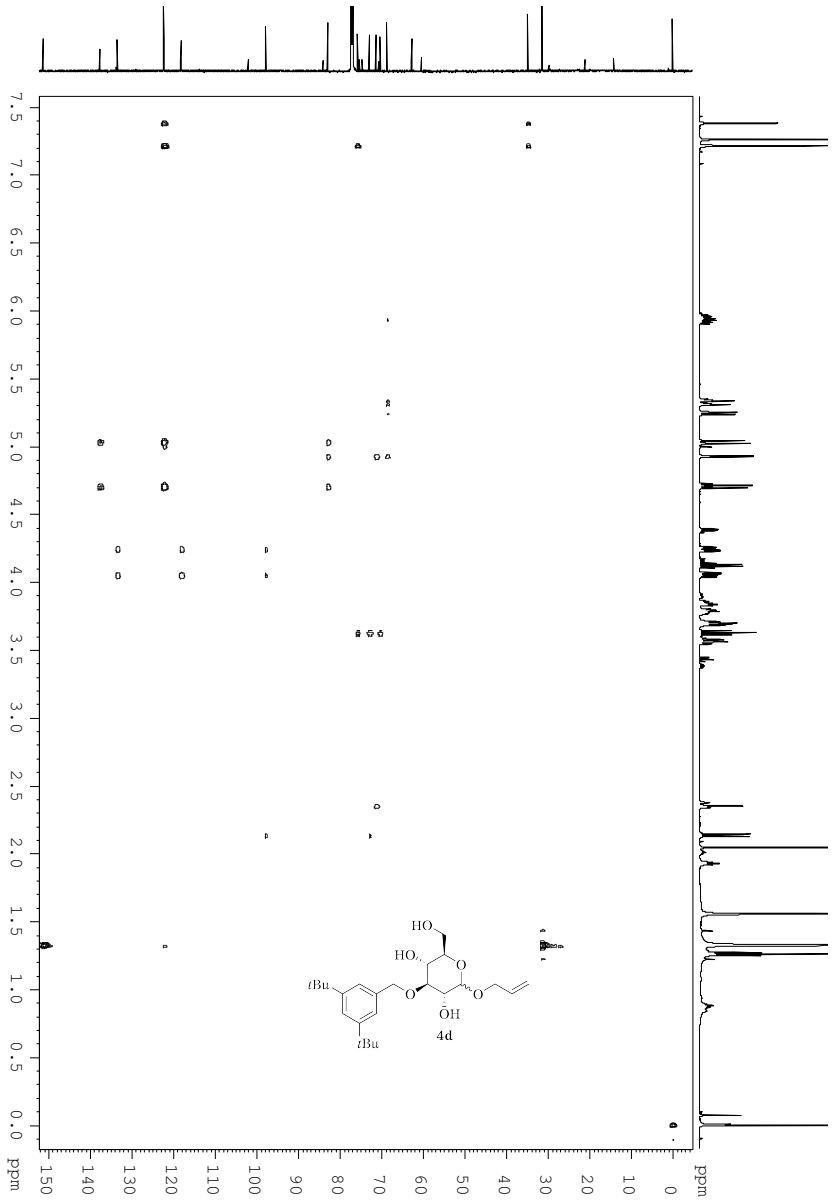

Figure 253: HMBC spectrum of anomeric mixture of **4d**.

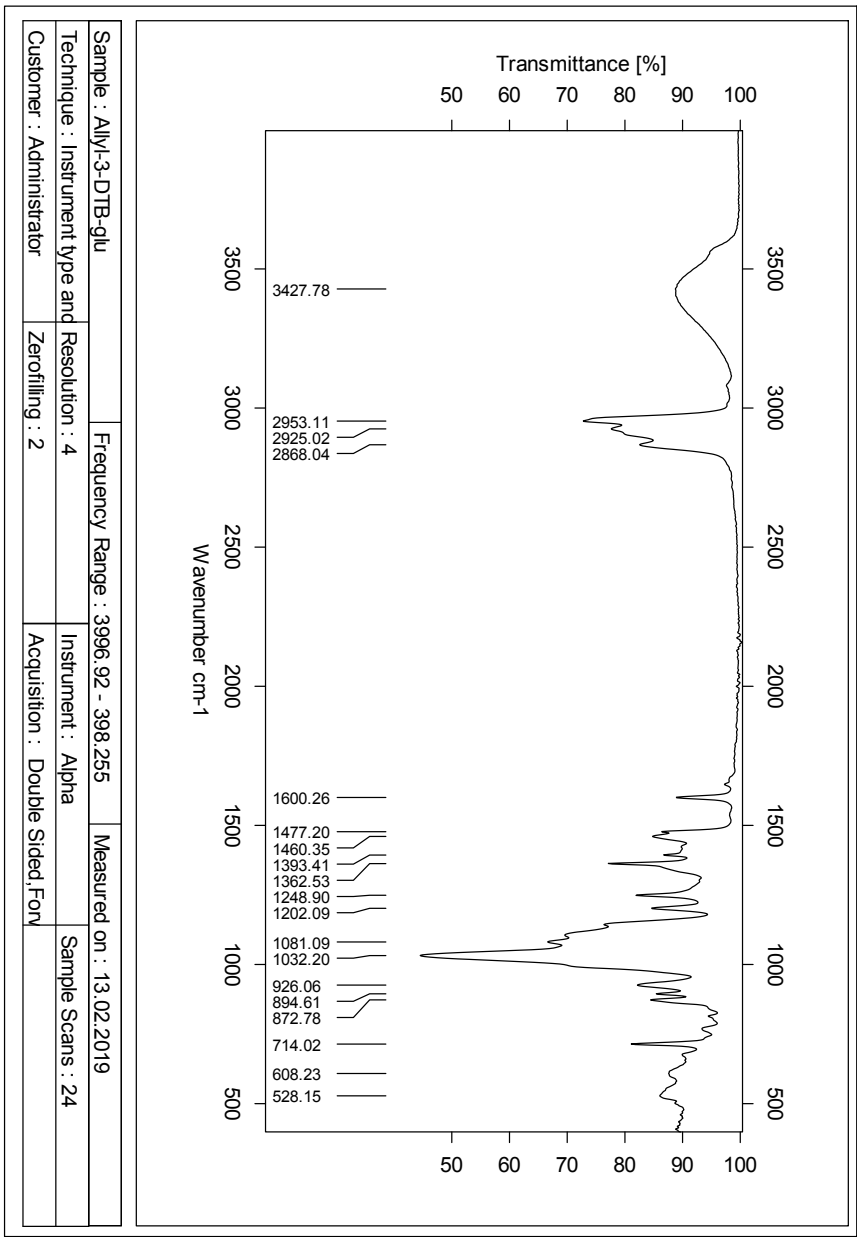

Figure 254: IR spectrum of anomeric mixture of **4d**.

B.33 Spectroscopic data for compound 4f-α

Elemental Composition Report **Page 1**

Tolerance = 2.0 PPM / DBE: min = -50.0, max = 50.0
Element prediction: Off
Number of isotope peaks used for i-FIT = 3

Monoisotopic Mass, Even Electron Ions
803 formula(e) evaluated with 2 results within limits (all results (up to 1000) for each mass)
Elements Used:
C: 2-100 H: 0-150 O: 0-10 Na: 0-1 Si: 0-2
2019_578 46 (0.525) AM2 (Ar,35000.0,0.00,0.00); ABS; Cm (38:46)
1: TOF MS ES+

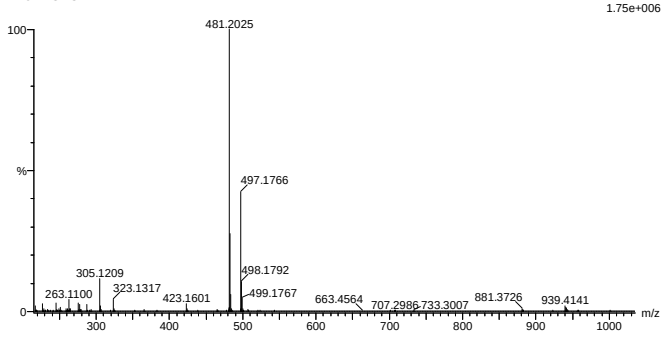

Minimum:	80.00				-50.0				
Maximum:	100.00		5.0	2.0	50.0				
Mass	RA	Calc. Mass	mDa	PPM	DBE	i-FIT	Norm	Conf(%)	Formula
481.2025	100.00	481.2022	0.3	0.6	9.5	1055.3	0.004	99.64	C25 H34 O6 Na Si
		481.2019	0.6	1.2	16.5	1060.9	5.622	0.36	C30 H33 O2 Si2

Figure 255: HRMS (ESI+) of **4f-α**.

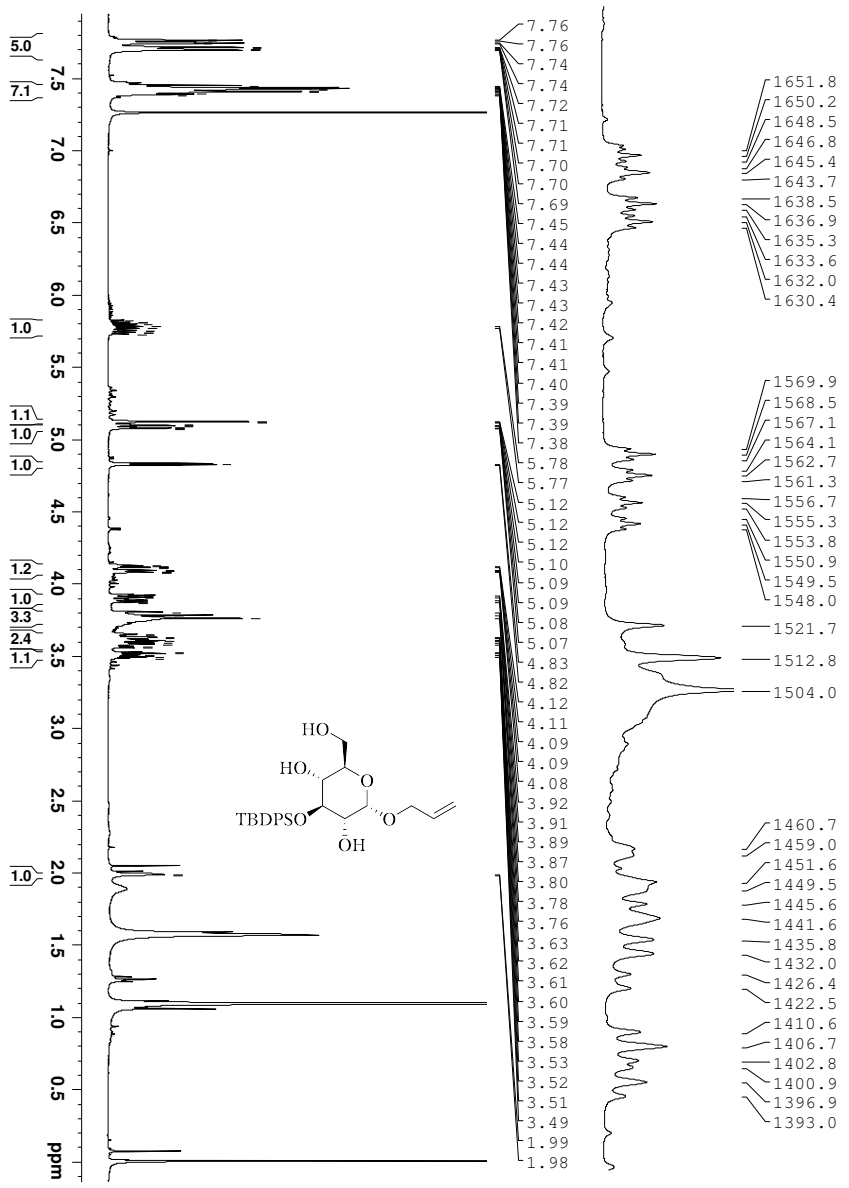

Figure 256: ^{1}H NMR (400 MHz) spectrum of **4f-α**.

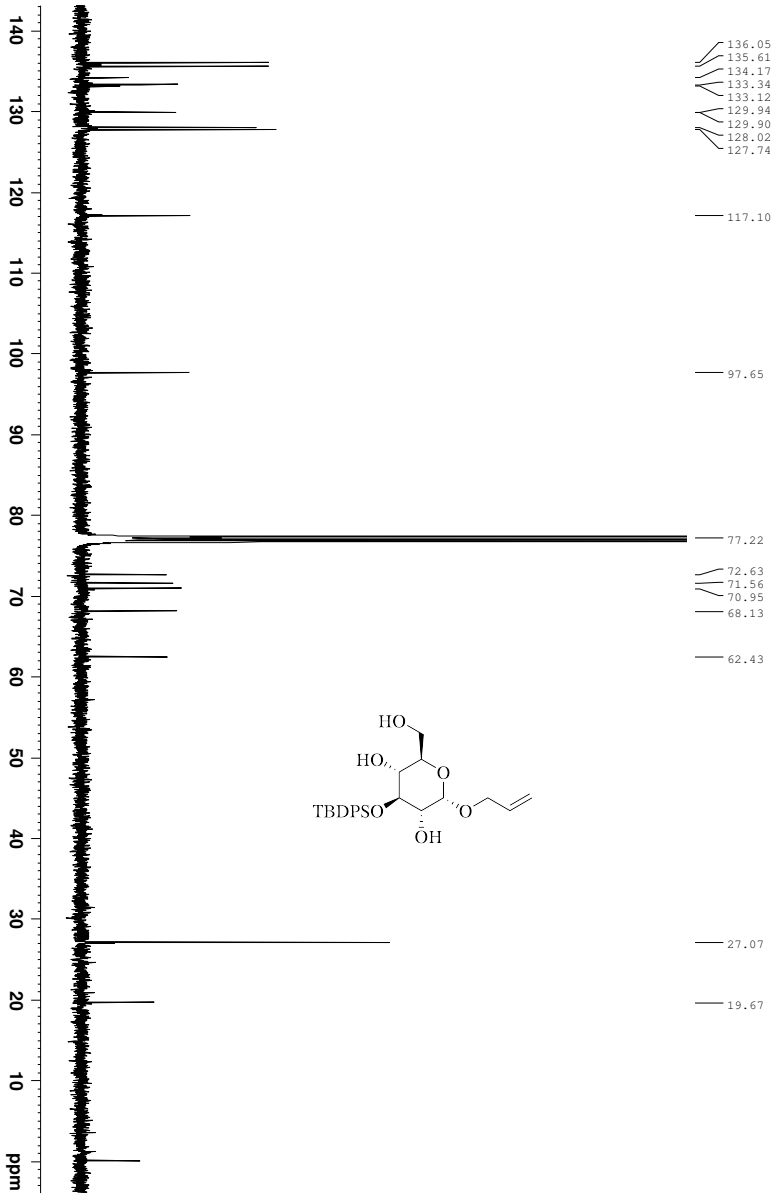

Figure 257: ^{13}C NMR (100 MHz) spectrum of **4f-α**.

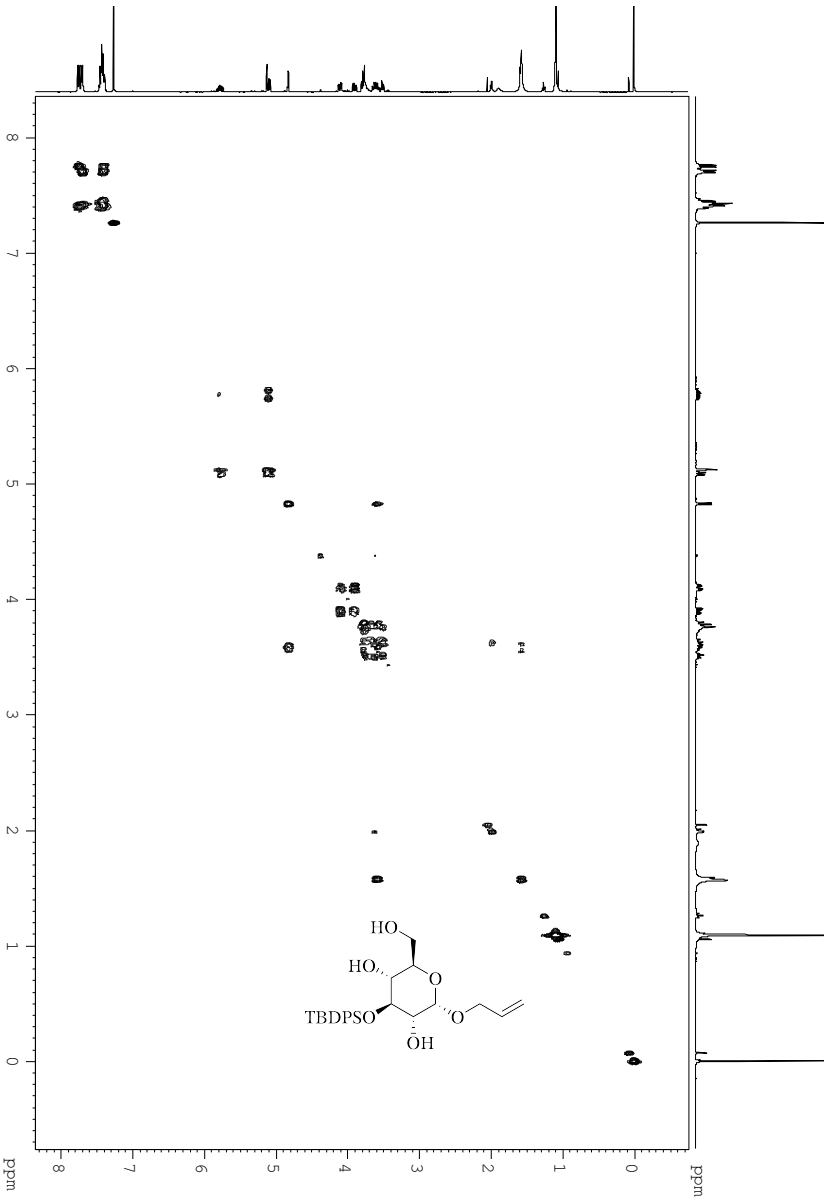

Figure 258: COSY (400 MHz) spectrum of **4f-α**.

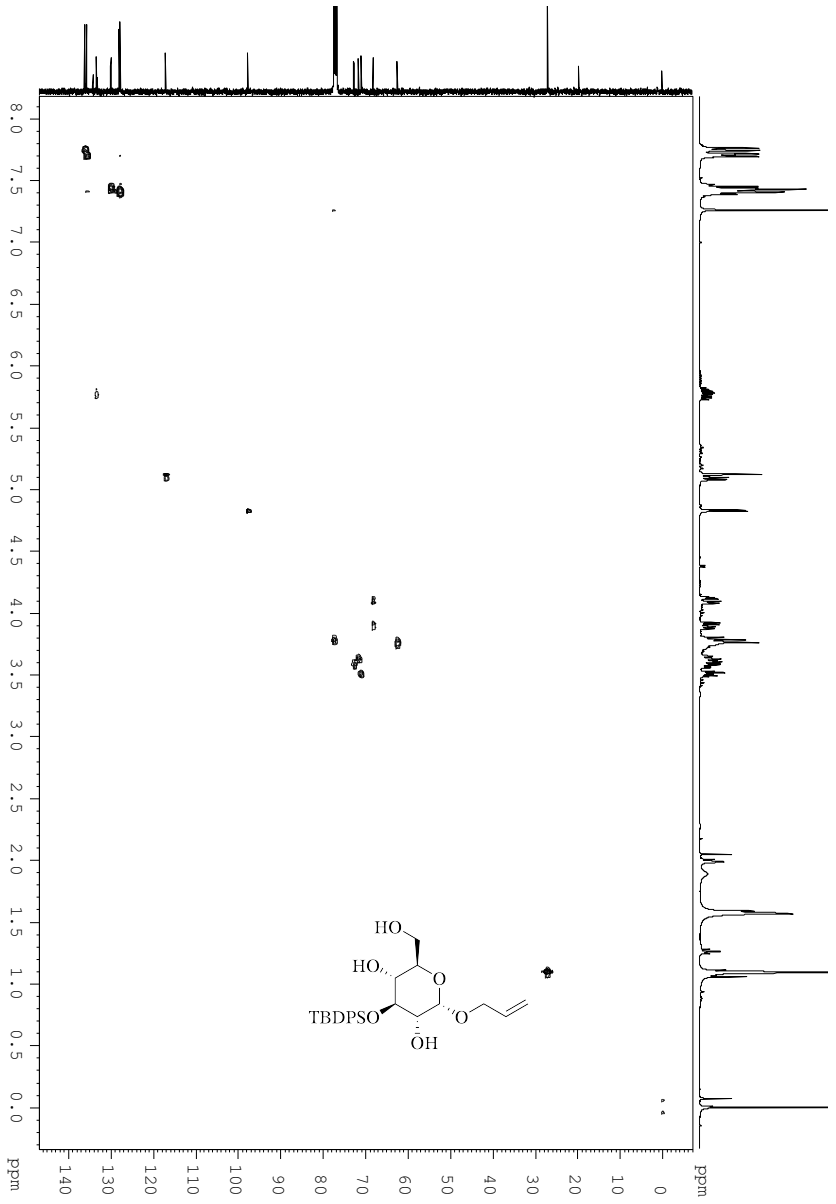

Figure 259: HSQC (400 MHz) spectrum of **4f-α**.

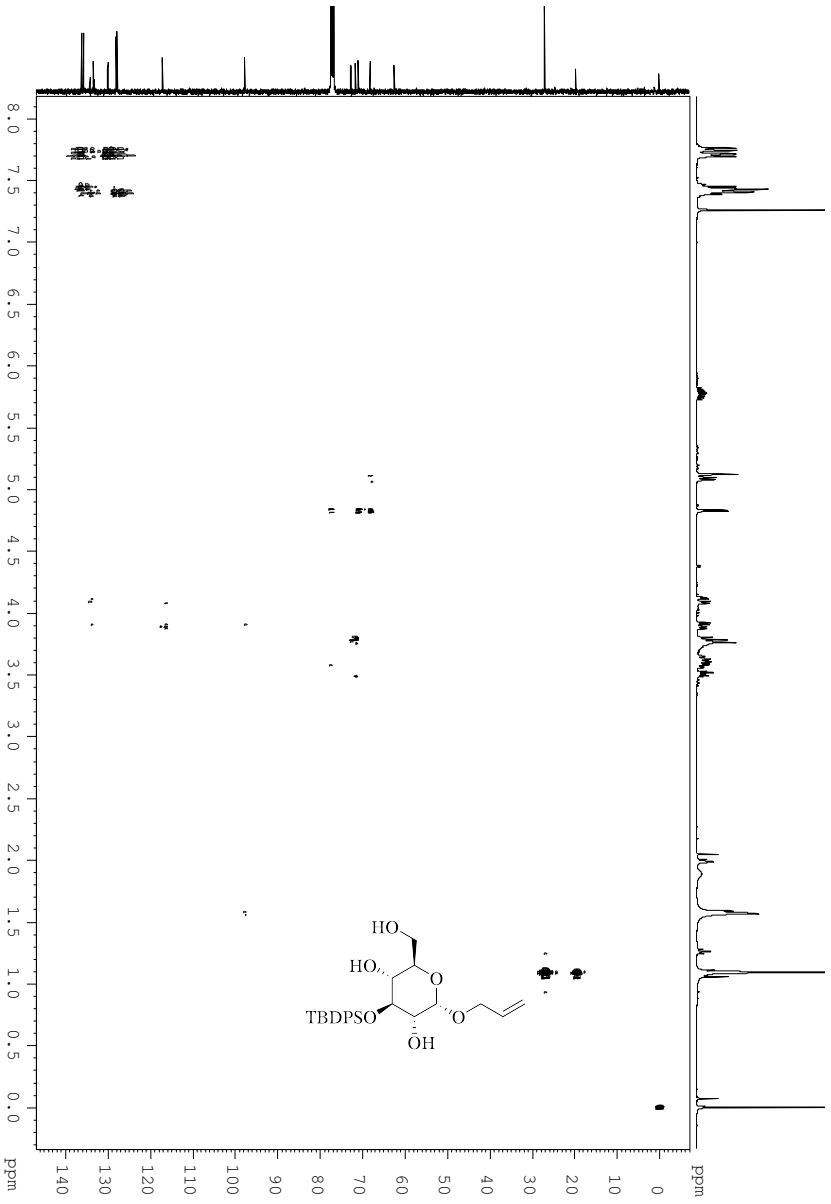

Figure 260: HMBC (400 MHz) spectrum of **4f-α**.

B.34 Spectroscopic data for compound 4f-β

Elemental Composition Report **Page 1**

Single Mass Analysis
Tolerance = 5.0 PPM / DBE: min = -50.0, max = 50.0
Element prediction: Off
Number of isotope peaks used for i-FIT = 3

Monoisotopic Mass, Even Electron Ions
803 formula(e) evaluated with 3 results within limits (all results (up to 1000) for each mass)
Elements Used:
C: 2-100 H: 0-150 O: 0-10 Si: 0-2 Na: 0-1

2019_576_rerun 58 (0.660) AM2 (Ar,35000.0,0.00,0.00); ABS; Cm (57:62)
1: TOF MS ES+

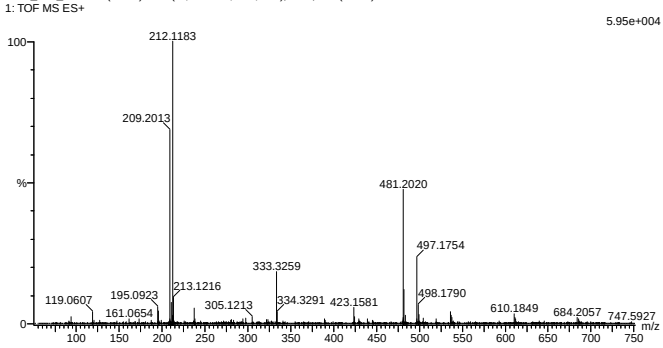

Minimum:				-50.0				
Maximum:		5.0	5.0	50.0				
Mass	Calc. Mass	mDa	PPM	DBE	i-FIT	Norm	Conf(%)	Formula
481.2020	481.2019	0.1	0.2	16.5	500.8	2.769	6.28	C30 H33 O2 Si2
	481.2022	-0.2	-0.4	9.5	498.1	0.068	93.40	C25 H34 O6 Si Na
	481.2015	0.5	1.0	17.5	503.8	5.745	0.32	C31 H29 O5

Figure 261: HRMS (ESI+) of **4f-β**.

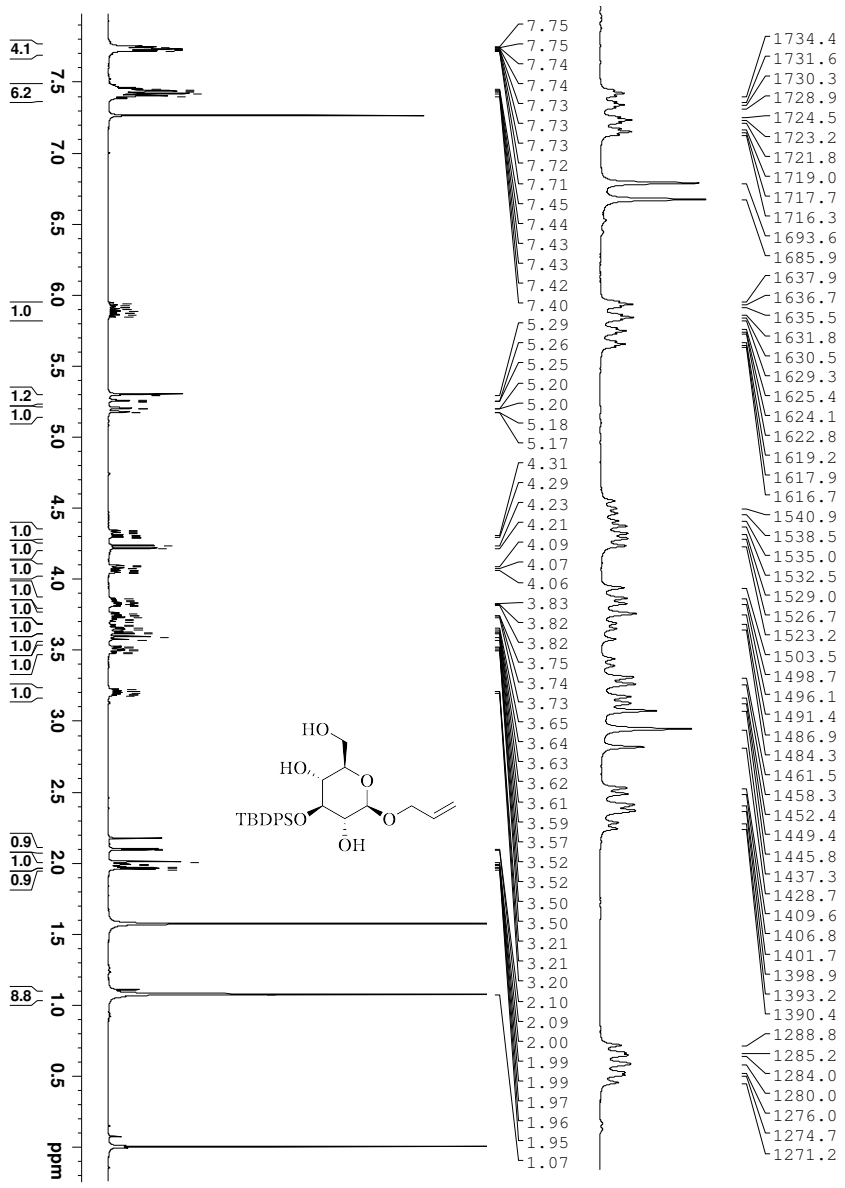

Figure 262: ^{1}H NMR (400 MHz) spectrum of **4f-β**.

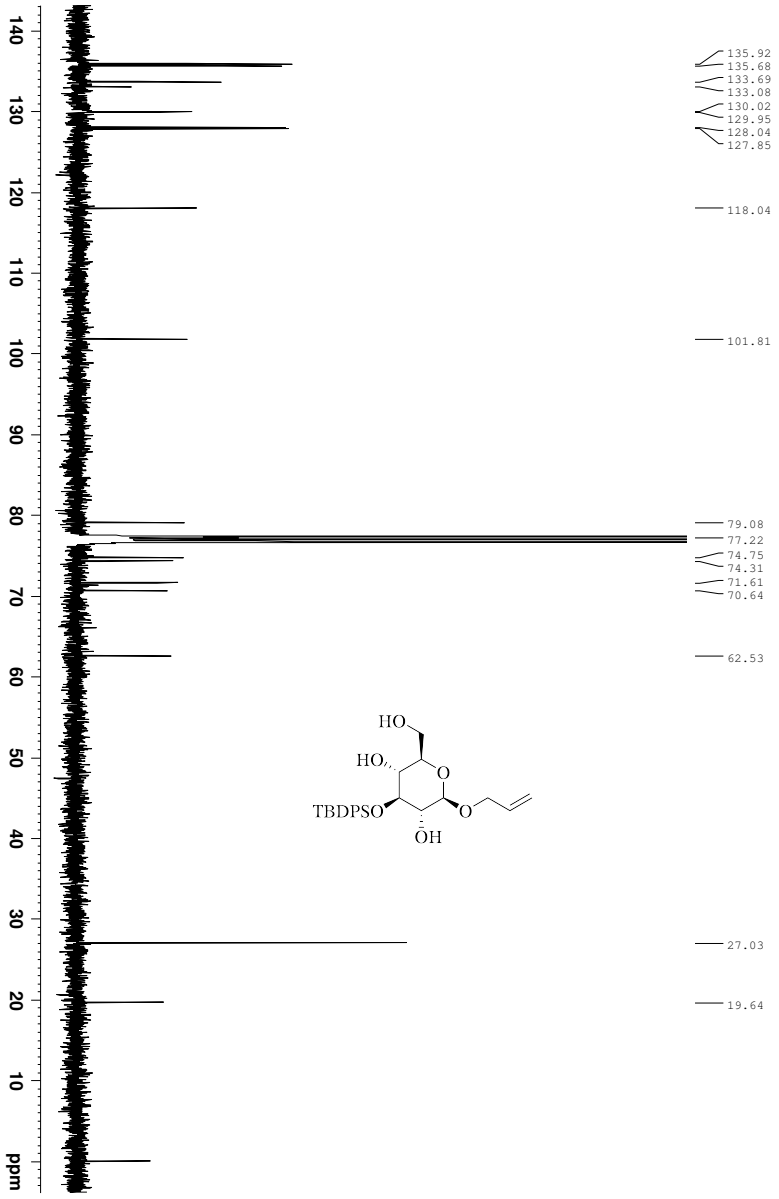

Figure 263: ^{13}C NMR (100 MHz) spectrum of **4f-β**.

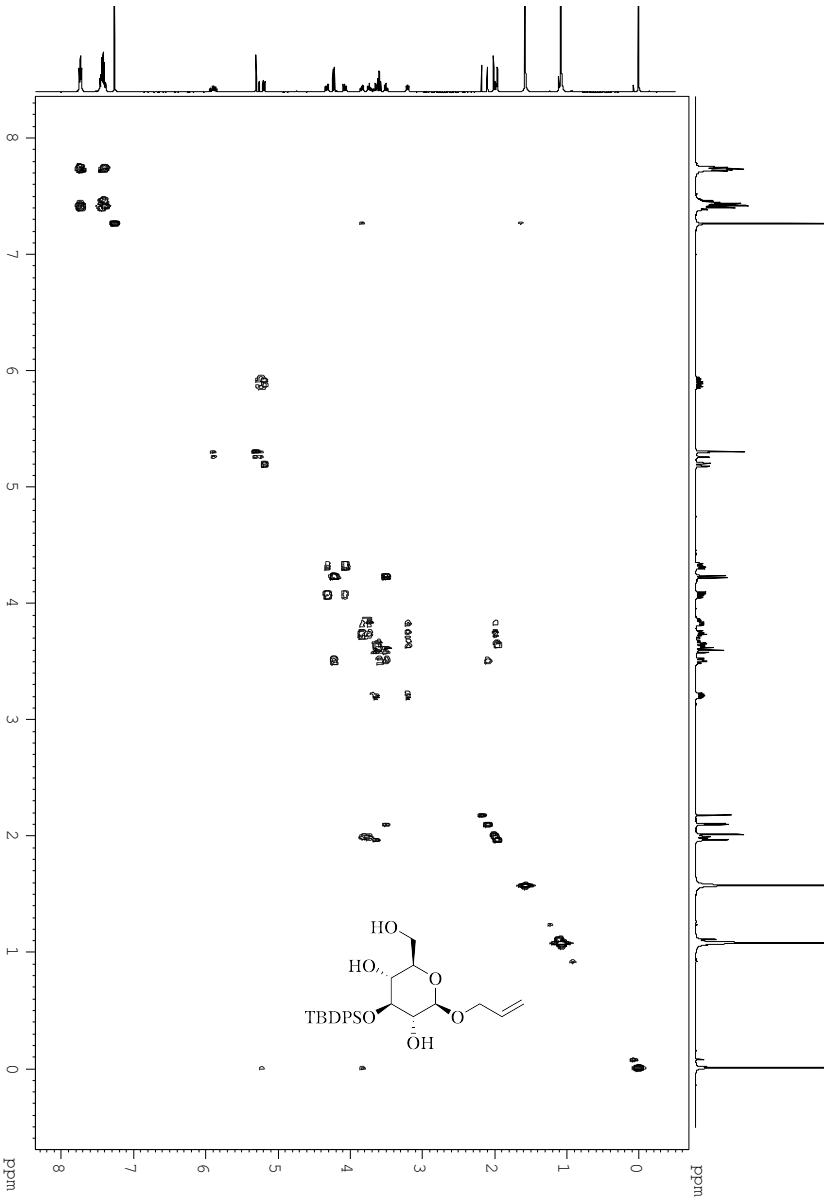

Figure 264: COSY (400 MHz) spectrum of **4f-β**.

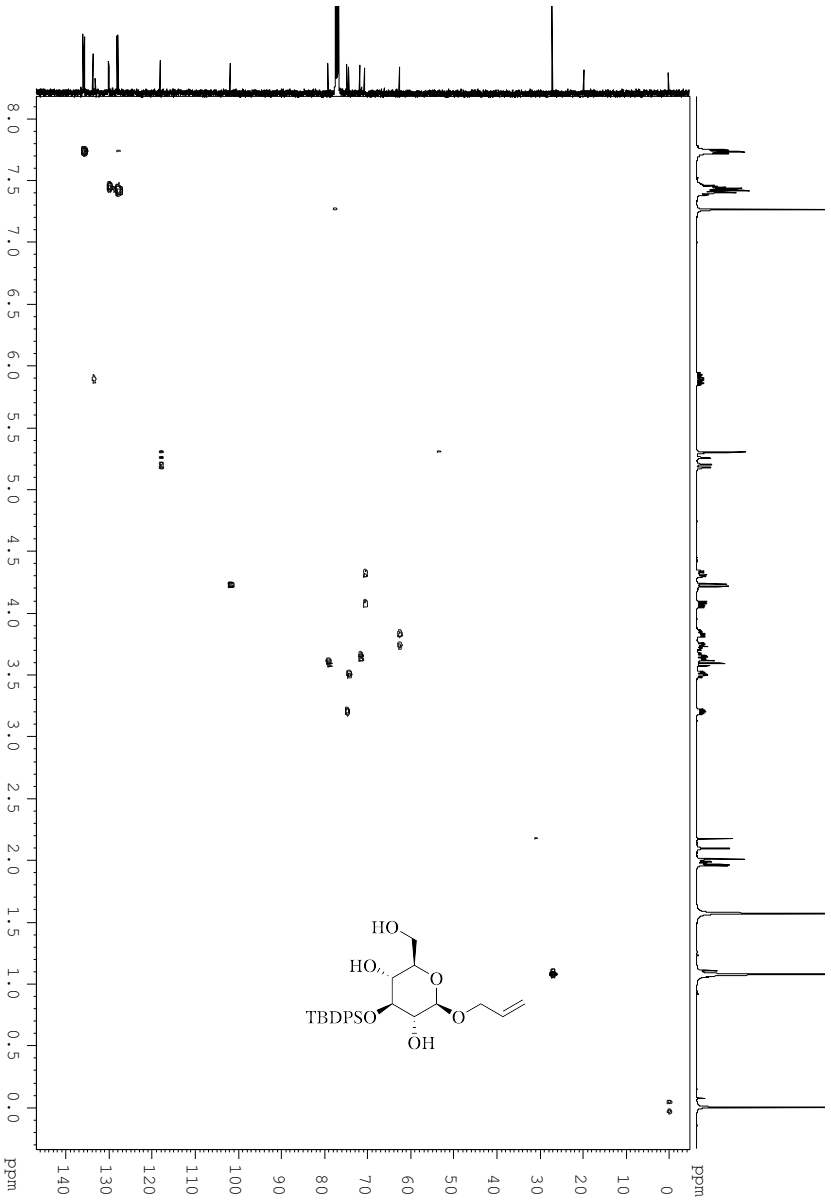

Figure 265: HSQC (400 MHz) spectrum of **4f-β**.

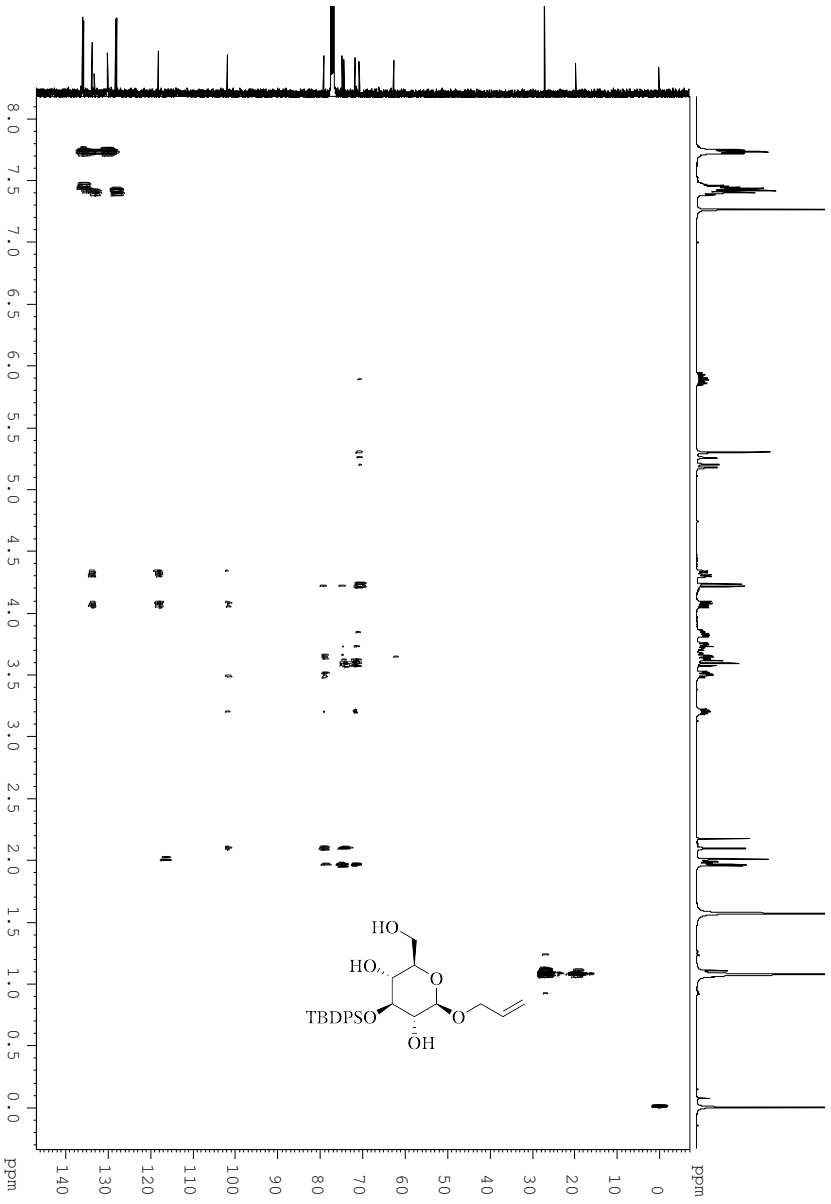

Figure 266: HMBC (400 MHz) spectrum of **4f-β**.

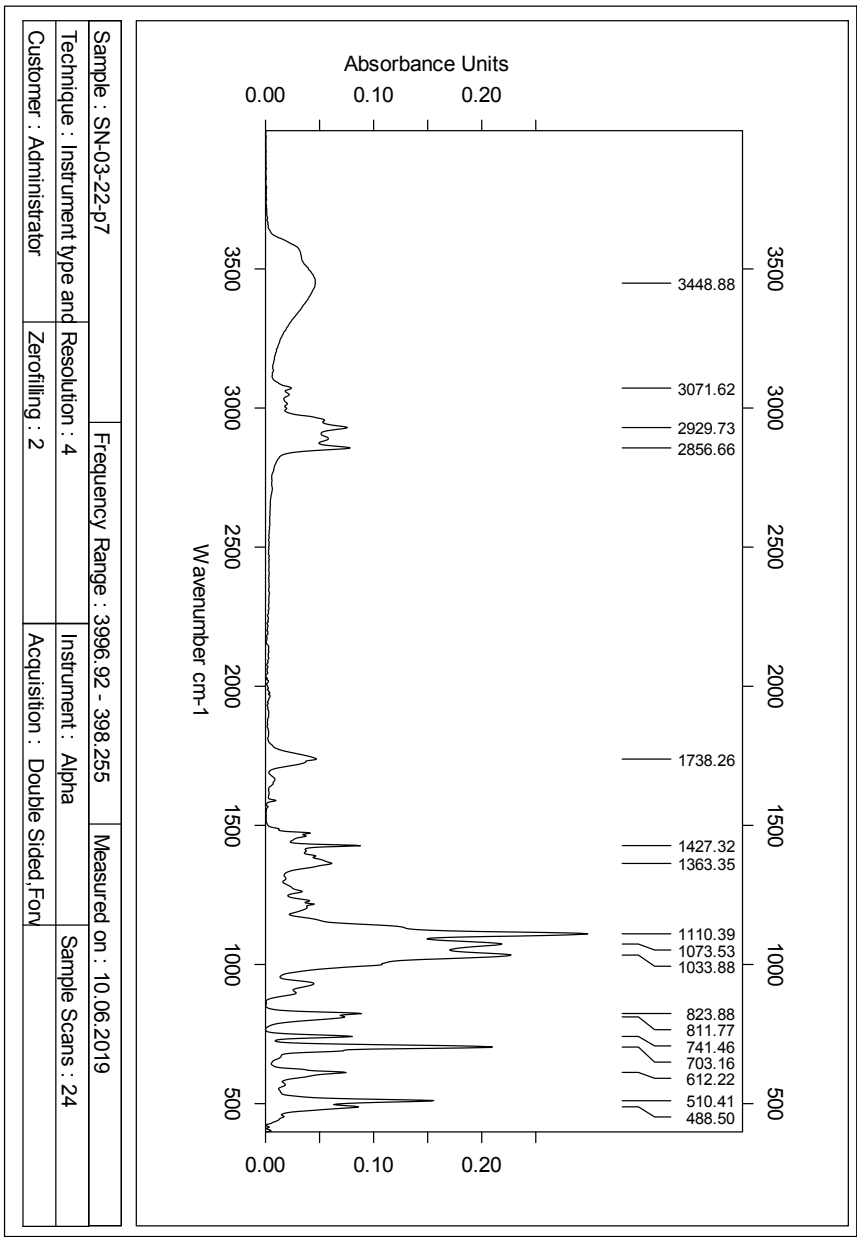

Figure 267: IR spectrum of **4f-β**.

B.35 Spectroscopic data for compound 4i

Elemental Composition Report **Page 1**

Single Mass Analysis
Tolerance = 5.0 PPM / DBE: min = -2.0, max = 50.0
Element prediction: Off
Number of isotope peaks used for i-FIT = 3

Monoisotopic Mass, Even Electron Ions
966 formula(e) evaluated with 4 results within limits (all results (up to 1000) for each mass)
Elements Used:
C: 0-100 H: 0-150 N: 0-10 O: 0-10 Na: 0-1

svg_20190211_84 28 (0.533) AM2 (Ar,35000.0,0.00,0.00); Cm (28:31)
1: TOF MS ES+

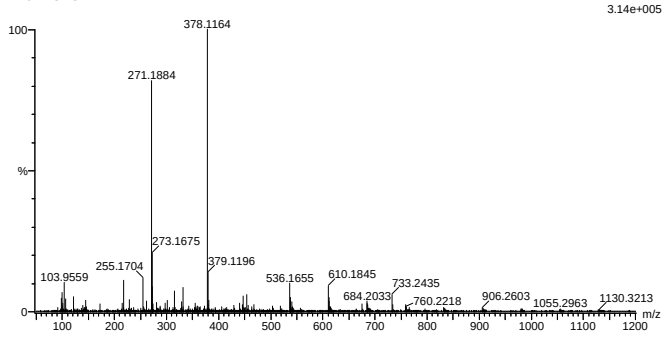

Minimum:				-2.0				
Maximum:		5.0	5.0	50.0				
Mass	Calc. Mass	mDa	PPM	DBE	i-FIT	Norm	Conf(%)	Formula
378.1164	378.1165	-0.1	-0.3	6.5	876.3	0.392	67.58	C16 H21 N O8 Na
	378.1162	0.2	0.5	10.5	878.2	2.311	9.92	C14 H16 N7 O6
	378.1178	-1.4	-3.7	11.5	878.7	2.798	6.09	C17 H17 N5 O4 Na
	378.1149	1.5	4.0	5.5	877.7	1.808	16.40	C13 H20 N3 O10

Figure 268: HRMS (ESI+) of anomeric mixture of **4i**.

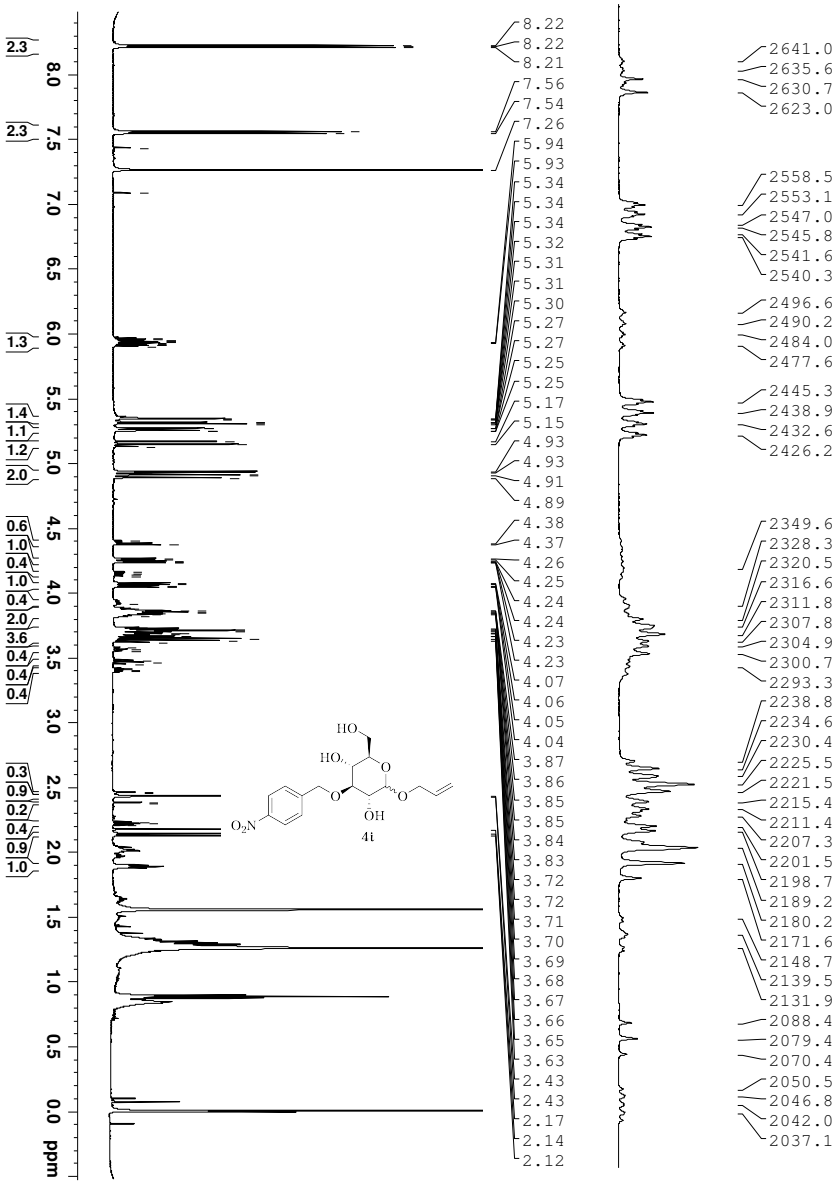

Figure 269: ^{1}H NMR spectrum of anomeric mixture of **4i**.

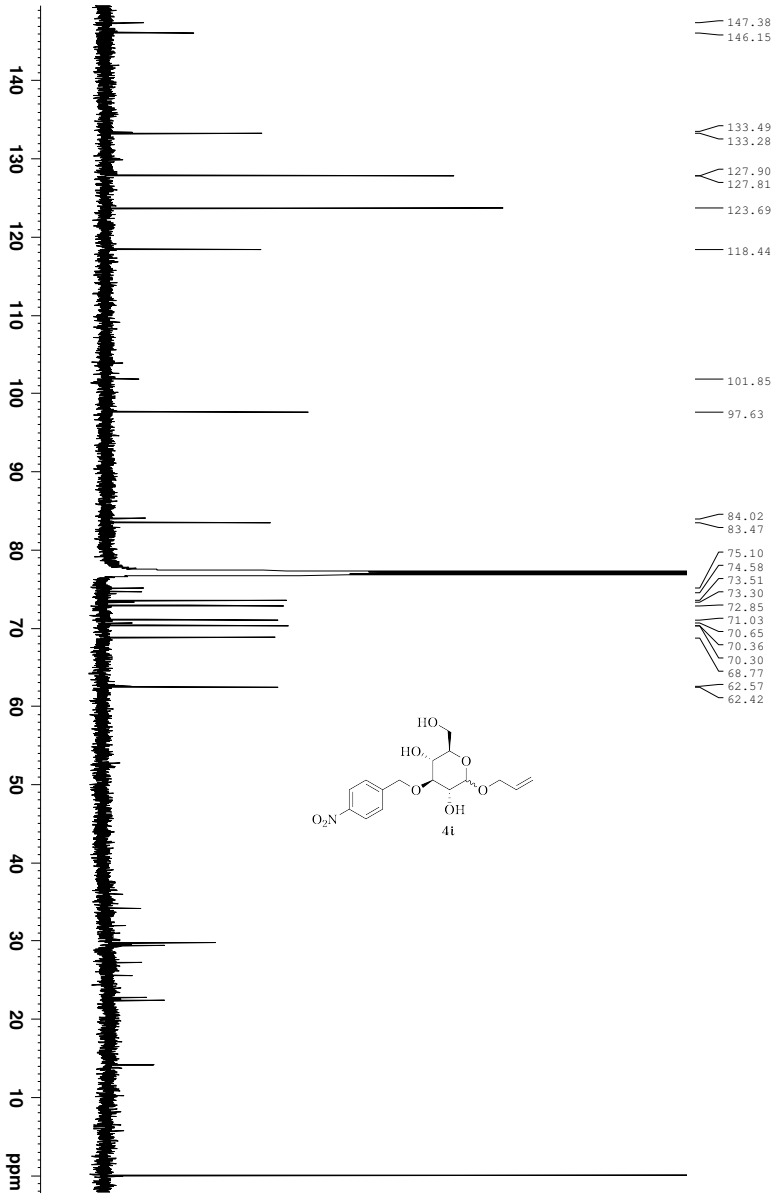

Figure 270: ^{13}C NMR spectrum of anomeric mixture of **4i**.

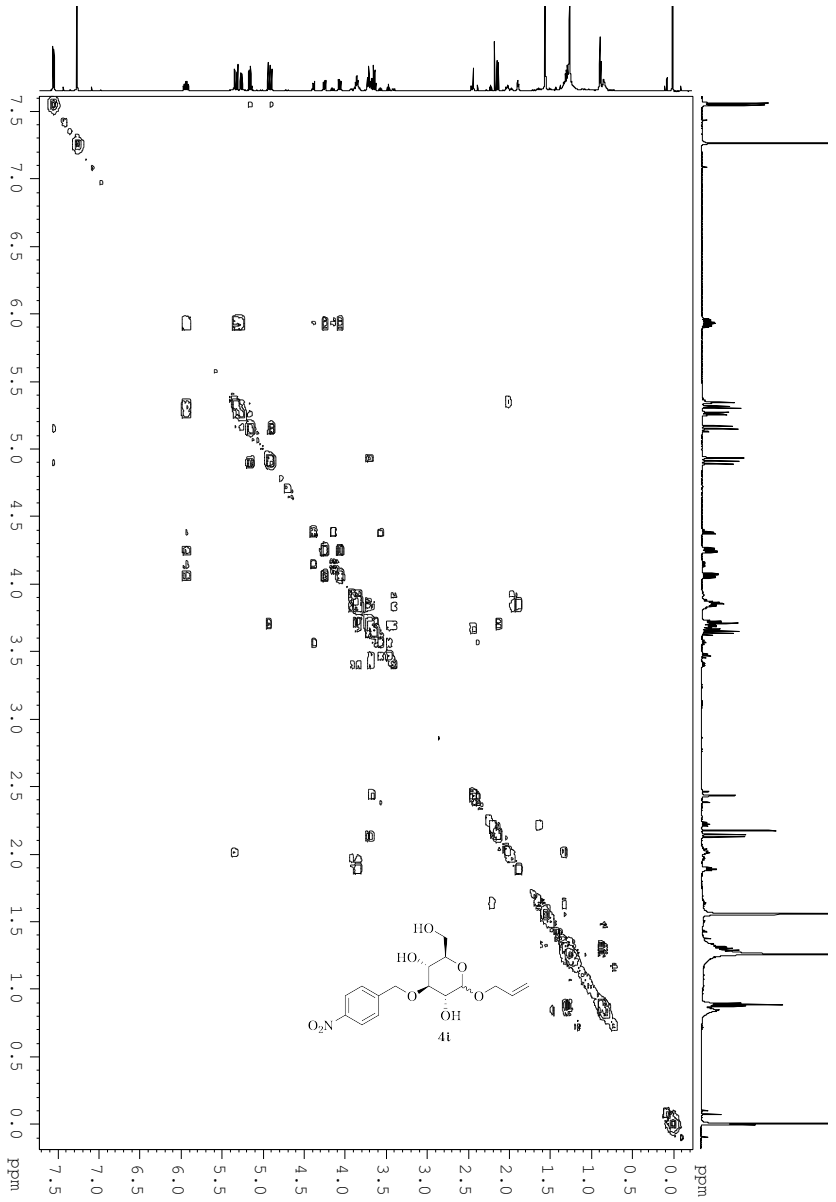

Figure 271: COSY spectrum of anomeric mixture of **4i**.

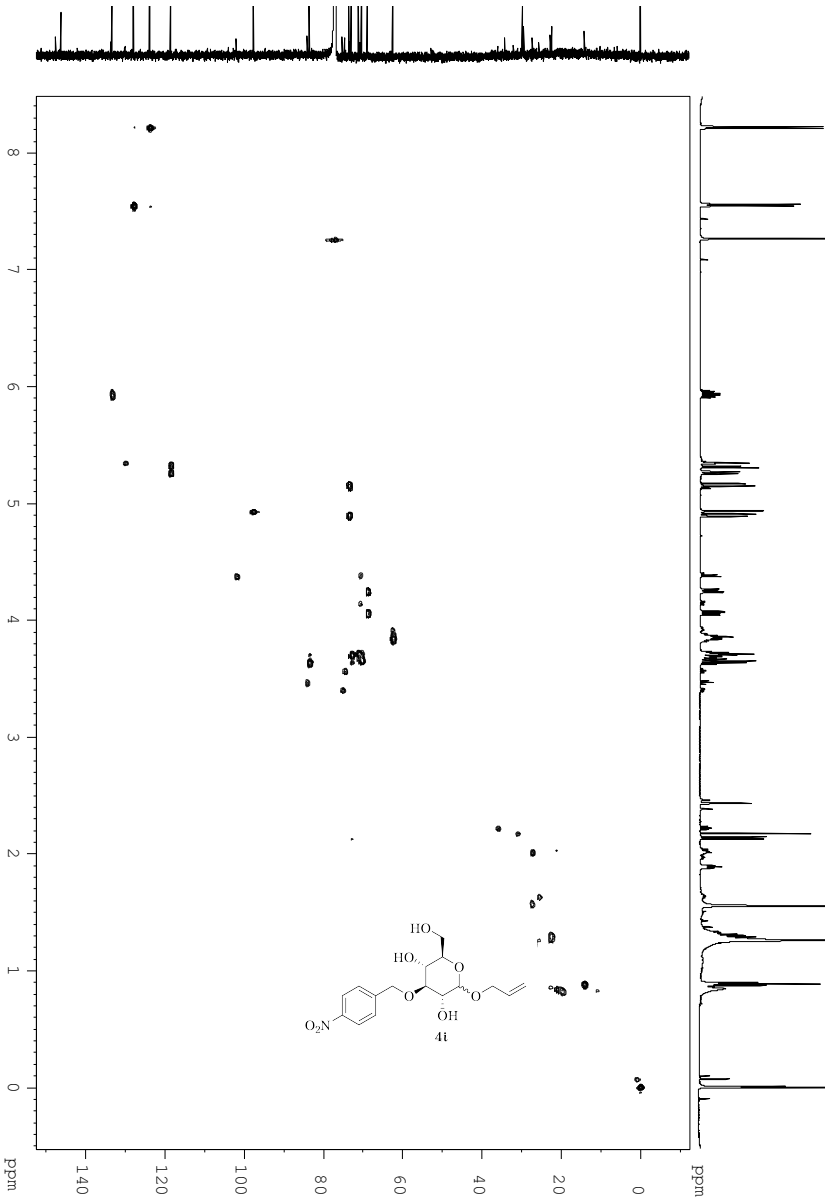

Figure 272: HSQC spectrum of anomeric mixture of **4i**.

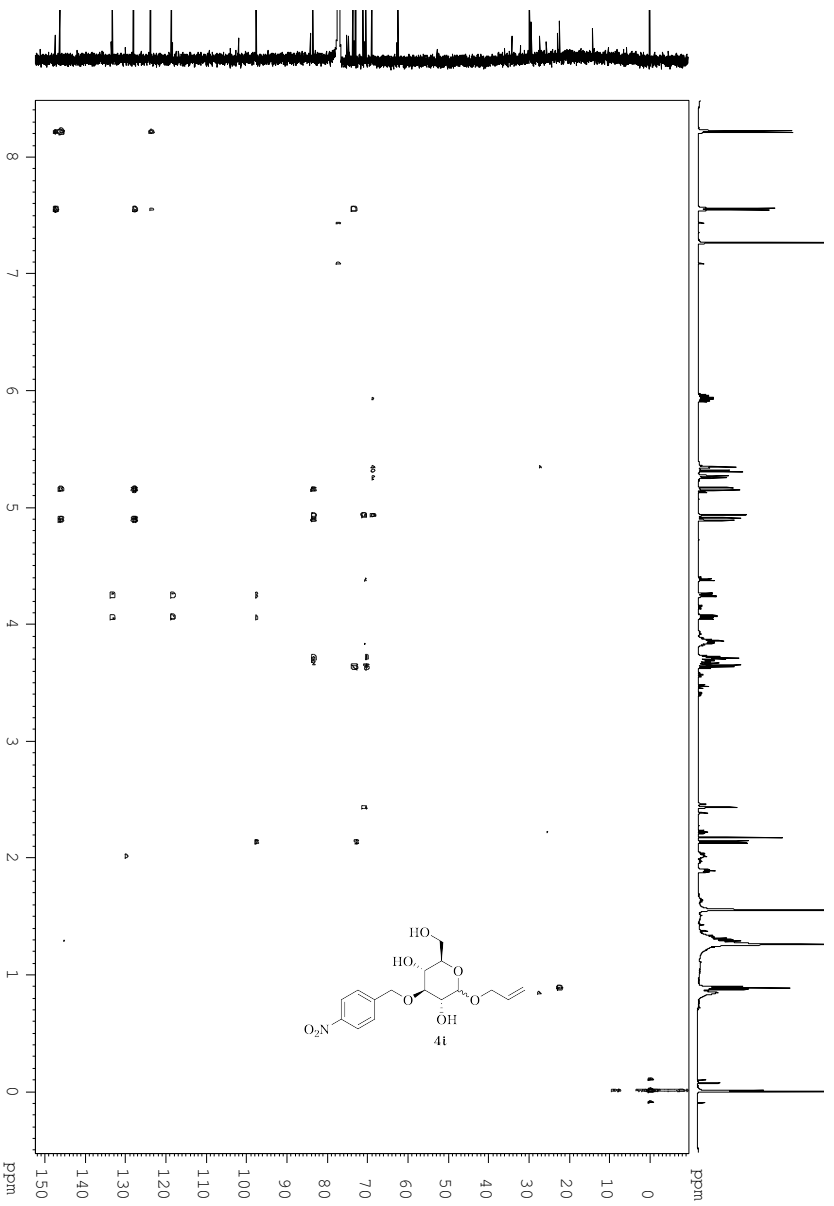

Figure 273: HMBC spectrum of anomeric mixture of **4i**.

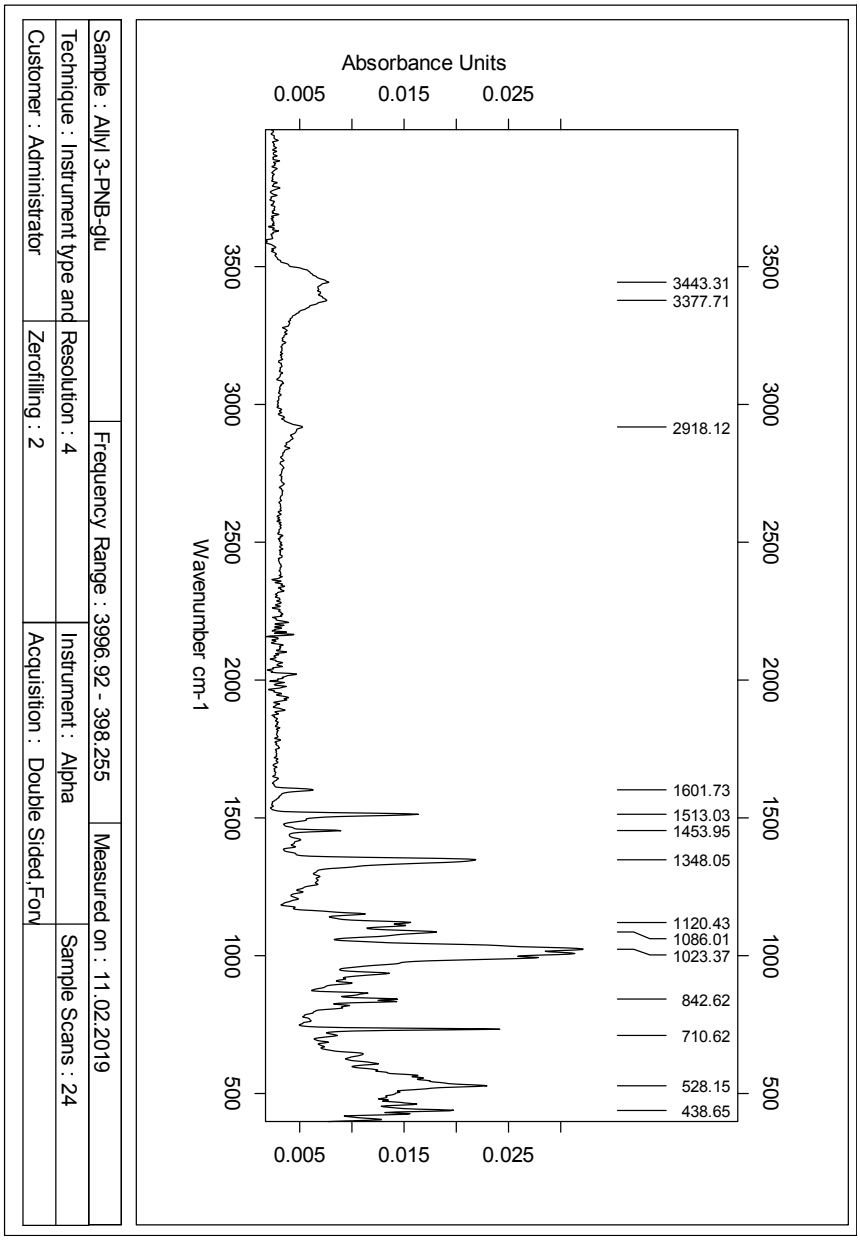

Figure 274: IR spectrum of anomeric mixture of **4i**.

B.36 Spectroscopic data for compound 4μ-α

Elemental Composition Report **Page 1**

Single Mass Analysis
Tolerance = 3.0 PPM / DBE: min = -50.0, max = 50.0
Element prediction: Off
Number of isotope peaks used for i-FIT = 3

Monoisotopic Mass, Even Electron Ions
2362 formula(e) evaluated with 3 results within limits (all results (up to 1000) for each mass)
Elements Used:
C: 0-100 H: 0-150 N: 0-6 O: 0-6 Br: 0-2 Na: 0-1

svg_20190328_2019_228 31 (0.585) AM2 (Ar,35000.0,0.00,0.00); Cm (29:36)
1: TOF MS ES+

9.21e+004

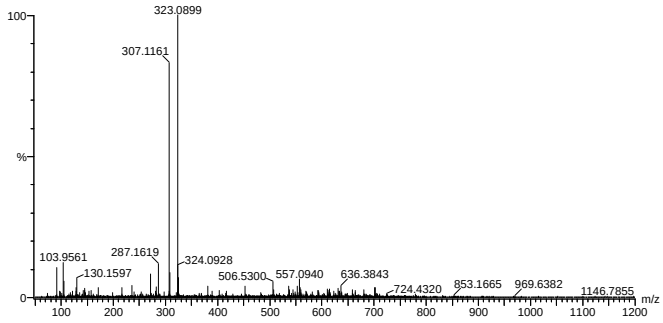

Minimum:				-50.0				
Maximum:		5.0	3.0	50.0				
Mass	Calc. Mass	mDa	PPM	DBE	i-FIT	Norm	Conf(%)	Formula
307.1161	307.1158	0.3	1.0	4.5	696.6	0.019	98.07	C14 H20 O6 Na
	307.1155	0.6	2.0	8.5	700.5	3.949	1.93	C12 H15 N6 O4
	307.1168	-0.7	-2.3	-10.5	715.4	18.838	0.00	C2 H29 N4 O6 Br Na

Figure 275: HRMS (ESI+) of **4μ-α**.

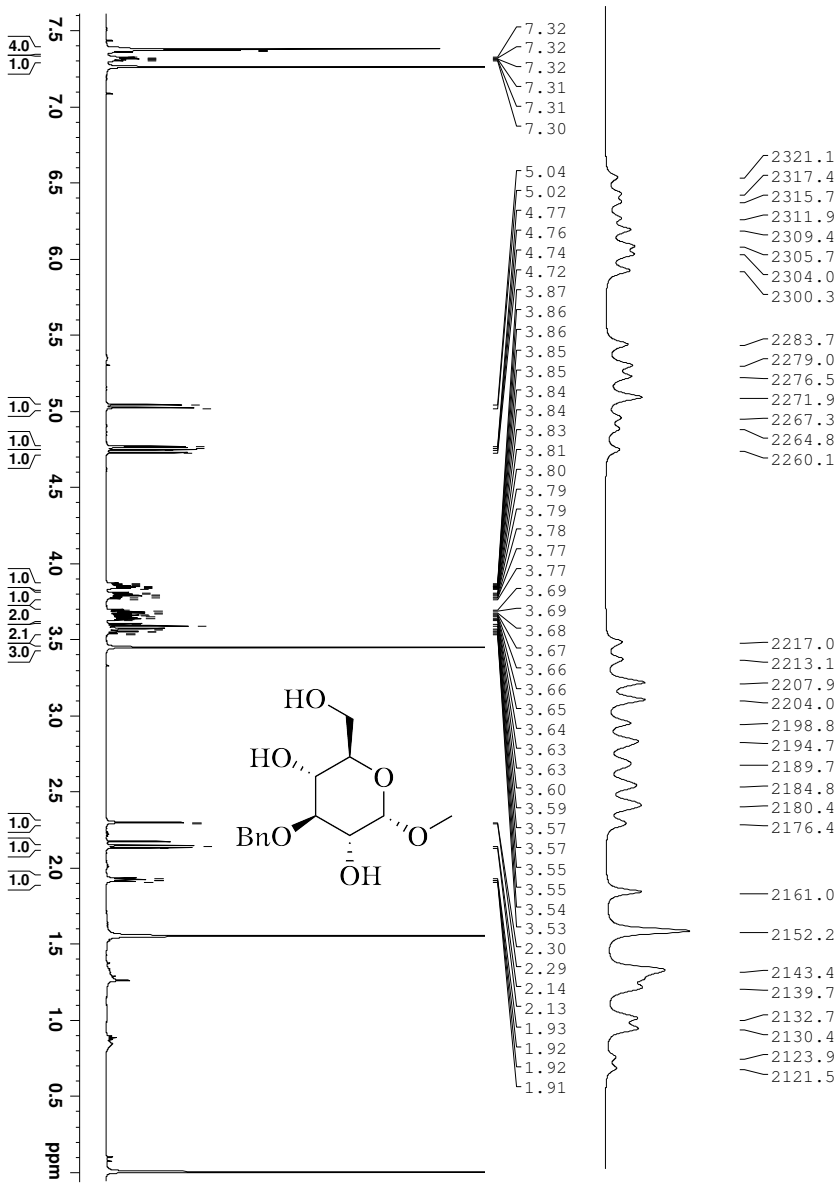

Figure 276: ^{1}H NMR spectrum of **4μ-α**.

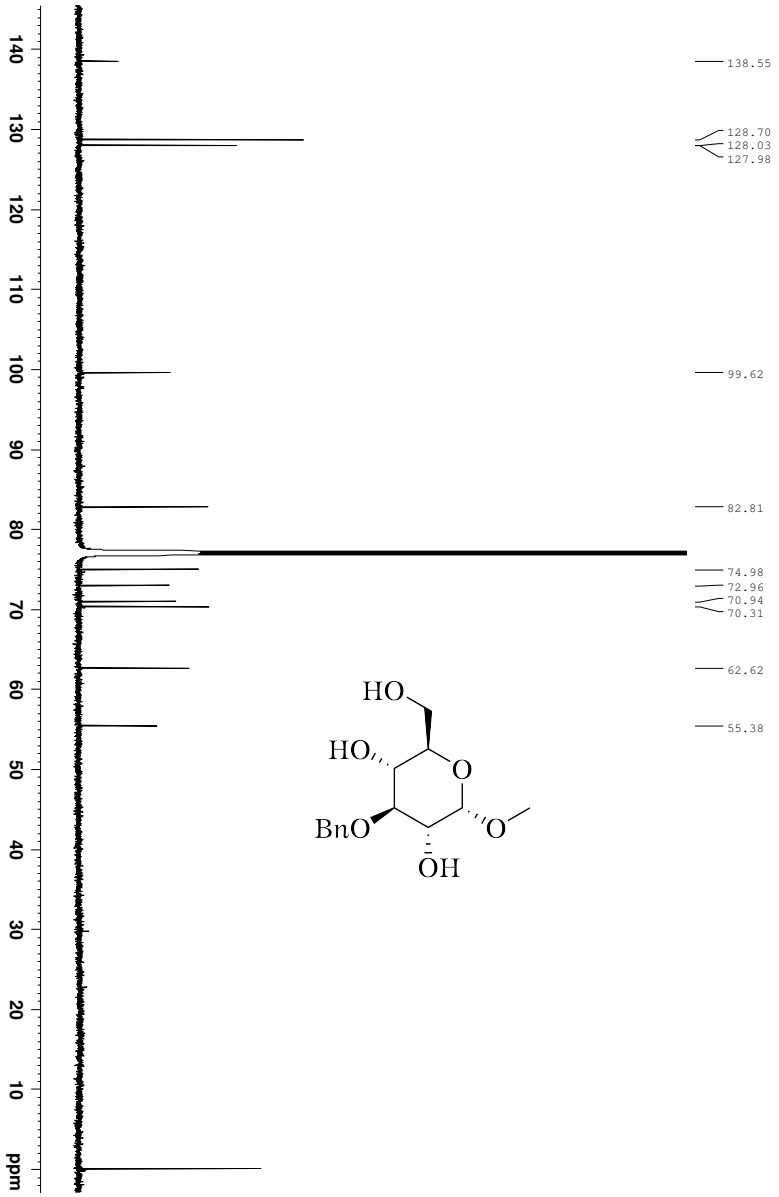

Figure 277: ^{13}C NMR spectrum of **4μ-α**.

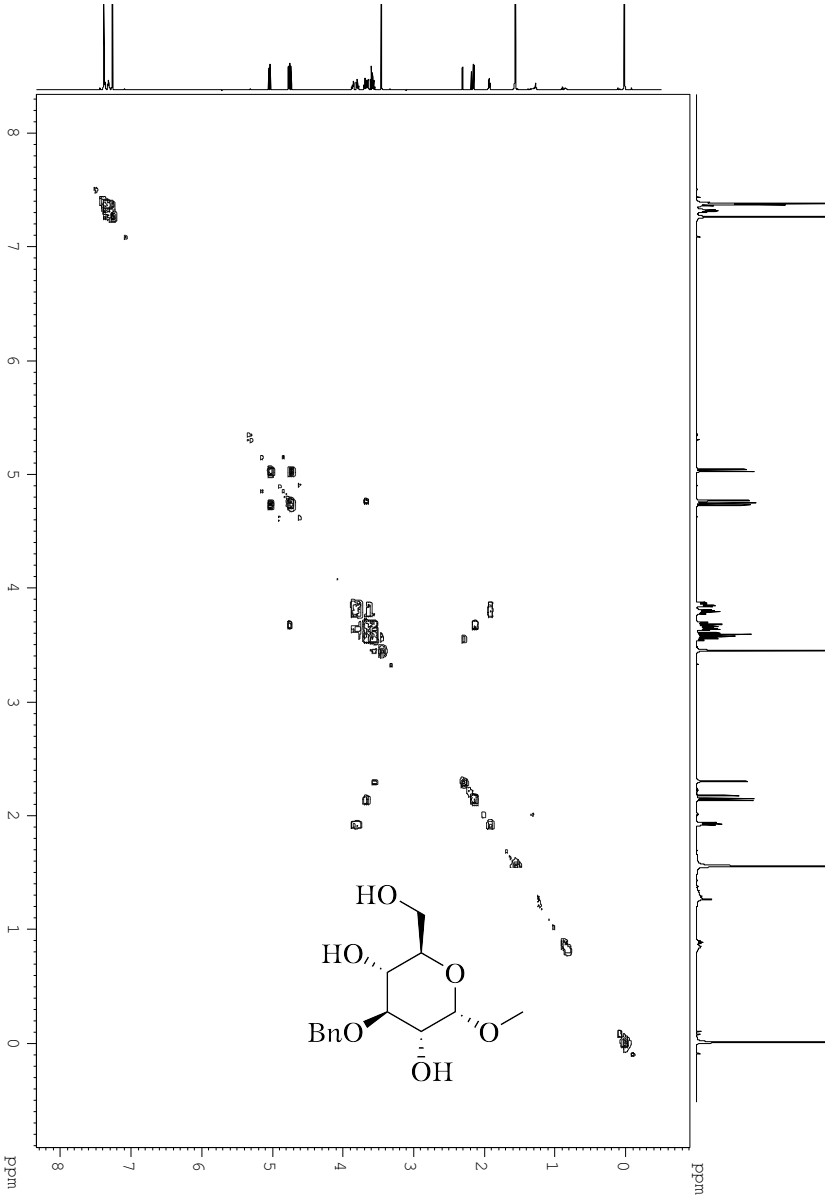

Figure 278: COSY spectrum of **4μ-α**.

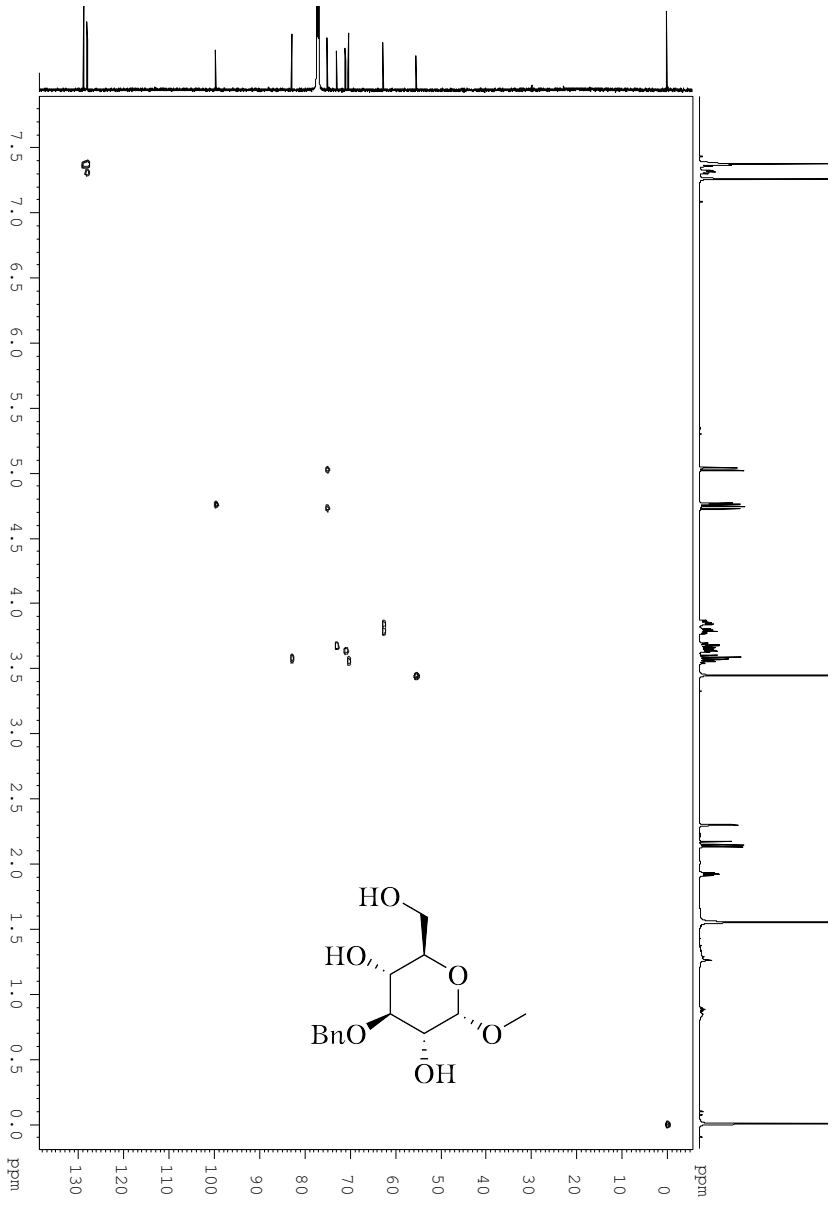

Figure 279: HSQC spectrum of **4μ-α**.

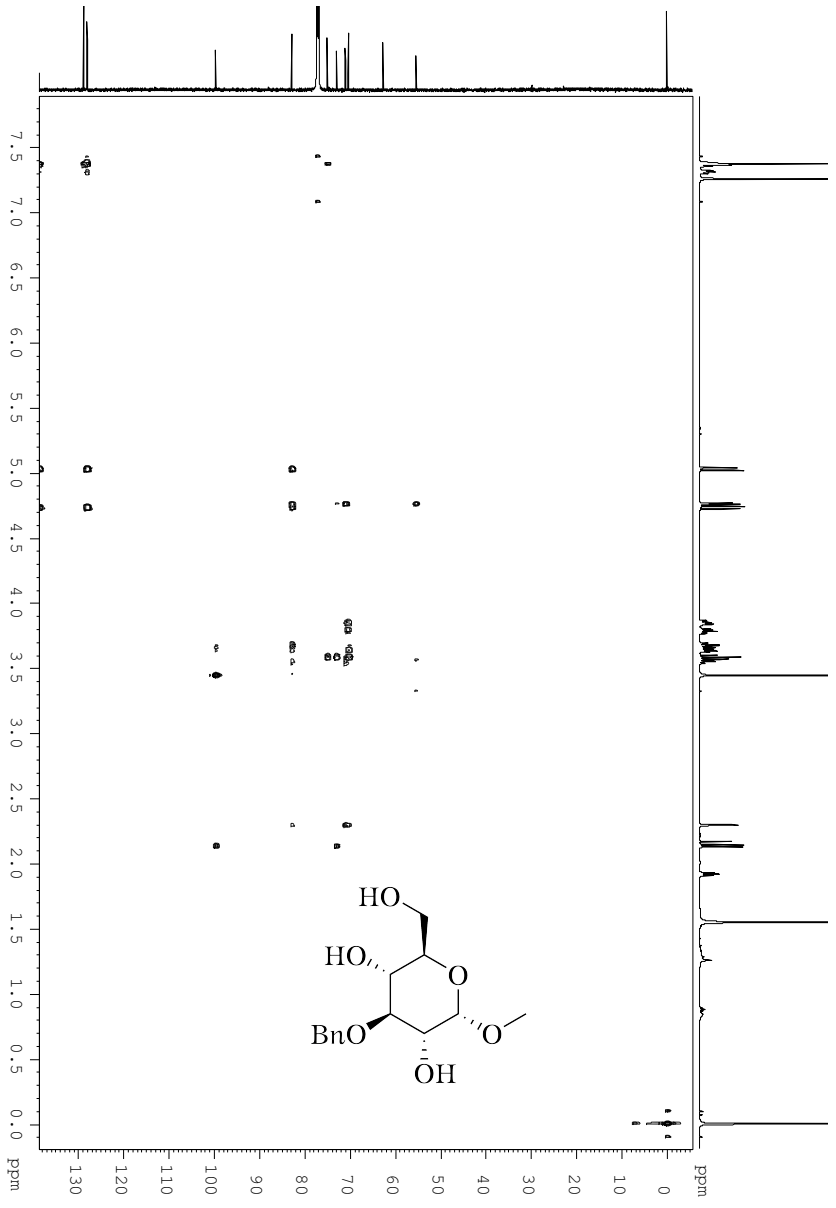

Figure 280: HMBC spectrum of **4μ-α**.

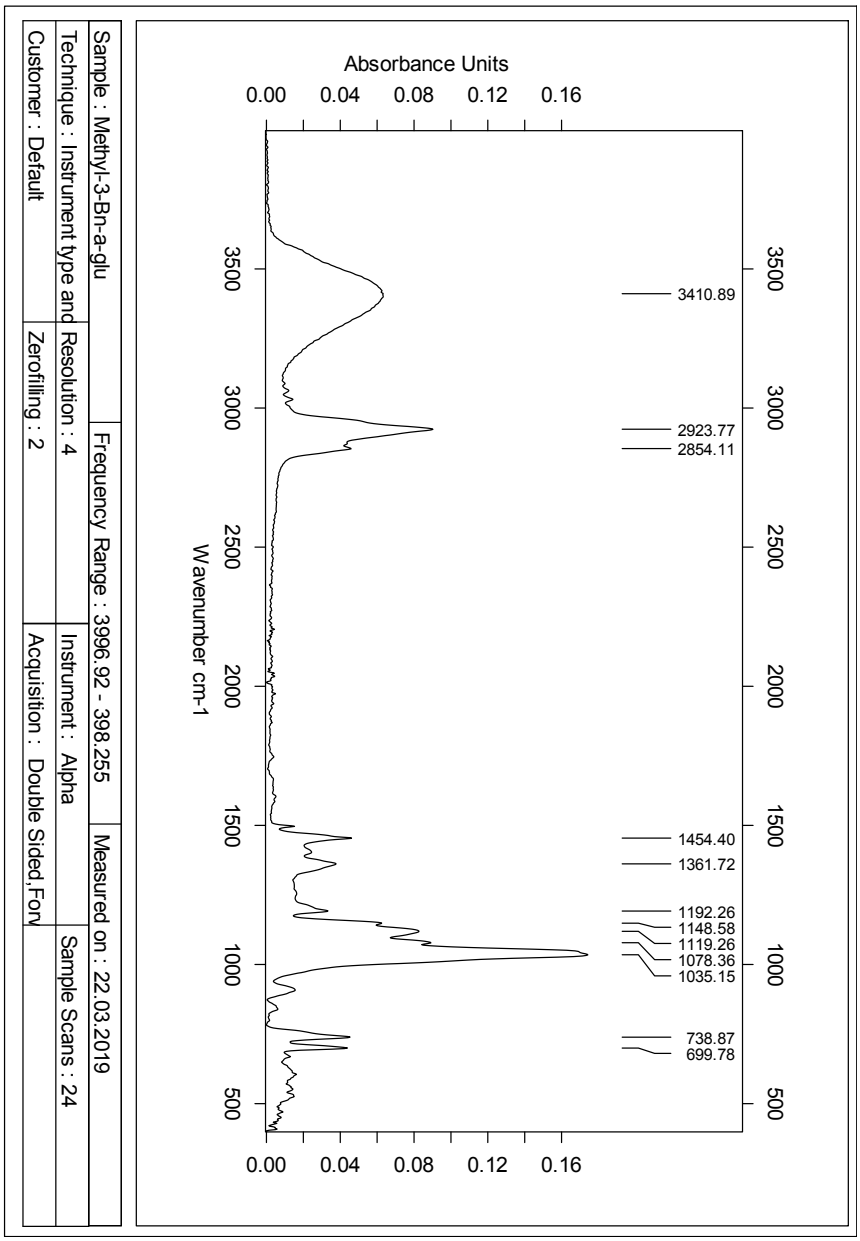

Figure 281: IR spectrum of **4μ-α**.

B.37 Spectroscopic data for compound 4μ-β

Elemental Composition Report **Page 1**

Single Mass Analysis
Tolerance = 2.0 PPM / DBE: min = -50.0, max = 50.0
Element prediction: Off
Number of isotope peaks used for i-FIT = 3

Monoisotopic Mass, Even Electron Ions
2195 formula(e) evaluated with 2 results within limits (all results (up to 1000) for each mass)
Elements Used:
C: 0-100 H: 0-150 N: 0-10 O: 0-10 Na: 0-1
svg_20190328_2019_233 34 (0.636) AM2 (Ar,35000.0,0.00,0.00); Cm (34:35)
1: TOF MS ES+

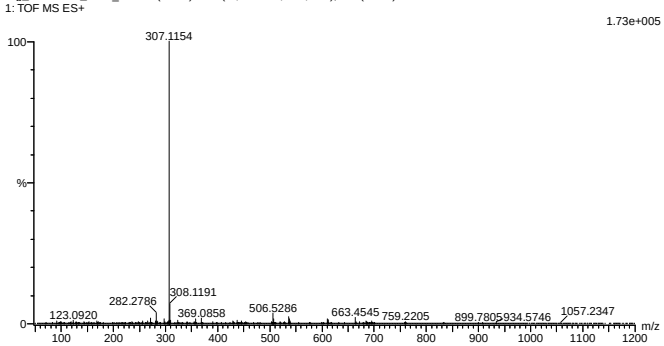

Minimum:				-50.0				
Maximum:		5.0	2.0	50.0				
Mass	Calc. Mass	mDa	PPM	DBE	i-FIT	Norm	Conf(%)	Formula
307.1154	307.1155	-0.1	-0.3	8.5	748.6	0.794	45.19	C12 H15 N6 O4
	307.1158	-0.4	-1.3	4.5	748.4	0.601	54.81	C14 H20 O6 Na

Figure 282: HRMS (ESI+) of **4μ-β**.

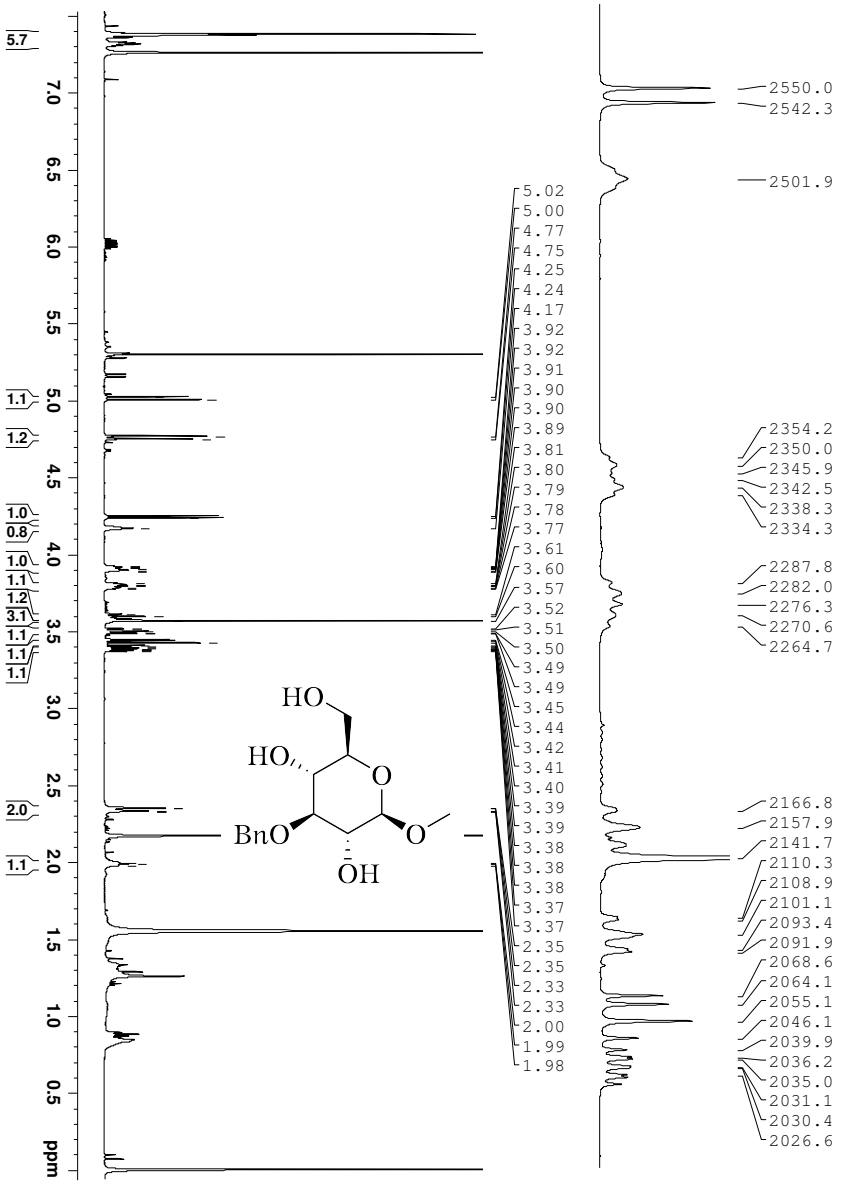

Figure 283: ^{1}H NMR spectrum of **4μ-β**.

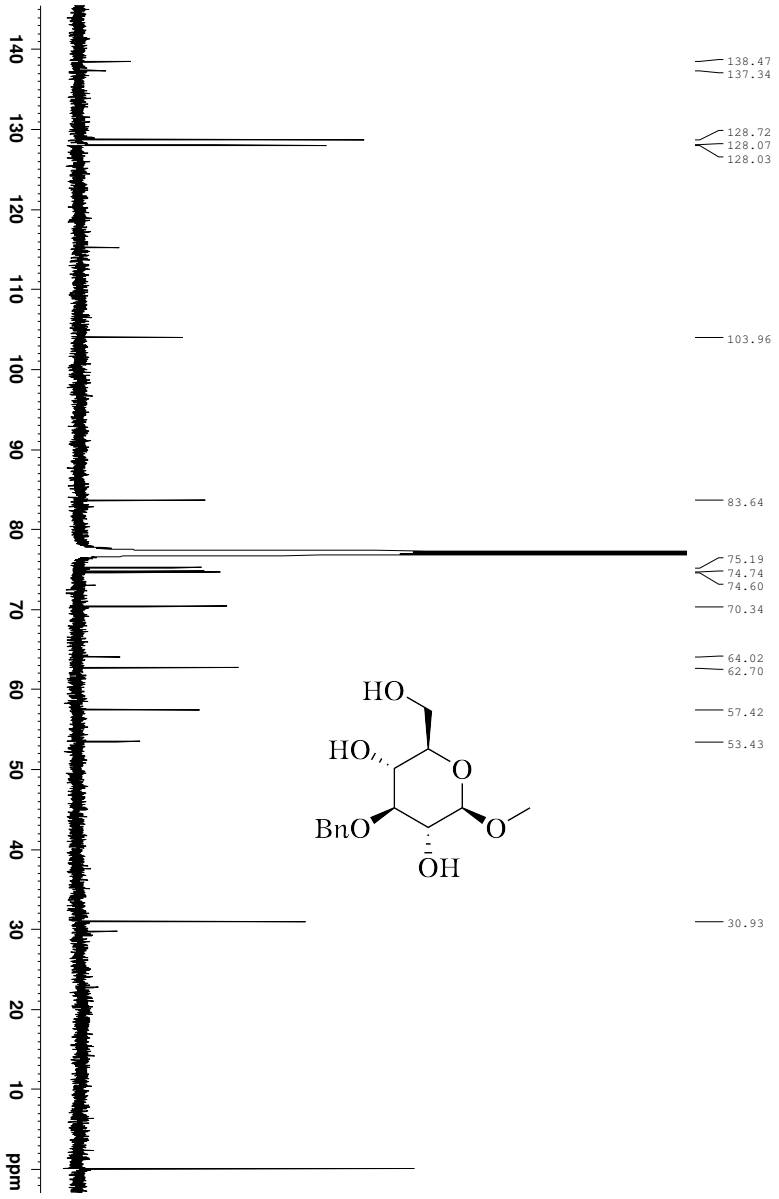

Figure 284: ^{13}C NMR spectrum of **4μ-β**.

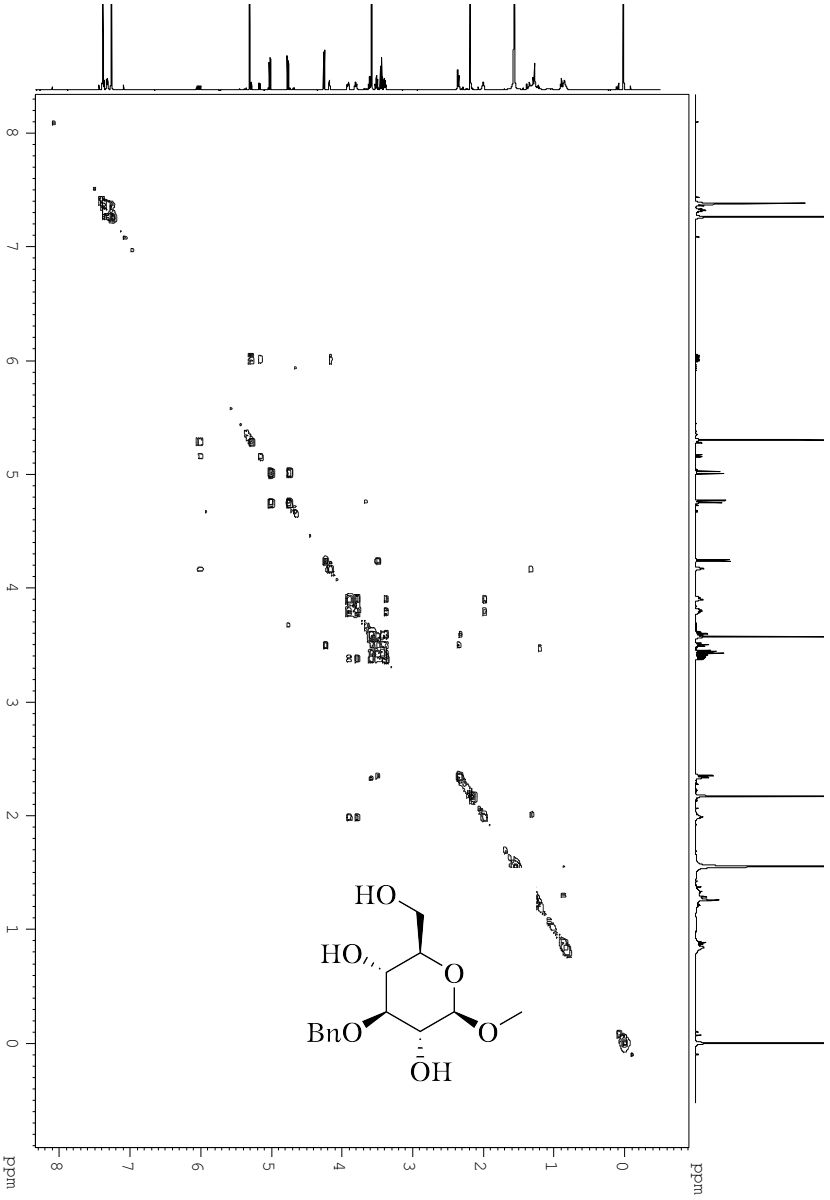

Figure 285: COSY spectrum of **4μ-β**.

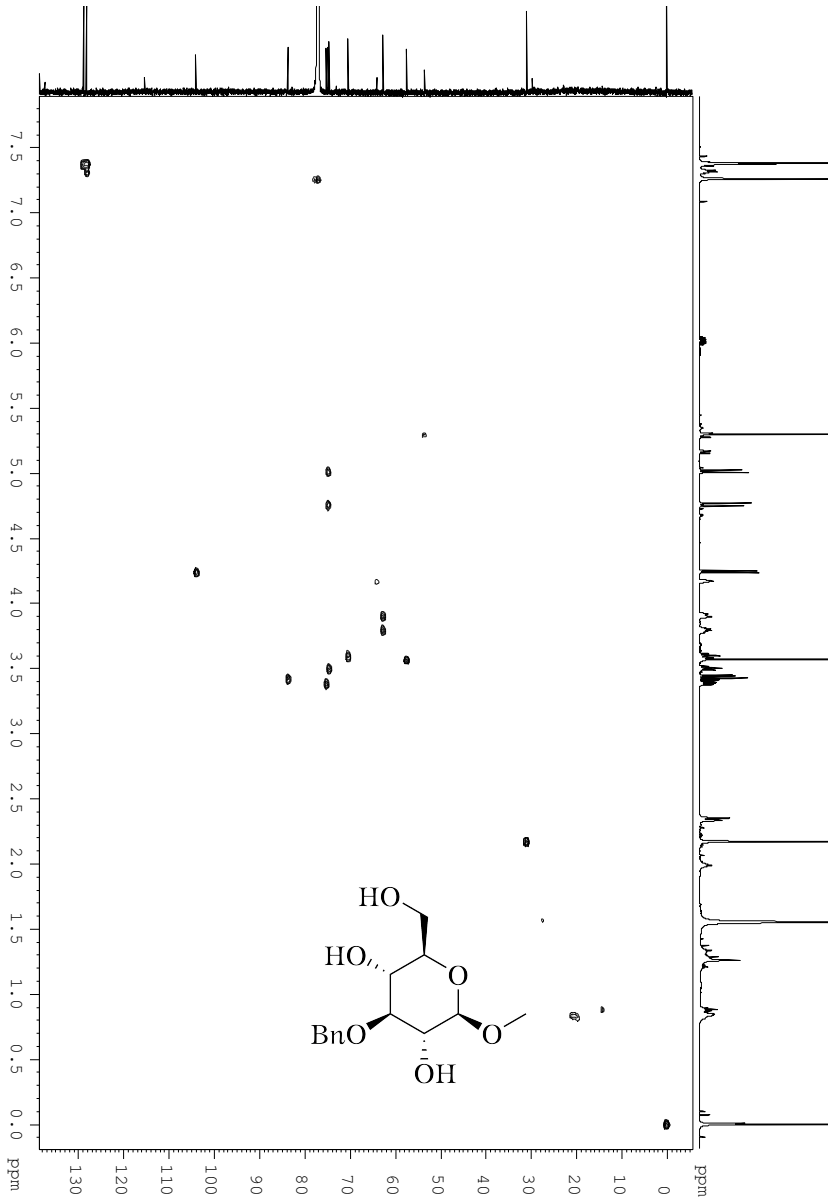

Figure 286: HSQC spectrum of **4μ-β**.

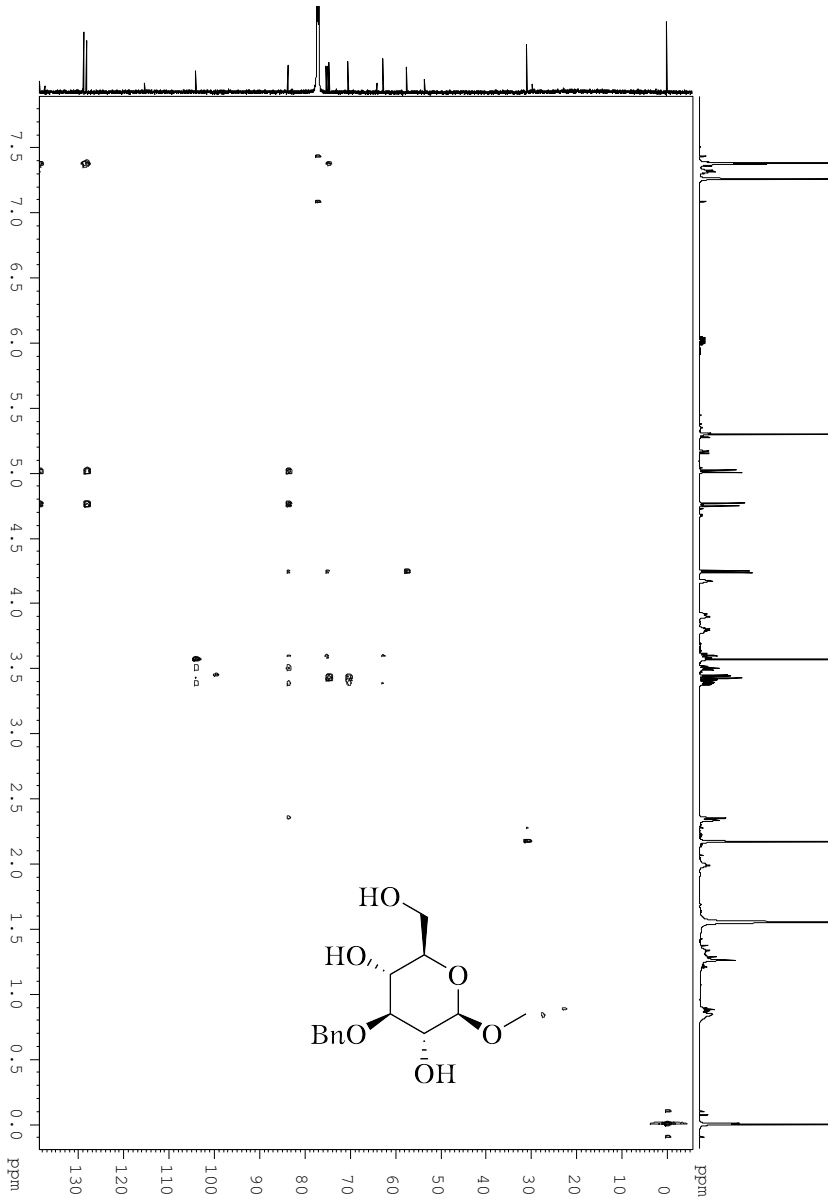

Figure 287: HMBC spectrum of **4μ-β**.

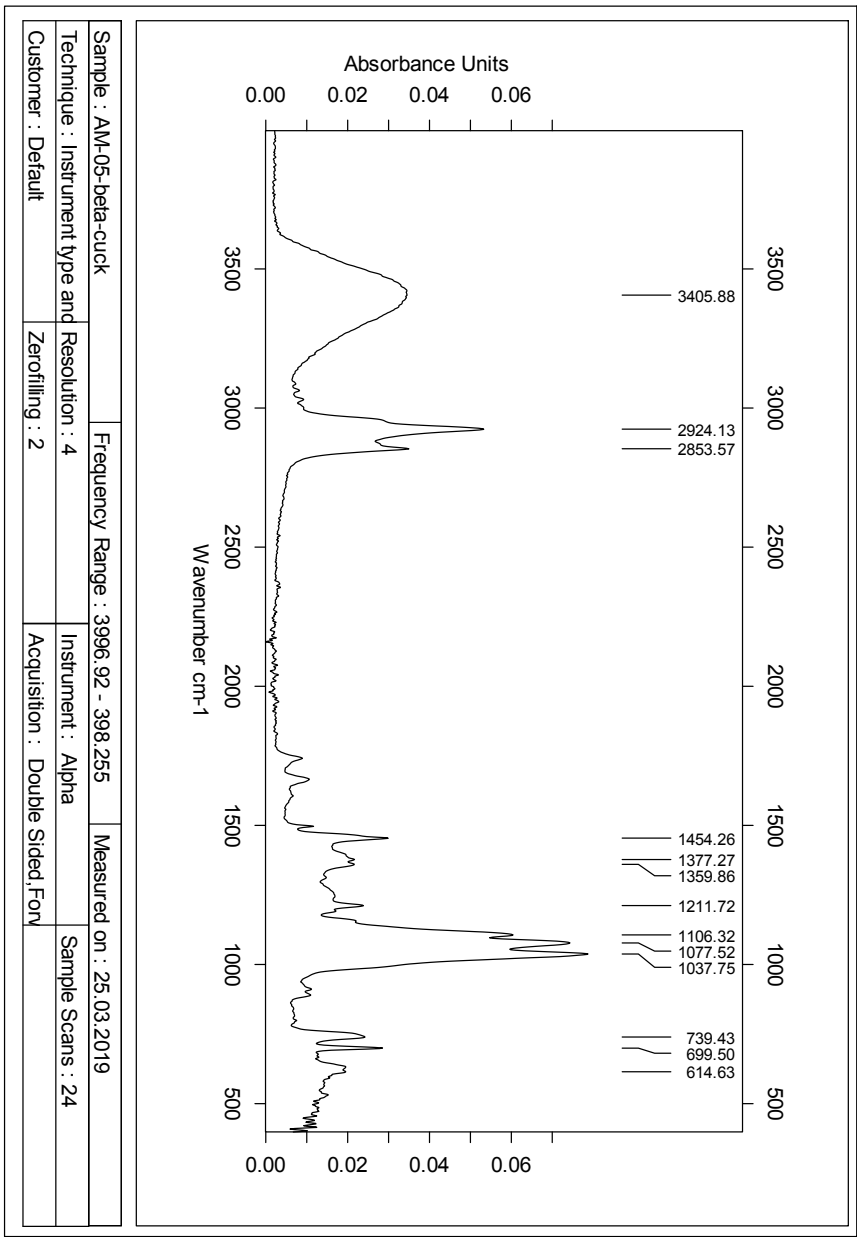

Figure 288: IR spectrum of **4μ-β**.

B.38 Spectroscopic data for compound 4ø

Elemental Composition Report **Page 1**

Single Mass Analysis
Tolerance = 2.0 PPM / DBE: min = -2.0, max = 50.0
Element prediction: Off
Number of isotope peaks used for i-FIT = 3

Monoisotopic Mass, Even Electron Ions
745 formula(e) evaluated with 2 results within limits (all results (up to 1000) for each mass)
Elements Used:
C: 0-100 H: 0-150 N: 0-10 O: 0-10 Na: 0-1

svg_20190214_96 43 (0.802) AM2 (Ar,35000.0,0.00,0.00); Cm (43:45)
1: TOF MS ES+

5.29e+006

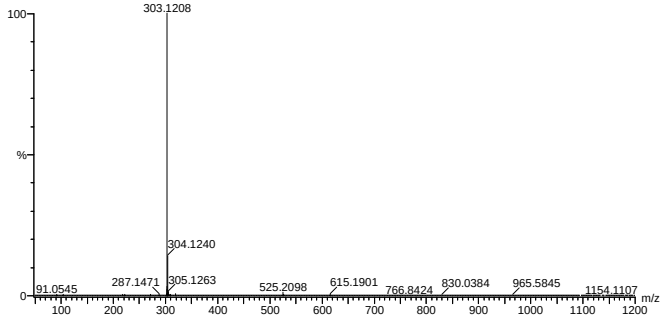

Minimum:				-2.0				
Maximum:		5.0	2.0	50.0				
Mass	Calc. Mass	mDa	PPM	DBE	i-FIT	Norm	Conf(%)	Formula
303.1208	303.1208	0.0	0.0	5.5	1391.1	0.110	89.56	C15 H20 O5 Na
	303.1206	0.2	0.7	9.5	1393.2	2.260	10.44	C13 H15 N6 O3

Figure 289: HRMS (ESI+) of **4ø**.

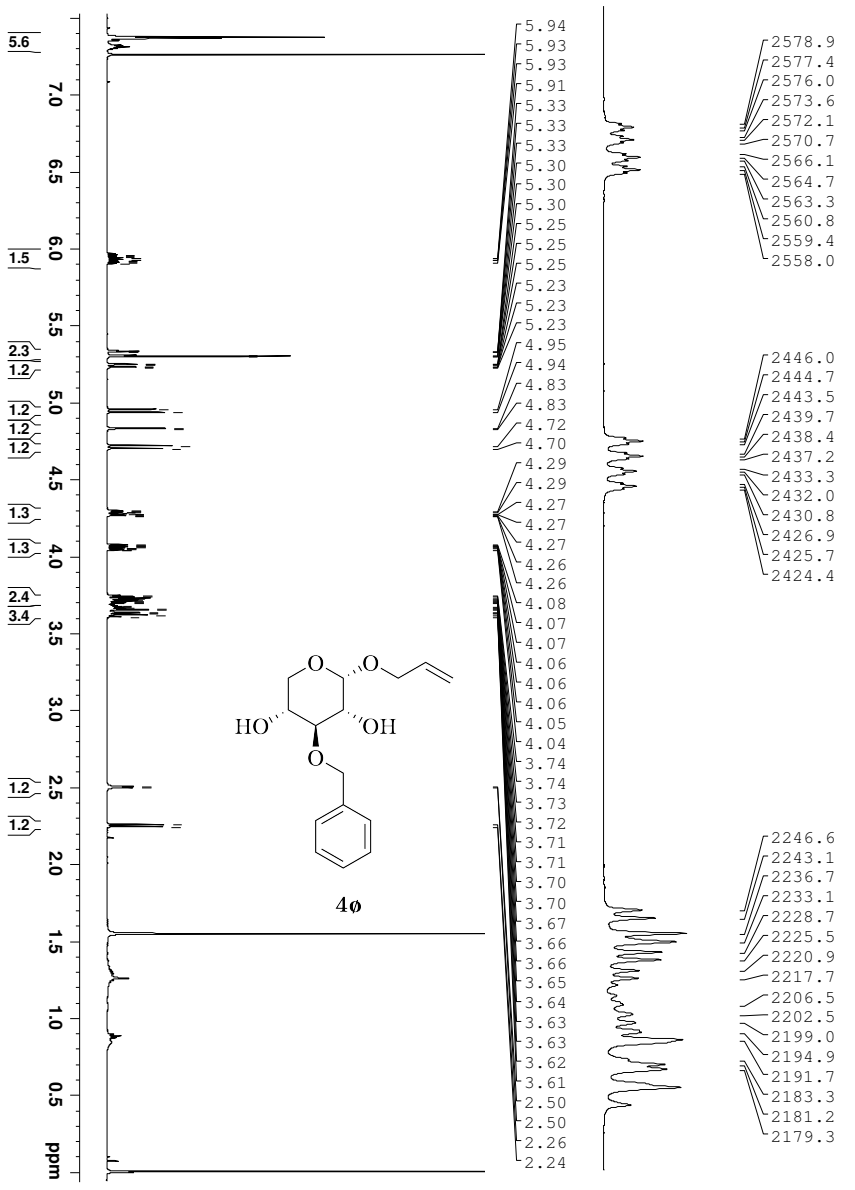

Figure 290: ^{1}H NMR spectrum of **4ø**.

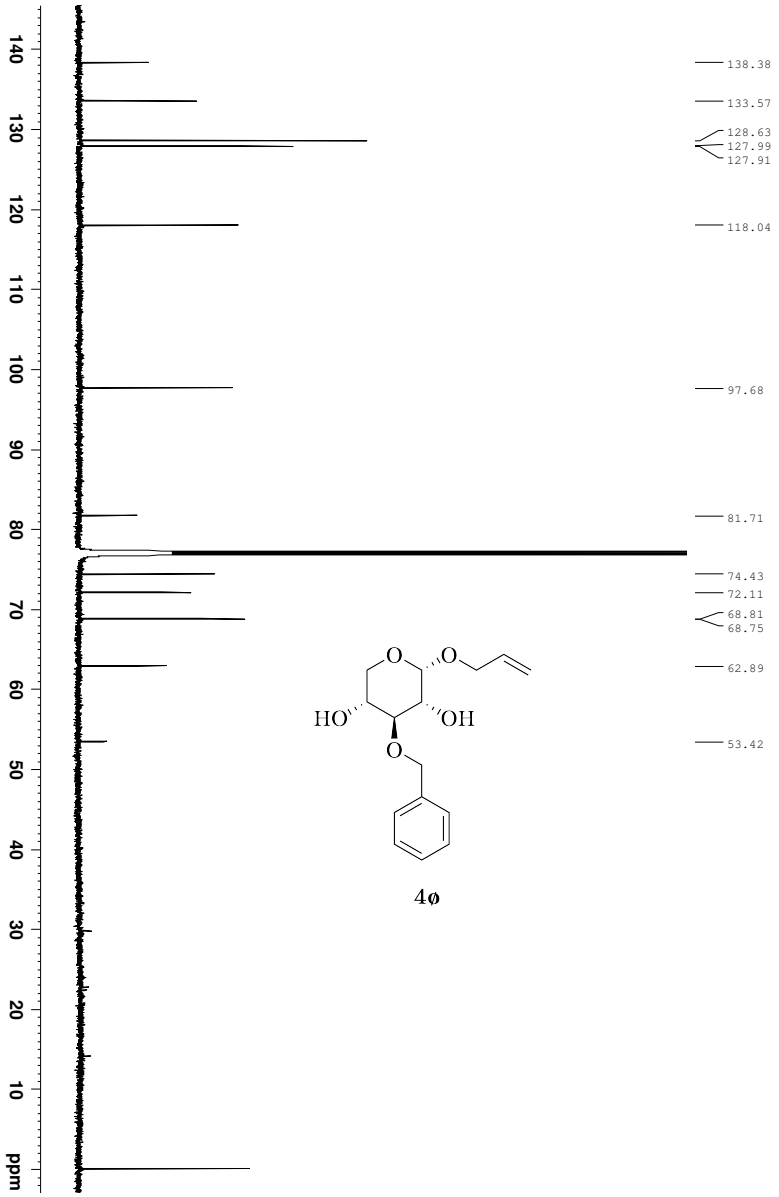

Figure 291: ^{13}C NMR spectrum of **4ø**.

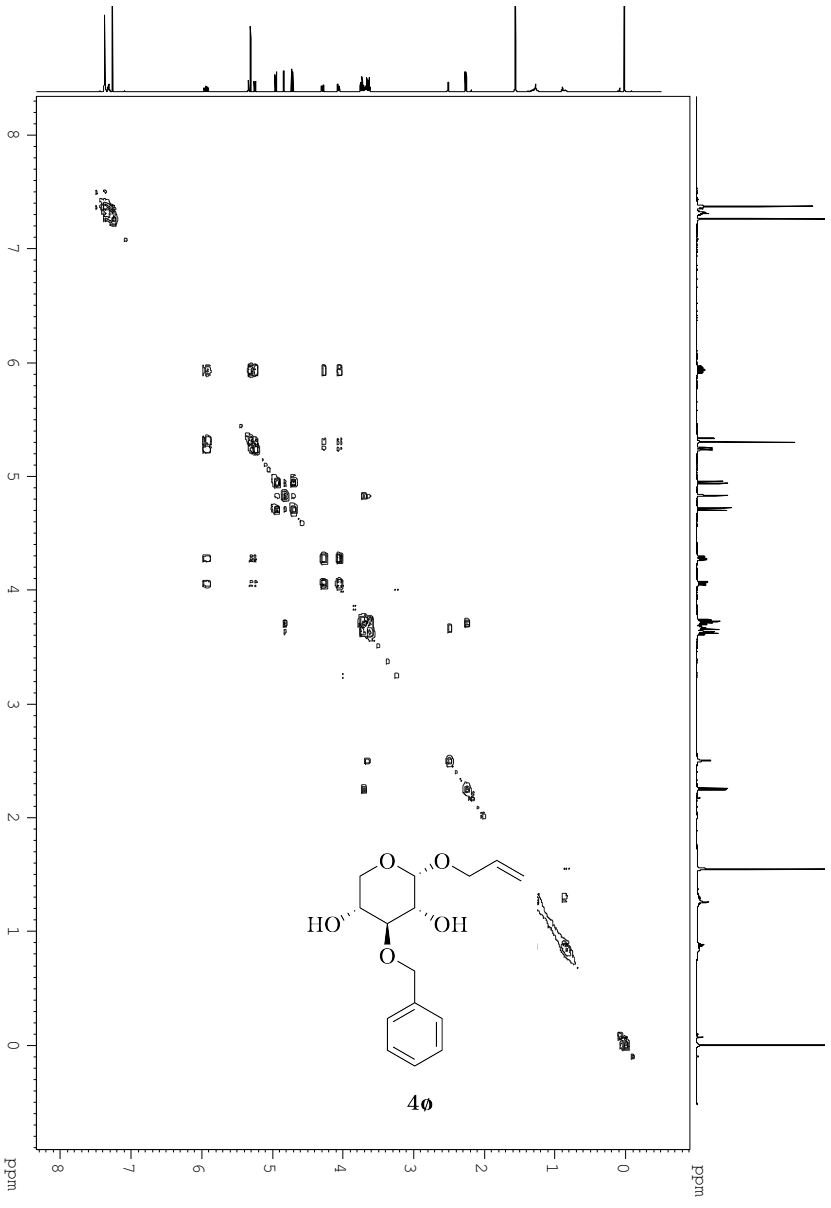

Figure 292: COSY spectrum of **4ø**.

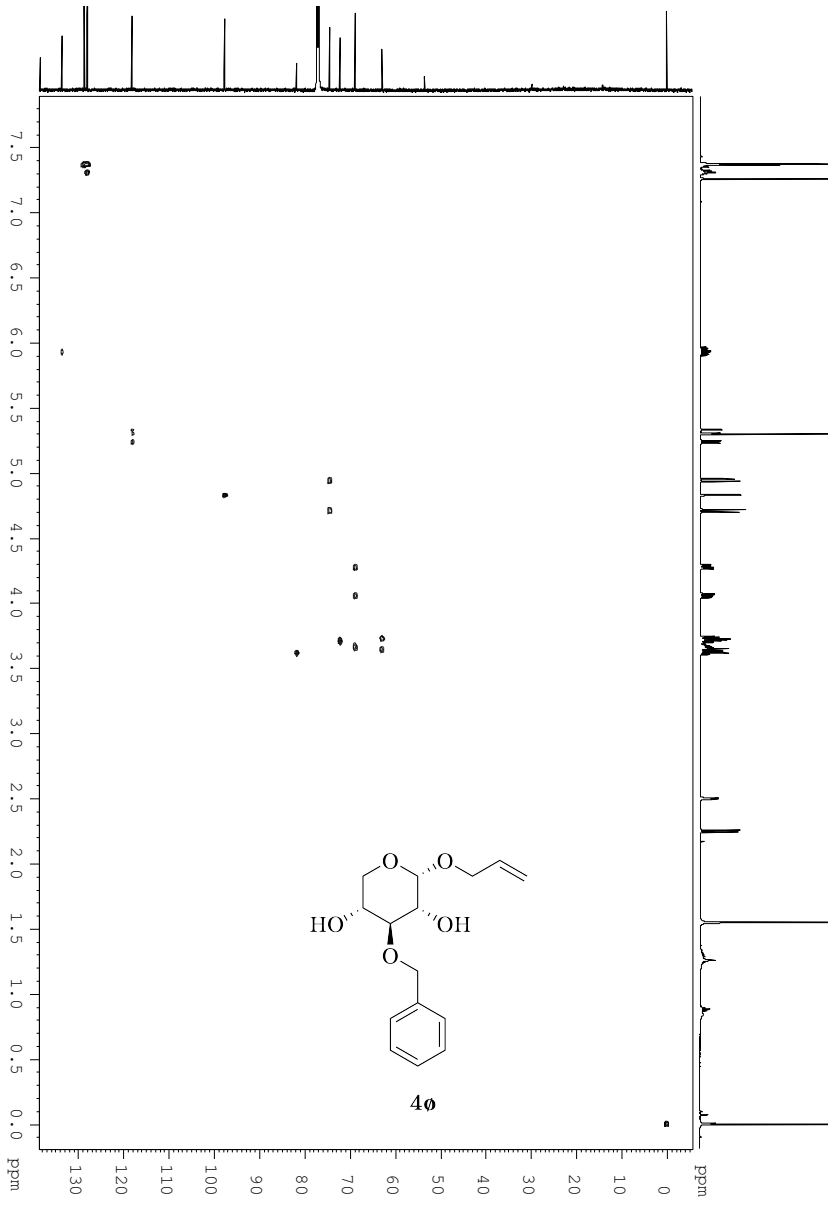

Figure 293: HSQC spectrum of **4ø**.

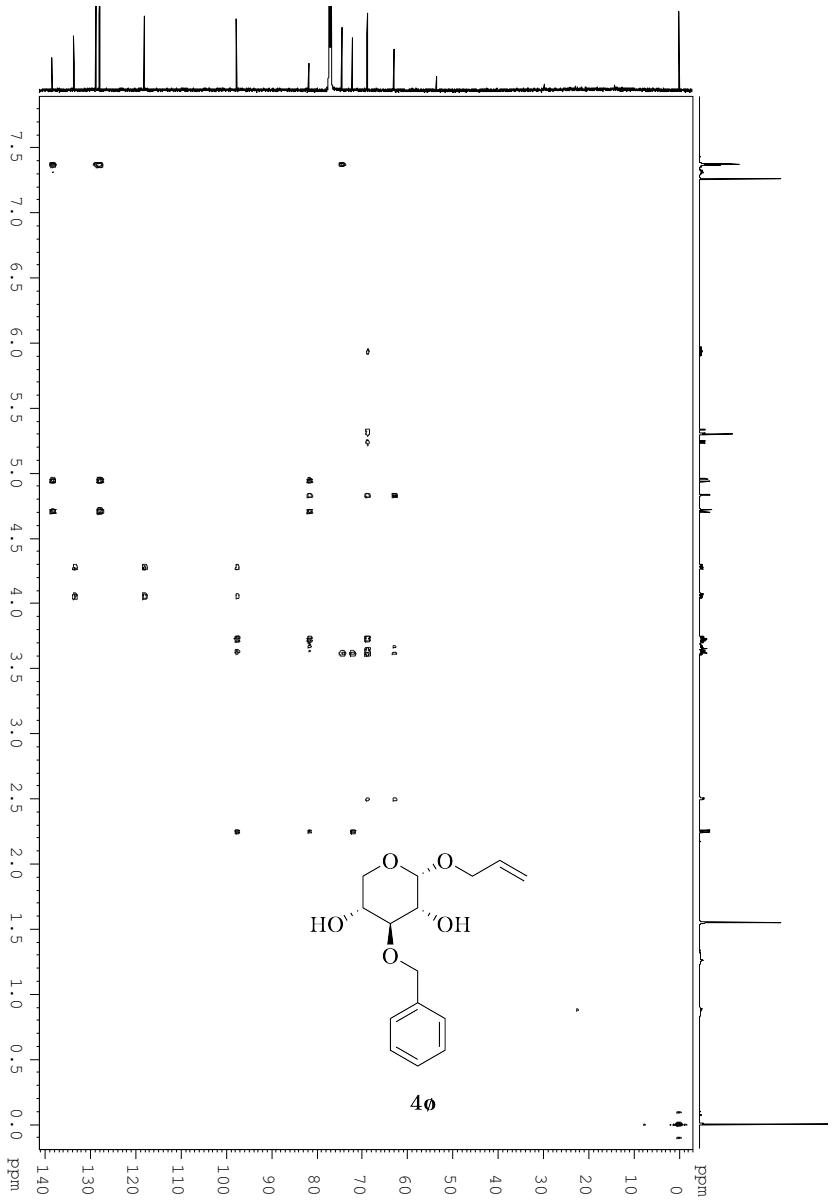

Figure 294: HMBC spectrum of **4ø**.

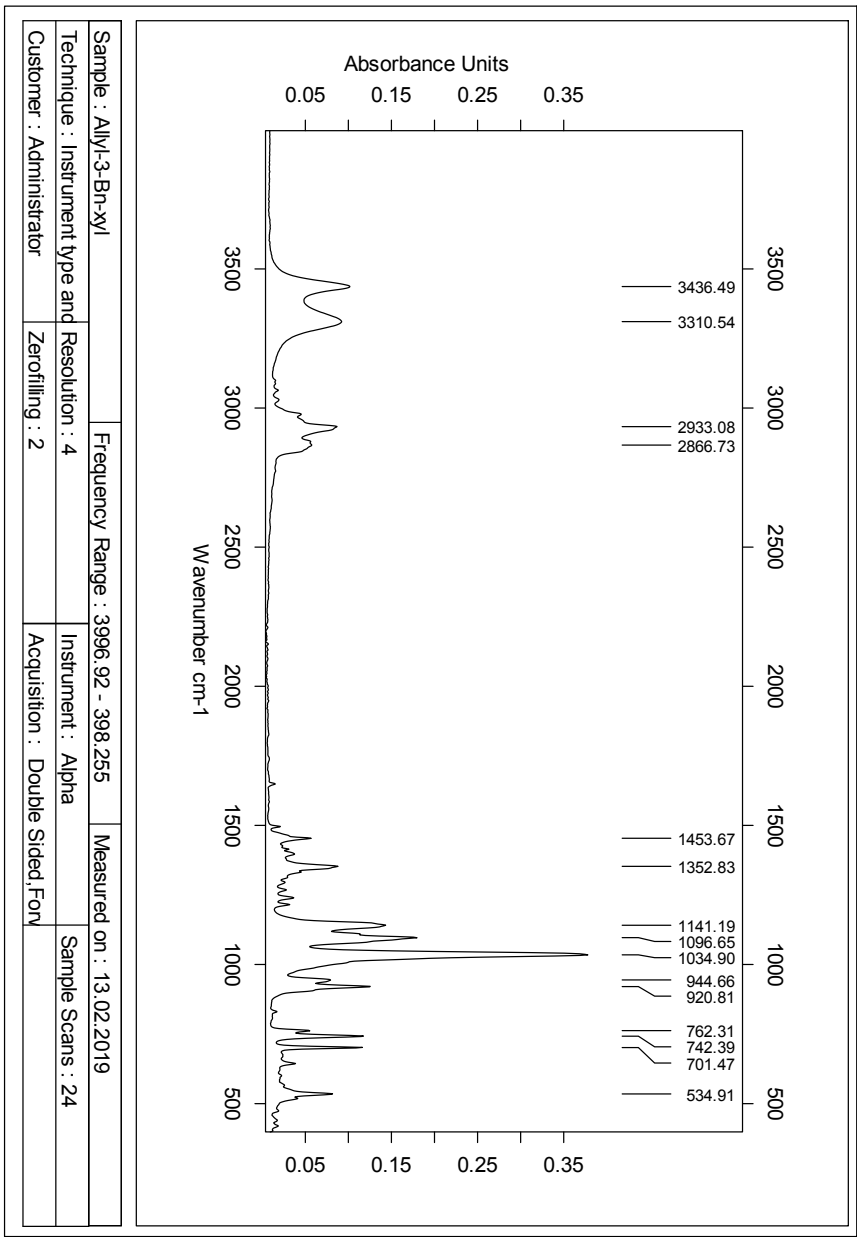

Figure 295: IR spectrum of **4ø**.

B.39 Spectroscopic data for compound 4ð

Elemental Composition Report **Page 1**

Single Mass Analysis
Tolerance = 2.0 PPM / DBE: min = -2.0, max = 50.0
Element prediction: Off
Number of isotope peaks used for i-FIT = 3

Monoisotopic Mass, Even Electron Ions
834 formula(e) evaluated with 2 results within limits (all results (up to 1000) for each mass)
Elements Used:
C: 0-100 H: 0-150 N: 0-10 O: 0-10 Na: 0-1
2019-116 152 (1.423) AM2 (Ar,35000.0,0.00,0.00); Cm (149:155)
1: TOF MS ES+

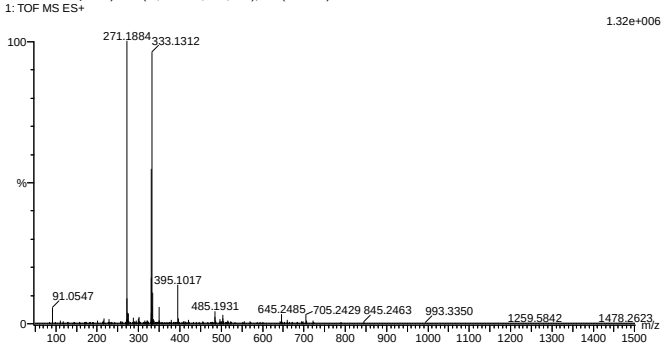

Minimum:				-2.0				
Maximum:		5.0	2.0	50.0				
Mass	Calc. Mass	mDa	PPM	DBE	i-FIT	Norm	Conf(%)	Formula
333.1312	333.1311	0.1	0.3	9.5	1283.8	2.383	9.23	C14 H17 N6 O4
	333.1314	-0.2	-0.6	5.5	1281.5	0.097	90.77	C16 H22 O6 Na

Figure 296: HRMS (ESI+) of **4ð**.

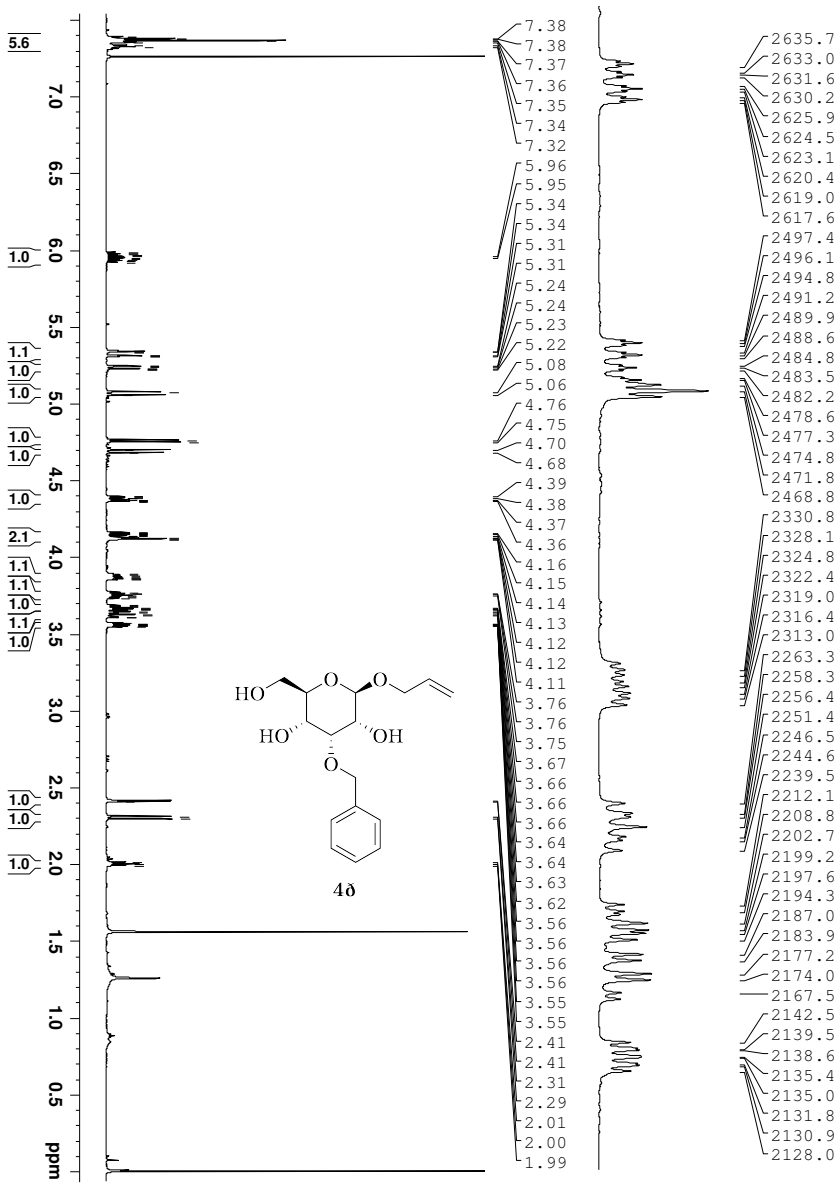

Figure 297: ^{1}H NMR spectrum of **4ð**.

4ð

Figure 298: ^{13}C NMR spectrum of **4ð**.

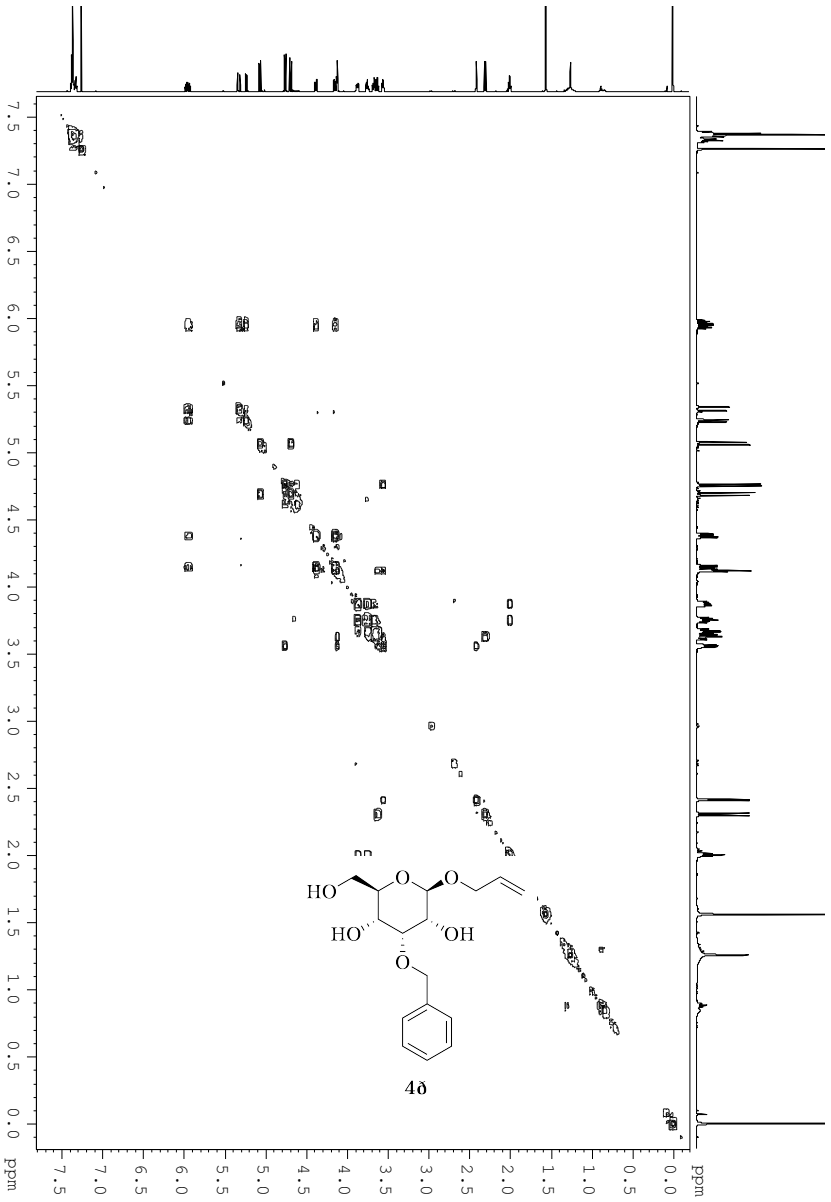

Figure 299: COSY spectrum of **4ð**.

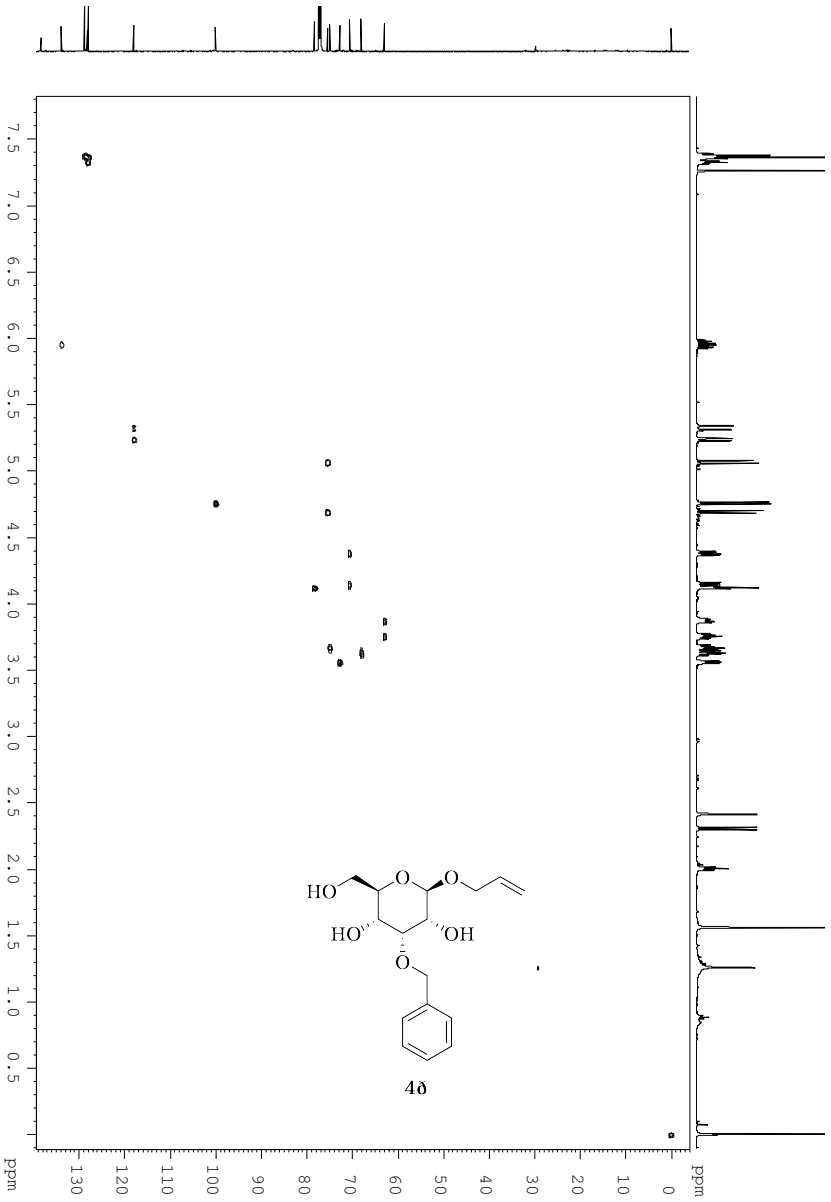

Figure 300: HSQC spectrum of **4ð**.

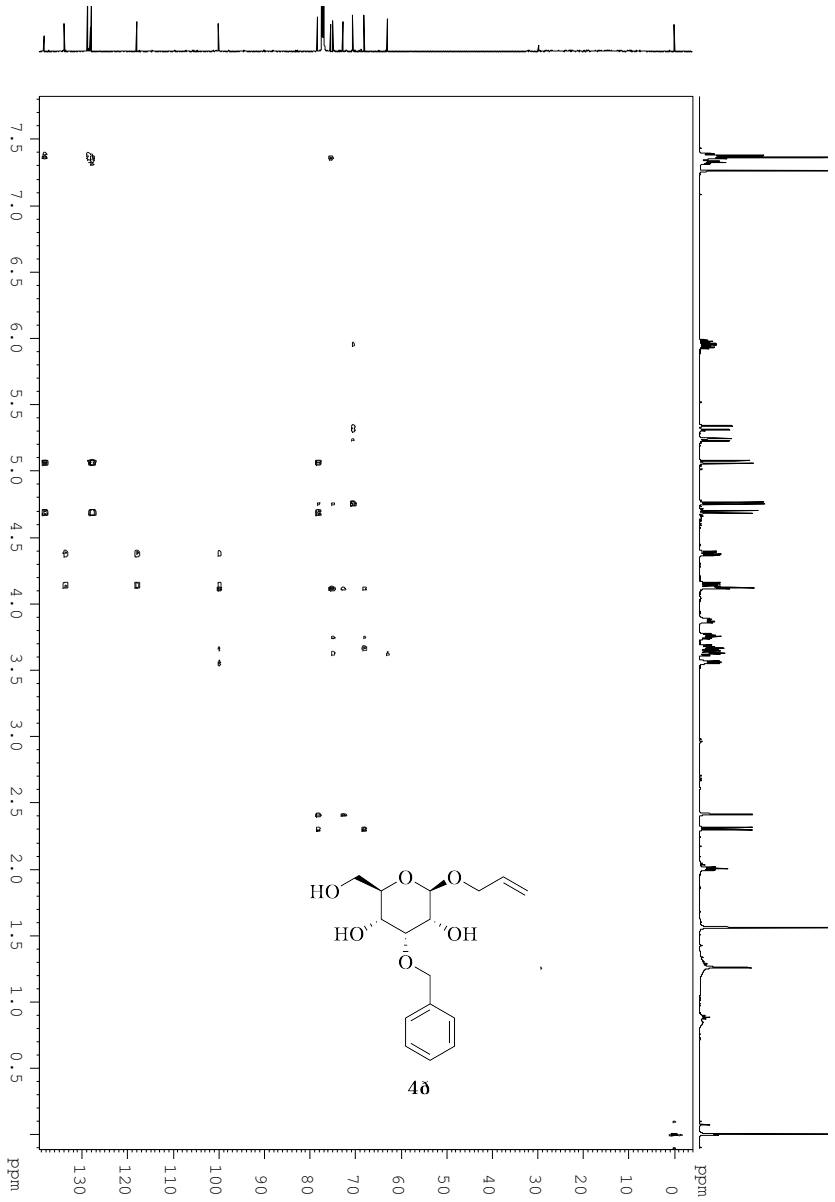

Figure 301: HMBC spectrum of **4ð**.

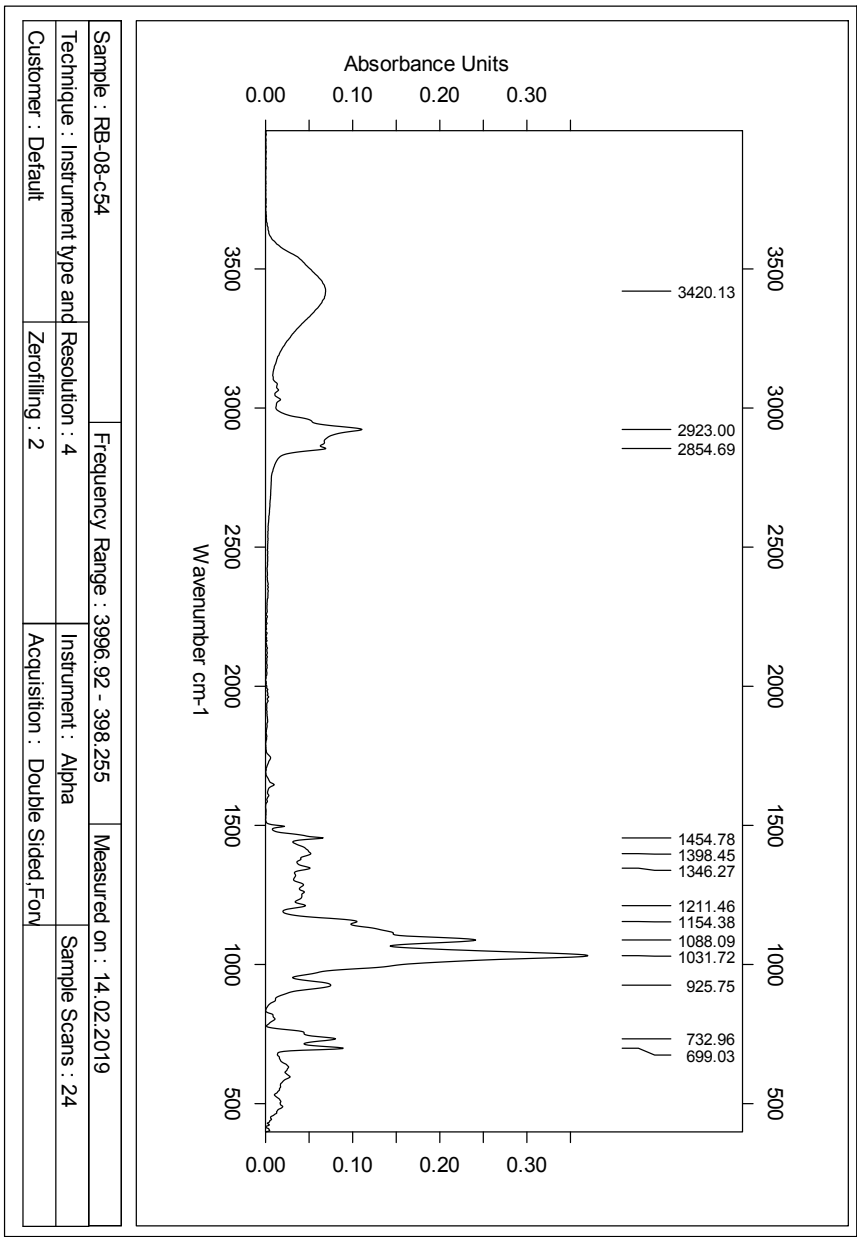

Figure 302: IR spectrum of **4ð**.

B.40 Spectroscopic data for compound 8a-α

Elemental Composition Report **Page 1**

Single Mass Analysis
Tolerance = 5.0 PPM / DBE: min = -2.0, max = 50.0
Element prediction: Off
Number of isotope peaks used for i-FIT = 3

Monoisotopic Mass, Even Electron Ions
490 formula(e) evaluated with 1 results within limits (all results (up to 1000) for each mass)
Elements Used:
C: 0-100 H: 0-150 O: 0-10 Na: 0-1 Br: 0-3 Au: 0-3

2019-125 37 (0.368) AM2 (Ar,35000.0,0.00,0.00); Cm (26:45)
1: TOF MS ES+

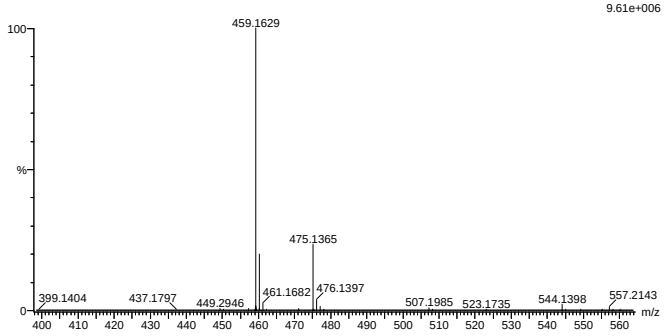

Minimum:				-2.0				
Maximum:		5.0	5.0	50.0				
Mass	Calc. Mass	mDa	PPM	DBE	i-FIT	Norm	Conf(%)	Formula
459.1629	459.1631	-0.2	-0.4	8.5	1099.6	n/a	n/a	C22 H28 O9 Na

Figure 303: HRMS (ESI+) of **8a-α**.

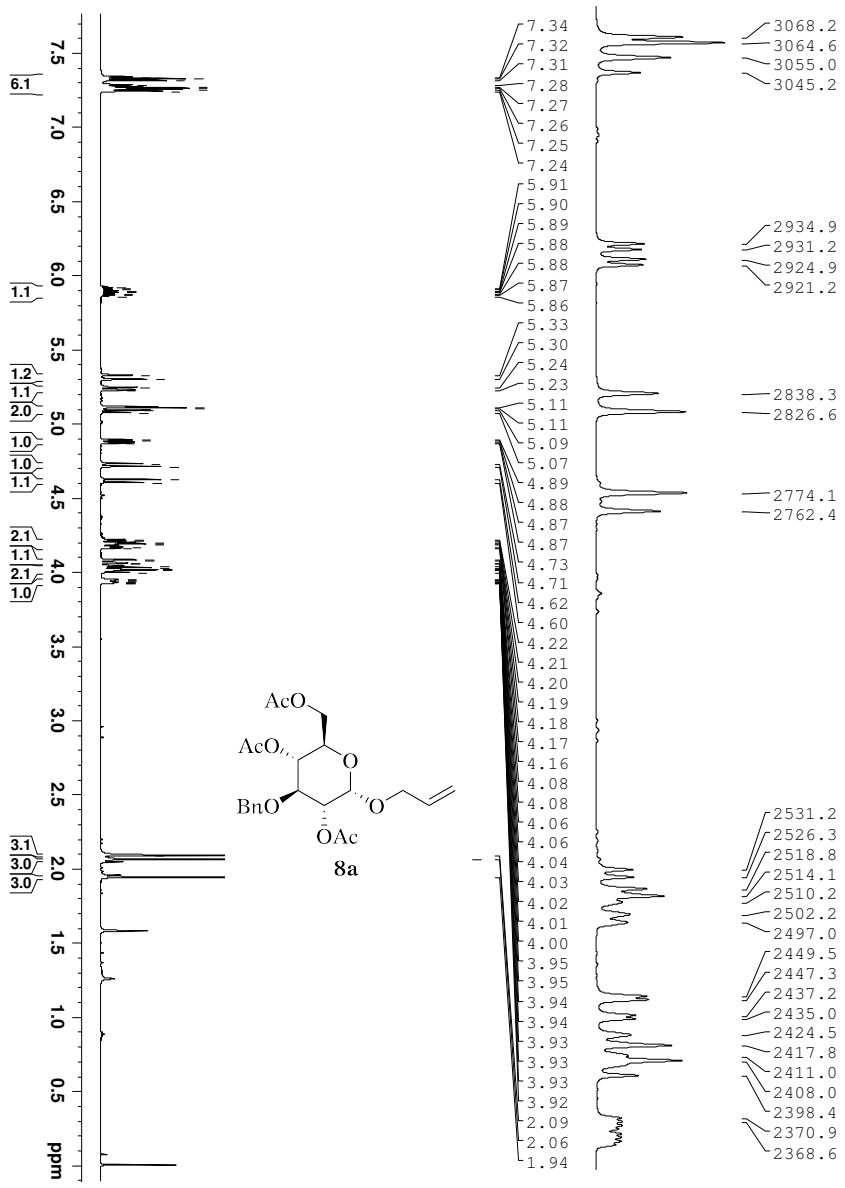

Figure 304: ^{1}H NMR spectrum of **8a-α**.

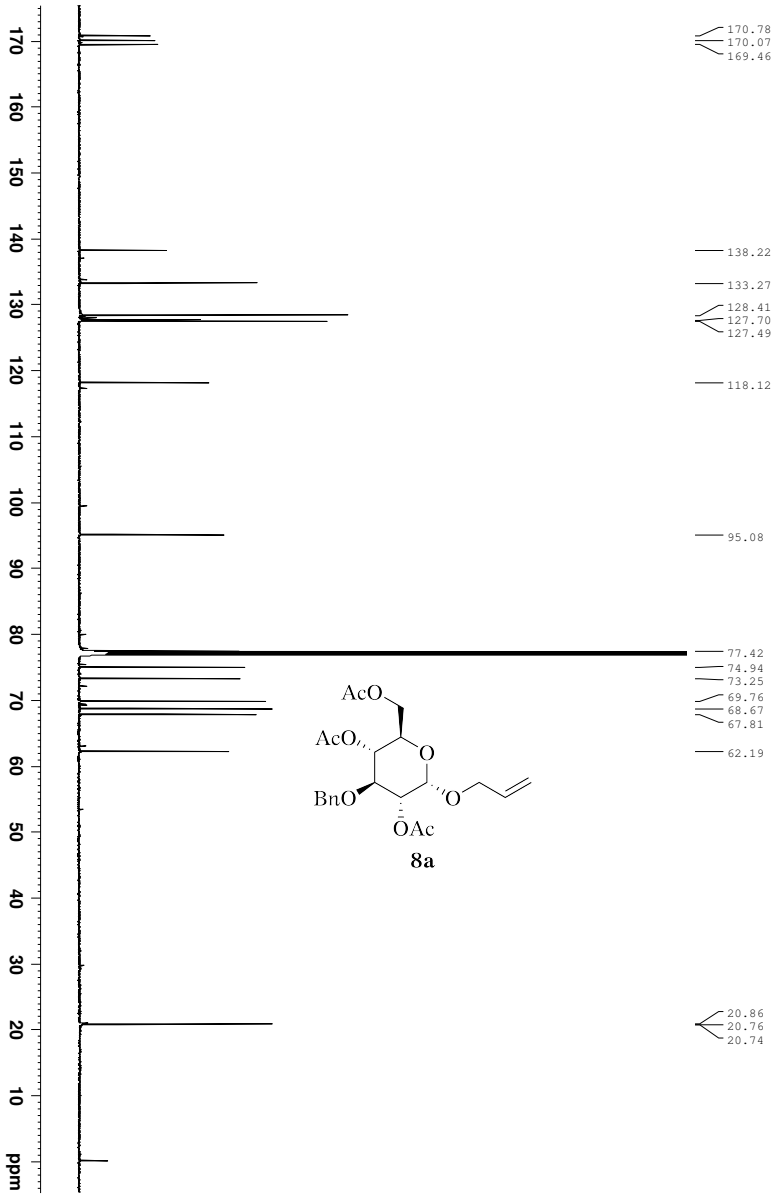

Figure 305: ^{13}C NMR spectrum of **8a-α**.

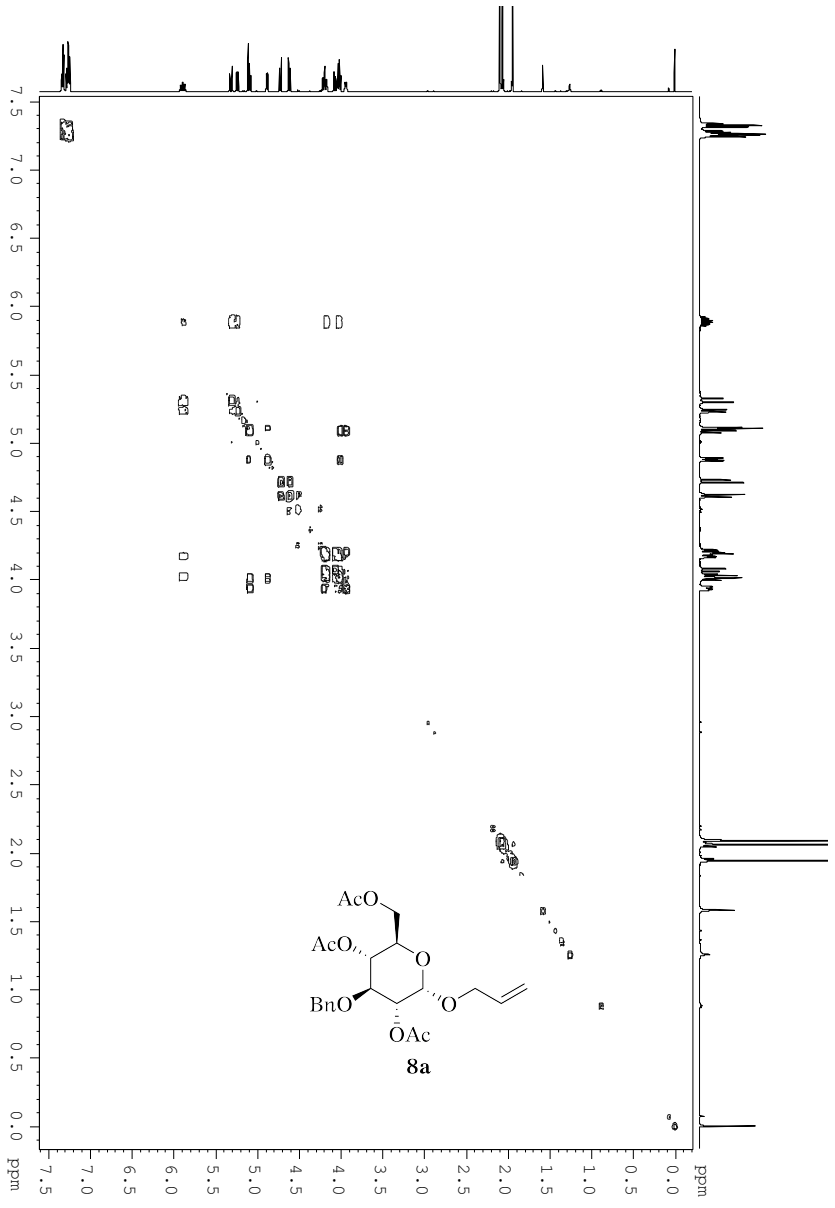

Figure 306: COSY spectrum of **8a-α**.

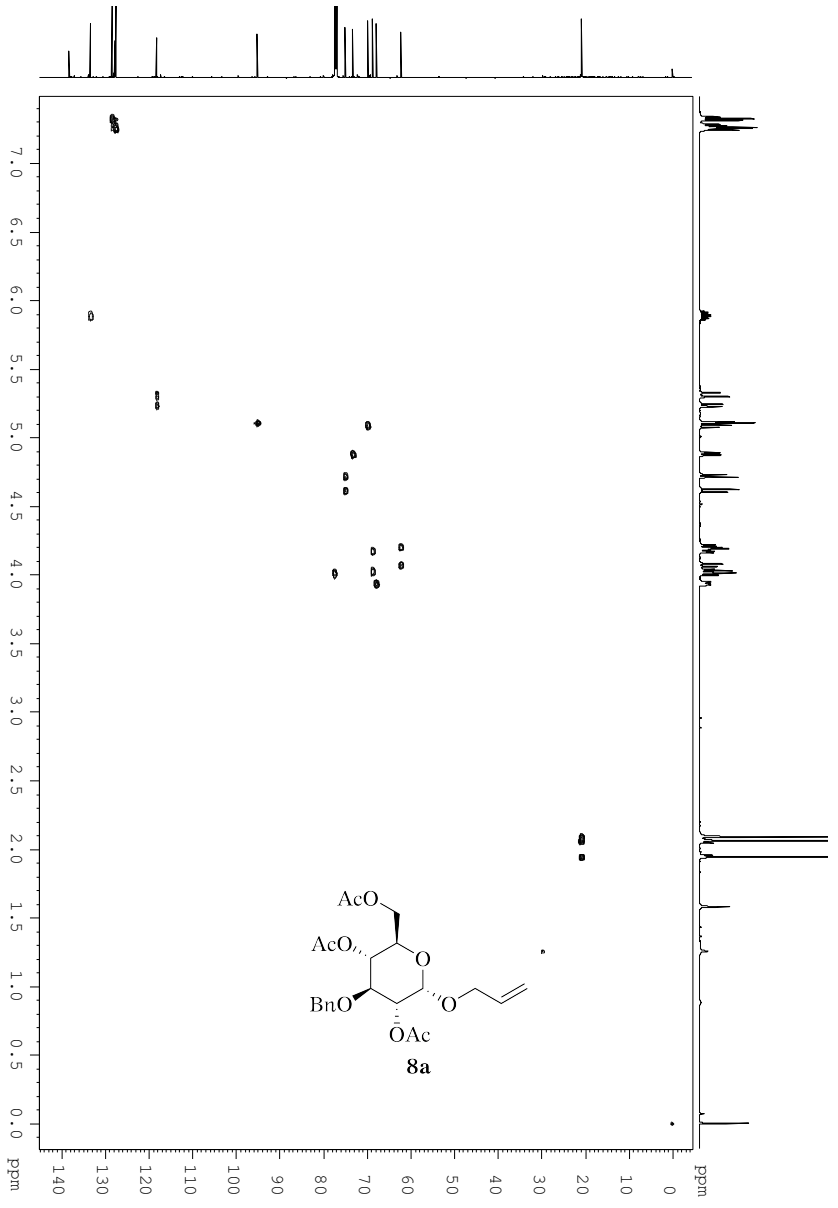

Figure 307: HSQC spectrum of **8a-α**.

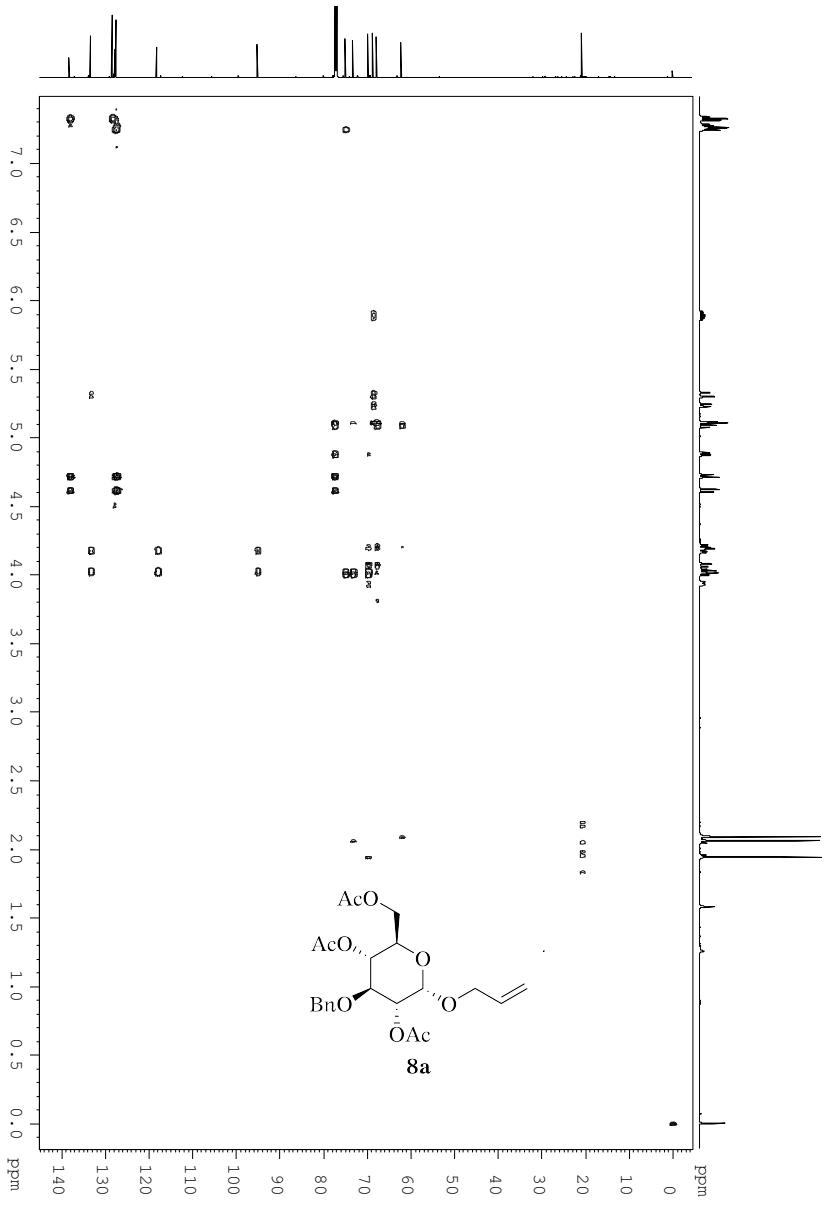

Figure 308: HMBC spectrum of **8a-α**.

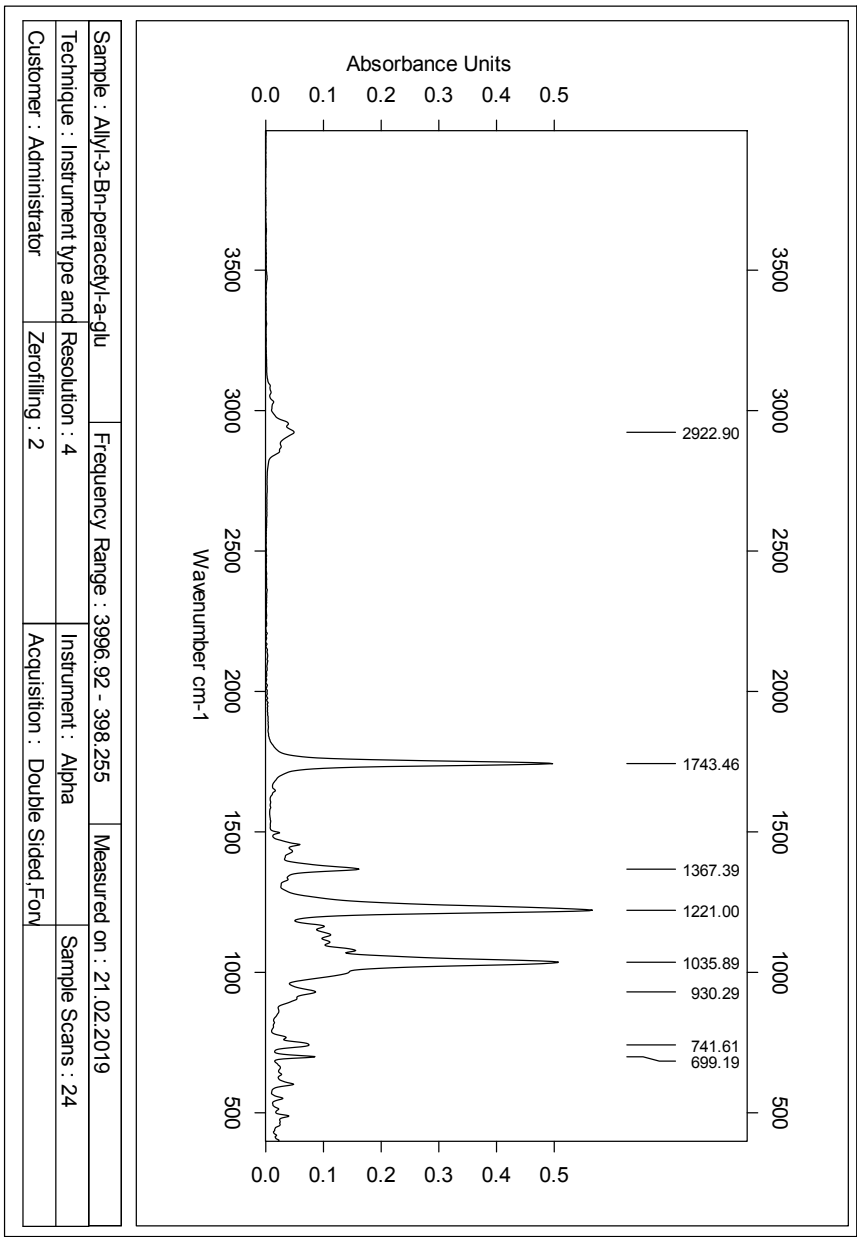

Figure 309: IR spectrum of **8a-α**.

B.41 Spectroscopic data for compound 8a-β

Elemental Composition Report **Page 1**

Single Mass Analysis
Tolerance = 3.0 PPM / DBE: min = -2.0, max = 50.0
Element prediction: Off
Number of isotope peaks used for i-FIT = 3

Monoisotopic Mass, Even Electron Ions
231 formula(e) evaluated with 2 results within limits (all results (up to 1000) for each mass)
Elements Used:
C: 0-100 H: 0-150 O: 0-10 Na: 0-1 K: 0-1
2019-126 9 (0.105) AM2 (Ar,35000.0,0.00,0.00)
1: TOF MS ES+

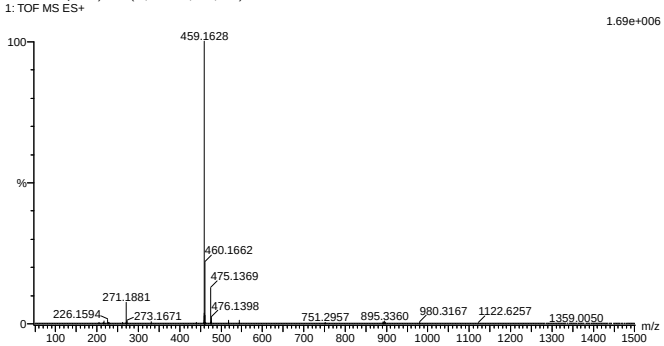

Minimum:				-2.0				
Maximum:		5.0	3.0	50.0				
Mass	Calc. Mass	mDa	PPM	DBE	i-FIT	Norm	Conf(%)	Formula
459.1628	459.1631	-0.3	-0.7	8.5	967.0	0.000	100.00	C22 H28 O9 Na
	459.1633	-0.5	-1.1	3.5	980.5	13.549	0.00	C19 H32 O10 K

Figure 310: HRMS (ESI+) of **8a-β**.

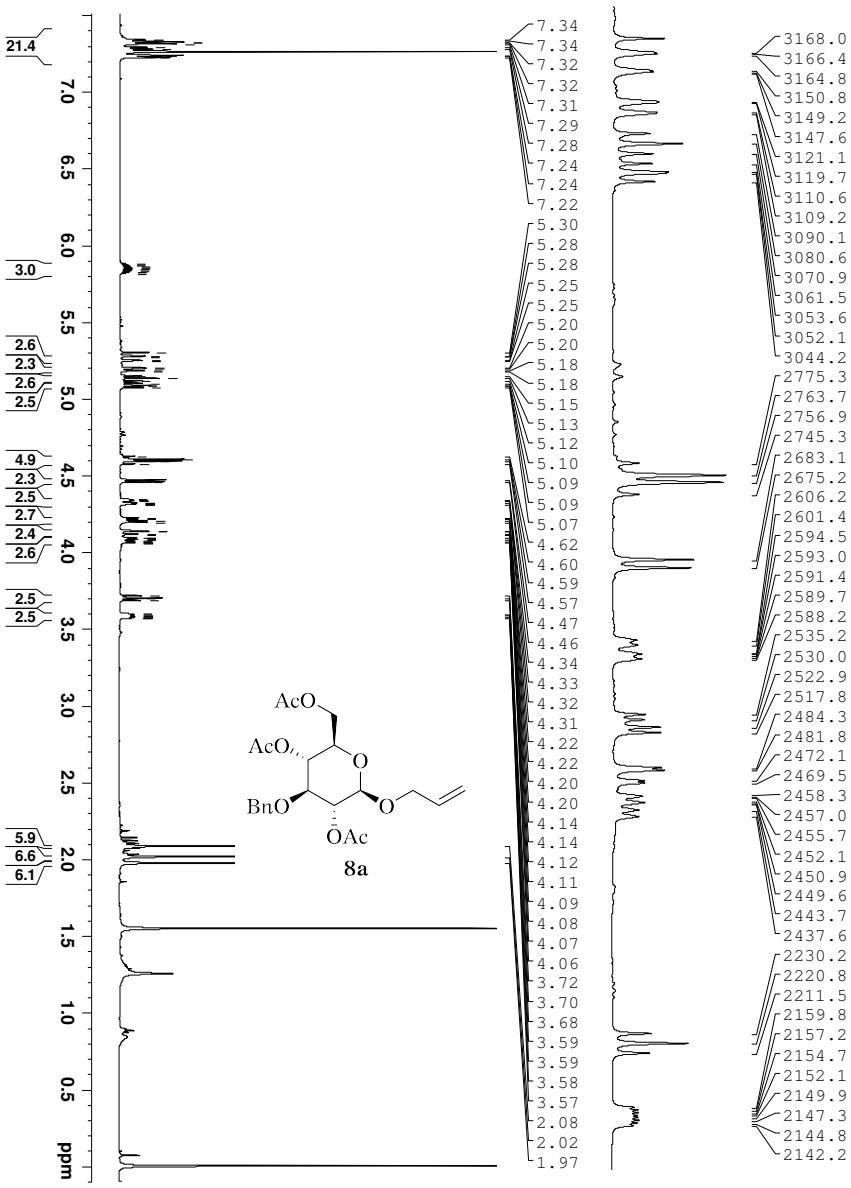

Figure 311: ^{1}H NMR spectrum of **8a-β**.

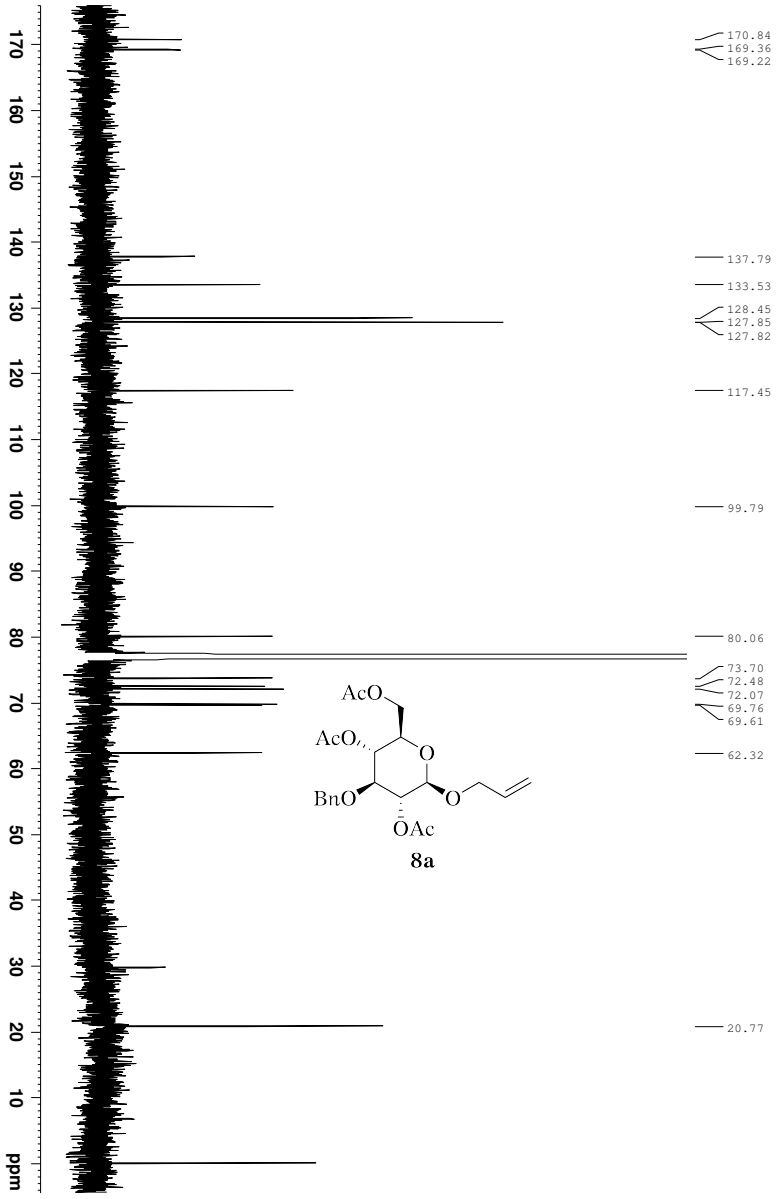

Figure 312: ^{13}C NMR spectrum of **8a-β**.

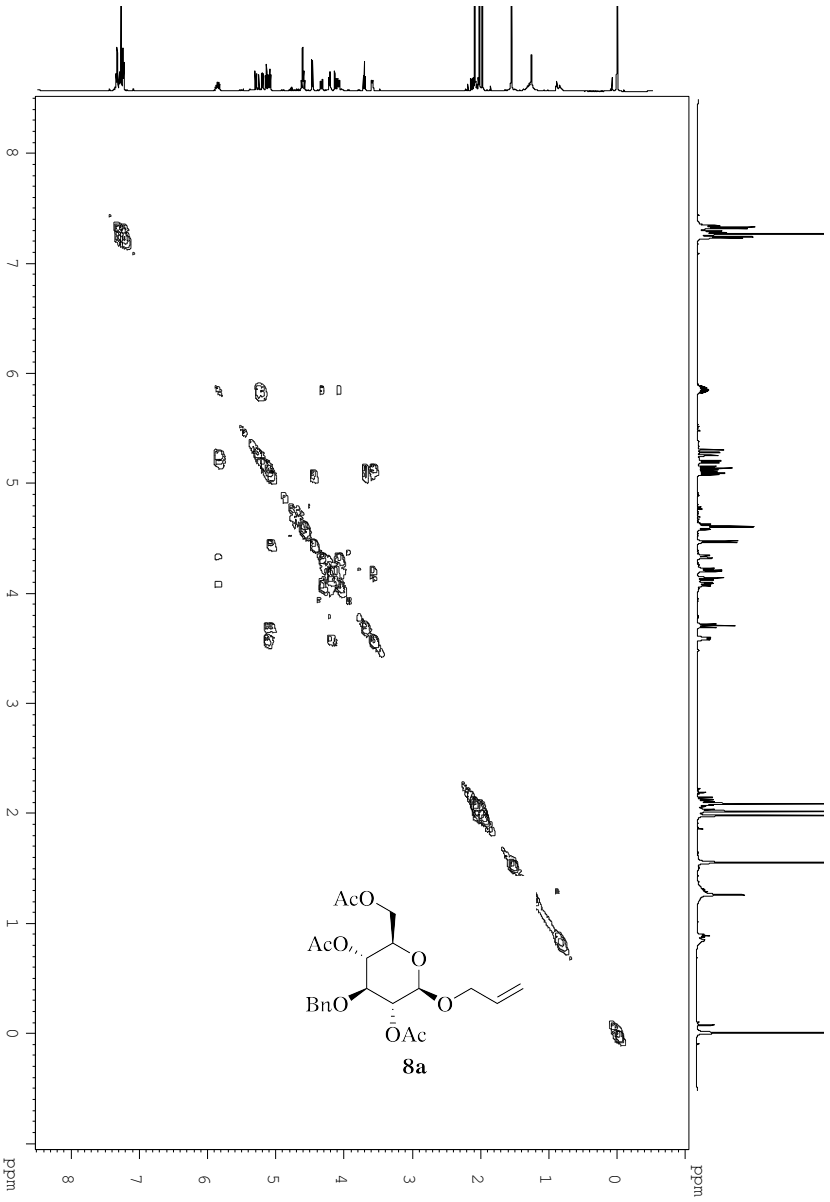

Figure 313: COSY spectrum of **8a-β**.

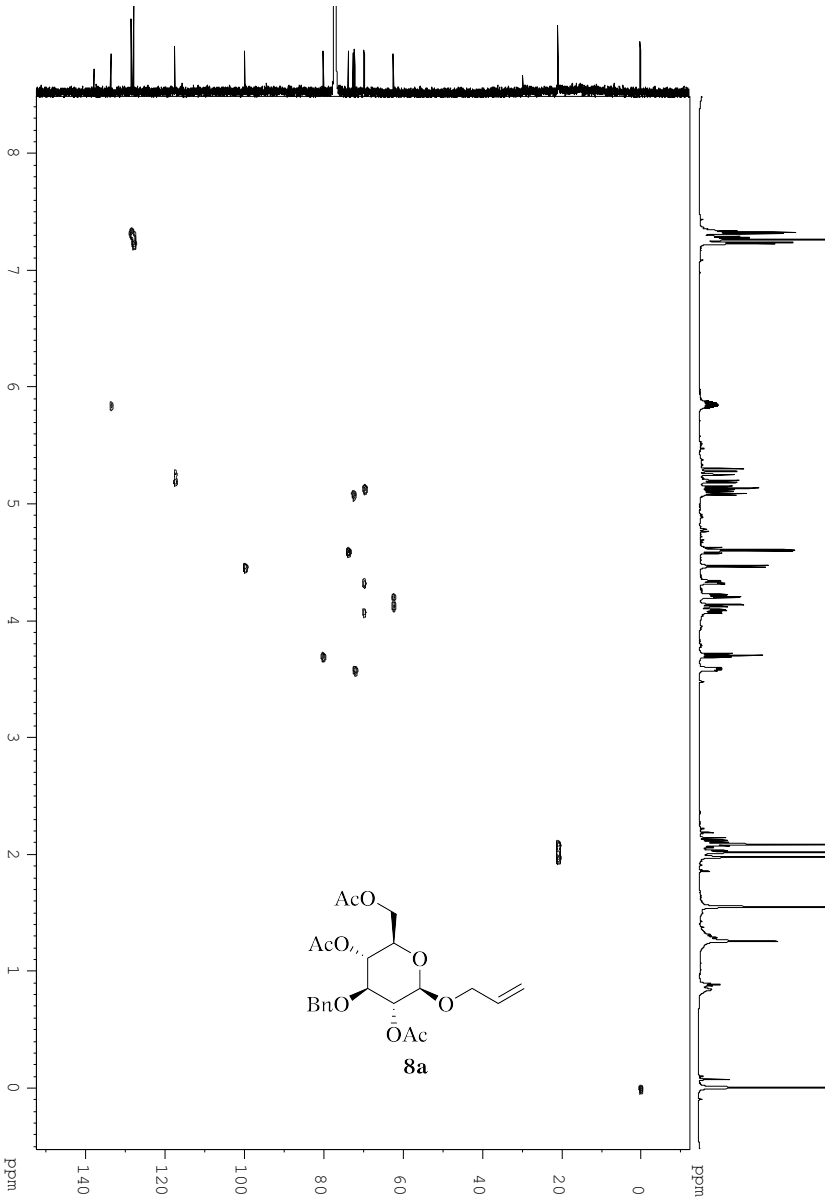

Figure 314: HSQC spectrum of **8a-β**.

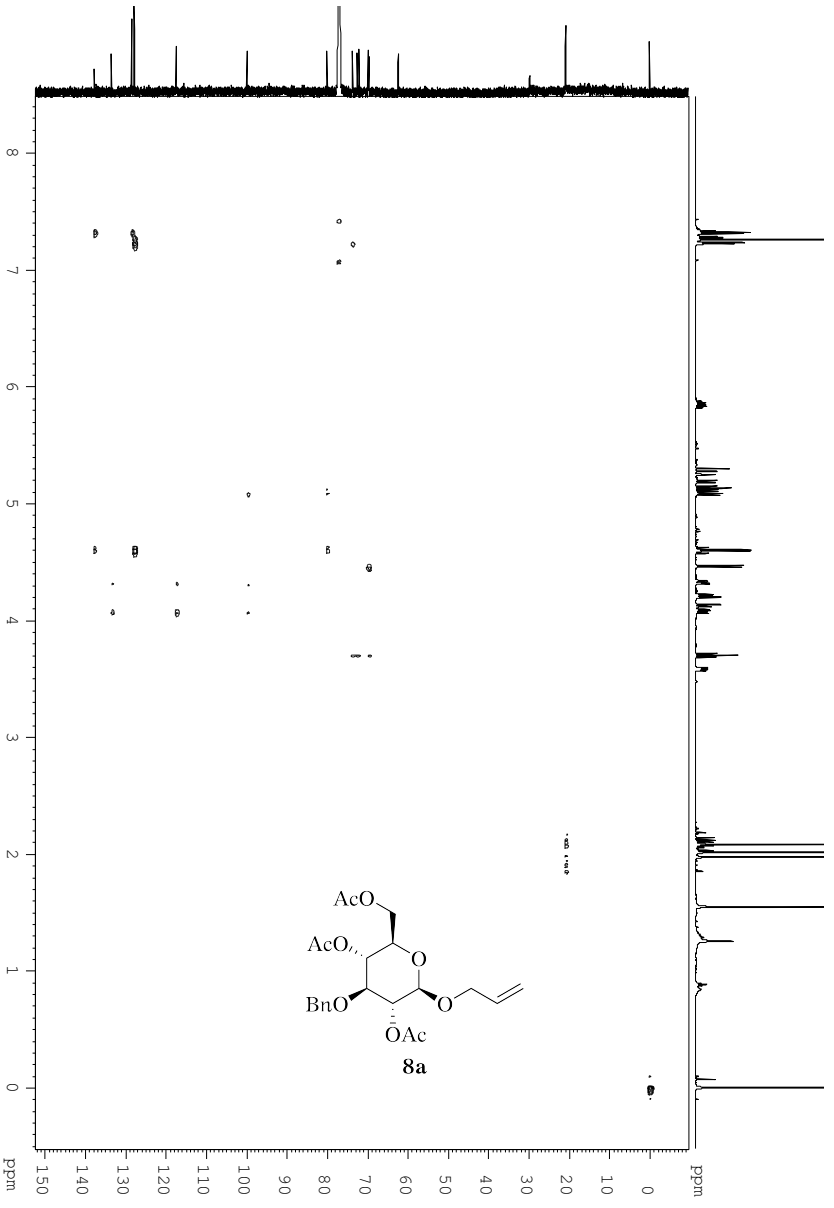

Figure 315: HMBC spectrum of **8a-β**.

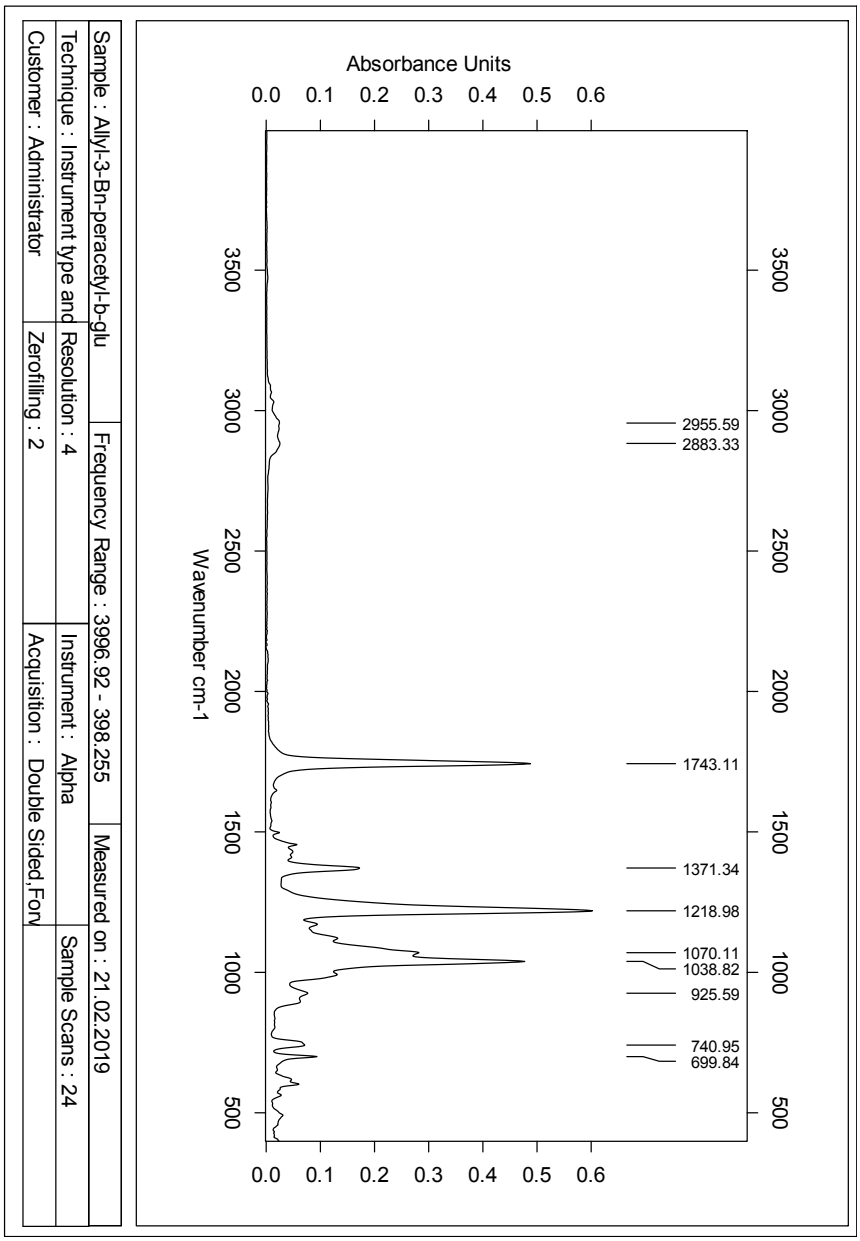

Figure 316: IR spectrum of **8a-β**.

B.42 Spectroscopic data for compound 8μ-α

Elemental Composition Report **Page 1**

Single Mass Analysis
Tolerance = 2.0 PPM / DBE: min = -2.0, max = 50.0
Element prediction: Off
Number of isotope peaks used for i-FIT = 3

Monoisotopic Mass, Even Electron Ions
1123 formula(e) evaluated with 2 results within limits (all results (up to 1000) for each mass)
Elements Used:
C: 0-100 H: 0-150 N: 0-10 O: 0-10 Na: 0-1

svg_20190306_2019_159 31 (0.585) AM2 (Ar,35000.0,0.00,0.00); Cm (31:32)
1: TOF MS ES+

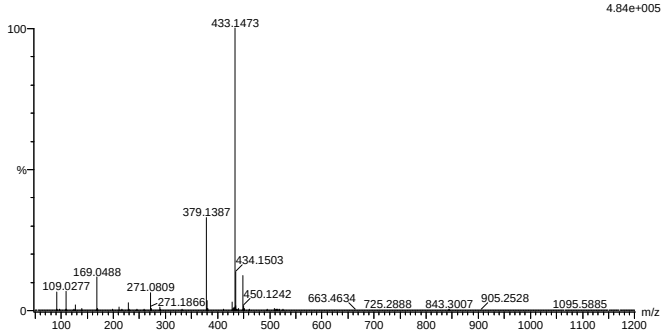

Minimum:				-2.0				
Maximum:		5.0	2.0	50.0				
Mass	Calc. Mass	mDa	PPM	DBE	i-FIT	Norm	Conf(%)	Formula
433.1473	433.1472	0.1	0.2	11.5	906.7	0.100	90.52	C18 H21 N6 O7
	433.1475	-0.2	-0.5	7.5	909.0	2.356	9.48	C20 H26 O9 Na

Figure 317: HRMS (ESI+) of **8μ-α**.

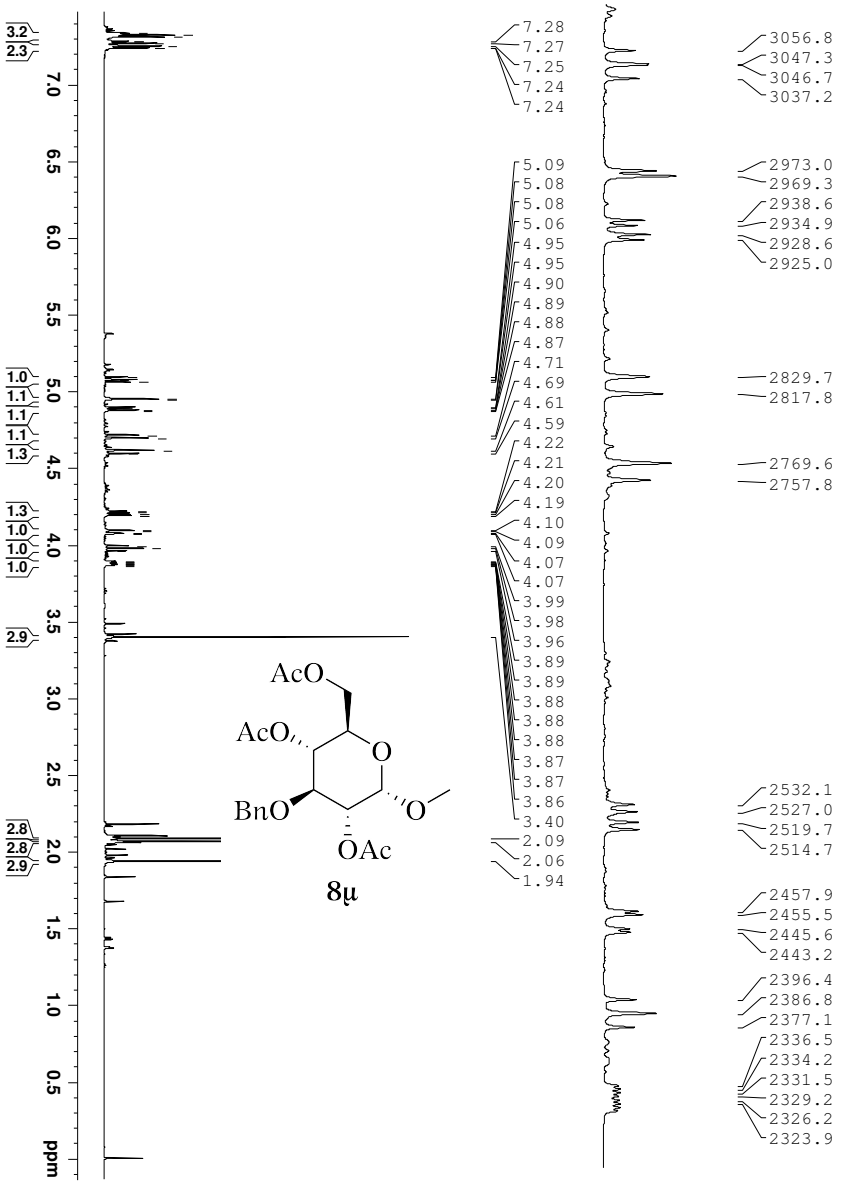

Figure 318: ^{1}H NMR spectrum of **8μ-α**.

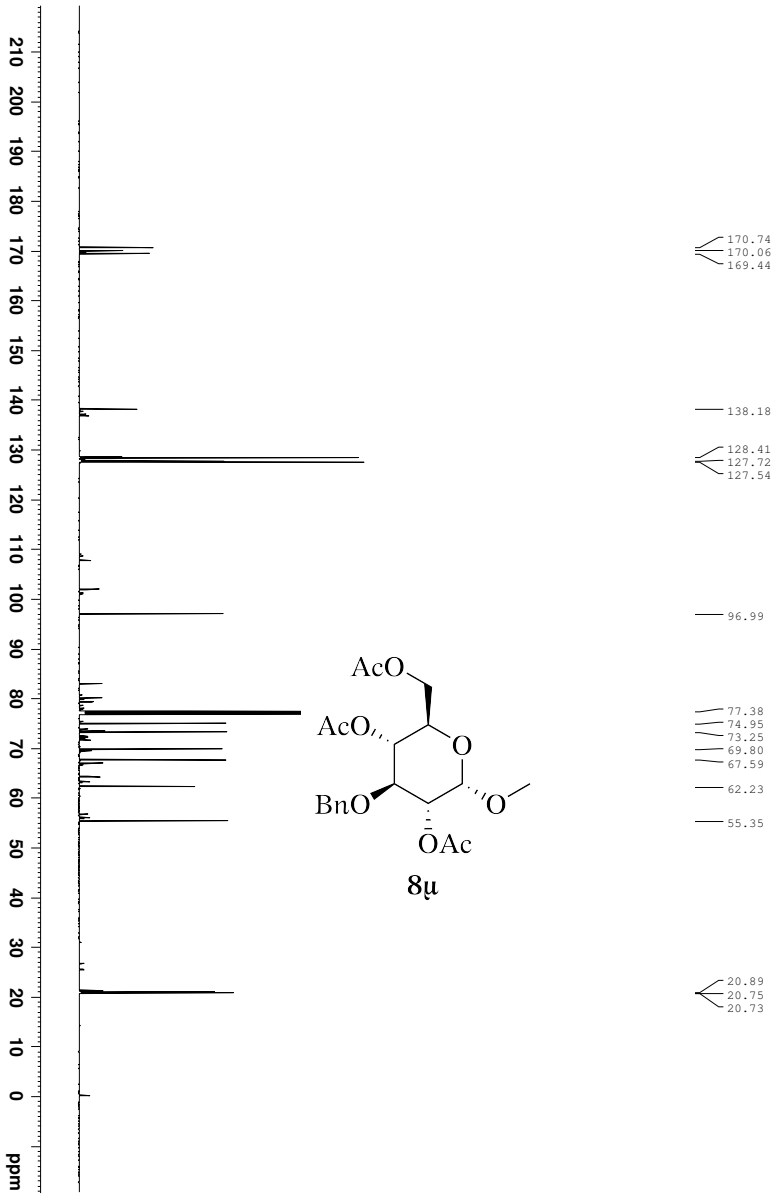

Figure 319: ^{13}C NMR spectrum of **8μ-α**.

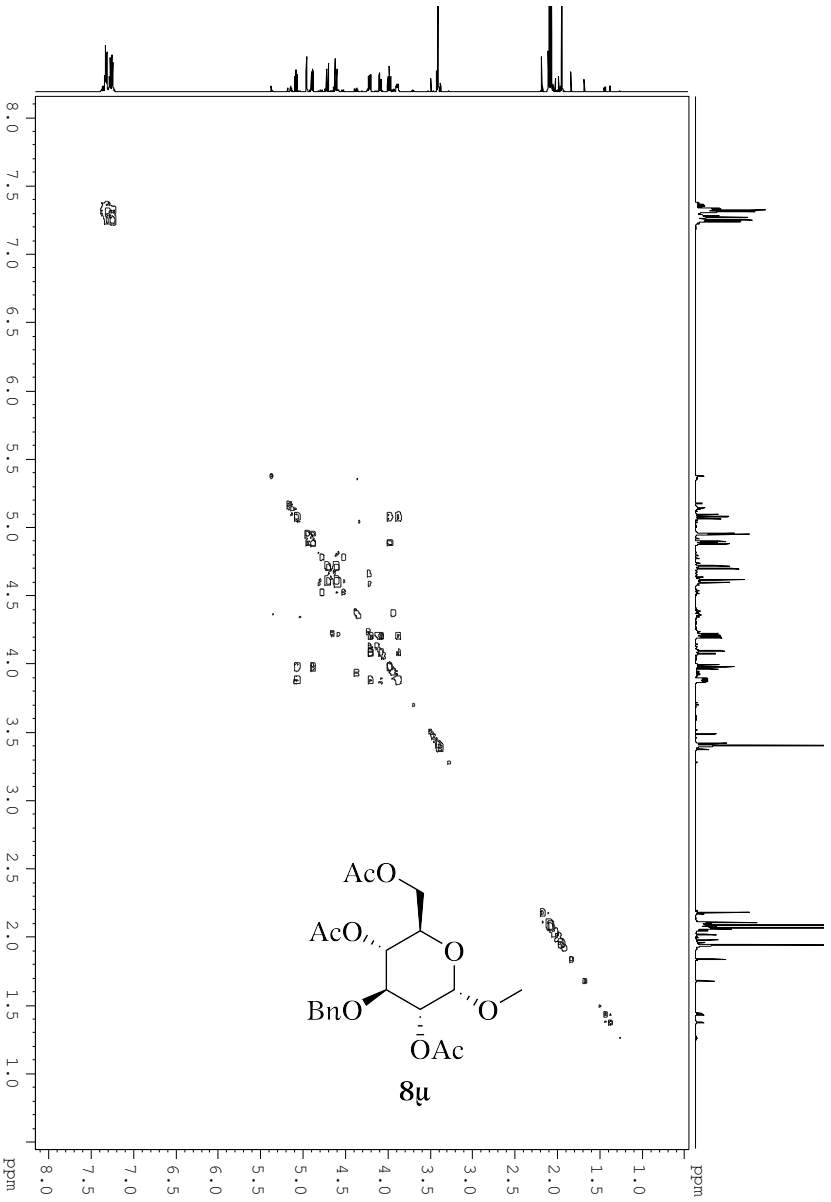

Figure 320: COSY spectrum of **8µ-α**.

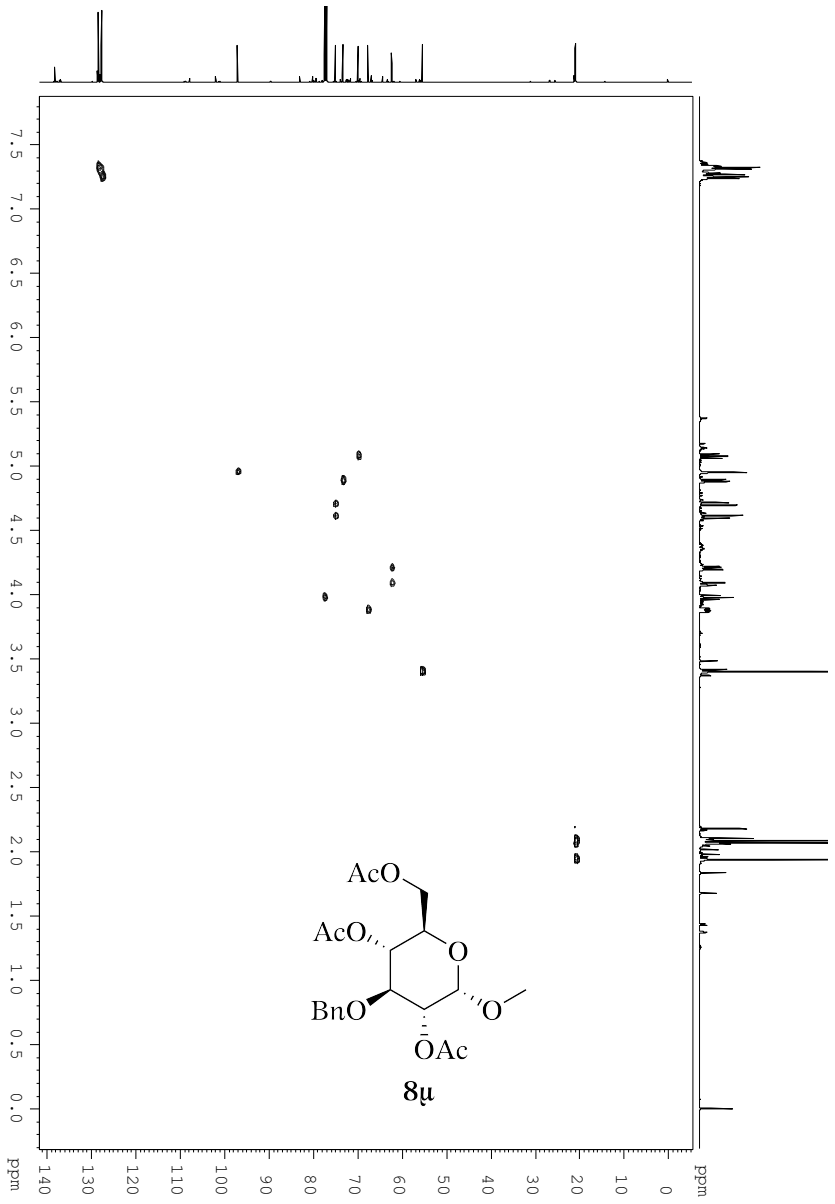

Figure 321: HSQC spectrum of **8μ-α**.

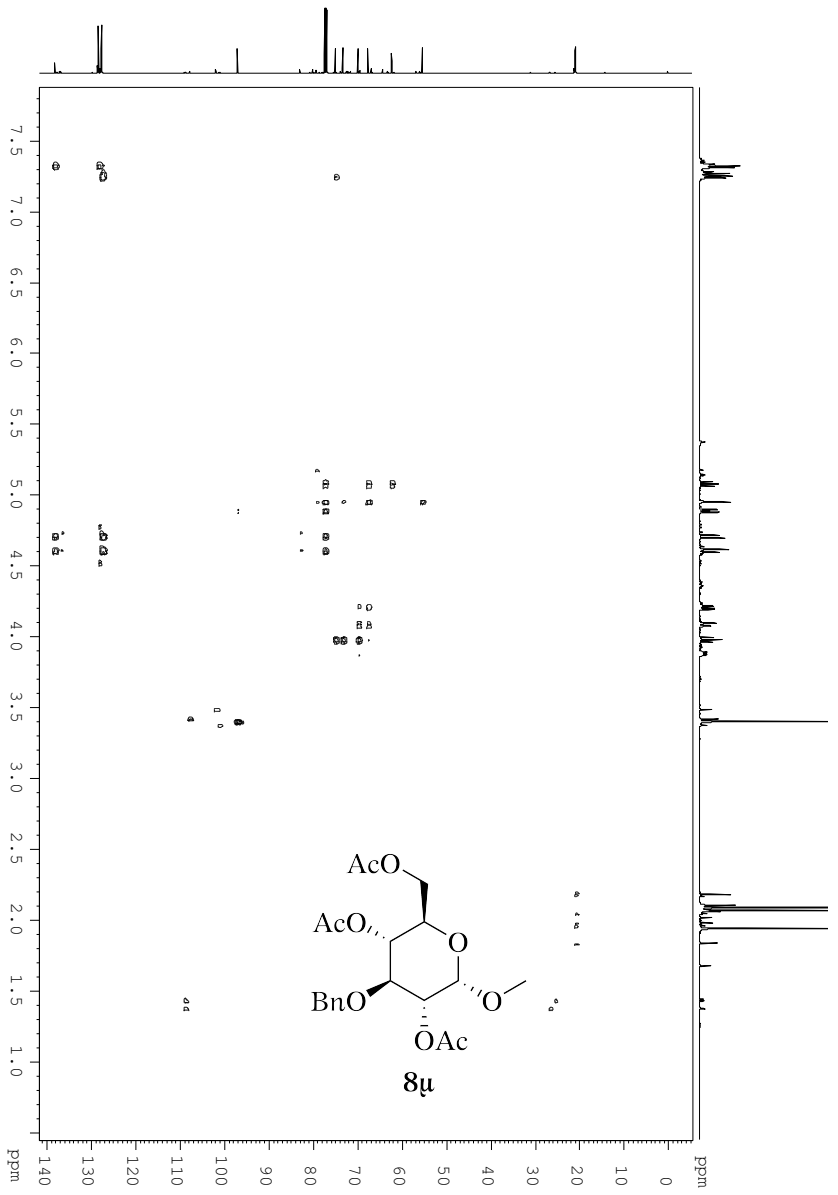

Figure 322: HMBC spectrum of **8μ-α**.

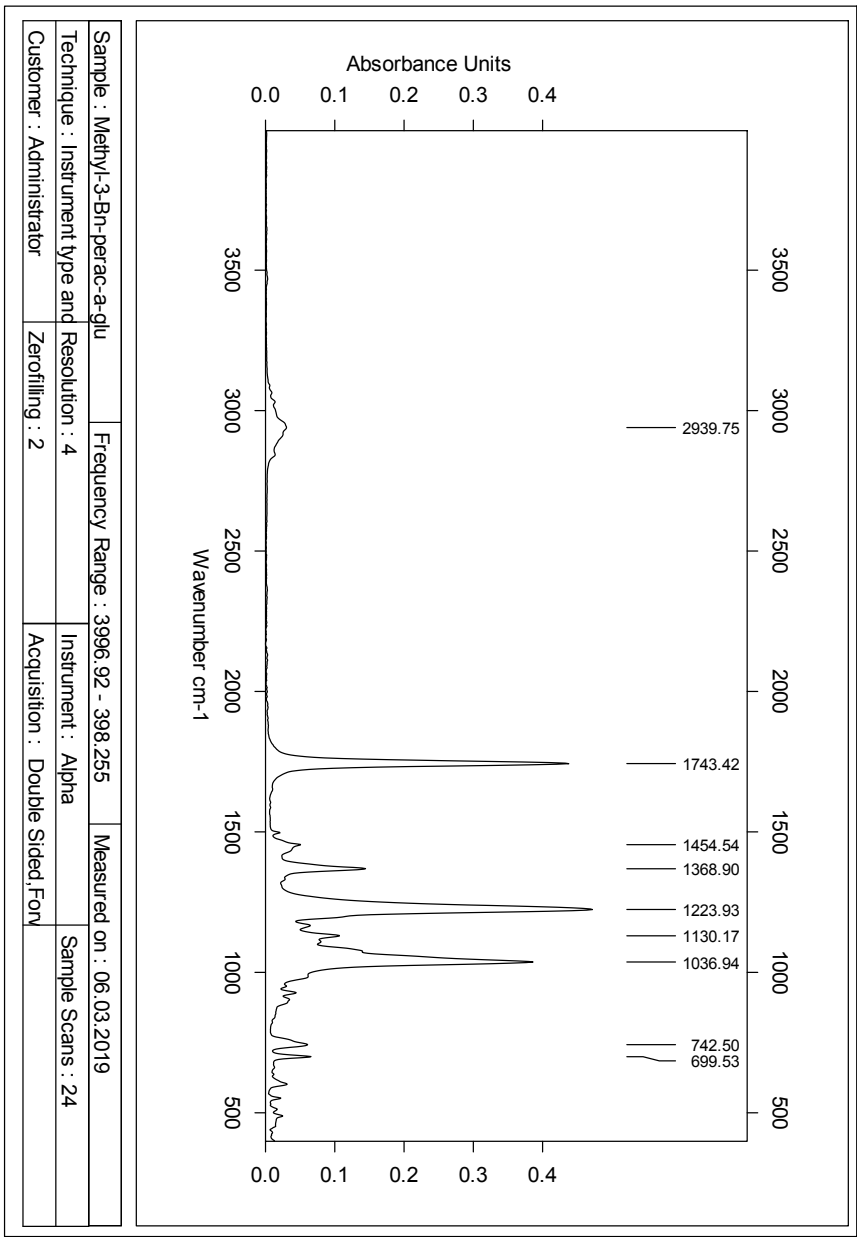

Figure 323: IR spectrum of **8μ-α**.

B.43 Spectroscopic data for compound 8μ-β

Elemental Composition Report **Page 1**

Single Mass Analysis
Tolerance = 2.0 PPM / DBE: min = -2.0, max = 50.0
Element prediction: Off
Number of isotope peaks used for i-FIT = 3

Monoisotopic Mass, Even Electron Ions
1123 formula(e) evaluated with 2 results within limits (all results (up to 1000) for each mass)
Elements Used:
C: 0-100 H: 0-150 N: 0-10 O: 0-10 Na: 0-1
svg_20190306_2019_160 31 (0.585) AM2 (Ar,35000.0,0.00,0.00); Cm (28:31)
1: TOF MS ES+

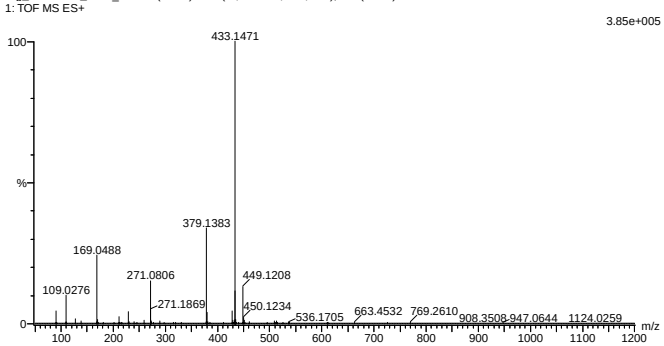

Minimum:				-2.0				
Maximum:		5.0	2.0	50.0				
Mass	Calc. Mass	mDa	PPM	DBE	i-FIT	Norm	Conf(%)	Formula
433.1471	433.1472	-0.1	-0.2	11.5	891.2	0.135	87.41	C18 H21 N6 O7
	433.1475	-0.4	-0.9	7.5	893.1	2.072	12.59	C20 H26 O9 Na

Figure 324: HRMS (ESI+) of **8μ-β**.

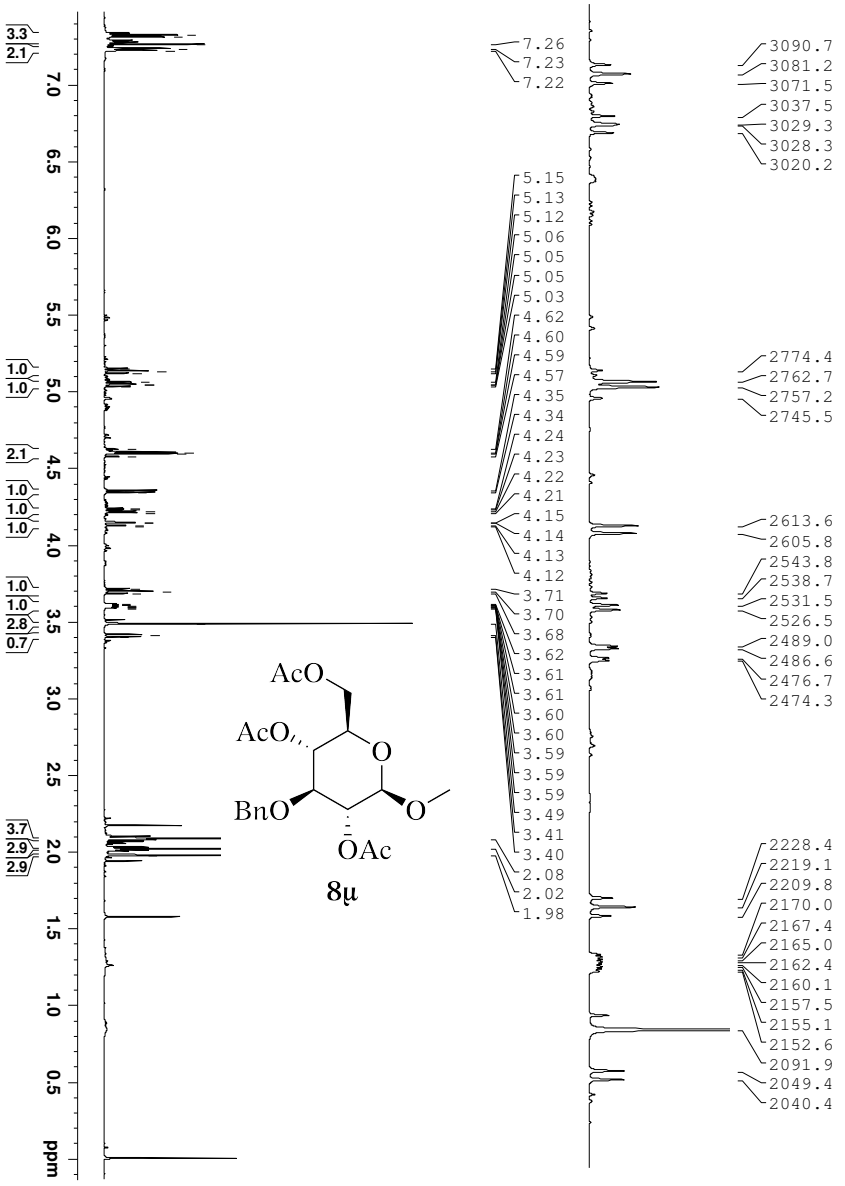

Figure 325: ^{1}H NMR spectrum of **8μ-β**.

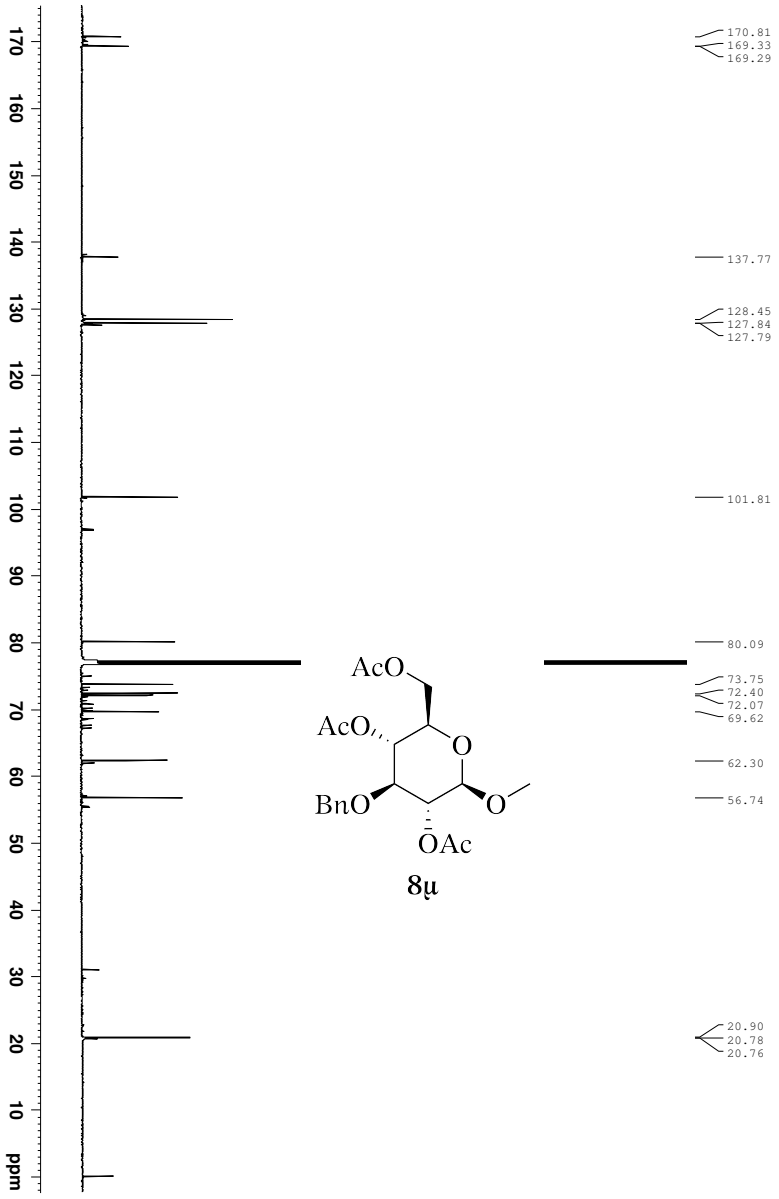

Figure 326: ^{13}C NMR spectrum of **8μ-β**.

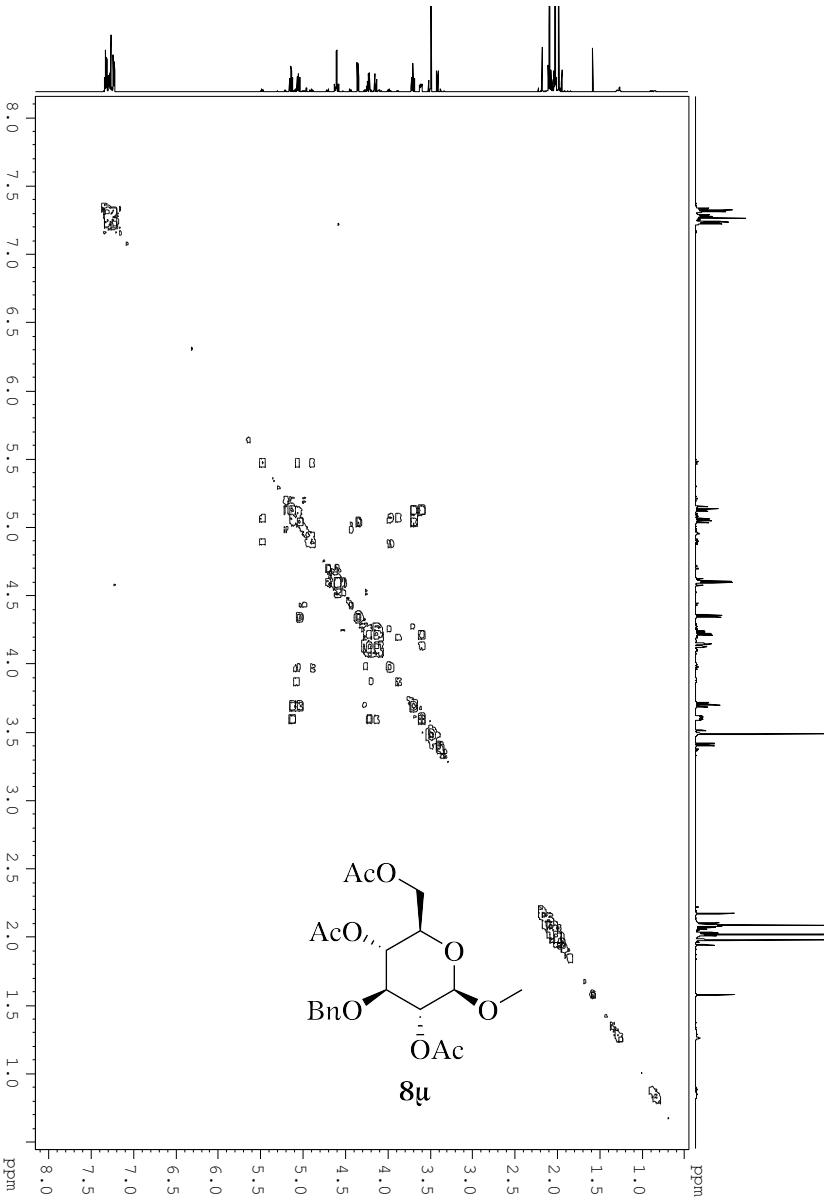

Figure 327: COSY spectrum of **8μ-β**.

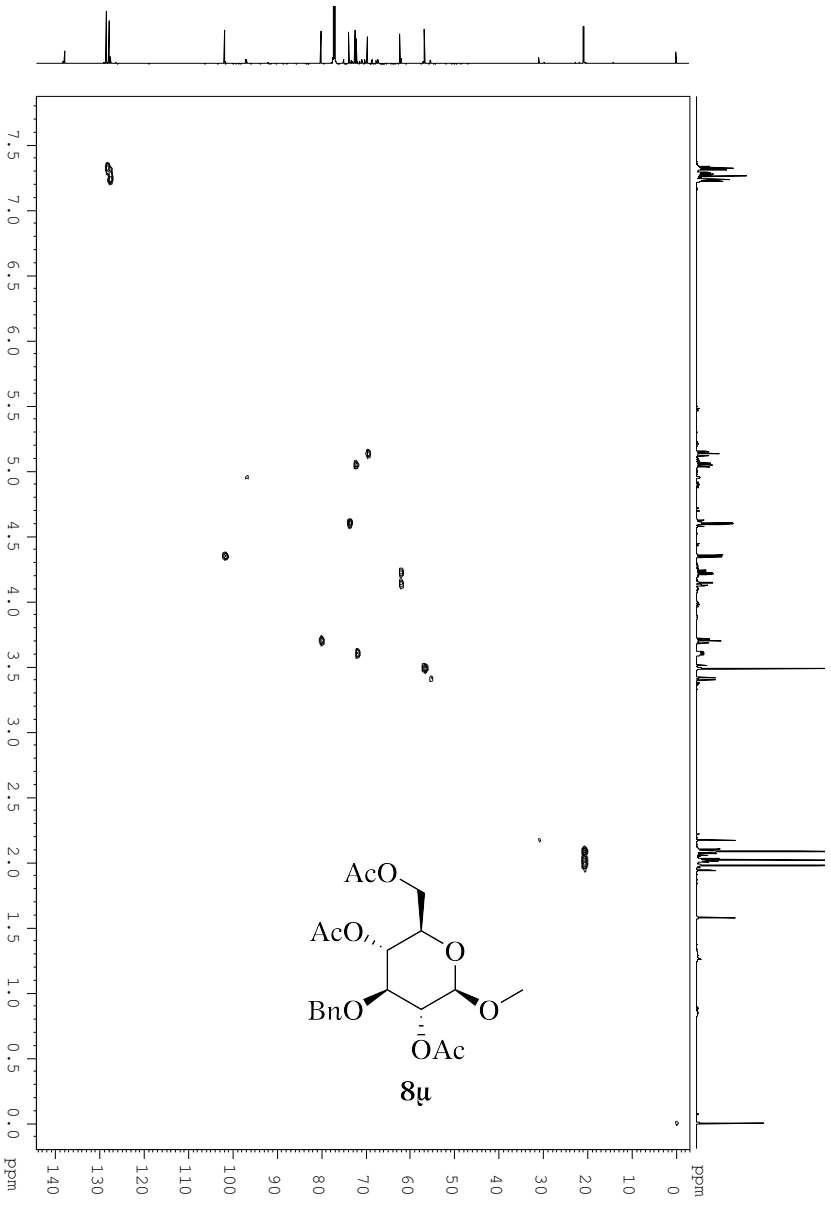

Figure 328: HSQC spectrum of **8μ-β**.

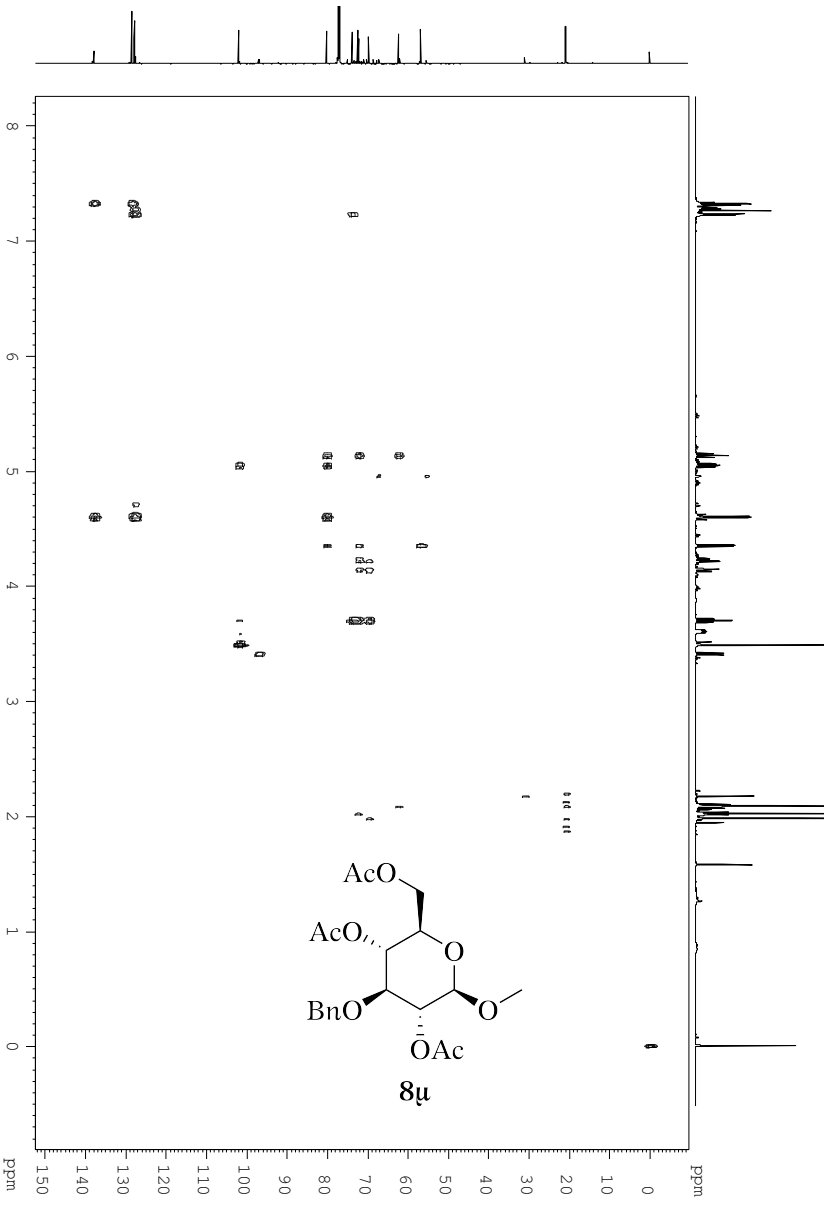

Figure 329: HMBC spectrum of **8μ-β**.

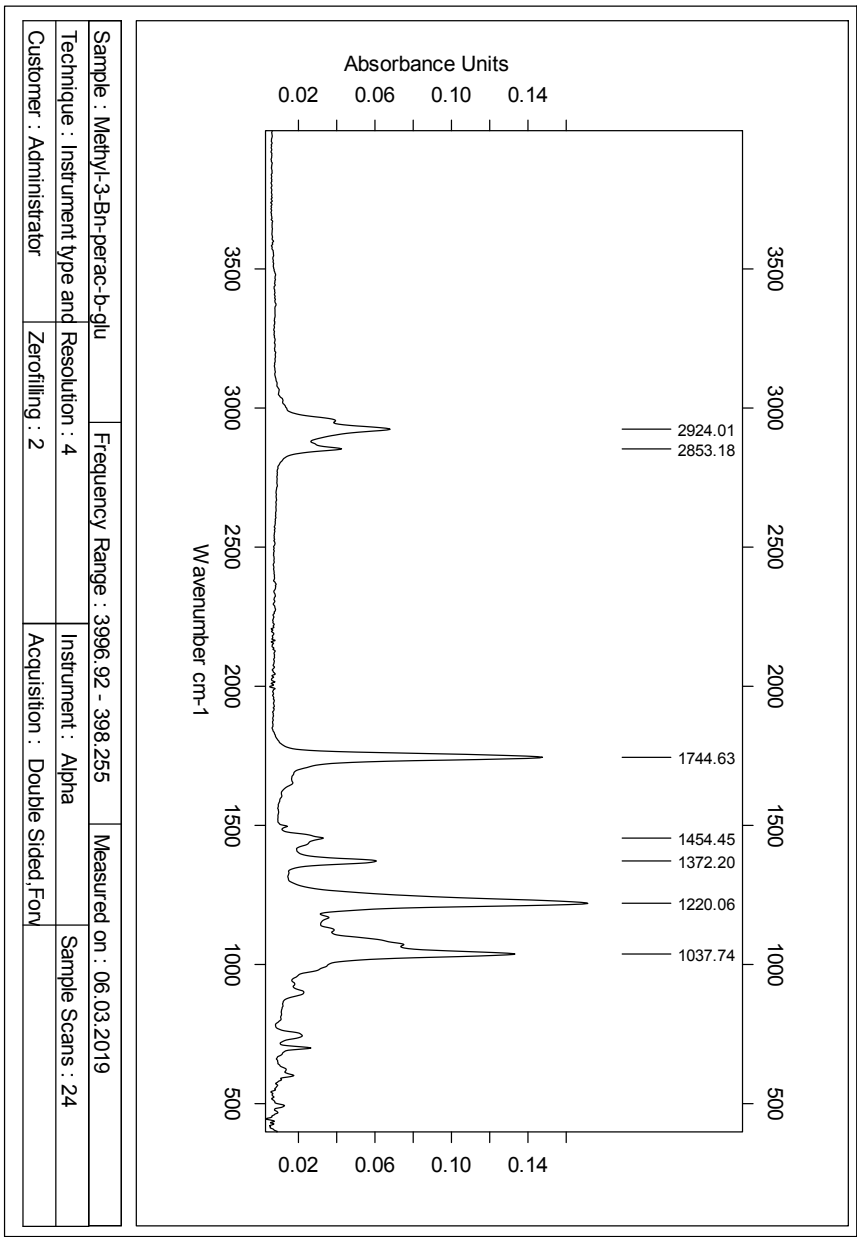

Figure 330: IR spectrum of **8μ-β**.

B.44 Spectroscopic data for compound 8b-α

Elemental Composition Report **Page 1**

Single Mass Analysis
Tolerance = 10.0 PPM / DBE: min = -2.0, max = 50.0
Element prediction: Off
Number of isotope peaks used for i-FIT = 3

Monoisotopic Mass, Even Electron Ions
132 formula(e) evaluated with 3 results within limits (all results (up to 1000) for each mass)
Elements Used:
C: 0-100 H: 0-150 O: 0-10 Na: 0-1
2019-133 37 (0.368) AM2 (Ar,35000.0,0.00,0.00); Cm (36:40)
1: TOF MS ES+

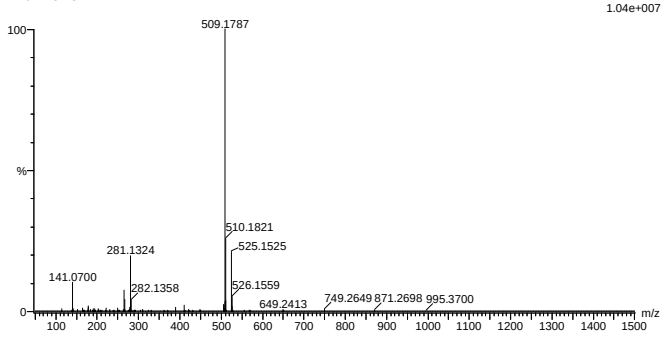

Minimum:				-2.0				
Maximum:		5.0	10.0	50.0				
Mass	Calc. Mass	mDa	PPM	DBE	i-FIT	Norm	Conf(%)	Formula
509.1787	509.1788	-0.1	-0.2	11.5	1129.5	0.087	91.63	C26 H30 O9 Na
	509.1812	-2.5	-4.9	14.5	1131.9	2.516	8.08	C28 H29 O9
	509.1753	3.4	6.7	23.5	1135.3	5.835	0.29	C35 H25 O4

Figure 331: HRMS (ESI+) of **8b-α**.

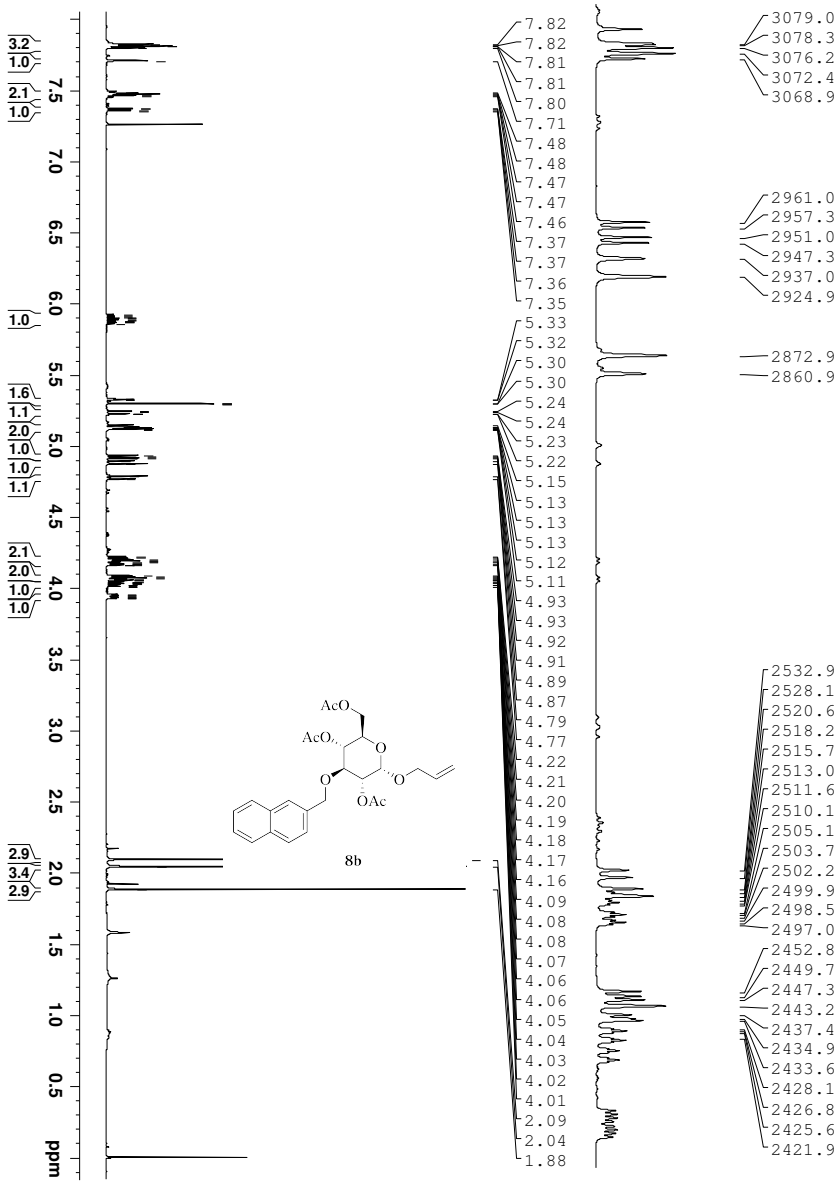

Figure 332: ^{1}H NMR spectrum of **8b-α**.

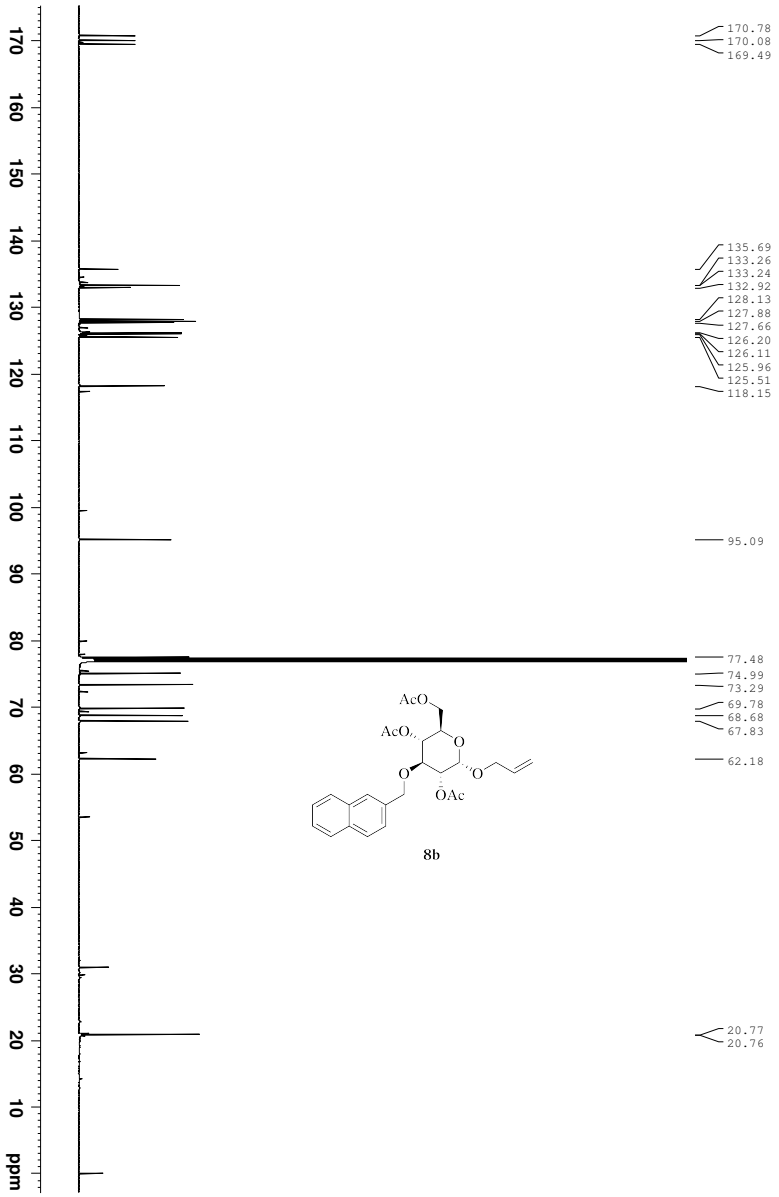

Figure 333: ^{13}C NMR spectrum of **8b-α**.

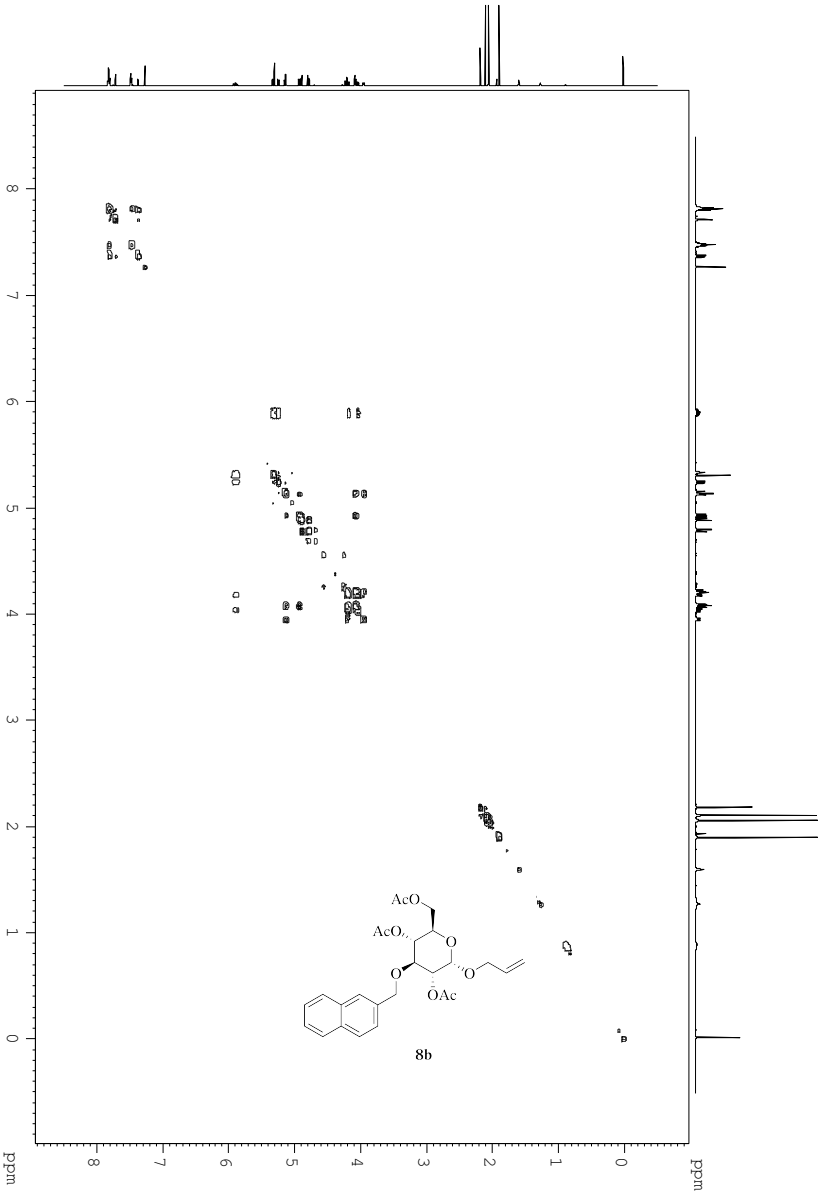

Figure 334: COSY spectrum of **8b-α**.

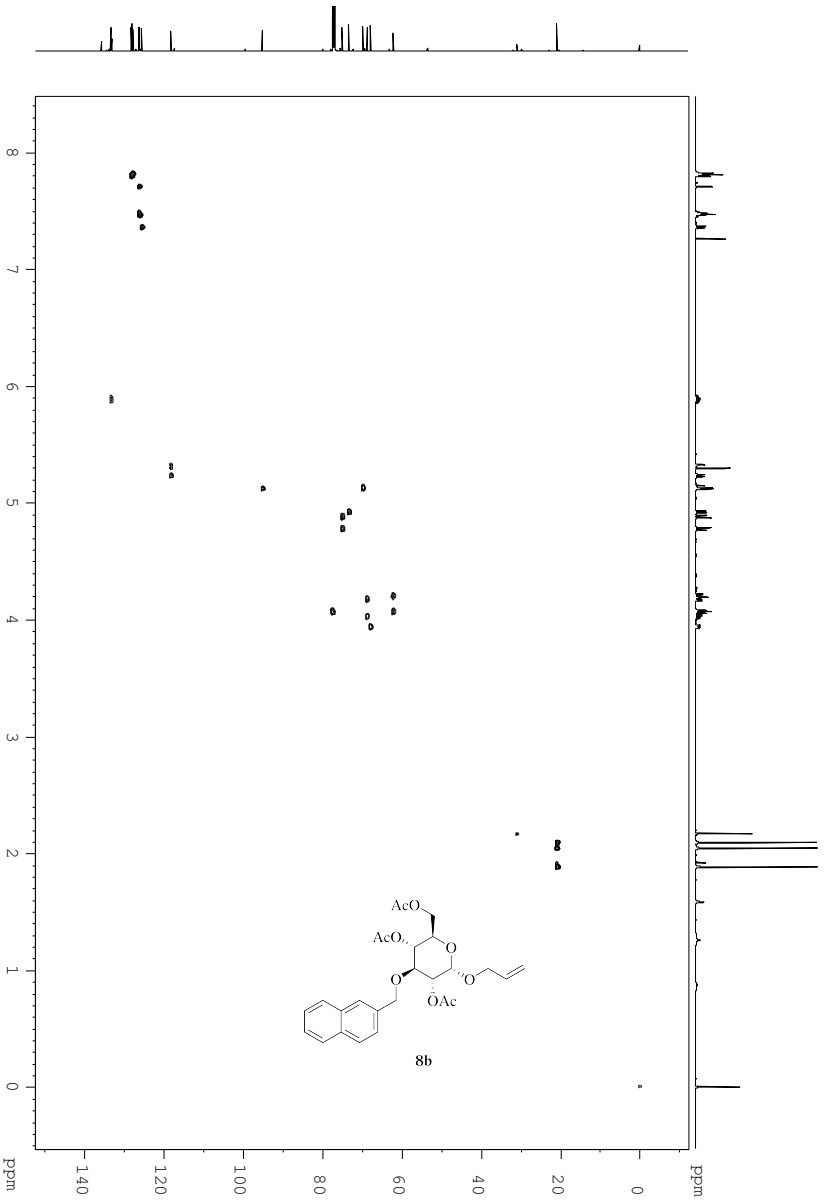

Figure 335: HSQC spectrum of **8b-α**.

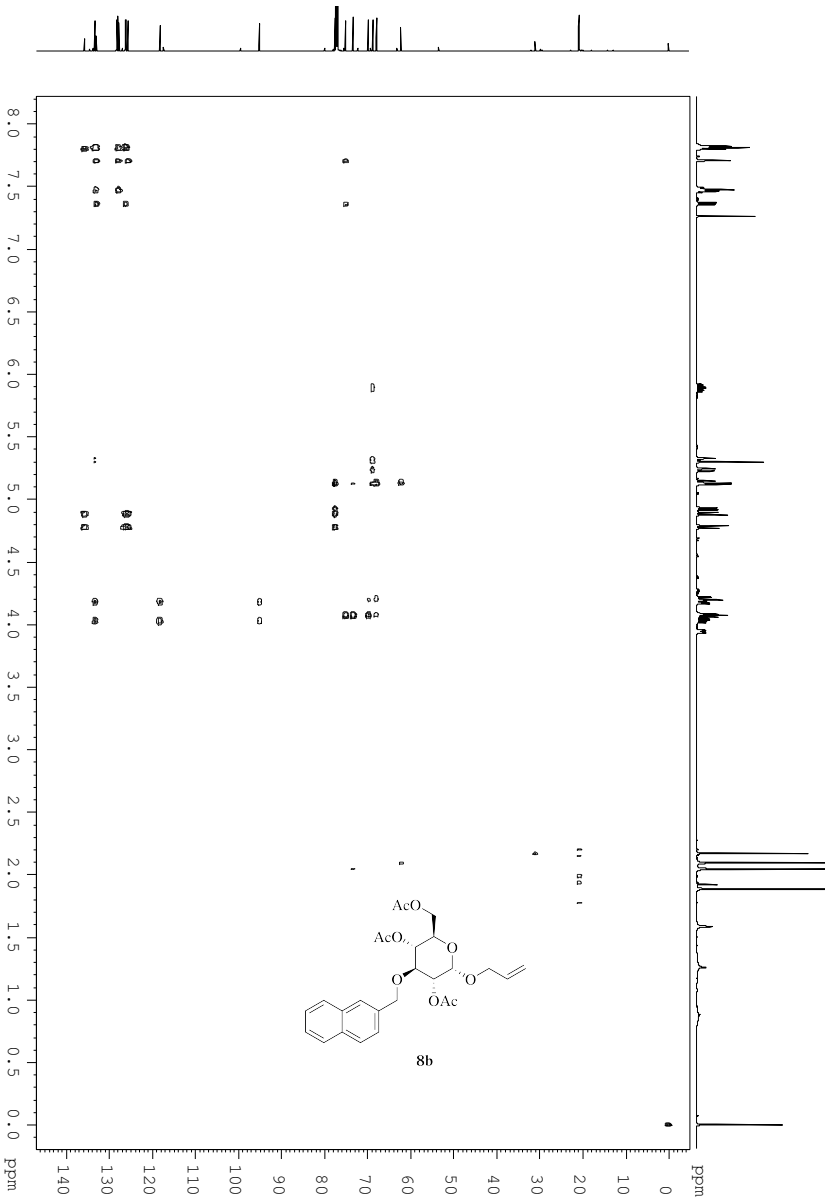

Figure 336: HMBC spectrum of **8b-α**.

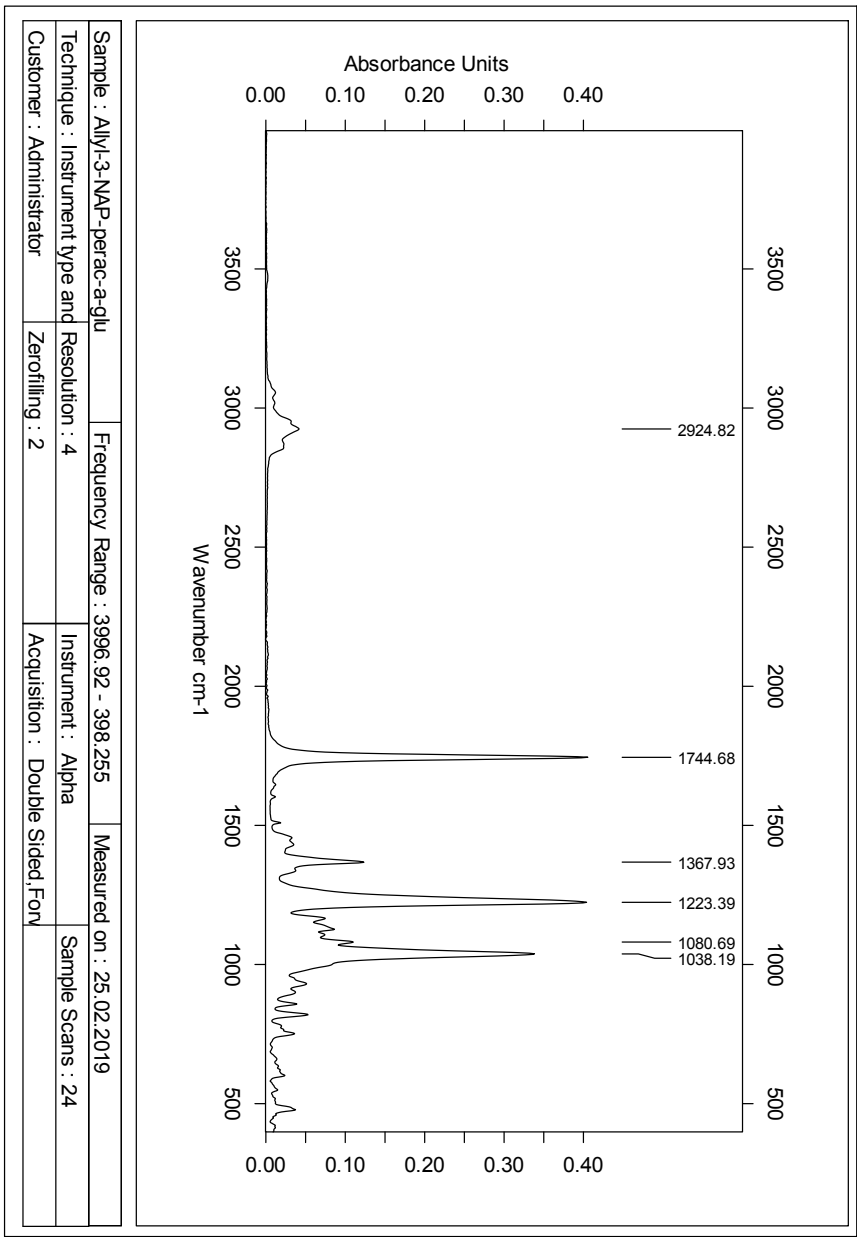

Figure 337: IR spectrum of **8b-α**.

B.45 Spectroscopic data for compound 8b-β

Elemental Composition Report **Page 1**

Single Mass Analysis
Tolerance = 10.0 PPM / DBE: min = -2.0, max = 50.0
Element prediction: Off
Number of isotope peaks used for i-FIT = 3

Monoisotopic Mass, Even Electron Ions
132 formula(e) evaluated with 3 results within limits (all results (up to 1000) for each mass)
Elements Used:
C: 0-100 H: 0-150 O: 0-10 Na: 0-1
2019-132 169 (1.580) AM2 (Ar,35000.0,0.00,0.00); Cm (166:173)
1: TOF MS ES+

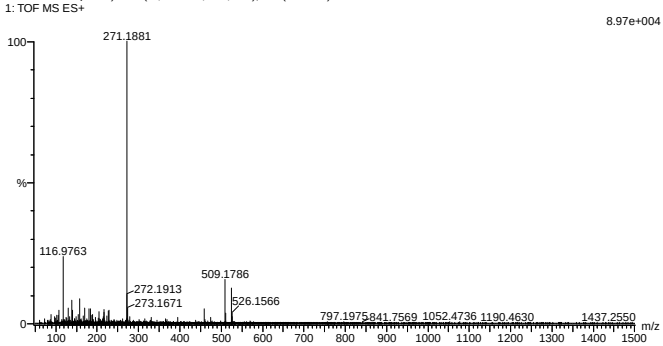

Minimum:				-2.0				
Maximum:		5.0	10.0	50.0				
Mass	Calc. Mass	mDa	PPM	DBE	i-FIT	Norm	Conf(%)	Formula
509.1786	509.1788	-0.2	-0.4	11.5	547.8	0.102	90.34	C26 H30 O9 Na
	509.1812	-2.6	-5.1	14.5	550.1	2.411	8.97	C28 H29 O9
	509.1753	3.3	6.5	23.5	552.7	4.976	0.69	C35 H25 O4

Figure 338: HRMS (ESI+) of **8b-β**.

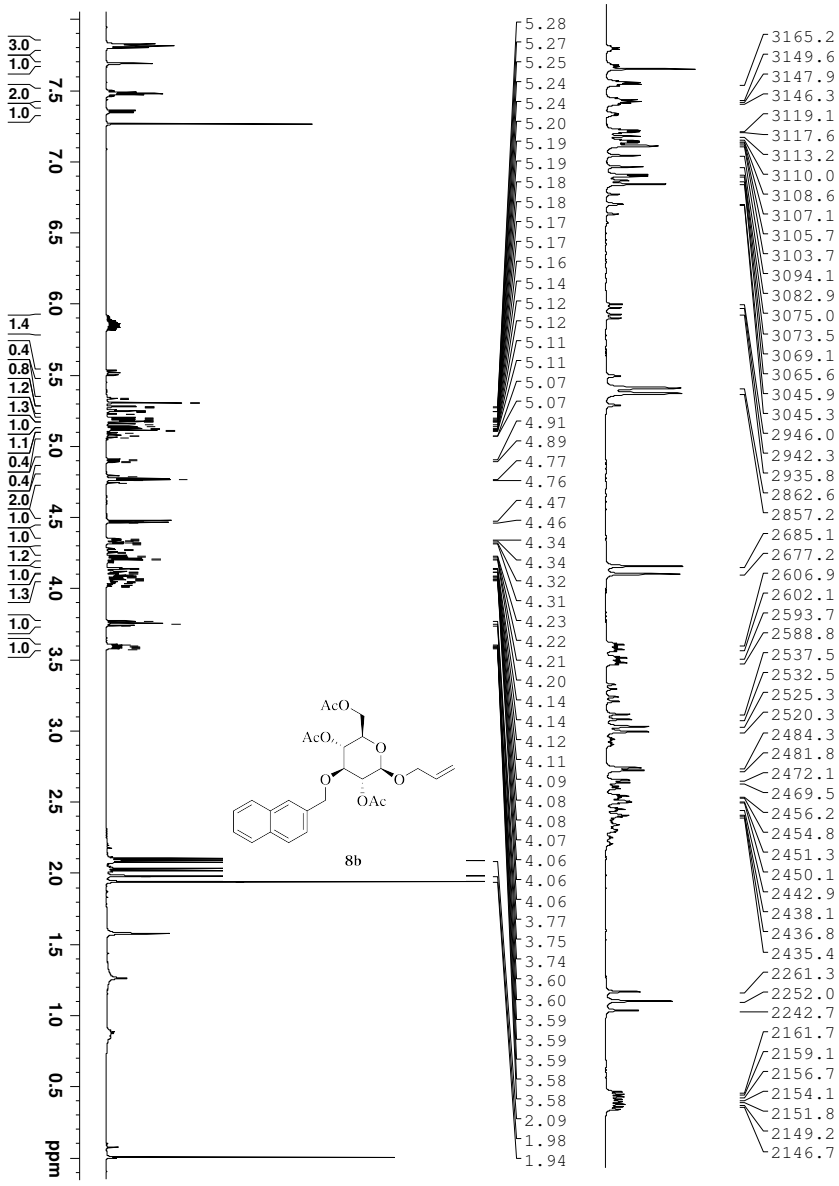

Figure 339: ^{1}H NMR spectrum of **8b-β**.

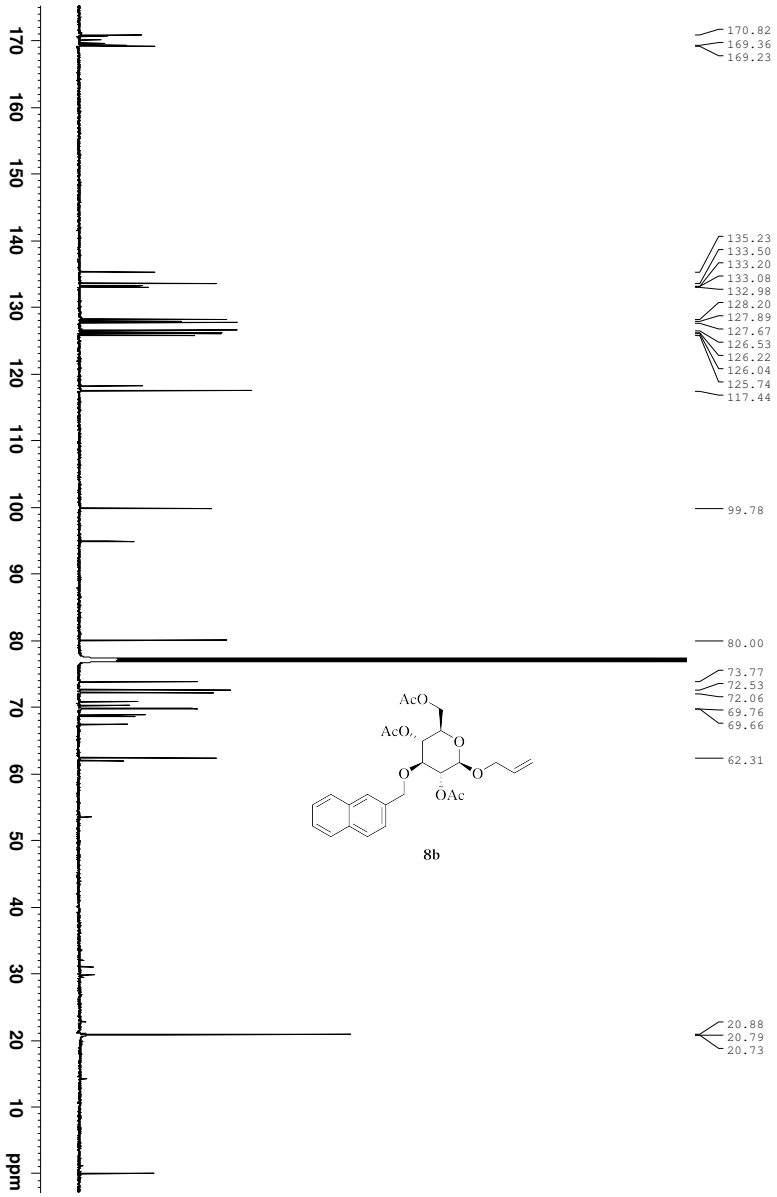

Figure 340: ^{13}C NMR spectrum of **8b-β**.

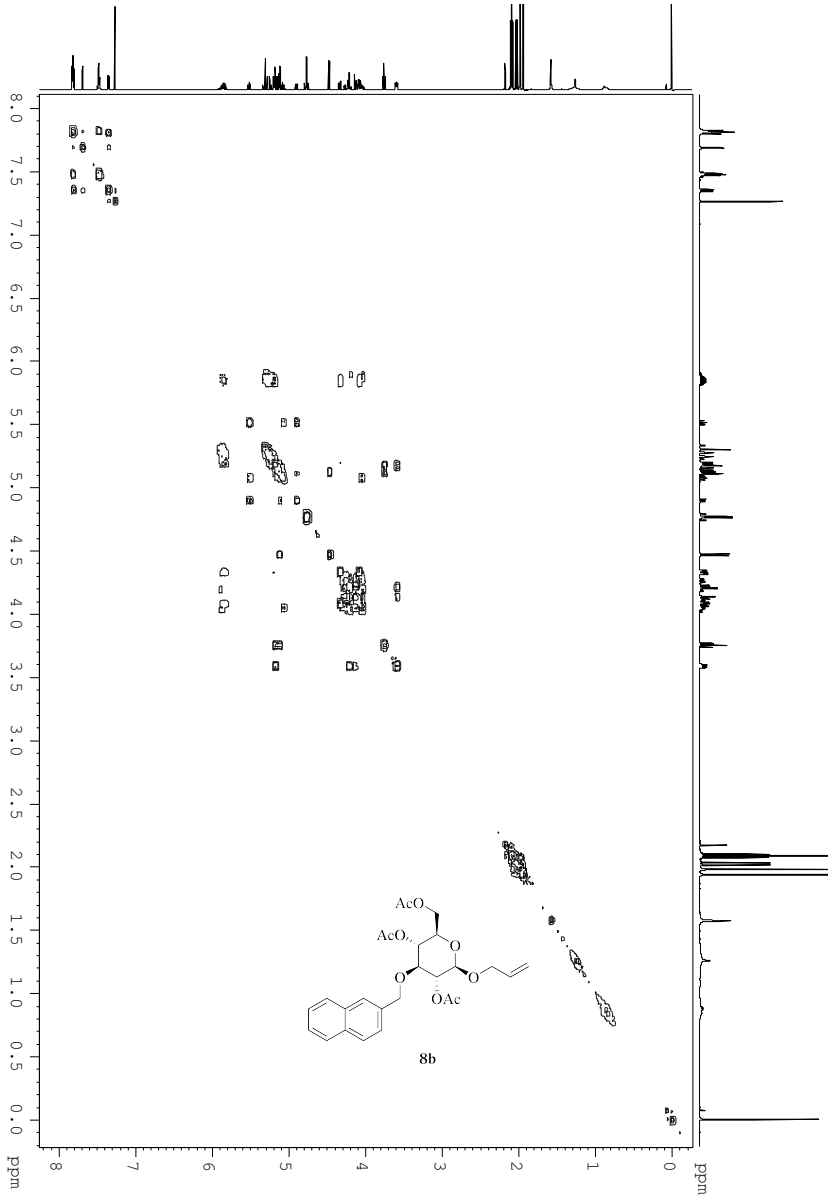

Figure 341: COSY spectrum of **8b-β**.

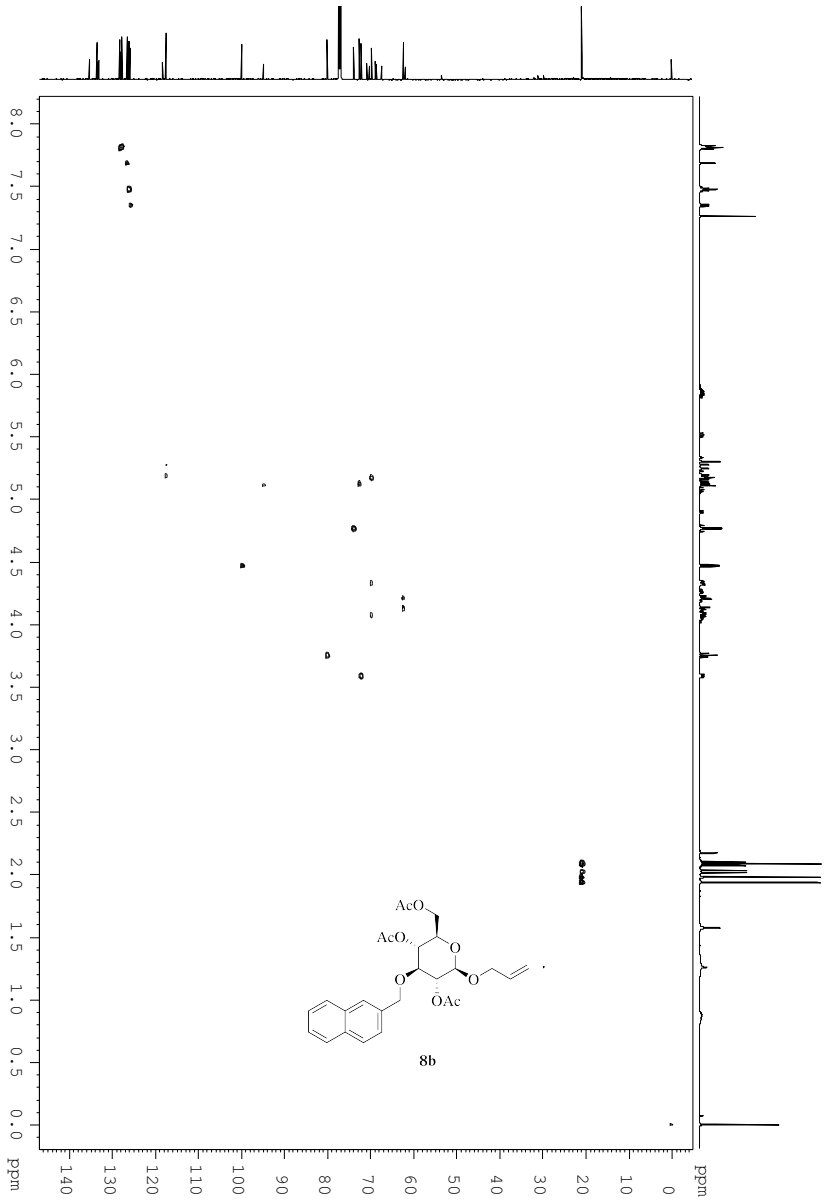

Figure 342: HSQC spectrum of **8b-β**.

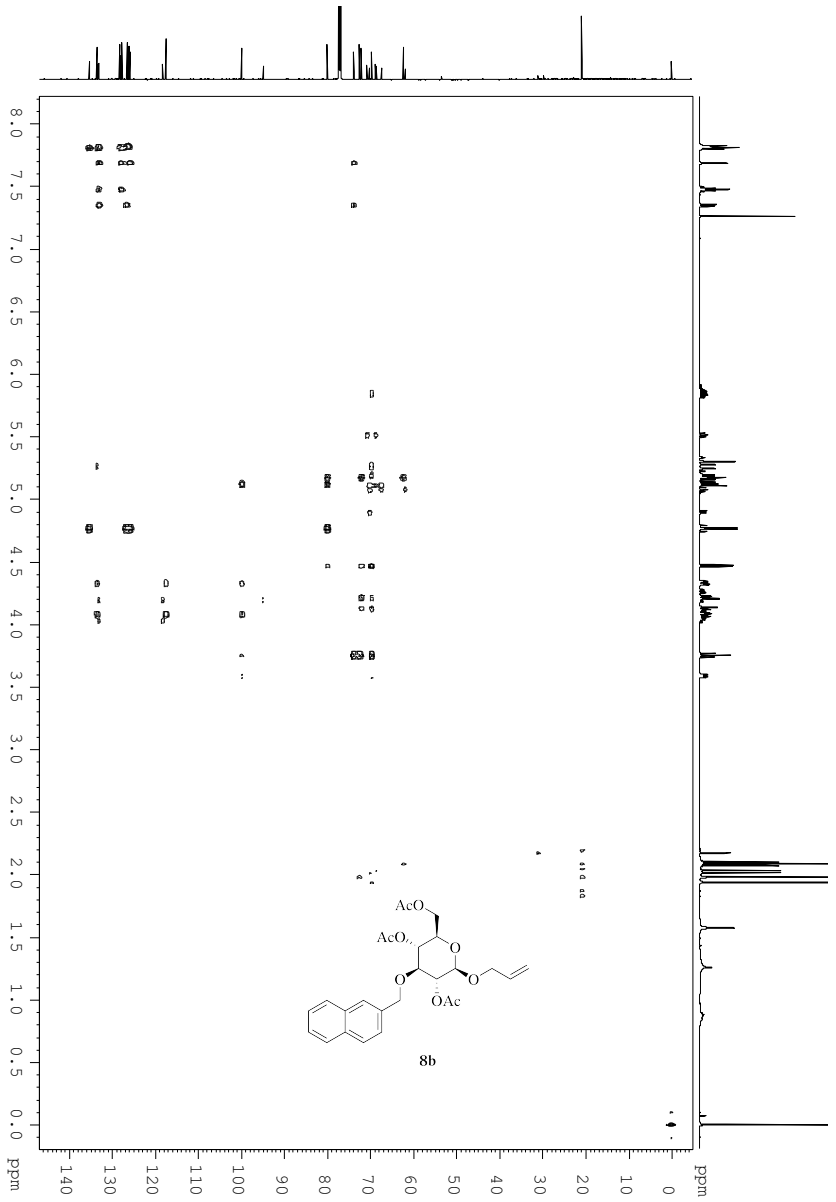

Figure 343: HMBC spectrum of **8b-β**.

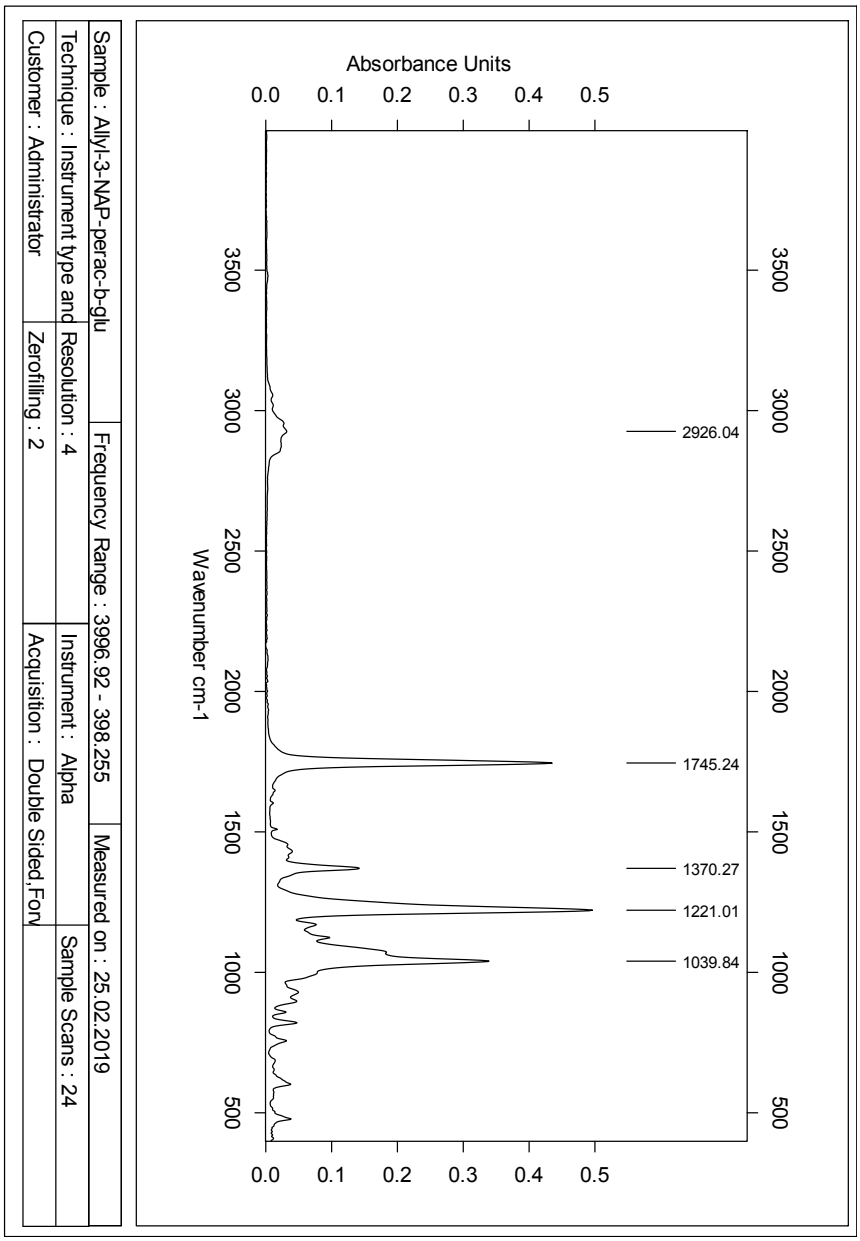

Figure 344: IR spectrum of **8b-β**.

B.46 Spectroscopic data for compound IC-3

Elemental Composition Report **Page 1**

Single Mass Analysis
Tolerance = 2.0 PPM / DBE: min = -50.0, max = 50.0
Element prediction: Off
Number of isotope peaks used for i-FIT = 3

Monoisotopic Mass, Even Electron Ions
2857 formula(e) evaluated with 3 results within limits (all results (up to 1000) for each mass)
Elements Used:
C: 0-100 H: 0-150 N: 0-10 O: 0-10 Na: 0-1
svg_20190328_2019_231 37 (0.699) AM2 (Ar,35000.0,0.00,0.00); Cm (37:41)
1: TOF MS ES+

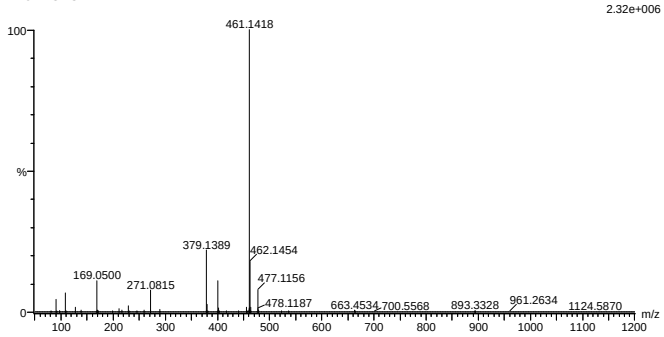

Minimum:				-50.0				
Maximum:		5.0	2.0	50.0				
Mass	Calc. Mass	mDa	PPM	DBE	i-FIT	Norm	Conf(%)	Formula
461.1418	461.1421	-0.3	-0.7	12.5	994.7	0.466	62.75	C19 H21 N6 O8
	461.1424	-0.6	-1.3	8.5	995.4	1.145	31.83	C21 H26 O10 Na
	461.1410	0.8	1.7	14.5	997.1	2.915	5.42	C18 H18 N10 O4 Na

Figure 345: HRMS (ESI+) of anomeric mixture of **IC-3**.

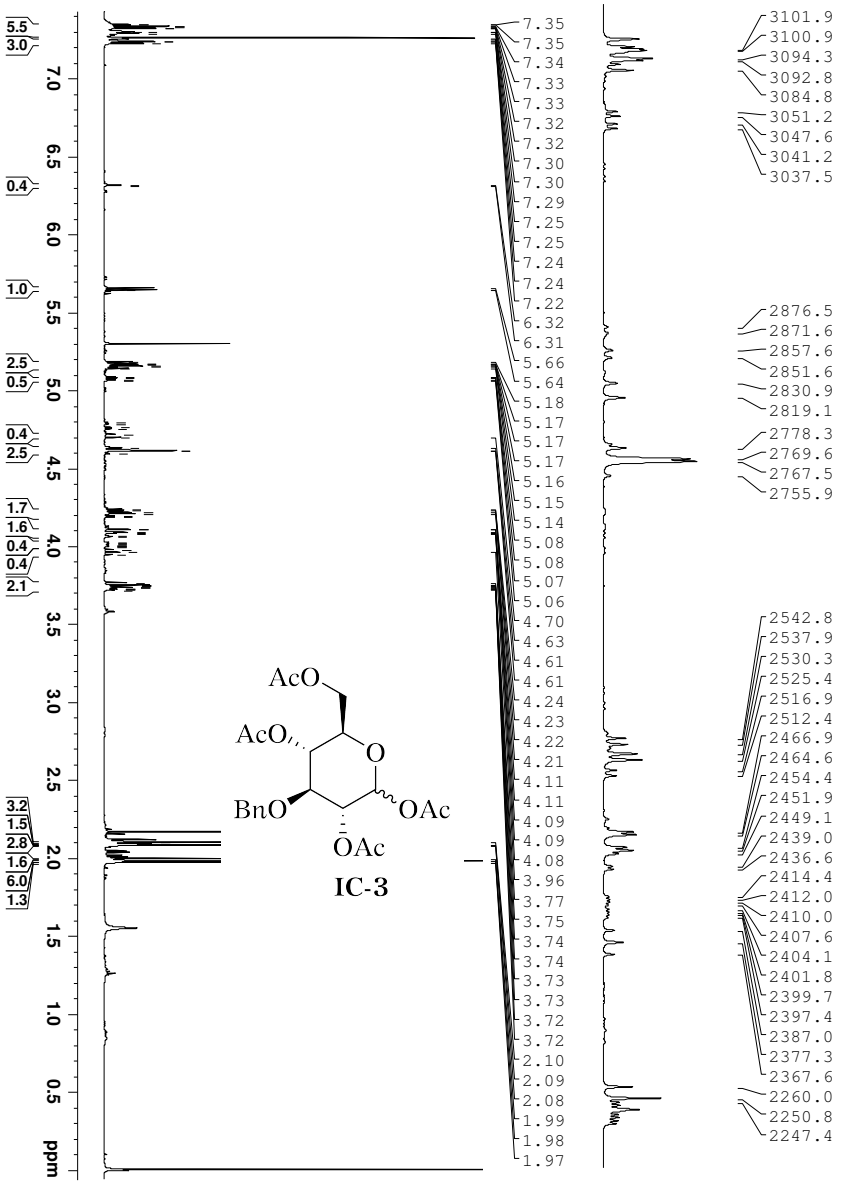

Figure 346: ^{1}H NMR spectrum of anomeric mixture of **IC-3**.

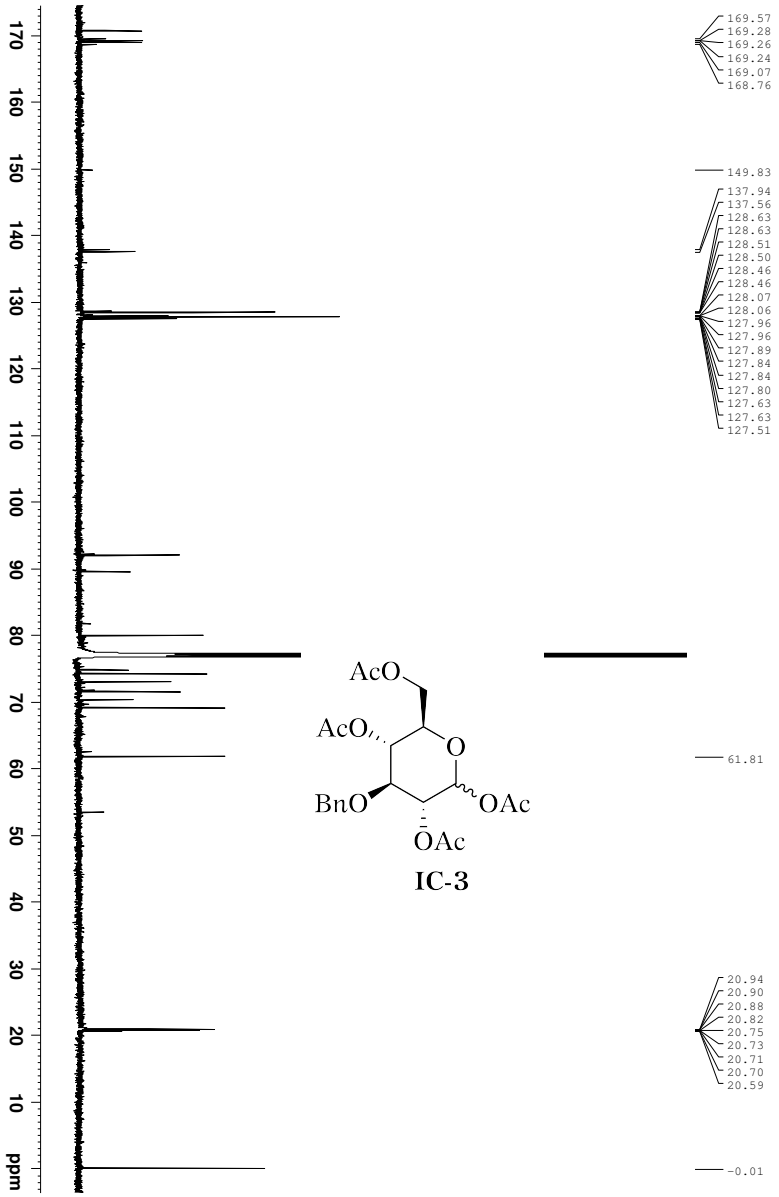

IC-3

Figure 347: ^{13}C NMR spectrum of anomeric mixture of **IC-3**.

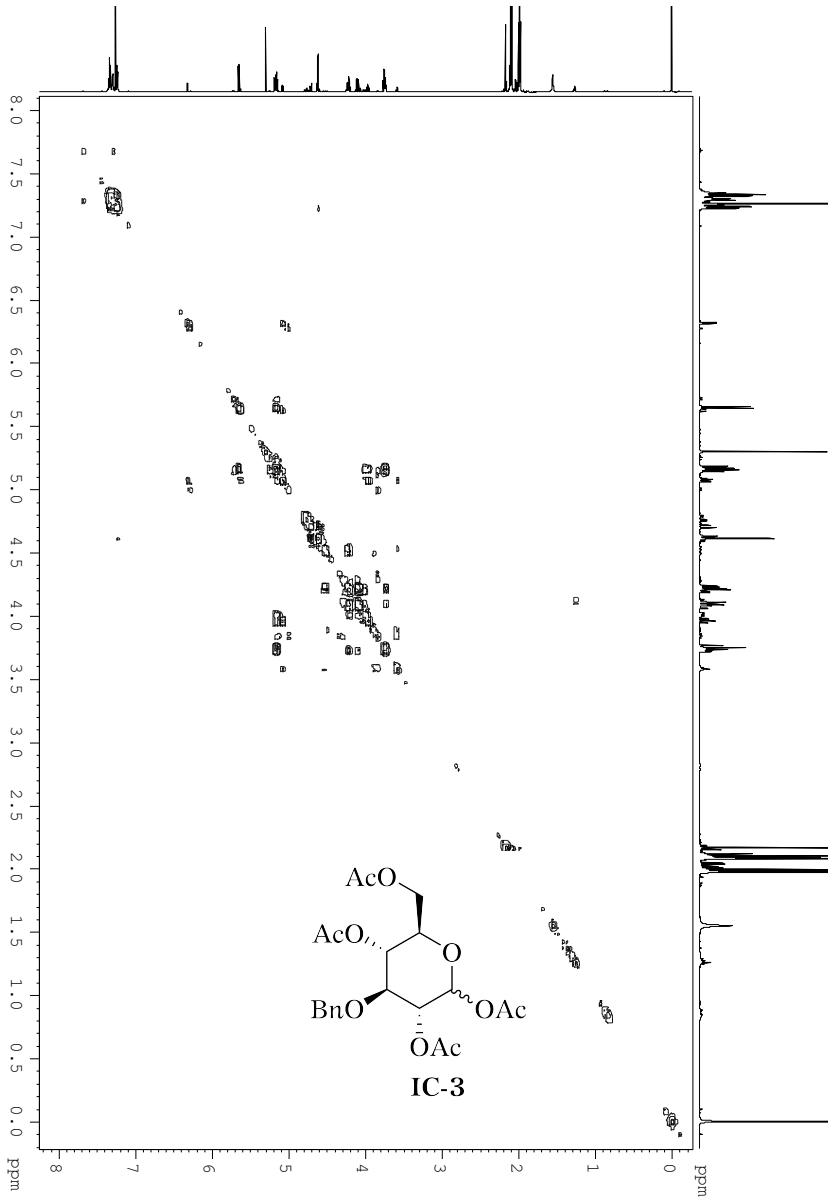

Figure 348: COSY spectrum of anomeric mixture of **IC-3**.

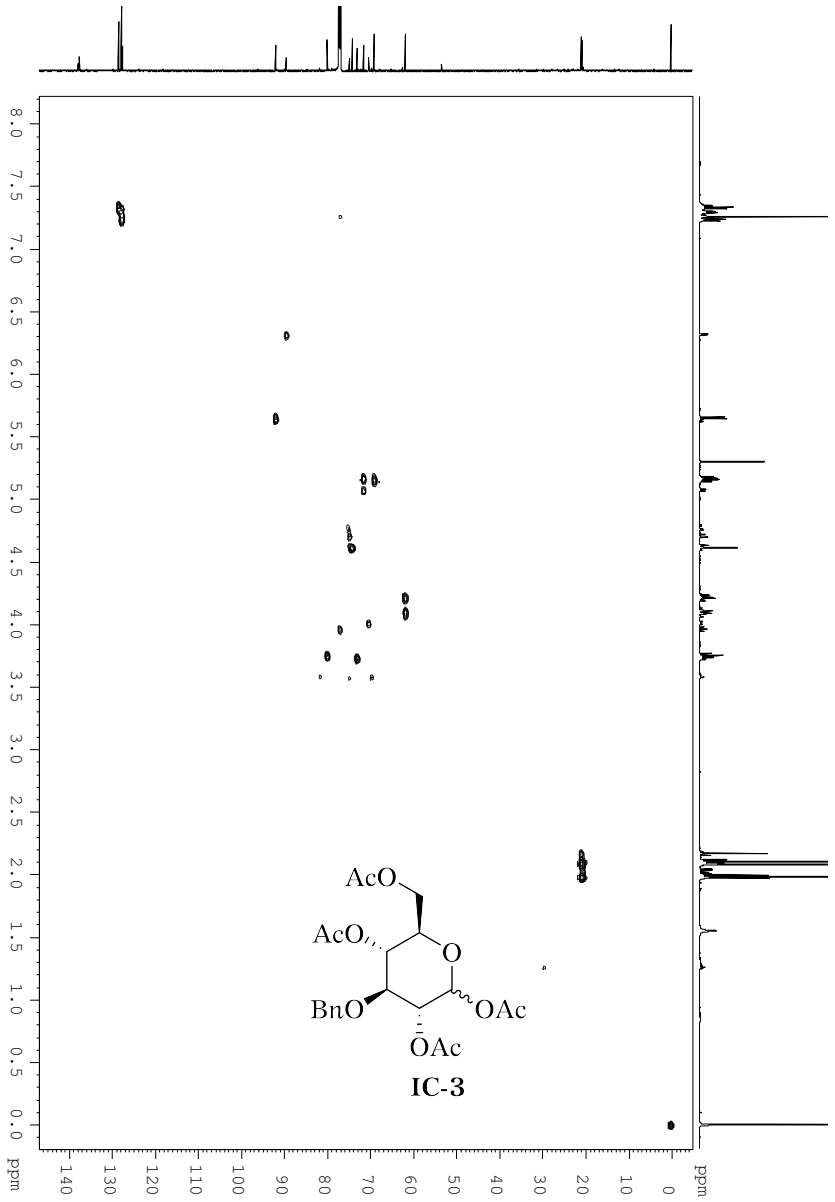

Figure 349: HSQC spectrum of anomeric mixture of **IC-3**.

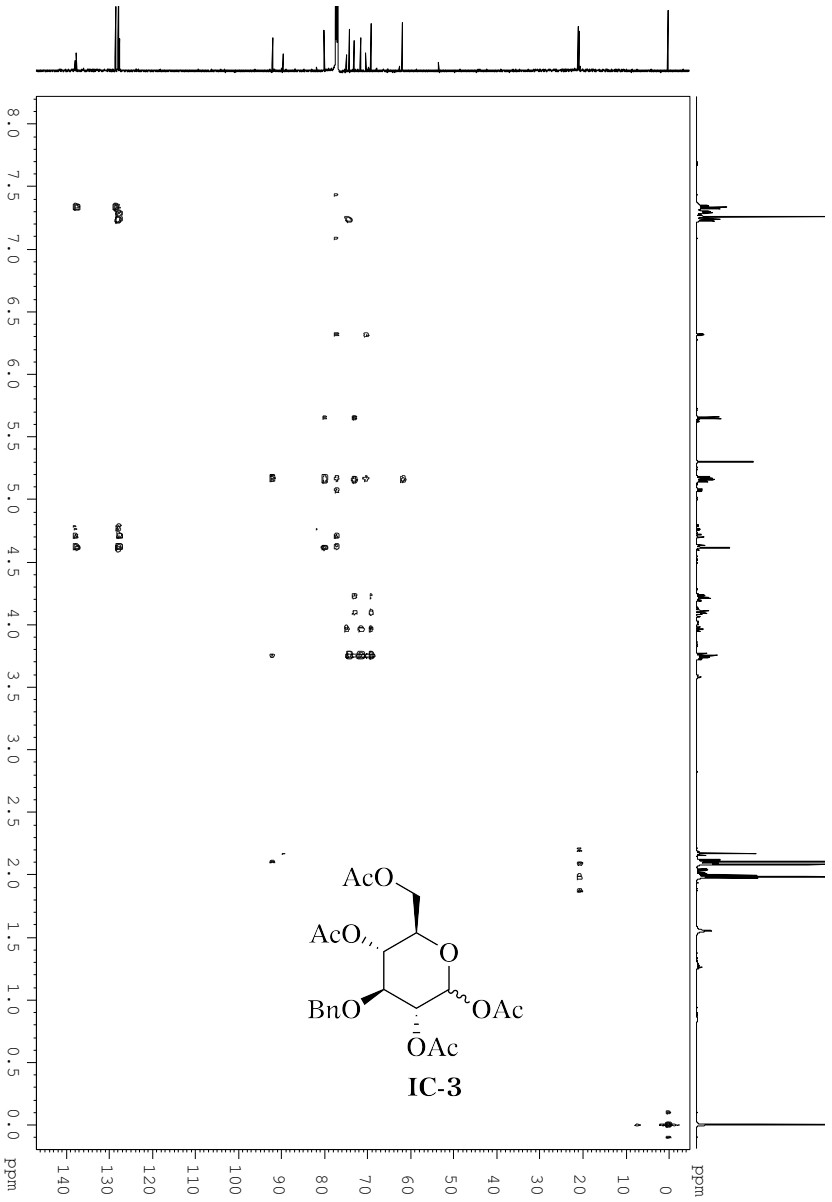

Figure 350: HMBC spectrum of anomeric mixture of **IC-3**.

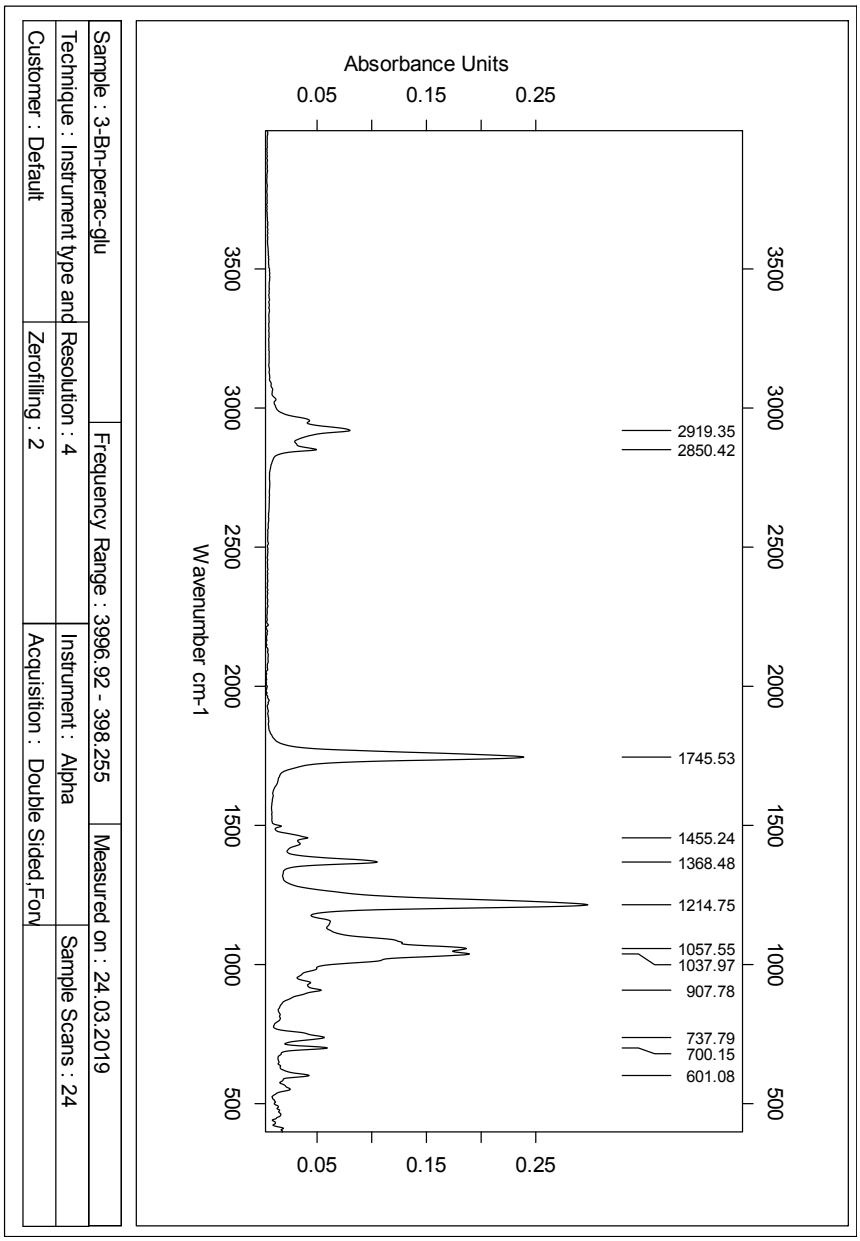

Figure 351: IR spectrum of anomeric mixture of **IC-3**.

B.47 Spectroscopic data for compound IC-4

Elemental Composition Report **Page 1**

Single Mass Analysis
Tolerance = 2.0 PPM / DBE: min = -50.0, max = 50.0
Element prediction: Off
Number of isotope peaks used for i-FIT = 3

Monoisotopic Mass, Even Electron Ions
262 formula(e) evaluated with 1 results within limits (all results (up to 1000) for each mass)
Elements Used:
C: 0-100 H: 0-150 O: 0-10 Na: 0-1
2019-446X 53 (0.599) AM2 (Ar,35000.0,0.00,0.00); Cm (52:55)
1: TOF MS ES+

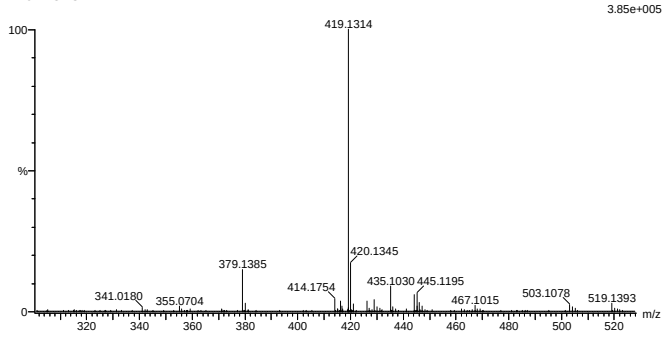

Minimum:				-50.0				
Maximum:		5.0	2.0	50.0				
Mass	Calc. Mass	mDa	PPM	DBE	i-FIT	Norm	Conf(%)	Formula
419.1314	419.1318	-0.4	-1.0	7.5	913.1	n/a	n/a	C19 H24 O9 Na

Figure 352: HRMS (ESI+) of anomeric mixture of **IC-4**.

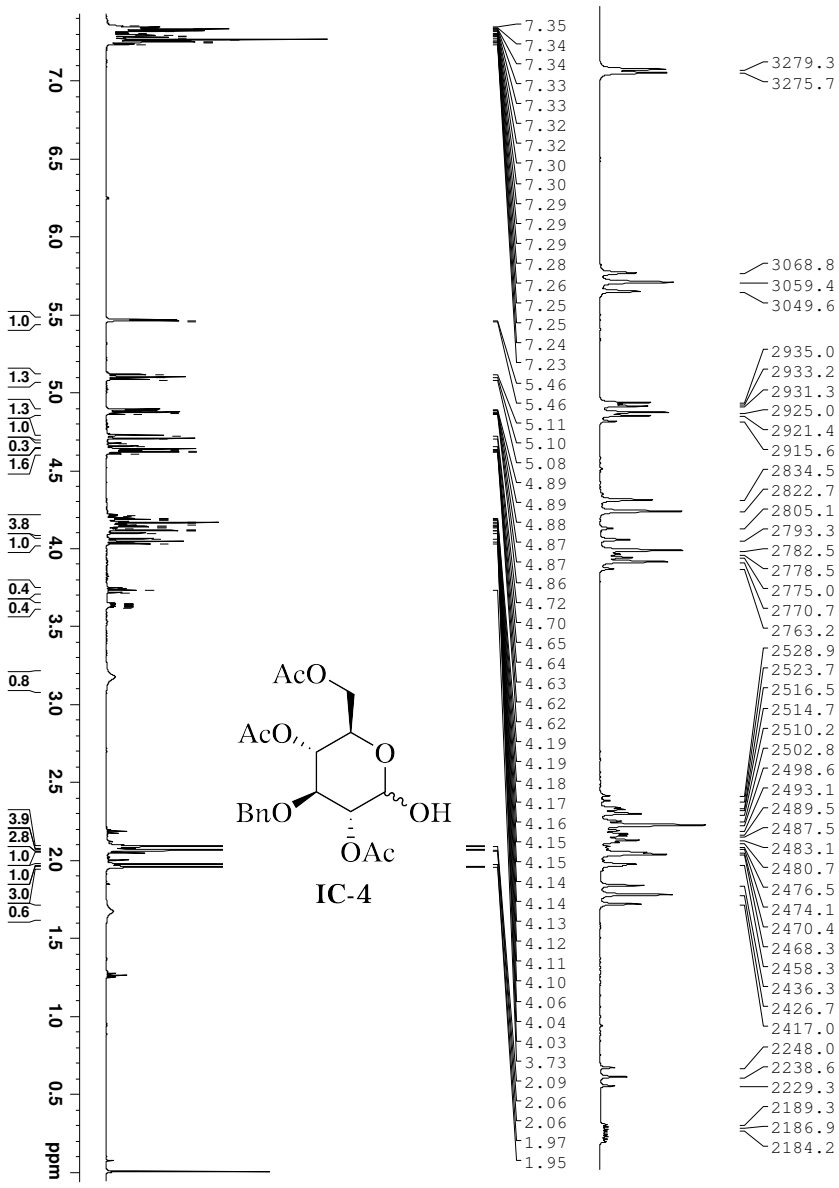

Figure 353: ^{1}H NMR spectrum of anomeric mixture of **IC-4**.

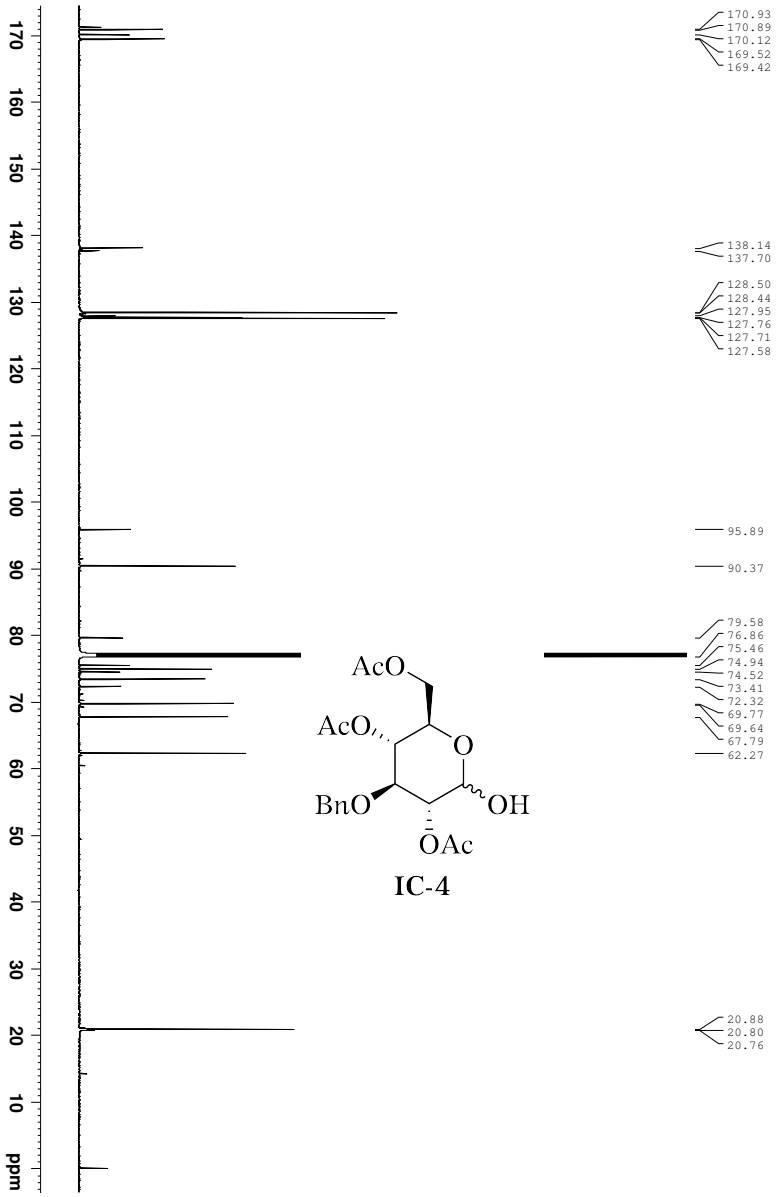

IC-4

Figure 354: ^{13}C NMR spectrum of anomeric mixture of **IC-4**.

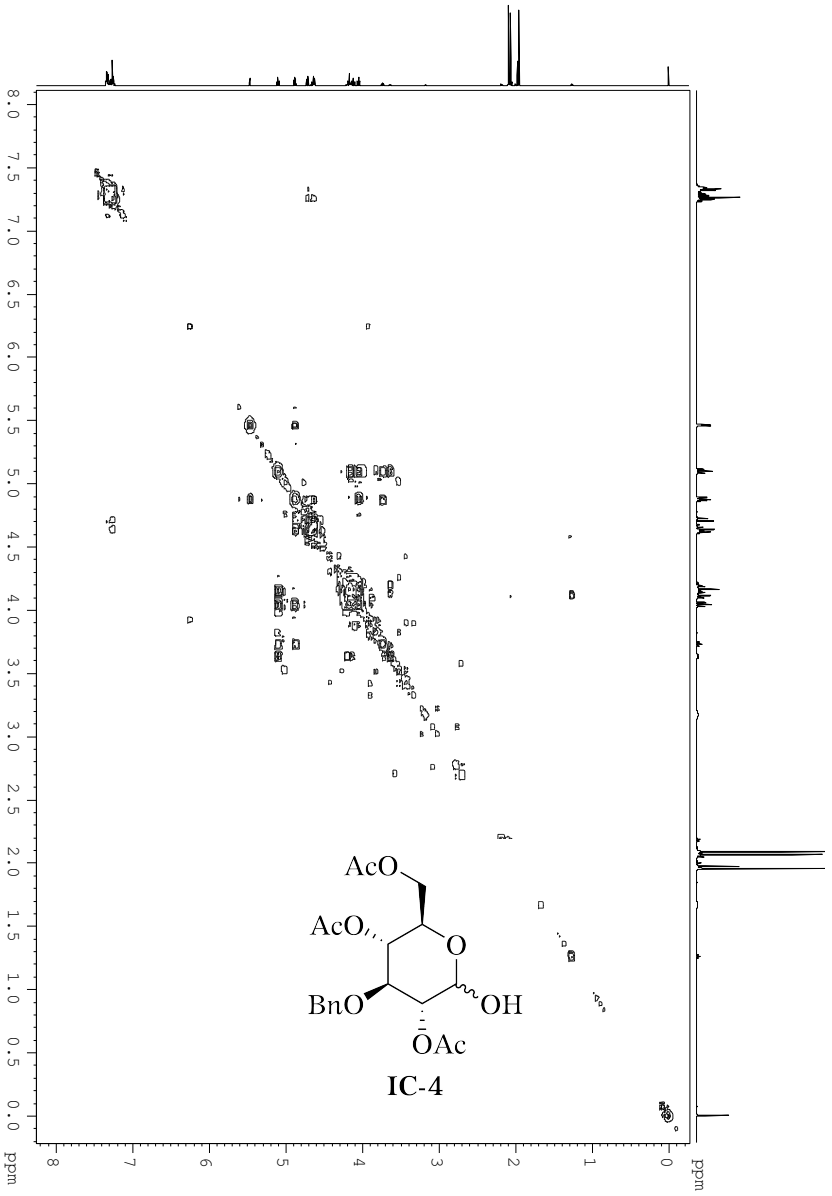

Figure 355: COSY spectrum of anomeric mixture of **IC-4**.

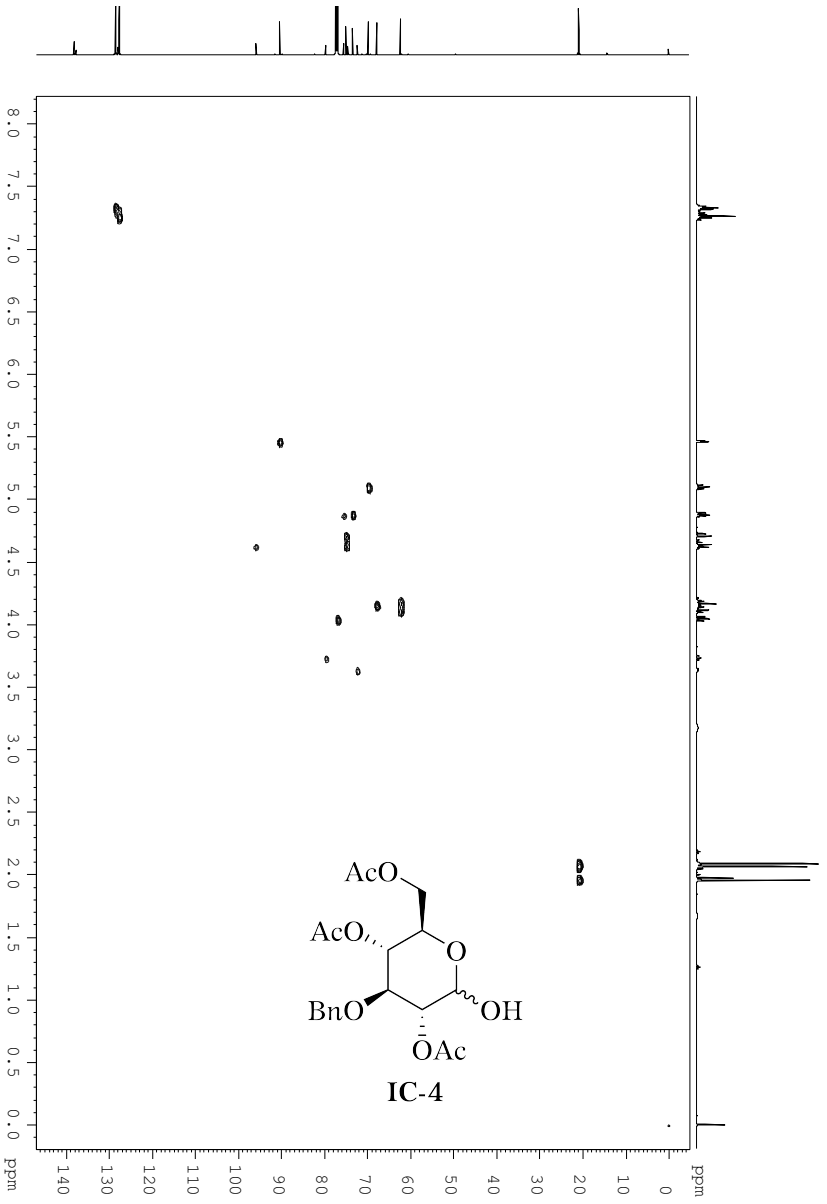

Figure 356: HSQC spectrum of anomeric mixture of **IC-4**.

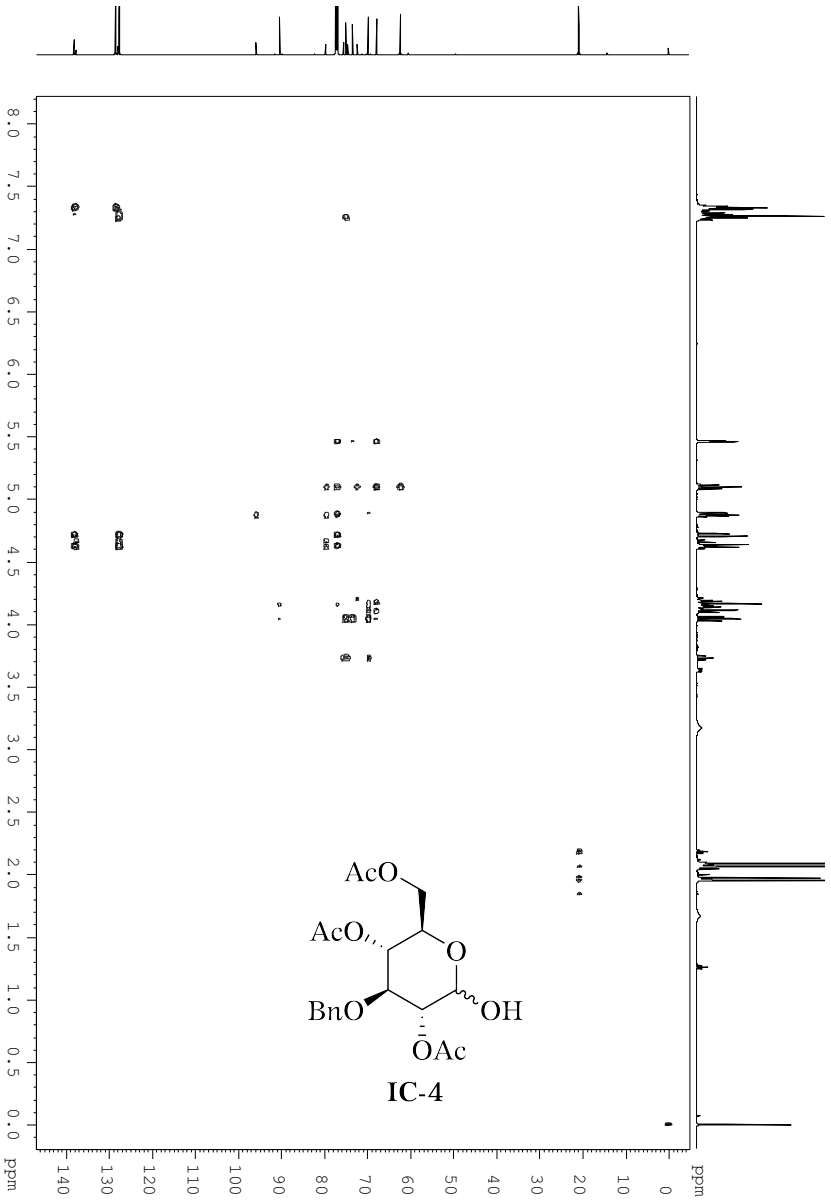

Figure 357: HMBC spectrum of anomeric mixture of **IC-4**.

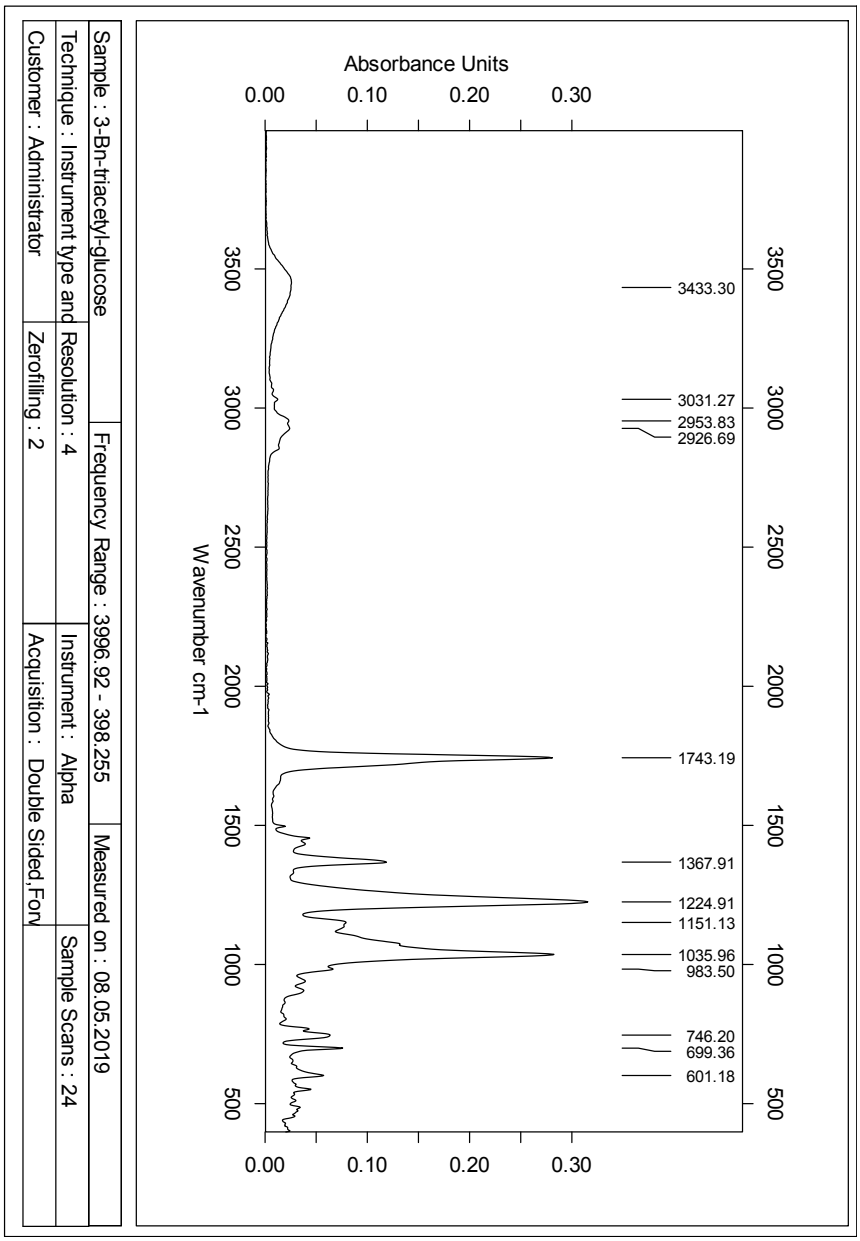

Figure 358: IR spectrum of anomeric mixture of **IC-4**.

B.48 Spectroscopic data for compound IC-5

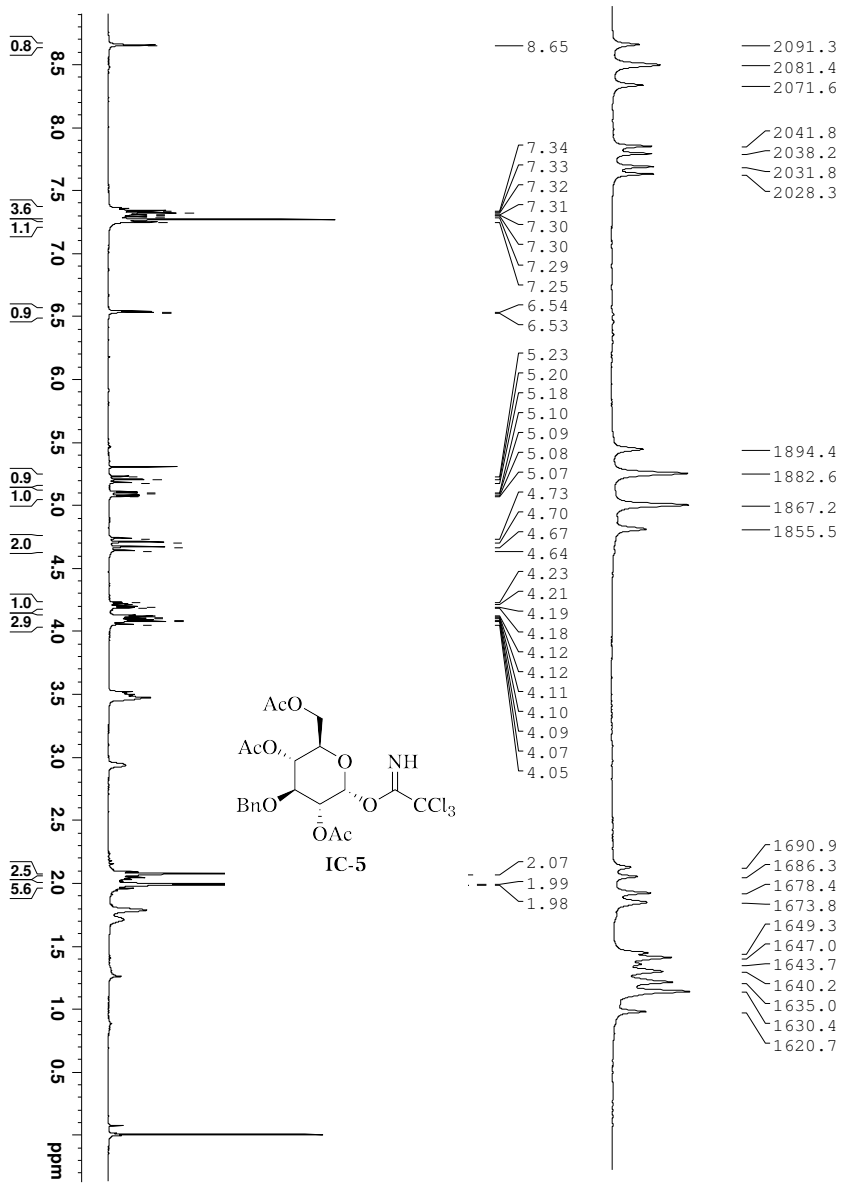

Figure 359: ^{1}H NMR spectrum of **IC-5**.

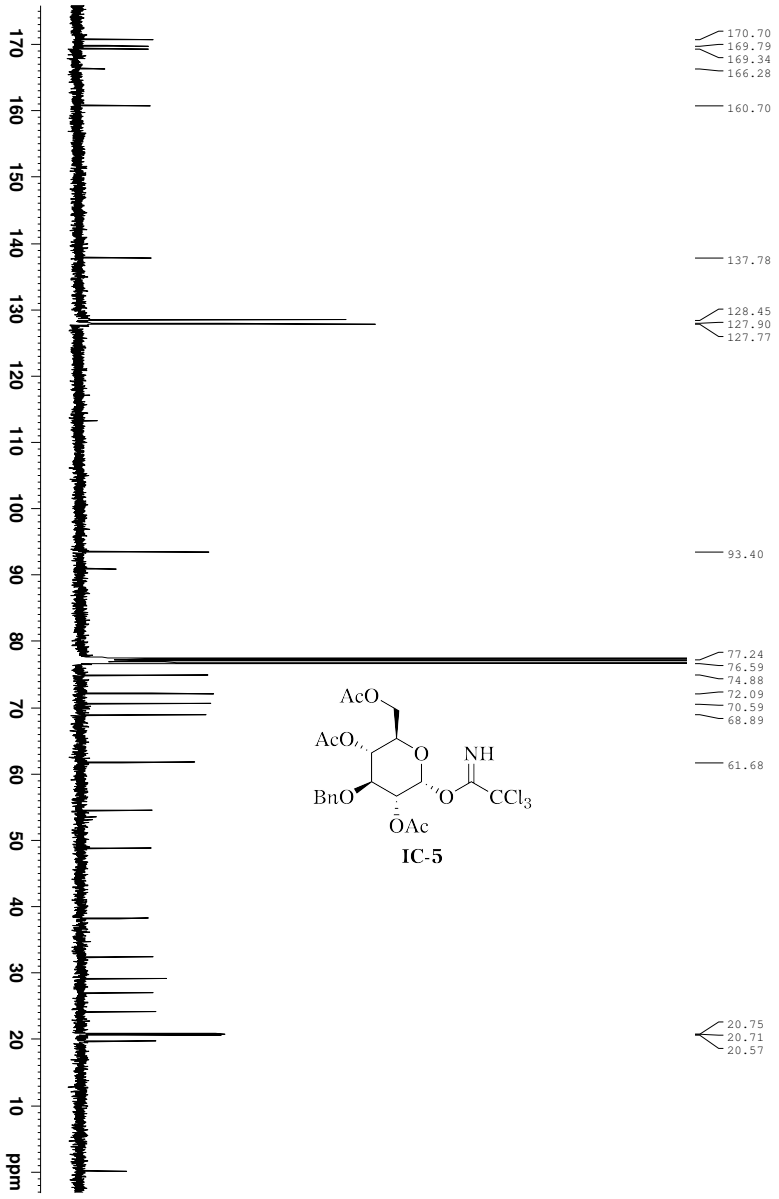

Figure 360: ^{13}C NMR spectrum of **IC-5**.

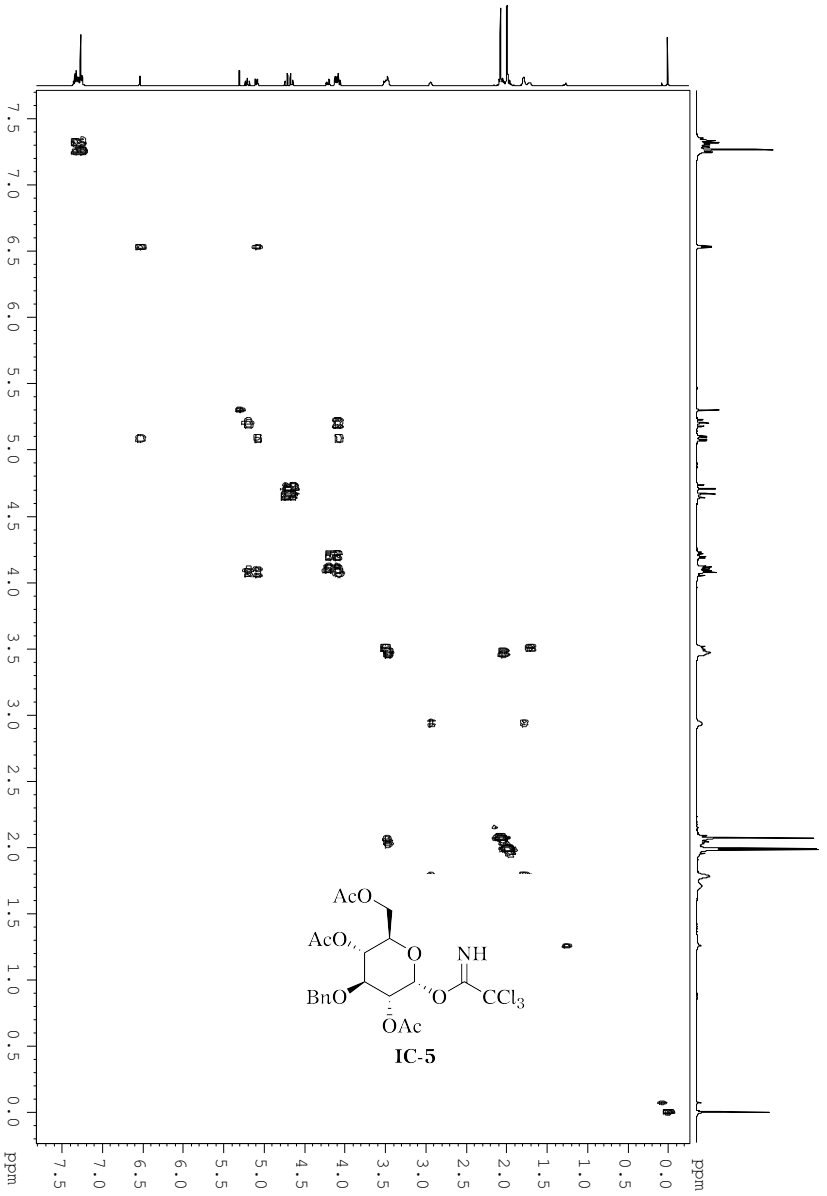

Figure 361: COSY spectrum of **IC-5**.

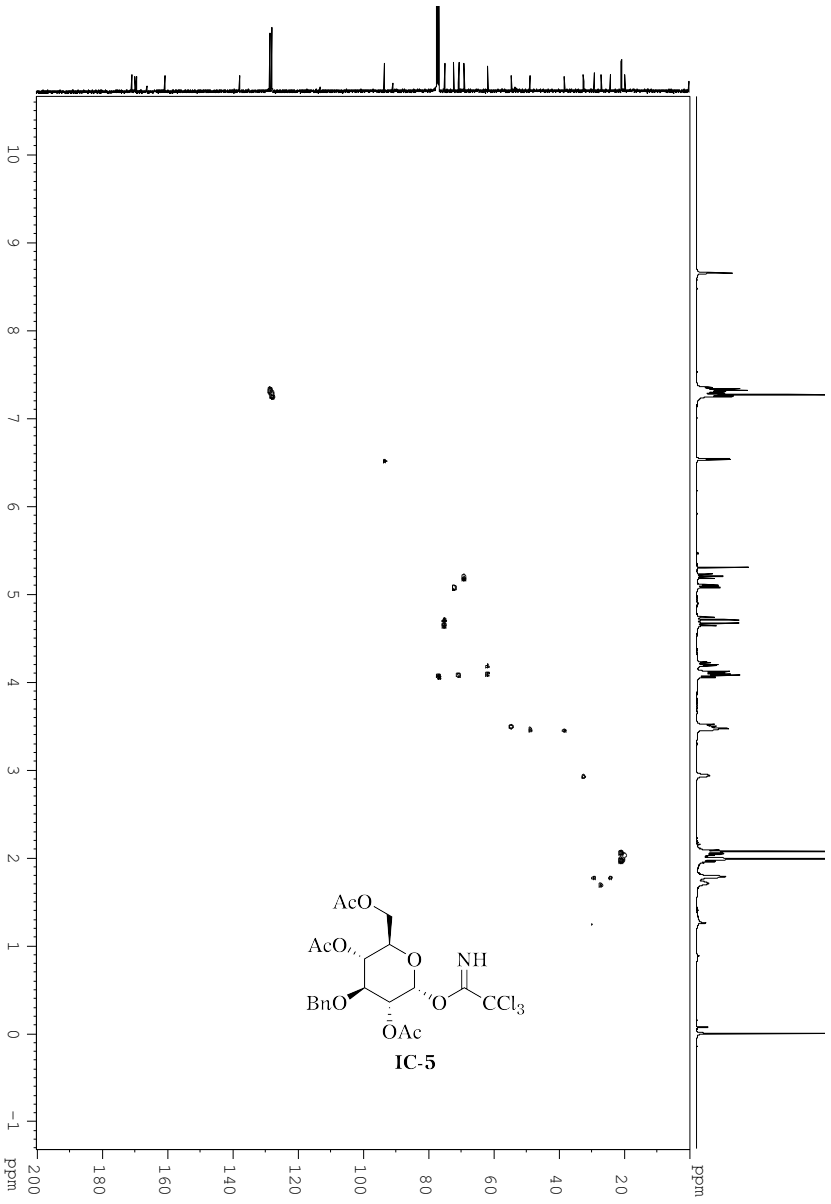

Figure 362: HSQC spectrum of **IC-5**.

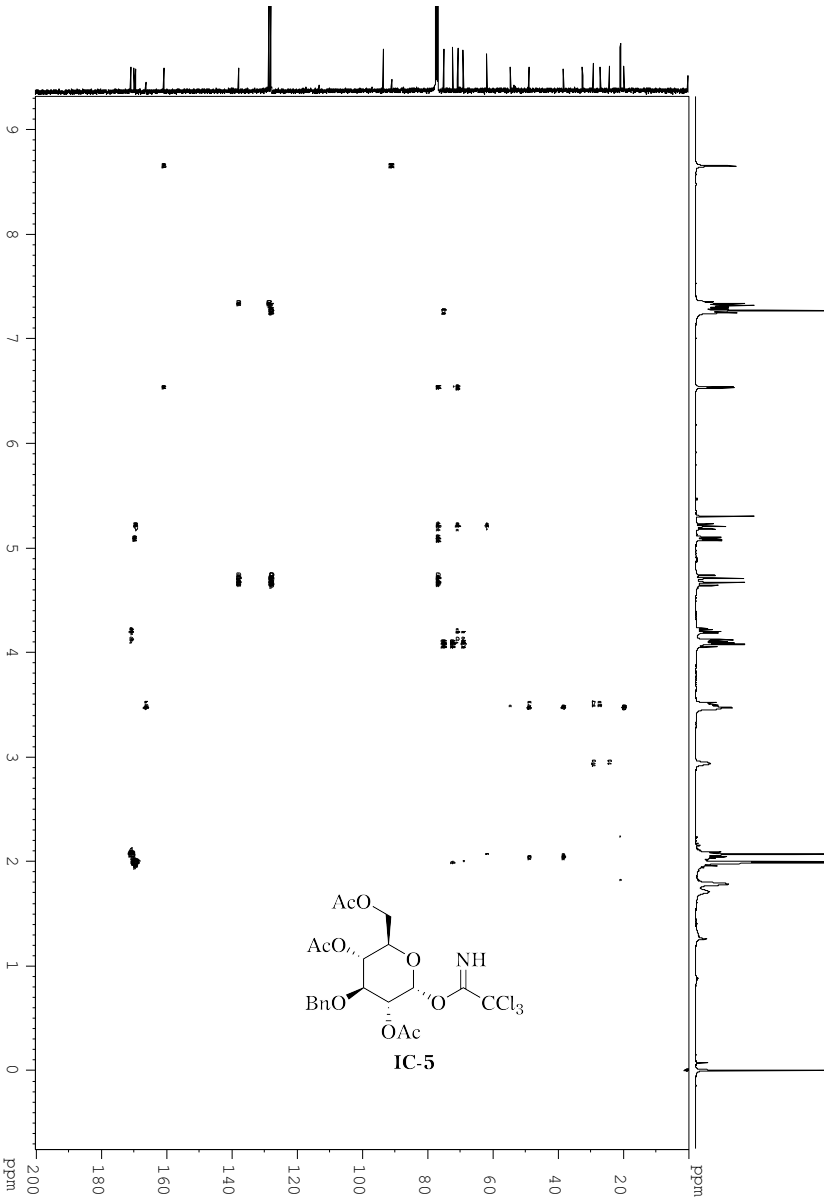

Figure 363: HMBC spectrum of **IC-5**.

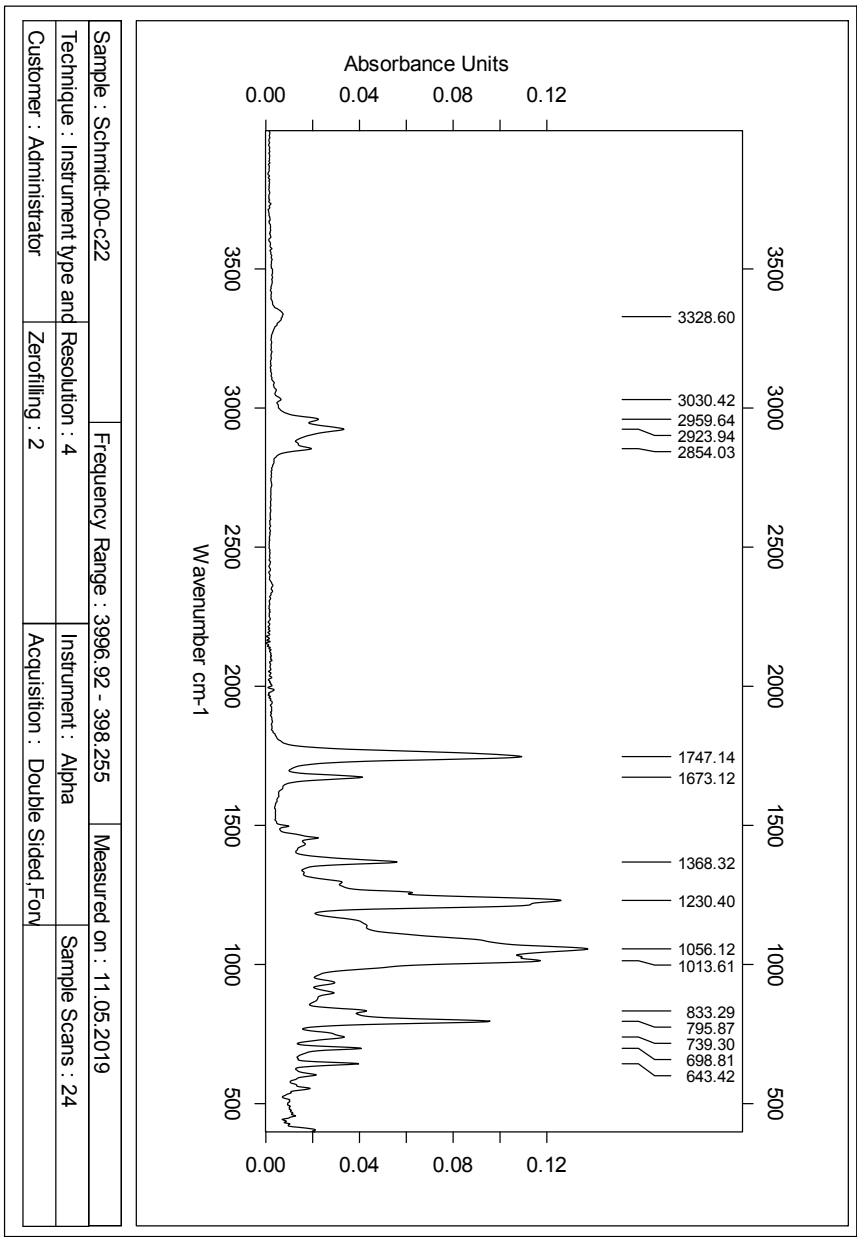

Figure 364: IR spectrum of **IC-5**.

B.49 Spectroscopic data for compound 9j

Elemental Composition Report **Page 1**

Single Mass Analysis
Tolerance = 2.0 PPM / DBE: min = -50.0, max = 50.0
Element prediction: Off
Number of isotope peaks used for i-FIT = 3

Monoisotopic Mass, Even Electron Ions
1500 formula(e) evaluated with 1 results within limits (all results (up to 1000) for each mass)
Elements Used:
C: 0-100 H: 0-150 N: 0-10 O: 0-10

2019-462 42 (0.477) AM2 (Ar,35000.0,0.00,0.00); Cm (40:44)
1: TOF MS ES+

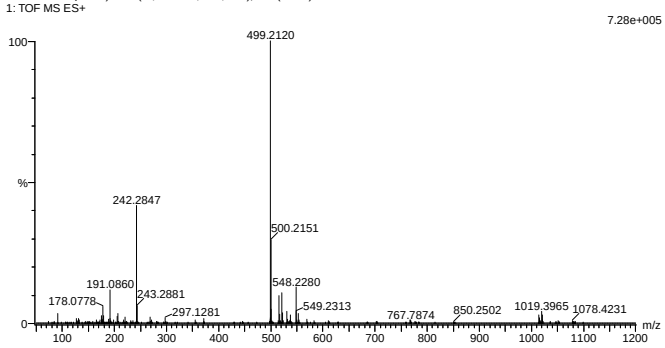

Minimum:				-50.0				
Maximum:		5.0	2.0	50.0				
Mass	Calc. Mass	mDa	PPM	DBE	i-FIT	Norm	Conf(%)	Formula
499.2120	499.2121	-0.1	-0.2	16.5	885.4	n/a	n/a	C31 H31 O6

Figure 365: HRMS (ESI+) of anomeric mixture of **9j**.

B.50 Spectroscopic data for compound 9j-α

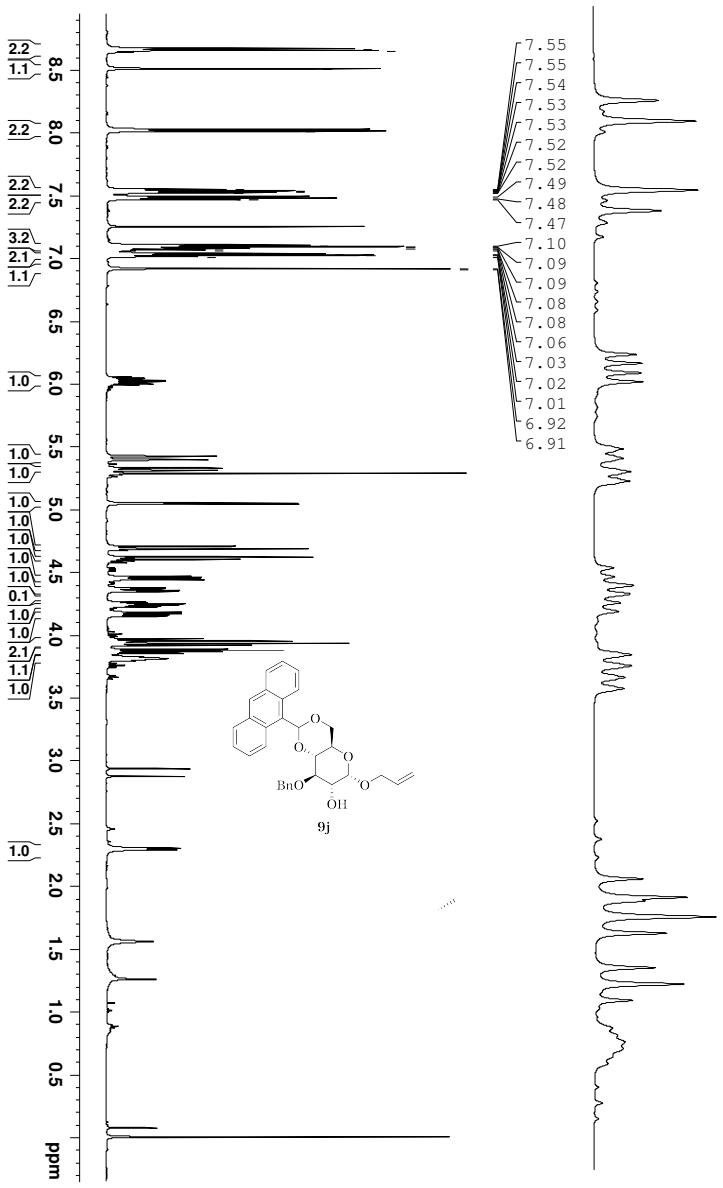

Figure 366: ^{1}H NMR spectrum of **9j-α**.

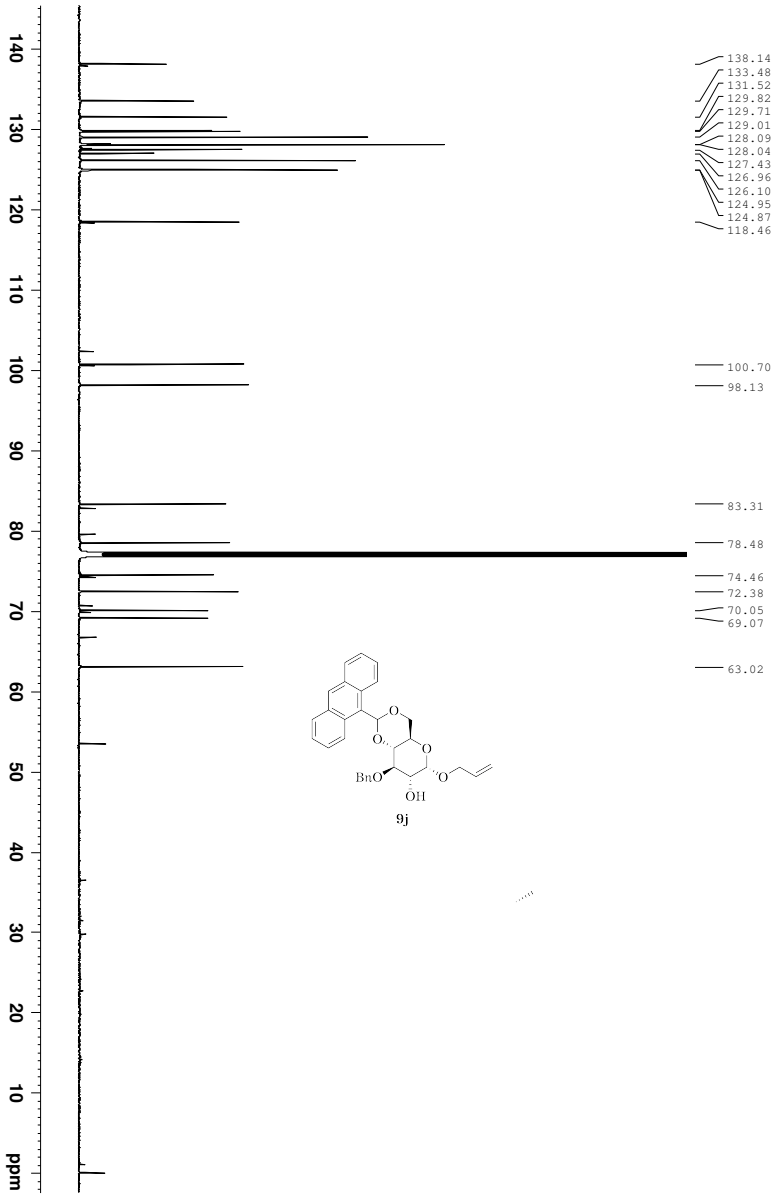

Figure 367: ^{13}C NMR spectrum of **9j-α**.

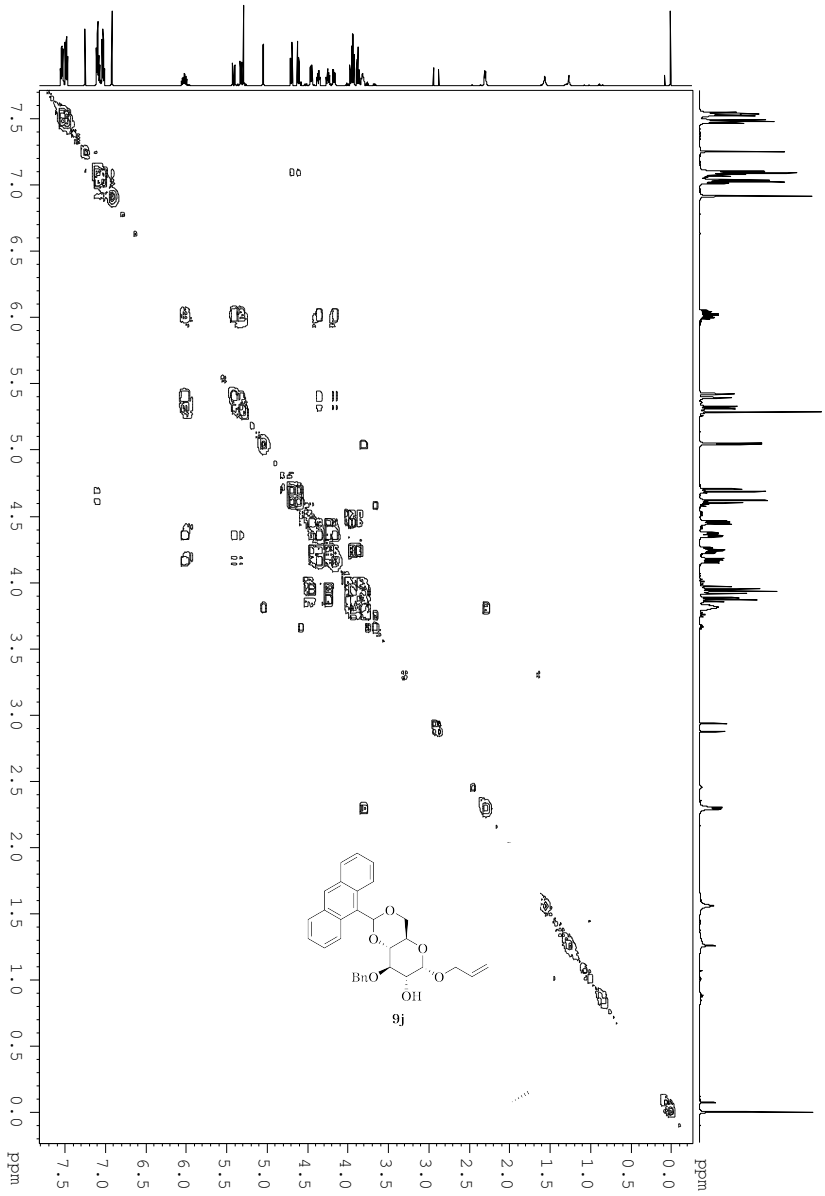

Figure 368: COSY spectrum of **9j-α**.

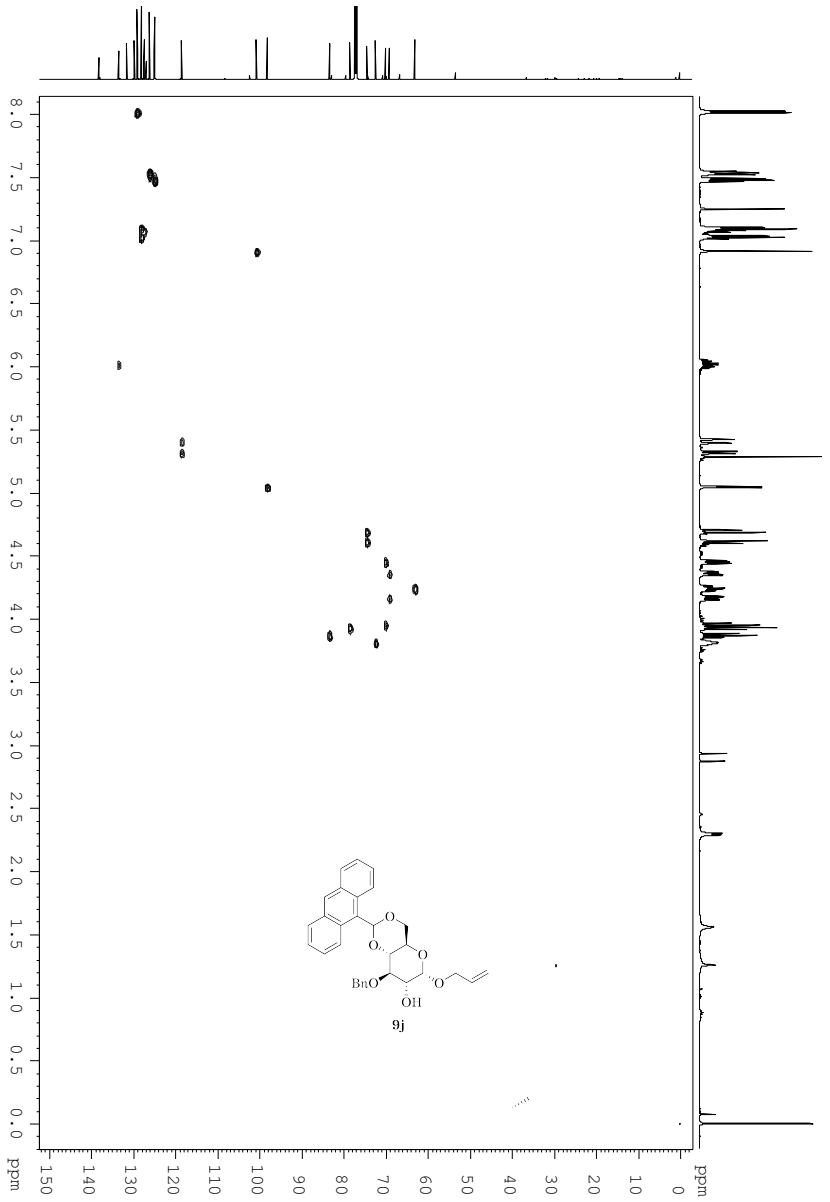

Figure 369: HSQC spectrum of **9j-α**.

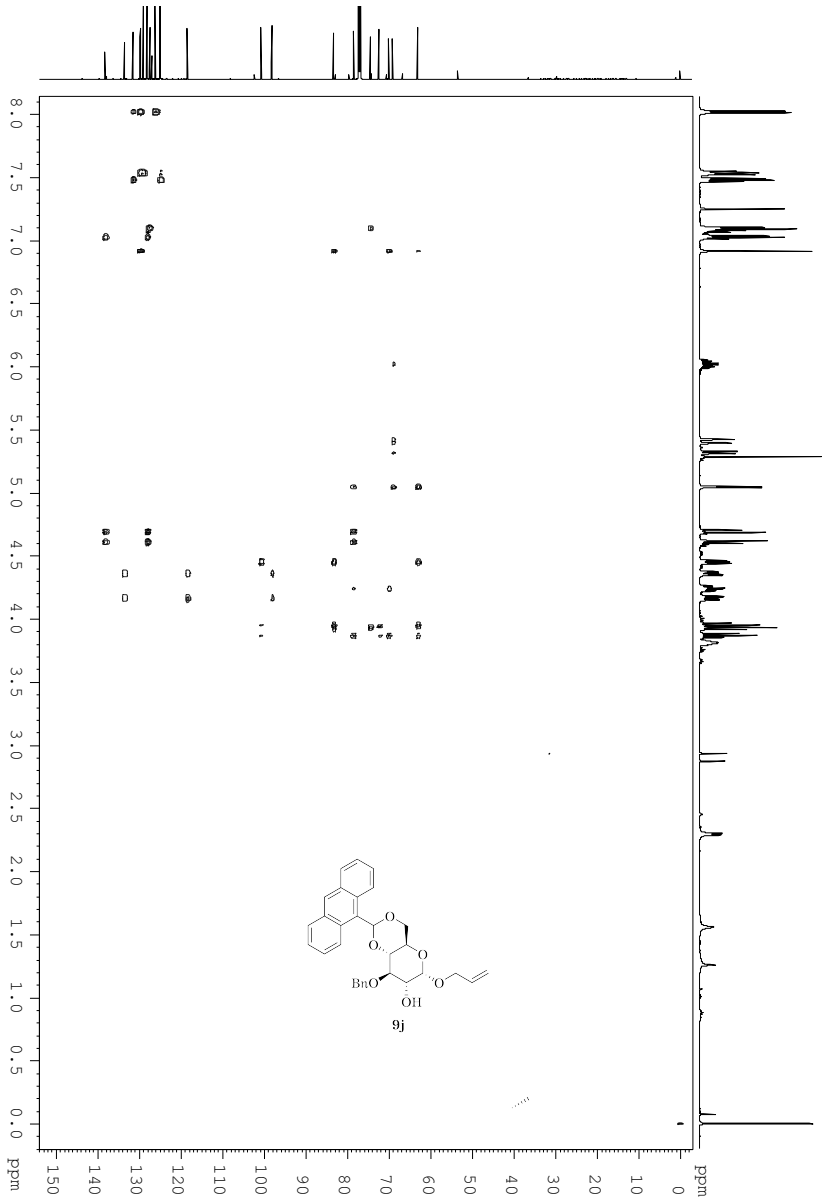

Figure 370: HMBC spectrum of **9j-α**.

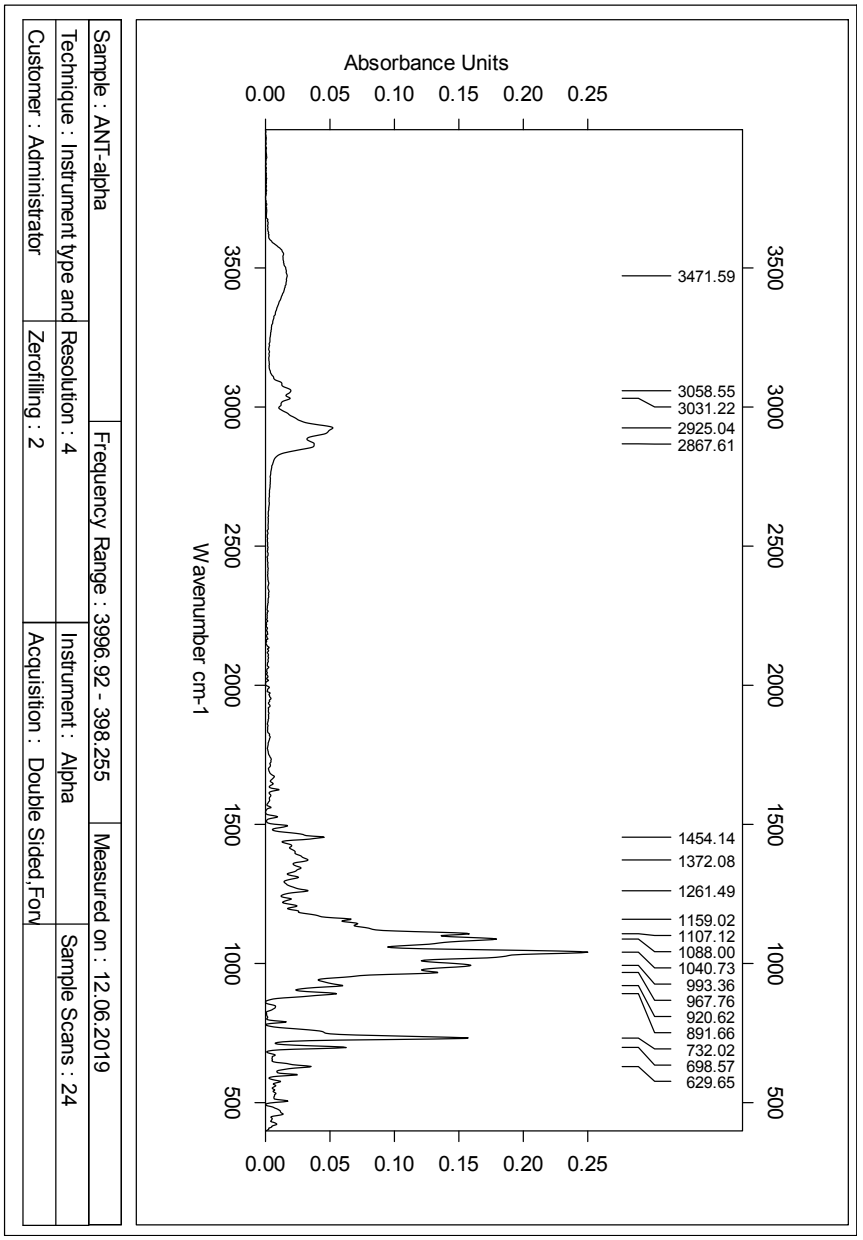

Figure 371: IR spectrum of **9j-α**.

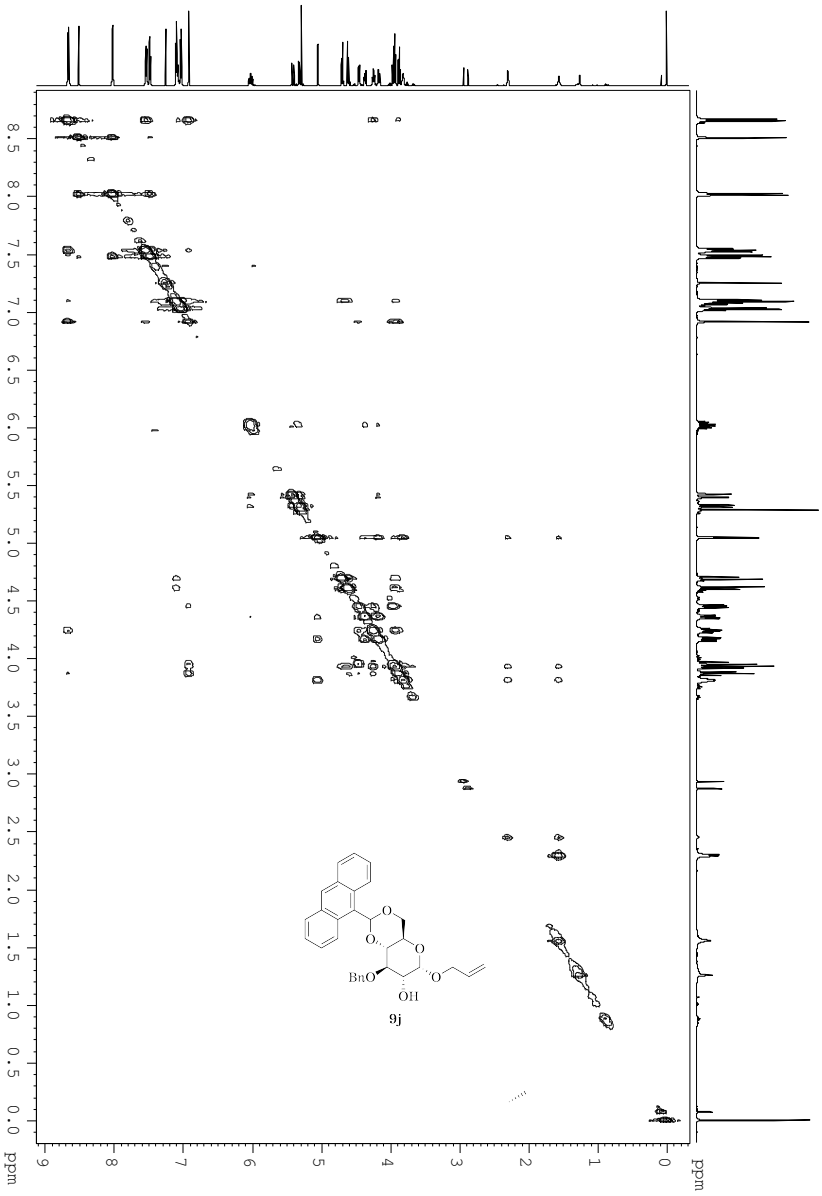

Figure 372: NOESY spectrum of **9j-α**.

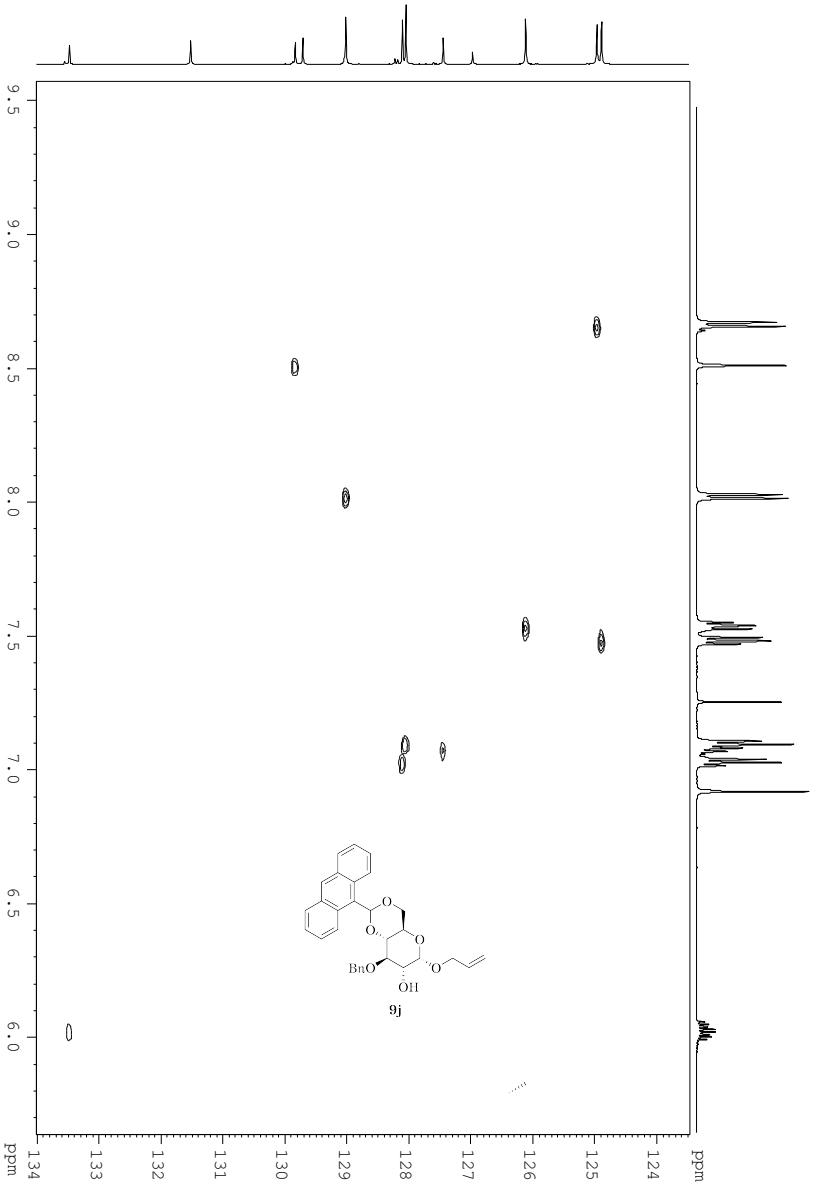

Figure 373: Selective HSQC spectrum of **9j-α**.

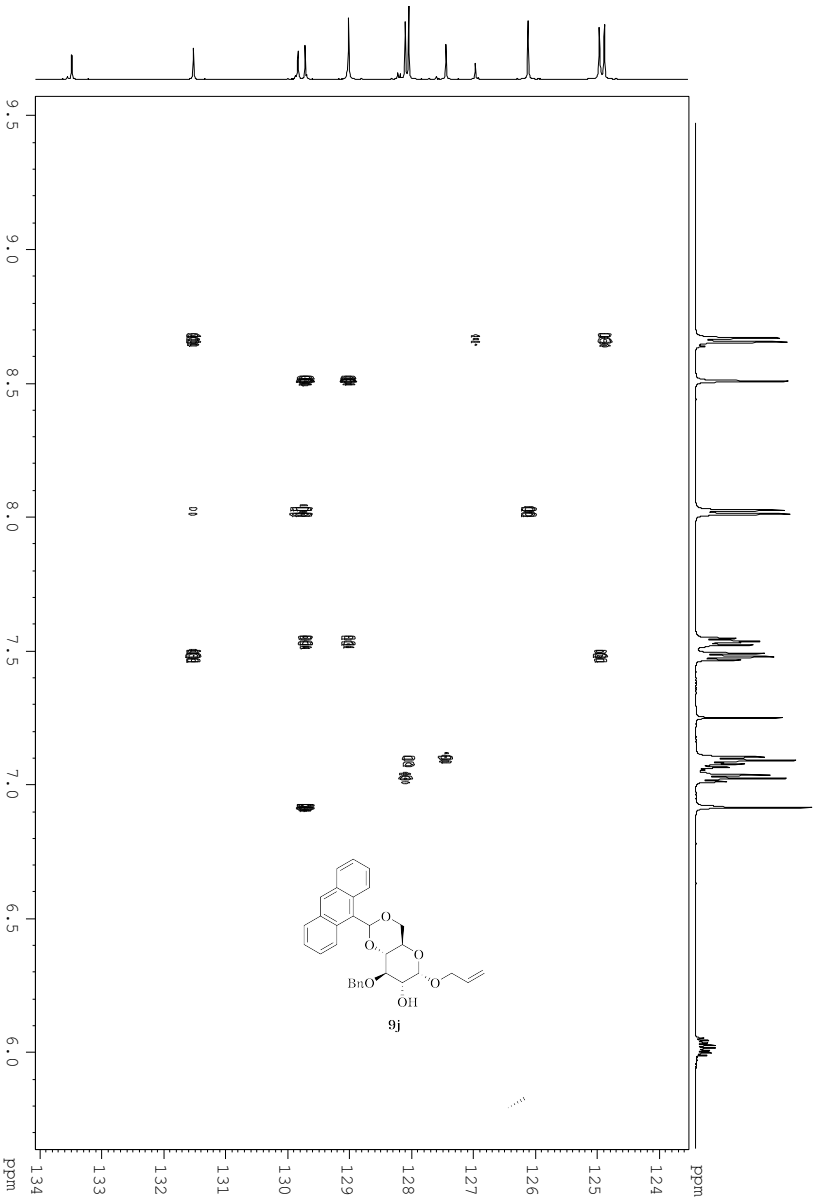

Figure 374: Selective HMBC spectrum of **9j-α**.

B.51 Spectroscopic data for compound 9j-β

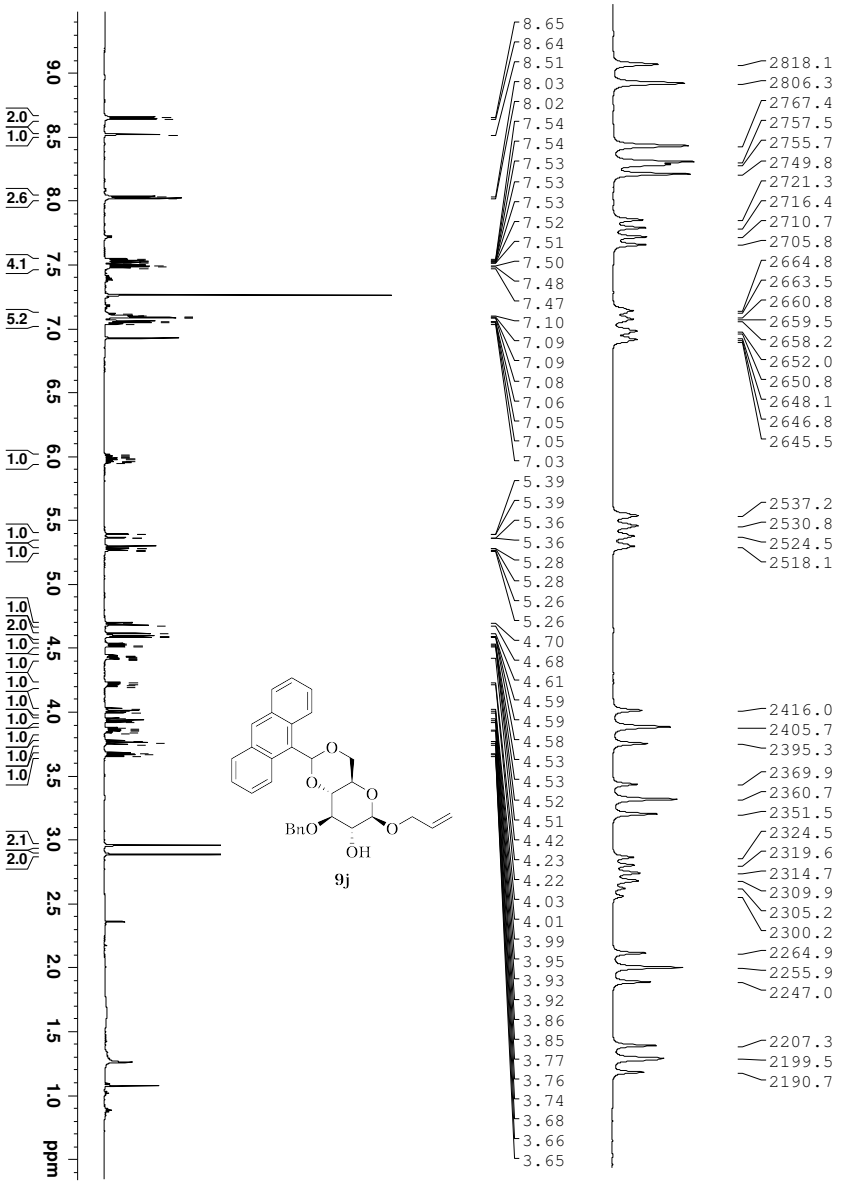

Figure 375: ^{1}H NMR spectrum of **9j-β**.

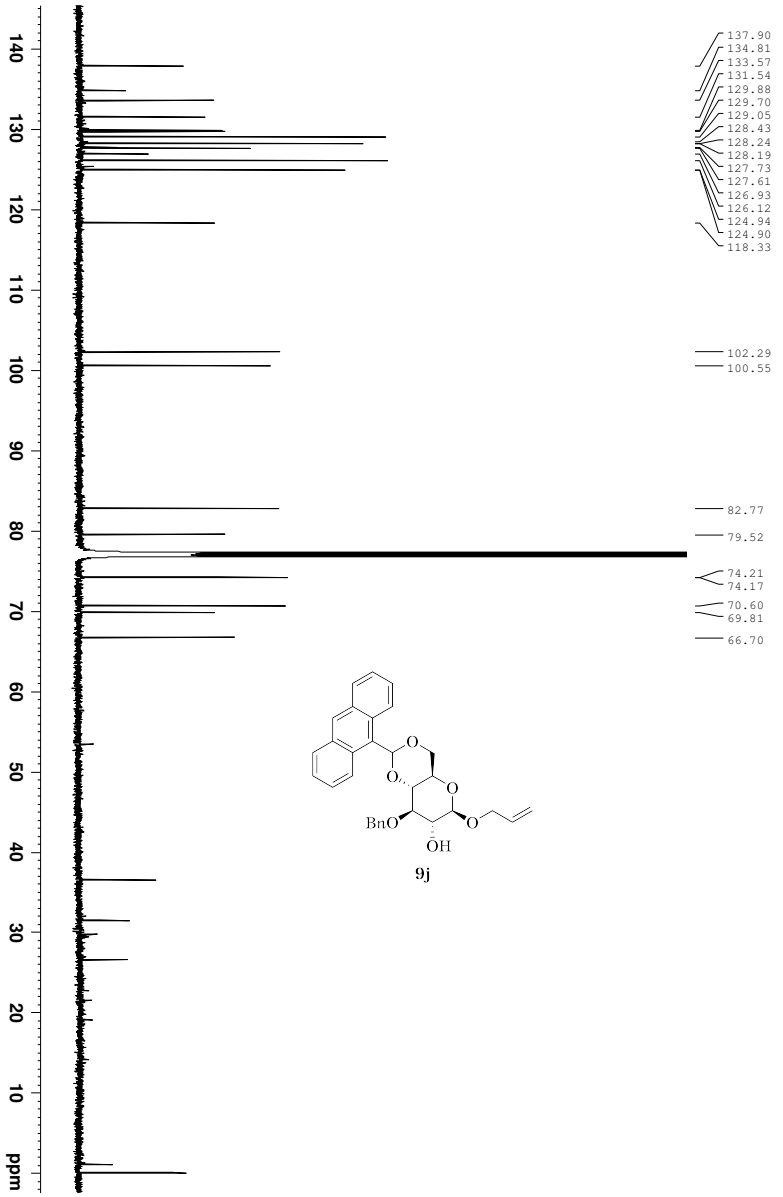

Figure 376: ^{13}C NMR spectrum of **9j-β**.

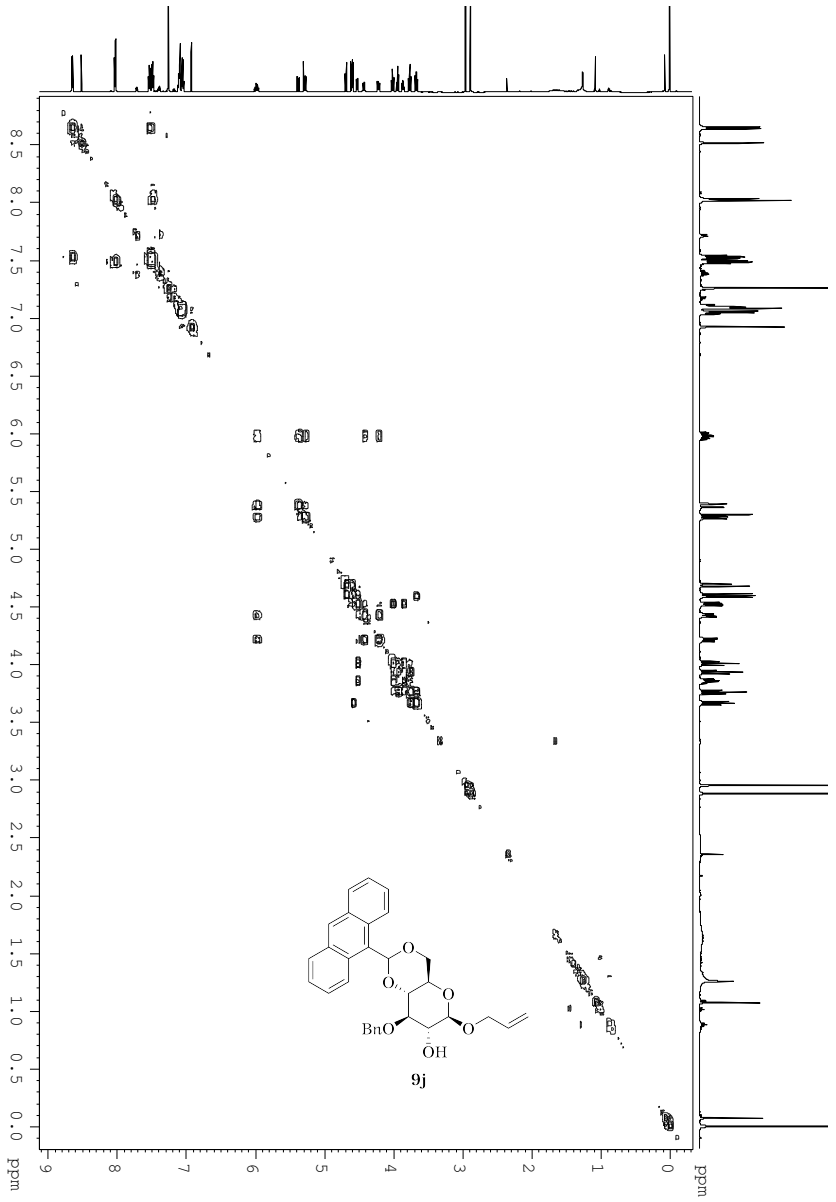

Figure 377: COSY spectrum of **9j-β**.

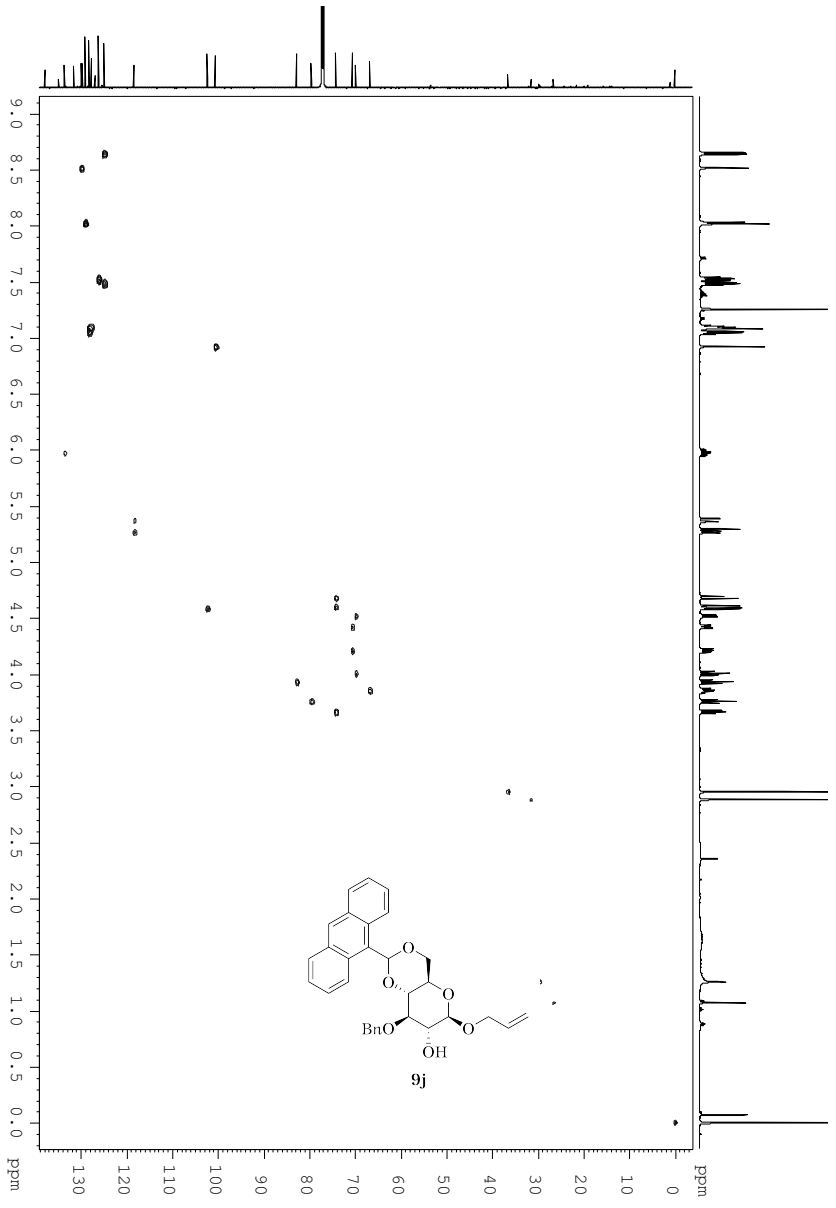

Figure 378: HSQC spectrum of **9j-β**.

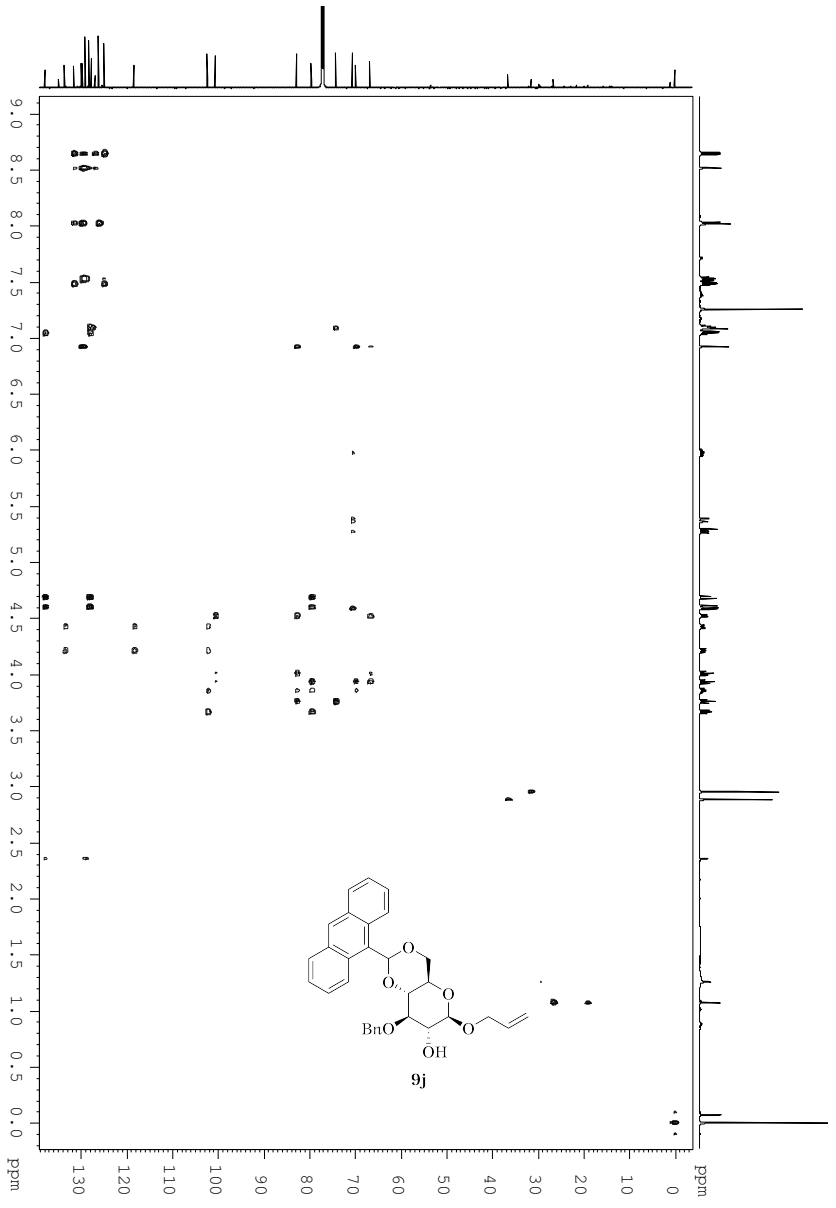

Figure 379: HMBC spectrum of **9j-β**.

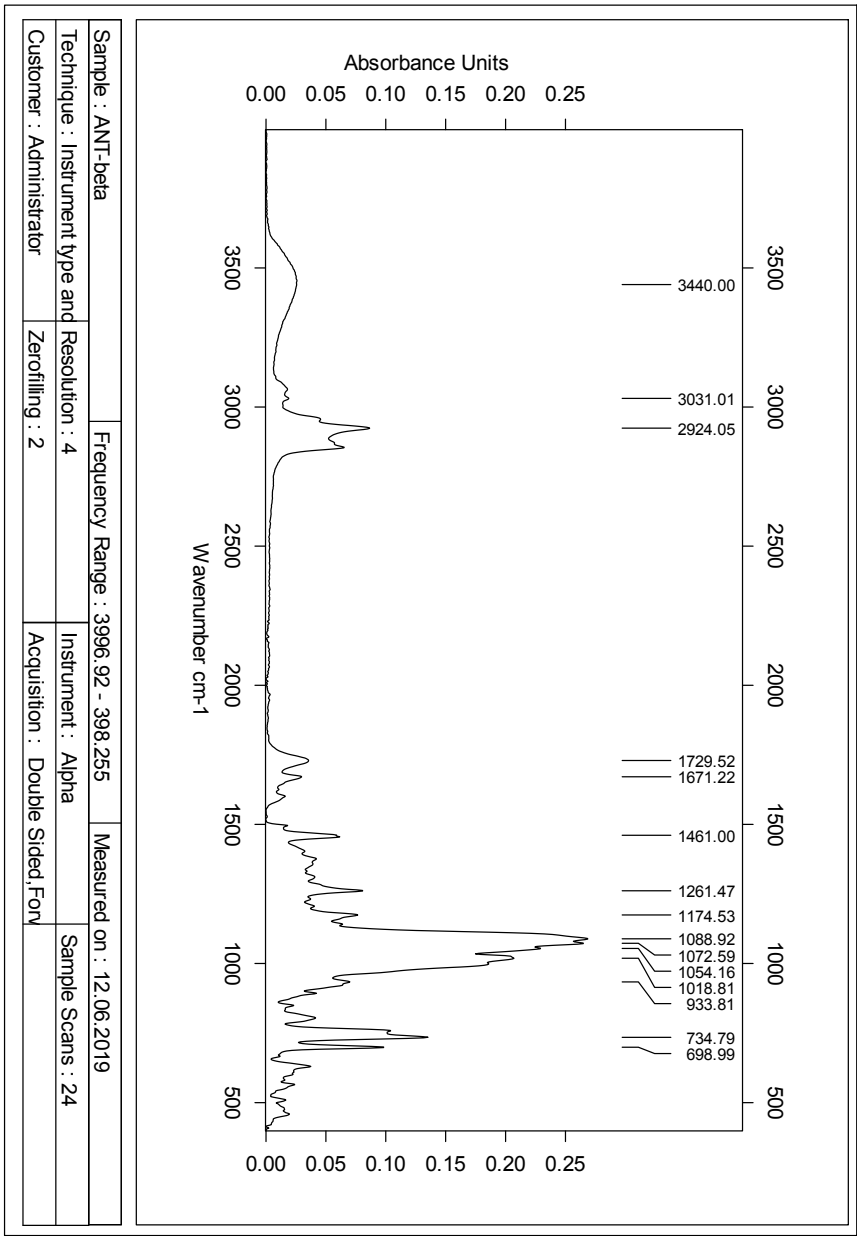

Figure 380: IR spectrum of **9j-β**.

B.52 Spectroscopic data for compound 9i-α

Elemental Composition Report **Page 1**

Single Mass Analysis
Tolerance = 2.1 PPM / DBE: min = -50.0, max = 50.0
Element prediction: Off
Number of isotope peaks used for i-FIT = 3

Monoisotopic Mass, Even Electron Ions
4094 formula(e) evaluated with 6 results within limits (all results (up to 1000) for each mass)
Elements Used:
C: 0-100 H: 0-150 N: 0-3 O: 0-10 Na: 0-1 S: 0-3
2019-379 25 (0.470) AM2 (Ar,35000.0,0.00,0.00); Cm (22:28)
1: TOF MS ES+

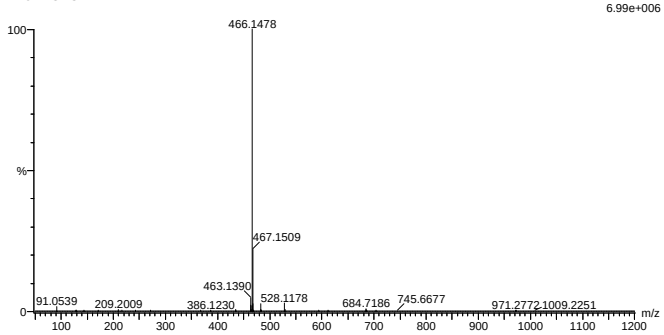

Minimum:				-50.0				
Maximum:		5.0	2.1	50.0				
Mass	Calc. Mass	mDa	PPM	DBE	i-FIT	Norm	Conf(%)	Formula
466.1478	466.1478	0.0	0.0	11.5	1175.5	0.000	100.00	C23 H25 N O8 Na
	466.1477	0.1	0.2	18.5	1186.6	11.129	0.00	C29 H24 N O3 S
	466.1480	-0.2	-0.4	1.5	1191.3	15.805	0.00	C16 H33 N3 O5 Na S3
	466.1471	0.7	1.5	2.5	1187.4	11.889	0.00	C15 H29 N3 O10 Na S
	466.1470	0.8	1.7	9.5	1189.9	14.404	0.00	C21 H28 N3 O5 S2
	466.1487	-0.9	-1.9	10.5	1189.5	13.959	0.00	C24 H29 N O3 Na S2

Figure 381: HRMS (ESI+) of **9i-α**.

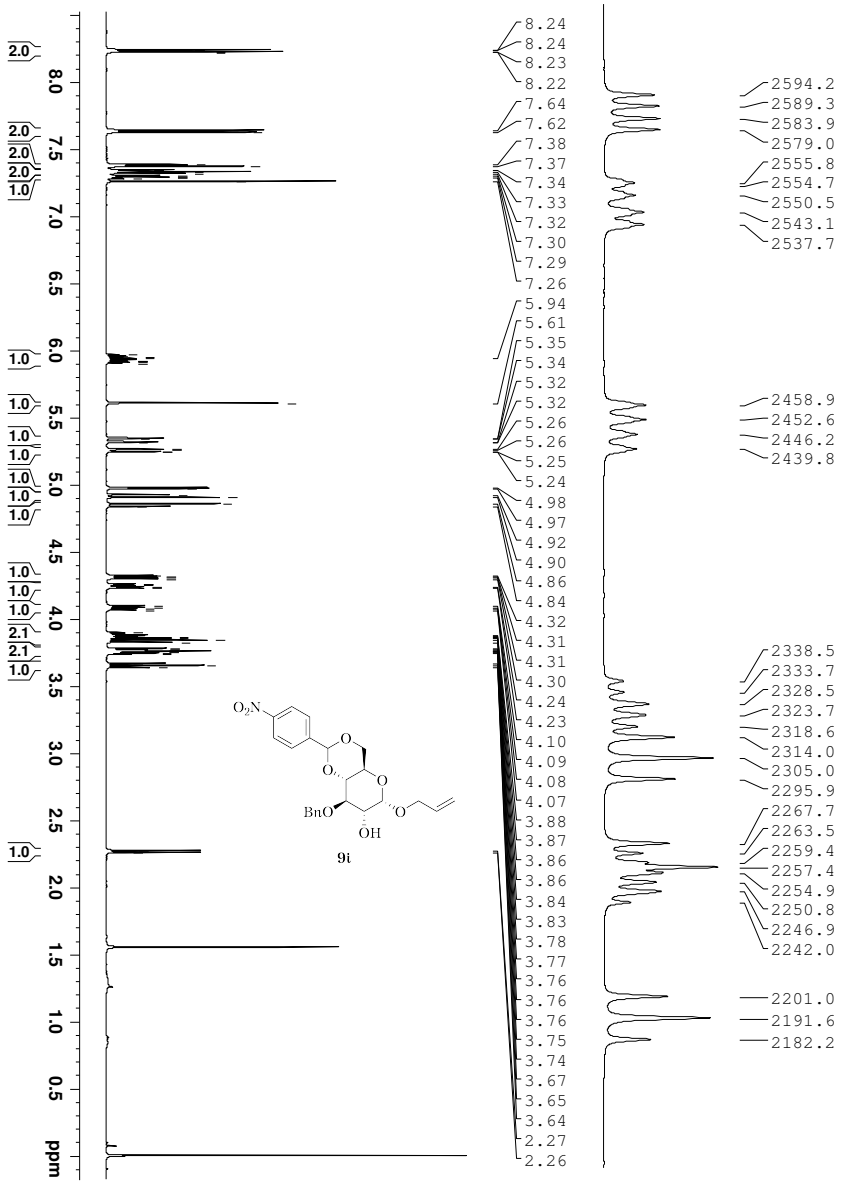

Figure 382: ^{1}H NMR spectrum of **9i-α**.

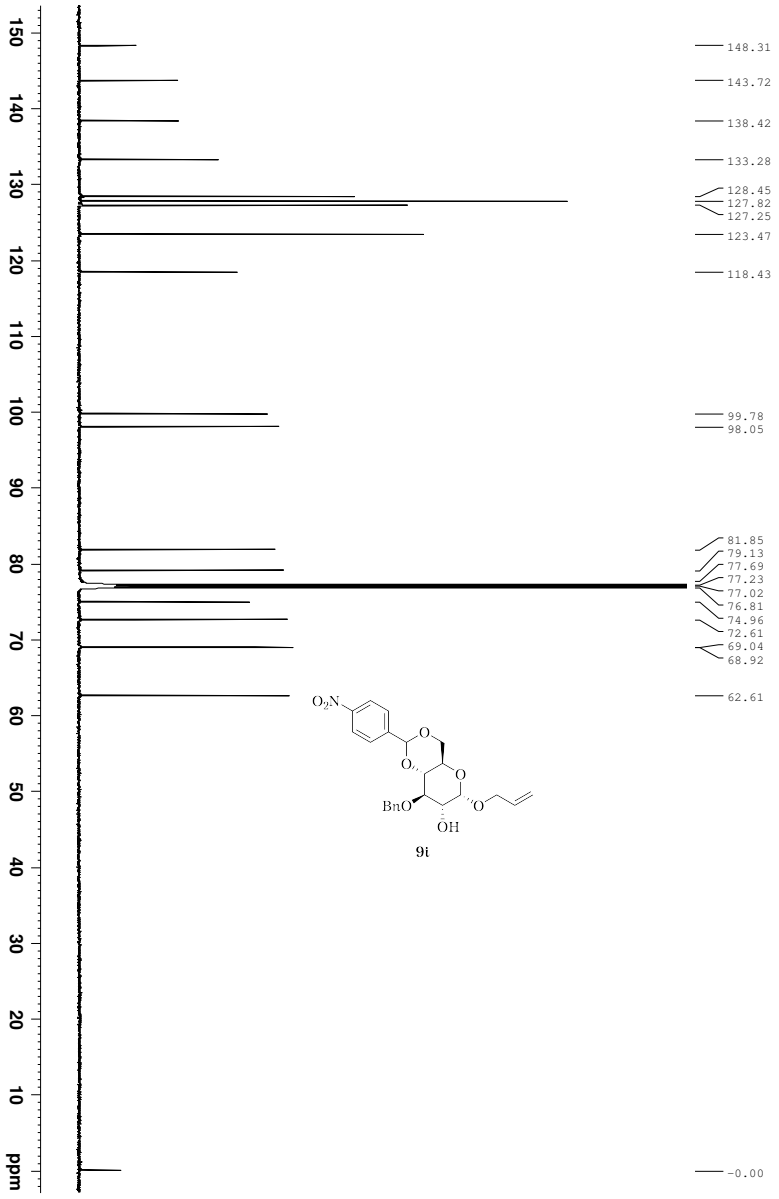

Figure 383: ^{13}C NMR spectrum of **9i-α**.

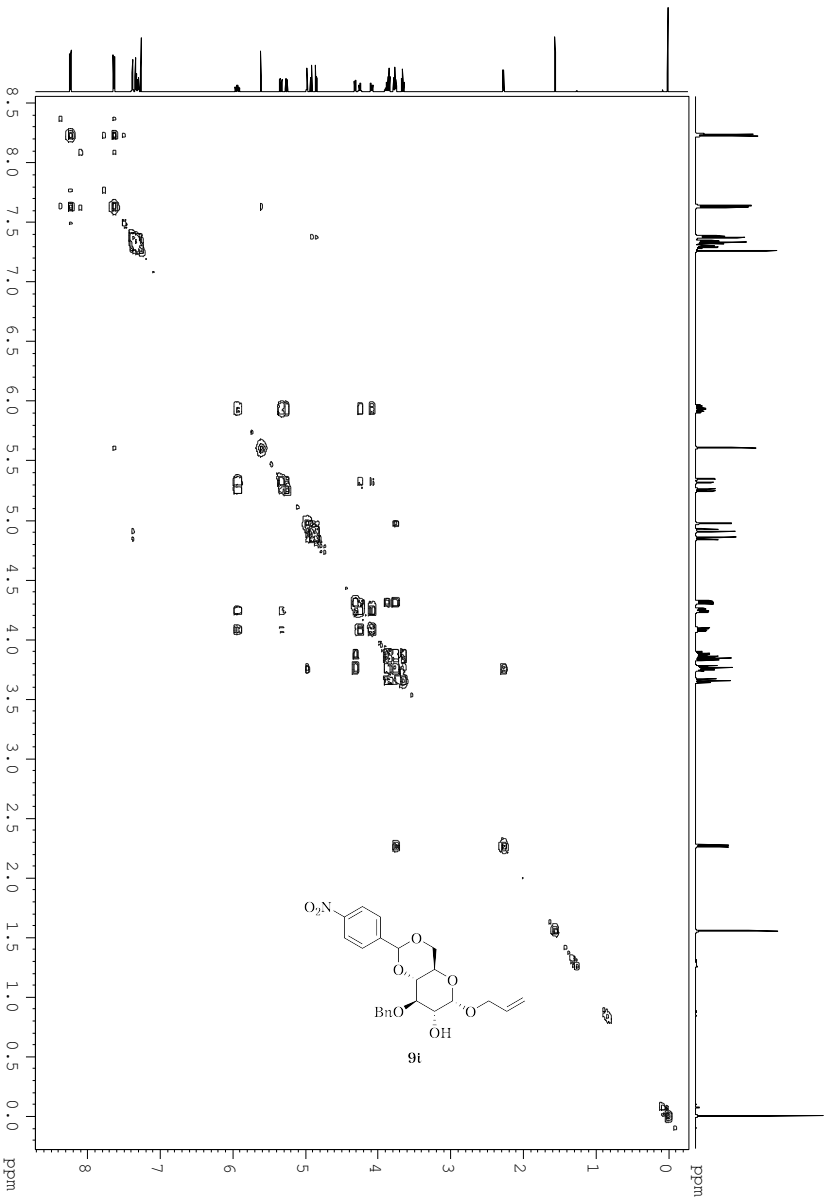

Figure 384: COSY spectrum of **9i-α**.

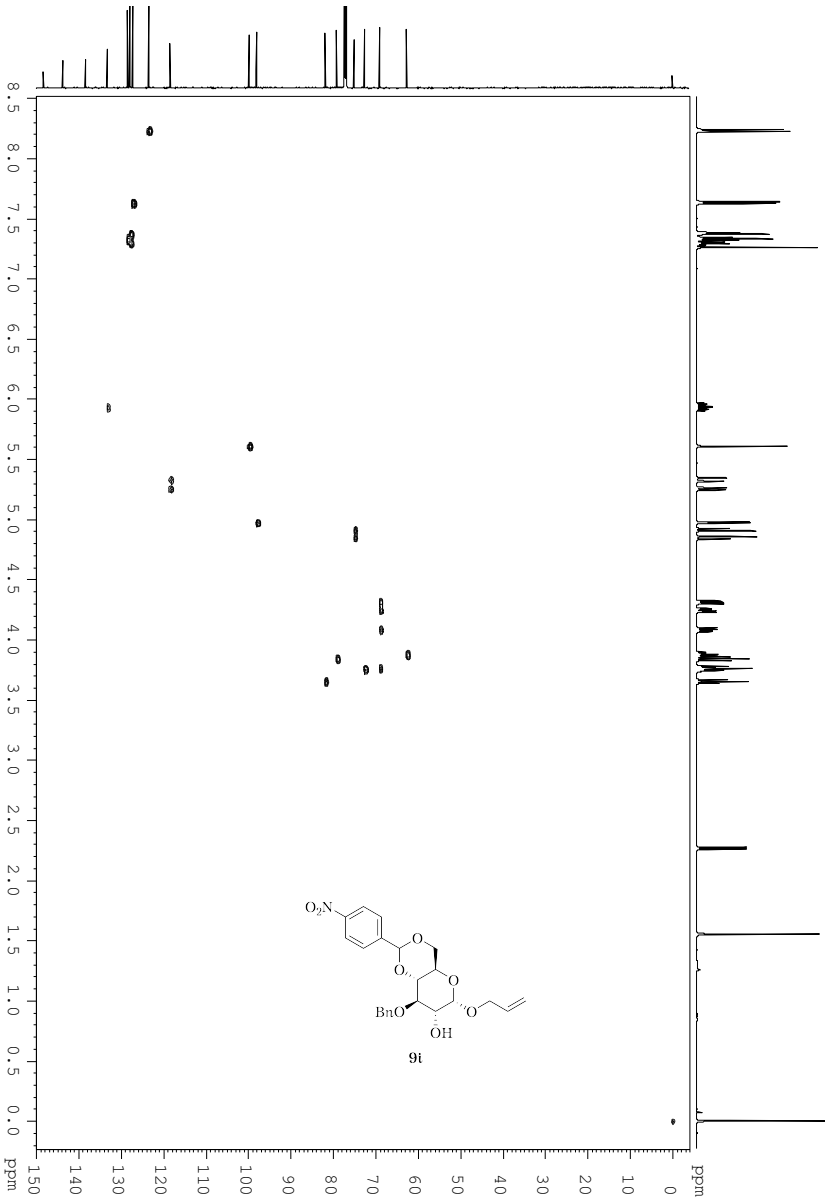

Figure 385: HSQC spectrum of **9i-α**.

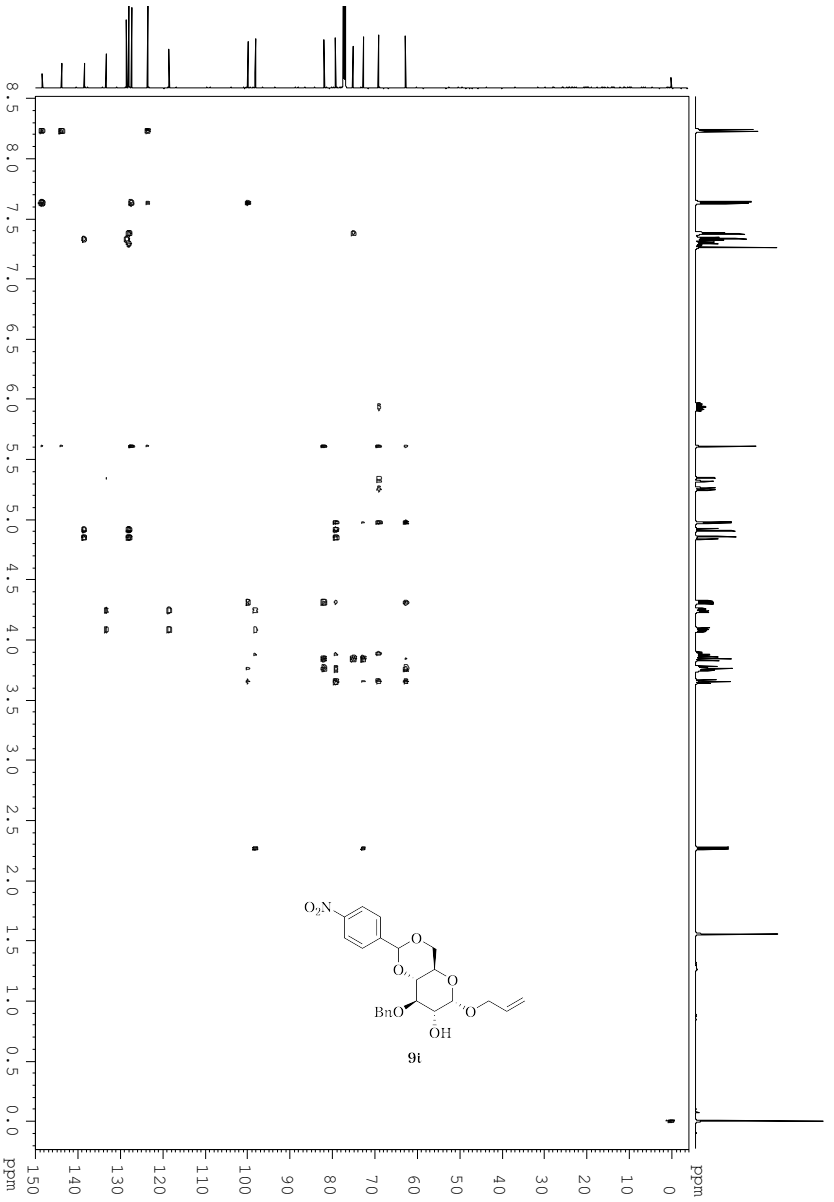

Figure 386: HMBC spectrum of **9i-α**.

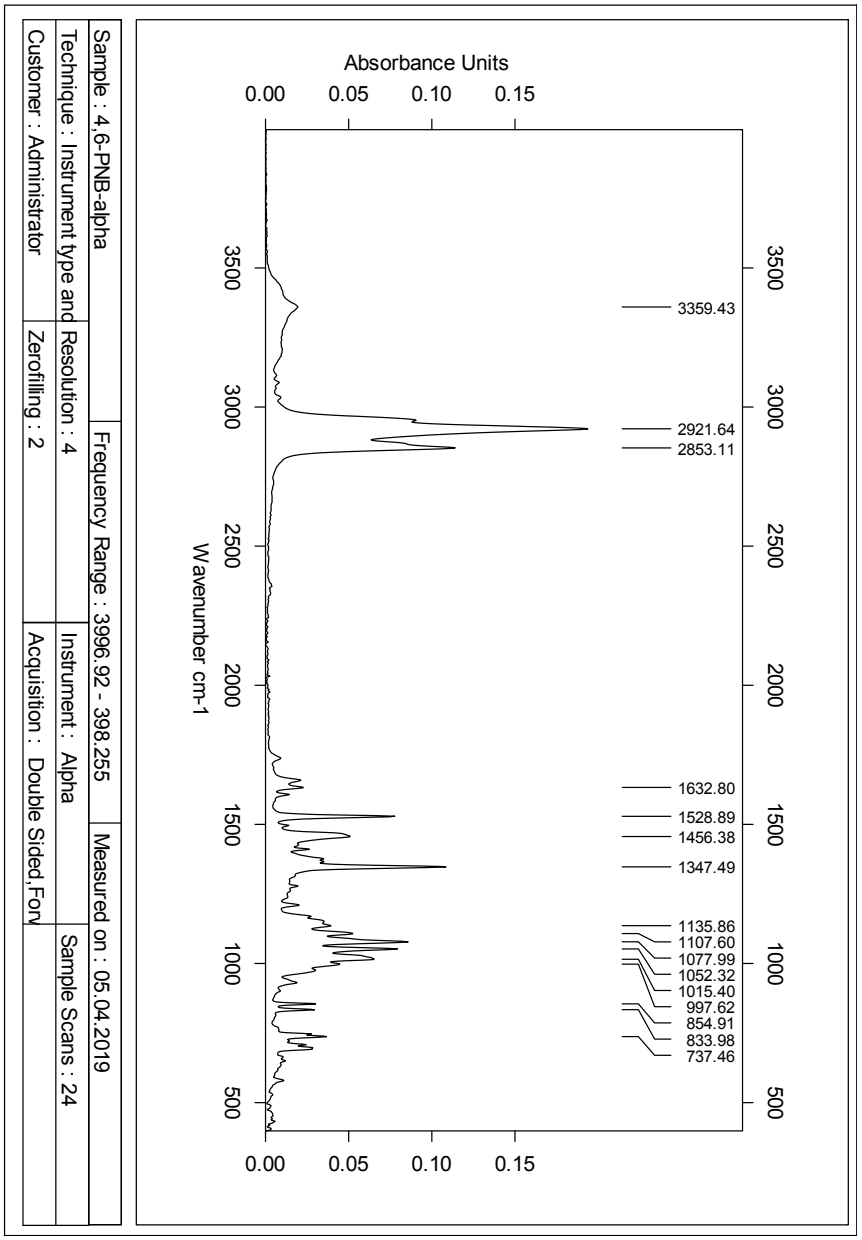

Figure 387: IR spectrum of **9i-α**.

B.53 Spectroscopic data for compound 9i-β

Elemental Composition Report **Page 1**

Single Mass Analysis
Tolerance = 2.1 PPM / DBE: min = -50.0, max = 50.0
Element prediction: Off
Number of isotope peaks used for i-FIT = 3

Monoisotopic Mass, Even Electron Ions
4094 formula(e) evaluated with 6 results within limits (all results (up to 1000) for each mass)
Elements Used:
C: 0-100 H: 0-150 N: 0-3 O: 0-10 Na: 0-1 S: 0-3
2019-380 25 (0.470) AM2 (Ar,35000.0,0.00,0.00); Cm (19:25)
1: TOF MS ES+

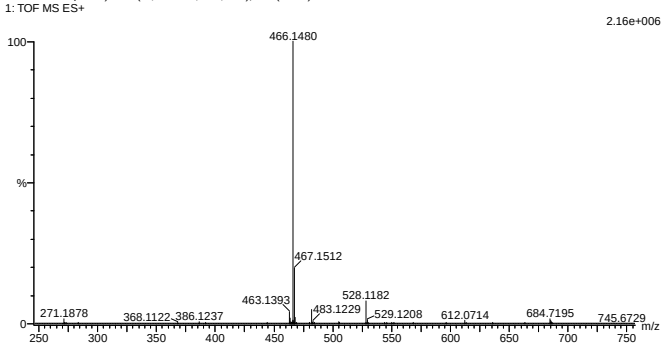

Minimum:				-50.0				
Maximum:		5.0	2.1	50.0				
Mass	Calc. Mass	mDa	PPM	DBE	i-FIT	Norm	Conf(%)	Formula
466.1480	466.1480	0.0	0.0	1.5	1048.6	14.614	0.00	C16 H33 N3 O5 Na S3
	466.1478	0.2	0.4	11.5	1034.0	0.000	99.99	C23 H25 N O8 Na
	466.1477	0.3	0.6	18.5	1044.2	10.145	0.00	C29 H24 N O3 S
	466.1487	-0.7	-1.5	10.5	1046.9	12.847	0.00	C24 H29 N O3 Na S2
	466.1471	0.9	1.9	2.5	1045.0	10.931	0.00	C15 H29 N3 O10 Na S
	466.1470	1.0	2.1	9.5	1047.4	13.335	0.00	C21 H28 N3 O5 S2

Figure 388: HRMS (ESI+) of **9i-β**.

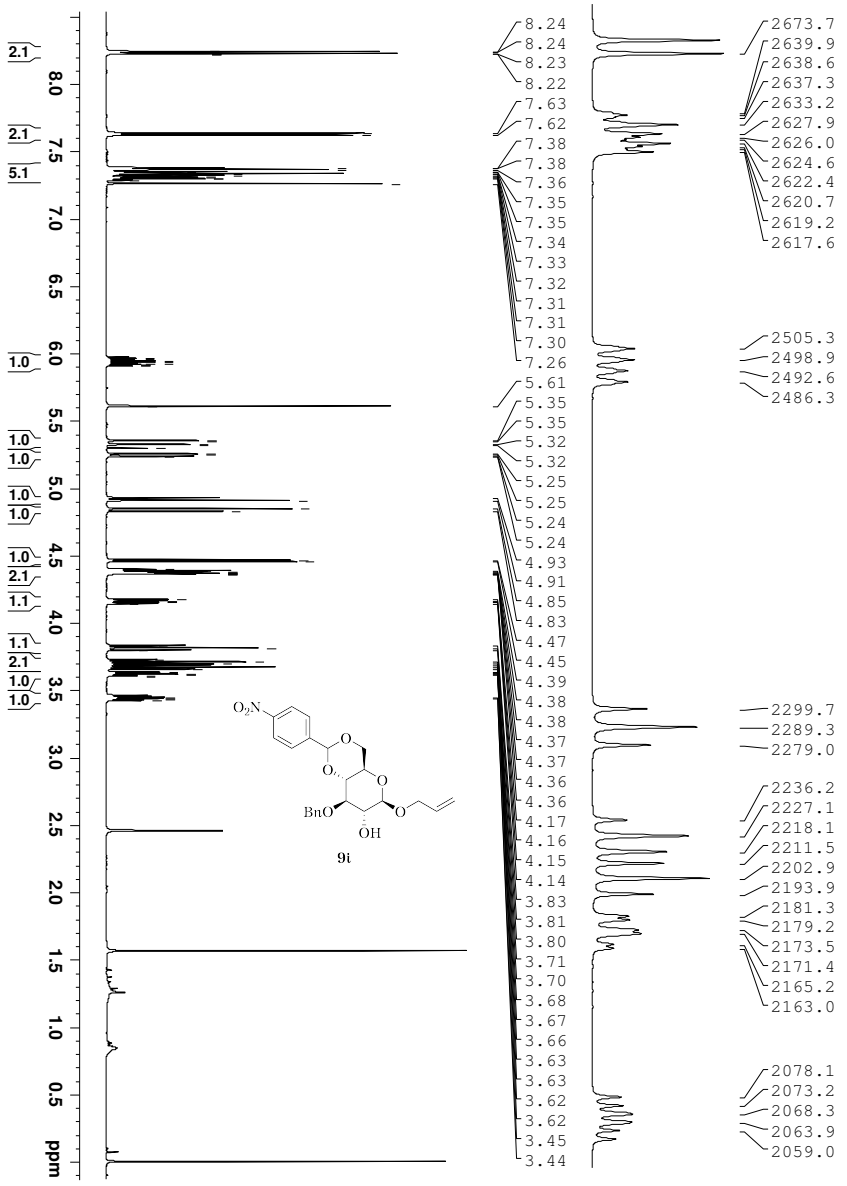

Figure 389: ^{1}H NMR spectrum of **9i-β**.

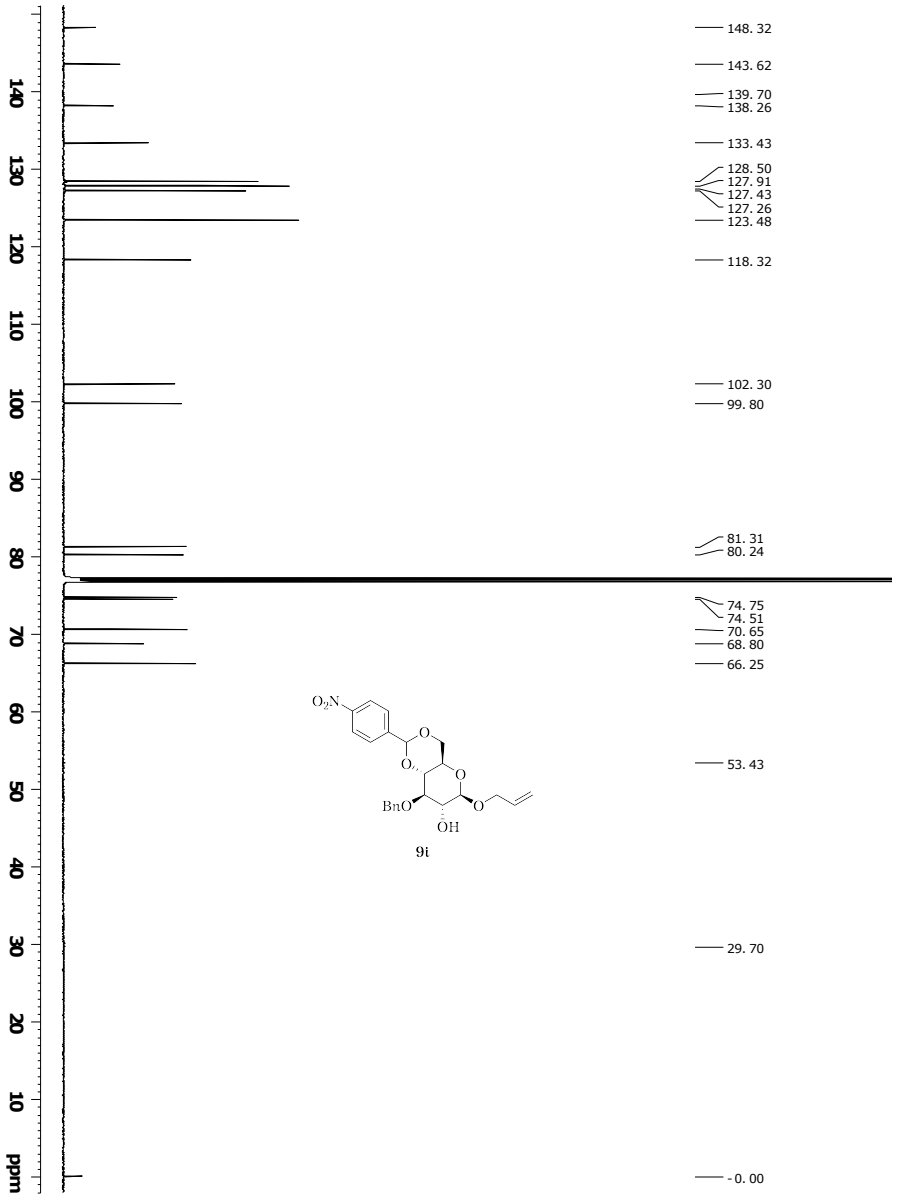

Figure 390: ^{13}C NMR spectrum of **9i-β**.

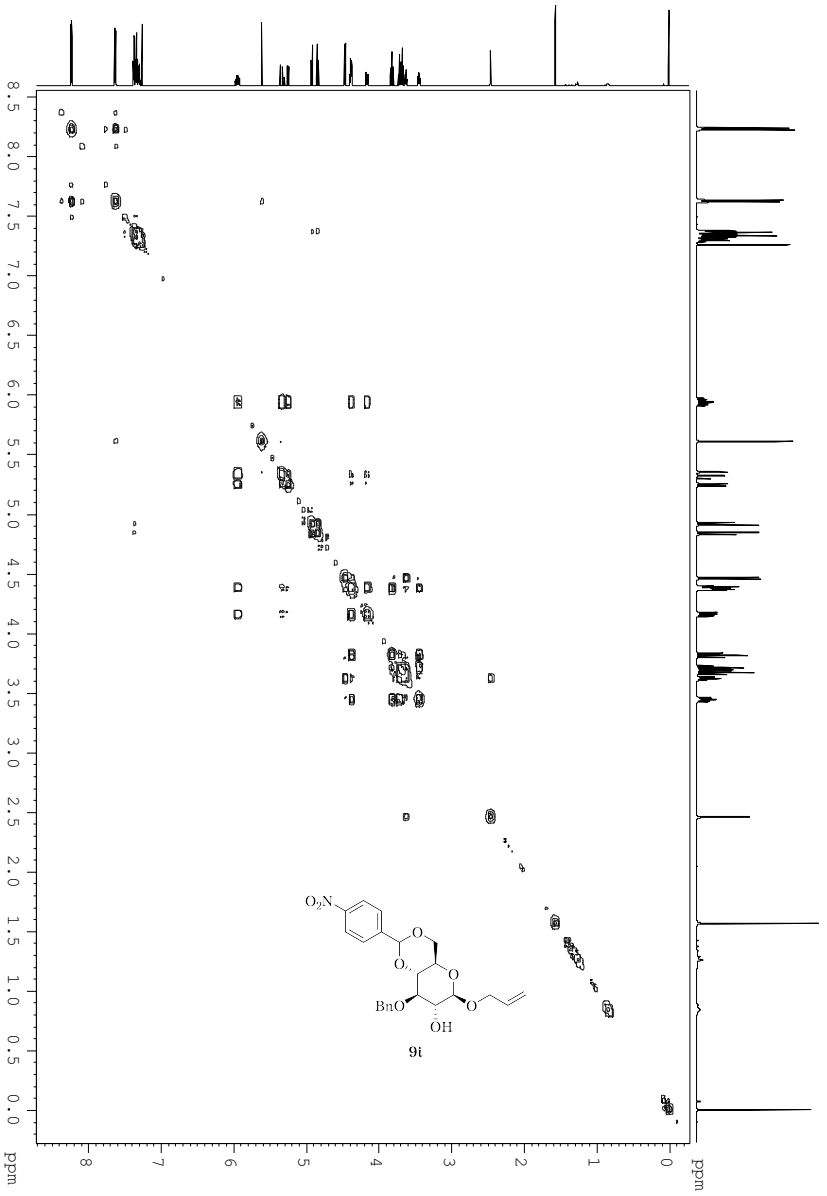

Figure 391: COSY spectrum of **9i-β**.

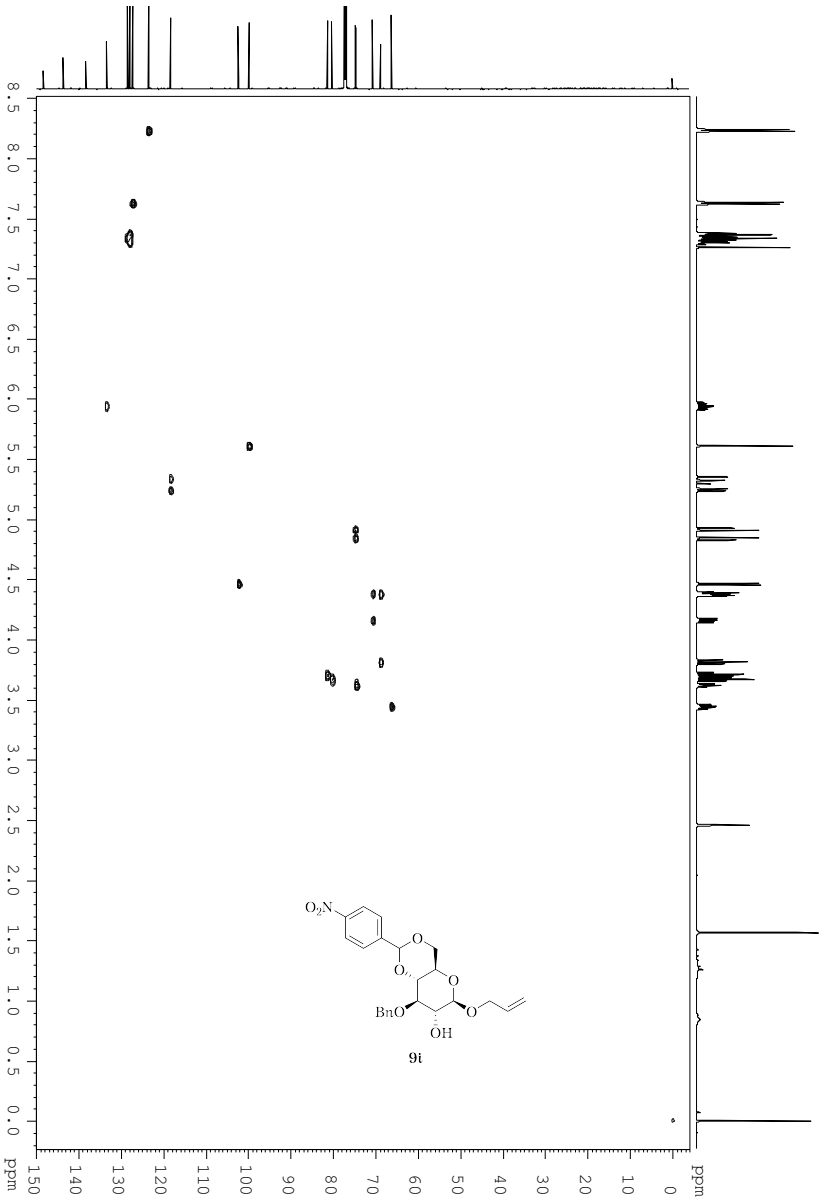

Figure 392: HSQC spectrum of **9i-β**.

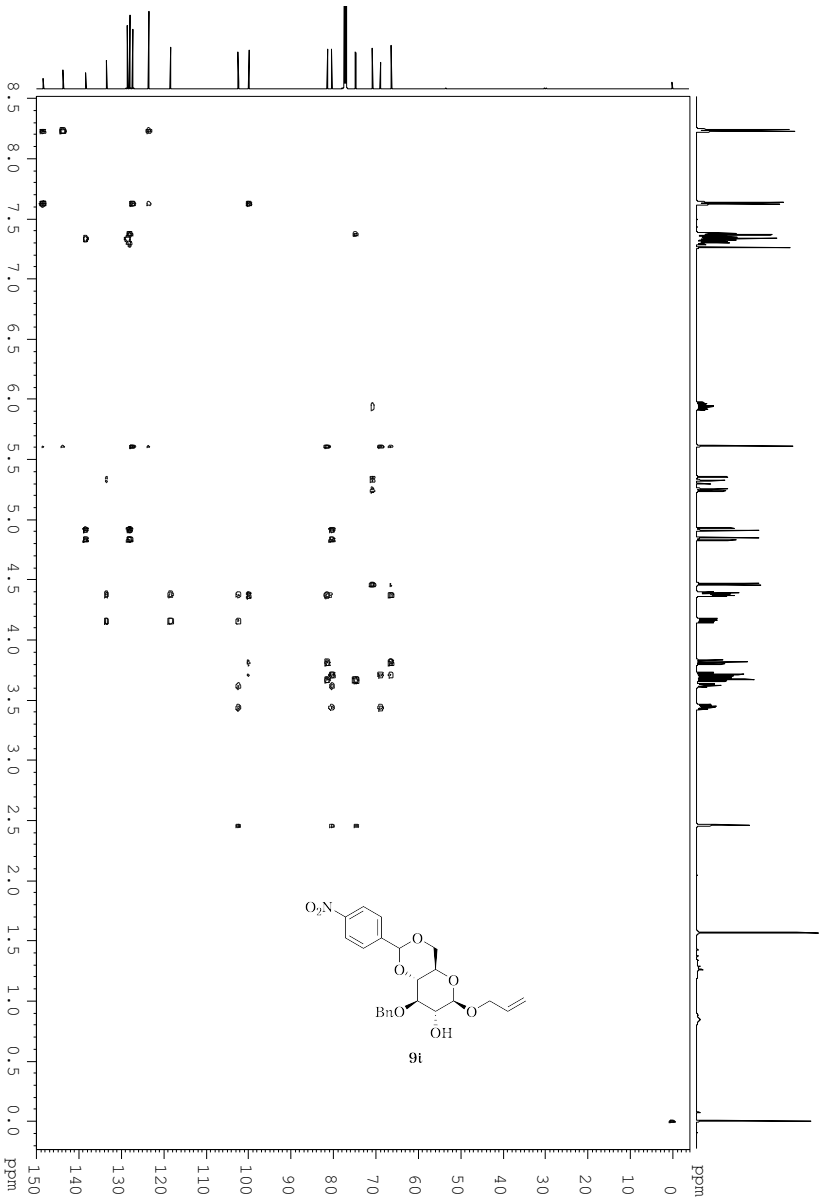

Figure 393: HMBC spectrum of **9i-β**.

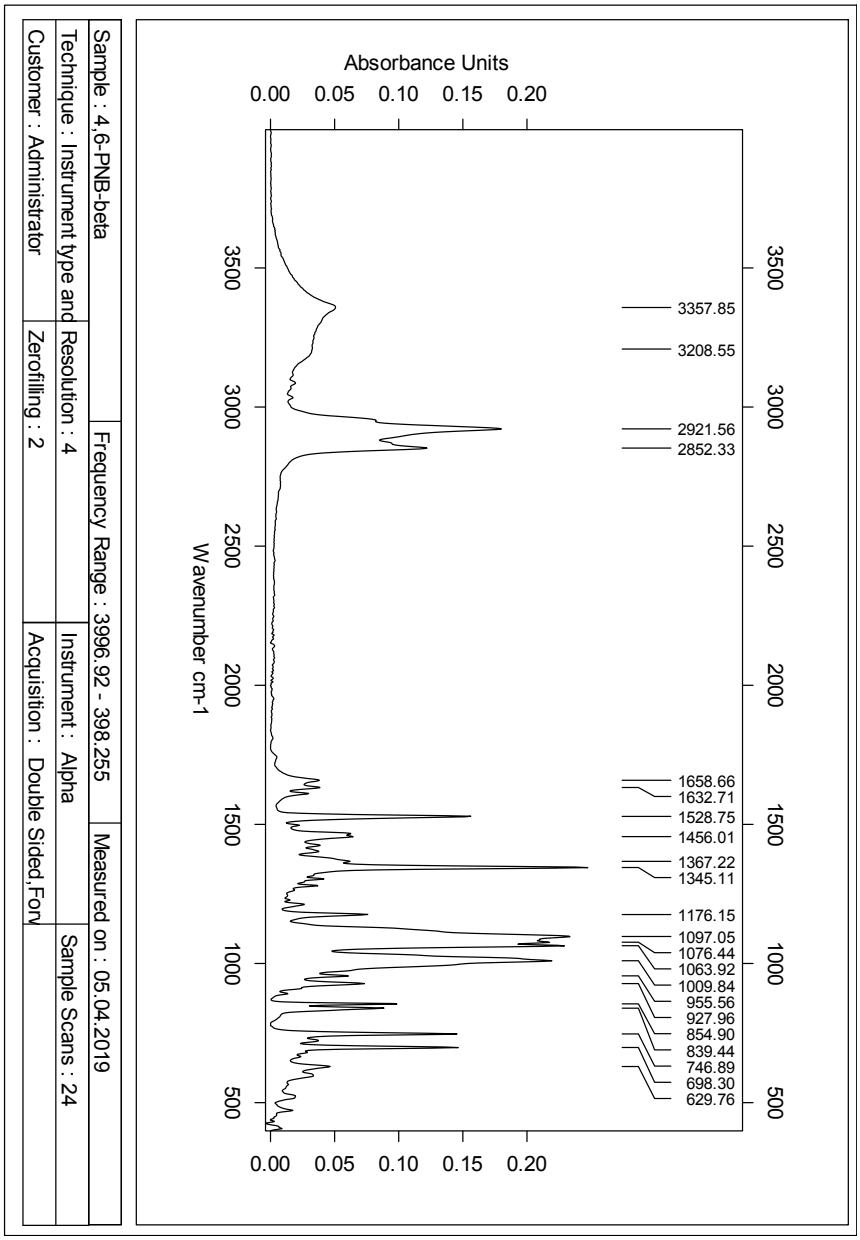

Figure 394: IR spectrum of **9i-β**.

B.54 *N*-Benzyl-3-*O*-benzyl-4,6-di-*O*-acetyl-β-D-glucopyranosylamine

Elemental Composition Report **Page 1**

Single Mass Analysis
Tolerance = 2.0 PPM / DBE: min = -50.0, max = 50.0
Element prediction: Off
Number of isotope peaks used for i-FIT = 3

Monoisotopic Mass, Even Electron Ions
654 formula(e) evaluated with 1 results within limits (all results (up to 1000) for each mass)
Elements Used:
C: 0-100 H: 0-150 N: 0-2 O: 0-8 Na: 0-1
2019-445 35 (0.403) AM2 (Ar,35000.0,0.00,0.00); Cm (23:35)
1: TOF MS ES+

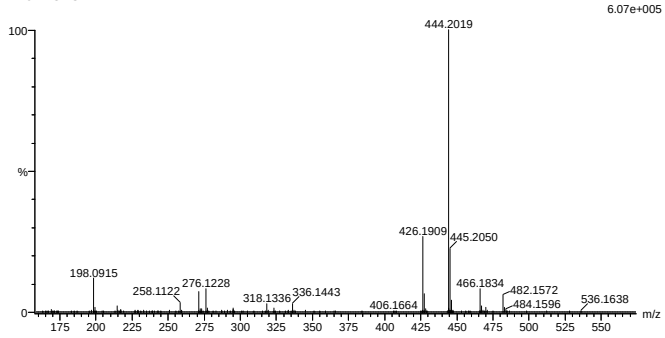

Minimum:				-50.0				
Maximum:		5.0	2.0	50.0				
Mass	Calc. Mass	mDa	PPM	DBE	i-FIT	Norm	Conf(%)	Formula
444.2019	444.2022	-0.3	-0.7	10.5	1047.1	n/a	n/a	C24 H30 N O7

Figure 395: HRMS (ESI+) of *N*-benzyl-3-*O*-benzyl-4,6-di-*O*-acetyl-β-D-glucopyranosylamine.

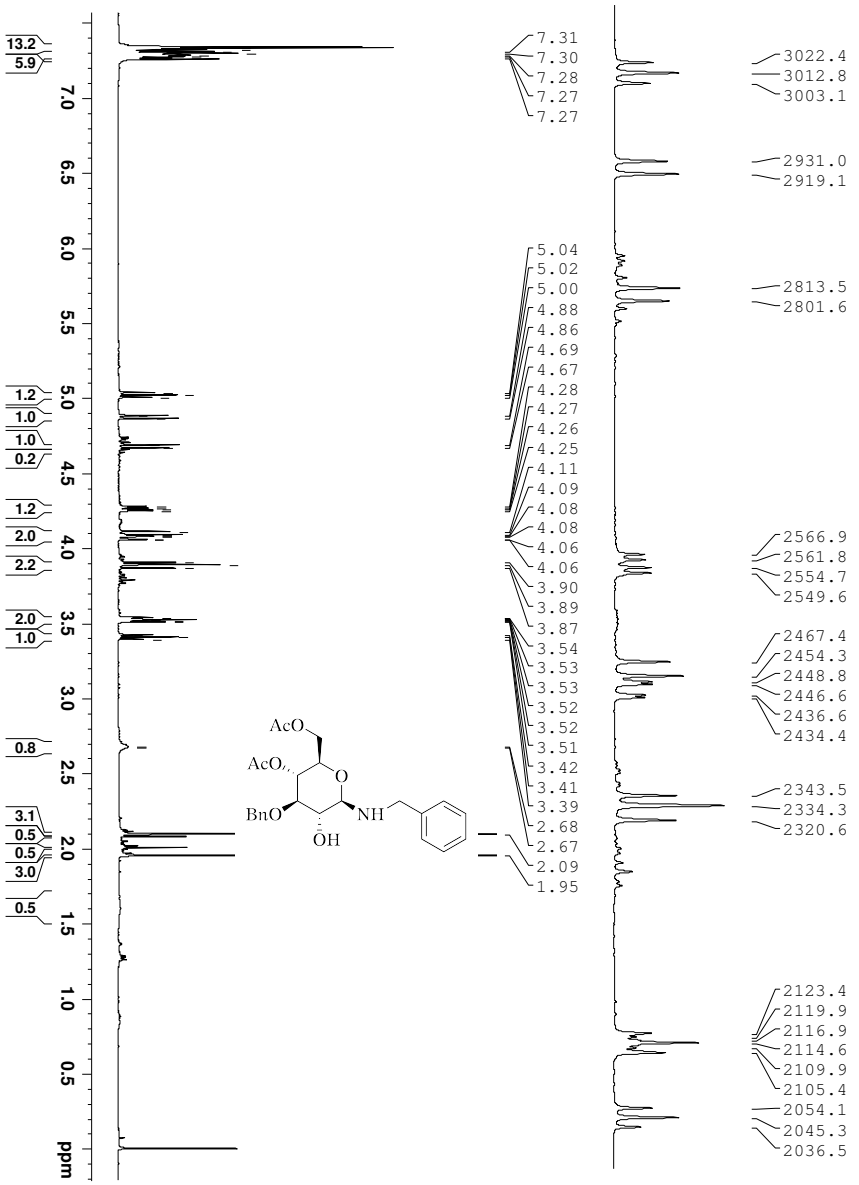

Figure 396: ^{1}H NMR spectrum of *N*-benzyl-3-*O*-benzyl-4,6-di-*O*-acetyl-β-D-glucopyranosylamine..

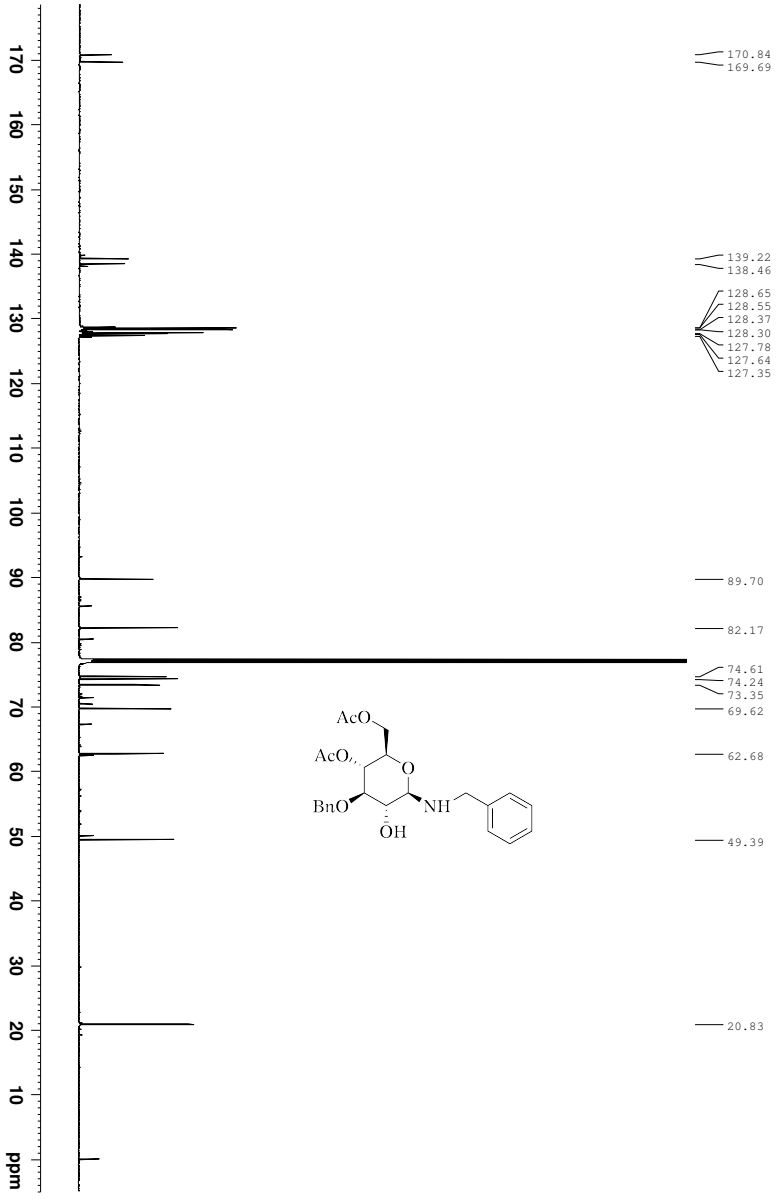

Figure 397: ^{13}C NMR spectrum of *N*-benzyl-3-*O*-benzyl-4,6-di-*O*-acetyl-β-D-glucopyranosylamine.

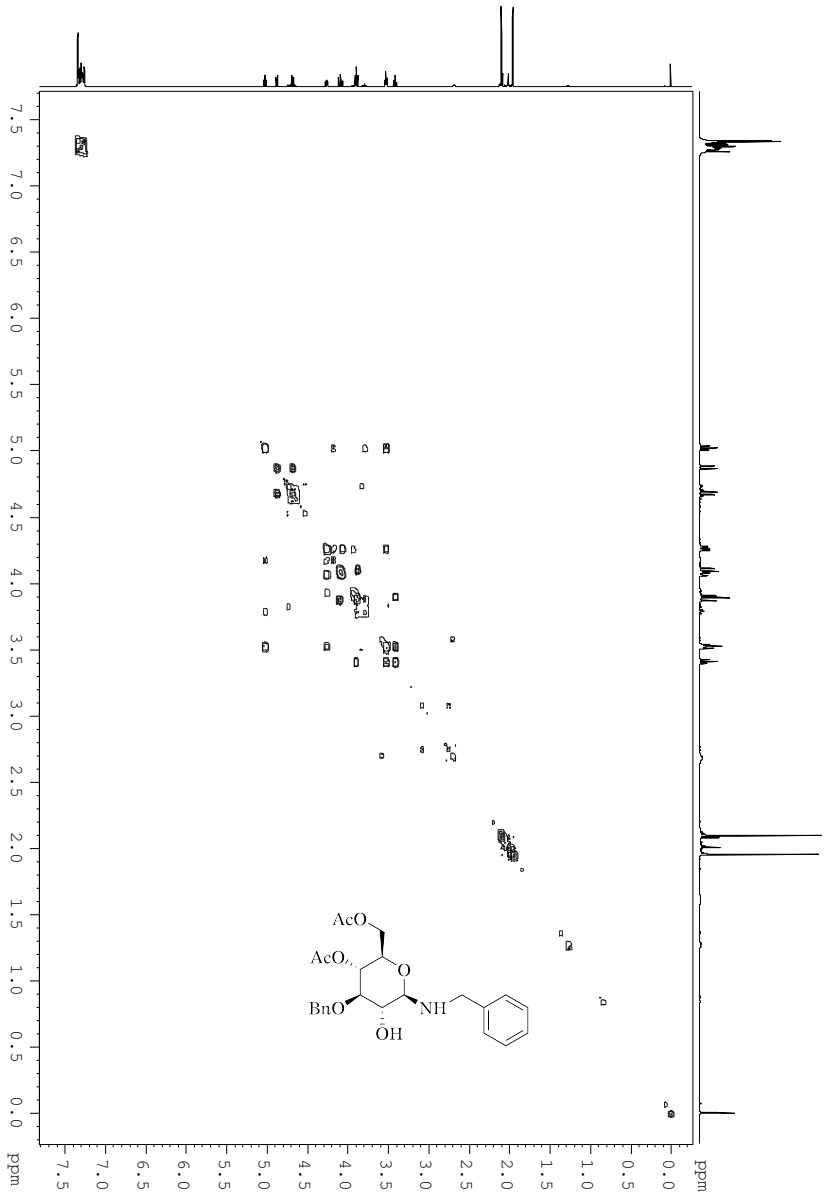

Figure 398: COSY spectrum of *N*-benzyl-3-*O*-benzyl-4,6-di-*O*-acetyl-β-D-glucopyranosylamine.

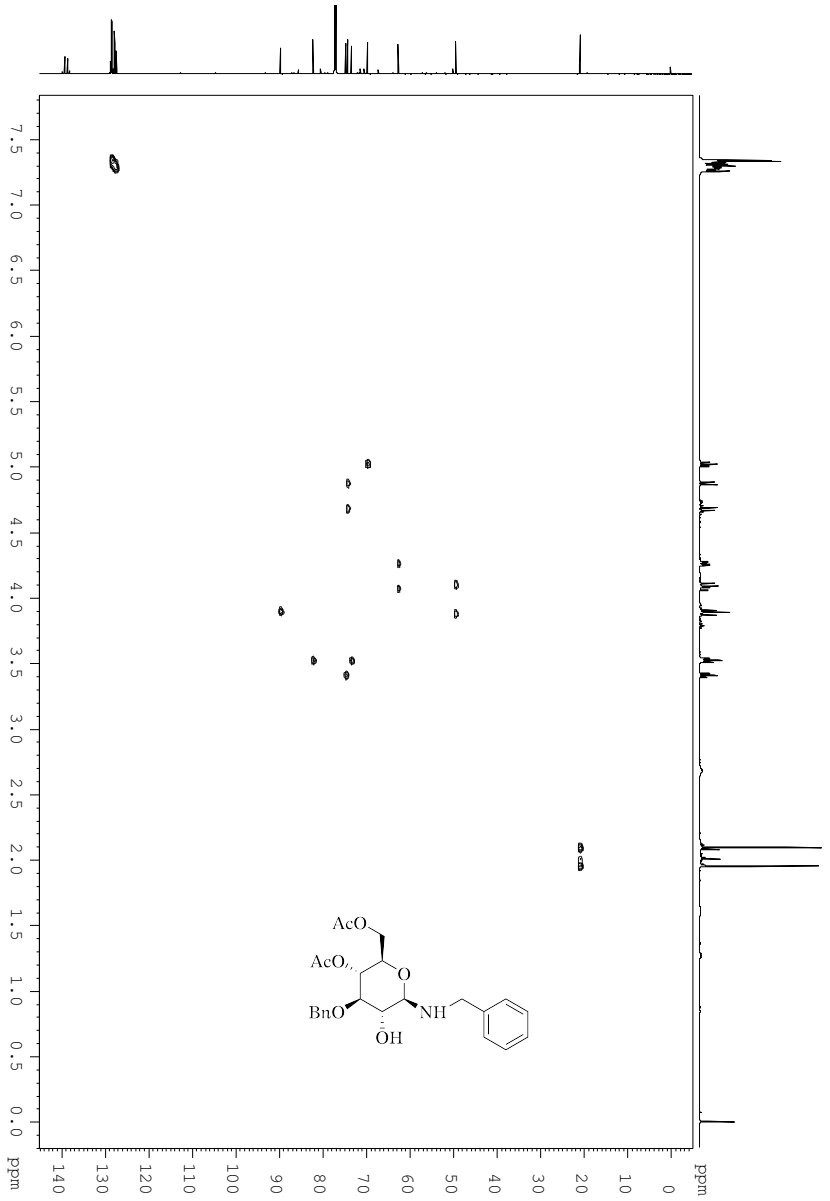

Figure 399: HSQC spectrum of *N*-benzyl-3-*O*-benzyl-4,6-di-*O*-acetyl-β-D-glucopyranosylamine.

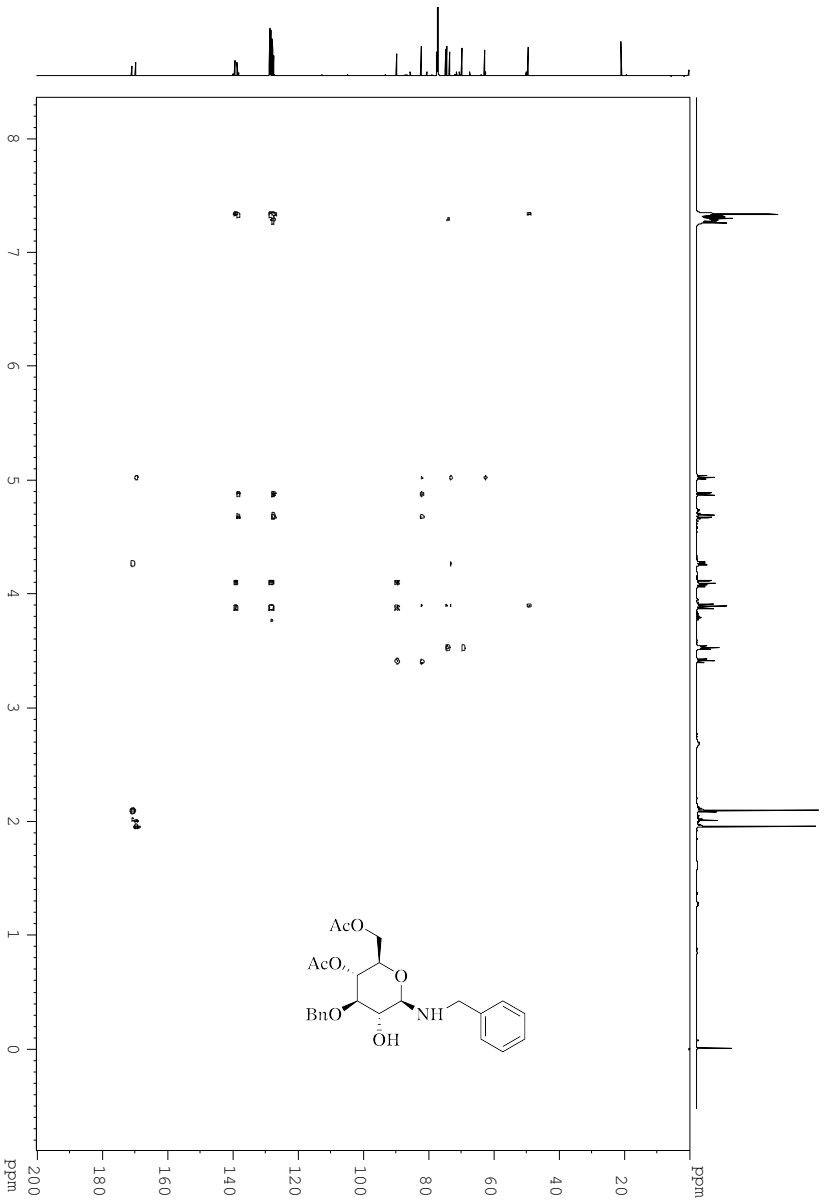

Figure 400: HMBC spectrum of *N*-benzyl-3-*O*-benzyl-4,6-di-*O*-acetyl-β-D-glucopyranosylamine.

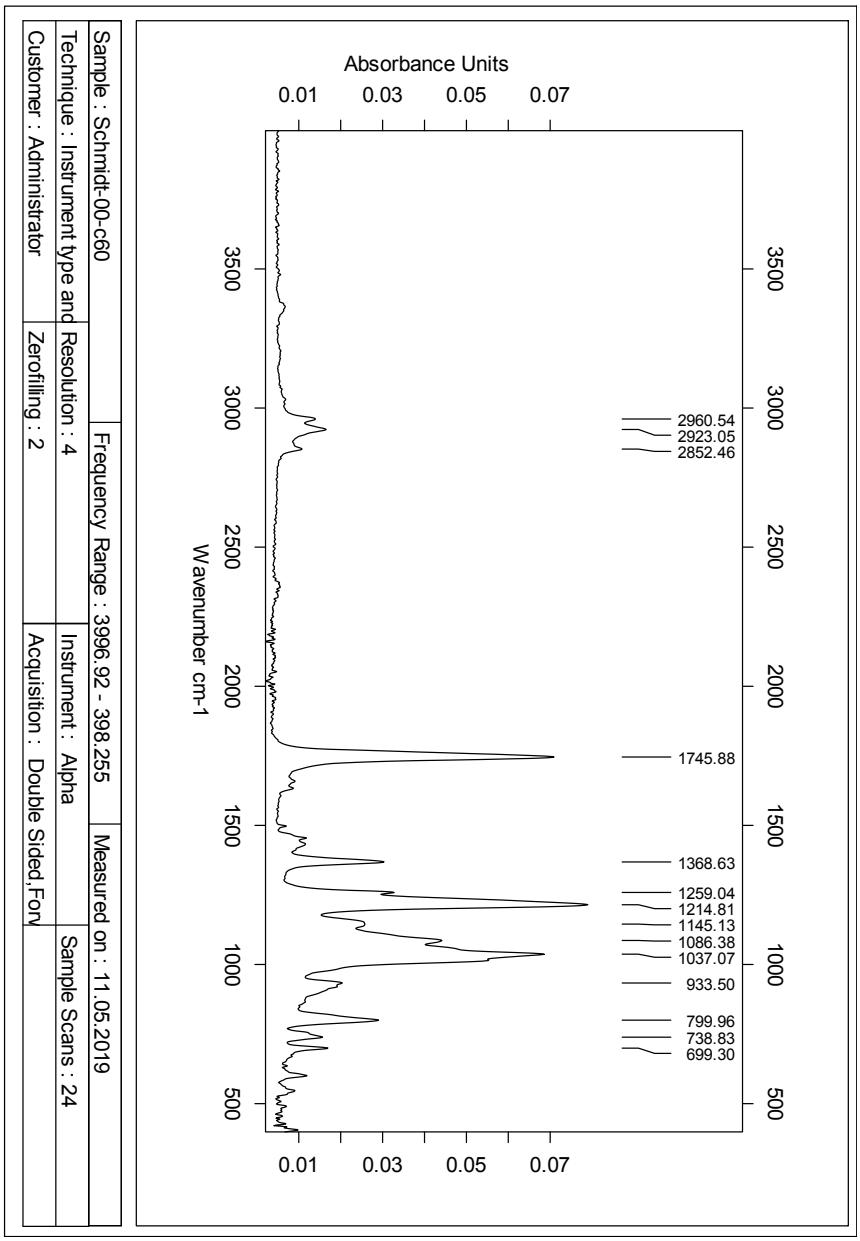

Figure 401: IR spectrum of **n-βn**.

B.55 Spectroscopic data for compound RC-3

Elemental Composition Report **Page 1**

Single Mass Analysis
Tolerance = 2.0 PPM / DBE: min = -2.0, max = 50.0
Element prediction: Off
Number of isotope peaks used for i-FIT = 3

Monoisotopic Mass, Even Electron Ions
295 formula(e) evaluated with 1 results within limits (all results (up to 1000) for each mass)
Elements Used:
C: 0-100 H: 0-150 N: 0-10 O: 0-10 Au: 0-2

2019-12 33 (0.674) AM2 (Ar,35000.0,0.00,0.00); Cm (31:33)
1: TOF MS ASAP+

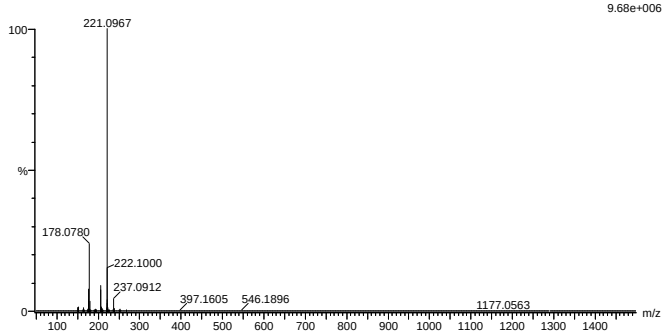

Minimum:				-2.0				
Maximum:		5.0	2.0	50.0				
Mass	Calc. Mass	mDa	PPM	DBE	i-FIT	Norm	Conf(%)	Formula
237.0912	237.0916	-0.4	-1.7	10.5	1416.9	n/a	n/a	C16 H13 O2

Figure 402: HRMS (ASAP+) [M-CH_3] of **RC-3**.

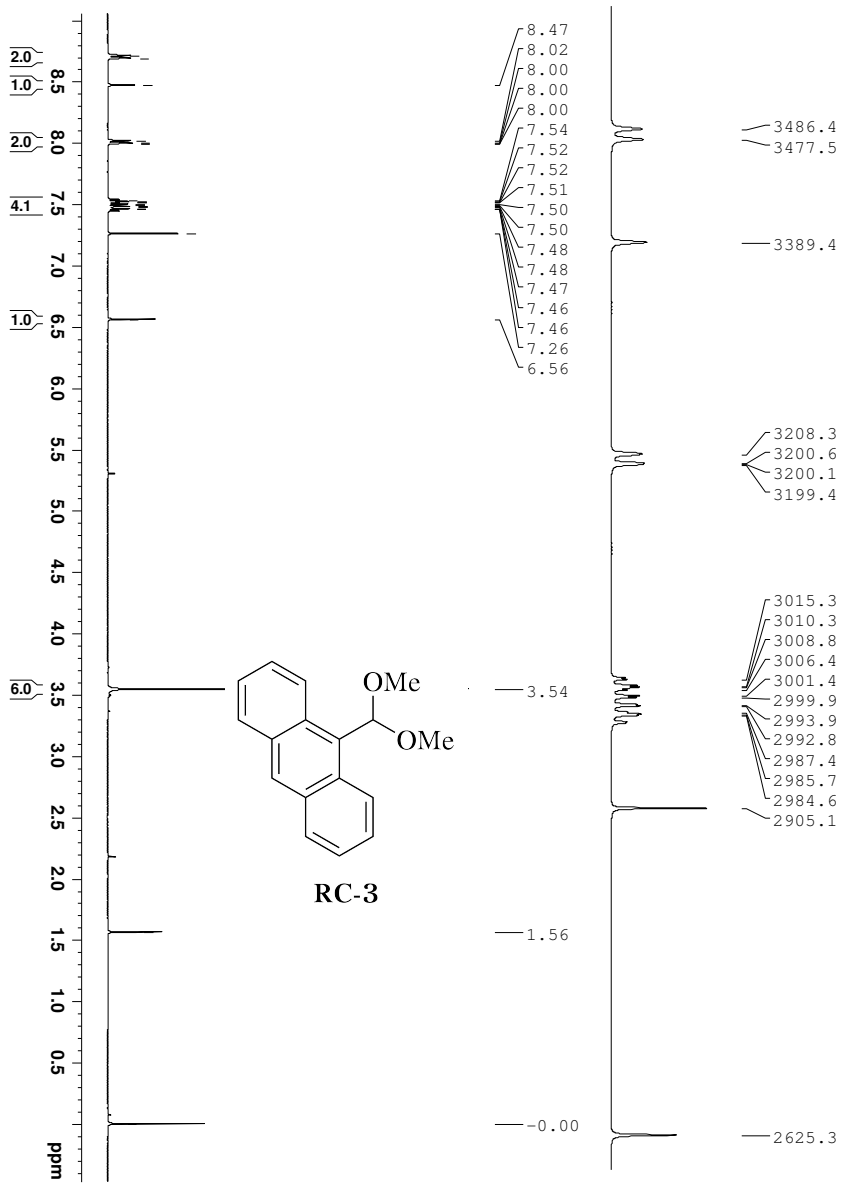

Figure 403: ^{1}H NMR (400 MHz) spectrum of **RC-3**.

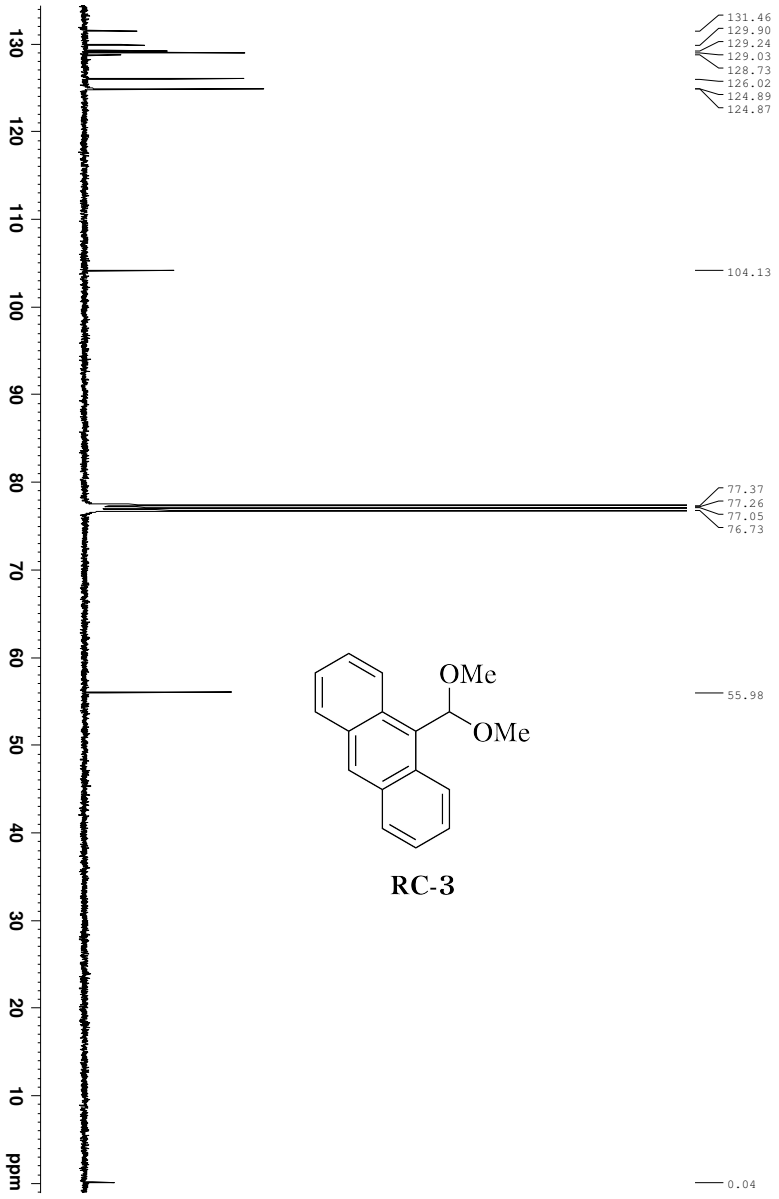

Figure 404: ^{13}C NMR (100 MHz) spectrum of **RC-3**.

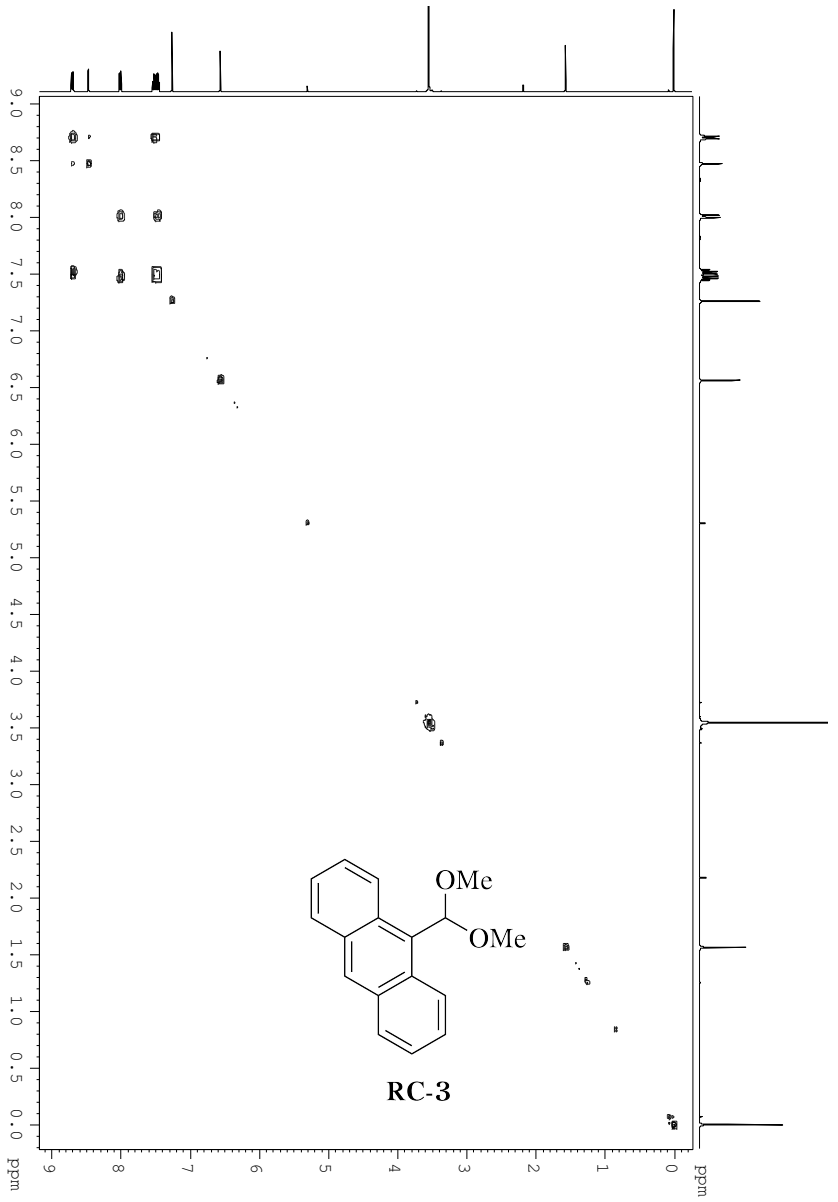

Figure 405: COSY (400 MHz) spectrum of **RC-3**.

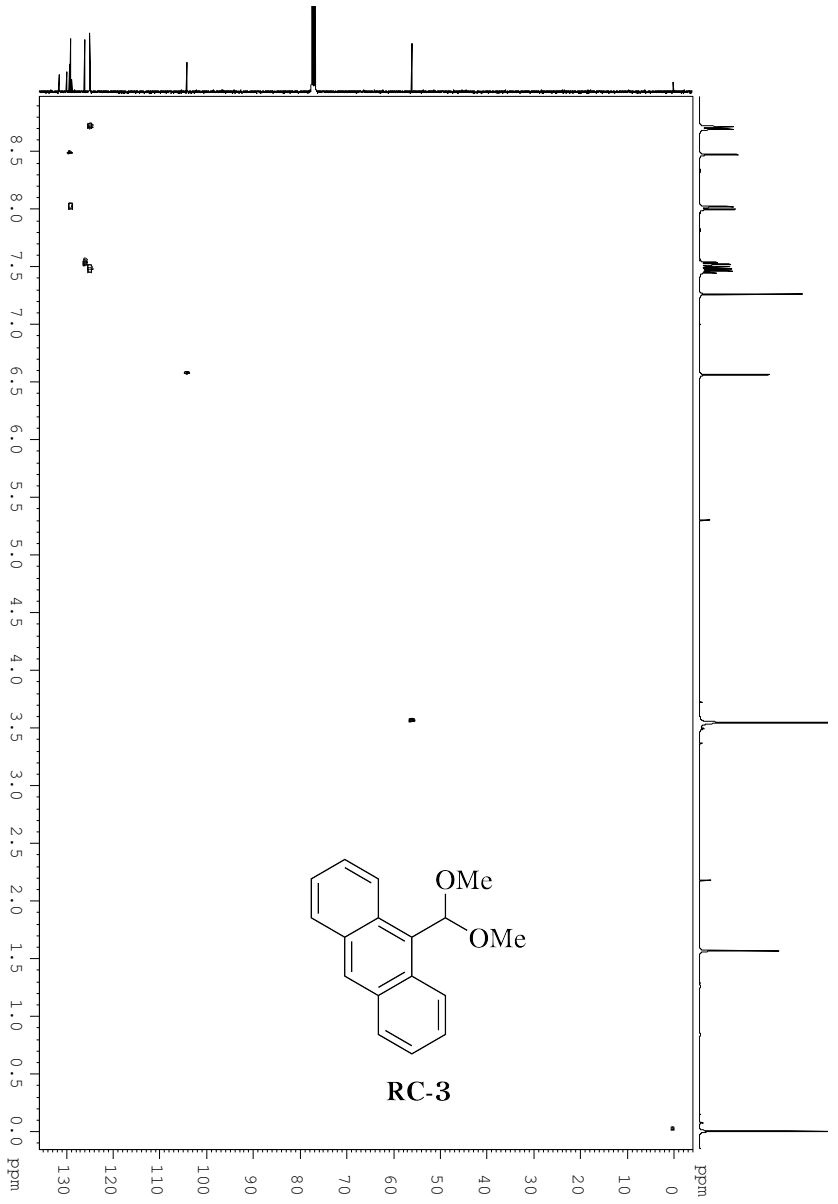

Figure 406: HSQC (400 MHz) spectrum of **RC-3**.

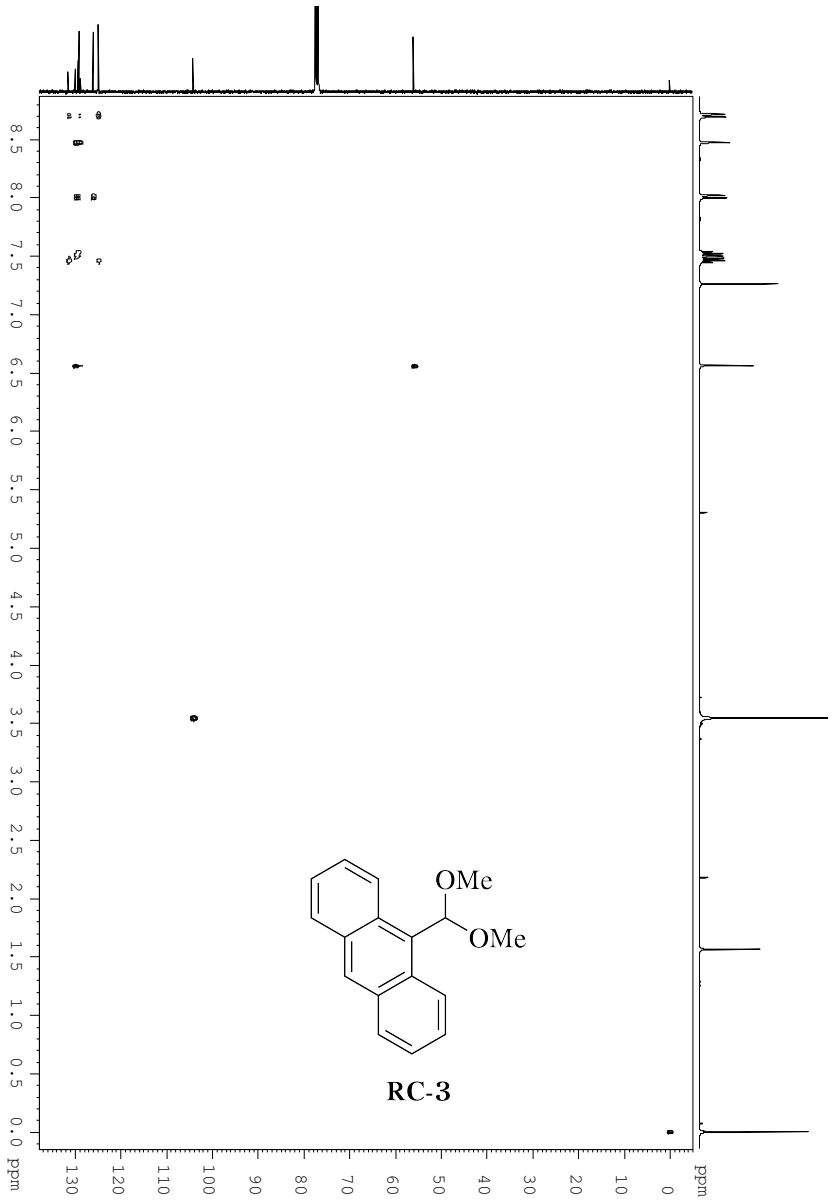

Figure 407: HMBC (400 MHz) spectrum of **RC-3**.

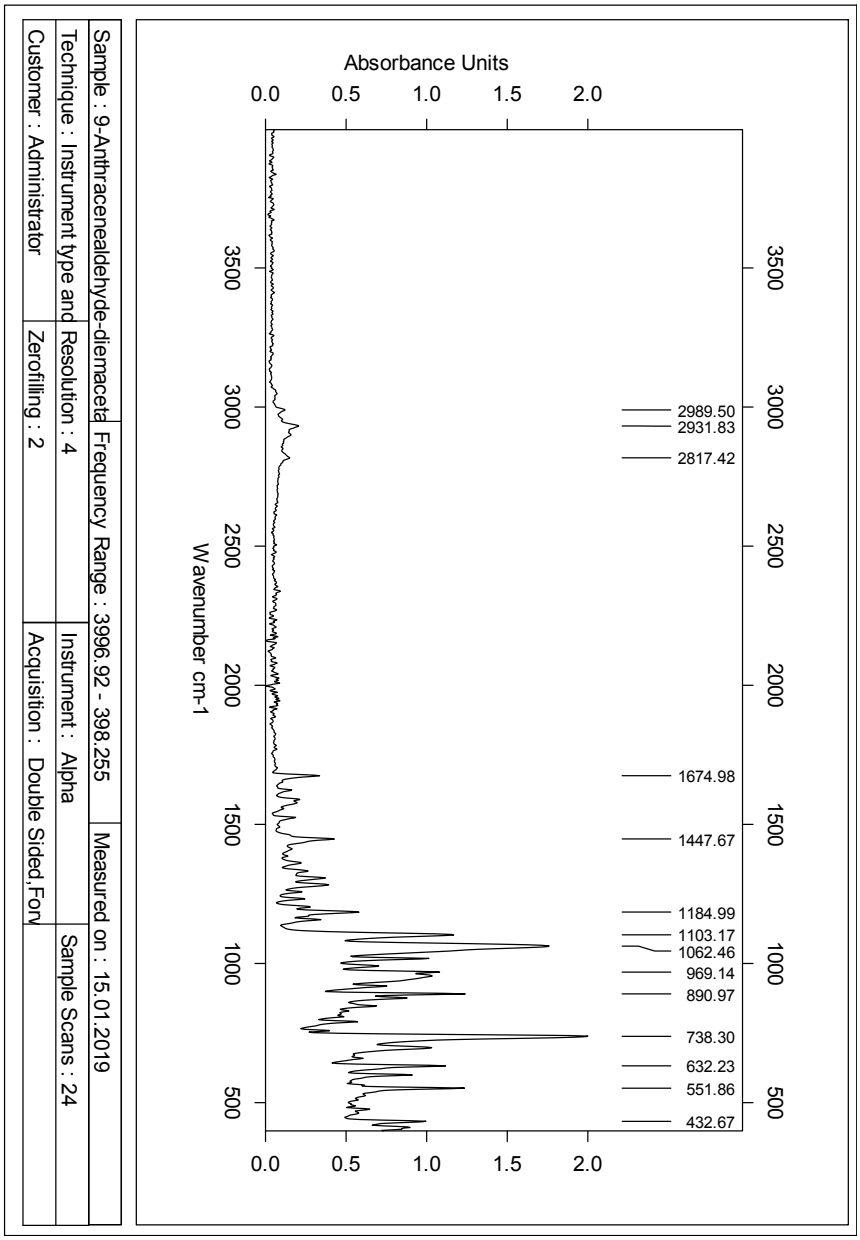

Figure 408: IR spectrum of **RC-3**.

B.56 Spectroscopic data for compound RC-2

Elemental Composition Report **Page 1**

Single Mass Analysis
Tolerance = 10.0 PPM / DBE: min = -1.5, max = 50.0
Element prediction: Off
Number of isotope peaks used for i-FIT = 3

Monoisotopic Mass, Even Electron Ions
241 formula(e) evaluated with 1 results within limits (up to 50 closest results for each mass)
Elements Used:
C: 0-500 H: 0-1000 N: 0-10 O: 0-10 Na: 0-1
2019-11esi 53 (0.505) AM2 (Ar,35000.0,0.00,0.00); Cm (53:55)
1: TOF MS ES+

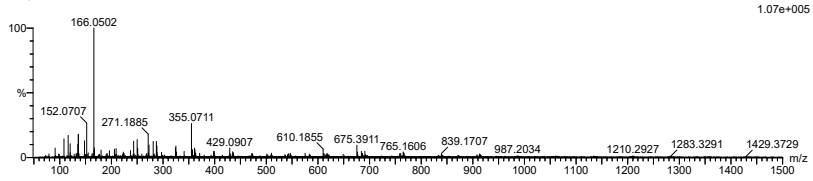

Minimum:				-1.5				
Maximum:		5.0	10.0	50.0				
Mass	Calc. Mass	mDa	PPM	DBE	i-FIT	Norm	Conf(%)	Formula
166.0502	166.0504	-0.2	-1.2	5.5	1294.8	n/a	n/a	C8 H8 N O3

Figure 409: HRMS (ESI+) [M+Na-CH_3] of **RC-2**.

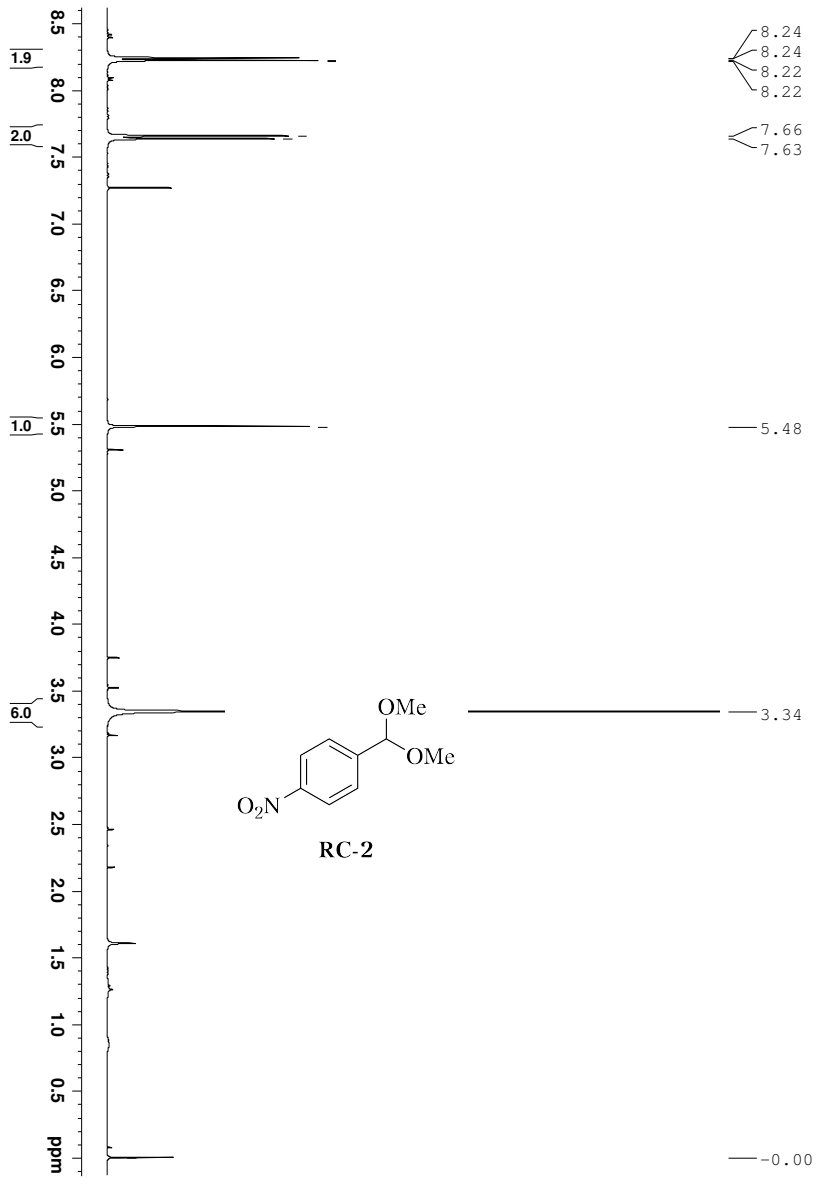

Figure 410: ^{1}H NMR (400 MHz) spectrum of **RC-2**.

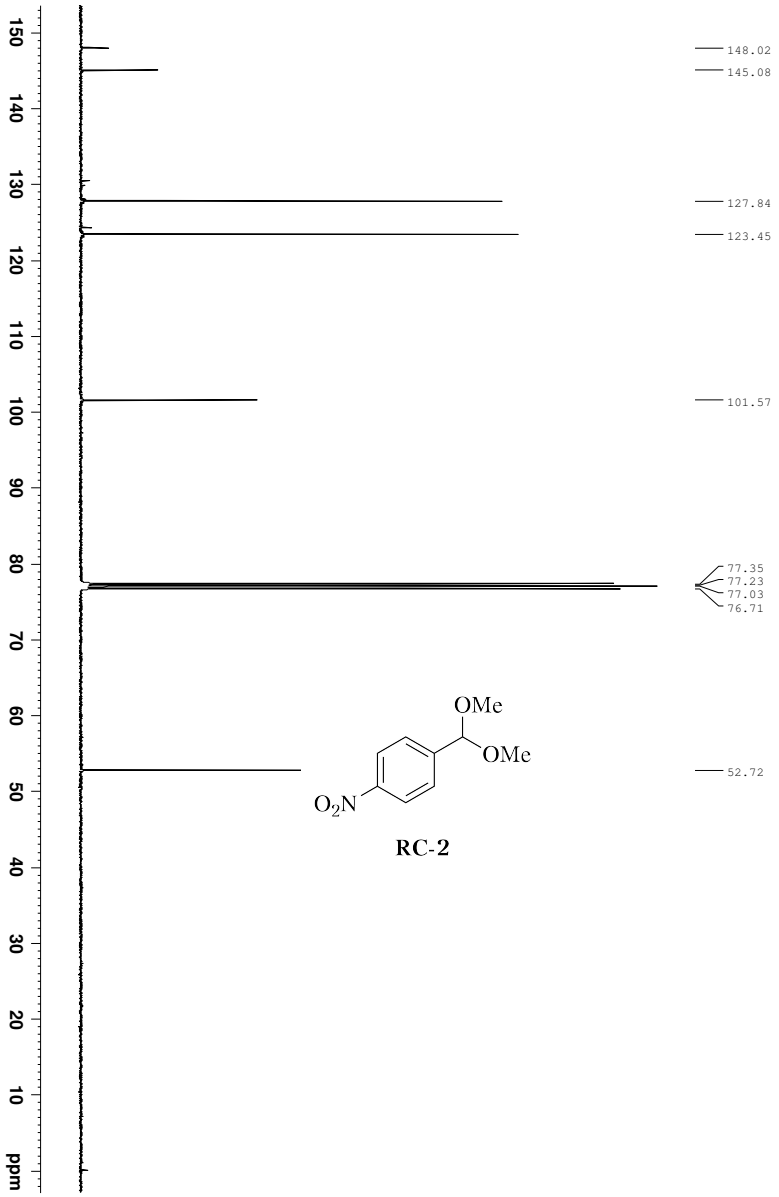

Figure 411: ^{13}C NMR (100 MHz) spectrum of **RC-2**.

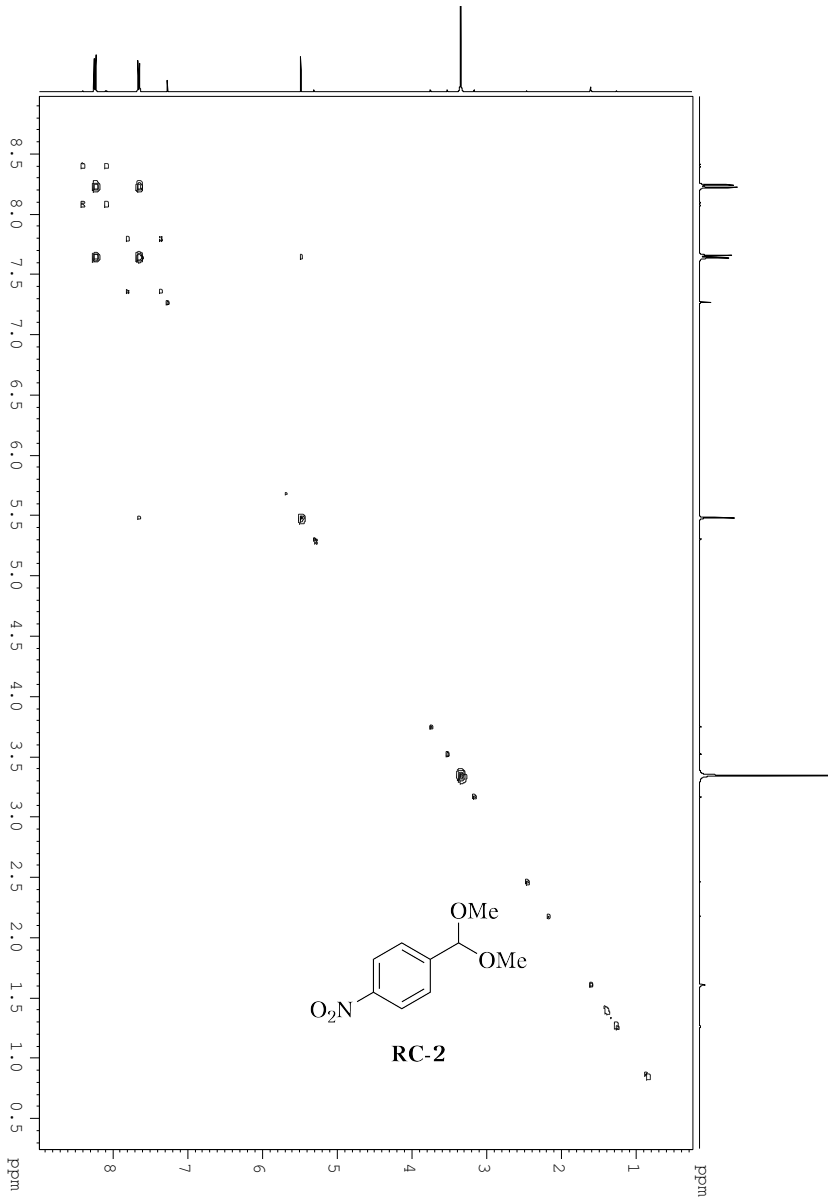

Figure 412: COSY (400 MHz) spectrum of **RC-2**.

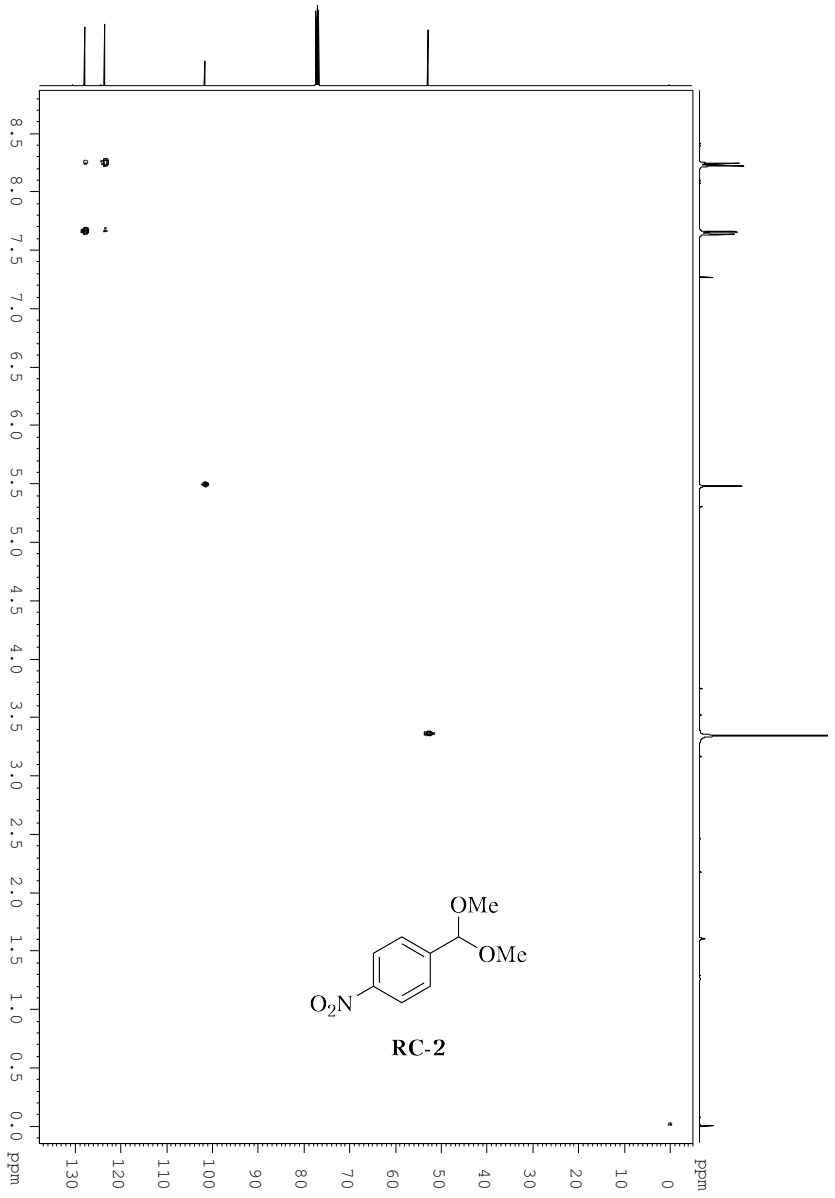

Figure 413: HSQC (400 MHz) spectrum of **RC-2**.

cd

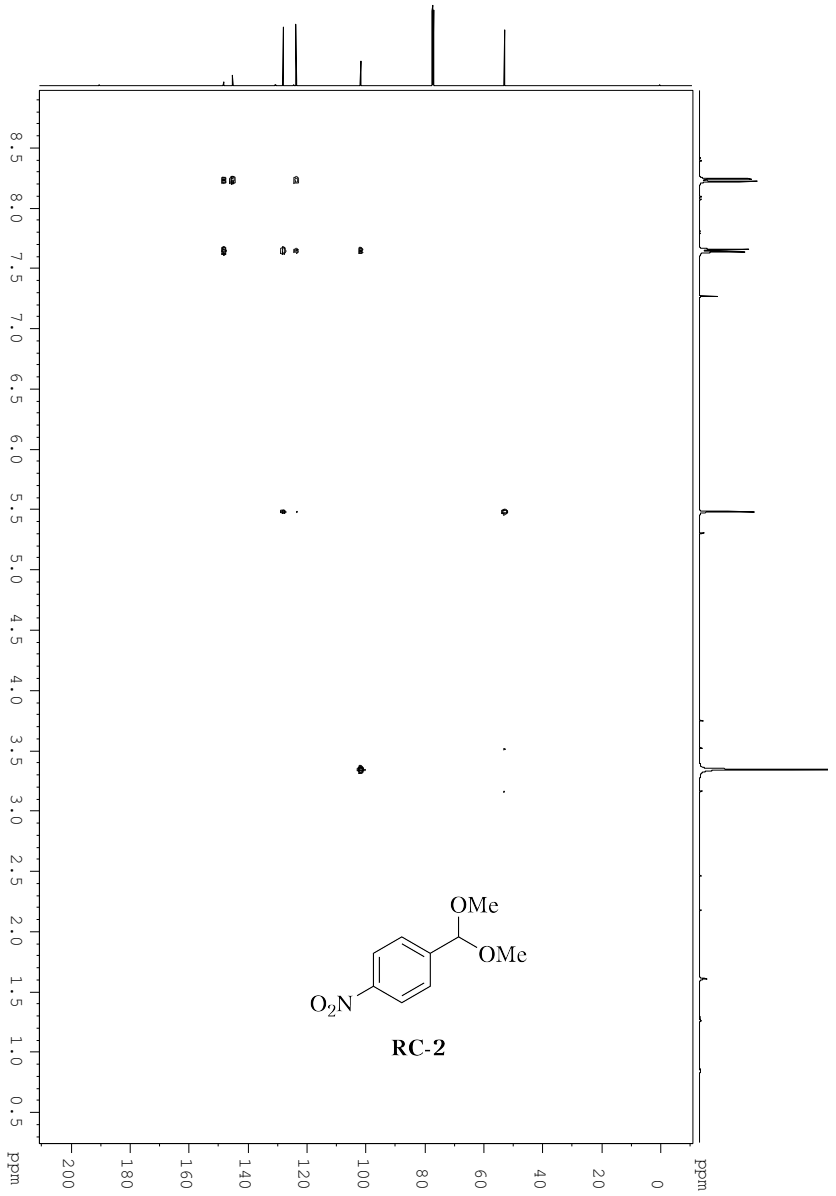

Figure 414: HMBC (400 MHz) spectrum of **RC-2**.

cdi

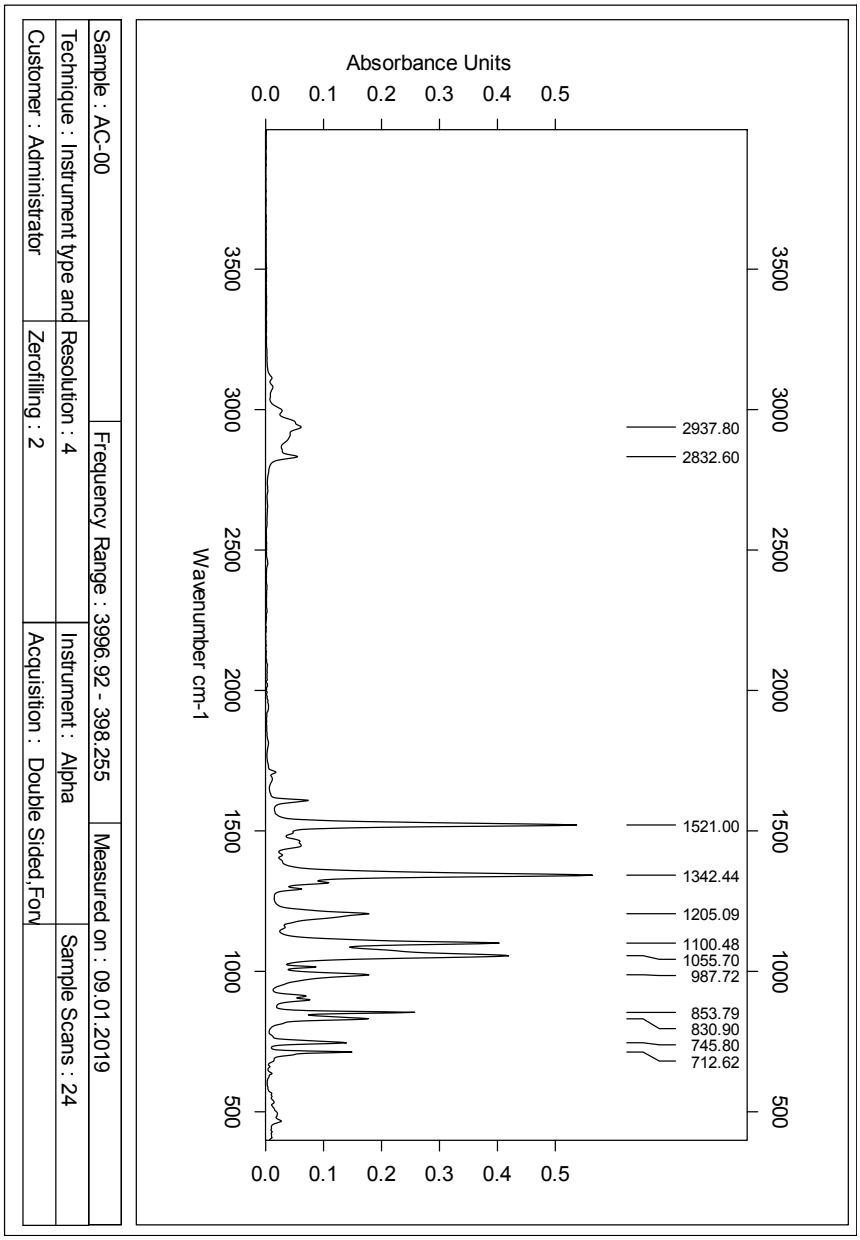

Figure 415: IR spectrum of **RC-2**.

B.57 Spectroscopic data for compound RC-1

Elemental Composition Report **Page 1**

Single Mass Analysis
Tolerance = 2.0 PPM / DBE: min = -50.0, max = 50.0
Element prediction: Off
Number of isotope peaks used for i-FIT = 3

Monoisotopic Mass, Odd Electron Ions
913 formula(e) evaluated with 1 results within limits (all results (up to 1000) for each mass)
Elements Used:
C: 0-100 H: 0-150 N: 0-5 O: 0-5 Cl: 0-2
2019-207 37 (0.741) AM2 (Ar,35000.0,0.00,0.00); Cm (33:39)
1: TOF MS ASAP+

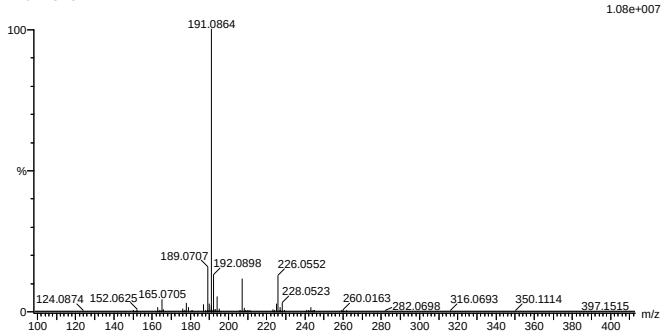

Minimum:				-50.0				
Maximum:		5.0	2.0	50.0				
Mass	Calc. Mass	mDa	PPM	DBE	i-FIT	Norm	Conf(%)	Formula
226.0552	226.0549	0.3	1.3	10.0	1560.3	n/a	n/a	C15 H11 Cl

Figure 416: HRMS (ASAP+) [M] of **RC-1**.

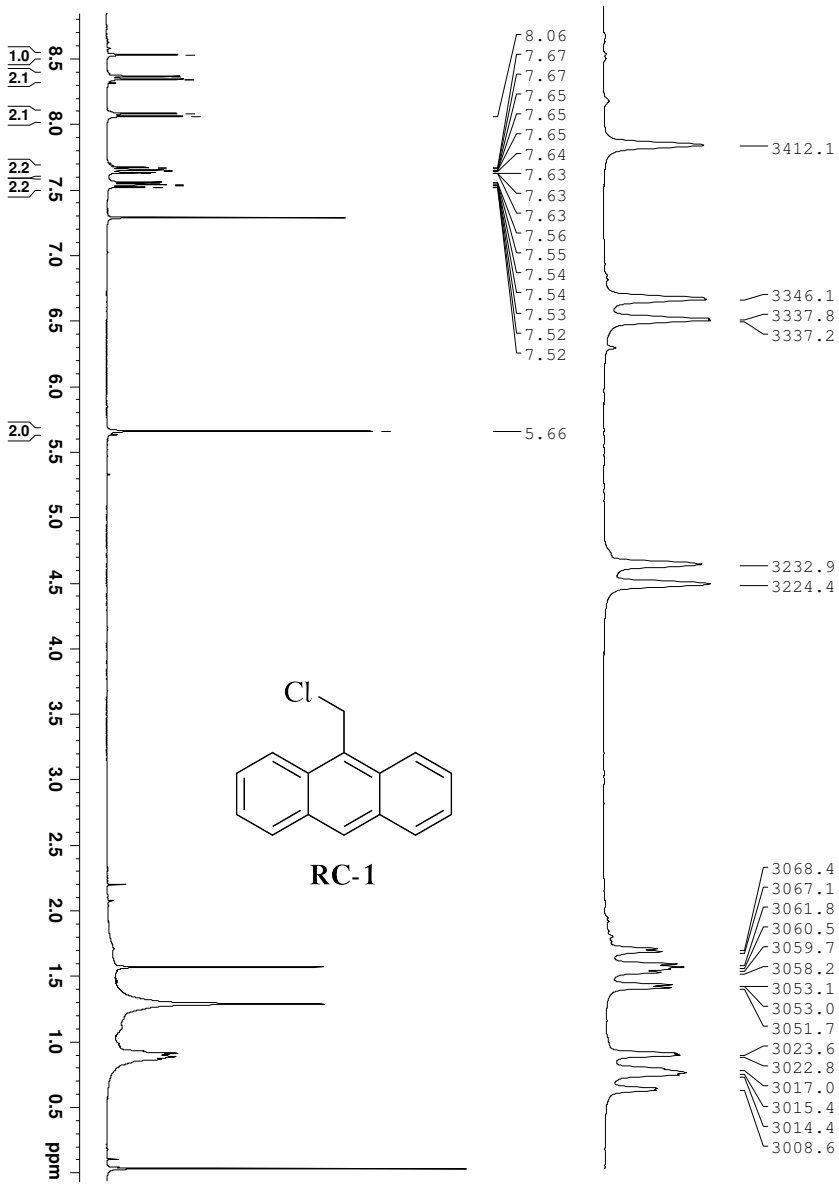

Figure 417: ^{1}H NMR (400 MHz) spectrum of **RC-1**.

cdiv

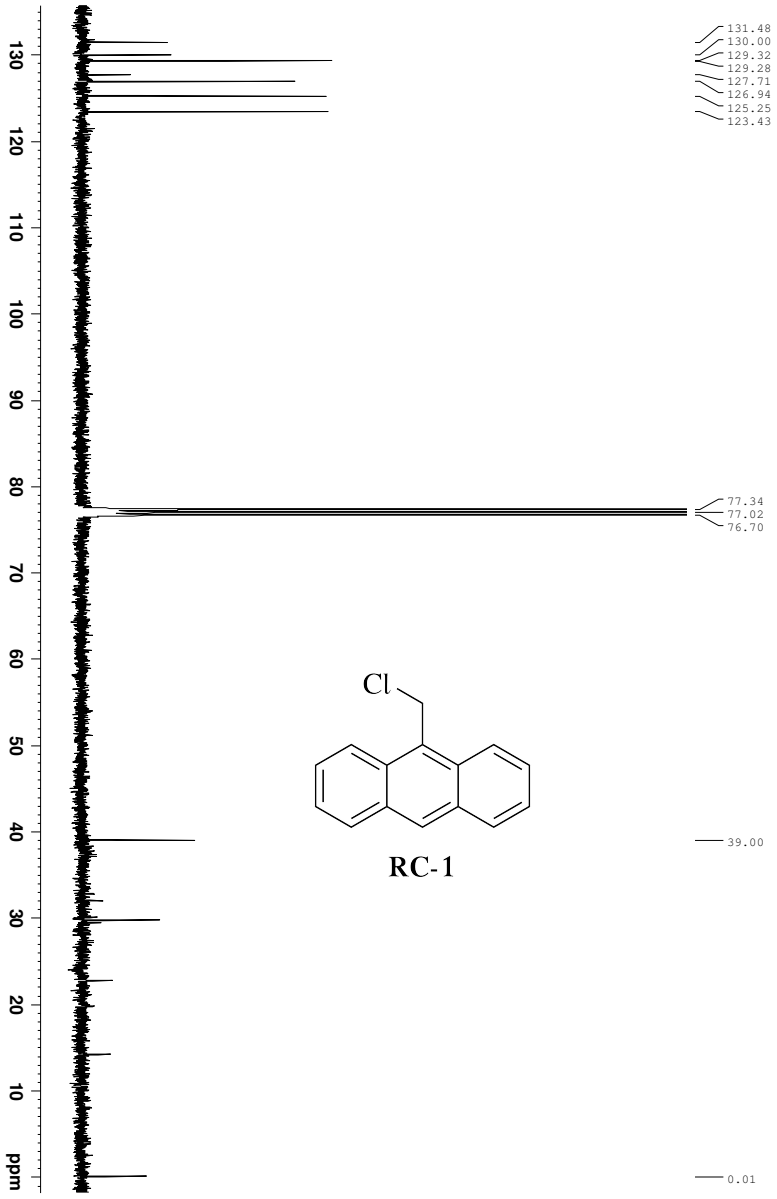

Figure 418: ^{13}C NMR (100 MHz) spectrum of **RC-1**.

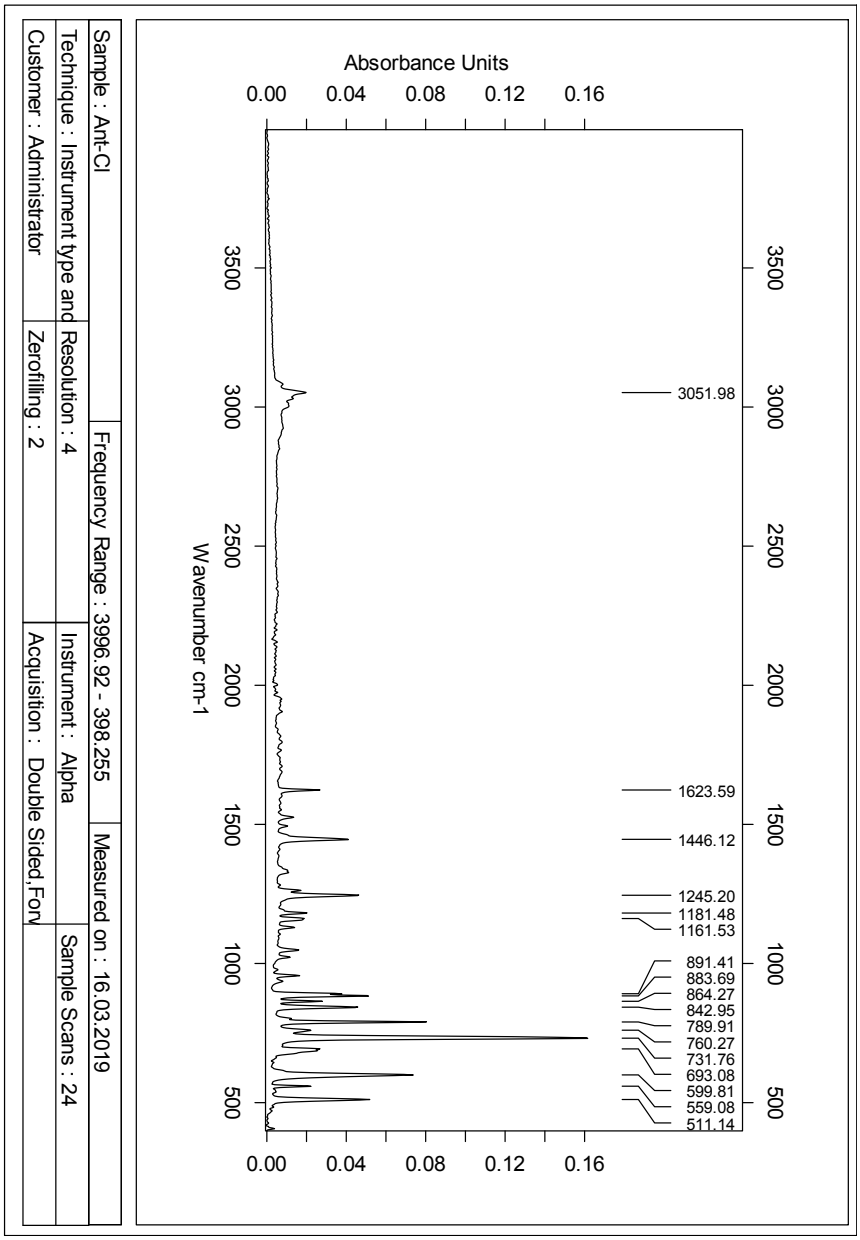

Figure 419: IR spectrum of **RC-1**.

B.58 Spectroscopic data for 3-*O*-Benzyl-4-*O*-trichloroacetimidate-1,2,6-tri-*O*-acetyl-α, β-D-glucopyranose

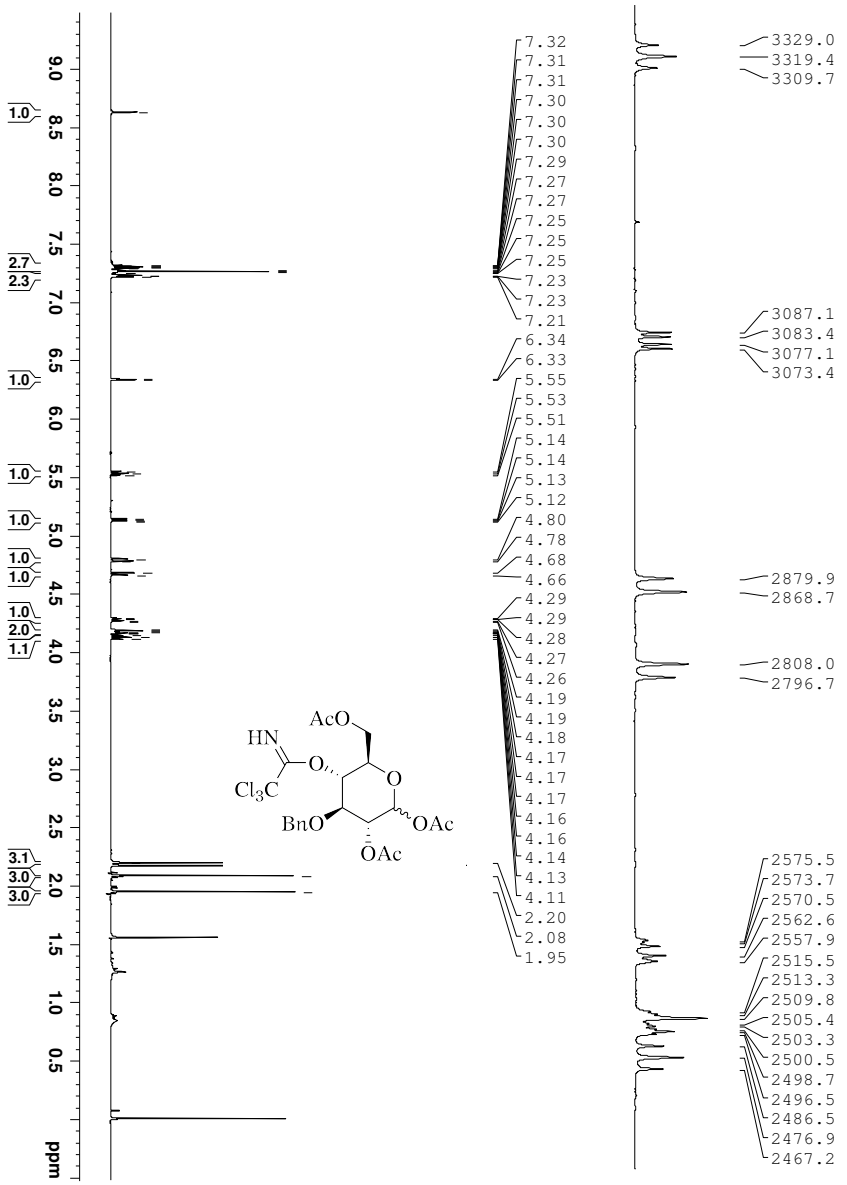

Figure 420: ^{1}H NMR spectrum of 3-*O*-Benzyl-4-*O*-trichloroacetimidate-1,2,6-tri-*O*-acetyl-α-D-glucopyranose.

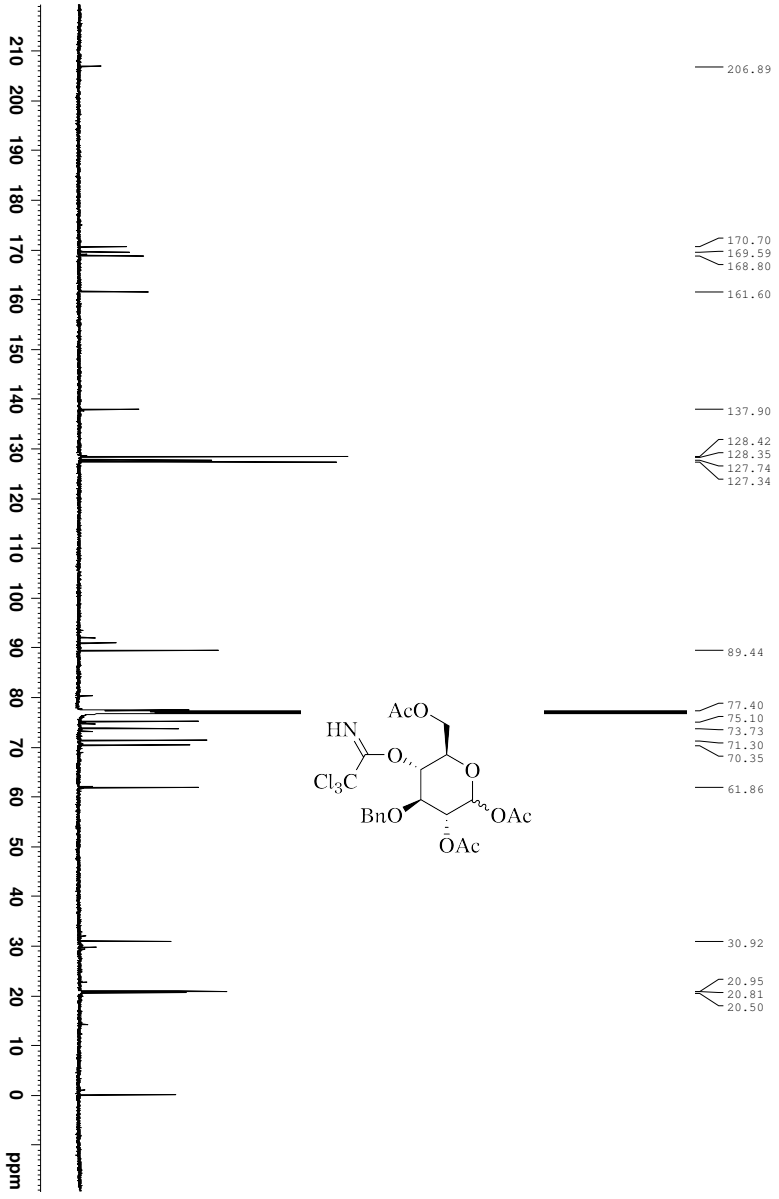

Figure 421: ^{13}C NMR spectrum of 3-*O*-Benzyl-4-*O*-trichloroacetimidate-1,2,6-tri-*O*-acetyl-α-D-glucopyranose.

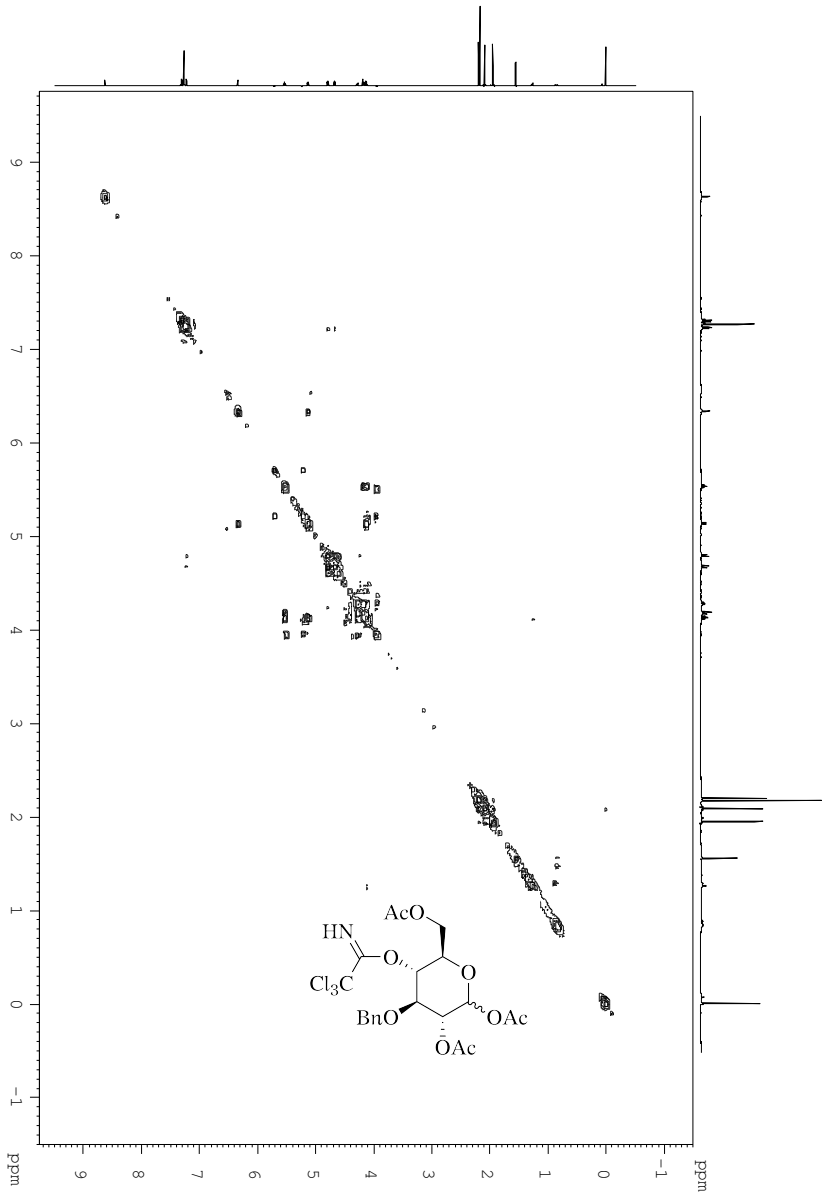

Figure 422: COSY spectrum of 3-*O*-Benzyl-4-*O*-trichloroacetimidate-1,2,6-tri-*O*-acetyl-α-D-glucopyranose.

cdx

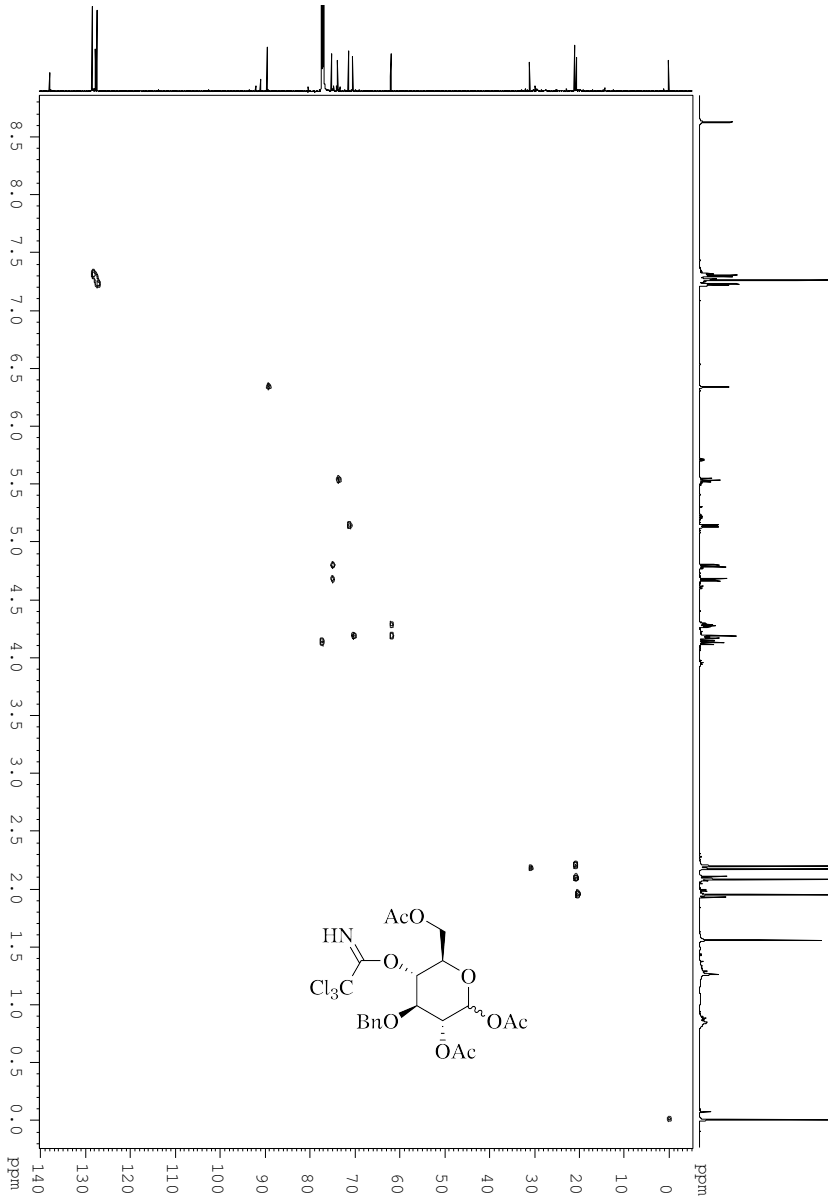

Figure 423: HSQC spectrum of 3-*O*-Benzyl-4-*O*-trichloroacetimidate-1,2,6-tri-*O*-acetyl-α-D-glucopyranose.

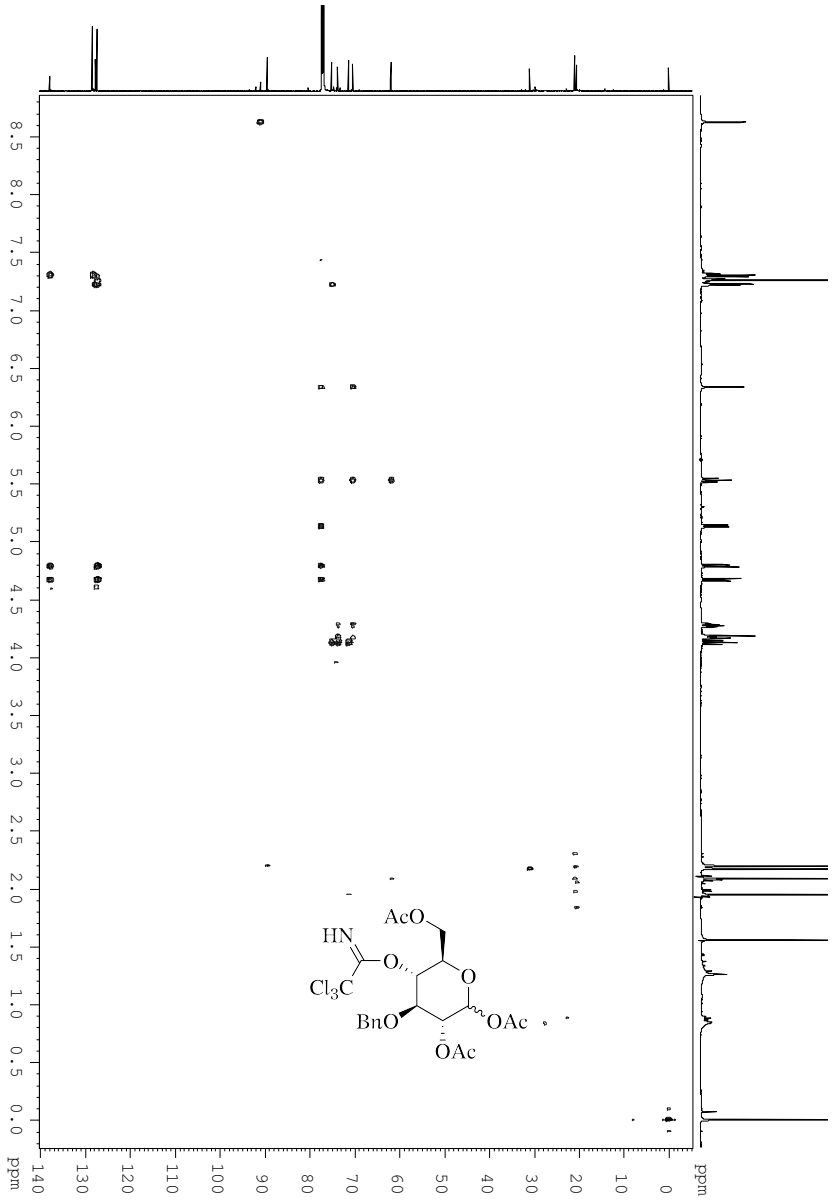

Figure 424: HMBC spectrum of 3-*O*-Benzyl-4-*O*-trichloroacetimidate-1,2,6-tri-*O*-acetyl-α-D-glucopyranose.

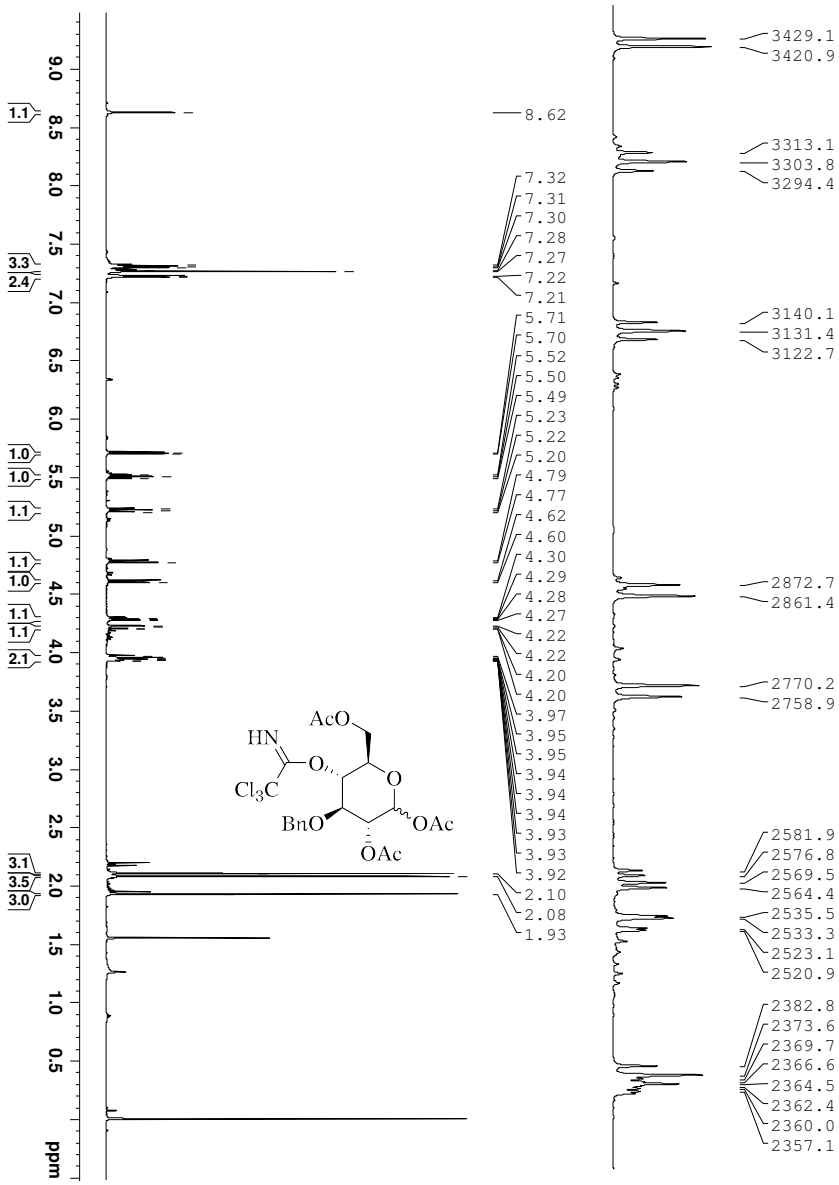

Figure 425: ^{1}H NMR spectrum of 3-*O*-Benzyl-4-*O*-trichloroacetimidate-1,2,6-tri-*O*-acetyl-β-D-glucopyranose.

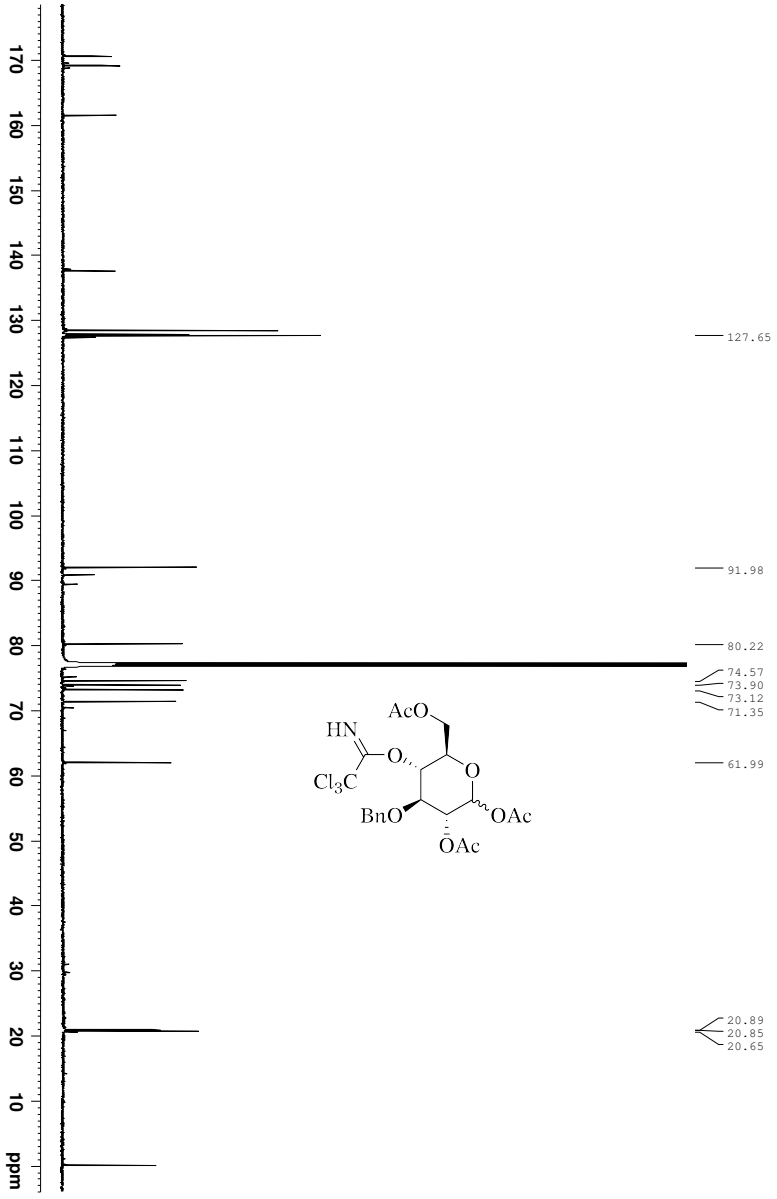

Figure 426: ^{13}C NMR spectrum of 3-*O*-Benzyl-4-*O*-trichloroacetimidate-1,2,6-tri-*O*-acetyl-β-D-glucopyranose.

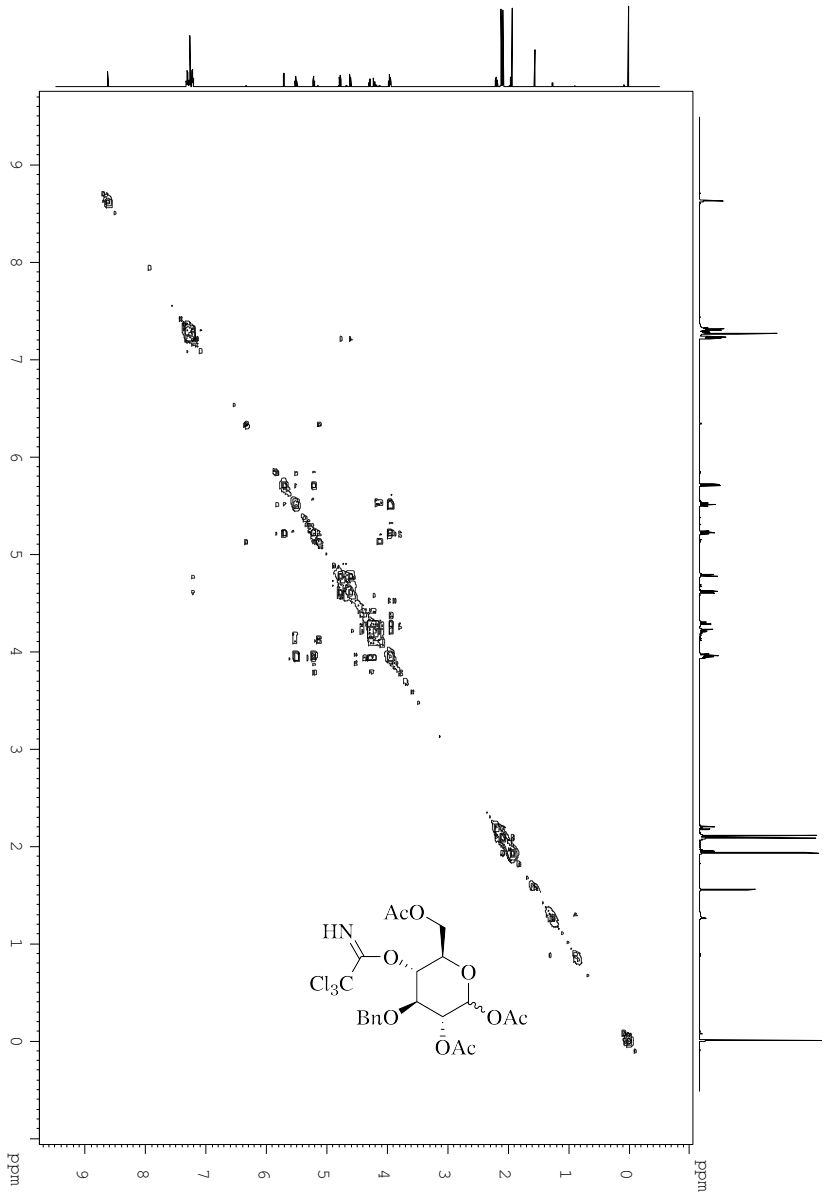

Figure 427: COSY spectrum of 3-*O*-Benzyl-4-*O*-trichloroacetimidate-1,2,6-tri-*O*-acetyl-β-D-glucopyranose.

cdxv

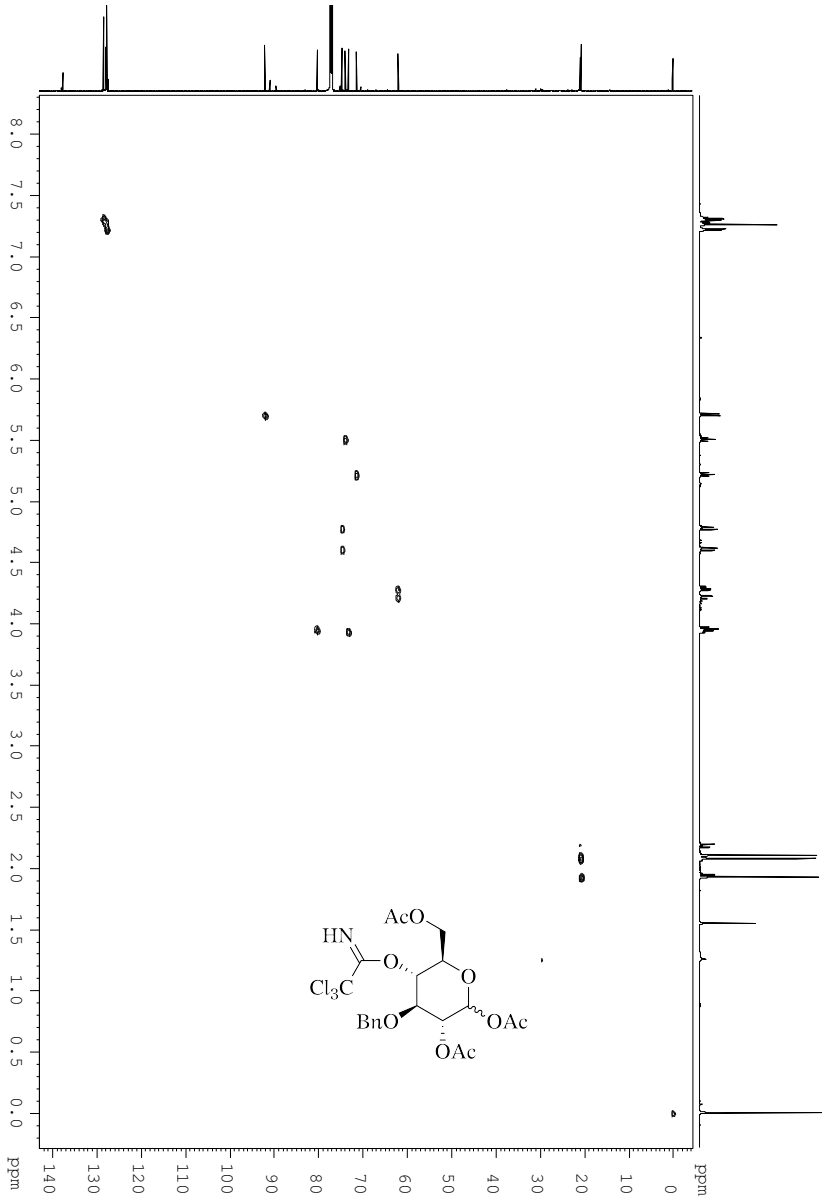

Figure 428: HSQC spectrum of 3-*O*-Benzyl-4-*O*-trichloroacetimidate-1,2,6-tri-*O*-acetyl-β-D-glucopyranose.

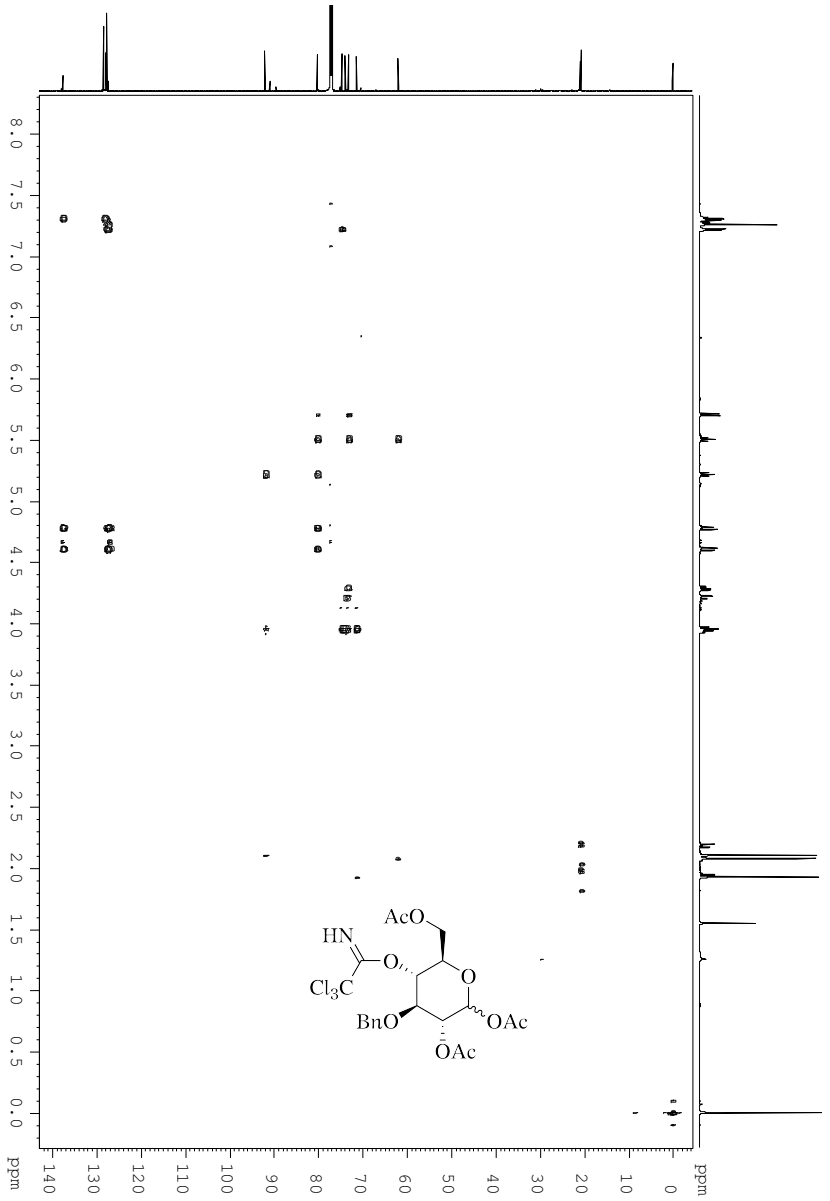

Figure 429: HMBC spectrum of 3-*O*-Benzyl-4-*O*-trichloroacetimidate-1,2,6-tri-*O*-acetyl-β-D-glucopyranose.